Agronomy Research

Established in 2003 by the Faculty of Agronomy, Estonian Agricultural University

Aims and Scope:
Agronomy Research is a peer-reviewed international Journal intended for publication of broad-spectrum original articles, reviews and short communications on actual problems of modern biosystems engineering incl. crop and animal science, genetics, economics, farm- and production engineering, environmental aspects, agro-ecology, renewable energy and bioenergy etc. in the temperate regions of the world.

***Agronomy Research* online:**
Agronomy Research is available online at: https://agronomy.emu.ee/

Acknowledgement to Referees:
The Editors of *Agronomy Research* would like to thank the many scientists who gave so generously of their time and expertise to referee papers submitted to the Journal.

Abstracted and indexed:
SCOPUS, EBSCO, DOAJ, CABI Full Paper and Clarivate Analytics database: (Zoological Records, Biological Abstracts and Biosis Previews, AGRIS, ISPI, CAB Abstracts, AGRICOLA (NAL; USA), VINITI, INIST-PASCAL.)

Subscription information:
Institute of Technology, EMU
Fr.R. Kreutzwaldi 56,
51006 Tartu,
ESTONIA
E-mail: timo.kikas@emu.ee

Journal Policies:
Estonian University of Life Sciences, Latvia University of Life Sciences and Technologies, Vytautas Magnus University Agriculture Academy, Lithuanian Research Centre for Agriculture and Forestry, and Editors of *Agronomy Research* assume no responsibility for views, statements and opinions expressed by contributors. Any reference to a pesticide, fertiliser, cultivar or other commercial or proprietary product does not constitute a recommendation or an endorsement of its use by the author(s), their institution or any person connected with preparation, publication or distribution of this Journal.

ISSN 1406-894X

CONTENTS

Agronomy Research **18**(4), 2291–2302, 2020
https://doi.org/10.15159/AR.20.173

Assessment of management effect on grasslands characteristics in an area of the Apennines (North Italy)

G. Argenti[1,*], F. Del Serra[1], N. Staglianò[1] and I. Battaglini[2]

[1]University of Florence, School of Agriculture, DAGRI, P.le delle Cascine 18, IT50144 Firenze, Italy
[2]Unione di Comuni Valdarno e Valdisieve, Via XXV Aprile, 10, IT50068 Rufina (FI), Italy
[*]Correspondence: giovanni.argenti@unifi.it

Abstract. In many regions of Europe, semi-natural grasslands not properly utilized face different threats, concerning changes in botanical composition and structural evolution, which can lead to a reduction of the qualitative value of forage biomass or, in the mid-long term, forest recovery. The present paper assesses various semi-natural grasslands within a mountain public property located in Tuscany (North Apennines, Italy) subjected to different types of utilization. Some of them are managed through cattle grazing during summer, whereas some others are only periodically mowed and utilization is performed only by wildlife occurring in the area. The paper analyses the importance of resource management and its impact on botanical composition and on qualitative value of forage production. Data collection of studied areas was conducted by means of vegetation assessment performed with a fast procedure that simplifies the botanical composition sampling. Results show the relevance of some environmental factors on grasslands evolution and on their composition (such as altitude and slope) and the importance of management on grassland quality and on level of shrub encroachment.

Key words: botanical composition, grazing, mowing, pastoral value, habitat improvement.

INTRODUCTION

Grasslands are one of the most widespread land use in the world (Dixon et al., 2014) and in Europe they cover more than 50 million ha (Stypinski, 2011). They provide a great number of ecosystem services that go beyond the mere productive function traditionally acknowledged to these resources (Conant et al., 2017; Targetti et al., 2018). Rational management of grasslands and pastures can, in turn, maintain services related to soil protection, to preservation of landscape and endangered species linked to open spaces, to conservation of areas useful for wildlife, to enhancement of the environment for touristic activity (Hopkins & Holz, 2006; Komac et al., 2014; Primi et al., 2016; Hao et al., 2017; Bengtsson et al., 2019).

Nowadays, in many Italian regions, these resources are threatened by a reduction of utilization or abandonment (Argenti et al., 2011; Probo et al., 2013). This evolution is ongoing since the middle of the last century and it is particularly evident in mountain areas (Faccioni et al., 2019) where depopulation and ageing led to remarkable changes in the employment of the agricultural territory and the landscape (Giustini et al., 2007; Orlandi et al., 2016). The causes of the abandonment of mountain agricultural and pastoral land are to be found in the socio-economic changes that have taken place in Italy and in many other European countries since the 1950s (Pittarello et al., 2020). In marginal areas, one of the most evident consequences of reduced utilization or land abandonment is the encroachment performed by shrubs and trees (Grau et al., 2019) and, consequently, the contraction of surface occupied by open habitats and grasslands (Urbina et al., 2020). Disappearance of grasslands presents a fundamental environmental significance (Rook & Tallowin, 2003), which is of extremely importance especially in mountain areas (Moudrý et al., 2009), where animal utilization can be represented not only by domestic herbivores, but also by wildlife, with consequent reduction of available forage biomass also for these animals' species (Ponzetta et al., 2010).

Taking into account the above-reported considerations, it is, therefore, necessary to protect the integrity and ecological quality of grasslands, as they are functional elements for maintaining biodiversity, both at local and territorial level (Gusmeroli et al., 2013). Following the progressive reduction of traditional agricultural practices, the landscape is slowly changing with a consequent increase in environmental uniformity (Burrascano et al., 2016) and such loss of heterogeneity can reduce its value as it is perceived by the general public (Lamarque et al., 2011). In this way, rational management performed by mowing or by animal grazing should be accurately carried out in order to optimize and to valorise the utilization of these resources, for forage production and/or for biodiversity conservation (Tälle et al., 2016). According to these issues, maintenance of grasslands is one of the key aims of European Agricultural policy (Viira et al., 2020) and to achieve this objective some mechanical interventions can be performed to maintain and recover grasslands and the ecosystem services they provide and to prevent them from afforestation ((Wahlman & Milberg, 2002), but they are time and money consuming (Cervasio et al., 2016), and, for this reason, the more suitable and sustainable management could be that carried out by direct animal grazing (Papanastasis, 2009). Thus, management and conservation of grasslands are really difficult to perform in mountain or marginal areas for technical and physical constraints present in these territories (Porqueddu et al., 2017).

As stated before, the possible manners to manage and maintain these resources are represented by mowing or grazing, and these two kinds of utilization can affect grassland traits in a very different way. Both of them can influence botanical composition (Tälle et al., 2016), by homogeneous herbage removal performed with cutting (Čop & Eler, 2019), or by higher animal intake on the most palatable species, which may decrease depending on management techniques and stocking rate (Mc Donald et al., 2020). Grazing effects on vegetation are also affected by species of animal grazing, as they are characterized by different impact on the herbaceous canopy in terms of selectivity and intensity (Osoro et al., 2017). Many studies were carried out to compare the two methods of grasslands utilization but conclusions on which is the best management choice were sometimes contradictory and site-specific (Tälle et al., 2016).

Following the previously reported issues, the main aim of the present paper is to compare, in an Apennine territory, some grasslands paddocks grazed by cattle with others subjected to periodical mowing, trying to understand the relationships between botanical composition or quality of pastures and type of management, and how some physical factors can affect botanical characteristics of areas under investigation.

MATERIALS AND METHODS

Assessment of grasslands was carried out inside the regional forest of Rincine, a public property located in the province of Florence (Tuscany, North Apennines, Italy) with a total extension of approximately 1,448 ha. Grasslands occur on poor and shallow soils, mainly developed on sandstone, with reaction from neutral to acid. Climate is characterized by a mean annual temperature of 8.4 and by an average precipitation of about 1700 mm, with a remarkable amount of rain during summer (Viciani et al., 2010).

Grasslands survey was performed on 9 different areas, 3 of them were managed through Limousine cattle grazing during summer, whereas the lasting 6 were only periodically mowed, and eventually utilized only by wildlife and not by domestic livestock. The studied areas are located between 800 and 1,300 m asl, with a different surface (between 0.25 and 1.80 ha), with a general southern aspect and a slope ranging from mainly flat to about 35%. Sampled grasslands were inside a rectangular area delimited by vertices characterized by the following coordinates (decimal degrees): 43,869492 N/11,630492E and 43,878030N/11,650362E.

Data collection of botanical composition was carried out according to the simplified method proposed in pasture vegetation assessment for forest planning (Argenti et al., 2006). This procedure provides the composition of an herbaceous community by means of visual estimation of ground cover of six different botanical categories instead of detecting all the species through a complete vegetation analysis (Table 1). Categories chosen for botanical surveys according to this approach are the following:

Table 1. Botanical categories used for assessing grasslands, acronym and Specific Index of each category (SIc) according to Argenti et al. (2006)

Botanical category	Acronym	SIc
Palatable grasses	PG	1.95
Not palatable grasses	NG	0
Legumes	LE	2.99
Species belonging to other botanical families	OT	0.29
Spiny or poisonous species	SP	0
Trees and shrubs	TS	0.03

– palatable grasses
– not palatable grasses
– legumes
– species belonging to other botanical families
– spiny or poisonous species
– trees and shrubs.

The six categories were proposed in order to take into account their relevance to affect qualitative forage potentiality of a pasture and, in turn, to potential stocking rate of a pastoral area (Argenti et al., 2006). In fact, some of them are deeply correlated to a high quality of pasture, such as palatable grasses or legumes, while others can outline reduction of forage value (not palatable grasses) or irrational management related to underutilization (such as the presence of shrubs). According to these considerations, this simplified approach is useful not only to describe the actual state of the analysed pasture but also to identify possible ongoing evolution (Argenti et al., 2017).

Moreover, the proposed method permits the calculation, in a synthetic way, of the pastoral value (Daget & Poissonet, 1972), a parameter derived from the percentage presence of each species occurring in the canopy and which is directly related to carrying capacity (Cavallero et al., 2007). According to the simplified approach utilized in this research, the pastoral value is calculated with the following formula:

$$PV = \frac{\sum SC_c \times SI_c}{5} \quad (1)$$

where SC_c is the percentage occurence in the sward of each botanical categories previously defined, and SI_c is a synthetic index that describes, for each category, its forage value (Bagella et al., 2013). Indices range between 0 (no forage interest) and 5 (excellent forage interest) and, following this method, the PV values range between 0 and 100 (Cavallero et al., 2002). SI for each of the six categories used to estimate pastoral value is reported in Table 1 according to values proposed originally by Argenti et al. (2006) and derived from about 1,000 botanical samples scattered in different mountain areas of Italy.

Results of survey were utilized to compare areas subjected to different management by means of ANOVA. Moreover, they were used to find out possible relationships among investigated variables and topographical features. All analyses were performed using statistical software SPSS (release 26, IBM, 2019).

RESULTS AND DISCUSSION

Results of botanical assessment, according to different botanical categories, are reported for both grazed and mowed areas in Fig. 1.

In grazed areas, palatable grasses (PG) represent the most occurring category, with a cover of more than 50%, significantly higher than what detected in mowed areas. The same trend is observed for legumes, with higher value in areas utilized by animals which is more than three times with regard to what occurred in mowed sectors. Not palatable grasses (NG) are more frequent in grazed areas as well but difference in ground cover is less evident than what observed for palatable ones. On the contrary, occurrence of species belonging to other botanical families (OT) is significantly higher in mowed grasslands compared to those grazed, and the same is for shrubs and woody species (TS), with a percentage presence in mowed areas (roughly 13%) significantly higher than grazed ones (about 3%). Among observed categories, only presence of thorny or poisonous species (SP) is not significantly different among treatments.

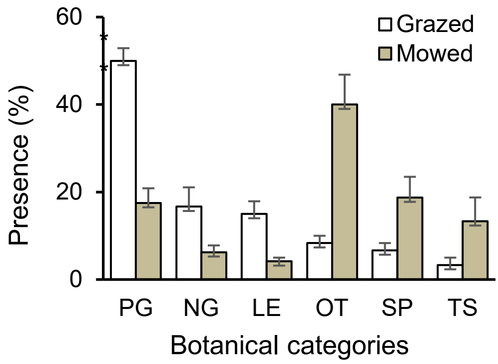

Figure 1. Botanical composition of assessed categories for grazed and mowed areas.

Significance: **: $P < 0.01$; *: $P < 0.05$; ns: not significant. Bars represent standard errors. PG: palatable grasses; NG: not palatable grasses; LE: legumes; OT: other botanical families; SP: Spiny or poisonous species; TS: trees and shrubs.

Grazing and mowing are the two considered an appropriate technique to recovery pasture after a long period of abandonment and it is often able to maintain also the botanical value of a grassland way to utilize grasslands. Grazing is (Perotti et al., 2018), even if a previous mowing action is necessary before restoring direct animal utilization (Tardella et al., 2020). Management practices can affect vegetation, functional traits and related ecosystem services that are linked to grasslands (Targetti et al., 2013; Silva et al., 2019), even if the effects on botanical composition are not always stable (Sullivan et al., 2017) and depend on specific ecological features (Stammel et al., 2003). Mowing generally can produce a higher cover of forbs and our findings are consistent with previous researches (Valkó et al., 2012), even if very important characteristics of mowing that can affect botanical composition are frequency and period of cutting (Cervasio et al., 2016; Tälle et al., 2018). Our results highlighted higher presence of legumes in grazed areas compared to mowing, as grazing can favour species with a reduced height and characterized by a creeping growth, such as *Trifolium repens* (Cavallero et al., 2002). Ganjurjav et al. (2019) also highlighted a higher resilience of legumes to heavy grazing with respect to no utilization. On the other hand, in our situation, grasses (palatable or not) were favoured also by grazing as mowing was performed not every year, thus confirming what found by Catorci et al. (2011) in a similar Apennine environment, whereas other researches highlighted the importance of a continuous and regular cutting regime to efficiently affect botanical composition of grasslands (Socher et al., 2013). Pierik et al. (2017) highlighted also the importance of number of cuts on botanical composition and biodiversity, even if this issue is deeply correlated also to climatic conditions. The irregular management on mowed areas can explain the higher presence of shrubs and trees as well, as it is clearly documented the narrow relationship among reduced level of utilization and woody species development on grasslands and pastures (Urbina et al., 2020). According to these issues, assessment of vegetation inside a grassland is of extremely importance to identify how grazing or mowing can affect not only botanical composition but also ecosystem services they provide, which are remarkably affected by management (Johansen et al., 2019).

The pastoral value for different managements is reported in Fig. 2. Grazed areas presented an average value significantly higher than mowed ones (28.9 *vs*. 11.7 respectively) and this result is a direct outcome of previously analysed botanical composition, as grazed areas were dominated by the most relevant species from a qualitative point of view (palatable grasses and legumes). Pastoral value is usually calculated in order to obtain carrying capacity for a pasture (Argenti et al., 2017) but it can be also considered an index that represents the overall forage potentiality of a grassland (Pittarello et al., 2020) and in this way we used it to compare grazed areas to mowed ones that are not subjected to animal utilization. Grazing is acknowledged to maintain microenvironments of grasslands due to its patchy utilization (Funk et al., 2018) and to permit a proper plants turnover (Niu et al., 2016) and thus it can be considered a way to enhance conservation

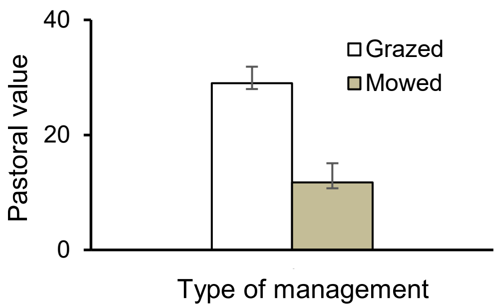

Figure 2. Pastoral value for grazed and mowed areas.

Significance: ** : $P < 0.01$; * : $P < 0.05$; ns: not significant. Bars represent standard errors.

of grasslands (Tälle et al., 2016). Adoption of specific management techniques is important also to improve the ecological status of a grassland: Perotti et al. (2018) reported a significant increase in floristic richness and diversity index after implementation for five years of rotational grazing.

Grazing was recognized also to favour some species belonging to grasses (Sebastià et al., 2008) and able, consequently, to improve directly grassland quality as reported by Hao & He (2019). Moreover, grazing can enhance the presence of specific clonal species with a reduced height and a prostrate growing structure, such as white clover, and this can contribute to improve forage value of the sward (Enriquez-Hidalgo et al., 2016). Results shown in the present work are also in line with the findings of Yoshihara et al. (2016) that highlighted the importance of grazing, when balanced in terms of stocking rate and animal pressure, to maintain a high level of forage quality in the long term. Other researches in the Apennines reported an improvement of pastoral value under grazing compared to mowing. Catorci et al. (2011) recorded an improvement of this parameter from 18 (in mowed areas) to 23 (in grazed areas). The different extent concerning our results can be reasonably attributed to the simplified way of calculation of pastoral value with respect to the original method, even if this approach was successfully adopted in other assessments on grasslands (Bolzan, 2009; Argenti et al., 2017).

The presence of different botanical categories was grouped in relation to different altitudinal classes in order to identify an eventual relationship with elevation (Fig. 3). Altitudinal classes were identified as follows: i) less than 1,000 m asl (Lower areas); ii) between 1,000 and 1,200 asl (Medium areas); iii) more than 1,200 m asl (Higher areas). It is evident the effect of elevation on different botanical categories: grasses presented a decreasing trend, more evident for palatable ones (PG) than for not palatable (NG). At the same time, legumes were extremely more frequent in lower areas with respect to those located at medium or higher elevations. In these areas, botanical classes with a greater occurrence were species belonging to other families (OT, remarkably reduced in lower areas), poison and spiny species (PS), and woody plants (TS).

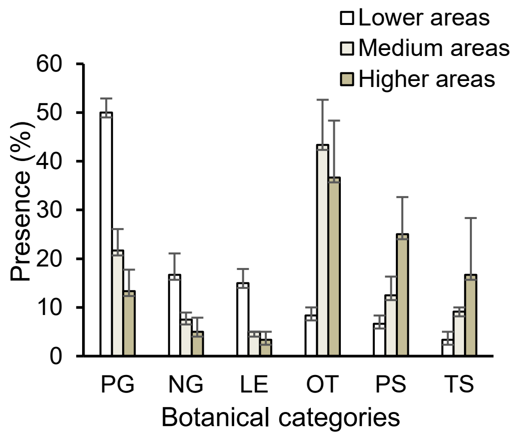

Figure 3. Botanical composition of assessed categories in relation to different altitudes. Bars represent standard errors. PG: palatable grasses; NG: not palatable grasses; LE: legumes; OT: other botanical families; SP: Spiny or poisonous species; TS: trees and shrubs.

Effects of some topographical features can be remarkably correlated to botanical composition or overall quality of the grasslands under investigation The most relevant regressions were those reflecting the effect of altitude on pastoral value, which is inversely correlated to elevation (Fig. 4), and the trend of percentage of woody species spread on grassland (trees and shrubs, TS) directly related to values of slope (Fig. 5).

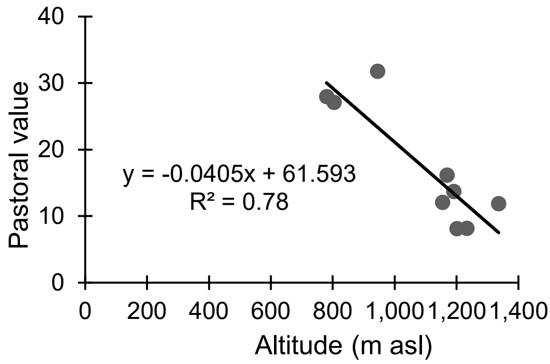

Figure 4. Regression between altitude and pastoral value.

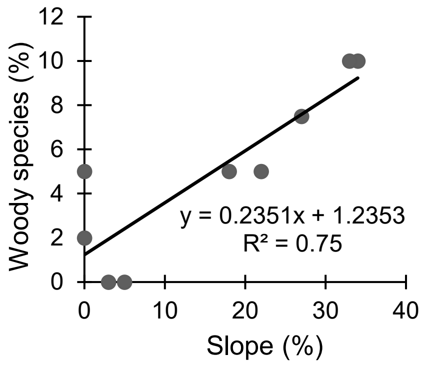

Figure 5. Regression between slope and presence of woody species.

Effects of different environmental factors on botanical composition and forage characteristics of grasslands are well documented in mountain areas (Gusmeroli et al., 2013) and in many cases, coupled with climatic features, topography and soil conditions, they are among the main key drivers able to describe distribution of grassland types on a wide territory (Dibari et al., 2016). Our data are consistent with previous researches. Argenti et al. (2020) reported the reduction of pastoral value, as a consequence of remarkable changes in vegetation composition, at increasing elevation in a rangeland mountain area. This can, in turn, affect the forage quality of herbaceous biomass that is highly related to botanical composition as affected by altitudinal location of pastures (Leiber et al., 2006). Moreover, Pornaro et al. (2019) recognized in alpine pastures a direct and significant correlation between pastoral value and crude protein content. Topographical characteristics can affect remarkably structural characteristics of grasslands, and, coupled with land utilization, can influence presence of woody species, and this is especially true for slope according to Tasser et al. (2007). On the contrary, elevation not always was considered significant in determining woody species cover, as reported by Parolo et al. (2011). Slope is thus considered one of the main drivers of accessibility of a grassland and it can influence type and frequency of management, both for grazing and mowing (Orlandi et al., 2016). Effect of slope is particularly evident in mountain and marginal regions, especially if characterized by reduced number of grazing animals. In this condition, steep slopes are the first areas to face a limited animal presence and to experience a relevant density of encroaching shrubs as a result of decreased animal pressure (Argenti et al., 2020). Also in our case the most significant effect induced by slope was the higher presence of shrubs and trees on steeper areas, confirming the findings of other researches (Homburger et al., 2015). Moreover, slope can influence soil characteristics and nutrient content and, consequently, it can induce changes in vegetation (Bennie et al., 2006).

Finally, the two most important botanical categories (PG and LE) were used as predictors to estimate PV, in single and multiple regressions (Table 2). Palatable grasses resulted more suitable than legumes to predict the pastoral value in single regression, both of them with highly significant determination coefficients (R^2). A combination of both predictors in a multiple regression was rather completely able to predict the total amount

Influence of these two main botanical categories on pastoral value is due to their high specific index, whereas other categories are not so relevant according to the reduced or null specific index that is not able to produce PV increasing (Pittarello et al., 2020). This could permit to further simplify data collection if the aim is just pastoral value evaluation, such as analysis performed in territorial planning with not specific pastoral assessment purposes (Paletto et al., 2012). Anyway, the extreme simplification in vegetation analysis can produce loosing of information and of thematic features of grasslands, such as grassland vegetation types, which are relevant for their characterization and accurate management and planning (Cavallero et al., 2007). The use of a simplified method should not be considered an alternative to the ordinary pasture assessment as already pointed out previously (Argenti et al., 2017) but it can represent a good agreement between opposite needs, *i.e.* simplification of the botanical survey and obtainable information that is acceptably accurate.

Table 2. Single and multiple regressions between PG and/or LE and PV. All determinant coefficients are significant with $P < 0.0001$

Predictors	Equation	R^2
PG	PV = 3.42 + 0.49 PG	0.92***
LE	PV = 7.02 + 1.34 LE	0.82***
PG and LE	PV = 3.43 + 0.33 PG + 0.59 LE	0.99***

CONCLUSIONS

Results of the study highlighted how mowing and grazing affected some features of grasslands, such as botanical composition and quality, in the case study. Grazing was superior in terms of occurrence of the most important forage categories, namely palatable grasses and legumes, and, in turn, of overall quality of herbaceous resources recorded by means of pastoral value. Mowing was recognized to be less useful to conserve a productive and efficient ground cover in grassland areas, but this was due to its occasional occurrence and to its irregular frequency, as in other conditions benefits of cutting were different than those observed in our survey.

The main constraints of mowing in our situation are due to the extremely marginal location of the areas, far from roads and rather problematic with regard to their accessibility. For these reasons, cutting or shrubs clearing are always difficult to perform and money consuming, and costs are often improved by the reduced surface of each open area.

Thus, especially in these conditions, grazing can represent the most efficient and economical way of utilization of grasslands, and availability of simplified methods to assess pastoral resources, such as that involved in this research, can help to provide information for different aims. In fact, one of the major findings of the research was the positive assessment of the fast procedure for vegetation sampling. This approach could be valuable in similar contexts, to attain data for pasture planning and management issues, such as for carrying capacity calculation, but also to evaluate the role of grasslands also under an ecological point of view, in order to obtain useful information for conservation purposes, such as those related to ecosystem services grasslands provide.

REFERENCES

Argenti, G., Bianchetto, E., Ferretti, F. & Staglianò, N. 2006 Proposal of a simplified method for pastures assessment in forest planning. *Forest@* **3**, 275–80 (in Italian).

Argenti, G., Bottai, L., Chiesi, M., Maselli, F., Staglianò, N. & Targetti, S. 2011. Analysis and assessment of mountain pastures by integration of multispectral and ancillary data. *Rivista Italiana di Telerilevamento/Italian Journal of Remote Sensing* **43**, 45−57 (in Italian).

Argenti, G., Bianchetto, E. & Ferretti, F. 2017. Proposal of a simplified method for pastoral value assessment inside forest planning. *Annals of Silvicultural Research* **41**, 67–73.

Argenti, G., Staglianò, N., Bellini, E., Messeri, A. & Targetti, S. 2020. Environmental and management drivers of alpine grassland vegetation types. *Italian Journal of Agronomy* **15**, 156–164.

Bagella, S., Salis, L., Marrosu, GM., Rossetti, I., Fanni, S., Caria, MC. & Roggero, P.P. 2013. Effects of long-term management practices on grassland plant assemblages in Mediterranean cork oak silvo-pastoral systems. *Plant Ecology* **214**, 621–631.

Bengtsson, J., Bullock, J.M., Egoh, B., Everson, C., Everson, T., O'Connor, T., O'Farrell, P.J., Smith, H.G. & Lindborg, R. 2019. Grasslands−more important for ecosystem services than you might think. *Ecosphere* **10**(2), e02582.

Bennie, J., Hill, M.O., Baxter, R. & Huntley, B. 2006. Influence of slope and aspect on long-term vegetation change in British chalk grasslands. *Journal of Ecology* **94**, 355–368.

Bolzan, A. 2009. *Analysis of vegetation parameters and functional characteristics of dominant species, as tools for studying grassland communitie*. PhD Dissertation, Bologna, Italy, 163 pp, (in Italian).

Burrascano, S., Chytrý, M., Kuemmerle, T., Giarrizzo, E., Luyssaert, S., Sabatini, F.M. & Blasi, C. 2016. Current European policies are unlikely to jointly foster carbon sequestration and protect biodiversity. *Biological Conservation* **201**, 370–376.

Catorci, A., Ottaviani, G., Ballelli, S. & Cesaretti, S. 2011. Functional differentiation of central Apennine grasslands under mowing and grazing disturbance regimes. *Polish Journal of Ecology* **59**, 115–128.

Cavallero, A., Rivoira, G. & Talamucci, P. 2002. Pastures. In: R. Baldoni and L. Giardini (eds.) *Herbaceous crops. Forage crops and turfgrasses*. Patron Editore, Bologna, pp. 239–294 (in Italian).

Cavallero, A., Aceto, P., Gorlier, A., Lombardi, G., Lonati, M., Martinasso, B. & Tagliatori, C. 2007. *Pasture vegetation types of Alps of Piedmont.* Alberto Perdisa Editore, Bologna, Italy, 467 pp. (in Italian).

Cervasio, F., Argenti, G., Genghini, M. & Ponzetta, M.P. 2016. Agronomic methods for mountain grassland habitat restoration for faunistic purposes in a protected area of the northern Apennines (Italy). *iForest* **9**, 490−496.

Conant, R.T., Cerri, C.E., Osborne, B.B. & Paustian, K. 2017. Grassland management impacts on soil carbon stocks: A new synthesis. *Ecological Applications* **27**, 662–668.

Čop, J. & Eler, K. 2019. Effect of fertiliser application and cutting regime on temporal differentiation of mesic semi-natural grassland vegetation. *Italian Journal of Agronomy* **14**, 153–161 (in French).

Daget, P. & Poissonet, J. 1972. A procedure to assess pastoral value of pastures. *Fourrages* **49**, 31–40.

Dibari, C., Bindi, M., Moriondo, M., Staglianò, N., Targetti, S. & Argenti, G. 2016. Spatial data integration for the environmental characterization of pasture macrotypes in the Italian Alps. *Grass Forage Science* **71**, 219–234.

Dixon, A.P., Faber-Langendoen, D., Josse, C., Morrison, J. & Loucks, C.J. 2014. Distribution mapping of world grassland types. *Journal of Biogeography* **41,** 2003–2019.

Enriquez-Hidalgo, D., Gilliland, T.J. & Hennessy, D. 2016. Herbage and nitrogen yields, fixation and transfer by white clover to companion grasses in grazed swards under different rates of nitrogen fertilization. *Grass and Forage Science* **71**, 559–574.

Faccioni, G., Sturaro, E., Ramanzin, M. & Bernués, A. 2019. Socio-economic valuation of abandonment and intensification of Alpine agroecosystems and associated ecosystem services. *Land Use Policy* **81**, 453–462.

Funk, F.A., Peter, G., Leder, C.V., Loydi, A., Kröpfl, A. & Distel, R.A. 2018. The impact of livestock grazing on the spatial pattern of vegetation in north-eastern Patagonia, Argentina. *Plant Ecology and Diversity* **11**, 219–227.

Ganjurjav, H., Zhang, Y., Gornish, E.S., Hu, G., Li, Y., Wan, Y. & Gao, Q. 2019. Differential resistance and resilience of functional groups to livestock grazing maintain ecosystem stability in an alpine steppe on the Qinghai-Tibetan Plateau. *Journal of environmental management* **251**, 109579.

Giustini, L., Acciaioli, A. & Argenti, G. 2007. Apparent balance of nitrogen and phosphorus in dairy farms in Mugello (Italy). *Italian Jouranl of Animal Science* **6**, 175–185.

Grau, O., Saravesi, K., Ninot, J.M., Geml, J., Markkola, A., Ahonen, S. & Peñuelas, J. 2019. Encroachment of shrubs into subalpine grasslands in the Pyrenees modifies the structure of soil fungal communities and soil properties. *FEMS Microbiology Ecology* **95**, 1–16.

Gusmeroli, F., Della Marianna, G., Fava, F., Monteiro, A., Bocchi, S. & Parolo, G. 2013. Effects of ecological, landscape and management factors on plant species composition, biodiversity and forage value in Alpine meadows. *Grass Forage Science* **68**, 437–447.

Hao, Y. & He, Z. 2019. Effects of grazing patterns on grassland biomass and soil environments in China: A meta-analysis. *PloS one* **14**, e0215223.

Hao, R., Yu, D., Liu, Y., Liu, Y., Qiao, J., Wang, X. & Du, J. 2017. Impacts of changes in climate and landscape pattern on ecosystem services. *Science of Total Environment* **579**, 718–728.

Homburger, H., Lüscher, A., Scherer-Lorenzen, M. & Schneider, M.K. 2015. Patterns of livestock activity on heterogeneous subalpine pastures reveal distinct responses to spatial autocorrelation, environment and management. *Movement Ecology* **3**, 1–15.

Hopkins, A. & Holz, B. 2006. Grassland for agriculture and nature conservation: production, quality and multi-functionality. *Agronomy Research* **4**, 3–20.

IBM, 2019. IBM SPSS Statistics for Windows, Version 26.0. IBM Corp., Armonk, NY, USA.

Komac, B., Domènech, M. & Fanlo, R. 2014. Effects of grazing on plant species diversity and pasture quality in subalpine grasslands in the eastern Pyrenees (Andorra): Implications for conservation. *Journal of Nature Conservation* **22**, 247–255.

Johansen, L., Taugourdeau, S., Hovstad, K.A. & When, S. 2019. Ceased grazing management changes the ecosystem services of semi-natural grasslands. *Ecosystems and People* **15**, 192–203.

Lamarque, P., Tappeiner, U., Turner, C., Steinbacher, M., Bardgett, R.D., Szukics, U., Schermer, M. & Lavorel, S. 2011. Stakeholder perceptions of grassland ecosystem services in relation to knowledge on soil fertility and biodiversity. *Regional Environmental Change* **11**, 791–804.

Leiber, F., Kreuzer, M., Leuenberger, H. & Wettstein, H. R. 2006. Contribution of diet type and pasture conditions to the influence of high altitude grazing on intake, performance and composition and renneting properties of the milk of cows. *Animal Research* **55**, 37–53.

Mc Donald, S.E., Reid, N., Smith, R., Waters, C.M., Hunter, J. & Rader, R. 2020. Comparison of biodiversity and ground cover between a commercial rotationally grazed property and an adjacent nature reserve in semi-arid rangeland. *Austral Ecology* **45**, 60–69.

Moudrý, J., Konvalina, P., Moudrý, J., Friebel, L. & Friebelová, J. 2009. Perennial grasslands and agroenvironmental programme effects. *Agronomy Research* **7**(Special issue I), 419–424.

Niu, K., He, J.S. & Lechowicz, M.J. 2016. Grazing-induced shifts in community functional composition and soil nutrient availability in Tibetan alpine meadows. *Journal of Applied Ecology* **53**, 1554–1564.

Osoro, K., Ferreira, L.M.M., García, U., Martínez, A. & Celaya, R. 2017. Forage intake, digestibility and performance of cattle, horses, sheep and goats grazing together on an improved heathland. *Animal Production Science* **57**, 102–109.

Orlandi, S., Probo, M., Sitzia, T., Trentanovi, G., Garbarino, M., Lombardi, G. & Lonati, M. 2016. Environmental and land use determinants of grassland patch diversity in the western and eastern Alps under agro-pastoral abandonment. *Biodiversity and Conservation* **25**, 275–293.

Paletto, A., Ferretti F., Cantiani, P. & De Meo, I. 2012. Multifunctional approach in forest landscape management planning: an application in Southern Italy. *Forest Systems* **21**, 68–80.

Papanastasis, V. 2009. Restoration of degraded grazing lands through grazing management: Can it work? *Restoration Ecology* **17**, 441–445.

Parolo, G., Abeli, T., Gusmeroli, F. & Rossi, G. 2011. Large-scale heterogeneous cattle grazing affects plant diversity and forage value of Alpine species-rich *Nardus* pastures. *Grass Forage Science* **66**, 541–550.

Perotti, E., Probo, M., Pittarello, M., Lonati, M. & Lombardi, G. 2018. A 5-year rotational grazing changes the botanical composition of sub-alpine and alpine grasslands. *Applied Vegetation Science* **21**, 647–657.

Pierik, M.E., Gusmeroli, F., Della Marianna, G., Tamburini, A. & Bocchi, S. 2017. Meadows species composition, biodiversity and forage value in an Alpine district: relationships with environmental and dairy farm management variables. *Agriculture Ecosystem and Environment* **244**, 14–21.

Pittarello, M., Lonati, M., Enri, S.R. & Lombardi, G. 2020. Environmental factors and management intensity affect in different ways plant diversity and pastoral value of alpine pastures. *Ecological Indicators* **115**, 106429.

Ponzetta, M.P., Cervasio, F., Crocetti, C., Messeri, A. & Argenti, G. 2010. Habitat improvements with wildlife purposes in a grazed area on the Apennine mountains. *Italian Journal of Agronomy* **5**, 233–238.

Pornaro, C., Basso, E. & Macolino, S. 2019. Pasture botanical composition and forage quality at farm scale: A case study. *Italian Journal of Agronomy* **14**, 214–221.

Porqueddu, C., Melis, R.A.M., Franca, A., Sanna, F., Hadjigeorgiou, I. & Casasús Pueyo, I. 2017. The role of grasslands in the less favoured areas of Mediterranean Europe. *Grassland Science in Europe* **22**, 3–22.

Primi, R., Filibeck, G., Amici, A., Bückle, C., Cancellieri, L., Di Filippo, A., Gentile, C., Guglielmino, A., Latini, R., Mancini, L.D., Mensing, S.A., Rossi, C.M., Rossini, F., Scoppola, A., Sulli, C., Venanzi, R., Ronchi, B. & Piovesan, G. 2016. From Landsat to leafhoppers: a multidisciplinary approach for sustainable stocking assessment and ecological monitoring in mountain grasslands. *Agriculture Ecosystem and Environment* **234,** 118−133.

Probo, M., Massolo, A., Lonati, M., Bailey, D.W., Gorlier, A., Maurino, L. & Lombardi, G. 2013. Use of mineral mix supplements to modify the grazing patterns by cattle for the restoration of sub-alpine and alpine shrub-encroached grasslands. *Rangeland Journal* **35**, 85–93.

Rook, A.J. & Tallowin, J.R.B. 2003. Grazing and pasture management for biodiversity benefit. *Animal Research* **52**, 181–189.

Sebastià, M.T., de Bello, F., Puig, L. & Taull, M. 2008. Grazing as a factor structuring grasslands in the Pyrenees. *Applied Vegetation Science* **11**, 215–222.

Silva, V., Catry, F.X., Fernandes, P.M., Rego, F.C., Paes, P., Nunes, L., Caperta, A.D., Sergio, C. & Bugalho, M.N. 2019. Effects of grazing on plant composition, conservation status and ecosystem services of Natura 2000 shrub-grassland habitat types. *Biodiversity and conservation* **28**, 1205–1224.

Socher, S.A., Prati, D., Boch, S., Müller, J., Baumbach, H., Gockel, S., Hemp, A., Schöning, I., Wells, K., Buscot, F., Kalko, E.K.V., Linsenmair, K.E., Schulze, E.D., Weisser, W.W. & Fischer, M. 2013. Interacting effects of fertilization, mowing and grazing on plant species diversity of 1500 grasslands in Germany differ between regions. *Basic and Applied Ecology* **14**, 126–136.

Stammel, B., Kiehl, K. & Pfadenhauer, J. 2003. Alternative management on fens: Response of vegetation to grazing and mowing. *Applied Vegetation Science* **6**, 245–254.

Stypinski, P. 2011. The effect of grassland-based forages on milk quality and quantity. *Agronomy Research* **9** (Special Issue II), 479–488.

Sullivan, E.R., Powell, I. & Ashton, P.A. 2017. Regional stability versus fine scale changes in community composition of mesotrophic grasslands over 25 years. *New Journal of Botany* **7**, 25–38.

Tälle, M., Deák, B., Poschlod, P., Valkó, O., Westerberg, L. & Milberg, P. 2016. Grazing vs. mowing: A meta-analysis of biodiversity benefits for grassland management. *Agriculture Ecosystem and Environment* **222**, 200–212.

Tälle, M., Deák, B., Poschlod, P., Valkó, O., Westerberg, L. & Milberg, P. 2018. Similar effects of different mowing frequencies on the conservation value of semi-natural grasslands in Europe. *Biodiversity and Conservation* **27**, 2451–2475.

Tardella, F.M., Bricca, A., Goia, I.G. & Catorci, A. 2020. How mowing restores montane Mediterranean grasslands following cessation of traditional livestock grazing. *Agriculture Ecosystem and Environment* **295**, 106880.

Targetti, S., Messeri, A, Staglianò, N. & Argenti, G. 2013. Leaf functional traits for the assessment of succession following management in semi-natural grasslands: a case study in the North Apennines, Italy. *Applied Vegetation Science* **16**, 325−332.

Targetti, S., Messeri, A., Argenti, G. & Staglianò, N. 2018. A comparative analysis of functional traits in semi-natural grasslands under different grazing intensities. *Agronomy Research* **16**, 2179–2196.

Tasser, E., Walde, J., Tappeiner, U., Teutschc, A. & Noggler, W. 2007. Land-use changes and natural reforestation in the Eastern Central Alps. *Agriculture Ecosystem and Environment* **118**, 115–129.

Urbina, I., Grau, O., Sardans, J., Ninot, J.M. & Peñuelas, J. 2020. Encroachment of shrubs into subalpine grasslands in the Pyrenees changes the plant-soil stoichiometry spectrum. *Plant Soil* **448**, 37–53.

Valkó, O., Török, P., Matus, G. & Tóthmérész, B. 2012. Is regular mowing the most appropriate and cost-effective management maintaining diversity and biomass of target forbs in mountain hay meadows? *Flora - Morphology, Distribution, Functional Ecology of Plants* **207**, 303–309.

Viciani, D., Gonnelli, V., Sirotti, M. & Agostini, N. 2010. An annotated check-list of the vascular flora of the "Parco Nazionale delle Foreste Casentinesi, Monte Falterona e Campigna" (Northern Apennines Central Italy). *Webbia* **65**, 3–131.

Viira, A.H., Ariva, J., Kall, K., Oper, L., Jürgenson, E., Maasikamäe, S. & Põldaru, R. 2020. Restricting the eligible maintenance practices of permanent grassland – a realistic way towards more active farming? *Agronomy Research* **18**(S2), 1556–1572.

Yoshihara, Y., Furusawa, S. & Sato, S. 2016. Recent pasture management determines biodiversity and productivity, and past management determines forage quality. *Ecoscience* **23**, 89–96.

Wahlman, H. & Milberg, P. 2002. Management of semi-natural grassland vegetation: evaluation of a long-term experiment in southern Sweden. *Annales Botanici Fennici* **39**, 159–166.

Agronomy Research **18**(4), 2303–2316, 2020
https://doi.org/10.15159/AR.20.202

Mapping performance of irrigation schemes in Turkey

F. Arslan[1,*], H. Değirmenci[2], S. Kartal[1] and F. Alcon[3]

[1]Alanya Alaaddin Keykubat University, Gazipaşa MRB Vocational School, Animal and Plant Production Department, TR07350 Antalya, Turkey
[2]Department of Biosystem Engineering, Kahramanmaraş Sütçü İmam University, 251/A, TR46040 Kahramanmaraş, Turkey
[3]Escuela Técnica Superior de Ingeniería Agronómica, Universidad Politécnica de Cartagena, Paseo Alfonso XIII 48, ES30203 Cartagena, Spain
[*]Correspondence: firat.arslan@alanya.edu.tr

Abstract. Water is a crucial resource and approximately 70% usage of it in the agriculture sector in Turkey. Water user associations are in charge of irrigation water management. The core aim of this study is to assess water user associations have command area more than 1,000 ha (WUAs) within the districts of DSI (State Hydraulic Works) and to create spatial maps to show the distribution of the performance indicators used constantly by researchers especially around Mediterranean countries during the period from 2011 to 2015. Frequency and panel data analysis are used to figure out the relationship among performance indicators and attributes such as water diversion type, management type, source of water and district no. Panel data analysis was applied to examine statistical assessment over time. As a result, current performance indicators show that excessive irrigation water used due to low technology and management problem. Performance indicators show high differences among districts due to climate, water resources, and crop pattern. Moreover, low irrigation efficiency can be increased with a transition to pressurized irrigation systems, so more are can be irrigated with less water.

Key words: panel data analysis, performance indicators, water management, water user associations.

INTRODUCTION

Effective water management is one of the most important issues since water is a limited source in agriculture (Gündoğdu et al., 2002) especially in semi-arid areas such as Mediterranean region (Lamaddalena et al., 2015). Estimated 65 per cent of global water use is consumed in the agricultural sector (Postel, 2014). Water is scarce and requires sustainable management at WUAs (Water User Associations) level due to water controlled by these organizations. To evaluate WUAs, performance indicators are used (Burt, 2001; Malano & Burton 2001). Performance indicators give general information about WUA evaluated (Molden et al., 1998; Burt 2001; Malano et al., 2004; Renault et al., 2007). The application of performance indicators to improve WUAs performance is a relatively recent phenomenon (Rodríguez-Díaz et al., 2008). The benchmarking technique, which is based on the comparison between different WUAs allow to determine the best practices in each of them (Córcoles et al., 2010). These indicators are also useful for water policies (Alcon et al., 2017) and can be used to measure effects of modernization of irrigation management (Değirmenci et al., 2003; Soto-García et al., 2013), land consolidation (Sönmezyildiz & Çakmak, 2013), water-scarce impact (Alcon et al., 2017), evaluation in years (Córcoles et al., 2010) and differences between management types among WUAs (Tanrıverdi et al., 2011). The methodology is also popular to assess WUAs in Mediterranean Countries (Borgia et al., 2013; Zema et al., 2015 and 2018; Kartal et al., 2019 and 2020).

The studies conducted with performance indicators in Turkey comprise a group of WUAs (Değirmenci et al., 2003; Değirmenci, 2004; Tanrıverdi et al., 2011; Akkuzu & Mengü, 2011) or a WUA (Çakmak et al., 2004; Nalbantoğlu & Çakmak, 2007; Tanrıverdi & Değirmenci, 2011; Sönmezyıldız & Çakmak, 2013; Çakmak et al., 2014; Arslan & Değirmenci, 2018) except Merdun & Değirmenci (2004) studied on 239 irrigation schemes but only for a year 2001. In these studies, WUAs compared in the discussions do not reflect a whole or not give sufficient comparison. Therefore, there is a need overall performance indicators in order to compare them.

The main aim of the present study is to determine reference performance indicators using 5 years of data between 2011 and 2015 from 244 WUAs. In this regard, panel data analysis is applied to analyse the data. This study also investigates the effects of a score of parameters such as water resources (river, lake, underground etc.), water diversion type (gravity, pumped or both), management type on performance. Other purposes of the study include recommendations to improve the performance of WUAs to managers, engineers and policymakers.

MATERIAL AND METHODOLOGY

Case study description

The current study was carried out with 244 irrigation schemes have more than 1,000 ha command area (except 2 of them) in 23 DSI (State Hydraulic Works) of 26 districts based on river basins between 2011 and 2015 irrigation seasons data. The total area of WUAs evaluated covers 20,195.222 km^2 whose sample size presents 89.4% of all WUAs. The sample size was not 100 per cent due to the available data. Fig. 1 shows that spatial distribution of DSI districts. As it is given in Table 1, each district has different features such as precipitation, water potential etc.

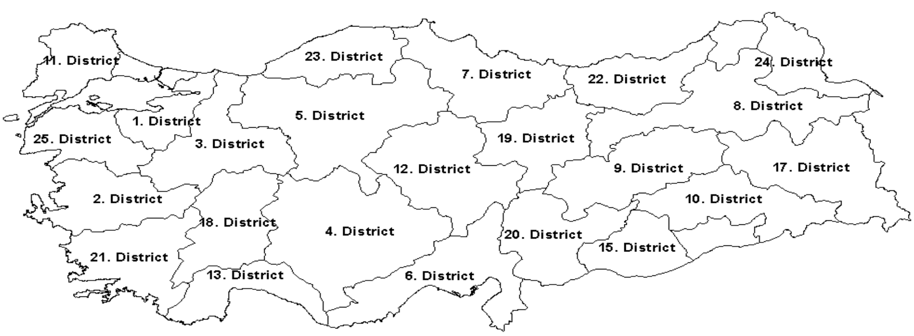

Figure 1. Spatial distribution of DSI districts in Turkey.

Table 1. Main features of DSI districts

District No.	Mean annual precipitation (mm)	Total water potential (hm^3 year^{-1})	Irrigable area (ha)	Evaluated area (ha)	Evaluated area (%)
1	738	8,018.5	61,410	54,175	88.2
2	605	4,508	133,258	122,561	91.9
3	548	5,469.29	67,713	64,659	95.5
4	398.4	8,353	188,976	169,866	89.9
5	493.6	11,862	43,540	42,130	96.8
6	812	23,292	347,219	301,814.2	86.9
7	713	10,944	104,877	91,377	87.1
8	438	12,118	83,356	77,634	93.1
9	720	11,202	74,164	60,542	81.6
10	645	20,500	48,928	44,226	90.4
11	621	9,921.9	57,145	54,852	95.9
12	720	11,202	82,161	69,769	84.9
13	1,009	15,907.13	80,046	78,980	98.7
15	425	33,582	226,677	195,187	86.1
17	662.6	13,038.08	71,132	59,214	83.2
18	529.5	4,690.7	93,499	80,929	86.6
19	902	11,202	22,966	18,390	80.1
20	620.6	9,614.8	78,541	54,534	69.4
21	720	11,202	205,482	203,482	99
22	10,180	15,755	15,647	15,647	100
23	713	8,649	20,987	18,987	90.5
24	720	11,202	68,792	68,400	99.4
25	663	5,867	83,107	72,167	86.8

Turkey has 4 types of climate; continental climate (summers are hot and arid, winters are cold and snowy); Mediterranean climate (summers are hot and dry, winters are warm and rainy); transition climate (characteristic between continental, Mediterranean and Black sea climate); Black sea climate (winters are warm and summers are cool) within regions (FL, 2017). These climate types help to interpret performance indicators within districts.

Methodology

Calculation of performance indicators

A set of performance indicators related to water, land and finance are used to evaluate WUAs. The performance indicator is used to improve system operation, better understand the performance determinants and to compare the performance of a system over time with others or the same system (Molden et al., 1998; Malano & Burton, 2001). These assessment methods are also used as a part of the modernization process by FAO (Renault et al., 2007). Available data-limited number of performance indicators to calculate. Selected performance indicators are given in Table 2.

Value of production of Turkish currency (Turkish Lira) are changed into Euro based on the consumer price index of Turkey according to Newbold (2009) and the year 2011 is selected reference year.

To show spatial distribution of performance of the districts, a district map was created using ESRI ArcMAP GIS package program. After calculation of performance indicators of WUAs within each district, the data entry was made to the program. And, the ranges of performance indicators were given in legent.

Table 2. Formulas of calculation irrigation performance indicators selected

Performance indicator	Formula
Irrigation intensity (%)	$\frac{\text{Irrigated area} \cdot 100}{Command\ area}$
Annual irrigation water supplied to users per unit command area ($m^3\ ha^{-1}$)	$\frac{\text{Annual volume of irrigation water supplied to users}}{Command\ area\ of\ the\ irrigation\ schemes}$
Annual irrigation water supplied to users per unit irrigated area ($m^3\ ha^{-1}$)	$\frac{\text{Annual volume of irrigation water supplied to users}}{Irrigated\ area\ of\ the\ irrigation\ schemes}$
Irrigation efficiency (%)	$\frac{\text{Conveyance efficiency} \cdot \text{field application efficiency}}{100}$
Total MOM cost per unit command area (€ ha^{-1})	$\frac{\text{Total MOM cost}}{Command\ area}$
Total MOM cost per unit irrigated area (€ ha^{-1})	$\frac{\text{Total MOM cost}}{Irrigated\ area}$
Total MOM cost per unit water supplied to users (€ m^{-3})	$\frac{\text{Total MOM cost}}{Annual\ volume\ of\ the\ irrigation\ water\ supplied\ to\ users}$
Output per unit command area (€ ha^{-1})	$\frac{\text{Total annual value of production}}{Command\ area}$
Output per unit irrigated area (€ ha^{-1})	$\frac{\text{Total annual value of production}}{Irrigated\ area}$
Output per unit water supplied to users (€ m^{-3})	$\frac{\text{Total annual value of production}}{\text{Annual volume of irrigation water supplied to users}}$

Data collection

Data used for the study was obtained from irrigation facilities evaluation reports and crop count reports of DSI related years. Data required including irrigated and command area, annual volume of irrigation water supplied to users, total maintenance and operation cost were taken from irrigation facilities reports and the total annual value of production was taken from crop count reports. WUAs have data less than 3 years were not taken into consideration.

Some WUAs' features were selected for consideration effect on performance indicators. Water diversion type (gravity, pumped and both), management type (transferred and non-transferred), crop pattern and source of water (river, lake, underground etc.) are these properties.

Statistical evaluation

Panel data analysis is used to assess relation performance indicators and WUAs facilities over time. The data is evaluated over time and the same individuals with panel data analysis and then a regression is run over these two dimensions. A panel dataset is one in which each of $N > 1$ units (sometimes called 'individuals' or 'groups') is observed over time. In a balanced panel, there are $T > 1$ observations on each unit; more generally the number of observations may differ by the unit. In the following, we index units by i and time by t. To allow for imbalance in a panel we use the notation T_i to refer to the number of observations for unit or individual i. In this context, effects of attributes (performance indicators, management type, source of water etc.) and time (2011–2015) are allowed to determine effects on performance indicators by the analysis. In this study, two techniques are used to analyse panel data: random and fixed effects. In general, a linear panel data model may be written as

$$Y_{it} = \beta_{0it} + \beta_{1it}X_{1it} + \beta_{2it}X_{2it} \dots \dots + \beta_{kit}X_{kit} + \upsilon_{it}$$

where $i = 1, 2, \dots,$ N is the cross-sectional unit and $t = 1,2, \dots\dots, T$ is time, Y_{it} is a dependent variable, X_{it} is explanatory variable for i^{th} observation at the period t, and υ_{it} is the error term is assumed to be independent and normally distributed $N =\sim (0, \sigma_i^2)$. When 1_{it} mean the first observation and the first time period and kit means the latest observation and the latest time period (Torres-Reyna, 2007).

RESULTS AND DISCUSSION

Table 3 shows the mean and standard deviation values of performance indicators for the districts. When we examine average values of indicators, irrigation intensity (IRRINT) was 45.3%, annual irrigation water supplied to users per unit command area (WATCOM) was 4,966.55 m^3 ha^{-1}, annual irrigation water supplied to users per unit irrigated area (WATIRR) was 12,907 m^3 ha^{-1}, and irrigation efficiency (IRREFF) was 43.4%for overall water delivery performance indicators. For financial indicators, mean values of total MOM (maintenance, operation and management) cost per unit command area (MOMCOM) was found as 81.4 € ha^{-1}, total MOM cost per unit irrigated area (MOMIRR) was 262.9 € ha^{-1}, total MOM cost per unit water supplied to users (MOMWAT) was 0.1 € m^{-3}. Production indicators are output per unit command area (outputCOM), output per unit irrigated area (outputIRR) and output per unit per unit water supplied to users (outputWAT) were found as 2,468.3 € ha^{-1}, 6,486.8 € ha^{-1} and 1.6 € m^{-3}, respectively.

Irrigation intensity was calculated considering all area irrigated including aftercrop areas. Fig. 2 shows average irrigation intensity (IRRINT) of irrigation schemes within 23 districts ranges from 7.4 to 86.7% and the mean was 43.3% during the experimental period. When it comes to irrigation schemes, mean IRINT was found 48.82%. Over irrigated areas (more than 100%) found because of after crops and irrigated areas out of command area of the WUAs. Irrigation schemes in 22th District had lowest IRRINT due to farmers who thought precipitation was adequate and no demand for water (20%), the inadequacy of irrigation facilities (11%), fallow (24%) and social and economic reasons (45%). Only irrigation intensity does not indicate the success of a WUA because of distinction diverted from the reservoir. Even though WUAs irrigate whole command area, they may use overabundance amount of water. For example, even if the highest rate of IRRINT was found in 15th District, the highest amount of water was used by WUAs in the district. Average IRRINT of 15th District was 86.7% and 451.10 million cubic meter water used 775.86% much more than average (58.14 million cubic meters) of DSI Districts. The lowest IRINT was seen in 22th District due to high rate of precipitation (10,180 mm) which was adequate and no irrigation water demand from WUAs according to farmers.

Table 3. Mean and standard deviation values of performance indicators

District no	IRRINT*	WATCOM	WATIRR	IRREFF	MOMCOM	MOMIRR	MOMWAT	outputCOM	outputIRR	outputWAT
1	46.77	3,299.35	8,051.37	59.47	178.80	424.81	0.09	3,190.90	6,822.49	1.52
	(23.79)	(1,679.52)	(3,715.09)	(0.26)	(147.22)	(369.79)	(0.08)	(2,215.63)	(3,418.92)	(0.83)
2	42.33	3,811.11	9,771.10	55.84	166.05	548.43	0.10	2,967.09	7,610.98	1.59
	(21.37)	(1,712.14)	3,542.22	(0.19)	(210.44)	(809.18)	(0.14)	(2,032.95)	(4,831.75)	(1.13)
3	37.27	4,048.96	14,250.97	34.70	72.11	270.28	0.06	1,819.62	7,056.75	1.44
	(27.58)	(2,916.42)	(14,592.40)	(0.18)	(73.90)	(273.88)	(0.07)	(1,321.77)	(8,018.65)	(1.26)
4	54.85	4,032.96	10,394.89	54.22	52.99	144.78	0.04	1,947.52	4,178.97	0.85
	(38.75)	(2,831.69)	(12,120.36)	(0.26)	(35.21)	(114.47)	(0.03)	(1,338.38)	(2,966.46)	(0.43)
5	24.25	3,971.62	17,922.50	30.74	33.71	428.93	0.11	1,653.98	6,652.34	1.67
	(15.31)	(3,012.28)	(8,739.43)	(0.18)	(24.97)	(1,107.7)	(0.29)	(1,272.88)	(6,122.31)	(1.50)
6	59.05	7,747.92	18,286.94	43.77	140.02	583.64	0.05	4041.16	13,735.46	1.19
	(29.62)	(4,746.67)	(22,468.84)	(0.21)	(208.81)	(1,443.5)	(0.07)	(2,859.52)	(2,2101.9)	(0.80)
7	45.67	2,881.02	7,022.72	57.43	43.62	102.85	0.03	1,984.66	4,771.50	1.17
	(23.91)	(1,863.02)	(3,770.20)	(0.27)	(29.08)	(66.98)	(0.02)	(1,164.31)	(2,352.66)	(0.58)
8	31.39	2,480.06	8,559.02	32.63	35.89	138.25	0.06	697.19	2,149.29	1.15
	(14.44)	(1,510.86)	(4,330.43)	(0.12)	(22.56)	(93.68)	(0.05)	(465.77)	(807.19)	(1.37)
9	48.53	5,624.54	13,399.19	40.29	133.56	360.63	0.37	4,128.14	7,748.83	6.35
	(27.87)	(4,571.89)	(9,699.78)	(0.20)	(314.20)	(646.83)	(1.57)	(4,341.64)	(5,658.86)	(21.16)
10	58.85	7,903.21	13,974.04	36.61	63.18	108.93	0.02	1,648.81	2,829.66	0.62
	(22.89)	(4,238.02)	(6,782.70)	(0.15)	(64.83)	(98.02)	(0.02)	(856.77)	(1,289.60)	(0.26)
11	58.26	8,197.54	11,957.48	52.45	129.42	193.47	0.03	3035.63	3,021.54	0.79
	(34.31)	(8,761.55)	(5,170.11)	(0.21)	(126.59)	(141.67)	(0.02)	(2,401.54)	(3,260.13)	(0.45)
12	45.58	4,044.23	9,923.92	41.21	59.06	145.36	0.04	2263.17	4,725.61	1.38
	(24.08)	(2,189.97)	(6,193.99)	(0.20)	(50.34)	(145.34)	(0.03)	(2,327.18)	(2,952.08)	(0.80)
13	54.17	5,534.37	10,001.85	55.07	128.71	265.86	0.06	7692.71	1,5005.64	3.10
	(19.46)	(3,137.69)	(4,271.38)	(0.23)	(95.69)	(218.50)	(0.05)	(5,593.48)	(1,3278.0)	(3.60)
15	86.66	10,570.20	11,548.18	50.73	131.09	176.66	0.03	2,925.94	3,498.49	0.60
	(30.16)	(6,682.49)	(4,889.91)	(0.22)	(98.61)	(162.42)	(0.03)	(838.51)	(839.26)	(0.22)
17	29.97	3,826.20	15,669.61	32.40	56.32	192.67	0.05	962.56	3,535.66	0.94
	(20.39)	(2,677.75)	(10,491.32)	(0.17)	(65.04)	(189.09)	(0.05)	(934.95)	(2,507.66)	(0.84)
18	47.14	4,194.41	11,024.16	45.54	77.11	176.53	0.04	3,059.39	5,752.88	1.30
	(28.72)	(3,313.47)	(7,781.65)	(0.23)	(72.45)	(160.61)	(0.04)	(3,700.81)	(4,049.91)	(0.91)
19	34.75	4,121.01	13,699.83	32.06	34.95	106.53	0.03	1,850.85	4,972.19	1.46
	(17.94)	(2,090.07)	(9,171.95)	(0.15)	(23.73)	(68.12)	(0.02)	(1627.60)	(2,787.78)	(0.78)
20	54.78	5,718.24	11,266.92	41.71	61.08	131.18	0.03	1,522.64	2,967.36	0.70
	(27.11)	(2,723.39)	(4,954.51)	(0.17)	(35.16)	(83.04)	(0.02)	(839.04)	(1,129.96)	(0.24)
21	68.73	7,618.15	26,870.80	48.37	92.67	305.40	0.03	3,279.78	15,124.52	0.93
	(33.68)	(4,690.02)	(71,897.28)	(0.22)	(50.09)	(701.66)	(0.02)	(1717.44)	(51,161.8)	(0.51)
22	7.40	773.67	11,985.18	42.70	10.03	151.09	0.06	442.47	6,106.35	2.17
	(1.69)	(585.46)	(11,058.82)	(0.29)	(6.91)	(122.33)	(0.05)	(499.41)	(6,475.63)	(2.21)
23	21.64	2,001.57	1,1307.73	30.04	30.91	139.72	0.05	1,529.11	7,080.85	2.60
	(11.62)	(951.67)	(7,484.01)	(0.14)	(21.78)	(76.44)	(0.03)	(1,080.94)	(4,166.51)	(1.53)
24	27.93	4,985.02	15,456.65	35.82	42.53	700.76	0.07	1,050.05	4,924.44	1.30
	(19.00)	(4,107.49)	(11,653.42)	(0.24)	(30.55)	(933.52)	(0.12)	(623.62)	(2,495.48)	(1.05)
25	56.79	6,844.38	14,226.21	45.38	109.73	180.20	0.04	3,076.55	5,460.36	1.07
	(23.02)	(2,380.49)	(8,175.09)	(0.20)	(175.32)	(190.07)	(0.04)	(1,790.88)	(2,224.10)	(0.52)
Av	45.3	4,966.5	12,937.0	43.4	81.9	262.9	0.1	2,468.3	6,486.8	1.6

*IRRINT:irrigation intensity; WATCOM: annual irrigation water supplied to users per unit command area; WATIRR: annual irrigation water supplied to users per unit irrigated area; IRREFF: irrigation efficiency; MOMCOM: total MOM cost per unit command area; MOMIRR: total MOM cost per unit irrigated area; MOMWAT: total MOM cost per unit water supplied to users; outputCOM: output per unit command area; outputIRR: output per unit irrigated area; outputWAT: output per unit per unit water supplied to users.

Irrigation intensity was 32.2% in Daphan plain in 24th District in 2013 (Demir et al., 2014), 62.43% in Aydın province in 2th District between the years 2006–2014 (Akçay, 2016), 27.33% in Gevrekli WUA in 4th District between the period 2008–2013 (Eliçabuk & Toprak, 2017).

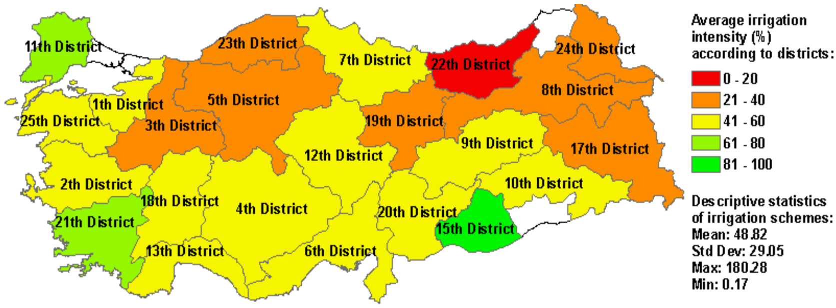

Figure 2. Irrigation intensity.

Values of WCOM changed between 10,570.20 and 773.70 m^3 ha^{-1} and the average value was found 4,966.50 m^3 ha^{-1} within the districts while WIRR was 7,022.70, 26,870.80 and 12,937.00 m^3 ha^{-1}, respectively. WUAs' WCOM values changed between 33.25 and 49,958.78 m^3 ha^{-1} while mean value was 5,185.88 m^3 ha^{-1}. WIRR values of irrigation schemes changed between 224.86 and 416,459.18, and the mean of the value was 13,403.47 m^3 ha^{-1}. WIRR is highly effected by water diversion type to users. The average WIRR was 1,173.74 m^3 ha^{-1} for WUAs with gravity water diversion type, 523.34 m^3 ha^{-1} for WUAs with pumped water diversion type, and 430.63 m^3 ha^{-1} for WUAs with both diversion types. The indicator also affected dramatically by management type. Mean WIRR of WUAs managed by DSI was 708.64 m^3 ha^{-1} while managed by WUAs their self has an average value of 1,570.94 m^3 ha^{-1} (Fig. 3). Besides that, the resource of water effects on WIRR, mean values of the indicator according to river, lake, underground, river and lake, river and underground, other were 1,085.52, 756.43, 258.26, 858.14, 725.26 and 535.03 m^3 ha^{-1}, respectively. Statistically significant correlation was found between WIRR and crop pattern ($P < 0.05$) except some crops (cereals, citrus, sunflower, sugar beet, strawberry, banana, forage crops and arboriculture). To be able to prepare a water distribution plan more realistically, the amount of water required for the crop pattern should be calculated as accurately as possible. The water distribution system also should be suitable to distribute water to users with pumped irrigation systems instead of gravity.

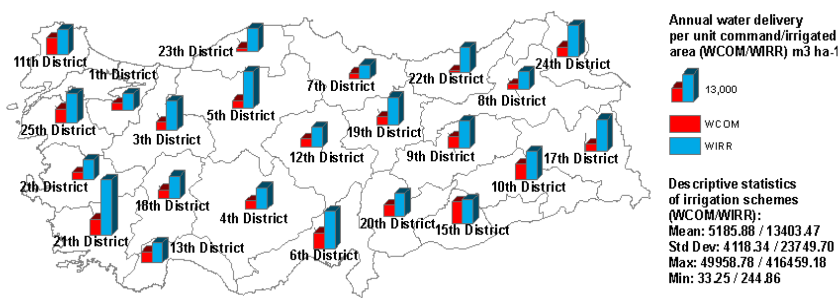

Figure 3. Annual irrigation water delivery per unit command area and irrigated area.

Financial indicators

These financial indicators show expenses in the field of irrigation schemes. This indicator does not tell us MOM requirement. A high value of MOM does not mean sustainable system. MOM expenditures may be low to encounter current MOM necessity. This indicator highly changed from 10.00 to 178.80 € ha^{-1} for MOMCOM, and 102.90 to 700.80 € ha^{-1} for MOMIRR within the districts. Average of MOMCOM and MOMIRR values of WUAS were 89.96 and 264.57 € ha^{-1}, respectively. Average, maximum and minimum values of the indicator were 89.96, 2,429.72 and 0.45 for MOMCOM, 254.57, 10,679.01 and 0.47 for MOMIRR within irrigation schemes (Fig. 4). Average MOMCOM of irrigation schemes with pumped distribution system was 265% more than gravity distribution systems. Non-transferred irrigation schemes have 177% more MOM expenditure than transferred irrigation schemes. The highest value of MOMCOM was found irrigation schemes getting water from underground. Energy bill and water tariff of these irrigation schemes highly likely increased MOM expenditure.

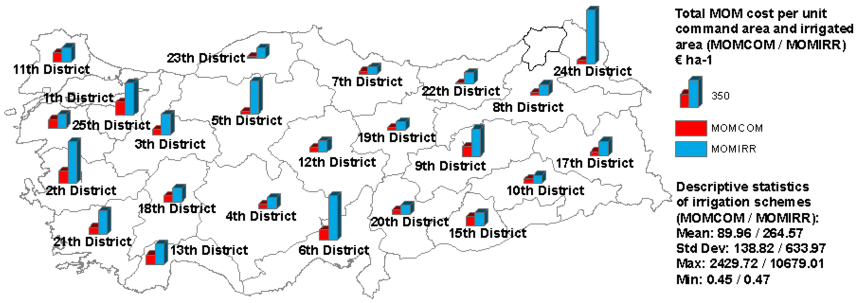

Figure 4. Total MOM cost per unit command and irrigated area.

Fig. 5 shows spatial distribution of MOMWAT within the districts. Average MOMWAT value is 0.06 when the maximum is 0.37 and minimum is 0.02 € m^{-3} within the districts. Mean MOMWAT value of irrigation schemes was 0.07, max was 12.18 and min was 0.0001 € m^{-3}. MOMWAT values were not affected highly by water diversion type but management type affected the indicator. Transferred irrigation schemes had a mean value of 0.045 while non-transferred irrigation schemes had a value of 0.081 € m^{-3}. The highest value was seen WUAs pumping water from underground.

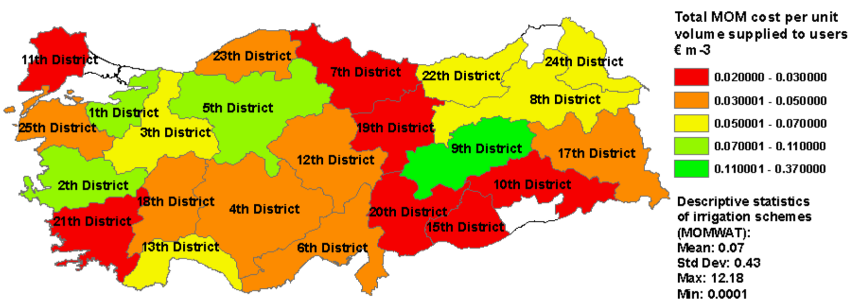

Figure 5. Total MOMWAT cost per unit volume supplied to users.

Production

Production indicators show the efficiency of farmer economic activity (Alcon et al., 2017). The average value of outputCOM and outputIRR were 2,468.30 and 6,486.80 € ha^{-1} within the districts. The values of the indicator changed from 442.50 to 7,692.70 € ha^{-1} for outputCOM, from 2,149.30 to 15,124.50 € ha^{-1} for outputIRR within the districts. The highest value of outputCOM was 28,019.33 while the lowest value was 2.18 € ha^{-1} and mean was 2,868.85 € ha^{-1} among irrigation schemes (Fig. 6). The highest and lowest values of outputIRR were 37,6536.75 and 48.46 € ha^{-1} (mean 7,384.79 € ha^{-1}). Seferihisar irrigation scheme had the highest value of over 16,000 € ha^{-1} in 2013. The indicators related to output had fluctuation because the situation seen among farmers planning crop pattern according to crops made money more last year (DSI 2016). Mean value of outputIRR according to water diversion type; gravity, pumped and both were found 7,587.39, 9,718.37 and 5,532.63 € ha^{-1}, respectively. There were big differences between transferred irrigation schemes and non-transferred irrigation schemes for the indicator. Mean of the indicator of transferred irrigation schemes was 2,909.49 € ha^{-1} while non-transferred irrigation schemes had value 677.37 € ha^{-1}.

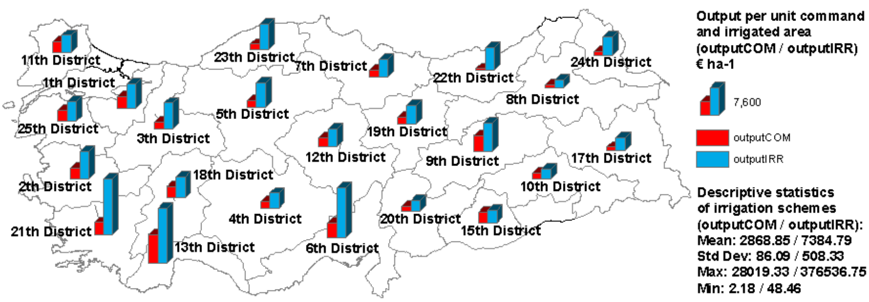

Figure 6. Output per unit command and irrigated area.

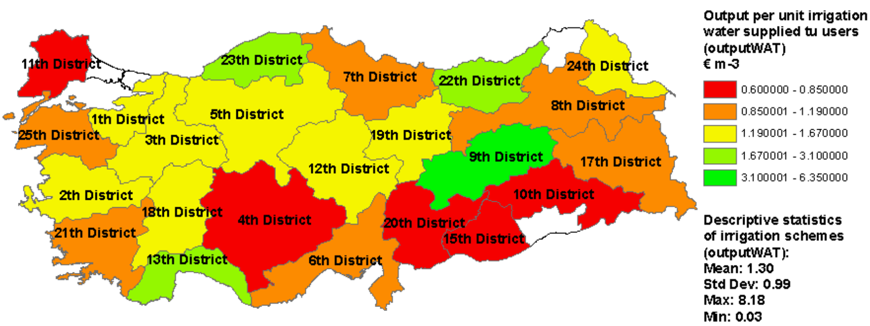

Figure 7. Output per unit irrigation water supplied to users.

Output per unit irrigation supplied to users can be seen as a measure of whether farmers are using the water efficiently or not. Average outputWAT was 1.60 € ha^{-1} within the districts. The highest value was seen in 9th District on average thanks to planting 42.93% of fruits. Average, maximum and minimum values were 1.30, 8.18 and 0.03 € ha^{-1} among irrigation schemes (Fig. 7). The maximum value was seen in Sarıgöl has crop pattern consist of almost 100% of the vineyard. When inputs (water) decrease and production increase the indicator go up. Irrigation efficiency and crop pattern play an important role in delivering water to users.

Average, IRREFF of the districts was 40%, the highest value was seen in 1th and 2td Districts and the lowest value was seen in 24th District. Mean value of IRREFF found in the current study was 0.45% same as the long term data according to reports (DSI, 2011), the highest value was 97 and min value was 0.04% according to calculations. Main system water delivers efficiency was 45% on average of all irrigation schemes between the study years (Fig. 8).

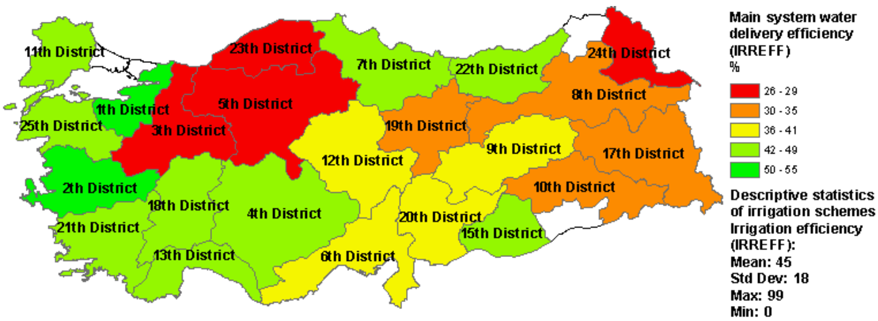

Figure 8. Main system water deliver efficiency.

Low irrigation efficiency was seen in the figure below for most of the irrigation schemes. Earth lined delivery system mainly used to deliver water. This causes that losing a lot of water before farmers get it. Average main system delivery efficiency is 55.84% for all irrigation schemes between the years (2011–2015). To improve water delivery efficiency, more pipe delivery system should be used by associations and farmers should courage to use drip, sprinkler etc. systems on their fields.

General view of water usage for the study period was given in Fig. 9. While water demand indicates (blue line) the total volume of water needed, water diverted (red line) demonstrate the total volume of water diverted or pumped from the source (dam, river, underground etc.) and water delivered (green line) point the total volume of water delivered to farmers. The graph shows WUAs consume water excessively which is about 2 times more than the water needed for irrigation.

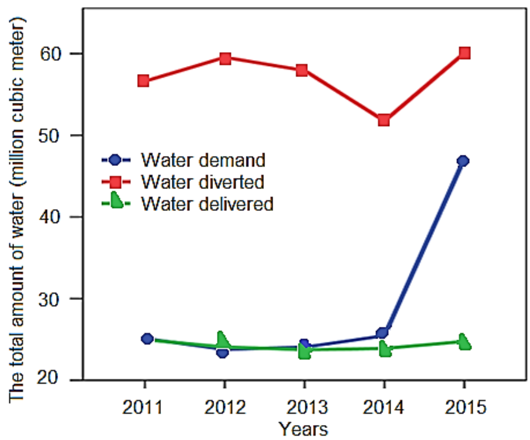

Figure 9. General view of water usage of the current study.

Statically assessment

Which panel method should be used such as fixed effects or random effects? One way of answering this question is concerning the nature of the data set. If the panel comprises observations on a fixed and relatively small set of units of interest, there is a presumption of fixed effects. If it comprises observations on a large number of randomly selected individuals, there is a presumption of random effects (Cottrell & Lucchetti, 2012).

To decide between fixed or random effects, a hausman test is run where the null hypothesis is that the preferred model is random effects vs. the alternative the fixed effects. It tests whether the unique errors are correlated with the regressors, the null hypothesis is they are not (Torres-Reyna, 2007). According to the hausman test, fixed effect method is chosen if *p*-value smaller than 0.05, otherwise random effect method is chosen which is given in Table 4 and Table 5. P is an important value to choose which method should be used.

Table 4. Panel data analysis between performance indicators and attributes

Indicator		Water diversion	Management type	Source of water	District no	Hausman test *P*-value (model)
IRRINT	*p*-value	0.67	0.06^{*}	0.39	0.27	0.10
	Coef	(0.81)	(11.35)	(0.73)	(0.27)	(Random)
IRREFF	*p*-value	0.44	0.02^{**}	0.01^{**}	0.03^{**}	0.08
	Coef	(0.01)	(0.11)	(0.01)	(-0.003)	(Random)
WATIRR	*p*-value	0.51	0.65	0.30	0.23	0.87
	Coef	(-998.70)	(-2,455.65)	(-716.35)	(248.24)	(Random)
MOMCOM	*p*-value	0.03^{**}	0.17	0.82	0.06	0.92
	Coef	(6.97)	(40.84)	(0.71)	(-1.69)	(Random)
outputIRR	*p*-value	0.09^{*}	0.31	0.01^{**}	0.90	0.39
	Coef	(-0.48)	(1.18)	(0.29)	(-0.004)	(Random)

IRRINT:irrigation intensity; WATCOM: annual irrigation water supplied to users per unit command area; WATIRR: annual irrigation water supplied to users per unit irrigated area; IRREFF: irrigation efficiency; MOMCOM: total MOM cost per unit command area; MOMIRR: total MOM cost per unit irrigated area; MOMWAT: total MOM cost per unit water supplied to users; outputCOM: output per unit command area; outputIRR: output per unit irrigated area; outputWAT: output per unit per unit water supplied to users; Significant level at $*p < 0.10$; $**p < 0.05$; $***p < 0.001$.

IRRINT is affected by WATIRR significantly negatively according to analysis but IRRINT increases 1%, WATIRR decrease just 0.0002 m^3 ha^{-1} which is very few. But the relation may be explained by using modern irrigation techniques decrease the usage of water and more area can be irrigated considering it may increase IRRINT. A similar situation was seen with IRREFF. Positive relation between IRREFF and outputIRR may explain where production more, water delivery systems are more improved. WATIRR is affected negatively by IRREFF and IRRINT, positively by MOMCOM and outputIRR. There is a positive significant relation between MOMCOM and IRREFF, WATIRR and negative significant relation with outputIRR. And IRREFF and WATIRR increase outputIRR considerably but MOMCOM expenditures decrease outputIRR.

Table 5. Panel data analysis among performance indicators

Indicator		IRREFF	WATIRR	MOMCOM	outputIRR	IRRINT	Hausman test *P*-value (model)
IRRINT	*p*-value Coef.	0.22 (5.00)	0.03** (-0.0002)	0.14 (0.006)	0.73 (-3.21e-05)	-	3.06e-006 (Fixed)
IRREFF	*p*-value Coef.	-	1.45-030*** (-8.60e-06)	0.56 (2.16e-05)	7.46e-05*** (3.72e-06)	0.22 (0.0005)	1.84e-05 (Fixed)
WATIRR	*p*-value Coef.	1.45e-030*** (-22,579.8)	-	0.01** (4.73)	7.93e-012*** (0.33)	0.03** (-46.19)	1.22e-077 (Fixed)
MOMCOM	*p*-value Coef.	0.056* (25.97)	0.01** (0.002)	-	0.052* (-0.002)	0.14 (-0.0002)	0.0003 (Fixed)
outputIRR	p-value Coef.	7.46e-05*** (6,807.86)	7.93e-012*** (0.23)	0.05* (-3.05)	-	0.73 (-5.85)	6.07e-025 (Fixed)

IRRINT: irrigation intensity, WATCOM: annual irrigation water supplied to users per unit command area; WATIRR: annual irrigation water supplied to users per unit irrigated area; IRREFF: irrigation efficiency; MOMCOM: total MOM cost per unit command area; MOMIRR: total MOM cost per unit irrigated area; MOMWAT: total MOM cost per unit water supplied to users; outputCOM: output per unit command area; outputIRR: output per unit irrigated area; outputWAT: output per unit per unit water supplied to users; Significant level at *$p < 0.10$; **$p < 0.05$; ***$p < 0.001$.

CONCLUSION

According to this experimental study, the performance of WUAs during the period notably range among the districts due to climatic, social, economic, crop pattern, management type, source of water. Water delivered to crops is overused since low technology is used both management level and farm level. WUAs managed by DSI show low performance according to results. Irrigation management transfer may increase the performance of the WUAs. Modern delivery of water technology ought to be used to enhance irrigation efficiency and not to lose water. And another important view of the current study, data management and collection are very important for decision-makers and researchers to evaluate WUAs. Main water delivers efficiency can be increased by using pressurized irrigation systems. Policies, improvements and innovations show that Turkey will eventually handle the transition to these systems to do not waste water even a drop in the future. Finally, it would be advisable to more focus on the transition of irrigation schemes into pressurized irrigation schemes with help policy and organizational works such as interdigitate of water management, land consolidation, energy production and climate change precautions. Without a systematic process, inefficient management and data collection, convenient irrigation methods, irrigation schemes of Turkey will proceed slightly.

REFERENCES

Akçay, S. 2016. Aydin Ili Sulama Kooperatiflerinde Su Saglama Oranlarinin Belirlenmesi/Evaluation of Water Supply Status of Irigation Cooperatives in Aydin Province. *Journal of Tekirdag Agricultural Faculty* **13**(2), 135.

Akkuzu, E. & Mengü, G.P. 2011. Evaluation of water user associations in Alasehir region in terms of land-water productivity and water supply. *Journal of Agriculture Faculty of Ege University* **48**(2), 119–126 (in Turkish, English abstr.).

Alcon, F., García-Bastida, P.A., Soto-García, M., Martínez-Alvarez, V., Martin-Gorriz, B. & Baille, A. 2017. Explaining the performance of irrigation communities in a water-scarce region. *Irrigation science* **35**(3), 193–203.

Anonymous, 2017. Climate types in Turkey. Available at https://tr.wikipedia.org/wiki/T%C3%BCrkiye%27deki_iklim_%C3%A7e%C5%9Fitleri

Arslan, F. & Değirmenci, H. 2017. Rating of some irrigation projects operated by DSI in Turkey. *In International Advanced Researches & Engineering Congress*, Osmaniye Korkutata University, Osmaniye, Turkey, pp. 16–18 (in Turkish, English abstr.)

Arslan, F. & Değirmenci, H. 2018. RAP-MASSCOTE Aproach of Modernizing OperatıonMaintanence and Management of Irrigation Schemes: A Case Study of Kahramanmaraş Left Bank Irrigation Scheme. *Atatürk University Journal of the Agricultural Faculty* **49**(1), 45–51 (in Turkish, English abstr.).

Borgia, C., García-Bolaños, M., Li, T., Gómez-Macpherson, H., Comas, J., Connor, D. & Mateos, L. 2013. Benchmarking for performance assessment of small and large irrigation schemes along the Senegal Valley in Mauritania. *Agricultural Water Management* **121**, 19–26.

Burt, C.M. 2001. Rapid Appraisal Process (RAP) and benchmarking, explanation and tools. Food and Agriculture Organisation of the United Nations, Bangkok, Thailand. Available at http://www.fao.org/3/a-aq443e.pdf

Çakmak, B., Beyribey, M., Yildirim, Y.E. & Kodal, S. 2004. Benchmarking performance of irrigation schemes: a case study from Turkey. *Irrigation and Drainage* **53**(2), 155–163.

Çakmak, B., Gökalp, Z. & Demir, N. 2014. Assessment of Agricultural Water Use in Trans-Boundary River Basins. *Journal of Tekirdag Agricultural Faculty* **11**(2), 119–130 (in Turkish, English abstr.).

Córcoles, J.I., De Juan, J.A. Ortega, J.F., Tarjuelo, J.M. & Moreno, M.A. 2010. Management evaluation of Water Users Associations using benchmarking techniques. *Agricultural Water Management* **98**(1), 1–11.

Değirmenci, H. 2004. Assessment of Irrigation Schemes with Comparative Indicators in Kahramanmaraş Region. *KSU Journal of Science and Engineering* **7**(1), 104–110 (in Turkish, English abstr.)

Değirmenci, H., Büyükcangaz, H. & Kuşçu, H. 2003. Assessment of irrigation schemes with comparative indicators in the Southeastern Anatolia Project. *Turkish Journal of Agriculture and Forestry* **27**(5), 293–303.

Demir, O., Demir, N., Tekin, M. & Yalçın, Z. 2014. Effects of Irrigation Investment of Erzurum Daphan Plain on Agricultural Production. *COMU Journal of Agriculture Faculty* **2**(2), 97–103. (in Turkish, English abstr.).

DSI. 2016. Assesment Report of Transferred and Non-Transferred Irrigation Schemes by DSI in Turkey in 2015. Ankara (in Turkish).

Eliçabuk, C. & Topak, R. 2017. Evaluation of Irrigation Performance in Gevrekli Irrigation Association. *Selcuk Journal of Agriculture and Food Sciences* **3**(2), 191–199 (in Turkish, English abstr.).

Gündoğdu, K., Değirmenci, H. & Demirtaş, Ç. 2002. Creation of Gis Supported Database In Irrigation Project Management. *AGROENVIRON* 2002, Cairo, Egypt (October), pp. 26–29.

IM, 2017. Agricultural Irrigated Land (% of total agricultural land). Index Mundi. Available at 'https://www.indexmundi.com/facts/indicators/AG.LND.IRIG.AG.ZS

Kartal, S., Arslan, F. & Değirmenci, H. 2019. Ranking irrigation schemes based on principle component analysis in the arid regions of Turkey. *Agronomy Research* **17**(2), 456–465.

Kartal, S., Değirmenci, H. & ARSLAN, F. 2020. Assessment of Irrigation Schemes with Performance Indicators in Southeastern Irrigation District of Turkey. *Journal of Agricultural Sciences* **26**(2), 138–146.

Lamaddalena, N., Khadra, R. & Fouial, A. 2015. Use of localized loops for the rehabilitation of on-demand pressurized irrigation distribution systems. *Irrigation science* **33**(6), 453–468.

Malano, H. & Burton, M. 2001. IPTRID Secretariat, Food and Agriculture Organization of the United Nations, Rome, 2001. Guidelines for Benchmarking Performance in the Irrigation and Drainage Sector.

Merdun, H. & Degirmenci, H. 2004. Topology of performance indicators of all irrigation schemes in Turkey. *Pakistan Journal of Biological Sciences* **7**(2), 163–173.

Molden, D. 1998. IWMI Research Report 20 Indicators for Comparing Performance of Irrigated Agricultural Systems. Available at http://books.google.com/books?hl=en&lr=&id=y2PRIcLsyg0C&oi=fnd&pg=PR5&dq=Indicators+for+Comparing+Performance+of+Irrigated+Agricultural+Systems&ots=usn_6-_at0&sig=_zeDC3oQ9xrPfRw1JVLkE263W1w

Nalbantoğlu, G & akmak, B. 2007. Benchmarking of Irrigation Performance in Akıncı Irrigation District. *Journal of Agricultural Sciences* **13**(3), 213–223.

Postel, S. 2014. The last oasis: facing water scarcity. Routledge. Available at https://www.routledge.com/The-Last-Oasis-Facing-Water-Scarcity-1st-Edition/Postel/p/book/9781853831485

Renault, D., Facon, T. & Wahaj, R. 2007. *Modernizing Irrigation Management: The MASSCOTE Approach--Mapping System and Services for Canal Operation Techniques* (Vol. **63**). Food & Agriculture Organization.

Rodríguez-Díaz, J.A., Camacho-Poyato, E., López-Luque, R. & Pérez-Urrestarazu, L. 2008. Benchmarking and Multivariate Data Analysis Techniques for Improving the Efficiency of Irrigation Districts: An Application in Spain. *Agricultural Systems* **96**(1–3), 250–59.

Shah, T., Van Koppen, B., de Lange, D.M.M. & Samad, M. 2002. Institutional alternatives in African smallholder irrigation: Lessons from international experience with irrigation management transfer (Vol. **60**). IWMI. Available at https://books.google.com.tr/books?hl=en&lr=&id=nWHUBAAAQBAJ&oi=fnd&pg=PP1&dq=Institutional+alternatives+in+African+smallholder+irrigation:+Lessons+from+international+experience+with+irrigation+management+transfer+&ots=v1wSWEwwsv&sig=docSjpPTDMI5361pjG07NiXz8Rk&redir_esc=y#v=onepage&q=Institutional%20alternatives%20in%20African%20smallholder%20irrigation%3A%20Lessons%20from%20international%20experience%20with%20irrigation%20management%20transfer&f=false

Sönmezyildiz, E. & Çakmak, B. 2013. Assessment of Irrigation Performance in Land Consolidation Area of Eskişehir Beyazaltın Village. *Mediterranean Agricultural Sciences* **26**, 33–40. *(in Turkish, English abstr.)*

Soto-García, M., Martin-Gorriz, B., García-Bastida, P.A. Alcon, F. & Martínez-Alvarez, V. 2013. Energy consumption for crop irrigation in a semiarid climate (south-eastern Spain). *Energy* **55**, 1084–1093.

Tanriverdi, C. & Degirmenci, H. 2011. Assessment of management transfer of Kahramanmaras irrigation system. *Scientific Research and Essays* **6**(3), 522–528.

Tanriverdi, Ç., Degirmenci, H. & Sesveren, S. 2011. Assessment of Irrigation Schemes in Turkey Based on Management Types. *African Journal of Biotechnology* **10**(11), 1997–2004.

Torres-Reyna, O. 2007. *Panel data analysis fixed and random effects using Stata* (v. 4.2). Data & Statistical Services, Priceton University, pp. 1–40.

Vermillion, D.L. & Sagardoy, J.A. 1999. *Transfer of irrigation management services:* Guidelines (No. **58**). Food & Agriculture Org. Available at http://www.fao.org/3/ah859e/ah859e00.htm

Zema, D.A., Nicotra, A., Mateos, L. & Zimbone, S.M. 2018. Improvement of the irrigation performance in Water User Associations integrating Data Envelopment Analysis and multiregression models. *Agricultural Water Management* **205**, 38–49.

Zema, D.A., Nicotra, A., Tamburino, V. & Zimbone, S.M. 2015. Performance assessment of collective irrigation in Water Users' Associations of Calabria (Southern Italy). *Irrigation and Drainage* **64**(3), 314–325.

Agronomy Research 18(4), 2317–2327, 2020
https://doi.org/10.15159/AR.20.175

A method for obtaining plastid pigments from the biomass of *Chlorella* microalgae

J. Bazarnova*, T. Kuznetsova, E. Aronova, L. Popova and E. Pochkaeva

Peter the Great St. Petersburg Polytechnic University, Graduate School of Biotechnology and Food Science, Polytechnicheskaya, 29, RU195251 St. Petersburg, Russia
*Correspondence: j.bazarnova@spbstu.ru

Abstract. Microalgae are distinguished from land plants by the high content of plastid pigments and the biodiversity of carotenoids. The aim of this study is to develop a technology for extracting a pigment complex from the biomass of the microalgae of the genus Chlorella and to determine the extracted pigments' composition. To obtain biomass, a crude cell suspension of microalgae was used, which was obtained under laboratory conditions for pre-culture cultivation of *C. sorokiniana* (strain 211-8k). The extraction of plastid pigments from air-dry biomass after disintegration of cell membrane was performed in the 40 kHz mode. It was found that the highest pigment content in ethanol extracts was observed after 30 min (870.0 ± 27.1 mg L^{-1}) at 45−50 °C. The pigments' composition in the resulting total extracts was determined by spectrophotometry and the Reverse Phase HPLC method. The established content of chlorophyll *a* in the obtained extracts was 537.5 ± 10.0 mg L^{-1}, the content of chlorophyll *b* was 182.5 ± 27.5 mg L^{-1}; the maximum output of the amount of carotenoids in extracts was 150.0 ± 10.0 mg L^{-1}. Thus, the main identified forms of carotenoids in extracts from the biomass of microalgae *C. sorokiniana* were xanthophylls: lutein and fucoxanthin (18.6 and 4.7% of the amount of pigment in extract, respectively) and β-carotene (1.8% of the amount of pigment). It is planned to further fractionate the obtained total extracts of the pigment complex to obtain various forms of chlorophylls and carotenoids to study the spectrum of physiological activity of plastid pigments.

Key words: *Chlorella* microalgae, pre-culture cultivation, disintegration, extraction, chlorophyll, carotenoids.

INTRODUCTION

To increase the nonspecific resistance of the body, it is advisable to use multicomponent preparations of natural origin, characterized by a balanced composition of biologically active substances that have a normalizing effect on the plastic, energy and informational types of metabolism (Baunthiyal et al., 2017; Nilova & Malyutenkova, 2018). At the same time, medical practice has a very limited list of pharmacopoeias used as antioxidants, including ascorbic acid, vitamin E and some bioflavonoids (quercetin, rutin, ascorutin, dihydroquercetin) (Nilova et al., 2017).

Algae are a unique source of phytochemical compounds with antioxidant properties (McQuistan et al., 2012; Dymova & Golovko, 2018). Microalgae *Chlorella sorokiniana* is a promising producer of valuable components: proteins (up to 40% dry biomass), lipids (up to 20% dry biomass), carbohydrates (up to 30% dry biomass) and biologically active substances (Lizzul et al., 2018), which can be obtained by cultivation in laboratory and industrial conditions (Politaeva et al., 2017). The relative content of microalgae components depends on cultivation conditions and age of the population (Sathasivam & Ki, 2018).

The content of plastid pigments, chlorophylls and carotenoids in microalgae can be up to 3.5% in dry biomass, which exceeds their content in land plants (Galasso et al., 2019). The authors (Mishra et al., 2011) noted the antioxidant activity of chlorophyll and its derivatives: chlorins, pheophytins and pyrophyophytins (Lanfer-Marquez et al., 2005).

Microalgae are distinguished by biodiversity of carotenoids, their high content (Ambrosino et al., 2019), as well as the possibility of targeted biosynthesis of carotenoids under intensive cultivation of microalgae in the laboratory. It is noted that β-carotene, zeaxanthin, anteroxanthin, violaxanthin, neoxanthin and lutein are characteristic of both microalgae and higher land plants. However, astaxanthin, loroxanthin, fucoxanthin, diadinoxanthin, diatoxanthin, siphonin are found only in the algae biomass (Galasso et al., 2019; Sathasivam 2018).

It is reported that consumption of any available source of carotenoids to significantly reduces photo-oxidative damage to biomembranes, the integrity of cells and tissues initiated by UV radiation (Dymova & Golovko, 2018). In this regard, it is promising to obtain pigment complex concentrates from *Chlorella* biomass in food (Bazarnova et al., 2019a; Kuznetsova, et al., 2019) and pharmaceutical industries.

When extracting pigments from the microalgae biomass, several features should be considered. It is known that photosynthetic pigments are localized in chloroplast thylakoids (Ladygin, 2014) (Fig. 1, a), while the cell membrane of the microalgae *Chlorella* is trilameolar and consists mainly of glycoproteins (Fig. 1, b). Therefore, it is necessary to use methods to increase the availability of valuable components of unicellular algae *Chlorella* (Viera, 2018), due to the processes of cell wall disintegration.

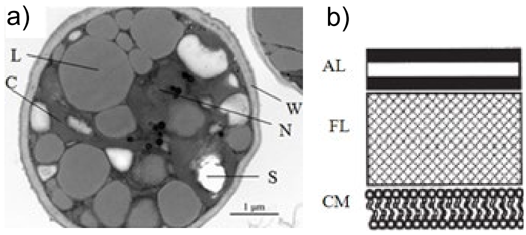

Figure 1. Ultrastructure of C. *sorokiniana* cell. a) – the image was obtained using a scanning electron microscope: L – lipid drops; S – starch granules; C – chloroplast; N – nucleolus; W – cell wall (Jiang, 2018); b) – cell membrane scheme (D'Hondt, 2017): AL – alginate-based layer; FL – fibrillar layer; CM – cell membrane.

Another problem is the instability of extracted plastid pigments, which are characterized by oxidative degradation under the influence of environmental factors: light, temperature, etc. (Albrecht et al., 2001).

The use of polar solvents is recommended for extraction of the amount of plastid pigments from plant materials: 95.6% ethanol, acetone, 1,4-dioxane, etc. (Dymova & Kuzivanova, 2018). Polar proton solvents (ethanol and acetone) are capable of forming hydrogen bonds and stabilizing ionized chlorophyll particles in biomass extracts. Polar aprotic solvents (1,4–dioxane) retain the ability to dissolve ions, but don't contain acidic hydrogen (Jaffer et al., 2019).

Ultrasonic extraction has a significant advantage over intensive extraction methods, for example, under the influence of microwaves or autoclaving (Jaeschke et al., 2017), as the recoverable substances are not exposed to high temperatures. Sound chemical reactions (Patel et al., 2018) and the phenomenon of cavitation (Antusheva, 2013) are considered as the main mechanism of the effect of ultrasound on biological objects.

The purpose of the research is to develop technologies for extracting the pigment complex from the biomass of microalgae *Chlorella* and to study the composition of the extracted pigments.

MATERIALS AND METHODS

The biomass of *C. sorokiniana* (strain 211-8k) was obtained by cultivation in a laboratory bioreactor (Bazarnova et al., 2019b; Politaeva et al., 2017). Universal nutrient medium balanced by micro- and macroelements (Crofcheck et al., 2012) was used. Cultivation temperature -20–22 °C, daylight illumination - 2,000–2,500 Lux (day-night mode) (Bazarnova et al., 2019c), bubbling mode - 1.5 L h^{-1}. The initial concentration of C. *sorokiniana* uterine culture cells was 4.14×10^{6} mL^{-1} cells.

The biomass was concentrated by autoflocculation (pH 10–11), followed by centrifugation at 6,000 rpm min^{-1} for 5 min (Bazarnova et al., 2018). The liquid phase was separated by decantation, the precipitate was dehydrated in air without access of light at a temperature of (20 ± 2) °C. The moisture content in the air-dry biomass was (2.5 ± 0.3) %.

A portion of dehydrated biomass of 0.025 g was poured with 10 mL of solvent and subjected to mechanical disintegration using a high-speed Silent Crusher M homogenizer (IKA® Werke, T25 Basic) at 10,000 rpm min^{-1} for 5 min, after which a glass container with homogenate was placed in a water-filled bath WUC-A01H (DAIHAN Scientific, South Korea, power 170 W). The extraction was performed under the conditions of voice-over at a frequency of 40 kHz (constant in the experiment) in the temperature range from 40 to 70 °C for 30 min (Bazarnova et al., 2019d).

When studying the effect of the composition of extracting solvent mixtures on the pigment yield, extractants recommended for extraction of plastid pigments from the phototroph biomass were used: ethanol, acetone, 1,4-dioxane (Amin et al., 2018).

After extraction, the mixture was centrifuged at 3,500 rpm min^{-1} for 3 min, the volume of the obtained supernatant was adjusted to 50 mL, and then filtered through a Nylon 66 Membranes 0.45×47 mm filter (SUPELCO) under pressure (105 Pa, VP 18R LabTech pump).

Spectrophotometry of the extracts was carried out in the visible and UV spectral ranges in the wavelength range 350–700 nm with a step of 0.2 on a UV-1240 instrument (Shimadzu corporation Analytical division). Calibration was carried out using 96% ethyl alcohol, a 10 mm cuvette.

The analysis of the total composition of pigments in the extracts was carried out according to the absorption maxima of 470, 649 and 664 nm. The concentrations of chlorophyll *a* (*Cha*), chlorophyll *b* (*Chb*) and carotenoids in extracts were determined according to the methodology (Nayek et al., 2014; Bazarnova et al., 2018).

To separate and identify the composition of chlorophylls and carotenoids in extracts, was used the method of reverse phase high performance liquid chromatography (RP HPLC, Reverse Phase HPLC) on a ZORBAX Original column with reverse phase ODS (C18) Analytical, 4.6 m × 150 mm × 5 μm, 883952−702, sorbent characteristic: specific surface area (Sp) - 350 m^2 g^{-1}, pore diameter - 7 nm, particle diameter - 8 nm, particle shape – spherical. The methodology (Gupta et al., 2015) was taken as the basis.

Optimization of the chromatographic separation of pigments requires compatibility between the injection solvent and the mobile phase. For this, the obtained extracts were thickened using a vacuum rotary evaporator (5 kPa, 40 °C) and the dry residue was redissolved in acetone. The resulting mixture was further used for chromatography at a dilution of 5 times.

An autonomous modular device with a simple piston pump for HPLC Varian 03-919000-00 9010 Gradient HPLC Pump DT VAC Case Scratched, Discolored REF VA248 was used as HPLC pump. The speed of passing the eluent is 1 mL min^{-1}.

To identify carotenes and xanthophylls in the obtained extracts, standard samples of β-carotene (Merck, Germany) and fucoxanthin (Shanxi Fuhen Biotechnology Co., Ltd.) were used.

Detection was carried out spectrophotometrically (Kratos Spectroflow 783 detector) at wavelengths of 440 nm and 650 nm. Identification and quantitative analysis of the components of the analyzed mixture was carried out according to the retention time and intensity of the analytical signal (height and peak area), followed by recalculation of concentrations according to the formula taking into account dilution, as well as using a computer-based data acquisition and processing system according to the method (Gupta, 2015). The value of the analytical signal for the fractions of identified pigments varied from 0.5 to 3.0.

The optical density of the eluate was measured in a specially designed microcuvette at wavelengths corresponding to the absorption maxima of the analytes under study.

Statistical processing of research results was carried out using the Microsoft Office

Excel software and the one-way analysis of variance Analysis of Variance (ANOVA).

The obtained experimental data are presented with the reference to confidence interval calculated using the t-criteria. The confidence probability is 0.95 and statistical significance of the given results is $p < 0.05$. The samples were examined in 3-fold repeatability mode.

RESULTS AND DISCUSSION

Choice of solvent system for extraction of plastid pigments

As a result of the study, it was found that the absorption spectrum of chlorophylls *a* and *b* is characterized by the presence of pronounced maxima: in the red, respectively, 660 and 640 nm and blue-violet, 430 and 450 nm spectral regions (Fig. 2).

The minimum absorption of carotenoids is fixed in the zone of green rays. Carotenes and xanthophylls absorb light only in the blue-violet part of the spectrum. In chlorophyll and carotenoid molecules, a system of conjugated double bonds determines the absorption of blue-violet rays (Borello & Domenici, 2019).

The obtained absorption spectrum of the ethanol extract of *C. sorokiniana* pigments (Fig. 2) is typical for phototroph pigments. The absorption band in the blue-violet region of 380–470 nm has absorption maximums (shoulder 1–380 nm, peak 2–420 nm, shoulder 3–440 nm, peak 4–470 nm), which are characteristic of carotenoids, chlorophylls *a* and *b*. The absorption band in the red region of the spectrum 640–680 includes the maximum (6), which is characteristic of chlorophyll *a* and *b* forms, as well as (5), which corresponds to protochlorophyll (Clayton, 1984).

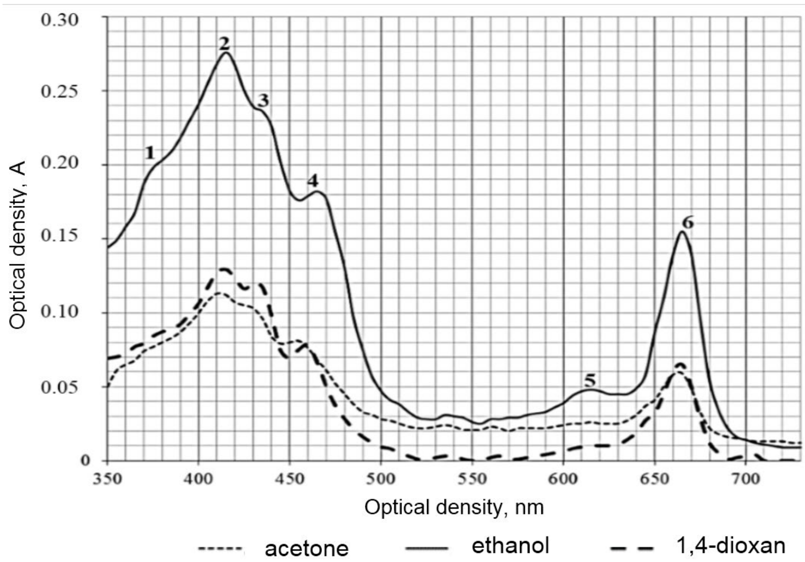

Figure 2. Spectral profiles of total extracts from biomass *C. sorokiniana.*

It was found that under conditions of extraction (40 kHz), ethanol is the most effective as extractant (Table 1) and the most complete extraction of the pigment complex from the biomass of microalgae *C. sorokiniana* is achieved at a temperature of 50 °C (Table 2).

Table 1. The effect of extractants on the pigment content in extracts from the biomass of *C. sorokiniana*

Extractants	The pigment content in the extracts, mg L^{-1}				
	∑ pigments	*Cha*	*Chb*	*Cha Chb^{-1}*	*Carotinoids*
Acetone	517.5 ± 25.0	285.5 ± 20.0	210.0 ± 10.0	1.4	22.5 ± 2.5
1,4-dioxane	607.5 ± 30.0	302.5 ± 15.0	280.0 ± 15.0	1.1	25.0 ± 2.5
Ethanol	870.0 ± 27.1	537.5 ± 10.0	182.5 ± 10.5	2.9	150.0 ± 10.0

Note: in 40 kHz mode, at 50 °C for 30 min.

The maximum yield of the amount of pigments in the extract was (870.0 ± 27.1) mg L^{-1}. The maximum yield of chlorophyll *a* - (537.5 ± 10.0) and the amount of carotenoids - (150.0 ± 10.0) mg L^{-1}.

An important characteristic of extractants used to work with biological objects is their toxicity. Ethyl alcohol and acetone, according to the safety data sheet, are not classified as acutely toxic, unlike 1,4-dioxane. Ethanol has the least toxicity, which expands the possibilities of its use for pigment extraction in biotechnology of algae biomass processing.

Table 2. The effect of the temperature of extraction on the pigment content in extracts from the biomass of *C. sorokiniana*

Extraction temperature, °C	The pigment content in the extracts, mg L^{-1}				
	∑ pigments	*Cha*	*Chb*	*Cha Chb*$^{-1}$	*Carotinoids*
40	742.5 ± 37.5	462.5 ± 0.6	145.0 ± 1.3	3.2	135.0 ± 2.5
50	870.0 ± 25.0	537.5 ± 0.4	182.5 ± 1.1	3.0	150.0 ± 7.5
60	827.5 ± 22.5	492.5 ± 0.7	217.5 ± 0.2	2.3	117.5 ± 5.0
70	605.0 ± 27.5	352.5 ± 0.5	170.0 ± 0.5	2.1	82.5 ± 5.0

Note: in 40 kHz mode, for 30 min.

With an increase in the extraction temperature to 60–70 °C, a decrease in the total content of chlorophylls and carotenoids in the obtained extracts is observed, which can be explained by their oxidative degradation (Ötleş, 2016). This process is accompanied by a simultaneous decrease in the ratio of chlorophyll *a* to chlorophyll *b*, indicating the oxidation of chlorophylls and the appearance of their derivatives: pheophytin, pheophorbide, chlorophyllide, chlorin and their oligomers (Antonov & Jagodin, 2006).

In Table 3 presents the results of studies on the effect of the duration of extraction of pigments from air-dry biomass of *C. sorokiniana* with 96% ethanol (40 kHz, 50 °C). It was found that the highest pigment content in the extracts was observed after 30 min.

Table 3. The effect of the duration of extraction on the content of pigments in extracts from biomass of *C. sorokiniana*

Extraction time, min	The pigment content in the extracts, mg L^{-1}			
	∑ pigments	*Cha*	*Chb*	Carotinoids
10	597.5 ± 20.0	270.0 ± 12.5	222.5 ± 12.5	105.0 ± 5.0
20	720.0 ± 22.5	335.0 ± 15.0	252.5 ± 12.5	130.0 ± 5.2
30	847.5 ± 27.5	350.0 ± 17.5	385.0 ± 20.0	147.5 ± 7.3
40	847.5 ± 25.0	350.0 ± 17.5	362.5 ± 17.5	137.5 ± 7.3

Note: in 40 kHz mode, at 50 °C.

When choosing the mobile phase and the conditions of chromatographic separation of carotenoids and their isomers by the Reverse Phase HPLC method, a gradient mobile phase consisting of methanol, water and acetone was used. The best separation was achieved by the consistent use of a mixture of solvents as an eluent: (A) 0–7 min - methanol : water (75:25); (B) 7−9 min - methanol; (B) 9−19 min - methanol : acetone (80:20); (D) 19-30 min - methanol : acetone (65:35). Maximum selectivity was obtained at a column temperature of 20 °C. The time required for chromatography is 30–40 min.

In Fig. 3 shows a fragment of a chromatogram of carotenoids used as standards.

The results of spectral and chromatographic analysis of the component composition of pigments in extracts of *C. sorokiniana* are presented in Fig. 4 and Table 4.

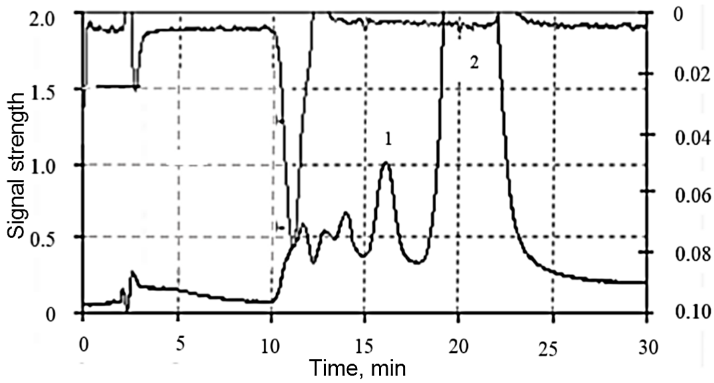

Figure 3. Chromatographic profiles of carotenoids used as standards. Detection at 440 nm – lower curve, left axis; at 650 nm – upper curve, the right axis: 1 – fucoxanthin; 2 – β-carotene.

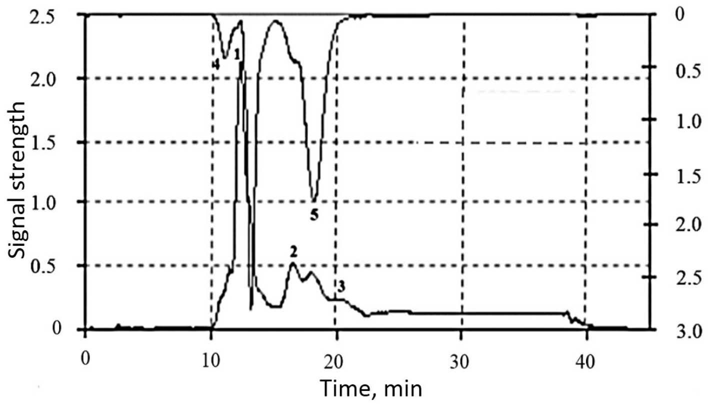

Figure 4. Chromatographic profiles of the main pigments of *C. sorokiniana* (lower curve, left axis, 440 nm; upper curve, right axis, 650 nm): 1 – lutein; 2 – fucoxanthin; 3 – β-carotene; 4 – chlorophyll *b*; 5 – chlorophyll *a*.

Fucoxanthin, lutein, β-carotene, chlorophyll *a* and *b* were identified by retention times (Fig. 4).

Thus, carotenoids of extracts from the biomass of microalgae *C. sorokiniana* are mainly represented by xanthophylls – lutein and fucoxanthin (18.6 and 4.7% of the amount of pigments in extract, respectively) and β-carotene (1.8% of the amount of pigments).

Table 4. The composition of pigments in extracts from biomass *C. sorokiniana*, mg L^{-1}

Pigments	Reverse Phase HPLC	Spectroscopy
∑ pigments	869.9 ± 89.3	352.9 ± 43.3
Cha	270.1 ±84.5	199.1 ± 24.4
Chb	239.2 ±28.6	113.1 ± 13.8
∑ carotenoids	–	40.7 ± 7.1
Lutein	161.6 ± 14.5	–
Fucoxanthin	40.9 ± 3.8	–
β-carotene	15.7 ± 1.4	–

Fig. 5 presents the technological scheme of the developed technology for producing pigment extracts from dry biomass of *C. sorokiniana*, including the process of obtaining air-dry biomass, its activation and extraction of pigments.

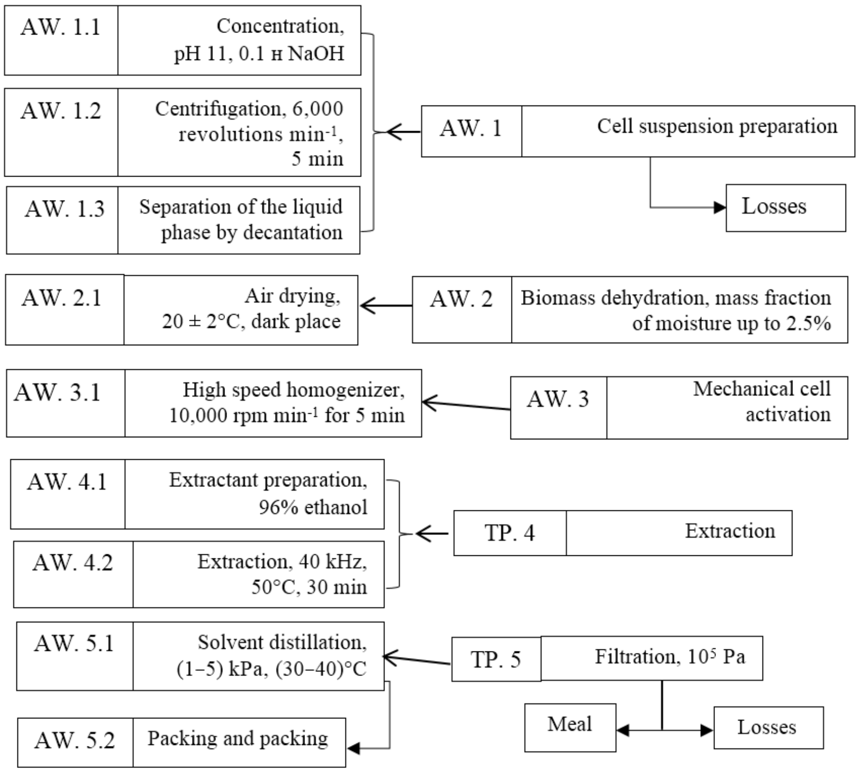

Figure 5. Technological scheme for obtaining extracts of pigments from biomass of microalgae *C. sorokiniana*: AW – Auxiliary work, TP – Technological process.

CONCLUSIONS

The search for alternative sources of biologically active substances is a promising area of research in biotechnology. The development of technology for the extraction of these substances from plant materials, the determination of their composition and properties is also a key issue (Gomez-Zavaglia et al., 2019). Microalgae of the genus *Chlorella* are considered as alternative sources of carotenoids (Liu et al., 2014).

To extract the amount of pigments from the air-dry biomass of *C. sorokiniana* obtained by cultivation in a laboratory bioreactor, the optimal extraction mode was selected. As the most effective and safe extractant, 96% ethanol is recommended (4 parts by volume of extractant are used for 1 part of dry biomass).

Under the conditions of extraction (40 kHz), the temperature and duration of extraction of pigments from the biomass of microalgae *C. sorokiniana* (50 °C, 30 min) were selected, at which their content in the extracts was (870.0 ± 27.1) mg L^{-1}, which agrees well with the results obtained by the authors (Villarruel-López A. et al., 2017). The content of chlorophyll *a* in the obtained extracts was (537.5 ± 10.0) mg L^{-1}, chlorophyll *b* - (182.5 ± 10.5) mg L^{-1}; the content of the amount of carotenoids - (150.0 ± 10.0) mg L^{-1}.

Xanthophylls – lutein (18.6%), fucoxanthin (4.7%) and β-carotene (1.8%) of the total pigment content were identified in extracts from the biomass of microalgae *C. sorokiniana* by the Reverse Phase HPLC method. It is good agreement with the data on the carotenoid content obtained by the authors (Matsukawa et al., 2000; Villarruel-López et al., 2017; Lizzul et al., 2018) for microalgae of *C. sorokiniana* cultivated in laboratory conditions. So, for example, as a result of studies (Matsukawa et al., 2000) in the biomass of *C. sorokiniana*, lutein and β-carotene were identified, the content of which was 62% (lutein) and 9% (β-carotene) of the total amount of carotenoids. Researchers (Raman & Mohamad, 2012) report that astaxanthin is present in *C. sorokiniana* (4.0 to 9.5 mg L^{-1} microalgae suspension).

Thus, a promising area for further study of the obtained total extracts of pigments of microalgae *C. sorokiniana* is their fractionation for the separation of chlorophylls and carotenoids and the study of the spectrum of their physiological activity, whereas this is relevant for their use in the field of biopharmacy (Xu et al., 2017).

ACKNOWLEDGEMENTS. The analysis of the composition of the pigments of the microalga *C. sorokiniana* using using the Reverse Phase HPLC method was carried out on the basis of MIP 'Analytics. Materials Technologies' Peter the Great St. Petersburg Polytechnic University. We would like to express our gratitude to Igor Vadimovich Kruchin-Bogdanov, Director of the small innovative enterprise 'Analytics. Materials. Technologies' Peter the Great St. Petersburg Polytechnic University.

REFERENCES

Albrecht, M., Steiger, S. & Sandmann, G. 2001. Expression of a ketolase gene mediates the synthesis of canthaxanthin in Synechococcus leading to tolerance against photoinhibition. pigment degradation and UV-B sensitivity of photosynthesis. *Photochemistry and Photobiology* **73**(5), 551−555.

Ambrosino, L., Tangherlini, M., Colantuono, C., Esposito, A., Sangiovanni, M., Miralto, M., Sansone, C. & Chiusano, M.L. 2019. Bioinformatics for Marine Products: An Overview of Resources. Bottlenecks. and Perspectives. *Marine Drugs* **17**(10), 1−30.

Amin, V., Chetpattananondh, P. & Khan, M.N. 2018. Extraction and Quantification of Chlorophyll from Microalgae Chlorella sp. *IOP Conf. Series: Materials Science and Engineering* **414**, 012025.

Antonov, V.I. & Jagodin, V.I. 2006. Transformations of green pigments during the extraction processing of coniferous green wood. *Chemistry of plant raw materials* **1**, 41–44 (in Russian).

Antusheva, T.I. 2013. Some features of the effect of ultrasound on microorganisms. Living and biocos systems 4. URL: http://www.jbks.ru/archive/issue- 4/article-11 (in Russian).

Baunthiyal, M., Singh, V. & Dwivedi, S. Review 2017. Article Insights of Antioxidants as Molecules for Drug Discovery. *Pharmacol* **13**(7), 874−889.

Bazarnova, J., Kuznetsova, T., Aronova, E. & Toumi, A. 2019b. Use of lipids of Chlorella microalgae in poultry meat marinades and sauces recipes. *Agronomy Research* **17**(S2), 1287–1298.

Bazarnova, Y., Kuznetsova, T. & Boysen, H.E. 2018. Methods for concentrating the cell suspension of *Chlorella* microalgae for obtaining pigment complex. *International Journal of Civil Engineering and Technology* **9**(10), 340−350.

Bazarnova, J., Kuznetsova, T. & Smyatskaya, Y. 2019d. A method of obtaining a pigment complex from the biomass of unicellular algae of the genus Chlorella. RF patent 2695879 (in Russian).

Bazarnova, Yu., Kuznetsova, T. & Trukhina, E. 2019a. Aquabiotechnology of directed cultivation of microalgae *Chlorella sorokiniana* biomass In: *IOP Conference Series: Earth and Environmental Science* **288**(1), 012037.

Bazarnova, J., Lyskova, N., Kuznetsova, T. & Trukhina, E. 2019c. Illumination influence on *Chlorella sorokiniana* biomass synthesis. *Biotechnologia acta* **12**(3). http://biotechnology.kiev.ua/index.php?option=com_content&view=article&id=957%3A-hlorella-sorokiniana-&catid=140%3A2019--3&Itemid=159&lang=en.

Borello, E. & Domenici, V. 2019 Determination of pigments in virgin and extra-virgin olive oils: A comparison between two near UV-vis spectroscopic techniques. *Foods* **8**(1), 1−13.

Clayton R. 1984. Photosynthesis. Physical mechanisms and chemical models. Moscow. 350 pp. (in Russian).

Crofcheck, C.L., Shea, A, Montross, M., Crocker, M. & Andrews, R. 2012. Influence of media composition on the growth rate of Chlorella vulgaris and Scenedesmus acutus utilized for CO_2 mitigation. *Biochem Tech*. **4**(2), 589−594.

D'Hondt, E., Martín-Juárez, J., Bolado, S., Kasperoviciene, J., Koreiviene, J, Sulcius, S., Elst, K. & Bastiaens, L. 2017. Cell disruption technologies. Microalgae-Based Biofuels and Bioproducts: From Feedstock Cultivation to End-Products. New York. NY. USA, pp. 133–154.

Dymova, O.V. & Golovko, T.K. 2018. Photosynthetic pigments: functioning. ecology. biological activity. *Bulletin of the Ufa Scientific Center for Wounds* **3**(4), 5–16 (in Russian).

Dymova, O.V. & Kuzivanova, O.A. 2018. The optimization of extraction routine of photosynthetic pigments and its content in lichens thalli. *Himiya rastitelnogo syrya* **2**, 137–144. doi: 10.14258/jcprm.2018023013 (in Russian).

Galasso, C., Gentile, A., Orefice, I., Ianora, A., Bruno, A., Noonan, D.M., Sansone, C., Albini, A. & Brunet, C. 2019. Microalgal Derivatives as Potential Nutraceutical and Food Supplements for Human Health: A Focus on Cancer Prevention and Interception. *Nutrients* **11**(6), E1226. doi: 10.3390/nu11061226

Gomez-Zavaglia, A., Prieto Lage, M.A., Jimenez-Lopez, C., Mejuto, J.C. & Simal-Gandara, J. 2019. The Potential of Seaweeds as a Source of Functional Ingredients of Prebiotic and Antioxidant Value. *Antioxidants* **8**(9), 406.

Gupta, P., Sreelakshmi, Y. & Sharma, R. 2015. A rapid and sensitive method for determination of carotenoids in plant tissues by high performance liquid chromatography. *Plant Methods* **11**(5). doi 10/1186/s13007-015-0051-0

Jaffer, M., Shaheen, S., Ashraf, H. & Hanif, U. 2019. Green vegetation: A promising source of color dyes. *Green Processing and Synthesis* **8**(1), 215−222.

Jaeschke, D.P., Rech, R., Marczak, L.D.F. & Mercali, G.D. 2017. Ultrasound as an alternative technology to extract carotenoids and lipids from Heterochlorella luteoviridis. *Bioresource Technology* **224**, 753–757.

Jiang, L., Zhang, L., Nie, C. & Pei, H. 2018. Lipid productivity in limnetic *Chlorella* is doubled by seawater added with anaerobically digested effluent from kitchen waste. *Biotechnology for Biofuels* **11**(68), 1−14.

Kuznetsova, T., Ivanchenko, O., Kiseleva, A. & Le Huong, T. 2019. Study of the influence of disintegrated biomass of Chlorella sorokiniana on the state of yeast Saccharomyces cerevisiae In: *E3S Web of Conferences 140*. EECE. Saint Petersburg, 01005.

Ladygin, V.G. 2014 Ways of biosynthesis. localization. metabolism and functions of carotenoids in chloroplasts of various species of algae: monograph. *Questions of modern algology* **2**, 7–19 (in Russian).

Lanfer-Marquez, U.M., Barros, R.M.C. & Sinnecker, P. 2005. Antioxidant activity of chlorophylls and their derivatives. *Food Research International* **38**, 885–891.

Liu, J., Sun, Z., Gerken, H., Liu, Z., Jiang, Y. & Chen, F. 2014. Chlorella zofingiensis as an Alternative Microalgal Producer of Astaxanthin: Biology and Industrial Potential. Mar. Drugs 12, 3487–3515.

Lizzul, A.M., Lekuona-Amundarain, A., Purton, S. & Campos, L.C. 2018. Characterization of *Chlorella sorokiniana*. UTEX 1230. *Biology* **7**, 1−25.

McQuistan, T.J., Simonich, M.T., Pratt, M.M., Pereira, C.B., Hendricks, J.D., Dashwood, R.H., Williams, D.E. & Bailey, G.S. 2012. Cancer chemoprevention by dietary chlorophylls: A 12.000-animal dose–dose matrix biomarker and tumor study. Food Chem. Toxicol 50, 341–352.

Matsukawa, R., Hotta, M., Masuda, Y., Chihara, M. & Karube, I. 2000. Antioxidants from carbon dioxide fixing *Chlorella sorokiniana*. *J. Appl. Phycol*. **12**, 263–267.

Mishra, V.K., Bacheti, R.K. & Husen, A. 2011. Medicinal Uses of Chlorophyll: A Critical Overview. In book: *Chlorophyll: Structure, Function and Medicinal Uses, Publisher: Nova Science Publishers*, Inc., Hauppauge, NY 11788, Editors: Hua Le and and Elisa Salcedo, pp. 177−196.
https://www.novapublishers.com/catalog/product_info.php?products_id=22468)

Nayek, S., Haque, C.I., Nishika, J. & Suprakash, R. 2014. Spectrophotometric Analysis of Chlorophylls and Carotenoids from Commonly Grown Fern Species by Using Various Extracting Solvents. *Research Journal of Chemical Sciences* **4**(9), 63−69.

Nilova, L. & Malyutenkova, S. 2018. The possibility of using powdered sea-buckthorn in the development of bakery products with antioxidant properties. *Agronomy Research* **16**(S2), 1444–1456.

Nilova, L, Pilipenko, T. & Malyutenkova, S. 2017. An investigation into the effects of bioactive substances from vegetable oils on the antioxidant properties of bakery products. *Agronomy Research* **15**(S2), 1399–1410.

Ötleş, S. 2016. Methods of Analysis of Food Components and Additives. *CRC Press Taylor & Francis*. 534 pp.

Patel, A., Mikes, F. & Matsakas, L. 2018. An Overview of Current Pretreatment Methods Used to Improve Lipid Extraction from Oleaginous Microorganisms. *Molecules* **23**(7), 1562.

Politaeva, N., Kuznetsova, T., Smyatskaya, Y. & Trukhina, E. 2017. Impact of various physical exposures on Chlorella sorokiniana microalgae cultivation. *International Journal of Applied Engineering Research* **12**(21), 11488−11492.

Raman, R. & Mohamad, S.E. 2012. Astaxanthin production by freshwater microalgae *Chlorella sorokiniana* and marine microalgae tetraselmis sp. *Pakistan Journal of Biological Sciences* **15(**24), 1182–1186.

Sathasivam, R. & Jang-Seu, Ki. A 2018. Review of the Biological Activities of Microalgal Carotenoids and Their Potential Use in Healthcare and Cosmetic Industries. *Mar Drugs.* **16**(1), 26.

Viera, I., Pérez-Gálvez, A. & Roca, A. 2018. Bioaccessibility of Marine Carotenoids. *Marine Drugs* **16**(10), 397, 1−21.

Villarruel-López, A., Felipe Ascencio, F. & Nuño, K. 2017. Microalgae, a Potential Natural Functional Food Source – a Review. *Pol. J. Food Nutr. Sci*. **67**(4), 251–263.

Xu, D.P., Li, Y., Meng, X., Zhou, T., Zhou, Y., Zheng, J., Zhang, J.J. & Li, H.B. 2017. Natural Antioxidants in Foods and Medicinal Plants: Extraction, Assessment and Resources *Int. J. Mol. Sci*. **18**, 96.

Agronomy Research **18**(4), 2328–2339, 2020
https://doi.org/10.15159/AR.20.201

Seasonal variation of macro- and micro- nutrients in leaves of fig (*Ficus carica* L.) under Mediterranean conditions

J.N. Bougiouklis, Z. Karachaliou, J. Tsakos, P. Kalkanis, A. Michalakos and N. Moustakas*

Agricultural University of Athens, Department of Natural Resources Management and Agricultural Engineering, Laboratory of Soil Science and Agricultural Chemistry, Iera Odos 75, GR11855 Athens, Greece
*Correspondence: nmoustakas@aua.gr

Abstract. Leaves of 'Smyrna' fig (*Ficus carica* L.), variety 'Smyrneiki', were collected at four stages of the annual growth cycle, namely (1) at flowering, (2) during fruit development, (3) at fruit maturity and (4) after fruit harvest, during two consecutive years (2018 and 2019) and the leaf macro-(N, P, K, Ca, Mg) and micro-(Fe, Zn, Cu, Mn, B) nutrient concentrations were determined. Mean concentrations of N, P, K, Ca and Mg ranged between 14.4–28.6, 0.5–1.7, 2–31.2, 22–80.3 and 2.1–6.7 g kg^{-1} (on a dry weight basis-d.w.), respectively, while concentrations of Fe, Zn, Cu, Mn, and B, ranged between 84–280, 11–70, 2–86, 40–206, and 18–39 mg kg^{-1} d.w., respectively. The mean leaf concentration of N decreased significantly at each successive growth stage, whereas those of P, K, Fe and Zn, also decreased progressively, but not always to a statistically significant level between each stage. In contrast, the mean leaf concentration of Ca increased significantly throughout the season, while the concentrations of Mg and Cu also increased, but not to a statistically significant level at each stage. The Mn concentration of fig leaves decreased significantly at fruit maturity, then increased significantly after fruit harvest. Overall, the nutrient concentration of fig leaves varies throughout the period from flowering to fruit harvest, suggesting that trees may need different amounts of nutrients depending on the developmental stage. The seasonal variation of the nutrient concentration in fig leaves confirmed the need for reference values for each phenological stage for leaf analysis interpretation and for developing an efficient fertilization program.

Key words: developmental stages, fig nutrition, reference nutrient values.

INTRODUCTION

The common fig (*Ficus carica* L.) belongs to the Moraceae family; it is native to Asia Minor, Iran and Syria and currently grows as a wild or domesticated species in most of the Mediterranean countries (Therios & Dimassi-Theriou, 2013). Figs are cultivated in the Mediterranean Basin, Iran and northern India, as well as in many regions with similar climatic conditions, such as the USA and Mexico (Flaishman et al., 2008). Its edible fruits are consumed fresh or dried and are used to prepare fig jam and syrup. Greece supplies more than 6% of global exports of dried figs. The mean annual production in Greece in the last 20 years is about 38,200 kg of dried figs from orchards covering an area of approximately 6,000 ha (FAO, 2017). Depending on the fruit pollination requirements, figs can be from several types. In the current study, the fig belongs to the ‘Smyrn’ type, and the variety is called ‘Smyrneiki’. The fruit of this variety is medium-large, spherical with a small neck, green-yellow, thin peel and has a rich flavor. It is mostly consumed dried but can also be eaten fresh. The tree is deciduous, reaching a height of 2–5 m; it is productive and has a lifespan of 50–60 years (Therios & Dimassi-Theriou, 2013). In Greece, it is cultivated in warm coastal areas, particularly in Evia (207.2 ha) and Messinia (83.3 ha) (https://www.statistics.gr).

In each plant tissue the nutrient concentrations depend on the uptake, vitality, transport, and movement of nutrients within the plant. All these processes may be affected by climatic factors. The content in macro and micronutrients of both leaves and other plant tissues varies with the age of the tissue and the time of sampling (Stylianidis et al., 2002). Leaves are organs in which nutritional elements accumulate and major metabolic processes occur. Thus, leaf analysis is the best means of diagnosing tree nutritional status, as well as indicating nutrient deficiency, toxicity, or imbalance, as reported for other woody crops (Arrobas et al., 2018; Cancela et al., 2018). Smith et al. (1987) reported that deciduous crops show seasonal changes in the mineral composition of the leaves and this can have important implications in relation to the diagnosis of nutrient disorders, the post-harvest storage of the fruit and in the timing of fertilizer applications. The nutrient accumulation curves throughout the growing season are good indicators of fruit tree nutrient demands for any developmental stage. They are also a useful tool to evaluate orchard nutritional status and to estimate the amount of soil nutrient removal (Nachtigall & Dechen, 2006). It is well known that leaf analysis must be based on standardized sampling methods and that results must be compared only with standard values obtained by those procedures. Standard values for figs are scarce and only two studies, namely those of Brown (1994), and Ersoy et al. (2003) are available. These values refer to nutrient concentrations in leaves sampled from the youngest, fully expanded, exposed leaves on non-fruiting branches in the fruit development stage (Brown, 1994) and from the third node, which was counted from the base of the shoots (Ersoy et al., 2003). The seasonal variations in fig leaf-nutrient concentration are necessary to understand and interpret the physiological aspects of fig nutrition. These seasonal changes are not available for all cultivars and varieties of figs. The most detailed nutrition survey of figs was conducted by Proebsting & Warner (1954) in commercial southern California ‘Adriatic’ and ‘Calimyrna’ orchards in the 1940s and 1950s. Also, many studies have been carried out in Turkey (Anac et al., 1982; Aksoy et al., 1987; Askin et al., 1998; Hakerlerler et al., 1998).

To achieve maximum production and high quality, the nutritional status of cultivated trees must be optimal throughout the growing season (Chatzissavvidis, 2005). Due to the lack of information on fig nutrition during the growing period in Greece and other countries in the Mediterranean region (except for Turkey), we determined the leaf concentrations of N, P, K, Ca, Mg, Fe, Zn, Cu, Mn, and B in the fig tree variety ‘Smyrneiki’ over different stages during the annual growth cycle. The objective of this study was to provide valuable information of macro and micro elements in fig leaves at different developmental stages for the design of a more efficient fertilization program under Mediterranean climatic conditions.

MATERIALS AND METHODS

Experimental site

This experiment was carried out in Istiaia (38° 56' 7.96" N 23° 08' 38" E), a province in the North of the Evia island, Greece. The island is characterized by a Mediterranean climate with hot dry summers and cold wet winters. The average annual temperature of the area is 17.2 °C. The hottest and the coldest months are July and January with mean temperatures of 27.4 and 7.5 °C, respectively. The mean annual precipitation is 445 mm. The highest precipitation occurs in December with an average of 60.6 mm. The total dry period lasts for approximately three months (June-August).

Plant sampling and analytical methods

The fig orchard was non-irrigated, occupied an area of about 2.5 ha and consisted of 260 mature (22 years old) trees. The trees were in a 10 m intra-row and 8.5 m inter-row spacing arrangement. The mean yield of marketable fig for this orchard during the last ten years was approximately 40,000 kg ha^{-1} $year^{-1}$. The yield of marketable fig from the orchard in 2018 and 2019 was approximately 30,000 kg ha^{-1} and 44,000 kg ha^{-1}, respectively. The low yield in 2018 was caused by a high incidence of fruit cracking due to the occurrence of rainfall at fruit maturity. All trees received the same fertilizers for 10 years at least; i.e. each tree received 1.5 kg of mono ammonium phosphate (12–52–0) and 1.5 kg of potassium sulphate (0–0–50) in mid-November in 2017 and 2018, respectively. At the end of the following March in each year, 1.5 kg 'nutrimore winner' (commercial name of fertilizer containing 40% total N (35.5% Uric Nitrogen and 5% Ammoniacal Nitrogen)) was applied to each tree.

Fifteen uniform, healthy trees were selected for sampling. The sampled trees were marked (2018) to be sampled again the next year (2019). Fifty young, fully expanded and exposed leaves on non-fruiting branches were collected from the perimeter of each tree at 1.8 m height, as proposed by Beutel et al. (1983). Leaf samples were collected on mid- to late May, June, late August, and October; these dates corresponded to the flowering, fruit development, fruit maturity and postharvest stages of the growth cycle, respectively. Extremely vigorous or weak shoots were avoided at all samplings. Leaves were stored in paper bags and refrigerated at 15 °C for 1 day. Once in the laboratory, the leaves were washed with deionized water, dried at 55 °C for 48 h, ground in a stainless steel Wiley mill, passed through a 250 µm plastic sieve and stored in covered plastic test tubes until analysis. Total nitrogen was determined by the Kjeldahl method (Bremner & Mulvaney, 1982). For determination of other elements, 0.5 g of the ground material was dry-ashed in a muffle furnace at 550 °C for 3.5 h. Then, the ash was dissolved in 3 mL 6N HCl and diluted to 50 mL with distilled water. The concentrations of Mg, Fe, Mn, and Zn in the clear solution were determined by flame atomic absorption spectrophotometry (Varian, A–300; Varian Techtron Pty. Ltd., Australia), using an air–acetylene flame, while Ca concentration was determined using an acetylene–N_2O flame. Potassium was measured using flame photometry (Microprocessor Flame photometer model 1332, Esica Ltd., India). Total P was determined using the Murphy & Riley (1962) method with a PG T60 UV/VIS Spectrophotometer (PG Instruments Ltd., United Kingdom), at 880 nm. Boron was determined using the azomethine–H method (Wolf, 1971) employing the above-mentioned spectrophotometer at 420 nm. The methods of leaf analysis used are described with further details in Klute, (1986).

Soil sampling and analytical methods

Equidistant around the circumference of a circle of 0.5 m radius from the trunk of each selected tree, three samples of soil were taken at depths of 0–30 and 30–60 cm. Then the three samples from each depth and each tree were combined and mixed separately, resulting in 15 mixed soil samples from the depth of 0–30 cm and 15 from the depth of 30–60 cm. Soil samples were taken in October 2017, transferred to the laboratory and dried at room temperature, after which they were ground and passed through a 2 mm sieve (fine earth fraction) for the determination of the following properties: the pH was determined in a soil:water (1:1) suspension (Mclean, 1982); soil texture was determined using the hydrometer method (Gee & Bauder, 1986); organic matter was determined using a modified Walkley–Black method (Nelson & Sommers, 1982); the $CaCO_3$ equivalent by using the quantity of CO_2 produced on reaction with HCl (Nelson, 1982); the cation exchange capacity (CEC) was determined with ammonium acetate method at pH 7.0 (Rhoades, 1982); exchangeable bases were determined using an NH_4OAc (1N, pH 7) method (Thomas, 1982); total nitrogen was estimated by the Kjeldahl procedure (Bremner & Mulvaney, 1982); total P was determined using the Olsen's method (Murphy & Riley, 1962); Fe, Mn, Cu and Zn were estimated by the DTPA method (Linsday & Norvell, 1978); while B was extracted by hot water and determined by colorimetry (420 nm) using the azomethine–H method (Gupta, 1979).

Statistical analysis

According to the Hartley's F max test, variance of leaf nutrient concentrations at a given developmental stage between the two cultivated years were homogeneous so the data of the two years were pooled for each developmental stage and analysis of variance performed. Where a significant difference was found, Duncan's multiple range test at the 5% level of probability was used to compare mean nutrient concentration at different developmental stages. Statistical analysis and graph preparation were carried out with STATISTICA (Statsoft, 2007). The mean leaf nutrient concentration data are expressed as the mean of the two years studied.

RESULTS AND DISCUSSION

Soil analysis

Table 1 shows the values of the different soil properties determined in the current study. The texture of all soil samples at both depths was clay loam (CL). The pH values were slightly alkaline. Equivalent calcium carbonate content was greater than 100 g kg^{-1}, which characterizes marl soils. Organic matter content was very low, but CEC was greater than 21.5 $cmol_{(+)}kg^{-1}$ in the 0–30 cm soil layer, indicating the soil to be fertile. However, the levels of soil N were low, implying that fertilization would be required to replenish N consumed by the trees. Total P concentration was at threshold limits (total P threshold limits are 15 mg kg^{-1}). Potassium was low, but calcium and magnesium concentrations were high: 33.75 $cmol_{(+)}kg^{-1}$ soil and 1.95 $cmol_{(+)}kg^{-1}$ soil, respectively. Levels of micronutrients (Fe, Zn, Cu, Mn, B) ranged within their corresponding threshold limits. The evaluation of soil nutrient status was based on Landon (1991).

Table 1. Physical and chemical properties of the soil samples collected under the fig trees

Depth	Units	0–30 cm	30–60 cm
Sand	g kg^{-1}	342	381
Silt		312	291
Clay		346	328
Texture		CL*	CL
pH		7.65	7.7
Eq. $CaCO_3$	g kg^{-1}	132.5	165.5
Org. matter		0.8	0.3
Total N		1.25	0.65
P-Olsen		17.8	15.6
Exch. Ca	cmol$_{(+)}$kg^{-1}	33.75	33.3
Exch. Mg		1.95	1.6
Exch. K		0.45	0.3
Exch. Na		0.3	0.3
CEC*		23.8	21.4
$Fe_{(DTPA)}$		2.3	2.05
$Zn_{(DTPA)}$		0.75	0.5
$Cu_{(DTPA)}$	mg kg^{-1}	4.55	2.3
$Mn_{(DTPA)}$		0.55	0.3
$B_{(zeon\ H2O)}$		3.8	2.7

*CEC = cation exchange capacity; CL = Clay loam.

Plant analysis

Macronutrients

Table 2. Mean, minimum, and maximum concentrations of the macronutrients N, P, K, Ca and Mg in the leaves of the fig variety 'Smyrneiki' over the sampling period (2018–2019)

	N	P	K	Ca	Mg
	G kg^{-1} d.w.				
Mean	20.3	1.0	13.1	43.3	4.1
Minimum	14.4	0.5	2.0	22.0	2.1
Maximum	28.6	1.7	31.2	80.3	6.7

Nitrogen (N)

Mean leaf N concentrations were 24.6, 21.4, 17.7, and 16.1 g kg^{-1} d.w. for the flowering, fruit development, fruit maturity and postharvest stages, respectively, and the mean value for the total sampling period was 20.3 g kg^{-1} d.w. (Table 2). The mean N in the leaves of the studied fig variety decreased significantly between each stage until the end of the sampling period (Fig. 1), probably due to utilization of N by the trees. Similar patterns of N leaf content in 'Sarilop' and 'Yesilguz' fig leaves were found by Brown (1994) and Ersoy et al. (2003), respectively, while Vemmos et al. (2013) reported that the leaf N concentration of three fig cultivars ('Kalamon', 'Mission' and 'Farkasana') decreased with plant age. In contrast, Cruz et al. (2019) reported that N concentration in fig leaves decreased, but not significantly, throughout the growing season.

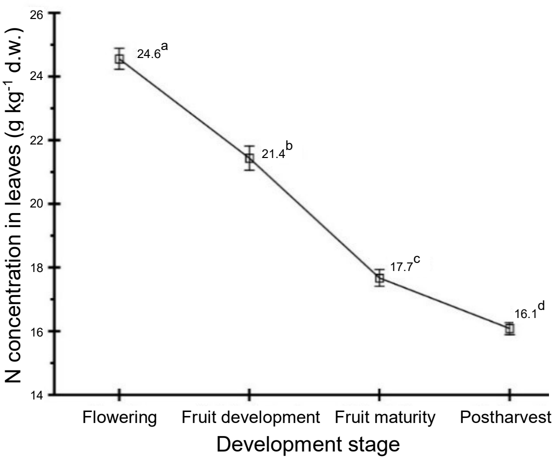

Figure 1. Nitrogen (N) concentration in leaves of the fig variety 'Smyrneiki' at four stages in the annual growth cycle of the tree on average for two consecutive years. Error bars represent standard error of the mean (± 0.5*SE). Means at different sampling time followed by the same letter are not significantly different according to Duncan's multiple range test at $P \leq 0.05$.

Phosphorus (P)

Leaf P mean concentrations were 1.3, 1.0, 0.9, and 0.9 g kg^{-1} d.w. for the flowering, fruit development, fruit maturity and postharvest stages, respectively, and the mean value for the total sampling period was 1.0 g kg^{-1} d.w. (Table 2). Mean leaf P content decreased sharply from flowering to the fruit development stage, but then remained constant (Fig. 2). The mean P values were greater than 0.9 g kg^{-1} in the late spring sampling (flowering) but low compared to most other tree crops (Beutel et al., 1983; Reuter & Robinson, 1986). Other woody crops, such as grapevines, can have even lower P leaf contents (Romero et al., 2014; Cancela et al., 2018). Proebsting & Warner (1954), Ersoy et al. (2003), and Brown (1994) reported that P concentrations in fig leaves decreased over the growing season, whereas Cruz et al. (2019) reported that fig leaf P concentration increased and decreased throughout the growing season.

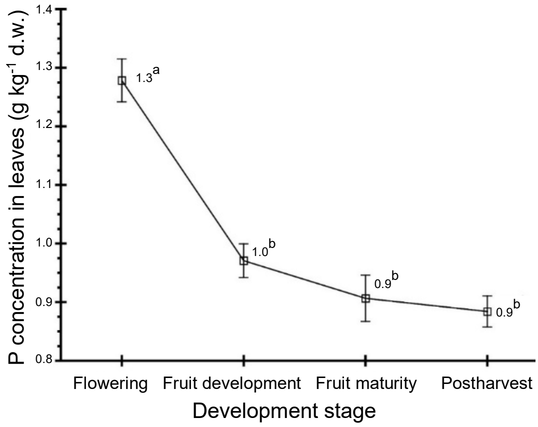

Figure 2. Phosphorus (P) concentration in leaves of the fig variety 'Smyrneiki' at four stages in the annual growth cycle of the tree on average for two consecutive years. Error bars represent standard error of the mean (± 0.5*SE). Means at different sampling time followed by the same letter are not significantly different according to Duncan's multiple range test at $P \leq 0.05$.

Potassium (K)

Mean leaf K concentrations were 20.2, 14.1, 8.9, and 7.0 g kg^{-1} d.w. for the flowering, fruit development, fruit maturity and postharvest stages, respectively, and the mean value for the total sampling period was 13.1 g kg^{-1} d.w. (Table 2). Mean leaf K concentration decreased markedly, by about 56%, from flowering to fruit maturity, 4–5 months after flowering (Fig. 3). A similar pattern of variation in mean leaf K concentration throughout the growing season was reported by Ersoy et al. (2003) and Brown (1994), as in most deciduous crop species (Smith et al., 1987, Nachtigall & Dechen, 2006; Mirdehghan & Rahemi, 2007; Cruz et al., 2019). Proebsting & Warner (1954) recorded similar mean K concentrations in fig leaves at fruit maturation.

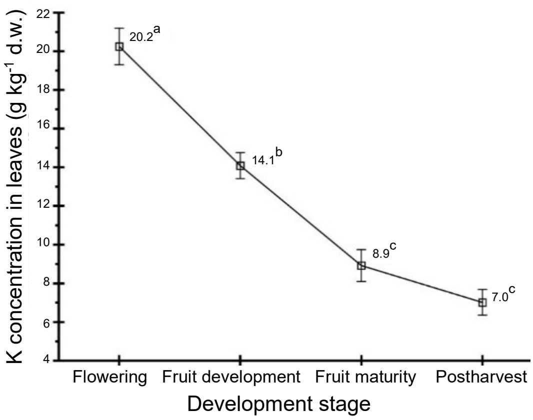

Figure 3. Potassium (K) concentration in leaves of the fig variety 'Smyrneiki' at four stages in the annual growth cycle of the tree on average for two consecutive years. Error bars represent standard error of the mean (± 0.5*SE). Means at different sampling time followed by the same letter are not significantly different according to Duncan's multiple range test at $P \leq 0.05$.

Calcium (Ca)

Mean leaf Ca concentrations were 30.7, 38.0, 51.8, and 57.2 g kg^{-1} d.w. for the flowering, fruit development, fruit maturity and postharvest stages, respectively, and the mean value for the total sampling period was 43.3 g kg^{-1} d.w. (Table 2). The mean leaf Ca concentration increased significantly from flowering to postharvest (Fig. 4). Ersoy et al. (2003), reported that the Ca concentration of leaves of 'Yesilguz' figs increased rapidly until the leaves were 3 to 4 months of age, after which there was very little change.

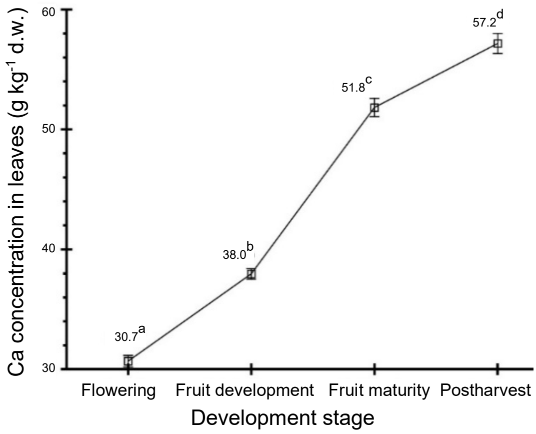

Figure 4. Calcium (Ca) concentration in leaves of the fig variety 'Smyrneiki' at four stages in the annual growth cycle of the tree on average for two consecutive years. Error bars represent standard error of the mean (± 0.5*SE). Means at different sampling time followed by the same letter are not significantly different according to Duncan's multiple range test at $P \leq 0.05$.

Magnesium (Mg)

Mean leaf Mg concentrations were 3.9, 3.9, 4.4, and 4.4 g kg^{-1} d.w. for the flowering, fruit development, fruit maturity and postharvest stages, respectively, with a mean value of 4.11 g kg^{-1} d.w.for the total sampling period (Table 2). Mean leaf Mg concentration increased from fruit development to fruit maturity, but then remained constant (Fig. 5). The same pattern for Mg in other fig cultivars was reported by Ersoy et al. (2003) and Brown (1994).

The leaf concentrations of N, P, K in the studied fig variety decreased during the growth cycle. This reduction should be related to a dilution effect occurred with leaf growth and to the nutrient redistribution to other plant organs (shoots, fruits) throughout the end of cycle. The increase in leaf Ca concentration from flowering to the postharvest stage was probably due to the immobility of Ca in plant tissues and no redistribution to other plant organs. The increase in leaf Mg concentration was likely a consequence of lower K competition since leaf K decreased during the growth period (Nachtigall & Dechen, 2006).

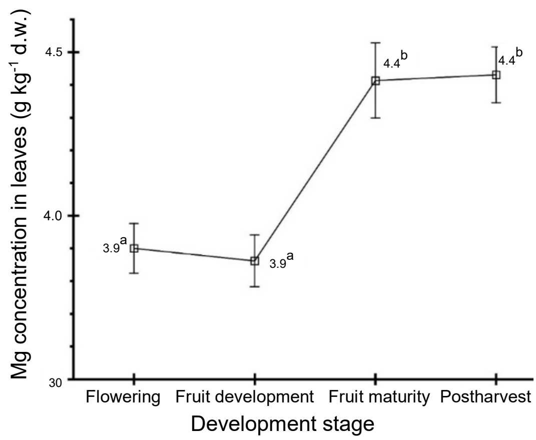

Figure 5. Magnesium (Mg) concentration in leaves of the fig variety 'Smyrneiki' at four stages in the annual growth cycle of the tree on average for two consecutive years. Error bars represent standard error of the mean (± 0.5*SE). Means at different sampling time followed by the same letter are not significantly different according to Duncan's multiple range test at $P \leq 0.05$.

Micronutrients

Iron (Fe)

Mean leaf Fe concentrations were 207, 164, 166, 112 mg kg^{-1} d.w. for the flowering, fruit development, fruit maturity and postharvest stages, respectively, and the mean value for the total sampling period was 161 mg kg^{-1} d.w. (Table 3). Mean leaf Fe concentration decreased from flowering to the fruit development stage, then remained constant until fruit maturity, followed by a significant decline (Fig. 6). The Fe concentration at the stage of fruit maturity (July) was greater than 70 µg g^{-1}, which is considered adequate for most tree species (Jones, 1998).

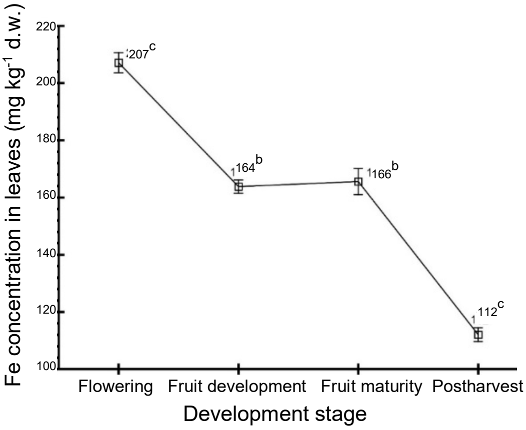

Figure 6. Iron (Fe) concentration in leaves of the fig variety ‘Smyrneiki’ at four stages in the annual growth cycle of the tree on average for two consecutive years. Error bars represent standard error of the mean (± 0.5*SE). Means at different sampling time followed by the same letter are not significantly different according to Duncan’s multiple range test at $P \leq 0.05$.

Table 3. Mean, minimum, and maximum concentrations of the micronutrients Fe, Zn, Cu, Mn and B in the leaves of the fig variety ‘Smyrneiki’ over the sampling period (2018–2019)

	Fe	Zn	Cu	Mn	B
	mg kg^{-1} d.w.				
Mean	161	27	12	91	29
Minimum	84	11	2	40	24
Maximum	280	70	86	206	39

Zinc (Zn)

Mean leaf Zn concentrations were 36, 26, 21, 22 mg kg^{-1} d.w for the flowering, fruit development, fruit maturity and postharvest stages, respectively, with a mean value for the total sampling period of 27 mg kg^{-1} d.w. (Table 3). The highest values of Zn concentration occurred at flowering, then decreased significantly to the fruit development stage and subsequently remained constant (Fig. 7). Similar patterns were obtained by Brown (1994) and Ersoy et al. (2003). The mean leaf Zn concentration was adequate for tree growth, according to Jones (1998).

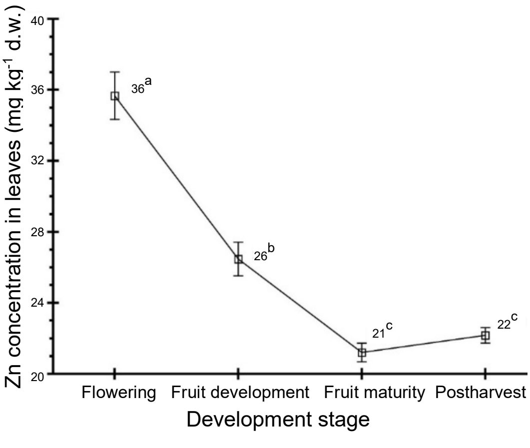

Figure 7. Zinc (Zn) concentration in leaves of the fig variety ‘Smyrneiki’ at four stages in the annual growth cycle of the tree on average for two consecutive years. Error bars represent standard error of the mean (± 0.5*SE). Means at different sampling time followed by the same letter are not significantly different according to Duncan’s multiple range test at $P \leq 0.05$.

Copper (Cu)

Mean leaf Cu concentrations were 6, 8, 14, and 21 mg kg^{-1} d.w. for the flowering, fruit development, fruit maturity and postharvest stages, respectively, with a mean value for the total sampling period 12 mg kg^{-1} d.w. (Table 3). The mean Cu concentration in fig leaves increased progressively with each stage, but only to a statistically significant level between flowering and postharvest (Fig. 8). Ersoy et al. (2003) reported that the Cu concentration in fig leaves decreased with increasing leaf age. Mean leaf Cu concentrations at all stages were higher than 6 mg kg^{-1}, which is considered adequate for most tree species (Jones, 1998).

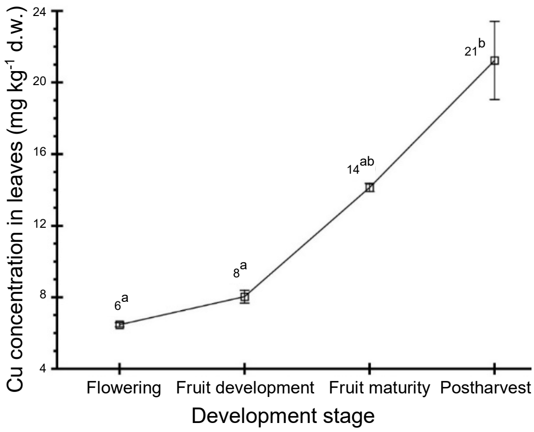

Figure 8. Copper (Cu) concentration in leaves of the fig variety 'Smyrneiki' at four stages in the annual growth cycle of the tree on average for two consecutive years. Error bars represent standard error of the mean (± 0.5*SE). Means at different sampling time followed by the same letter are not significantly different according to Duncan's multiple range test at $P \leq 0.05$.

Manganese (Mn)

Mean leaf Mn concentrations were 91, 87, 65, and 108 mg kg^{-1} d.w. for the flowering, fruit development, fruit maturity and postharvest stages, respectively, and the mean value for the total sampling period was 91 mg kg^{-1} d.w. (Table 3). Manganese concentration along the growing cycle follows a unique pattern, decreasing sharply from fruit development to fruit maturity and then increasing sharply to postharvest development stage (Fig. 9).

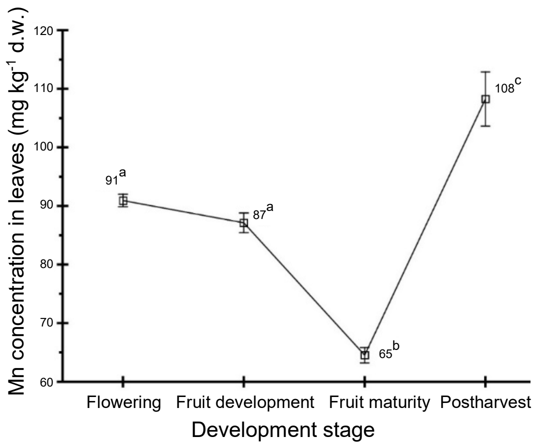

Figure 9. Manganese (Mn) concentration in leaves of the fig variety 'Smyrneiki' at four stages in the annual growth cycle of the tree on average for two consecutive years. Error bars represent standard error of the mean (± 0.5*SE). Means at different sampling time followed by the same letter are not significantly different according to Duncan's multiple range test at $P \leq 0.05$.

Boron (B)

Mean leaf B concentrations were 28, 28, 30, and 32 mg kg^{-1} d.w. for the flowering, fruit development, fruit maturity and postharvest stages, respectively and the mean value for the total sampling period was 29 mg kg^{-1} d.w. (Table 3). Mean leaf B concentration did not differ between flowering and fruit development, but thereafter increased significantly (Fig. 10). Brown (1994) reported that fig leaves are possible B accumulators, like walnut and pistachio. Boron requirements for most plant species are poorly defined because higher amounts of B are required for flowering and fruit production than for vegetative growth (Hansen et al., 1985).

The mean leaf values of N, P, K, Fe, Ca concentrations at the fruit development stage agree with those reported by Hakerlerler et al. (1998) from 10 fig cultigens. The mean values for macro- and micro-nutrients in fig leaves recorded here were higher than the threshold limits of deficiency (Reuter & Robinson, 1986) probably thanks to the correct time and dose of fertilizers. Mean leaf Fe, Zn, Cu, and B contents showed less intense fluctuation, decreasing (Fe, Zn) or increasing (Cu, B) throughout the sampling period, but not to statistically significantly levels at all stages. No deficiency was observed in any instance.

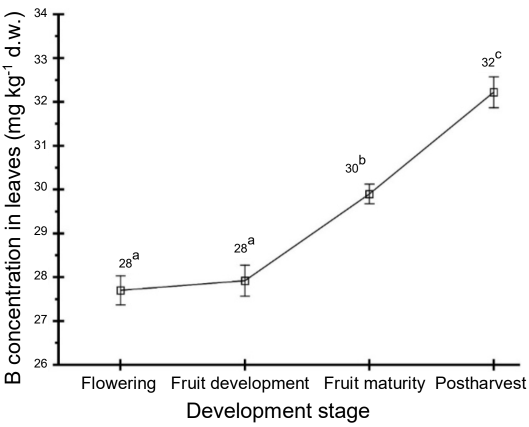

Figure 10. Boron (B) concentration in leaves of the fig variety 'Smyrneiki' at four stages in the annual growth cycle of the tree on average for two consecutive years. Error bars represent standard error of the mean (±0.5*SE). Means at different sampling time followed by the same letter are not significantly different according to Duncan's multiple range test at $P \leq 0.05$.

A classical method for developing a practical basis for fertilizing commercial plants is to define critical nutrient concentrations (reference values) in each species and tissue and relating them to yields (Smith, 1962).

In the studied fig orchard the yields of marketable fig, under the same fertilization treatment applied for 10 consecutive years, were at high levels (40–50 kg tree^{-1}); therefore the macro and micro nutrient concentrations in leaves at different tree developmental stages could be consider critical and hence be used as reference values for developing an efficient fertilization program under Mediterranean climatic conditions.

CONCLUSIONS

Fig leaf nutritional concentrations varied throughout the growing period, indicating that the plants have different nutrient requirements at different developmental stages. The sharp decrease in potassium from flowering until fruit maturity development stage is particularly remarkable and should be considered when developing a fertilization plan. The measured values of each nutrient plotted versus time can be useful in explaining several phenomena during the bearing cycle of the fig tree and can also be used to support decision making for the optimum fertilization of fig trees. Overall, the variation in nutrient contents of fig leaves is similar to that of most deciduous trees. The leaf nutrient concentrations observed at different developmental stages in the current study could be used as standard reference values for leaf analysis interpretation and for developing an optimum fertilization program.

REFERENCES

Aksoy, U., Anac, D., Eryuce, N. & Yoltas, T. 1987. Determination and evaluation of the nutrients status of fig orchards in the Aegean Region. *J. Ege Univ. Fac. Agric*. **24**(2), 21–35.

Anac, D., Aksoy, U., Hakerlerler, H. & Duzbastõlar, M. 1982. *Nutritional status of fig orchard in the small meander basin and relationships between soil and leaf nutrients and some yield and quality attributes*. Taris Research and Development Centre Project no:**4**.

Arrobas, M., Afonso, S. & Rodrigues, M.A. 2018. Diagnosing the nutritional condition of chestnut groves by soil and leaf analyses. *Sci. Hortic*. **228**, 113–121.

Askin, A., Ceyls, S. & Yener, H. 1998. A study on the national status of fig orchards in birgi-irimagzi. *Acta Hort.* **480**, 239–246.

Beutel, J., Uriu, K. & Lilleland, O. 1983. *Leaf analysis for Californian deciduous fruits*. Soil and Plant Tissue Testing in California Bull. 1879. Univ. of California, Berkeley, 17 pp.

Bremner, J.M. & Mulvaney, C.S. 1982. Salicilic acid thiosulfate modification of Kjieldahl method to include nitrate and nitrite. In A.L. Page (ed), *Methods of Soil Analysis*. Part 2. *Chemical and Microbiological Properties*. second ed. Amer. Soc. Agron. No **9** (Part 2) in the Agronomy Series. ASA, SSSA, Madison, WI., pp. 595–562.

Brown, P.H. 1994. Seasonal variations in fig *(Ficus carica* L.) leaf nutrient concentrations. *HortScience* **29**, 871–873.

Cancela, J.J., Fandiño, M., González, X.P., Rey, B.J. & Mirás-Avalos, J.M. 2018. Seasonal variation of macro and micronutrients in blades and petioles of *Vitis vinifera* L. cv. Mencía and Sousón. *J. Plant Nutr. Soil Sci.* **181**, 498–515.

Chatzissavvidis, C., Therios, I. & Molassiotis, A. 2005. Seasonal variation of nutritional status of olive plants as affected by boron concentration in nutrient solution. *J. Plant Nutr.* **28**, 309–21.

Cruz, A.F., Almeida, G.M de, Wadt, P.G.S., Pires, M. de C. & Ramos, M.L.G. 2019. Seasonal variation of plant mineral nutrition in fruit ttrees. *Braz. Arch. Biol. Technol.* **62**, e19180340. Epub October 24, 2019. https://dx.doi.org/10.1590/1678-4324-2019180340

Ersoy, N., Gözlekçi, S. & Kaynak, L. 2003. Seasonal variations in the content of nutrient elements in the leaves of fig (*Ficus carica* L. Yesilguz). *Acta Hortic.* **605**, 269–275.

FAO. 2017. Food and agriculture organization of the United Nations statistical databases. Available online: http://www.fao.org/faostat/en/ (accessed on 2 May 2020).

Flaishman, M.A., Rover, V. & Stover, E. 2008. The Fig: Botany, Horticulture, and Breeding. *Hortic Rev.* **34**, 113–197.

Gee, G.W. & Bauder, J.W. 1986. Particle-size Analysis. In A.L. Page (ed.). *Methods of soil analysis*, Part 1. *Physical and mineralogical methods*. second ed. Amer. Soc. Agron. No **9** (Part 1) in the Agronomy Series. ASA, SSSA, Madison, WI., pp. 383–411.

Gupta, U.C. 1979. Some factors affecting the determination of hot-water boron from potzol soils using azomethine –H. *Can. J. Soil Sci*. **59**, 241–247.

Hakerlerler, H., Saatçi, N., Hepaksoy, S. & Aksoy, U. 1998. Fruit and leaf nutritional status of some Fig clones and cultivars and relationships with some sugar fractions. *Acta Hortic.* **480**, 247–252.

Hansen, E.J., Chaplin, M.H. & Breen, P.J. 1985. Movement of foliar boron out of leaves and accumulation in flower buds and flower parts of 'Italian' prune. *Hortscience* **20**, 747–748.

Jones, B.J. Jr., 1998. *Plant Nutrition Manual*. CRC press, Boca Raton, FL., USA, 149 pp.

Klute, A. 1986. *Methods of Soil Analysis.* Part 1. *Physical and mineralogical methods.* second edition. Amer. Soc. Agron. No **9** (Part 1) in the Agronomy Series. ASA, SSSA, Madison, WI., pp. 1–1188.

Landon, R.J. 1991. *Booker Tropical Soil Manual. A Handbook for Soil Survey and Agricultural Land Evaluation in the Tropics and Subtropics*. Booker Agriculture International Ltd. Longman Publ. New York, 450 pp.

Linsday, W.L. & Norvell, W.A. 1978. Development of a DTPA soil test for zinc, iron, manganese, and copper. *Soil Sci. Soc. Am. J.* **31**, 421–428.

McLean, E. 1982 Soil pH and Lime Requirement. In A.L. Page (ed), *Methods of Soil Analysis*. Part 2. *Chemical and Microbiological Properties*. second ed. Amer. Soc. Agron. No **9** (Part 2) in the Agronomy Series. ASA, SSSA, Madison, WI., pp. 199–223.

Mirdehghan, S.H. & Rahemi, M. 2007. Seasonal changes of mineral nutrients and phenolics in pomegranate (*Punica granatum* L.) fruit. *Sci. Hortic.* **111**, 120–127.

Murphy, J. & Riley, J.P. 1962. A modified single solution method for the determination of phosphate in natural waters. *Anal. Chim. Acta* **27**, 31–36.

Nachtigall, G.R. & Dechen, A.R. 2006. Seasonality of nutrients in leaves and fruits of apple trees. *Sci. Agric.* **63**, 493–501.

Nelson, D.W. & Sommers, L.E. 1982. Total Carbon, Organic Carbon, and Organic Matter. In A.L. Page (ed), *Methods of Soil Analysis*. Part 2. *Chemical and Microbiological Properties*. second ed. Amer. Soc. Agron. No **9** (Part 2) in the Agronomy Series. ASA, SSSA, Madison, WI., pp. 539–577.

Nelson, R.E. 1982. Carbonate and gypsum. In A.L. Page (ed), *Methods of Soil Analysis*. Part 2. *Chemical and Microbiological Properties*. second ed. Amer. Soc. Agron. No **9** (Part 2) in the Agronomy Series. ASA, SSSA, Madison, WI., 181–196.

Proebsting, E.L. & Warner, R.M. 1954. The effect of fertilizers on yield, quality and leaf composition of figs. *Proc Am Soc Hortic Sci*. **63**, 10–18.

Reuter, D.J. & Robinson, J.B. 1986. *Plant Analysis: An interpretation manual.* Inkata Press. Melbourne, pp. 1–218.

Rhoades, J.D. 1982. Cation Exchange Capacity. In A.L. Page (ed), *Methods of Soil Analysis*. Part 2. *Chemical and Microbiological Properties*. second ed. Amer. Soc. Agron. No **9** (Part 2) in the Agronomy Series. ASA, SSSA, Madison, WI., pp. 149–157.

Romero, I., Benito, A., Dominguez, N., Escudero, EG. & Martin, I. 2014. Leaf blade and petiole nutritional diagnosis for *Vitis vinifera* L. cv. 'Tempranillo' by deviation from optimum percentage method. *Span. J. Agric. Res*. **12**(1), 206–214.

Smith, G.S., Clark, C.J. & Henderson, H.V. 1987. Seasonal accumulation of mineral nutrients by kiwifruit. *New Phytol*. **106**, 81–100.

Smith, P.F. 1962. Mineral analysis in plant tissue. Annual Review. *Plant Physiol*. **13**, 81–108.

StatSoft Inc. 2007. STATISTICA, ver. 8. Tulsa, OK.

Stylianidis, D.C., Simonis, A.D. & Syrgiannidis, G.D. 2002. *Nutrition-Fertilization of deciduous fruit trees.* Stamoulis publ., 675 pp. (in Greek).

Therios, J.N. & Dimassi-Theriou, K. 2013. *Pomology Deciduous Fruit Trees*. Published by A.S. Gartagani, Thessaloniki, Greece 844 pp. (in Greek).

Thomas, G.W. 1982. Exchangeable Cations. In A.L. Page (ed), *Methods of Soil Analysis*. Part 2. *Chemical and Microbiological Properties*. second ed. Amer. Soc. Agron. No **9** (Part 2) in the Agronomy Series. ASA, SSSA, Madison, WI., pp. 159–164.

Vemmos, S.N., Petri, E. & Stournaras, V. 2013. Seasonal changes in photosynthetic activity and carbohydrate contents in leaves and fruits of three fig cultivars. *Sci. Hort.* **160**, 198–207.

Wolf, B. 1971. The determination of boron in soil extracts, plant materials, composts, manures, water, and nutrient solutions. *Commun. Soil Sci. Plant Anal.* **2**, 363–374.

Agronomy Research **18**(4), 2340–2352, 2020
https://doi.org/10.15159/AR.20.183

Motion stability estimation for modular traction vehicle-based combined unit

V. Bulgakov[1], I. Holovach[1], V. Nadykto[2], O. Parakhin[2], H. Kaletnik[3], L. Shymko[1] and J. Olt[4,*]

[1]National University of Life and Environmental Sciences of Ukraine, Ukraine, 15 Heroyiv Oborony Str., UA 03041 Kyiv, Ukraine
[2]Dmytro Motornyi Tavria State Agrotechnological University, 18B, Khmelnytsky Ave, UA 72310, Melitopol, Zaporozhye Region, Ukraine
[3]Vinnytsia National Agrarian University of Ukraine, 3 Soniachna Str., UA 21008 Vinnytsia, Ukraine
[4]Estonian University of Life Sciences, Institute of Technology, 56 Kreutzwaldi Str., EE 51006 Tartu, Estonia
[*]Correspondence: jyri.olt@emu.ee

Abstract. One of the promising ways of efficiently applying high power intensity tractors is their design and utilisation in the form of modular traction vehicles comprising two modules: the power module and the process module. In order to provide for the sufficient manoeuvrability of the modular traction vehicle, when its process module passes a turn, the latter is equipped with vertical and horizontal hinge joints. The freedom of the process module's rotation with respect to the power module in the horizontal plane through the agency of the above-mentioned vertical hinge joint is restrained by a hydraulic cylinder, in which the chambers above and below the piston are connected via a throttle valve with a hydraulic resistance coefficient of about 1.03×10^6 N m s rad^{-1}. This paper is concerned with the theoretical and experimental research into the stability of motion (on turn spaces as well as in the transport mode) of a modular combined unit, when its velocity changes and/or the slip resistance coefficient of the tyres on the wheels of the process module, in which the hydraulic cylinder is equipped with a throttle valve with the above-mentioned hydraulic resistance coefficient, changes.

Key words: modular unit, oscillation, resistance, stability of motion, tractor.

INTRODUCTION

Increasing the power rating of the tractor's engine is one of the ways to improve the productive capacity of combined tractor-implement units. However, the greater the power rating is, the more problematic its utilisation through the agency of the traction effort becomes (Macmillan, 2002). The problem stands out most acutely with tractors in the power intensity category of over 15 kW t^{-1} (Kutkov, 2004).

One of the promising ways of efficiently employing the tractors with high power intensity is their design in the form of modular traction vehicles (Bulgakov et al., 2015, 2019, 2020). With this approach, the traction vehicle comprises two modules: the power

(PM) and the process (PrM) ones (Fig. 1). A wheeled tractor equipped with a ground-speed power take-off shaft is used as the power module. The process module is an additional axle, the wheels of which are driven by the ground-speed power take-off shaft of the power module, that is, the wheeled tractor.

In order to provide for the sufficient manoeuvrability of the modular traction vehicle, when it passes a turn (on turn spaces or during travel runs), its process module is equipped with vertical and horizontal hinge joints. The vertical hinge joint facilitates the angular displacement of the process module relative to the power module in the horizontal plane through angles of ± 30°, while the horizontal hinge joint - through angles of ± 15° in the transverse and vertical plane.

Figure 1. Modular traction vehicle: PM – power module; PrM – process module.

The details of the design of the connection between the power module and the process module are presented in Fig. 2.

Thus, the ability of the process module to turn relative to power module in the horizontal plane through the agency of the above-mentioned vertical hinge joint 2 is restrained by the hydraulic cylinder 1, in which the chambers above and under the piston are connected through a hose line (Fig. 2).

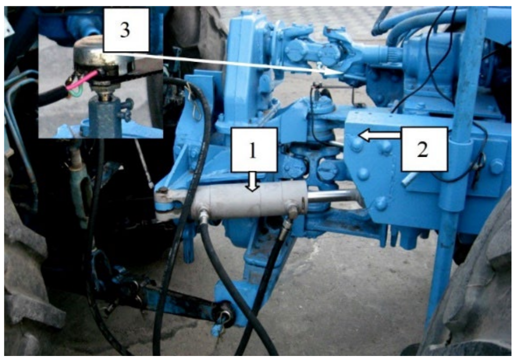

Figure 2. Connection between power and process modules in longitudinal and vertical plane: 1 – hydraulic cylinder; 2 – vertical hinge joint of process module; 3 – resistor SP-3A.

Besides that, when the modular traction vehicle travels from one field to another one, the process module together with the implement linkage-mounted on it can perform forced oscillations relative to the power module. In many cases, their amplitude is so great that it results in the reduced stability of motion of the process module in the horizontal plane. Eventually, that implies reducing the rate of travel of the whole combined unit, which is an undesirable development.

The issue of research into the stability of motion of articulated power units is extensively covered in the literature (Hac et al., 2008; Szakács, 2010; Yildiz, 2010; Demšar et al., 2012; Song et al., 2014; Pascuzzi, 2015; Li et al., 2016; Nadykto et al., 2019).

However, the earlier obtained results of research are not quite suitable for eliminating the problem under consideration. First of all, it has to be noted that the line of our research is defined by the scientific hypothesis, the essence of which is stated as follows: ‘The stability of motion in the travelling mode of a modular traction vehicle-based combined unit can be improved by means of damping the horizontal oscillations of the process module with respect to the power module, introducing for that purpose a hydraulic damper between the modules'. The said hydraulic damper can be implemented in the form of a throttle valve, which is installed on the line connecting the chambers above and under the piston of the hydraulic cylinder 1 (Fig. 2) and has a resistance coefficient of 1.03×10^6 N m s rad^{-1} (Bulgakov et al., 2019).

The aim of this completed theoretical and experimental research is to determine the stability of motion in the travelling mode of a modular combined unit in case of varying its rate of travel as well as in case of varying the slip resistance coefficients of the tyres on the wheels of the process module, the linkage hydraulic cylinder of which is equipped with a throttle valve with the earlier indicated hydraulic resistance coefficient.

THEORETICAL PREMISES

It is assumed that the modular combined unit together with the *YOX* plane performs plane-parallel motion at a constant velocity of V_o (Fig. 3). The practical experience of operating a multitude of different agricultural combined units has proved that the assumption about the invariance of their operating rate of travel is quite correct.

The above-mentioned plane is tied by its *OX* axis to the vertical hinge joint of the process module, the centreline of which passes through the point π, which is the effective centre of mass of the modular traction vehicle.

In the *YOX* plane, the modular traction vehicle-based combined unit has the following three degrees of freedom: 1) transverse displacement X_t of the point π; 2) course angle φ of the power module; 3) angular displacement β of the process module relative to the longitudinal axis of symmetry of the power module.

When the modular traction vehicle-based combined unit is in the transport mode of motion, the single force F_b (Fig. 3) generated by the rear axle of the power module is sufficient for its movement. Apart from the said force, the following inputs are acting on the modular combined unit: 1) rolling resistance forces applied to the front axle of the power module P_{fa} and to the axle of the process module P_{fc}; 2) lateral forces P_a, P_b and P_c applied at the points *A*, *B* and *C*, respectively; 3) resultant moment M_m and resultant vector R_m of the external perturbing forces. The latter one is represented here with its longitudinal R_v and transverse R_g components.

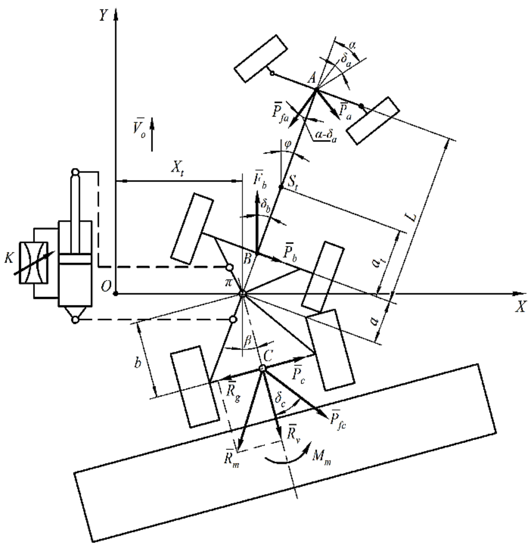

Figure 3. Equivalent schematic model of external forces and moments acting on modular combined unit in horizontal plane.

The slips of the tyres on the front and rear axles of the power module as well as the axle of the process module are represented by the angles δ_a, δ_b and δ_c , respectively.

As mentioned earlier, the mutual angular mobility of the process module and the power module in the horizontal plane is restrained by the hydraulic cylinder, in which the chambers above and under the piston are connected by a throttle valve with a resistance coefficient of K_m.

The mathematical model of the transport mode motion of the modular traction vehicle-based combined unit appears as the system of three differential equations (1). The following designations are used in the system: M_t, J_t – mass of the power module and its moment of inertia about the vertical axis that passes through the point π (Fig. 3); k_a, k_b, k_c – slip resistance coefficients of the tyres on the wheels of the front and rear axles of the power module and the axle of the process module, respectively; J_m – moment of inertia of the process module and the agricultural implement linkage-mounted on it about the axis that passes through the point π; L, a_m, b_m – design parameters of the modular traction vehicle, which are shown in Fig. 3.

$$\left.\begin{aligned} A_{11}\cdot\ddot{X}_t + A_{12}\cdot\dot{X}_t + A_{13}\cdot\dot{\varphi} + A_{14}\cdot\varphi + A_{15}\cdot\dot{\beta} + A_{16}\cdot\beta = B_{11}\cdot\alpha - R_g,\\ A_{21}\cdot\ddot{\varphi}_t + A_{22}\cdot\dot{X}_t + A_{23}\cdot\dot{\varphi} + A_{24}\cdot\varphi = B_{21},\\ A_{31}\cdot\ddot{\beta}_t + A_{32}\cdot\dot{X}_t + A_{35}\cdot\dot{\beta} + A_{15}\cdot\beta = M_0, \end{aligned}\right\} \tag{1}$$

The following components are the input variables in the system of differential Eqs (1):

1) control action in the form of the angular displacement α of the steer wheels of the power module in the modular traction vehicle;
2) perturbing action in the form of the resultant turning moment $M_o = R_g\cdot b_m - M_m$.

The following components are the output parameters in the functioning of the dynamic system under consideration: displacement X_t of the point π, which is the effective centre of mass of the modular traction vehicle; course angle φ of the power module; angular displacement β of the process module relative to the power module.

The analysis of the stability of motion of the dynamic system under study is best of all performed with the use of the amplitude and phase frequency response characteristics. Currently, these characteristics are efficiently applied for solving similar problems (Yildiz, 2010; Anche & Subramanian, 2018; Ghasemi, 2018). It has been found that just these characteristics represent best of all the stability of a dynamic system in the form of its response to the input perturbing action.

It is to pointed out that the amplitude frequency response characteristic shows the frequency distribution of the coefficient of the input action amplification by the dynamic system. The phase frequency response characteristic of a dynamic system shows the frequency distribution of the lag in its response to the input action expressed in terms of angle or time values.

In case of follow-up dynamic systems (the system under consideration falls exactly into this category), the ideal amplitude frequency response characteristic and phase frequency response characteristic exist. In particular, the amplification of the input perturbing action by the dynamic system (that is, its amplitude frequency response characteristic) has to be equal to 0 within the whole range of its frequencies (Rotach, 2008). The lag of the dynamic system's response to such an action has to be as great as possible, ideally - tending to infinity (Rotach, 2008).

With such an approach, the mathematical modelling of the stability of motion of a particular dynamic system amounts in essence to selecting such parameters of it, which provide for the best approximation of the ideal amplitude frequency response characteristic and phase frequency response characteristic by the actual ones.

The actual amplitude frequency response characteristic and phase frequency response characteristic can be obtained from the respective transfer functions. In the case under consideration the transfer function in terms of the turning moment M_o in relation to the course angle φ of the power module appears as follows:

$$W_1 = \frac{b_6 \cdot p + b_5}{a_6 \cdot p^4 + a_5 \cdot p^3 + a_4 \cdot p^2 + a_3 \cdot p + a_2}. \tag{2}$$

The similar function in terms of the same perturbing action (that is, the moment M_o), but in relation to the angular displacement β of the process module, is more complex:

$$W_2 = \frac{b_4 \cdot p^3 + b_3 \cdot p^2 + b_2 \cdot p + b_1}{a_6 \cdot p^4 + a_5 \cdot p^3 + a_4 \cdot p^2 + a_3 \cdot p + a_2}. \tag{3}$$

The following designations have been assumed in the Eqs (2) and (3):

$$b_6 = A_{15} A_{22},$$
$$b_5 = A_{16} A_{22},$$
$$b_4 = A_{11} A_{21},$$
$$b_3 = A_{12} A_{21} + A_{11} A_{23},$$
$$b_2 = A_{11} A_{24} + A_{12} A_{23} - A_{13} A_{22},$$
$$b_1 = A_{12} A_{24} - A_{22} A_{14},$$
$$a_6 = A_{11} A_{21} A_{31},$$
$$a_5 = A_{12} A_{21} A_{31} + A_{11} A_{31} A_{23} + A_{11} A_{21} A_{35},$$
$$a_4 = A_{11} A_{31} A_{24} + A_{12} A_{23} A_{31} - A_{13} A_{22} A_{31} + A_{11} A_{21} A_{36} + A_{12} A_{21} A_{35} - \\ - A_{21} A_{32} A_{15} + A_{11} A_{23} A_{35},$$
$$a_3 = A_{12} A_{31} A_{24} - A_{22} A_{31} A_{14} + A_{12} A_{21} A_{36} + A_{11} A_{23} A_{36} - A_{21} A_{32} A_{16} + \\ + A_{11} A_{24} A_{35} + A_{12} A_{23} A_{35} - A_{13} A_{22} A_{35} - A_{12} A_{31} A_{24},$$
$$a_2 = A_{11} A_{24} A_{36} + A_{12} A_{23} A_{36} + A_{12} A_{24} A_{35} - A_{13} A_{22} A_{36} - A_{22} A_{14} A_{35} - \\ - A_{23} A_{14} A_{35} - A_{23} A_{32} A_{16} - A_{32} A_{15} A_{24}.$$

The methods and algorithm of calculating the actual amplitude and phase frequency response characteristics of a particular dynamic system, when it responds to both the control and perturbing actions, are in considerable detail described in the book (Rotach, 2008) and many other literary sources. However, before the modelling can be started, it is necessary to verify the adequacy of the developed mathematical model (1). The procedure of this process is described in detail hereafter.

MATERIALS AND METHODS

The adequacy of the mathematical model (1) has been verified by comparing the two amplitude frequency response characteristics. One of them is the theoretical characteristic A_t calculated with the use of the transfer function (3). The second one A_e has been obtained by the authors as a result of their experimental investigation of the combined tractor-implement unit under consideration.

The latter characteristic has been determined in field conditions during the travelling of the modular traction vehicle with a plough mounted on it in the transport mode. The technical specifications of the combined unit under study is presented in Table 1.

Table 1. Technical specifications of modular traction vehicle with plough

Parameter	Designation	Unit	Value
Mass of power module	M_t	kg	3,820
Longitudinal wheel base of tractor	L	m	2.37
Mass of process module	M_m	kg	2,500
Mass of PLN-5-35 plough	M_p	kg	800
Moment of inertia of power module	J_t	kN m s^2	15.7
Moment of inertia of process module with plough	J_m	kN m s^2	15.9
Tyres on front wheels of power module:	9.00R20		
– width	b_a	m	0.24
– diameter	D_a	m	0.95
– air pressure	ρ_a	MPa	0.10
– vertical load on axle	Q_a	kN	12.70
Tyres on rear wheels of power module:	15.5R38		
– width	b_b	m	0.40
– diameter	D_b	m	1.57
– air pressure	ρ_b	MPa	0.12
– vertical load on axle	Q_a	kN	25.30
Tyres on wheels of process module:	16.9R38		
– width	b_c	m	0.43
– diameter	D_c	m	1.69
– air pressure	ρ_c	MPa	0.13
– vertical load on axle	Q_c	kN	32.70
Rolling resistance force by front wheels of power module	P_{fa}	kN	1.27
Tractive effort by rear axle of power module	F_b	kN	10.10
Rolling resistance force by wheels of process module	P_{fc}	kN	3.27
Design parameters shown in Fig. 3	a_m	m	1.22
	b_m	m	1.22
Resistance coefficient of throttle valve on hydraulic cylinder of process module	K_m	N m s rad^{-1}	1.03×10^6

During the experimental investigation, the modular traction vehicle complete with the five-bottom plough mounted on it travelled along the 250 m long record run at a constant speed. The agronomic background, on which the combined tractor-implement unit under consideration performed motion, was a scuffled stubble field of winter wheat. The moisture content of the soil was measured in the layer of 0–10 cm with the use of the MG-44 electronic moisture meter with the following specifications: soil moisture content measurement range - 1–40%; measurement error - ± 1%; duration of one measurement - below 3 seconds.

The time t_a spent by the combined unit under consideration to cover the 250 m long record run was recorded with the use of the electronic stop watch FS-8200 with a measurement accuracy of up to 0.1 s. Later, the rate of travel V_o of the combined unit under consideration was calculated with the use of the following formula: $V_0 = 250 \cdot (t_\alpha)$.

During the experimental investigations, the angular displacement β and the angular acceleration $\ddot{\beta}$ of the modular traction vehicle's process module with a PLN-5-35 five-bottom plough rear-mounted on it were recorded in the PC with the use of an 8-channel analogue-to-digital converter.

The angular displacement β of the process module in the horizontal plane was measured with the use of an SP-3A slide-wire gauge with a straight-line characteristic and a rated resistance of 470 Ohm. The slide-wire gauge was installed on the axle of the vertical hinge joint connecting the power and process modules in the modular traction vehicle (pos. 3, Fig. 2).

The angular acceleration of the process module was recorded with the use of an MMA 7260QT (Freescale Semiconductor) acceleration transducer. Its main specifications were as follows: output signal - analogue; acceleration measurement range - ± 1.5 g; sensibility - 300 mV g^{-1}; bandwidth - 150 Hz.

In order to use the measurements of the angular displacement β and the angular acceleration $\ddot{\beta}$ obtained as a result of the completed experimental investigations, the standard deviations and the normalized spectral densities have to be calculated with the use of the PC. The obtained statistical characteristics can be used for determining the actual amplitude frequency response characteristic in accordance with the following formula:

$$A_e = \frac{\sigma_\beta}{\sigma_m} \cdot \sqrt{\frac{S_\beta}{S_m}} \;, \tag{4}$$

where σ_β, σ_m – standard deviations of the oscillations of the angular displacement β of the process module and the turning moment M_o acting on it; S_β, S_m – normalized spectral densities of the oscillations of the angular displacement β of the process module in the modular traction vehicle and the perturbing moment acting on the process module.

The value of the latter is determined with the use of the following expression:

$$M_o = J_m \cdot \ddot{\beta}, \tag{5}$$

where J_m – moment of inertia of the process module complete with the mounted plough about the axis that is aligned with the vertical hinge joint of the process module (point π, Fig. 3). This parameter has been determined by way of calculation.

As already stated above, the experimental amplitude frequency response characteristic has been compared with the theoretical one calculated with the use of the transfer function (3). The parameters present in the said function include the slip resistance coefficients of the tyres on the wheels of the modular traction vehicle k_a, k_b and k_c. Their values depend on the vertical load Q acting on the tyre, its diameter D, width b and air pressure ρ.

In view of the fact that each of the axles of the modular traction vehicle is compliant with the following condition:

$$U = 0.42 \cdot \frac{Q}{\rho \cdot D^2} \cdot \sqrt{\frac{D}{b}} < 0.088 \,, \tag{6}$$

the values of the slip resistance coefficients of their tyres are calculated similarly (Xie, 1984) with the use of the following expression:

$$k = 145\left(1.7 \cdot U - 12.7 \cdot U^2\right) \cdot \rho \cdot b^2 \,. \qquad (7)$$

The values of the slip resistance coefficients of the tyres k_a, k_b and k_c are calculated by the formula (7) taking into account the data in Table 1. The values obtained as a result are used as one of the analysed parameters in the theoretical calculation of the specially developed mathematical model (1). The reason for choosing the above approach can be explained as follows. Knowing the pattern of the effect the aforesaid coefficients have on the stability of motion of the modules in the modular traction vehicle, it is not difficult to find out with the use of the formula (7) the required values of the air pressure in the tyres on all its wheels. Eventually, that can be efficiently implemented under the practical conditions of operation of the modular traction vehicle.

The second parameter that is variable in the process of theoretical investigations is the rate of travel of the modular traction vehicle-based combined unit in the transport mode. The parameter V_o varies from 2 to 5 m s^{-1} (7.2–18.0 km h^{-1}). The smaller speeds of moving in the transport mode are inefficient, while moving at greater rates is restricted by the operating specifications of the modular traction vehicle. These specifications stipulate that the maximum rate of travelling in the transport mode of such a modular vehicle may not exceed 5.5 m s^{-1}.

RESULTS AND DISCUSSION

During the experimental investigations, the soil moisture content of the agronomic background within the layer of 0–10 cm did not exceed 14.5%. The modular traction vehicle with the plough travelled at rates, the mean value of which was equal to 3.95 m s^{-1}. Exactly this value of the motion velocity V_o was used for calculating the theoretical amplitude frequency response characteristic (A_t) of the investigated tractor-implement combined unit in its response to the perturbing action (moment M_o) with the use of the transfer function (3). The comparison of the obtained characteristic with the experimental one (A_e) has proved their satisfactory convergence (Fig. 4).

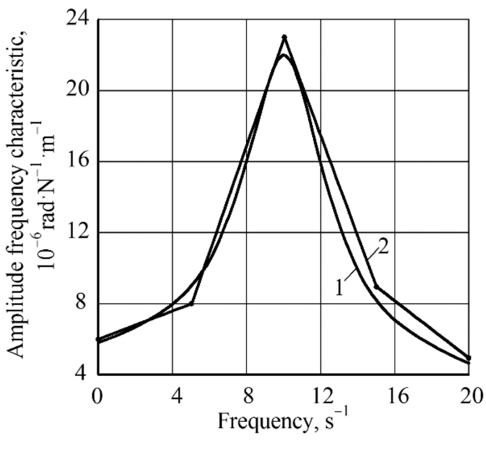

Figure 4. Amplitude frequency response characteristics of investigated combined unit: 1) theoretical A_t,; 2) experimental A_e.

Such convergence unequivocally indicates that the mathematical model (1) of the transport mode of travel of a modular traction vehicle with an agricultural implement (in this particular case - a plough) mounted on it is adequate, hence, perfectly suitable for further theoretical investigations.

The further theoretical analysis of the amplitude frequency response characteristic and the phase frequency response characteristic plotted with the use of the transfer function (3) has resulted in the following findings. As the rate of travel of the investigated combined unit rises from 2 to 5 m s^{-1}, the amplitude frequency response characteristics of the angular displacement β of the process module responding to the perturbing action (moment M_o) reach their resonance peaks at a frequency of 10 s^{-1} (Fig. 5).

At the same time, the amplitude frequency response characteristics themselves change very little, especially at travel rates of $V_o = 2$ m s^{-1} and higher. That can be explained by the inertia of the process module with the plough mounted on it that becomes more pronounced with the rise of the combined unit's speed.

As regards the phase frequency response characteristics, they vary little within the range of frequencies of 0-10 s^{-1} (Fig. 6). A substantial difference in the response lag of the process module responding to the perturbing action occurs at frequencies within the range of 10-20 s^{-1}, then, again, it disappears.

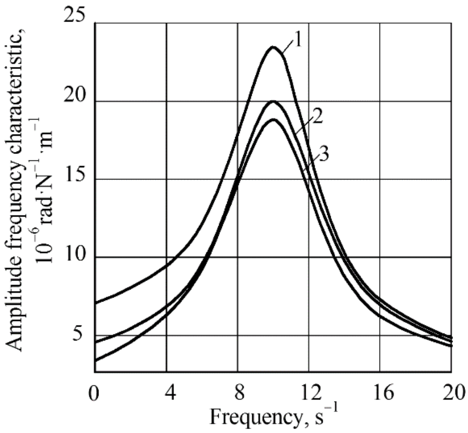

Figure 5. Amplitude frequency response characteristics of angular displacement β of process module responding to perturbing action at different travel rates of modular combined unit (V_o): 1) 2 m s^{-1}; 2) 3 m s^{-1}; 3) 5 m s^{-1}.

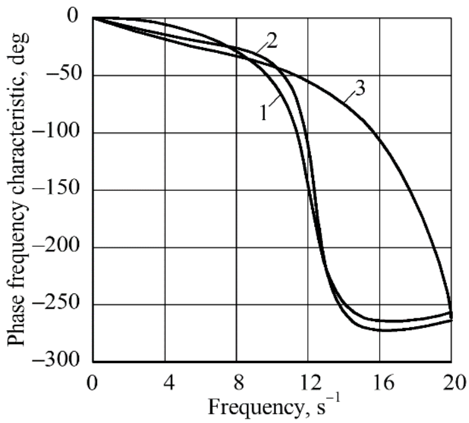

Figure 6. Phase frequency response characteristics of angular displacement β of process module responding to perturbing action at different travel rates of modular combined unit (V_o): 1) 2 m s^{-1}; 2) 3 m s^{-1}; 3) 5 m s^{-1}.

It should be reminded that the lag in the response of a dynamic system to a perturbing action has to be as great as possible. In view of that, it is desirable that, when the frequency of oscillations of the angle of the process module is within the range of 10–20 s^{-1} (1.6–3.2 Hz), the modular combined unit moves at a velocity not exceeding 3 m s^{-1} (Fig. 6). Although, that is applicable more theoretically, than in practice. Here is why.

At a frequency of about 15 s^{-1} the greatest phase difference is observed between the two modes of motion: 2 and 3 m s^{-1} (curves 1 and 2), on the one hand, and 5 m s^{-1} (curve 3), on the other hand. The said difference is specifically equal to about 200° or 3.5 rad. That means that, when V_o rises from 2 (or 3) m s^{-1} to 5 m s^{-1}, the lag in the response of the process module to the perturbing action decreases by mere $3.5\ 15^{-1} = 0.23$ s. At other frequencies within the range of 10–20 s^{-1} the difference is even smaller.

That brings to the conclusion that the rate of travelling in the transport mode of the modular combined unit under consideration within its variation range of 2 to 5 m s^{-1} has a negligible effect on the process of oscillation of the angular displacement of the process module in the modular traction vehicle, when it is under the action of the perturbing action in the form of the turning moment.

Essentially the same can be stated about the slip resistance coefficients of the tyres on the front k_a and rear k_b wheels of the power module.

As regards the slip resistance coefficient k_c of the tyres on the wheels of the process module, the result is different. When its value increases from 160 to 210 kN rad^{-1}, the maximum value of the amplitude frequency response characteristic of the dynamic system rises (curve 2, Fig. 7). The further growth of the value of the coefficient k_c results in the decrease of the said characteristic. At the same time, the resonance peaks of the amplitude frequency response characteristics (curves 3 and 4) shift to the area of higher frequencies.

Although the phase frequency response characteristics differ from each other at frequencies of over 6 s^{-1}, the difference is small (Fig. 8).

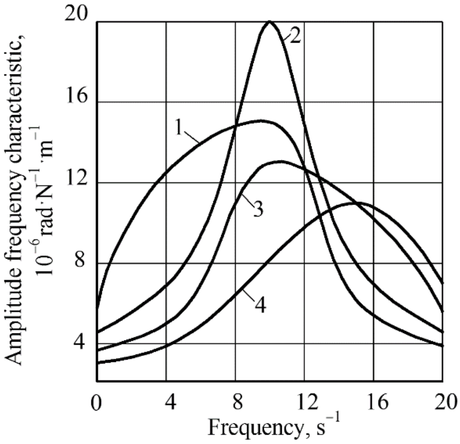

Figure 7. Amplitude frequency response characteristic of angle β of process module responding to perturbing action at different values of coefficient k_c:
1) 160 kN rad^{-1}; 2) 210 kN rad^{-1};
3) 260 kN rad^{-1}; 4) 310 kN rad^{-1}.

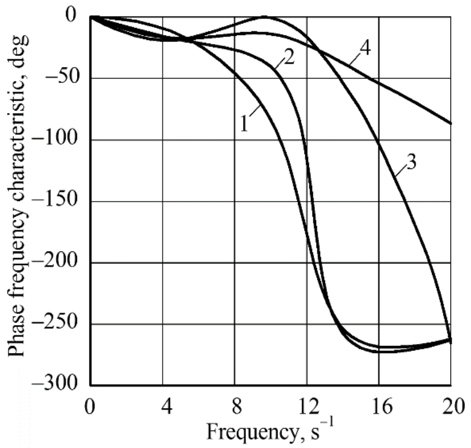

Figure 8. Phase frequency response characteristic of angle β of process module responding to perturbing action at different values of coefficient k_c:
1) 160 kN rad^{-1}; 2) 210 kN rad^{-1};
3) 260 kN rad^{-1}; 4) 310 kN rad^{-1}.

The final conclusion is that installing tyres with a slip resistance coefficient of about 260 kN rad^{-1} and higher on the wheels of the process module contributes to the reduction of the amplitude of the module's oscillation in the horizontal plane.

The following step is to analyse the impact that the turning moment M_o has on the dynamics of oscillation of the course angle φ of the power module in the modular traction vehicle. In this case, the amplitude and phase frequency response characteristics are generated with the use of the transfer function (2).

The same as in case of the process module, the variation of the rate, at which the modular combined unit under consideration travels in the transport mode, within the assumed range of 2–5 m s^{-1} has an insignificant effect on how the power module responds to the perturbing action in the form of the moment M_o (Fig. 9).

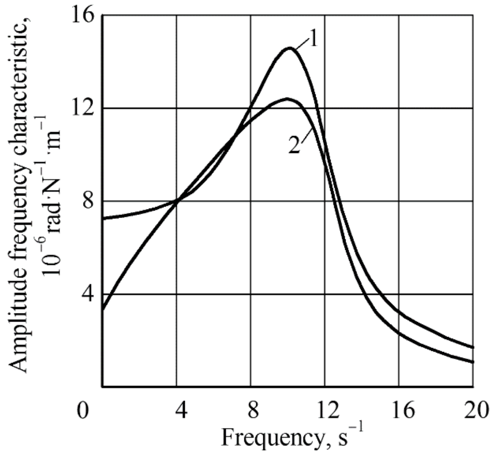

Figure 9. Amplitude frequency response characteristic of angle φ in response to perturbing action at different values of travel rate V_o: 1) 2 m s^{-1}; 2) 5 m s^{-1}.

Here, the same as in case of the process module, the resonance peaks of the amplitude frequency response characteristics are found at a frequency of 10 s^{-1}. But the amplitude of oscillations of the angle φ is smaller in comparison to the amplitude of oscillations of the angle β. For example, when the combined unit travels at a rate of 2 m s^{-1}, the maximum value of the amplitude frequency response characteristic of the oscillation of the course angle of the power module (curve 1, Fig. 9) is about 1.9 times smaller than that of the amplitude frequency response characteristic of the oscillation of the angular displacement of the process module (curve 1, Fig. 5). When the rate, at which the modular combined unit travels in the transport mode, is equal to 5 m s^{-1}, the amplitude of oscillations of the angle φ is reduced by factor of 1.5 in comparison to the oscillations of the angle β.

Essentially, such a result is quite logical, since the mass of the power module in the modular combined unit is by 520 kg greater, than the mass of the process module complete with the plough mounted on it. Moreover, the turning moment M_o acts on the process module with the plough directly, which is not the case for the power module.

The mentioned circumstances are exactly what explains the fact that changing the values of the slip resistance coefficients of the tyres on the wheels of the rear and especially front axles of the power module has little effect on the oscillation of its course angle under the action of the perturbing moment. Theoretically, the value of the discussed coefficient depends mostly on the air pressure in the tyre (Xie, 1984). That implies that in the selection of the value for this parameter (the value of ρ) the preference must be given not to the stability of the power module under the impact of the perturbing action, but to some other factors (for example, the kinematic mismatch between the drives of the axles in the power module).

The dynamics of the lag in the response of the power module to the oscillations of the moment M_o is as follows. When the perturbing action oscillates at a frequency of under 8.5 s^{-1}, the variation of the travel rate of the combined unit from 2 to 5 m s^{-1} has little effect on the dynamics of the oscillation of the course angle maintained by the power module of the modular traction vehicle (Fig. 10).

Theoretically, within the perturbing moment oscillation frequency range of 8.5–12.5 s^{-1} it is more advantageous for the modular combined unit to travel at a lower speed, because in that case the lag in the response of the power module to the perturbing action is greater. That is especially true for the perturbing moment oscillation frequencies that are close to 10 s^{-1} (curve 1, Fig. 10).

At perturbing moment oscillation frequencies of over 12 s^{-1} it is preferable for the modular combined unit to travel at a greater rate (up to 5 m s^{-1}, curve 2, Fig. 10). When that is complied with, especially at frequencies of over 16 s^{-1}, the desired lag in the response of the power module in the modular traction vehicle to the perturbing action grows by more than 0.5 rad. In terms of time, that is equal to about 0.1 s, which is exactly the expected result.

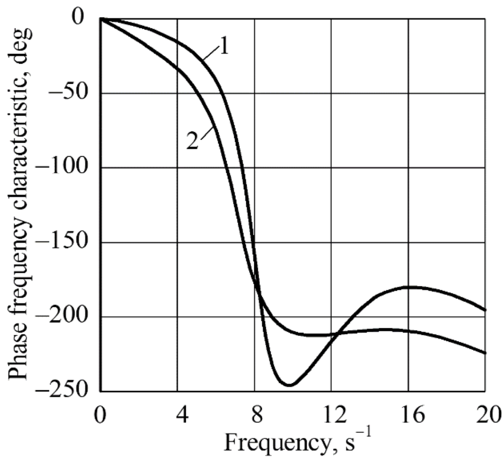

Figure 10. Phase frequency response characteristic of angle φ in response to perturbing action at different values of travel rate V_o: 1) 2 m s^{-1}; 2) 5 m s^{-1}.

CONCLUSIONS

The mathematical model of the modular traction vehicle-based combined unit moving in the transport mode that has been developed by the authors is adequate. The results of the investigations carried out with the use of this model reveal the following:

1. Changing the rate of travel of the combined unit within the range of 2 to 5 m s^{-1} does not impair the stability of motion of either the process module or, the more so, the power module in the modular traction vehicle. The characteristics of the modules' amplitude frequency response to the perturbing turning moment improve, although insignificantly, when the parameter V_o increases. The phase frequency characteristic of the process module in the modular traction vehicle responding to the mentioned moment somewhat deteriorates, but only at relatively high frequencies of its oscillation, that is, at frequencies of more than 10 s^{-1}. The response lag of the power module in the modular traction vehicle is virtually invariable with regard to the changes in the combined unit motion condition within the range of 2–5 m s^{-1}.

2. The values of the slip resistance coefficients of the tyres on the wheels of the power module do not have any noticeable effect on the response of the module to the oscillations of the perturbing moment. At the same time, the value of the slip resistance coefficient of the tyre on each of the wheels of the process module has to be equal to at least 130 kN rad^{-1}.

REFERENCES

Anche, M. & Subramanian, C., 2018. Model Based Compensator Design for Pitch Plane Stability of a Farm Tractor with Implement. *IFAC-PapersOnLine* **51**, 208–213. https://doi.org/10.1016/j.ifacol.2018.05.043

Bulgakov, V., Kyurchev, V., Nadykto, V. & Olt, J., 2015. Structure Development and Results of Testing a Novel Modular Power Unit. *Agriculture and Agricultural Science Procedia* **7**, 40–44. https://doi.org/10.1016/j.aaspro.2015.12.028

Bulgakov, V., Parakhin, O., Mitkov, V. & Chorna, T., 2019. The Coefficient Determination of a Damper Washer Hydraulic Resistance for Reducing a Technical Module Oscillation Amplitude, in: *Modern Development Paths of Agricultural Production*. Springer International Publishing, Cham, pp. 183–190. https://doi.org/10.1007/978-3-030-14918-5_20

Bulgakov, V., Kuvachov, V. & Olt, J. 2020. Theory of smoothness of movement of multiple-axle agricultural combined tractor-implement units, *Proceedings of the 31st DAAAM International Symposium*, 10 pp., B. Katalinic (Ed.), Published by DAAAM International, ISSN 1726-9679, Vienna, Austria.

Demšar, I., Bernik, R. & Duhovnik, J., 2012. A Mathematical Model and Numerical Simulation of the Static Stability of a Tractor. *Agric. Conspec. Sci*. **77**, 143–150.

Ghasemi, A., 2018. A New Current Controller Design for Tractor Active Suspension Using by Model Order Reduction. *Appl. Sci. Reports* 23–30. https://doi.org/10.15192/PSCP.ASR.2018.23.1.2330

Hac, A., Fulk, D. & Chen, H., 2008. Stability and Control Considerations of Vehicle-Trailer Combination. SAE *Int. J. Passeng. Cars - Mech. Syst.* **1**, 925–937. https://doi.org/10.4271/2008-01-1228

Kutkov, G.M. 2014. *Tractors and Automobiles: the theory and the technological properties*, Moscow, Kolos, 506 pp. (in Russian).

Li, Z., Mitsuoka, M., Inoue, E., Okayasu, T., Hirai, Y. & Zhu, Z., 2016. Parameter sensitivity for tractor lateral stability against Phase I overturn on random road surfaces. *Biosyst. Eng.* **150**, 10–23, https://doi.org/10.1016/j.biosystemseng.2016.07.004

Macmillan, R.H., 2002. *The Mechanics of Tractor - Implement Performance*. University of Melbourne, 165 pp. http://eprints.unimelb.edu.au.

Nadykto, V., Karaiev, O., Kyurchev, V. & Beloev, H. 2019. The Efficiency of Tractor Application with Articulated Frame for Cultivating Arable Crops, in: Nadykto, V. (Ed.), *Modern Development Paths of Agricultural Production*. Springer International Publishing, Cham, pp. 161–167. https://doi.org/10.1007/978-3-030-14918-5_17

Pascuzzi, S. 2015. A multibody approach applied to the study of driver injuries due to a narrow-track wheeled tractor rollover. *J. Agric. Eng.* **46**, 105–114. https://doi.org/10.4081/jae.2015.466

Rotach, V.Y. 2008. *Theory of automatic control.* Moscow Technical Universsity, Power Engineering Institute, 123 pp. (in Russian).

Song, P., Zong, C. & Tomizuka, M. 2014. *A terminal sliding mode based torque distribution control for an individual-wheel-drive vehicle*. *J. Zhejiang Univ. Sci. A* **15**, 681–693. https://doi.org/10.1631/jzus.A1400101

Szakács, T., 2010. Developing stability control theories for agricultural transport systems. *Acta Polytechnica Hungarica* **7**(2), 25–37.

Xie, L., 1984. *Simulation of tractor-trailer system stability*. SAE Tech. Pap. Iowa State University. https://doi.org/10.4271/851530

Yildiz, S. 2010. *Improving high speed lateral stability of longer and heavier vehicles by active steering*. Master´s Thesis, Eindhoven University og Technology, 78 pp., http://mate.tue.nl/mate/pdfs/12270.pdf

Agronomy Research **18**(4), 2353–2364, 2020
https://doi.org/10.15159/AR.20.231

Biological properties and fruit quality of sweet cherry (*Prunus avium* L.) cultivars from Romanian assortment

M. Corneanu, E. Iurea* and S. Sîrbu

Research Station for Fruit Growing, 175 Voineşti Str., RO707305 Iaşi, Romania
*Correspondence: iurea_elena@yahoo.com

Abstract. The paper presents a 4-year study of the valuable characteristics in 15 autochthonous and cosmopolitan sweet cherry cultivars grown in northeastern Romania, named Moldavia area. Tree's vigour, resistance to frost and anthracnosis, the fructification phenophases, epidermis colour, organoleptic and quality traits of fruits and also fruit's and stone's size were evaluated. Weak tree vigour was find at 'Tereza', 'Ştefan' and 'Golia' cultivars. From end of flowering to harvesting time were determined 39–40 days for the early cultivars ('Scorospelka', 'Cătălina'), while for the late cultivars as 'Marina' and 'George' were identified 71–83 days. Eight cultivars have presented fruits' resistance to cracking with low values between 1.3–9.3% fruits cracked. Fruit's weight have varied between 5.9 g ('Scorospelka') and 9.2 g ('Andreiaş'), while fruit's equatorial diameter have varied between 22.4 mm ('George') and 25.8 mm ('Paulică'). The cultivars with the largest fruit's size were 'Andreiaş', 'Bucium', 'Ştefan', 'Paulică', 'Golia', 'Van' and 'Stella'. The values of the soluble solids content range between 14.4°Brix ('Scorospelka') to 20.0°Brix ('Bucium'), the titratable acidity has been between 0.39 ('Andreiaş') and 0.87 ('Cătălina') mg malic acid 100^{-1} mL juice and the total content of polyphenols has recorded values between 314.93–584.95 mg GAE 100^{-1} mL of fruit juice. The studied sweet cherry cultivars showed high variability but some got remarked through earliness, low vigour of the tree, large fruit's size or fruit's resistance to cracking.

Key words: cherries, features, fruit, quality, resistance, vigour.

INTRODUCTION

Sweet cherry tree (*Prunus avium* L.) is a fruit growing species very important given by the nutraceutical features of the fruits (Höfer & Giovannini, 2017; Quero-Garcia et al., 2017; Ganopoulos et al., 2018). Also, the price of sweet cherries is higher having early ripening time when other fruits are missing on market (Grădinariu & Istrate, 2003). In the last years new cultivars suitable for constant production, with low vigour of the trees, self-fertile with resistance to biotic or abiotic factors and ripening time at the extremities of the cherries' maturation season were approved (Sansavini & Lugli, 2008; Kazantzis et al., 2011; Schuster et al., 2014). Although this species is distinguished by a rather high ecological plasticity, the novelty of the assortment and the claims regarding the intensification of the trees' crop made it necessary to put experiments that would respond to the behaviour of the cultivars under the ecological conditions (Istrate & Petre, 2003).

In Romania, the surface of cherries increased in the last five years with about 1,000 ha being now at 7,058 ha with 90,837 tonnes as total production (FAO, 2018). The new orchards were established with very different cultivars, the farmers being interested by quality of fruits, but also for good resistance at climate conditions from the area (Hedhly et al., 2007; Asănică et al., 2013). Climate changes are subject to the recent research on plants having great influence in the development of phenological stages (Ansari & Davarynejad, 2008). Salazar-Gutierrez et al., 2014 observed that the damages due to the low temperatures from early springs is highly dependent on the stages of development of the flower buds at sweet cherry cultivars.

The trees vigour of sweet cherry is an important feature for decide the growing systems of the orchards but is high influenced by genotype (Chatzicharissis et al., 2013; Di Matteo et al., 2017) and also by the rootstock used for grafting (Hrotkó et al., 2009; Bujdosó & Hrotkó, 2019; Zhang et al., 2019). Also, the resistance of the diseases of new sweet cherry cultivars have influence in recommendations for introducing in orchards (Damianov et al., 2011).

Bujdosó et al., 2020 showed that the consumers from many countries prefer sweet cherries with fruits not very sweet taste, large size with more than 25.6 mm diameter, red color, reniform shape and medium long stalk. Olmstead et al., 2007 showed that fruit size is depending by cell length which was significantly influenced by the environment.

The paper presents the sweet cherry tree's valuable features of some autochthonous and cosmopolitan cultivars that improve the assortment with cultivars that have various maturation stages of the fruits sequenced during the entire cherries' maturation season.

MATERIALS AND METHODS

The studies were performed during 2015–2018, the research material consisted of 11 sweet cherry cultivars which were approved by Research Station for Fruit Growing (RSFG) Iaşi ('Cătălina', 'Ştefan', 'Golia', 'Tereza', 'Paulică', 'Maria', 'Iaşirom', 'Bucium', 'Andreiaş', 'Marina', 'George') and four cosmopolitan cultivars ('Scorospelka', 'Van', 'Stella', 'Kordia'). There were a total of 15 cultivars. Among them, two cultivars ('Scorospelka', 'Cătălina') were early fruiting cultivars followed by nine cultivars ('Ştefan', 'Golia', 'Tereza', 'Paulică', 'Maria', 'Iaşirom', 'Bucium', 'Andreiaş', 'Van', 'Stella', 'Kordia') and two late fruiting cultivars ('Marina', 'George'). The experimental area is located in the Northeastern part of Romania, near of Iași city (6 km distance), from the climate point of view being distinguished by the average multiannual temperature of 10.5 °C and 560.8 mm multiannual rain fall, with the maximum absolute temperature during the study period reaching 37.7 °C (2017) and the minimum absolute reaching -18.5 °C (2015). The soil was on chernozem, eroded, on löess and clay tiles, with loose and sandy texture, with pH 6.3–6.9, index N 3.21, mobile phosphorus content 47–75 (ppm) and mobile potassium content 175–500 (ppm).

The studied cultivars were grafted on *Prunus mahaleb* L. seedlings as rootstock and planted in the experimental plot in RSFG Iaşi. Distances were 4×5 m, the fruit trees were trained as palmette crown shape limited in height and on the row's direction, without sustaining and irrigation system. Nine trees (3 replications × 3 trees) per cultivar for 4 years were evaluated. On the trees' row, the soil has been worked with the lateral disk with filler and between the rows, the soil has been grassed.

Procedure the data recording

To estimate the blooming and fructification phenophases, the Flekinger and BBCH systems has been used as follows: stage E (61) - when the first flowers (5%) are open; stage g (67) - when 75% of the petals of the flowers fall off (Fleckinger, 1960; Meier, 2001). Fertility index was determined by percentage of resulted fruits after 25–30 days by petals' fall; cultivars with more 30–35% are considered highly productive (Cociu & Oprea, 1989). The tree vigour and some fruits parameters as taste, epidermis colour, pulp firmness and fruit's shape were describe in accordance with UPOV questionnaire TG/35/7, 2006 (UPOV, 2006).

To estimate the resistance to anthracnosis, 300 leaves were observed, determining the frequency of the attack (F% = number of attacked leaves from the total of observed leaves), the intensity of the attack (I% = it has been represented in percentage of the number of attacked leaves (n) and the attack degree (AD) that represents the leaf attack in percentages as: AD% = F × I/100 (Roşca et al., 2011).

To estimate the resistance to frost, 100 flowers per cultivar, from each third of the crown (down, up and the medium third) were analysed for the pistil's viability (ovaries, style and stigma) (Szabó et al., 1996).

To determine the average weight of the fruit and stone (g), 30 fruits and 30 stones have been weighed in three repetitions with the electronical balance Radwag; the fruit's equatorial diameter (D) has been determined with the digital calliper Luumytools for 30 fruits in three repetitions. The pulp firmness, the pulp's adherence to the stone and the fruit's taste have been estimated through tasting with marks from 1 to 9 (UPOV test). The resistance of fruits to cracking was determined by counting the cracked fruits after six hours immersed in distilled water with temperature of 20 °C (Cristensen method described by Webster & Looney, 1996).

The soluble dry substance of the fruit has been determined using the portable digital refractometer Zeiss (Brix degrees); titratable acidity of the fruits has been determined using the potentiometric method (Ghimicescu, 1977); the total content of polyphenols has been performed by the Folin-Ciocâlteu method (Jayaprakasha et al., 2001). The experimental data was statistically interpreted by ANOVA using Microsoft Office Excel package by the multiple comparisons method (Duncan test, with *P* 5%).

RESULTS AND DISCUSSION

Among 15 sweet cherry cultivars, three cultivars registered weak tree vigour as follows 'Tereza', 'Ştefan' and 'Golia' (Table 1). Regarding resistance to frost, during 19th - 21st of April 2017, time period when the sweet cherry tree is in the phase of complete bloom, there were recorded minimum temperatures of -2.5 °C and the branches of the trees were covered with a snow layer of approx. 10 cm for a time period longer than 24 hours, amplifying the effect of frost. Thus, the effect of extremely low temperatures on the pistil of the sweet cherry flowers in the given conditions was between 49% for 'George' (calculated through the pistil's degree of damage) and 75% for 'Ştefan'. Hence, the most affected cultivars have been 'Ştefan' (75%), 'Golia' (69%) 'Scorospelka' (68%) and 'Cătălina' (66%) and the least affected ones have been 'George' (49%), 'Tereza' (54.5%) and 'Maria' (54.8%) (Table 1). The sweet cherry tree blooms quite early and it is frequently caught by frost or hoar-frost that compromise largely the fruits' production of the year, so the resistance to frost is an extremely important trait in cultivars (García et al., 2014). Under these conditions, the recently pollinated ovary was affected and at the same time, the production of fruits was largely compromised. These phenomenon were presented from others research too, so Prskavec & Kloutvor (1986) presented that the thermal limit of damages for cherry blossom was similar for different areas. Others researches showed that the cherry flowers are more affected by frost on bottom of the crown than the top (Iacobuţă, 1989; Budan & Grădinariu, 2000).

For the studied cultivars, the bloom phenological stage overlaps, allowing pollination even for the incompatible groups. García et al. (2014) has noticed that for the early and middle blooming types, it is important to produce enough flowers to have a normal production of sweet cherries. But, the phenological periods for the same sweet cherry cultivars are different and depending on the climatic conditions of each year (Darbyshire et al., 2012; Moghaddam et al., 2013). The order in which the sweet cherry cultivars grow into maturity is always kept the same, but the time interval between two sequencing cultivars can be longer or shorter. Also, Milić et al. (2015) showed that the fruit set could be different according with cultivar but Stepulaitienė et al. (2013) observed that generative organs of plants are most susceptible to spring frost and if these phenological phases are short, the damages will be lower.

Table 1. Tree's vigour, resistance to frost and anthracnosis in sweet cherry cultivars (RSFG Iasi; 2015–2018)

Cultivars	Tree's vigour[1]	Resistance to frost in the phenophase of full bloom (% affected ovaries)[2]	Resistance to anthracnosis (*Coccomyces hiemalis* Higg.)		
			F (%)	I (%)[3]	G.A. (%)
'Andreiaş'	5	58.3^{e}	3.6	4	0.14
'Bucium'	5	57.8^{e}	3.1	4	0.12
'Cătălina'	5	66.0^{d}	3.5	4	0.14
'George'	5	49.0^{f}	2.9	4	0.11
'Golia'	3	69.0^{b}	3.7	4	0.15
'Iaşirom'	5	60.0^{e}	2.9	4	0.11
'Kordia'	5	63.0^{d}	3.7	4	0.15
'Maria'	5	54.8^{f}	3.1	4	0.12
'Marina'	5	65.5^{d}	3.8	4	0.15
'Paulică'	5	64.0^{d}	3.6	4	0.14
'Scorospelka'	5	68.0^{c}	3.2	4	0.13
'Stella'	5	60.8^{e}	3.7	4	0.15
'Ştefan'	3	75.0^{a}	3.6	5	0.18
'Tereza'	3	54.5^{f}	3.2	4	0.13
'Van'	5	64.0^{d}	2.5	5	0.13

[1] – UPOV test: tree's vigour mark on a scale of 1–9: 3 = weak; 5 = average (***, 2006); [2] – different letters correspond with the significant statistical difference for $P \leq 5\%$, Duncan test; [3] – the attack intensity mark (1–6 scale): 1 = 1–3% attacked surface; 2 = 4–10%; 3 = 11–25%; 4 = 26–50%; 5 = 51–75%; 6 = 76–100% (Cociu & Oprea, 1989).

In regards with resistance to diseases, 2016 and 2018, rainy years (with a surplus of 173 mm in 2016 and 73.5 mm in 2018), favourable for pathogens evolution, the cultivars expressed a low sensitivity to *Coccomyces hiemalis* Higg. (the attack frequency was between 2.5–3.8%) (Table 1). Bloom as the main phase of fructification takes place closely related to the evolution of the climate factors and most importantly the series of active temperatures (temperatures above + 5 °C for sweet cherry). This phenological stage (bloom) took place during 03–28 April, between 7–12 days, crossed pollination being performed under good conditions (Table 2). During 2015–2018, the studied cultivars bloomed the earliest in 2016, at the beginning of April (2–7 April) and the latest in 2015, in the second half of April (15–18 April). All the studied cultivars are highly productive because the values of the natural fertility index are above 30% (Table 2).

The harvesting maturity was recorded in the second and third decades of May for the early cultivars (‘Cătălina’, ‘Scorospelka’), the first and second decades of June for the cultivars with middle fruit maturation season (‘Golia’, ‘Bucium’, ‘Ştefan’, ‘Iaşirom’, ‘Andreiaş’, ‘Stella’, ‘Van’, ‘Kordia’, ‘Paulică’, ‘Iaşirom’, ‘Maria’) and the first and second decades of July for the late cultivars (‘Marina’, ‘George’). The number of days from the end of bloom to the harvesting maturity has been between 39–40 days for the early cultivars (‘Scorospelka’, ‘Cătălina’), 47–57 days for the cultivars with middle maturation season (‘Golia’, ‘Bucium’, ‘Ştefan’, ‘Iaşirom’, ‘Andreiaş’, ‘Stella’, ‘Van’, ‘Kordia’, ‘Paulică’, ‘Iaşirom’, ‘Maria’) and 71–83 days for the late cultivars (‘Marina’, ‘George’) (Table 2).

Table 2. The fructification phenophases running in sweet cherry cultivars (RSFG Iasi; 2015–2018)

Cultivars	Beginning of bloom (stage E; date)	End of bloom (stage G; date)	Bloom duration (no. of days[1])	Natural fertility (%)	Harvesting maturity (date)	No. of days between end of bloom and harvesting maturity[1] n = 5
	Limit data (the earliest - the latest)					
‘Andreiaş’	04 IV–17 IV	14 IV–28 IV	12^{a}	49.8	06 VI–10 VI	47^{i}
‘Bucium’	06 IV–17 IV	14 IV–24 IV	9^{c}	35.3	07 VI–12 VI	51^{f}
‘Cătălina’	02 IV–15 IV	10 IV–22 IV	9^{c}	30.1	17 V–31 V	39^{j}
‘George’	04 IV–18 IV	14 IV–26 IV	10^{b}	32.1	06 VII–15 VII	83^{a}
‘Golia’	05 IV–17 IV	14 IV–24 IV	9^{c}	66.1	06 VI–12 VI	51^{f}
‘Iaşirom’	04 IV–17 IV	12 IV–23 IV	8^{c}	35.9	05 VI–10 VI	50^{g}
‘Kordia’	04 IV–16 IV	14 IV–19 IV	8^{c}	31.0	08 VI–18 VI	57^{c}
‘Maria’	04 IV–17 IV	11 IV–24 IV	8^{c}	42.5	06 VI–12 VI	52^{e}
‘Marina’	04 IV–17 IV	11 IV–26 IV	9^{c}	36.8	19 VI–06 VII	71^{b}
‘Paulică’	03 IV–16 IV	11 IV–25 IV	10^{b}	48.6	07 VI–16 VI	49^{h}
‘Scorospelka’	05 IV–15 IV	11 IV–21 IV	7^{c}	30.2	18 V–01 VI	40^{j}
‘Stella’	04 IV–18 IV	14 IV–25 IV	10^{b}	34.4	05 VI–16 VI	53^{d}
‘Ştefan’	07 IV–17 IV	14 IV–26 IV	9^{c}	38.4	06 VI–10 VI	48^{i}
‘Tereza’	05 IV–17 IV	14 IV–24 IV	9^{c}	38.5	07 VI–10 VI	50^{g}
‘Van’	04 IV–16 IV	14 IV–18 IV	7^{c}	41.8	08 VI–16 VI	56^{c}

[1] – different letters correspond with the significant statistical difference for $P \leq 5\%$, Duncan test.

The sequencing of fruits maturation for the studied sweet cherry cultivars ensure a varietal range for a period of 46–51 days, ensuring continuous market supply. To highlight the cultivars, there have been measurements concerning physical traits (epidermis colour, pulp firmness, fruit’s shape, pulp adherence to stone), organoleptic traits (taste) and quality traits (fruits’ resistance to cracking), average weight of fruit and stone, percentage of the stone from the fruit’s weight, fruit’s dimensions (equatorial diameter), chemical composition of fruits (content in soluble dry substance, titratable acidity, ration between soluble dry substance and titratable acidity, total content of polyphenols). In terms of physical and organoleptic traits of the fruits, the epidermis colour was from bi-coloured ('Paulică', 'Marina'), bright red ('Scorospelka'), shiny red ('Maria', 'Stella', 'George') to dark red ('Bucium', 'Van', 'Kordia', 'Ştefan', 'Golia', 'Tereza', 'Andreiaş', 'Cătălina', 'Iaşirom'). For the 'Scorospelka', 'Cătălina' and 'Stella' cultivars, the pulp firmness was medium, while, for the rest of the cultivars, it was firm. All the cultivars have a sweet taste and are deficient in pulp adherence to stone.

Regarding the resistance of fruits to cracking, eight cultivars have presented superior qualities with low values of cracked fruits between 1.3–9.3% (Table 3). The fruits' cracking is a phenomenon particular to cherry and can making to lose up to 90% from the fruits production (Milatović, 2011). Our results showed a good resistance to fruit cracking at 'Iașirom' and 'Paulică' with just 1.3% and respectively 3.3% fruits cracked compared with 'Stella' or 'Van' with 74% and respectively 46.8%. Balbontin et al., 2013 showed that sweet cherry cultivars have considerable differences in cracking susceptibility but no one cultivar totally tolerant to the problem.

Table 3. Epidermis colour, organoleptic and quality traits of fruits in sweet cherry cultivars (RSFG Iasi; 2015–2018)

Cultivars	Epidermis colour[1]	Pulp firmness[2]	Fruit's shape[3]	Pulp adherence to stone	Taste[4]	Fruit's resistance to cracking (%)[5]
'Andreiaş'	7	7	1	non-adherent	7	5.5^{g}
'Bucium'	7	7	1	non-adherent	7	17.8^{d}
'Cătălina'	7	5	1	non-adherent	7	6.0^{g}
'George'	5	7	1	non-adherent	7	5.8^{g}
'Golia'	7	7	1	non-adherent	7	7.5^{g}
'Iaşirom'	7	7	1	non-adherent	7	1.3^{g}
'Kordia'	7	7	1	non-adherent	7	22.1^{c}
'Maria'	5	7	1	non-adherent	7	9.3^{g}
'Marina'	2	7	1	non-adherent	7	13.3^{f}
'Paulică'	2	7	2	non-adherent	7	3.3^{g}
'Scorospelka'	4	5	3	adherent	5	17.5^{d}
'Stella'	5	5	1	non-adherent	7	74.0^{a}
'Ştefan'	7	7	1	non-adherent	7	15.8^{e}
'Tereza'	7	7	1	non-adherent	7	6.3^{g}
'Van'	7	7	4	non-adherent	7	46.8^{b}

[1] – UPOV test: mark for epidermis colour on the scale 1–8: 1 = yellow; 2 = yellow with red (bi-coloured); [4] = bright red; 5 = shiny red; 7 = dark red (***, 2006); [2] – UPOV test: mark for pulp firmness on the scale 3–9: 3 = soft; 5 = average; 7 = firm (***, 2006); [3] – UPOV test: mark for the fruit's shape on the scale 1–5: 1 = heart-shaped; 2 = kidney-shaped; 3 = oblong; [4] = circular (***, 2006); [4] – UPOV test: mark for fruit's taste on the scale 3–7: 5 = average sweet; 7 = very sweet (***, 2006); [5] – different letters correspond with the significant statistical difference for $P \leq 5\%$, Duncan test.

The average weight of the fruit and the equatorial diameter range between 5.9 g ('Scorospelka') and 9.2 g ('Andreiaş') and 22.4 mm ('George') and 25.8 mm ('Paulică'). Therefore, the cultivars with the highest fruit's dimensions have been 'Andreiaş', 'Bucium', 'Ştefan', 'Paulică', 'Golia', 'Van' and 'Stella' (Table 4). The weight and the equatorial diameter of the fruit are traits influenced by the climatic conditions, the applied technology, rootstock or the biological particularities of each cultivar (Ballistreri et al., 2013; Zeman et al., 2013; Maglakelidze et al., 2015). Our results are consistent with other research regarding the pomological characteristics of some sweet cherry cultivars (Radicevic et al., 2008; Faniadis et al., 2010; Kask et al., 2010; Fotirić Akšić & Nikolić, 2013; Pal et al., 2017). Bieniek et al. (2011) showed that the average over three years of the sweet cherry fruits' weight has ranged between 3.78 g and 6.45 g under the soil and climate conditions from Lithuania.

The small proportion (%) that the stone has for the studied cultivars is noteworthy (3.60–5.64%) (Table 4).

Table 4. Physical features of the fruit in sweet cherry cultivars (RSFG Iasi; average 2015–2018)

Cultivar	Fruit's average weight (g)[1]	Fruit's equatorial diameter (mm)[1]	Stone's average weight (g)[1]	Stone from the weight of the fruit (%)[1]
'Andreiaş'	9.2^{a}	24.6^{b}	0.33^{b}	3.61^{d}
'Bucium'	8.7^{b}	24.9^{b}	0.31^{f}	3.60^{d}
'Cătălina'	7.3^{f}	23.6^{c}	0.32^{e}	4.36^{d}
'George'	6.1^{f}	22.4^{c}	0.34^{a}	5.64^{a}
'Golia'	7.8^{d}	24.2^{b}	0.30^{g}	3.86^{d}
'Iaşirom'	6.4^{f}	23.3^{c}	0.27^{i}	4.27^{d}
'Kordia'	6.7^{f}	23.4^{c}	0.32^{c}	4.89^{b}
'Maria'	7.0^{f}	23.8^{c}	0.25^{j}	3.63^{d}
'Marina'	7.2^{f}	23.8^{c}	0.32^{e}	4.56^{c}
'Paulică'	7.8^{d}	25.8^{a}	0.32^{d}	4.15^{d}
'Scorospelka'	5.9^{f}	22.4^{c}	0.24^{k}	3.96^{d}
'Stella'	7.5^{e}	24.6^{b}	0.30^{g}	3.82^{d}
'Ştefan'	8.2^{c}	24.6^{b}	0.34^{a}	4.12^{d}
'Tereza'	7.0^{f}	24.2^{b}	0.27^{i}	3.86^{d}
'Van'	7.8^{d}	24.7^{b}	0.28^{h}	3.73^{d}

[1] – different letters correspond with the significant statistical difference for $P \leq 5\%$, Duncan test.

The chemical composition of the fruits represents a major source of antioxidant compounds (Coşofreţ et al., 2006; Beceanu, 2008; Usenik et al., 2008). The recorded data for the chemical composition of the fruits highlights the values for all the parameters studied for each cultivar (Table 5). The content in dry substance is extremely important in sweet cherries as the taste of the fruits depends highly on it. The soluble dry substance was between 14.4 °Brix ('Scorospelka') and 20.0 °Brix ('Bucium'). The values recorded in the soluble dry substance content of the fruits are according with other similar studies (Vursavus et al., 2006; Jänes et al., 2010; Papapetros et al., 2018). The titratable acidity range in large limits, the values being between 0.39% ('Andreiaş') and 0.87% ('Cătălina') (Table 5). The ratio between the soluble dry substance and the titratable acidity is considered important to determine the fruit taste, reflecting the balance between the sweet and the sour taste of fruits (Crisosto et al., 2002).

In this regard, the sweet cherry cultivars have recorded values between 18.00 at 'Scorospelka', an early cultivar and 43.59 at 'Andreiaş', an average ripening time cultivar being very appreciated. The total content of polyphenols is an important trait for determining the taste and the flavour of cherries and it has an antioxidant role with anticancer effect (Chaovanalikit & Wrolstad, 2004; Melicháčová et al., 2010; Skrzyński et al., 2016; Hallmann & Rozpara, 2017; Nizioł-Łukaszewska, 2019).

Table 5. Bio-chemical traits of the fruits in sweet cherry cultivars (RSFG Iasi; average 2015–2018)

Genotype	SDS (°Brix)[2]	Titratable acidity (mg malic acid 100^{-1} mL fruit juice)[3]	SDS: TA[4]	Total content of polyphenols (mg GAE 100^{-1} mL fruit juice)
'Andreiaş'	17.0^{c}	0.39^{n}	43.59^{a}	362.55^{g}
'Bucium'	20.0^{a}[1]	0.57^{k}	35.09^{c}	424.43^{b}
'Cătălina'	18.3^{b}	0.87^{a}	21.03^{h}	378.21^{f}
'George'	17.7^{b}	0.42^{m}	42.14^{b}	324.12^{i}
'Golia'	18.7^{b}	0.61^{i}	30.66^{e}	410.79^{c}
'Iaşirom'	19.4^{b}	0.47^{l}	41.27^{b}	584.95^{a}
'Kordia'	18.3^{b}	0.69f	26.52^{f}	400.12^{d}
'Maria'	19.9^{a}	0.65^{h}	30.61^{e}	404.36^{d}
'Marina'	16.3^{c}	0.75^{d}	21.73^{h}	369.85^{g}
'Paulică'	17.2^{c}	0.72^{e}	23.80^{g}	314.93^{j}
'Scorospelka'	14.4^{c}	0.80^{c}	18.00^{i}	343.27^{h}
'Stella'	18.7^{b}	0.81^{b}	23.09^{g}	335.18^{h}
'Ştefan'	19.1^{b}	0.72^{e}	26.53^{f}	381.46^{e}
'Tereza'	19.2^{b}	0.58^{j}	33.10^{d}	372.46^{f}
'Van'	17.5^{b}	0.66^{g}	26.52^{f}	398.22^{d}

[1] – different letters correspond with the significant statistical difference for $P \leq 5\%$, Duncan test; [2] – SDS = the soluble dry substance; [3] – TA = the titratable acidity; [4] – SDS/AT = the ratio between the soluble dry substance and titratable acidity.

All the cultivars got noted with a high content of polyphenols, the values being between 314.93 mg GAE 100^{-1} mL fruit juice ('Paulică') and 584.95 mg GAE 100^{-1} mL fruit juice ('Iaşirom'), recording statistical differences (Table 5). All the studied cultivars have a sweet taste and a pleasant flavour.

CONCLUSIONS

The studied sweet cherry cultivars ('Scorospelka', 'Cătălina', 'Ştefan', 'Golia', 'Tereza', 'Paulică', 'Maria', 'Iaşirom', 'Bucium', 'Andreiaş', 'Van', 'Stella', 'Kordia', 'Marina' and 'George') showed high variability of all the determined and analysed parameters.

The cultivars were remarked through earliness ('Scorospelka' and 'Cătălina') or lateness ('Marina' and 'George') with fruits production at the extremities of the harvesting time and then with good prices on market.

Cultivars with low vigour of the trees ('Ştefan', 'Golia' and 'Tereza') are suitable for the establishing the new orchards with high density of the trees.

Cultivars with high quality of fruits and fruits' resistance to cracking ('Iaşirom', 'Paulică', 'Andreiaş', 'George', 'Cătălina', 'Tereza', 'Golia', 'Maria', 'Marina' and 'Ştefan') can be recommended to be cropped in the Northeast areas of Romania and also for others areas with similar climate conditions.

ACKNOWLEDGEMENTS. This work was partially supported by the Romanian Ministry of Research and Innovation, Grant No. PN-III-P1-1.2.-PCCDI-2017-0662, with title 'Increasing the Institutional Capacity of Research-Development-Innovation in the Field of Ecological Fruit Growing'.

REFERENCES

Ansari, M. & Davarynejad, G. 2008. The Flower Phenology of Sour Cherry Cultivars. *American-Eurasian J. Agric. & Environ. Sci.* **4**(1), 117–124.

Asănică, A., Tudor, V. & Teodorescu, R. 2013. Distinctive behaviour of some sweet cherry cultivars related to rootstock type. *AgroLife Scientific Journal* **2**(1), 79–82.

Ballistreri, G., Continella, A., Gentile, A., Amenta, M., Fabroni, S. & Rapisarda, P. 2013. Fruit quality and bioactive compounds relevant to human health of sweet cherry (*Prunus avium* L.) cultivars grown in Italy. *Food Chem.* **140**, 630–638. doi: 10.1016/j.foodchem.2012.11.024.

Beceanu, D. 2008. Antioxidizing Properties of Fruits and Vegetables. *Lucr. Şt. USAMV Iasi*, seria Horticultură, **51**, 925–930.

Bieniek, A., Kawecki, Z., Kopytowski, J. & Zielenkiewicz, J. 2011. Yielding and fruit quality of Lithuanian sweet cherry cultivars grown under the climatic and soil conditions of Warmia. *Folia Horticulturae* **23**(2), 101–106.

Budan, S. & Grădinariu, G. 2000. *The cherry tree.* Edit. Ion Ionescu de la Brad, Iaşi, 262 pp. (in Romanian).

Bujdosó, G. & Hrotkó, K. 2019. Evaluation of Hungarian bred sweet cherry cultivars on Hungarian bred Mahaleb rootstocks. *Acta Hortic*. **1235**, 233–238. doi: 10.17660/ActaHortic.2019.1235.31

Bujdosó, G., Hrotkó, K., Feldmane, D., Giovannini, D., Demirsoy, H., Tao, R., Ercisli, S., Ertek, N. & Malchev, S., 2020. What kind of sweet cherries do the final consumers prefer?. *South-west J Hortic Biol Environ* **11**(1), 37–48.

Chaovanalikit, A. & Wrolstad, R.E. 2004. Total anthocyanins and total phenolics of fresh and processed cherries and their antioxidant properties. *J. Food Sci*. **69(**1), 67–72.

Chatzicharissis, I., Kazantzis, K., Sotiropoulos, T. & Koutinas, N. 2013. Evaluation of the Local Greek Sweet Cherry Cultivar 'Vasiliadi' Compared to the Cultivar 'Ferrovia'. *Acta Hort.* **981**, 119–122.

Cociu, V. & Oprea, Şt. 1989. *Research methods of breeding of the fruit tree species.* Edit. Dacia, Cluj-Napoca, 173 pp. (in Romanian).

Coşofreţ, S., Beceanu, D. & Radu, R.M. 2006. Studies for Determining and Identifying the Content of Antocyanic Pigments in Some Species of Wild Fruits Originated in Neamţ County. *Rev. Cercetări Agronomice în Moldova* **1**(125), 51–58.

Crisosto, C.H., Crisosto, G.M. & Ritenour, M.A. 2002. Testing the reliability of skin color as an indicator of quality forearly season 'Brooks' *(Prunus avium L)* cherry. *Postharvest Biol. Technol*. **24**, 147–154.

Damianov, S., Simeria, Gh., Grozea, I., Ştef, R., Vîrteiu, A.M., Fora, C. 2011. Researches regarding the introduction of anthracnose resistant varieties in cherry tree (*Coccomyces Hiemalis* sin *Blumeria Jaapi*) in the orchard centre Lugoj Herindeşti. *Research Journal of Agricultural Science* **43**(2), 28–33.

Darbyshire, R., Webb, L., Goodwin, I. & Barlow, E.W.R. 2012. Evaluation of recent trends in Australian pome fruit spring phenology. *International Journal of Biometeorology* **57**(3), 409–421.

Di Matteo, A., Russo, R., Graziani, G., Ritieni, A. & Di Vaio, C. 2017. Characterization of autochthonous sweet cherry cultivars (*Prunus avium* L.) of southern Italy for fruit quality, bioactive compounds and antioxidant activity. *J. Sci. Food Agric.* **97**, 2782–2794. doi 10.1002/jsfa.8106.

Faniadis, D., Drogoudi, P.D. & Vasilakakis, M. 2010. Effects of cultivar, orchard elevation, and storage on fruit quality characters of sweet cherry (*Prunus avium* L.). *Scientia Horticulturae* **125**, 301–304. doi:10.1016/j.scientia.2010.04.013

FAO (Food and Agriculture Organization of the United Nation). 2018. *http://www.fao.org/faostat/en/#data/QC.* Accesed 17.07.2020.

Fleckinger, J. 1960. Phenologie et arboriculture fruitiere. In: *Rev. Bon Jardinier*, tome **1**, pp. 362–372.

Fotirić Akšić, M. & Nikolić, T. 2013. Analysis of pomological traits in new promising sweet cherry genotypes. *Genetika* **45**(3), 873–880.

Ganopoulos, I., Farsakoglou, A.-M., Aravanopoulos, F., Molassiotis, A., Michailidis, M., Malliarou, E., Avramidou, E., Tsaftaris, A., Osanthanunkul, M., Madesis, P., Kazantzis, K. & Xanthopoulou, A. 2018. Towards sweet cherry (*Prunus avium* L.) breeding: phenotyping evaluation of newly developed hybrids. *Euphytica* **214**, 99. doi:10.1007/s10681-018-2179-2

García, F., Frutos, D., Lopez, G., Carrillo, A. & Cos, J. 2014. Flowering of sweet cherry (*Prunus avium* L.) cultivars in Cieza, Murcia, Spain. *Acta Horticulturae* **1020**, 191–196.

Ghimicescu, G. 1977. *Chemistry and analysis of food, beverages and spices.* Editura Junimea, Iaşi, 315 pp. (in Romanian).

Grădinariu, G. & Istrate, M. 2003. *Special crop of fruit-growing trees*. Editura Matrix Rom, Bucureşti, 528 pp. (in Romanian).

Hallmann, E. & Rozpara, E. 2017. The Estimation of Bioactive Compounds Content in Organic and Conventional Sweet Cherry (*Prunus Avium* L.). *Journal of Research and Applications in Agricultural Engineering* **62**(3), 141–145.

Hedhly, A., Hormaza & J.I., Herrero, M. 2007. Warm temperatures at bloom reduce fruit set in sweet cherry. *Journal of Applied Botany and Food Quality* **81**, 158–164.

Höfer, M. & Giovannini, D. 2017. Phenotypic Characterization and Evaluation of European Cherry Collections: A Survey to Determine the Most Commonly used Descriptors. *Scientific Pages Hortic*. **1**(1), 7–12.

Hrotkó, K., Magyar, L. & Gyeviki, M. 2009. Effect of Rootstocks on Growth and Yield of 'Carmen' Sweet Cherry. *Bulletin UASVM Horticulture* **66**(1), 143–148.

Iacobuţă, Gh. 1989. The effect of spring frost on sweet cherry in the area of Fălticeni. *Cercetări Agronomice în Moldova* **I**, 67–72. (in Romanian).

Istrate, M. & Petre, L. 2003. The improvement of assortments and the promoting of valuable cultivars in orchards from the NE area of Moldova. *Lucr. şt.USAMV*, seria Horticultură, **46,** 203–207 (in Romanian).

Jänes, H., Ardel, P., Kahu, K., Kelt, K. & Kikas, A. 2010. Some biological properties and fruit quality parameters of new sweet cherry cultivars and perspective selections. *Agronomy Research* **8**(Sp Iss III), 583–588.

Jayaprakasha, G.K., Singh, R.P. & Sakariah, K.K. 2001. Antioxidant activity of grape seed (*Vitis vinifera*) extracted on peroxidation models in vitro. *Food Chemistry* **73**, 285–290.

Kask, K., Jänes, H., Libek, A., Arus, L., Kikas, A., Kaldmäe, H., Univer, N. & Univer, T. 2010. New cultivars and future perspectives in professional fruit breeding in Estonia. *Agronomy Research* **8(**Special Issue III), 603–614.

Kazantzis, K., Chatzicharissis, I., Papachatzis, A., Sotiropoulos, T., Kalorizou, H. & Koutinas, N. 2011. Evaluation of Sweet Cherry Cultivars Introduced in Greece, *Univ. Craiova*, **XVI**(LII), 293–296.

Maglakelidze, E., Bobokasvili, Z., Kakashvili, V. & Tsigriasvili, L. 2015. Biological and Agricultural Properties of Sweet Cherry (*Prunus avium* L.) Cultivars in Georgia. *International Journal of Science and Research* **6**(9), 796–803. doi: 10.21275/art20176036

Meier, U. 2001. *Growth stages of mono- and dicotyledonous plants*. BBCH Monograph. Federal Biological Research Centre for Agriculture and Forestry, 158 pp.

Melicháčová, S., Timoracká, M., Bystrická, J., Vollmannová, A. & Čéry, J. 2010. Relation of total antiradical activity and total polyphenol content of sweet cherries (*Prunus avium* L.) and tart cherries (*Prunus cerasus* L.). *Acta Agriculturae Slovenica* **95**(1), 21–28.

Milatović, D. 2011. Oplemenjivanje i sorte višnje pomilor [Breeding and cultivars in cherry]. In: *Trešnja i višnja.* Ed. Naučno voćarsko društvo Srbije. Čačak. Srbije. 119–213 pp.

Milić, B., Keserović, Z., Dorić, M., Ognjanov, V. & Magazin, N. 2015. Fruit set and quality of self-fertile sweet cherries as affected by chemical flower thinning, *Hort. Sci.* **42**(3), 119–124. doi: 10.17221/288/2014-HORTSCI

Moghaddam, E.G., Ahmadi, Moghaddam, H. & Piri, S. 2013. Genetic variation of selected Siah Mashhad sweet cherry genotypes grown under Mashhad environmental conditions in Iran. *Crop Breeding Journal* **3**(1), 45–51. doi: http://dx.doi.org/10.22092/cbj.2013.100449

Nizioł-Łukaszewska, Z. 2019. Extracts of Cherry and Sweet Cherry Fruit as Active Ingredients of Body Wash Formulations. *Not Bot Horti Agrobo* **47**(1),100–107. doi:10.15835/nbha47111212

Olmstead, J.W., Iezzoni, A.F. & Whiting, M.D. 2007. Genotypic Differences in Sweet Cherry Fruit Size are Primarily a Function of Cell Number. *J. Amer. Soc. Hort. Sci*. **132**(5), 697–703.

Pal, M.D., Mitre, I., Asănică, A.C., Sestraş, A.F., Peticilă, A.G. & Mitre, V. 2017. The Influence of Rootstock on the Growth and Fructification of Cherry Cultivars in a High Density Cultivation System. *Not Bot Horti Agrobo*. **45**(2), 451–457. doi:10.15835/nbha45210826

Papapetros, S., Louppis, A., Kosma, I., Kontakos, S. & Kontominas, M.G. 2018. Characterization and differentiation of botanical and geographical origin of selected popular sweet cherry cultivars grown in Greece. *Journal of Food Composition and Analysis* **72**, 48–56. doi:10.1016/j.jfca.2018.06.006

Prskavec, K. & Kloutvor, J. 1986. 30 years survey of spring frost occurrence during cherry blossom period. In: *New Trends in Cherry Growing*, Sempra, Praga. 326 pp.

Radicevic, D., Cerovic, R., Mitrovic, M. & Glišic, I. 2008. Pomological characteristics and biochemical composition of some Canadian sweet cherry cultivars. *Acta Hort.* **795**, 283–286. doi:10.17660/Acta Hort. 2008.795.39

Roşca, I., Oltea, I. & Mitrea, I. 2011. *General and Special Entomology Treatise.* Editura ALPHA MDN, Buzău, 1055 pp. (in Romanian).

Quero-Garcia, J., Iezzoni, A., Pulawska, J. & Lang, G. 2017. *Cherries: Botany, Production and Uses*. CABI, 551 pp.

Salazar-Gutierrez, M.R., Chaves, B., Anothai, J., Whiting, M. & Hoogenboom, G. 2014. Variation in cold hardiness of sweet cherry flower buds through different phenological stages. *Scientia Horticulturae* **172**, 161–167. doi:10.1016/j.scienta.2014.04.002

Sansavini, S. & Lugli, S. 2008. Sweet Cherry Breeding Programs in Europe and Asia. In: Proc. 5thIS on Cherry; Eds. A. Eris et al. *Acta Hort.* **795**, 41–57.

Schuster, M., Grafe, C., Wolfram, B. & Schmidt, H. 2014. Cultivars Resulting From Cherry Breeding in Germany, *Erwerbsobstbau* **56**(2), 67–72.

Skrzyński, J., Leja, M., Gonkiewicz, A. & Banach, P. 2016. Cultivar effect on the sweet cherry antioxidant and some chemical attributes. *Folia Hort.* **28**(1), 95–102. doi: 10.1515/fhort-2016–0011

Stepulaitienė, I., Žebrauskienė, A. & Stanys, V. 2013. Frost resistance is associated with development of sour cherry (*Prunus cerasus* L.) generative buds. *Zemdirbyste-Agriculture* **100(**2), 175–178, doi 10.13080/z-a.2013.100.022

Szabó, Z., Nyéki, J. & Soltész, M. 1996. Frost Injury to Flower Buds and Flowers of Cherry Varieties. *Acta Hortic*. **410**, 315–322. doi: 10.17660/ActaHortic.1996.410.49

UPOV. 2006. Guidelines for the Conduct of Tests for Distinctness, Uniformity and Stability. Sweet Cherry (*Prunus avium* L.) Geneva, Switzerland: *International Union for the Protection of New Varieties of Plants*. 31 pp.

Usenik, V., Fabčič, J. & Štampar, F. 2008. Sugars, Organic Acids, Phenolic Composition and Antioxidant Activity of Sweet Cherry (*Prunus avium* L.). *Food Chemistry* **107**(1), 185–192.

Vursavus, K., Kelebek, H. & Selli, S. 2006. A study on some chemical and physico-mechanic properties of three sweet cherry varieties (*Prunus avium* L.) in Turkey. *J. Food Eng.* **74**(4), 568–575. doi:10.1016/j.jfoodeng.2005.03.059

Webster, A.D. & Looney, N.E. 1996. *Cherries: Crop Physiology. Production and Uses*. Wallingford, UK: KAB International, 513 pp.

Zeman, S., Jemrić, T., Čmelik, Z., Fruk, G., Bujan, M. & Tompić, T. 2013. The effect of climatic conditions on sweet cherry fruit treated with plant growth regulators. *Journal of Food, Agriculture & Environment* **11**(2), 524–28.

Zhang, K., Yan, G., Zhang, X., Wang, J. & Duan, X. 2019. Sweet cherry growing in China. *Acta Hortic.* **1235**, 133–140. doi 10.17660/ActaHortic.2019.1235.17

Agronomy Research **18**(4), 2365–2373, 2020
https://doi.org/10.15159/AR.20.170

Special features of *Pseudomonas aeruginosa* strains in animal and poultry farms in the regions with various levels of man-made pollution

I.M. Donnik[1], A.S. Krivonogova[2], A.G. Isaeva[1,2,*], I.A. Shkuratova[2], K.V. Moiseeva[1,2] and N.B. Musikhina[1]

[1]'Ural State Agrarian University' (FSBEI HE Ural SAU), Federal State Budgetary Educational Institution of Higher Education, 42, K. Liebknechta Str., RU620000 Ekaterinburg, Russia
[2]'Ural Federal Agrarian Scientific Research Centre, Ural Branch of the Russian Academy of Sciences' (FSBSI UrFASRC, UrB of RAS), Federal State Budgetary Scientific Institution, 112 A, Belinskogo Str., RU620000 Ekaterinburg, Russia
[*]Correspondence: isaeva.05@bk.ru

Abstract. The research on the *P. aeruginosa* strains in animal and poultry farms located in the areas with various levels of technogenic pollution were done. The content of *P. aeruginosa* in composition of opportunistic pathogenic microflora in dairy, pig-breeding and poultry farms was stated. Susceptibility of *P. aeruginosa* to fluoroquinolone antibiotics and carbapenems was defined. The enterprises were located in the areas with various levels of contamination of agrobiocenosis with Zn, Fe, Cd, Cu, As, Pb, ^{90}Sr, ^{137}Cs of technogenic origin. It was stated that content of *P. aeruginosa* in opportunistic pathogenic microbiota was the most in poultry farms. In man-made polluted areas *P. aeruginosa* was most often found in samples from oral cavity and cloaca of laying hens and broiler chickens, and in 'clean' areas' - mostly in wash-offs from cages and drinking pans. In dairy farms content of *P. aeruginosa* was higher in environmentally friendly areas, as compared to the areas with technogenic pollution. Analysis of antibiotic susceptibility has shown that in dairy farms average level of resistance of *P. aeruginosa* strains to carbapenems and fluoroquinolone was 12% and 6%, in pig-breeding farms - 9% and 13%, and in poultry farms - 6% and 18% correspondingly. At the same time, in environmentally neglected areas significant content of the strains with low susceptibility to the above-mentioned antibiotics was stated. The research is executed at the expense of a grant of the Russian scientific fund (project No. 18-16-00040).

Key words: animal farms, antibiotic susceptibility, opportunistic microbiota, poultry farms, *Pseudomonas aeruginosa*, technogenic pollution.

INTRODUCTION

Pseudomonas aeruginosa is widely spread in opportunistic microbiocenosis of animals and humans. Intensive adaptive potential of this microorganism is explained by a number of its unique special features, such as histolytic activity, genetic flexibility, quorum sensing, and ability to form biofilms, as well as high speed of development of resistance to antibiotics. A significant number of severe nosocomial diseases and complications is caused by *P. aeruginosa*, which is resistant to modern antibiotics. *P. aeruginosa* strains with 100% resistance are more and more often detected in medical enterprises all over the world (Ventola, 2015; von Wintersdorff et al., 2016).

In veterinary enterprises and animal farms *P. Aeruginosa*, as well as *S. aureus*, cause a significant number of purulent-septic infections and complications among fragile, ill and new-born animals, accompanied by injuries, stress, or during pre- or post-operation periods. Highly productive animals are also included into a risk-group because of their chronical physiological deterioration (Donnik et al., 2019). Circulation of *P. aeruginosa* in animal and poultry farms inevitably results in formation of strains resistant to antibiotics. In Russia public supervision over microbial resistance in veterinary and animal farming has been done only for a few last years. Earlier only veterinary specialists monitored microbial antibiotic susceptibility at the local level. Numerous data on opportunistic microbiocenosis in animal farms for the period of 2015–2018 prove a high level of resistant strains in enterprises with various profiles. One of the factors facilitating spread of dangerous strains of opportunistic pathogenic microflora is chronical secondary immunodeficiency of highly productive animals (Koba, 2018). Incompetence of the immune system leads to growing incidence of disease, and need in antibiotic treatment, and results in formation of resistant strains. In a number of regions of the Russian Federation agricultural enterprises are subject to man-made environmental pollution, including pollution of agrobiocenosis. They are mostly regions with developed industries or those damaged after serious man-made accidents (Luo et al., 2012; Alimova et al., 2015; Belykh et al., 2015). High concentrations of metals often are toxic to soil microflora, plants and animals. The toxicity of heavy metals depends on the type of metal element and its bioavailability on the soil (R. Imeri et al., 2019). Content of such man-made pollutants as Cd, Fe, Zn, Cu, Hg, As, Pb, and radionuclides in soil, water, plants, vegetable feedstuff, and in organisms of wild and productive animals is much higher than in the regions with favourable ecological situation (Ghiyasi et al., 2010; Abdulkhaliq et al., 2012). According to the data of various authors, agricultural animals in the regions with man-made pollution have secondary immunodeficiency because of frequent intoxication, chronical metabolitic stress, metabolic disorder and disbalance of processes of humoral regulation (Abdulkhaliq et al., 2012). Such situations cause higher risk of opportunistic infections, and growth of microbial resistance reduces the effect of medical-preventive activities. In order to improve quality of veterinary interventions, protect animals and prevent spread of dangerous resistant strains, a complex of activities, also including monitoring resistance in animal farms, is necessary. The aim of the work was to do the research on *P. aeruginosa* strains in animal and poultry farms located in the regions with various levels of environmental pollution. In order to achieve the aim, the following tasks were set: to determine content of *P. aeruginosa* in the composition of opportunistic pathogenic microflora in dairy, pig and poultry farms of meat- and egg-type; give the description of sensitivity of detected *P. aeruginosa* strains to antibiotics from groups of fluroquinolones and carbapenems.

MATERIALS AND METHODS

In order to achieve the tasks set, we have done the research on genus and species composition of microbiota in poultry farms of meat- and egg-type, dairy farms and pig farms. For the research enterprises with similar technological and production cycles, spices and breeds of animals, homotypic diet and veterinary maintenance were selected. All the enterprises were located in the Ural area, in the regions with various level of man-made contamination of agrobiocenosis with Zn, Fe, Cd, Cu, As, Pb, ^{90}Sr, ^{137}Cs. We did the preliminary analysis of contamination of feedstaff, soil and water with metals, using the methods of atomic absorption and atomic emission spectrometry (AA 6800 FG, Shimadzu); activity of samples of ^{90}Sr, ^{137}Cs were defined by radio-chemical methods. Totally 24 animal farms were researched, including 8 dairy farms (4 farms located in the area of Eastern Ural radioactive trail and border industrial districts, whereas other 4 farms - in the districts located not less than 100 km from the sources of technogenic emission). All the commercial dairy farms used yard housing, had similar technological profile and used their own feedstuff produced at their own agricultural lands. Total livestock numbers was 1,500–1,700 livestock units of Holstein black-and-white cows. The results of preliminary contamination of agrobiocenosis and feedstuff at the farms under research are given in Table 1.

Table 1. Average content of technogenic pollutants in ready-made feed mix at the commercial dairy farms in the regions with various level of man-made pollution

Pollutant	Regions with intensive man-made pollution	Regions with insignificant man-made pollution
^{90}Sr (Bqkg^{-1})	3.94	1.26
^{137}Cs (Bqkg^{-1})	3.15	0.19
Zn (mgkg^{-1})	52.51	33.38
Pb (mgkg^{-1})	6.14	2.23
Cd (mgkg^{-1})	0.42	0.11
Fe (mgkg^{-1})	123.14	49.65

In dairy farms wash-offs from mucosa, coat and udder of cows and calves, wash-offs from equipment, feed boxes, drinking pans, fence, surfaces, wash-offs from tools for cattle' maintenance, samples of litter, manure, water, feedstuff and air were taken. In every dairy farm the following departments were researched: maternity barn, calf-shed, and department for milking herd. 8 pig farms were researched, including the one located in the area of Eastern Ural radioactive trail; three farms located within a 50–80 km radius from large iron and non-ferrous industries, and four pig farms located in relatively favourable area, far from the sources of technogenic pollution. Pig farms were selected according to the following parameters: similar technological profile, bacon-pig production, Large White breed, total livestock numbers of 5,500–6,100 units, and their own feedstuff produced at their own agricultural lands and production facilities. According to the data of preliminary analysis of feedstuff of self-production, content of Cd in feedstuff at the pig farms in environmentally neglected regions was on average 0.48 mg kg^{-1}, Pb - 7.37 mg kg^{-1}, Fe - 69.5 mg kg^{-1}, the same data at the farms in the regions with low level of technogenic pollution were 2.5–6 times lower. In pig farms samples of air, feedstuff and premixes, litter, water, wash-offs from mucosa and dugs of pregnant and farrow sows, wash-offs from mucosa and skin of piggery from weaning cohort, nursery and fattening groups; wash-offs from equipment, fence, surfaces and tools in various places of premises were taken. The research was done on 4 poultry farms of meat-type (production locations of isolated raising with similar technological profile, cage housing, total cage flock of 0.9–1.2 million units of Cobb-500 and Ross-308 and 4 poultry farms of egg-type (with similar technological profile, cage housing, and total cage flock of 1.8–2.0 million of units of Lohman pedigree). Percent of home-grown feeder grain in all the farms under research was not less than 40%. 4 poultry farms were located in environmentally neglected regions with high content of metal pollutants in soil and water. Feeder grain grown in the lands of the poultry farms had high content of Zn (50.5–63.8 mg kg^{-1}), Pb (2.48–5.52 mg kg^{-1}), and Cd (0.26–0.38 mg kg^{-1}) that was 2–14 times higher than the same parameters of grain in the poultry farms located in the regions with low level of technogenic pollution. In poultry farms samples of feedstuff, water, air, litter, poultry manure, and wash-off from cages, feed-throughs, drinking pans and dung tape; wash-off from mucosa, feather and skin cover, and from cloaca of laying chicken from different age groups (in the poultry farms aimed at egg farming) and broiler chicken of antemortem age (in the poultry farms aimed at meat farming) were made. In total, 1,443 samples for microbiological research were taken. Selected samples were analyzed according to standard microbiological methods: inoculations of medium, cultivation, recovery of pure line, identification of microorganisms, and evaluation of their pathogenicity and antibiotic susceptibility by disk-diffusion method (Minimum Inhibitory Concentration) and serial dilution method (Clinical recommendations. Determination of the susceptibility of microorganisms to antimicrobials, 2015). The results obtained in the course of research were analyzed by methods of mathematical statistics in 'STATISTICA 10' including averaging, standard deviation, normality testing with Shapiro-Wilk criteria, estimation of verified differences between the groups according to various parameters by ANOVA methods and Mann-Whitney criteria.

RESULTS AND DISCUSSION

Analysis of structure of opportunistic pathogenic microflora in animal farms has shown that the most typical agents in all the objects were *Enterococcus faecium, Enterococcus faecalis, Enterococcus durans*, *Pseudomonas aeruginosa, Staphylococcus aureus, Staphylococcus epidermidis, Staphylococcus saprophyticus, Proteus vulgaris, Proteus mirabilis, Echerichia coli, Bacillius subtilis, Enterobacter spp., Citrobacter farmeri, Klebsiella spp., Candida albicans, Aspergillus spp., Mucor spp., Penicillium spp*, and *Fusaium spp*. Proportion of a number of detected strains varied depending on profile of an enterprise and its location. In general, content of *P. aeruginosa* was the biggest one in poultry farms of both meat- and egg-type and made up averagely 19% of all the detected microorganisms. In pig farms in environmentally neglected zones *P. aeruginosa* was detected more often (16%) than in dairy farms (12%), but not as often as in poultry farms.

Research on opportunistic pathogenic microflora of poultry farms have shown that the dominating microorganism detected in 63–100% of samples, was Enterococcus faecium. The second one, according to its frequency, was *Pseudomonas aeruginosa* detected in 29–100% of samples, depending on a definite enterprise. At the same time in the regions with man-made pollution *P. Aeruginosa* was mostly often detected in samples from mouth cavity and cloaca of laying chicken and chicken broilers, whereas in 'clean' regions - mostly in wash-offs from cages and drinking pans (Table 2). The fact may imply that in environmentally neglected zones birds have chronical toxic load on their digestive tract, caused by contamination of feedstuff with metal pollutant Fe, Cd, Cu, Pb and others.

Table 2. Quantity of positive *P. aeruginosa* tests in samples from various objects from poultry farms located in different regions

Object	Region with agrobiocenosis with man-made pollution (n = 221)	Ecologically favourable region (n = 219)
Mouth cavity	26	10
Cloaca	24	6
Outer coverings	14	13
Litter, manure	25	11
Cage	8	24
Feed-through	9	21
Drinking pan	17	26
Total amount of positive tests	123	111

In poultry farms of meat-type content of *P. aeruginosa* strains was averagely 18.6% of all the detected opportunistic pathogenic microorganisms. In poultry farms of egg-type - 19.7%. Therefore, in the poultry farms of both meat- and egg-type under research percent of *P. aeruginosa* in general opportunistic microflora was comparatively the same.

Results of the research on dairy farms have shown that structure of opportunistic pathogenic microbiota (without fungal microflora) in various regions significantly differs. Thus, in enterprises located in ecologically favourable regions *S. aureus* (23.2%) and *P. aeruginosa* (22.9%) were most often detected. In farms with high level of contamination of agrobiocenosis with metals and radionuclides of man-made nature proportion was the following: *Ent. faecium* (16.6%), *P. aeruginosa* (12.9%), and *S. aureus* (15.8%) (Table 3). In dairy farms proportion of samples, positive for *P. aeruginosa* was twice more in ecologically favourable regions than in regions with man-made pollution.

Table 3. Structure of opportunistic pathogenic microflora of dairy farms in ecologically favourable regions and in regions with man-made pollution (2018)*

Microorganism	Man-made pollution on the level of background pollution	Intensive man-made pollution
P.aeruginosa	22.9%	12.9%
Ent. faecalis	11.1%	13.7%
Ent. faecium	8.6%	16.6%
Ent. durans	10.2%	2.4%
P. mirabilis	6.2%	3.2%
P. vulgaris	5.0%	12.4%
E.coli	4.9%	5.3%
S. aureus	23.2%	15.8%
S. epidermidis	3.5%	2.5%
S. saprophyticus	< 0.5%	2.9%
C. farmer	2.3%	< 0.5%
S. marcescens	1.1%	< 0.5%
B. subtillis	< 0.1%	2.8%
Enterobacter	< 0.3%	8.4%
Other microorganisms	< 0.1%	< 0.1%
	100%	100%

**Distribution based on statistical analysis of structure of strains in selected samples, n = 492.*

It is especially important that more than a half of *Pseudomonas aeruginosa* positive tests were the tests taken from maternity barns of the farms. In calf-sheds and departments for milking herd *P. aeruginosa* was detected less often. *P. aeruginosa* was found in litter, on tools, fences and in manure. At the same time, in wash-offs from calves' coat *P. aeruginosa* with parameters of antibiotic susceptibility, similar to the ones of the strains from maternity barns was detected. This fact speaks for possible risk of insemination of a new-born calf with strains of opportunistic pathogenic microflora, which are low sensitive or resistant to antibiotics, that takes place during contact of a calf with litter or surfaces in a maternity barn. Circulation of resistant strains in maternity barn causes high risk of contamination of calves with them.

In samples taken from pig farms, there was the following distribution of strains according to average frequency: Ent. faecium (19%), *P. aeruginosa* (15%), *Aspergillus spp.* (14%), *S. aureus* (11%), *C. albicans* (8%), *Enterobacter* (8%), *Proteus spp.* (7%), *E.coli* (4%), *S. saprophyticus* (4%). Content of *S. epidermidis* and *Ent. faecalis* strains was not more than 0.2%. It was stated that in pig farms located in the regions with man-made pollution total number of detected *P. aeruginosa* strains did not have any statistically significant differences from ecologically favourable regions. All the enterprises under research had high level of contamination of pregnant sows with *P. aeruginosa*: more than a half of wash-offs from mucosa of mouth, nose and vagina were positive for this microorganism. Tools in all the enterprises under research was contaminated with *Enterococcus* and *P. aeruginosa*.

Analysis of antibiotic susceptibility has shown that in dairy farms average level of resistance of P. aeruginosa strains to carbapenems and fluroquinolones was 12% and 6%, in pig farms - 9% и 13%, in poultry farms - 6% and 18% respectively. Resistance of *P. aeruginosa* to carbapenems is explained by activation of a few mechanisms, such as formation of betalactamases, reduction of permeability of a membrane, and efflux-dependent elimination of antibiotic from a bacterial cell. These mechanisms can be activated separately or in complex. Resistance to fluroquinolones is explained by modification of targets, mostly type II and IV topoisomerases, fermentative inactivation of antibiotic, as well as by efflux systems (Jacoby, 2005; Wolter & Lister, 2013; Hong et al., 2015; Chebotar et al., 2017; Rostami, 2018).

In poultry farms there were mostly *P. aeruginosa* strains with low susceptibility to fluroquinolones and carbapenems. At the same time in the regions with intensive man-made pollution no strains with good susceptibility to these antibiotics were detected (Table 4). Resistant strains in environmentally neglected zones was detected twicemore often than in the regions with low man-made load.

Table 4. Proportion of *P. Aeruginosa* strains with various levels of susceptibility to to fluroquinolones and carbapenems in poultry farms from ecologically favourable and environmentally neglected regions

Status of man-made pollution of grobiocenosis	Proportion from all the strains researched in the object		
	Fluroquinolones		
	Susceptibility preserved	Low susceptibility	Resistance
Low	10%	80%	10%
Intensive	0%	70%	30%
	Carbapenems		
Low	20%	80%	0%
Intensive	0%	82.5%	16.5%

In pig farms in all the researched regions there were mostly *P. aeruginosa* with low susceptibility to antibiotics of fluroquinolones type and carbapenems. Reaction to carbapenems (meropenem, imipenem) was relatively similar in all the regions under research: strains with good susceptibility made up 34–36%, with low susceptibility - 56–58%, and resistant - 9%. In general, in pig farms sensitivity of *P. aeruginosa* to meropenem and Tienam was higher than to antibiotics of fluroquinolones type (enrofloxacin, ciprofloxacin, ofloxacin). At the same time, in the regions with man-made pollution proportion of strains resistant to fluroquinolones was less than in ecologically favourable regions. Thus, in polluted regions 10% of detected strains were non-sensitive to enrofloxacin and in conventionally 'clean' regions - 17% (Fig. 1).

On the other hand, pig farms located in ecologically favourable regions have more strains with good susceptibility to enrofloxacin (Fig. 2).

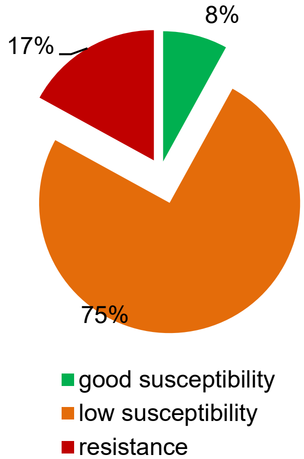

Figure 1. Susceptibility of *P. aeruginosa* strains to enrofloxacin in pig farms located in ecologically favourable regions (2018).

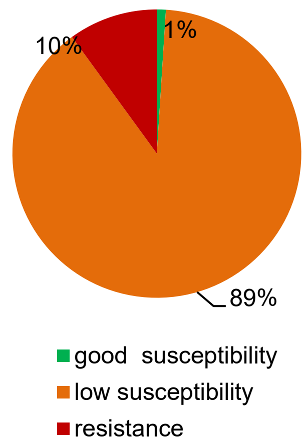

Figure 2. Susceptibility of *P. aeruginosa* strains to enrofloxacin in pig farms in the regions with man-made pollution (2018)

Research on antibiotic susceptibility of *P. aeruginosa* in dairy farms have shown that in the regions with man-made pollution quantity of strains resistant to fluroquinolones was 1.8 times less than in ecologically favourable regions. Both groups of regions had most strains with low susceptibility (their proportion made up 52–58% depending on a farm). Only in two from eight enterprises under research located in the regions with various levels of ecological load, *P. Aeruginosa* strains with good susceptibility to enrofloxacin and ofloxacin formed the most part (53% and 63% from all the detected strains). In these farms no strains resistant to fluroquinolones were detected. Probably, the reason for preserved antibiotic susceptibility of *P. aeruginosa* in these enterprises were special preventive measures taken against microbial resistance.

CONCLUSION

The research done have shown that content of *P. aeruginosa* in composition of opportunistic pathogenic microbiota was highest in poultry farms and lowest - in dairy farms. At the same time ecological well-being of agrobiocenosis correlated to a number of characteristics. Thus, in poultry farms in the regions with man-made pollution *P. aeruginosa* was more often found in mouth cavity and cloaca of chicken, whereas in ecologically favourable regions - in wash-offs from equipment. This fact implicits that in environmentally neglected areas microbiocenosis of poultry is affected by chronical alimentary intoxication related to contamination of feedstuff. In dairy farms difference in percentage of *P. aeruginosa* strains was stated - in ecologically favourable regions content of *P. aeruginosa* in structure of microbiocenosis was almost twice higher than in the regions with man-made pollution. *P. aeruginosa* was most often found in maternity barns - in samples from litter, and wash-offs from tools and equipment. High percentage of positive *P. aeruginosa* tests in maternity barns, as well as detected similarity of antibiotic-resistance profiles of *P. aeruginosa* strains from maternity barns and calf-sheds might speak for the possibility of insemination of newly-born calves with resistant strains of opportunistic microorganisms. In this case, risk of replacement of native microflora of a newly-born calf with more pathogenic and resistant microorganisms is significantly higher, that may cause a negative effect on calves' health and efficiency of antibiotic treatment in farms. Pig farms had high level of contamination of pregnant sows with *P. aeruginosa*. Total number of detected *P. aeruginosa* strains did not have any stastically significant differences depending on ecological status of territory. Average level of resistance of *P. aeruginosa* strains to carbapenems and fluroquinolones was in the commercial dairy farms 12% and 6%, in pig farms - 9% and 13%, in poultry farms - 6% and 18% respectively. In regions with man-made pollution *P. aeruginosa* strains with low susceptibility to carbapenems and fluroquinolones were dominating and there were practically no strains with good susceptibility to these antibiotics. In poultry farms quantity of resistant strains in environmentally neglected zones were detected 2.5 times more often than in the regions with low man-made load. In pig farms and dairy farms located in the regions with man-made pollution content of strains resistant to fluroquinolones and carbapenems was generally lower than in ecologically favourable regions.

ACKNOWLEDGEMENTS. The research was supported by a grant from the Russian Science Foundation (Project No. 18-16-00040).

REFERENCES

Abdulkhaliq, A., Swaileh, K.M. & Hussein, R.M. 2012. Levels of metals (Cd, Pb, Cu and Fe) in cow's milk, dairy products and hen's eggs from the West Bank, Palestine. *International Food Research Journal* **19**(3), 1089–1094.

Alimova, G.S., Korzhavin, A.V., Zemtsova, E.S., Dudareva, I.A., Tokareva, E.I., Popova, E.I. & Sulkarnaeva, R.M. 2015. Heavy metals accumulation in the riverside soil of samsonovskaya, lev and vandras minor rivers. *In the World of Scientific Discoveries*, Series B. **3**(2), pp. 22–33.

Belykh, E.S., Maystrenko, T.A., Grusdev, B.I., Vakhrusheva, O.M., Kaneva, A.V., Zainullin, V.G. & Trapeznikov, A.V. 2015. Species diversity of plant communities from territories anthropogenically contaminated with natural radionuclides. *Russian Journal of Ecology* **5**, 425–430.

Chebotar, I.V. Bocharova, Yu.A. & Maianski, N.A. 2017. Mechanisms of resistance of Pseudomonas aeruginosa to antibiotics and their regulation. *Clinical microbiology and antimicrobial chemotherapy* **19**(4), 308–319.

Clinical recommendations. Determination of the susceptibility of microorganisms to antimicrobials, 2015. Available at: *www.antibiotic.ru/minzdrav/files/docs/clrec-dsma2015*. (in Russian).

Donnik, I.M., Bykova, O., Krivonogova, A.S., Isaeva, A.G., Loretts, O.G., Baranova, A., Musikhina, H. & Romanova, A. 2019. Biological safety of cows' milk under the conditions of technogenic agricultural ecosphere when using biologically active substances *International Transaction Journal of Engineering, Management and Applied Sciences and Technologies* **10**(2), 203–209.

Ghiyasi, S., Karbassi, A., Moattar, F., Modabberi, S. & Sadough, M.B. 2010. Origin – and concentrations of heavy metals in agricultural land around aluminum industrial complex. *Food Agric. Environ*. **8**, 1237–40.

Hong, D.J., Bae, I.K., Jang, I.H., Jeong, S.H., Kang, H.K., Lee, K. 2015. Epidemiology and characteristics of metallo-β-lactamase-producing Pseudomonas aeruginosa. *Infect Chemother*. **47**(2), 81–97.

Imeri, R., Kullaj, E., Duhani, E. & Millaku, L. 2019. Impact of rootstock on heavy metal bioaccumulation in apple plant grown near an industrial source in Obiliq, Kosovo. *Agronomy Research* **17**(1), 100–110. https://doi.org/10.15159/AR.19.012

Jacoby, G.A. 2005. Mechanisms of resistance to quinolones. *Clin Infect Dis*. **41**(2), 120–126.

Koba, I.S., Lysenko, A.A., Koshchaev, A.G., Shantyz, A.K., Donnik, I.M., Dorozhkin, V.I. & Shabunin, S.V. 2018. Prevention of mastitis in dairy cows on industrial farms. *Journal of Pharmaceutical Sciences and Research* **10**(10), 2582–2585.

Luo, X.S., Yu, S, Zhu, Y.G. & Li, X.D. 2012. Trace metal contamination in urban soils of China. *Sci. Total Environ* **17**(30), 421–422.

Rostami, S., Sheikh, A.F., Shoja, S., Farahani, A., Tabatabaiefar, M.A., Jolodar, A., Sheikhi, R. 2018. Investigating of four main carbapenem–resistance mechanisms in high-level carbapenem resistant Pseudomonas aeruginosa isolated from burn patients. *J. Chin. Med. Assoc.* **81**(2), 127–132.

Ventola, L.C. 2015. The antibiotic resistance crisis. Part I: causes and threats. *Pharmacy and Therapeutics* **40**, 1–3.

von Wintersdorff, C.J.H., Penders, J., van Niekerk, J.M., Mills, N.D., Majumder, S., van Alphen, L.B., Savelkoul, P.H.M. & Wolffs, P.F.G. 2016. Dissemination of antimicrobial resistance in microbial ecosystems through horizontal gene transfer. *Frontiers in Microbiology* **7**, 173. https://doi.org/10.3389/fmicb.2016.00173

Wolter, D.J. & Lister, P.D. 2013.Mechanisms of β-lactam resistance among Pseudomonas aeruginosa. *Curr. Pharm. Des*. **19**(2), 209–222.

Agronomy Research **18**(4), 2374–2390, 2020
https://doi.org/10.15159/AR.20.188

Simulating the effect of tillage practices on the yield production of wheat and barley under dryland condition

A.N. El-Sadek[1], F.I. Abd EL-Ghany[1] and A.M. Shaalan[2,*]

[1]Ecology and Dry Land Agriculture Division, Desert Research Center, EG11753 El-Matarya, Cairo, Egypt
[2]Plant Production Department, Faculty of Desert and Environmental Agriculture, Matrouh University, EG51744 Matrouh, Egypt
[*]Correspondence: ahmedmahgoub@mau.edu.eg

Abstract. In arid and semiarid regions, soil tillage practices have major effects on soil water dynamics. In this study, we compared the effects of Zero Tillage (ZT) and Conventional Tillage (CT) on the grain yield of rainfed barley and wheat at three locations i.e. Barrani, El-Neguilla and Matrouh in the north western coast of Egypt. We also tested the performance of the DSSAT (Decision Support System for Agrotechnology Transfer). In the first season of 2017/2018, only barley plants in Barrani location were able to grow and produce yield due to insufficient rain. Results showed that ZT produced significantly higher grain yield (almost 200%) for barley as compared to the CT treatment. In the second season of 2018/2019, conventional tillage produced higher yields as compared to the zero tillage treatment over the three studied locations and for the two crops. The DSSAT model successfully simulated the grain yield, total biomass and harvest index with an excellent agreement between simulated and observed data with NSE values of 0.868 and 0.800 for grain yield and total biomass respectively and a satisfactory agreement with NSE of 0.431 in case of harvest index. Tillage had a noticeable impact on grain yield of barley and wheat and the DSSAT successfully simulated the effects of the tillage treatments.

Key words: wheat, barley, DSSAT, drylands, tillage, precipitation use efficiency.

INTRODUCTION

Tillage is defined as the soil disturbance process that provides an adequate physical condition for the plant growth (Ucgul et al., 2014; Busari et al., 2015), meanwhile it is an important crop production factor with a yield contribution of 20% (Khurshid et al., 2006). Conventional tillage is usually used to reduce the population of weed, diseases, insects and other pests, also to conserve the soil moisture during the fallow period. However, these aims may not be achieved efficiently and causes a significant damage in the soil structure resulting in compacting the soil and increasing the risk of soil erosion (Novak et al., 2019; Jordan et al., 2000). As a result, the strategy of zero tillage which ensures both minimal soil disturbance and moisture loss has been adopted worldwide (Saturnino & Landers 2002; Kassam et al., 2015). Under short term condition zero tillage treatment could improve the crop yield (Hemmat & Eskandari, 2004; Hemmat & Eskandari, 2006; Mrabet, 2008; Mokrikov et al., 2019) and improve the physical

(Anikwe & Ubochi, 2007), chemical (Rahman et al., 2008) and biological (Cookson et al., 2008) properties of the soil. However, some studies have reported that no tillage didn't increase the crop yield (Monneveux et al., 2006; Masek & Novak, 2018). Furthermore it could cause soil compaction, reduce infiltration (Schwartz et al., 2010; Ferreras et al., 2000), therefore the impact of conservational agriculture usually depends on some environmental and ecological factors (Yang et al., 2018), also soil characteristics such as soil texture, slope and mulching might affect the impact of tillage operations (Mhazo et al., 2016).

Crop production in the North Western Coast of Egypt is characterized by a continuous cultivation of barley and small areas of wheat. The traditional tillage practices include one or two tillage operations before sowing and one operation after sowing, for seed coverage, following the first effective rain. The grain yield of wheat and barley is highly variable in this area based on the amount of annual rain which falls between October and March and peaks in December and January with an average of 140 mm. Precipitation in the region have changed dramatically in the past decades in terms of amount and distribution, in particular a decrease in annual precipitation and an increased incidence of prolonged dry spells have been observed most often in the last few years (El-Sadek & Salem, 2016) making the successful crop production challenging and highly variable. Barley yield usually ranges from 200 to 1,400 kg ha^{-1}, while for wheat it ranges from 150 to 900 kg ha^{-1}. Many studies in the region have reported an increase in barley yield (Gomaa et al., 2013; Sayed et al., 2017) and wheat yield (Salem et al., 2003; El-Sadek & Salem, 2016; Ali & El-Sadek, 2016) using different varieties and crop management practices under rainfed conditions.

Crop growth models are used to simulate crop growth and yield as a response of different weather conditions, soil characteristics and crop management. The Decision Support System for Agrotechnology Transfer (DSSAT; Jones et al., 2003) is a widely used model to simulate different crops growth and yield under a broad range of conditions and crop management scenarios e.g. nitrogen fertilization (Banger et al., 2018; Prasad & Mailapalli, 2018; Tovihoudji et al., 2019), irrigation management (Jiang et al., 2016; Babel et al., 2019; Malik & Dechmi, 2019), climate change (Ngwira et al., 2014; Tyagi et al., 2019), yield forecasting and soil management and crop rotation (Soler et al., 2011; Li et al., 2015; Puntel et al., 2016; Araya et al., 2017). In Egypt, the model was applied with sufficient reliability to simulate the growth and yield of different Egyptian wheat varieties under varied sowing dates (Fayed et al., 2015), maize and broad bean (Harb et al., 2016) and climate change impact on wheat production (Kheir et al., 2019).

The main aim of this study was to evaluate the ability of the two models CERES-barley and CERES wheat (Crop-Environment Resource Synthesis) through DSSAT to estimate the grain yield of rainfed barley and wheat under different tillage practices (conventional tillage versus zero tillage) at different locations in the North Western Coast of Egypt.

MATERILAS AND METHODS

Experimental site

The experiment was conducted at three locations i.e. Barrani, El-Neguilla and Matrouh along the North Western Coast of Egypt. Data in Table 1 shows the

Coordinates and sowing and harvesting dates for each location. The agriculture in this region is mainly rainfed and the region is characterized by a Mediterranean type of climate with cold wet winter and hot dry summer. The average annual precipitation is 140 mm, however it is increasing towards the west to be 180 mm in Barrani. The mean annual maximum and minimum temperatures are 22.54 and 19.23 °C.

Table 1. Location of the experimental sites, total rainfall, date of sowing and harvesting date in the two growing seasons

Location	Coordinates		Total rainfall	Sowing	Harvesting
	N	E	(mm)	dates	dates
Barrani (2017/2018)	31° 36' 0"	25° 52' 48"	79.00	28/11/2017	17/4/2018
Matrouh (2018/2019)	31° 22' 27.88"	27° 03'19.6	159.25	28/11/2018	28/3/2019
El-Neguilla (2018/2019)	31° 24' 33.6"	26° 40' 32.3"	162.14	10/12/2018	16/5/2019
Barrani (2018/2019)	31° 36' 0"	25° 52' 48"	115.96	22/11/2018	2/5/2019

Precipitation data for the two seasons of 2017/2018 and 2018/2019 were downloaded from The Tropical Rainfall Measurement Mission (TRMM) data 3B43 Version 07 daily Rainfall product (Table 1 and Fig. 1), which is a collection of rainfall data accumulated in millimeters per day with a spatial resolution of 0.25°. The daily weather data required for the model simulation including minimum and maximum temperature, solar radiation, wind speed and relative humidity were obtained from the National Center for Environmental Prediction; Climate Forecast System Reanalysis NCEP/CFSR. The data set is available for direct download free of charge from this website: http://rda.ucar.edu/pub/cfsr.html. Fig. 2 shows the average maximum and minimum temperature at Matrouh station.

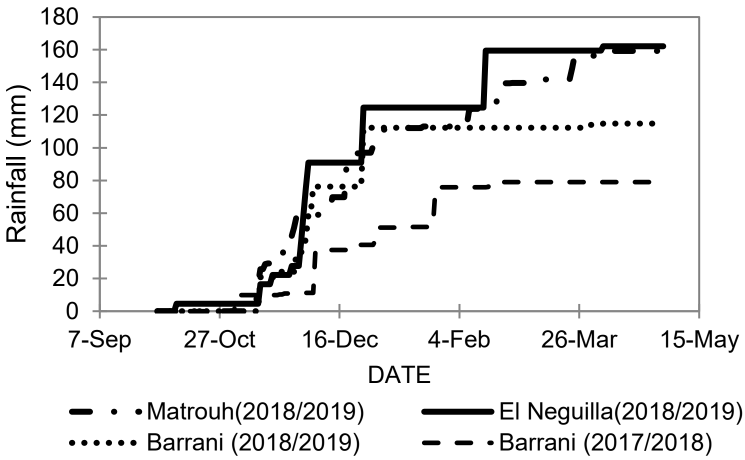

Figure 1. Cumulative rainfall for the study sites in the two growing seasons.

Total precipitation during the growing seasons (from October through April of the following year) was 79 mm in Barrani, 48.63 mm in El-Neguilla and 38 mm in Matrouh in the first season of 2017/2018, and was 115.96 mm in Barrani, 162.14 mm in El-Neguilla and 159.25 in Matrouh in the second season 2018/2019. The highest percentage of precipitation usually occurs in December and January. Cumulative precipitation for the study locations is presented in Fig. (1). The rainy season started very late in 2017 beginning in late November, and it was represented mostly by two excessive events; the first event of 25.75 mm in December, 6th and the second event was in 25/1/2018 with a 23.5 mm of rain.

The main soils of the region have been classified as Aridisols and Entisols, and are generally low in soil organic matter (SOM), nitrogen (N) and plant-available phosphorus (P). soils in the studied locations mostly have a coarse and moderately coarse soil texture. Soils are highly calcareous (~20% $CaCO_3$) with a pH ranges from 7.5–8 and EC around 0.7 ds m^{-1} (fresh soil). The soil is classified as Typic Torriorthents.

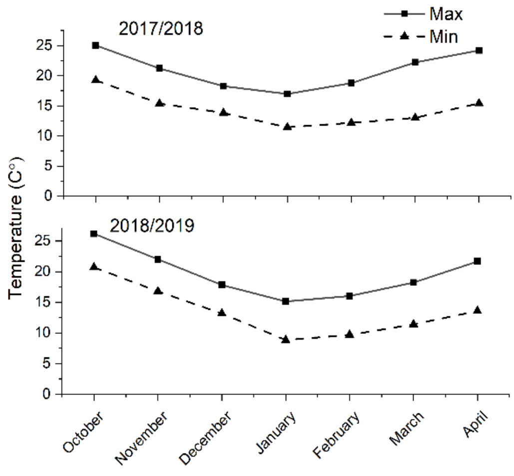

Figure 2. Average maximum and minimum monthly temperatures at Matrouh station.

Experimental design and treatments

In the first season of 2017/2018, only Barrani's barley was able to grow and produce yield due to insufficient rain in this season. The effects of two tillage treatments on barley's yield were investigated, including conventional tillage (CT) and Zero tillage (ZT). Each treatment was replicated four times in a randomized complete block design with a total of 8 plots. While in the second season of 2018/2019, for each crop the three locations of Matrouh, El-Neguilla and Barrani and the tillage treatments (CT and ZT) were arranged in a split plot design, where locations were allocated in the main plots, while the sub plots were assigned for the tillage treatments. In both seasons, each plot was 24 m^2 (4 m × 6 m) in area. There were 2-m spaces between adjacent blocks and 1-m spaces between adjacent plots.

Soil was plowed twice at a depth of 20 cm before and after sowing (CT) as a traditional practice performed by the local farmers. whereas no tillage was used for the ZT treatment, however the plots with the zero tillage had been tilled the previous years. The cultivars used in this study were Giza 171 for wheat and Giza 126 (six-rowed) for barley at a rate of 75 kg ha^{-1} for the two crops. In the CT treatment, seeds were broadcasted by hand, while for the ZT treatment, both crops were sown using a small no till seeder at 20 cm width. Neither chemical fertilizers nor pesticides were applied throughout the two growing seasons.

Grain yield, straw yield and biological yield (total dry biomass) were measured from hand- harvested plants from a 1 square meter quadrate. Plant height at maturity (harvest) was measured as the height from the soil surface to the tip of the head of the plant. To measure yield components, sub-samples of plants for wheat and barley were randomly selected and threshed and separated to calculate no of grains/spike from each single ear and 1,000-grain weight from a sub-sample of ears of each quadrate. Harvest index was calculated by dividing the grain yield by the biological yield. Precipitation

Using Efficiency (PUE) was calculated by dividing crop grain yield (kg ha^{-1}) by growing season precipitation.

All data were analyzed using analysis of variance (ANOVA) with a significance level of 5% to determine the significance of the main effects and their interaction. Least significant difference (*LSD*) test was performed to determine the significant differences between individual means. All statistical analyses were performed using the SAS statistical software (SAS institute 2007).

The DSSAT model

The two models CERES-barley (Otter-Nacke et al., 1991) and CERES wheat Godwin et al., 1989 were examined in this study within the framework of DSSAT 4.7 (Decision Support System for Agrotechnology Transfer). Model inputs include information about the conducted experiment (site soil profile and soil surface data, crop management data, preceding crop, residues,….etc), daily data for the climate parameters (precipitation, minimum and maximum temperature, solar radiation), soil physical and chemical parameters, and the cultivar specifications. The model simulates the phonological development and yield components of many crops, more information about the model can be found in Hoogenboom et al., 2012. Simulated model outputs can be calibrated against the real data by adjusting the cultivar genetic coefficients.

Model evaluation

To evaluate the model performance and to compare the simulated grain yield, biomass and harvest index versus the observed data, three statistical measurements were used: the coefficient of determination (R^2), Nash- Sutcliff efficiency (*NSE*) (Nash & Sutcliffe, 1970), and the root mean square error ($RMSE$)-observation's standard deviation ratio (*SR*) collectively called *RSR* (Eq. 1,2 and 3).

$$R^2 = \frac{[\sum_{i=1}^{n}(O_i - \bar{O})(P_i - \bar{P})]^2}{[\sum_{i=1}^{n}(O_i - \bar{O})^2][\sum_{i=1}^{n}(P_i - \bar{P})^2]} \quad (1)$$

where, P_i are the predicted values, O_i are the observed values, n is the total number of observations, is the mean of the observed data and is the mean of the predicted data. R^2 ranges from 0 to 1, with higher values indicating less error variance

$$NSE = \frac{\sum_{i=1}^{n}(O_i - \bar{O})^2 - \sum_{i=1}^{n}(P_i - O_i)^2}{\sum_{i=1}^{n}(O_i - \bar{O})^2} \quad (2)$$

NSE, ranges between –∞ and 1, The value of NSE = 1 corresponds to a perfect match between predicted and observed data

$$RSR = \frac{RMSE}{STDEV_{obs}} = \frac{\left[\sqrt{\sum_{i=1}^{n}(O_i - P_i)^2}\right]}{\left[\sqrt{\sum_{i=1}^{n}(O_i - \bar{O})^2}\right]} \quad (3)$$

where, $STDEV_{obs}$ is the standard deviation of observed values, the RSR value varies from the optimal value of 0, which indicates 0 $RMSE$ or residual variation and a perfect model simulation, to a large positive value.

Economic parameters

Production costs were calculated for each of the two tillage systems. Inputs such as seeds were purchased from the Central Administration for Seeds, Ministry of Agriculture and Land Reclamation, and the exact price was recorded. For labour and tillage operation costs, we used data from the local farmers. Gross margin ($ ha^{-1}) was calculated from net income for crop after deducting all variable costs.

RESULTS AND DISCUSSION

Precipitation

In the first season, the two early high events resulted in a poor grain yield for barley due to inappropriate timing of rain that missed the two critical growth stages of anthesis and grain filling. While, In the second growing season, the rainfall started as early as November, 13th. The rainfall was well distributed along the growing season having a significant event every month from November to March. Rainfall variation in quantity and time had a significant impact on plant growth and yield. In this season the high amount of rainfall and its proper distribution produced a higher yield. The proper delivery of plant water requirement, soil and crop management practices plays a critical role in the produced yield (Silungwe et al., 2019).

Tillage effects on grain yield

In the first season, there was a significant difference between the two tillage systems i.e., zero tillage and conventional tillage for spike length, number of grains/ spike, grain yield, straw yield, total dry biomass, harvest index and precipitation use efficiency (Table 2). Average grain yield for barley under zero tillage condition was more than double of that under conventional tillage. The superior average grain yield of no till as compared to other systems was also recorded by Hemmat & Eskandari (2006). The higher yield from zero tillage treatment may be due to the fact that zero tillage improved the soil water content which resulted in a better crop growth and yield (Morell et al., 2011). This positive impact of zero tillage was higher in dry years as compared to wet years. Same conclusion also was drawn by Bescansa et al. (2006) who reported that zero tillage positively increased the soil water storage. Also, the number of plants in the unit area was higher in zero-tillage treatment as compared to the conventional tillage. Farmers in the North Western Coast (NWC) of Egypt used to plow the soil before and after sowing, this usually increased the chance of the soil to be drier driven by moisture loss unless rain falls directly after sowing. This explains the good establishment of seedlings in case of ZT treatment.

In the second season of 2018/2019, conventional tillage produced a higher yield as compared to the zero tillage treatment over the studied locations (Table 2). Decreasing the grain yield in the second season for the zero tillage treatment, as compared to the conventional tillage, maybe due to the fact that conservation tillage (zero tillage in our case) usually reduces the leaching loss of calcium carbonate (which is very high in our study sites) as compared to the conventional tillage in rainfed areas (Murillo et al., 2004 and 2006). Tillage also improves the soil physical characteristics reducing the soil penetration resistance in the first 0–10 cm depth as a result of loosening the soil and macrospores formation (Jabro et al., 2009).

Table 2. Mean values of plant height, spike length, no. of plants/m^2, no. grains/spike, 1,000-grain weight, grain yield, straw yield, biological yield, harvest index and precipitation use efficiency in 2017/2018 and 2018/2019 seasons

Treatments	PH, cm	SL, cm	NP/ m^2	NGS	TGW, g	GY, kg ha^{-1}	SY, kg ha^{-1}	BY, kg ha^{-1}	HI, %	PUE, kg ha^{-1} /mm
	2017/2018 Season (barley only)									
ZT	42.38	5.67	67.00	40.00	24.88	571.20	1,220.2	1,849.4	30.88	13.09
CT	44.72	4.33	42.00	34.67	20.19	257.30	974.4	1,231.7	20.55	5.667
LSD 0.05	**NS**	**NS**	**1.29**	**NS**	**NS**	**26.67**	**126.40**	**114.66**	**6.24**	**1.39**
	2018/2019 season (barley)									
Locations										
Barani	25.50	3.50	163.17	27.00	30.71	716.46	1,059.6	1,776.0	40.42	6.13
Matrouh	25.000	3.17	116.33	14.83	29.65	243.07	886.43	1,129.5	21.44	1.53
El-Neguilla	39.333	5.67	116.67	38.17	43.63	1165.67	2,016.9	3,182.5	36.58	7.19
LSD 0.05	**2.37**	**0.66**	**22.94**	**1.42**	**1.38**	**67.40**	**116.13**	**132.08**	**3.14**	**0.54**
Tillage										
ZT	28.56	3.67	131.44	23.00	33.28	649.47	1,184.36	1,833.82	32.42	4.62
CT	31.33	4.56	132.67	30.33	36.06	767.33	1,457.56	2,224.89	33.75	5.28
LSD 0.05	**1.94**	**0.54**	**NS**	**1.16**	**1.13**	**55.03**	**94.82**	**107.84**	**NS**	**0.44**
	2018/2019 season (wheat)									
Locations										
Barani	48.33	6.00	154.67	25.67	31.77	537.73	1,501.3	2,039.0	26.41	4.60
Matrouh	47.33	7.00	136.67	28.00	29.43	471.77	1,454.6	1,926.3	24.43	2.96
El-Neguilla	60.33	6.83	163.33	28.50	45.12	1,315.17	1,552.6	2,867.8	45.25	8.11
LSD 0.05	**4.30**	**0.89**	**19.03**	**NS**	**1.94**	**70.55**	**NS**	**167.7**	**2.94**	**0.46**
Tillage										
ZT	49.11	5.11	147.78	19.44	33.88	593.89	1,236.73	1,830.6	31.13	4.11
CT	54.89	8.11	155.33	35.33	37.00	955.89	1,768.91	2,724.8	32.93	6.34
LSD 0.05	**3.51**	**0.73**	**NS**	**2.57**	**1.59**	**57.61**	**120.3**	**136.9**	**NS**	**0.38**

ZT: Zero Tillage; CT: Conventional Tillage; PH: plant height at harvest; SL: spike length, NP/m$^{2:}$ no. of plants/ m^2; NGS: number of grains per spike; TGW: thousand grain weight; GY: grain yield; SY: straw yield; BY: biological yield; HI: harvest index and PUE: precipitation use efficiency.

Tillage effects on yield components

The main components of grain yield for cereals are number of ears per square meter, number of kernels per ear and the kernel weight. Table (2) shows the response of various yield components to tillage systems for barley in the first season and for barley and wheat in the second season. Results show that, there was a significant effect of the tillage systems on the number of plants/m^2 in the first season. Zero tillage treatment produced more plants/m^2 as compared to the conventional tillage, these results are in agreement with those obtained by Moret et al. (2007) who concluded that no tillage practice increased the percentage of crop emergence for barley plants with no significant difference as compared to the other tillage systems. No significant effect was recorded for 1,000-grain weight as a result of the tillage treatments, Similar results were recorded on wheat by Hemmat & Eskandari (2006).

In the second season plant height, spike length, number of grains/spike and 1,000-grain (kernel) weight were significantly affected by the tillage systems, and were higher for the conventional tillage treatment in both crops. Plants were taller by 2.77 and 5.78 cm under conventional tillage as compared to zero tillage in barley and wheat, respectively (Table 2). Spike length was significantly affected by the tillage systems and recorded its highest values of 4.56 cm for barley and 8.11 cm for wheat under conventional tillage treatment. Highest values of number of grains/spike (30.33 and 35.33) and 1,000-grain weight (36.06 and 37.00 g) were observed under conventional tillage for barley and wheat, respectively (Table 2). Lower values of yield components under zero tillage treatment were probably due to the water deficit in the root zone resulted from low infiltration rate and high soil bulk density (Busari & Salako, 2012).

Tillage effects on total dry biomass and harvest index

In the dry season (2017/2018), zero tillage treatment produced a higher above ground biomass (biological yield; kg ha^{-1}) as compared to the conventional tillage. However, in the wetter season i.e., 2018/2019, biomass accumulation was greater in conventional tillage for both crops and over all the studied locations. A higher total biomass produced in the dry year is mainly due to the higher availability of soil moisture. HI was higher (30.88%) with the zero tillage as compared to the conventional tillage in the first season. However, the two treatments had a similar impact on harvest index in the second season for both wheat and barley overall the studied locations.

Tillage effects on precipitation use efficiency

The precipitation use efficiency was significantly influenced by the tillage systems in the two growing seasons. In the first season, zero tillage treatment recorded a higher PUE as compared to the conventional treatment. Similar results were obtained by Hemmat & Eskandari (2006) when the PUE was averaged across the growing seasons. However, in the second season, the conventional tillage treatment produced a slightly higher PUE as compared to the zero tillage for both crops (Table 2). There was also a significant effect of locations on PUE when averaged across the tillage systems and for the two studied crops. PUE depends mainly on the amount of precipitation (Fensholt & Rasmussen, 2011) and the crop rotation followed in the region as concluded by Hemmat & Eskandari (2004).

Crop performance in response to tillage and location

In the second season, we performed the interaction between the two studied factors i.e., location and tillage (Table 3). Results showed that there was a significant location × tillage interaction for all the studied characters in both crops. Plant height varied with location and recorded the highest values of 61 cm for wheat and 45 cm for barley in El-Neguilla, tending to be higher under the conventional tillage treatment. Spike length and number of plants /m^2 showed a significant location × tillage interaction (Table 3), spikes were taller in wheat as compared to barley with highest values in El-Neguilla location under the conventional tillage treatment (Table 3).

Number of grains per spike showed a significant location × tillage interaction with more grains in spike under the CT treatment at El-Neguilla location for barley and at Matrouh location for wheat. The 1,000-grain weight was significant in location × tillage interaction (Table 3), where the maximum values of 45.93 g for barley and 48.00 g for wheat were recorded in El-Neguilla with the conventional tillage treatment. The highest grain yields of barley and wheat of 1,351.3 and 1,691.8 kg ha^{-1} respectively were at El- Neguilla under conventional tillage treatment. Same trends were also for the straw and biological yields in barley and for the biological yield only in wheat. Precipitation use efficiency values were also higher at El-Neguilla location under the conventional tillage treatment with the highest rainfall recorded for this season of 162 mm. Bonfil et al. (1999) stated that the PUE changes according to the amount of precipitation.

Table 3. Effect of location × tillage interaction on plant height (cm), spike length (cm), no. of plants /m^2, no. grains/spike, 1,000-grain weight (g), grain yield (kg ha^{-1}), straw yield (kg ha^{-1}), biological yield (kg ha^{-1}), harvest index (%) and precipitation use efficiency (kg ha^{-1} per mm) in 2018/2019 season

Location	Tillage	PH	SL	NP/ m^2	NGS	TGW	GY	SY	BY	HI	PUE
Barley											
Barrani	ZT	26.00	3.00	177.0	20.00	29.37	762.9	969.3	1,732.3	43.99	6.52
	CT	25.00	4.00	149.3	34.00	32.07	670.0	1,149.8	1,819.8	36.85	5.73
Matrouh	ZT	26.00	3.00	105.3	15.67	29.13	205.5	848.5	1,054.0	19.50	1.29
	CT	24.00	3.33	127.3	14.00	30.17	280.7	924.3	1,205.0	23.38	1.76
El-Neguilla	ZT	33.67	5.00	112.0	33.33	41.33	980.0	1,735.2	2,715.2	36.13	6.04
	CT	45.00	6.33	121.3	43.00	45.93	1351.3	2,298.5	3,649.9	37.03	8.33
LSD 0.05		**3.55**	**0.94**	**31.81**	**2.01**	**1.96**	**95.31**	**164.2**	**186.8**	**4.44**	**0.77**
Wheat											
Barrani	ZT	42.67	4.33	158.7	19.33	30.67	542.3	1491.5	2,033.6	26.72	4.66
	CT	54.00	7.67	150.7	32.00	32.87	533.3	1511.1	2,044.4	26.10	4.56
Matrouh	ZT	45.00	6.00	128.0	17.67	28.73	301.0	930.9	1,231.9	24.44	1.89
	CT	49.67	8.00	145.3	38.33	30.13	642.5	1978.3	2,620.8	24.42	4.04
El-Neguilla	ZT	59.67	5.00	156.7	21.33	42.23	938.5	1287.9	2,226.4	42.24	5.79
	CT	61.00	8.67	170.0	35.67	48.00	1691.8	1817.4	3,509.2	48.27	10.43
LSD 0.05		**6.08**	**1.26**	**26.92**	**4.46**	**2.75**	**99.78**	**208.4**	**237.1**	**4.16**	**0.66**

ZT: Zero Tillage; CT: conventional tillage; PH: plant height at harvest; SL: spike length; NP m^{-2}: No. of plants per m^2; NGS: number of grains per spike; TGW: thousand grain weight; GY: grain yield; SY: straw yield;BY: biological yield; HI: harvest index and PUE: Precipitation Use Efficiency.

Previous studies drew different conclusions about the response of crop yield to different tillage systems. Piggin et al. (2015) found that wheat and barley were less responsive to zero tillage as compared to legumes in eleven seasons (five for wheat and six for barley). On the other hand, Mrabet (2000) found that, overall the growing seasons, wheat grain yield was maximum under No-tillage condition with no difference compared to chisel plow or deep tillage. However, under the dry condition (season 1998/1999) with a total rainfall of 195 mm, no tillage treatment produced the highest grain yield and total dry biomass as compared to the other tillage systems.

Traditional tillage may result in a better root growth, an increase in nutrient and water uptake and ultimately the agronomic yield, while ZT causes a soil compaction which impedes the root growth (Martinez et al., 2008). We believe that under our conditions, tillage can be more effective in case of implemented with other conservation agriculture treatments i.e. residue retention and crop rotation which found to increase the crop yield in dryland rainfed areas (Piggin et al., 2015; Pittelkow et al., 2015).

Being in a dryland Mediterranean environment, the amount and distribution of rainfall was the major driver for the crop performance in our study area. High and well distributed rainfall in Matrouh (159.25 mm) and El-Neguilla (162.14 mm) in the second season under CT treatment produced higher yields for wheat as compared to barley (Table 3). However, barley as a more drought resistant crop as compared to wheat, produced a better yield in Barrani (with less rainfall) in the second season. Moreover in the first season, barley was able to grow in at least one location where wheat couldn't survive.

In the present study, under very scarce rainfall 74 mm in the first season, the zero tillage was more productive than the conventional tillage, but in the second season, with rainfall between 116 and 169 mm, which is also a small amount, we found the reverse. One of the possible reasons of this apparent contradiction may rely on the fact that the beneficial effects of zero tillage on the structure of the soil will become more evident after several years of following the same soil management and, during the meantime, soil properties will pass through a transitional stage.

DSSAT model testing: barley and wheat yields

The variables used for calibration were grain yield, total produced biomass and harvest index. The calibration process revealed that the model predicted the grain yield and total biomass of both wheat and barley well, with NSE and R^2 values ≥ 0.8 (Table 4 and Fig. 3). The calibration results showed that RSR values were 0.098, 0.447 and 0.754 for grain yield, total biomass and HI respectively, which showed good model performance for the total biomass and HI and excellent performance for the crops grain yield. This implies that the model was successfully calibrated for the three treatments of the experiment i.e., location, crop and tillage. Similar results were obtained by another study of Soldevilla-Martínez et al. (2013), working under dryland condition with different crop rotations and tillage systems, concluded that CERES-Barley was able to accurately predict yield and total biomass of barley. The model showed a difference in yield and biomass associated with the tillage systems and locations.

Table 4. Simulated and observed values for barley and wheat and comparison statistics in the different locations and tillage systems

Crop, year and location	Tillage	Grain yield, kg ha^{-1}		Biomass, kg ha^{-1}		HI	
		Sim.	Obs.	Sim.	Obs.	Sim.	Obs.
Barley 2017/2018 (Barrani)	ZT	545	571	1,560	1,849	0.35	0.30
	CT	550	257	1,468	1,231	0.37	0.21
Barley 2018/2019 (Matrouh)	ZT	385	205	1,484	1,054	0.26	0.20
	CT	370	281	1,515	1,205	0.24	0.23
Wheat 2018/2019 (Matrouh)	ZT	386	301	1,003	930	0.38	0.24
	CT	655	642	2,414	2,620	0.27	0.24
Barley 2018/2019 (El-Neguilla)	ZT	927	980	2,587	2,715	0.36	0.36
	CT	1,123	1,351	3,263	3,649	0.34	0.37
Wheat 2018/2019 (El-Neguilla)	ZT	1,190	938	2,589	2,226	0.46	0.42
	CT	1,459	1691	2,902	3,504	0.50	0.48
Barley 2018/2019 (Barrani)	ZT	742	763	2,081	1,732	0.36	0.44
	CT	743	670	2,085	1,819	0.36	0.36
Wheat 2018/2019 (Barrani)	ZT	579	542	2,075	1,491	0.27	0.27
	CT	577	533	2,062	1,511	0.28	0.26
NSE		0.868		0.800		0.431	
R^2		0.909		0.856		0.552	
RSR		0.098		0.447		0.754	

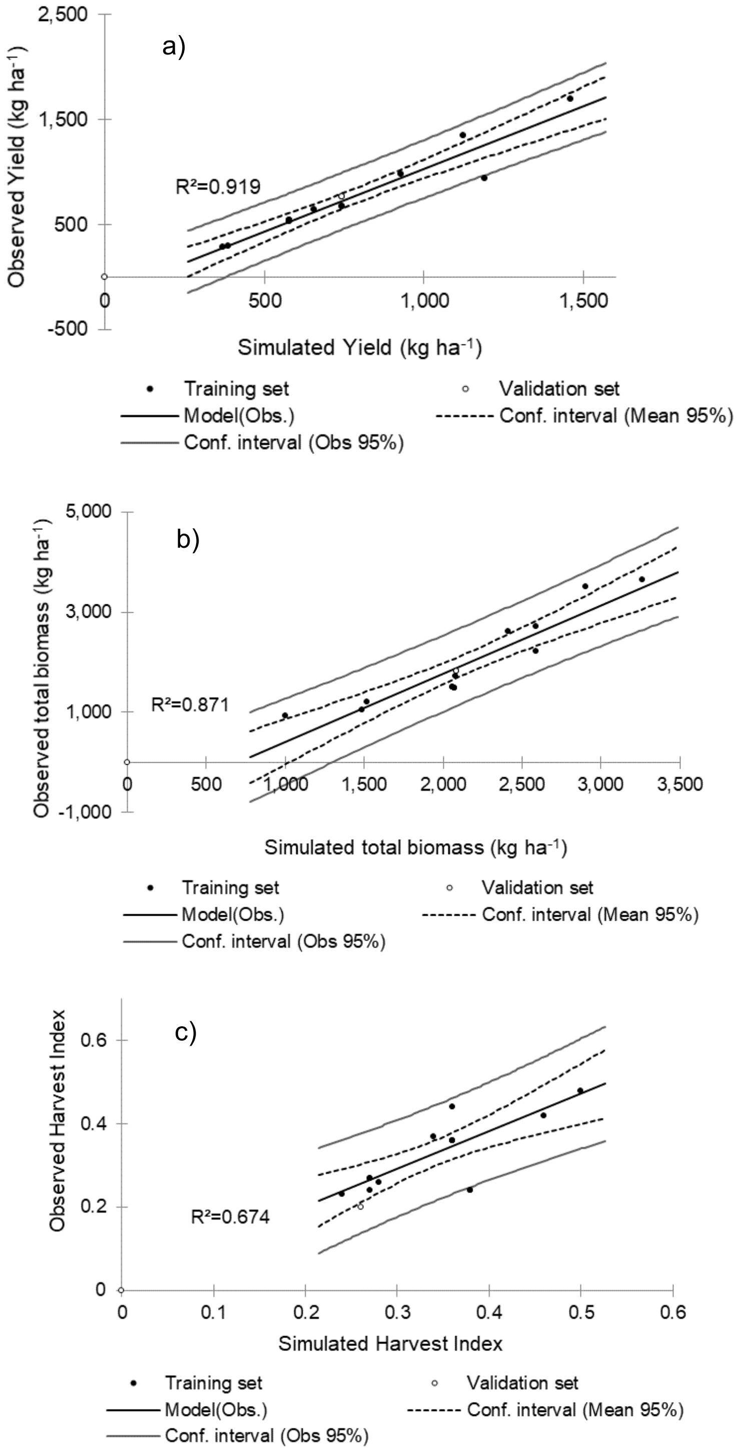

Figure 3. Barley and wheat grain yields (a) total biomass (b) and HI after calibration in the two growing seasons.

In the North Western Coast of Egypt, Mahmoud & Meselhy (2019) studied the impact of different sowing dates; 15th Nov, 30th Nov and 15th Dec, tillage treatments (conventional versus zero tillage) and three treatments of supplemental irrigation (0, 70, 140 mm) on barley yield. Results showed that under all the studied treatments, conventional tillage operation produced higher biomass and grain yields of 2.85 and 1.07 t ha^{-1} as compared to the No tillage operation. Barley yield was simulated using the Aqua Crop model (Raes et al., 2009; Steduto et al., 2009) under all the above mentioned treatments. The model adequately simulated the crop yield with an $R^2 > 0.85$ under the two tillage systems.

A sensitivity analysis was performed for the CENTURY-based soil module in DSSAT model inputs. Results showed that the model is less sensitive to tillage as compared to other factors (Porter et al., 2010). The model simulated higher yield and biomass for the CT in the second season which may be caused by a higher soil water storage in the CT treatment accompanied by higher precipitation in this season. The performance of the present simulation was therefore at the same order as that obtained by Soldevilla-Martínez et al. (2013) who used DSSAT to simulate different tillage systems and crop rotations under rainfed conditions in Spain. They found that the model simulated well the grain yield and biomass of barley and tended to overestimate both outputs for the conventional tillage and no-tillage systems. A study conducted by Liu et al. (2011) concluded that the model is having trouble in tracking the change in the soil physical properties over time caused by compaction, soil erosion and consolidation, and that finding was supported by Joshi et al., 2017.

Crop profitability in response to tillage over two years

Table 5. Comparison of gross margins of wheat and barley under different tillage treatments over the two growing seasons

Crop	Location and Season	Tillage	Total variable costs \$ ha^{-1}	Total income \$ ha^{-1}	Gross margin \$ ha^{-1}
Barley	Barrani (2017/2018) season	ZT	56.39	66.92	10.53
		CT	58.07	25.47	-32.6
	Matrouh (2018/2019) season	ZT	58.43	63.69	5.26
		CT	84.79	87.00	2.20
	El-Neguilla (2018/2019) season	ZT	138.46	303.08	165.33
		CT	202.32	439.58	237.25
	Barrani (2018/2019) season	ZT	116.03	236.50	120.47
		CT	125.03	207.07	82.66
Wheat	Matrouh (2018/2019) season	ZT	77.61	102.64	25.03
		CT	131.32	219.10	87.78
	El-Neguilla (2018/2019) season	ZT	150.08	320.04	169.96
		CT	254.30	576.90	322.60
	Barrani (2018/2019) season	ZT	105.02	184.86	79.84
		CT	122.62	181.86	59.24

The estimated mean of total cost, total income and gross margins for each treatment are presented in Table (5). In the first season ZT treatment was more profitable than CT treatment with an increase in the gross margins from -32.6 to 10.53 \$ ha^{-1} for barley. However, in the second season ZT was more profitable in Matrouh for barley and in

Barrani for barley and wheat. In El-Neguilla location, CT treatment had a gross margins almost double that recorded by ZT treatment for both crops because of the high grain yield produced in this location. The highest gross margins of 322.60 \$ ha^{-1} was recorded in El- Neguilla for the wheat crop under the CT treatment.

CONCLUSION

Barley and wheat yields are erratic in the rainfed area of the NWC of Egypt due to a highly year to year variable precipitation. Comparison of the two years revealed that higher yields were recorded in the second season due to a high and well distributed above average amount of precipitation. Two of the three studied locations failed to produce any yield in the first season due to the severe drought condition. In this year ZT produced a higher barley yield as compared to the CT. Long term study should be conducted to measure the effectiveness of the ZT system on the crop performance and profitability. Farmers will be keen to eliminate plowing when they feel that it saves their time and money.

ACKNOWLEDGMENTS. This research was conducted as a part of the project "Implementation of conservation agriculture systems to improve the productivity of small grains (wheat and and barley) and soil characteristics in the Arab countries funded by the Arabian Center of Studies in Arid zones and Drylands (ACSAD).

REFERENCES

Ali, M.B.& El-Sadek, A.N. 2016. Evaluation of Drought Tolerance Indices for Wheat (*Triticum aestivum* L.) under Irrigated and Rainfed Conditions. *Communications in Biometry and Crop Science* **11**(1),77–89.

Anikwe, M.A.N. & Ubochi, J.N. 2007. Short-term changes in soil properties under tillage systems and their effect on sweet potato (*Ipomea batatas* L.) growth and yield in an Ultisol in south-eastern Nigeria. *Soil Research* **45**(5), 351–358.

Araya, A., Kisekka, I., Gowda, P.H. & Prasad, P.V. 2017. Evaluation of water-limited cropping systems in a semi-arid climate using DSSAT-CSM. *Agricultural Systems* **150**, 86–98.

Babel, M.S., Deb, P. & Soni, P. 2019. Performance evaluation of AquaCrop and DSSAT-CERES for maize under different irrigation and manure application rates in the Himalayan region of India. *Agricultural Research* **8**(2), 207–217.

Banger, K., Nafziger, E.D., Wang, J., Muhammad, U. & Pittelkow, C.M. 2018. Simulating nitrogen management impacts on maize production in the U.S. Midwest. *PLos One* **13**(10). e0201825. https://doi.org/10.1371/journal.pone.0201825

Bescansa, P., Imaz, M.J., Virto, I., Enrique, A. & Hoogmoed, W.B. 2006. Soil water retention as affected by tillage and residue management in semiarid Spain. *Soil and Tillage Research* **87**(1), 19–27.

Busari, M.A., Kukal, S.S., Kaur, A., Bhatt, R. & Dulazi, A.A. 2015. Conservation tillage impacts on soil, crop and the environment. *International Soil and Water Conservation Research* **3**, 119–129.

Busari, M.A. & Salako, F.K. 2012. Effect of tillage and poultry manure application on soil infiltration rate and maize root growth in a sandy Alfisol. *Agro-science Journal of Tropical Agriculture, Food, Environment and Extension* **11**, 24–31.

Cookson, W.R., Murphy, D.V. & Roper, M.M. 2008. Characterizing the relationships between soil organic matter components and microbial function and composition along a tillage disturbance gradient. *Soil Biology and Biochemistry* **40**, 763–777.

El-Sadek, A.N. & Salem, E.M.M. 2016. Simulation of wheat yield using the RZWQM as affected by supplemental irrigation in the North Western Coast of Egypt. *Egyptian Journal of Agronomy* **38**(2), 279–292.

Fayed, T.B., El-Sarag, E.I., Hassanein, M.K. & Magdy, A. 2015. Evaluation and prediction of some wheat cultivars productivity in relation to different sowing dates under North Sinai region conditions. *Annals of Agriculture Science* **60**, 11–20.

Fenshol, R. & Rasmussen, K. 2011. Analysis of trends in the Sahelian 'rain-use efficiency' using GIMMS NDVI, RFE and GPCP rainfall data. *Remote Sensing of Environment* **115**, 438–451.

Ferreras, L.A., Costa, J.L., Garcia, F.O. & Pecorari, C. 2000. Effect of no-tillage on some soil physical properties of a structural degraded Petrocalcic Paleudoll of the southern 'Pampa' of Argentina. *Soil and Tillage Research* **54**(1–2), 31–39.

Godwin, D.C., Rithie, J.T. Singh, U. & Hunt, L. 1989. A User´s Guide to CERES Wheat-v2.10. International Fertilizer Development Center, Muscle Schoals, Al, 89 pp.

Gomaa, M.A., Radwan, F.I., Moselhy, N.M.M. & Abd-El-Kader, S.E. 2013. Evaluation of different rainfed barley genotypes across variable environments in Egypt Using GGE biplot analysis. *Journal of Advances in Agricultural Researches* **18**(4), 796–809.

Harb, O.M., Abd El-Hay, G.H., Hager, M.A. & Abou El-Enin, M.M. 2016. Calibration and Validation of DSSAT V.4.6.1, CERES and CROPGRO Models for Simulating No-Tillage in Central Delta, Egypt. *Agrotechnology* **5**, 143. doi:10.4172/2168-9881.1000143

Hemmat, A & Eskandari, I. 2004. Conservation tillage practices for winter wheat–fallow farming in the temperate continental climate of north-western Iran. *Field Crops Research* **89**, 123–133.

Hemmat, A. & Eskandari, I. 2006. Dryland winter wheat response to conservation tillage in a continuous cropping system in northwestern Iran. *Soil &Tillage Research* **86**, 99–109.

Hoogenboom, G., Jones, J.W., Wilkens, P.W., Porter, C., Boote, K., Hunt, L.D., Singh, U., Lizaso, J.I., White, J.M., Uryasev, O., Royce, F., Ogoshi, R., Gijsman, H., Tsuji, G., Koo, J., Jones, J.W., Wilkens, P., Porter, C., Hunt, L., White, J.L., Royce, F., Tsuji, G & Koo, J.C. 2012. Decision support system for agrotechnology transfer (DSSAT) version 4.5 [CD-ROM]. University of Hawaii, Honolulu, Hawaii.

Jabro, J.D., Sainju, U.M., Stevens, W.B., Lenssen, A.W. & Evans, E.G.2009. Long-term tillage influences on soil physical properties under dryland conditions in northeastern Montana, *Archives of Agronomy and Soil Science* **55**(6), 633–640. doi: 10.1080/03650340902804316

Jiang, Y., Zhang, L., Zhang, B., He, C., Jin, X. & Bai, X. 2016. Modeling irrigation management for water conservation by DSSAT-maize model in arid northwestern China. *Agricultural water management* **177**, 37–45.

Jones, J.W., Hoogenboom, G., Porter, C.H., Boote, K.J., Batchelor, W.D., Hunt, L.A., Wilkens, P.W., Singh, U., Gijsman, A.J. & Ritchie, J.T. 2003. The DSSAT cropping system model. *European Journal of Agronomy* **18**, 235–265.

Jordan, V.W., Leake, A.R. & Ogilvy, S.E. 2000. Agronomic and environmental implications of soil management practices in integrated farming systems. *Aspects of Applied Biology* **62**, 61–66.

Joshi, N., Singh, A.K. & Madramootoo, C.A. 2017. Application of DSSAT Model to Simulate Corn Yield under Long-Term Tillage and Residue Practices. *Transactions of the ASABE* **60**(1), 67–83.

Kassam, A., Friedrich, T., Derpsch R. & Kienzle, J. 2015. Overview of the Worldwide Spread of Conservation Agriculture. *Field Actions Science Reports* [Online], Vol. **8** URL: http://journals.openedition.org/factsreports/3966

Kheir, A.M.S., El Baroudy, A., Aiad, M.A., Zoghdan, M.G., Abd El-Aziz, M.A., Ali, M.G.M. & Fullen, M.A. 2019. Impact of rising temperature, carbon dioxide concentration, and sea level on wheat production in North Nile Delta. *Science of the Total Environment* **651**, 3161–3173.

Khurshid, K., Iqbal, M., Arif, M.S. & Nawaz, A. 2006. Effect of tillage and mulch on soil physical properties and growth of maize. *International Journal of Agriculture and Biology* **5**, 593–596.

Li, Z.T., Yang, J.Y., Drury, C.F. & Hoogenboom, G. 2015. Evaluation of the DSSAT-CSM for simulating yield and soil organic C and N of a long-term maize and wheat rotation experiment in the Loess Plateau of Northwestern China. *Agricultural Systems* **135**, 90–104.

Liu, H.L., Yang, J.Y., Drury, C.F., Reynolds, W.D., Tan, C.S., Bai, Y.L., He, P., Jin, J. & Hoogenboom, G. 2011. Using the DSSAT-CERES-Maize model to simulate crop yield and nitrogen cycling in fields under long-term continuous maize production. *Nutrient Cycling in Agroecosystem* **89**, 313–328.

Mahmoud, A.K. & Meselhy, A.A. 2019. Influence of different heat units and supplementary irrigation on barley production under Matrouh conditions-Egypt. *Journal of Natural Sciences Research* **9**(14) 21–30.

Malik, W. & Dechmi, F. 2019. DSSAT modelling for best irrigation management practices assessment under Mediterranean conditions. *Agricultural water management* **216**, 27–43.

Martınez, E., Fuentes, J., Silva, P., Valle, S. & Acevedo, E. 2008. Soil physical properties and wheat root growth as affected by no-tillage and conventional tillage systems in a Mediterranean environment of Chile. *Soil and Tillage Research* **99**, 232–244.

Masek, J. & Novak, P. 2018. Influence of soil tillage on oats yield in Central Bohemia Region. *Agronomy research* **16**(3), 838–845. https://doi.org/10.15159/AR.18.110

Mhazo, N., Chivenge, P. & Chaplot, V. 2016. Tillage impact on soil erosion by water: Discrepancies due to climate and soil characteristics. *Agriculture, Ecosystems & Environment* **230**, 231–241.

Mokrikov, G., Minnikova, T., Kazeev K. & Kolesnikov, S. 2019. Influence of precipitation and moisture reserves on the yield of crops under different tillage. *Agronomy Research* **17**(6), 2350–2358. https://doi.org/10.15159/AR.19.202

Monneveux, P., Quillérou, E., Sanchez, C. & Lopez-Cesati, J. 2006. Effect of Zero Tillage and Residues Conservation on Continuous Maize Cropping in a Subtropical Environment (Mexico). *Plant and Soil* **279**(1–2), 95–105. doi:10.1007/s11104-005-0436-3

Morell, F.J., Lampurlanés, J., Álvaro-Fuentes, J. & Cantero-Martínez, C. 2011. Yield and water use efficiency of barley in a semiarid Mediterranean agroecosystem: Long-term effects of tillage and N fertilization. *Soil and Tillage Research* **117**, 76–84. doi: 10.1016/j.still.2011.09.002

Moret, D., Arrúe, J.L., López, M.V. & Gracia, R. 2007. Winter barley performance under different cropping and tillage systems in semiarid Aragon (NE Spain). *European Journal of Agronomy* **26**(1), 54–63. doi: 10.1016/j.eja.2006.08.007

Mrabet, R. 2008. *No-tillage systems for sustainable dryland agriculture in Morocco*. INRA, France, Fanigraph Edition, 153 pp.

Mrabet, R. 2000. Differential response of wheat to tillage management systems in a semiarid area of Morocco. *Field Crops Research* **66**(2), 165–174. doi: 10.1016/s0378-4290(00)00074-5

Murillo, J., Moreno, F., Girón, I. & Oblitas, M. 2004. Conservation tillage: long term effect on soil and crops under rainfed conditions in South-West Spain (Western Andalusia). *Spanish Journal of Agricultural Research* **2**(1), 35–43.

Murillo, J., Moreno, F., Madejón, E., Girón, I. & Pelegrín, F. 2006. Improving soil surface properties: a driving force for conservation tillage under semi-arid conditions. *Spanish Journal of Agricultural Research* **4**(1), 97–104.

Nash, J.E. & Sutcliffe, J.V.1970. River flow forecasting through conceptual models. Part 1: discussion of principles. *Journal of Hydrology* **10**, 282–290.

Ngwira, A.R., Aune, J.B. & Thierfelder, C. 2014. DSSAT modelling of conservation agriculture maize response to climate change in Malawi. *Soil and Tillage Research* **143**, 85–94.

Novak, P., Kovaricek, P., Hula, J. & Buric, M. 2019. Surface water runoff of different tillage technologies for maize. *Agronomy Research* **17**(3), 754–760. https://doi.org/10.15159/AR.19.120

Otter-Nacke, S., Ritchie, J.T., Godwinm, D.C. & Singh, U. 1991. A user's guide to CERES Barley – V210 Inter - national Fertilizer Development Center Simulation manual IFDC-SM-3, pp. 87.

Prasad, L.R.V. & Mailapalli, D.R. 2018. Evaluation of Nitrogen Fertilization Patterns Using DSSAT for Enhancing Grain Yield and Nitrogen Use Efficiency in Rice. *Communications in Soil Science and Plant Analysis* **49**(12), 1401–1417.

Piggin, C., Haddad, A., Khalil, Y., Loss, S. & Pala, M. 2015. Effects of Tillage and Time of Sowing on Bread Wheat. Chickpea, Barley and Lentil Grown in Rotation in Rainfed Systems in Syria. *Field Crops Research* **173**, 57–67.

Pittelkow, C.M., Linquist, B.A., Lundy, M.E., Liang, X., van Groenigen, K.J., Lee, J. van Gestel, N., Six, J., Venterea, R.T. & van Kessel, C.2015. When does no-till yield more? A global meta-analysis, *Field Crops Research* **183**, 156–168.

Porter, C.H., Jones, J.W., Adiku, S., Gijsman, A. J., Gargiulo, O. & Naab, J. B. 2010. Modeling organic carbon and carbon-mediated soil processes in DSSAT v4.5. *Operational Research* **10**, 247–278.

Puntel, L.A., Sawyer, J.E., Barker, D.W., Dietzel, R., Poffenbarger, H., Castellano, M.J., Moore, K.J., Thorburn, P. & Archontoulis, S.V. 2016. Modeling long-term corn yield response to nitrogen rate and crop rotation. *Frontiers in plant science* **7**, doi: 10.3389/fpls.2016.01630

Raes, D., Steduto, P., Hsiao, T.C. & Fereres, E. 2009. AquaCrop–the FAO crop model to simulate yield response to water: II. Main algorithms and software description. *Agronomy Journal* **101**, 438–447.

Rahman, M.H., Okubo, A., Sugiyama, S. & Mayland, H.F. 2008. Physical, chemical and microbiological properties of an Andisol as related to land use and tillage practice. *Soil & Tillage Research* **101**, 10–19.

Salem, E.M., Ashoub, M.A., Salem, M.O. & Hamed, M.F. 2003. Response of wheat to supplemental irrigation and fertilizer under North Western Coast of Egypt. *Zagazig Journal of Agricultural Research* **30**(4), 1343–1363.

SAS Institute, Inc. 2007. SAS Technical Report SAS/STAT Software: Changes and Enhancements User's Guide, Volume 2, Version 9.1.3, Fourth Edition, Cary, NC: SAS Institute, Inc.

Saturnino, H.M. & Landers, J.N. 2002. The Environment and Zero Tillage. APDC-FAO, Brasilia, Brazil UDC 504:631/635, CDD 631.521

Sayed, M.S., El-Sadek, A.N., Bakry, A.B., Ali, M.B., Leon, J. & Salem, E.M. 2017. QTL mapping in barley across environments in Egypt. *Egyptian Journal of Agronomy* **39**(1), 53–71.

Schwartz, R.C., Baumhardt, R.L. & Evett, S.R. 2010. Tillage effects on soil water redistribution and bare soil evaporation throughout a season. *Soil & Tillage Research* **110**, 221–229.

Silungwe, F.R., Graef, F., Bellingrath-Kimura, S.D., Tumbo, S.D., Kahimba, F.C. & Lana, M.A. 2019. Analysis of intra and interseasonal rainfall variability and its effects on pearl millet yield in a semiarid agroclimate: significance of scattered fields and tied ridges. *Water* **11**, 578. doi:10.3390/w11030578

Soldevilla-Martínez, M., Martin-Lammerding, D., Tenorio, J.L., Walter, I., Quemada, M. & Lizaso, J.I. 2013. Simulating improved combinations tillage-rotation under dryland conditions. *Spanish Journal of Agricultural Research* **11**(3), 820–832.

Soler, C.M., Bado, V.B., Traore, K., Bostick, W.M., Jones, J.W. & Hoogenboom, G. 2011. Soil organic carbon dynamics and crop yield for different crop rotations in a degraded ferruginous tropical soil in a semi-arid region: a simulation approach. *The Journal of agricultural science* **149**(5), 579–593.

Steduto, P., Hsiao, T.C., Raes, D. & Fereres, E., 2009. AquaCrop–the FAO crop model to simulate yield response to water: I. Concepts and underlying principles. *Agronomy Journal* **101**, 426–437.

Tovihoudji, P.G., Akponikpè, P.B.I, Agbossou, E.K. & Bielders, C.L. 2019. Using the DSSAT Model to Support Decision Making Regarding Fertilizer Microdosing for Maize Production in the Sub-humid Region of Benin. *Frontiers in Environmental Science* **7**, 1–15.

Tyagi, S., Singh, N., Sonkar, G. & Mall, R.K. 2019. Sensitivity of evapotranspiration to climate change using DSSAT model in sub humid climate region of Eastern Uttar Pradesh. *Modeling Earth Systems and Environment* **5**(1), 1–11.

Ucgul, M., Fielke, J.M. & Saunders, C. 2014. Three-dimensional discrete element modelling of tillage: Determination of a suitable contact model and parameters for a cohesionless soil. *Biosystems Engineering* **121**, 105–117.

Yang, X., Zheng, L., Yang, Q., Wang, Z., Cui, S. & Shen, Y. 2018. Modelling the effects of conservation tillage on crop water productivity, soil water dynamics and evapotranspiration of a maize-winter wheat-soybean rotation system on the Loess Plateau of China using APSIM, *Agricultural Systems* **166**, 111–123.

Agronomy Research **18**(4), 2391–2409, 2020
https://doi.org/10.15159/AR.20.234

Development and examination of high-performance fluidised-bed vibration drier for processing food production waste

H. Kaletnik[1], I. Sevostianov[1], V. Bulgakov[2], I. Holovach[2], V. Melnik[3], Ye. Ihnatiev[4] and J. Olt[5,*]

[1]Vinnytsia National Agrarian University of Ukraine, 3 Soniachna Str., UA21008 Vinnytsia, Ukraine
[2]National University of Life and Environmental Sciences of Ukraine, 15 Heroyiv Oborony Str., UA03041 Kyiv, Ukraine
[3]Kharkiv Petro Vasylenko National Technical University of Agriculture, 44 Alchevskih Str., Kharkiv, UA61002, Ukraine
[4]Dmytro Motornyi Tavria State Agrotechnological University, 18B, Khmelnytsky Ave, UA72310 Melitopol, Zaporozhye Region,Ukraine
[5]Estonian University of Life Sciences, Institute of Technology, 56 Kreutzwaldi Str., EE51006 Tartu, Estonia
[*]Correspondence: jyri.olt@emu.ee

Abstract. Drying and processing wet particulate food production waste, such as distillery dreg, brewer's grains, beet pulp, spent coffee and barley slurry etc. for their further use as cattle fodder or fuel is an important and topical problem, which needs effective solutions. As a solution of the problem, the authors have developed improved equipment and a fluidised bed vibration drier, which ensures reaching the required output of the work process and final moisture content in the waste at a minimum power and material intensity and features the combination of the high feasibility with the high reliability of design. In order to validate the improved drying work process together with the optimum parameters of the vibration drier, theoretical investigations based on the mathematical model of the process developed by the authors have been carried out. The process of the vibration drier's frame oscillating together with the waste has been examined, which has resulted in the generation of the differential equation that analytically describes the said process. The work process under consideration has been researched into from the thermophysical point of view using the specific initial data typical for the specific food producer. The research has resulted in obtaining the following design and process parameters of the vibration drier, in particular, for its heating pipes: diameter $r_t = 0.1$ m; length $l_t = 5$ m; number $n_t = 20$, heat-transfer factor $K_p = 30$ and the final temperature of the dried food production waste $t_{o2} = 80$ °C. The listed parameters provide for reaching the required final moisture content in the dried food production waste. Also, new relations have been generated for determining the principal process parameters of the improved drier (productive capacity, heat consumption, mass of heat carrier, waste conveyance speed, sizes and masses of the drier's actuating elements). The obtained relations can be applied in the further theoretical and experimental research on the drier as well as the development of standard methods for its design and calculation.

Key words: drying, fluidized bed drier, mathematical modeling, moisture, reactor, vibration, waste.

INTRODUCTION

In the food producing companies of Ukraine and a number of other countries, the by-products generated as a result of food production, such as distillery dreg, brewer's grains, beet pulp, spent coffee and barley slurry, are mostly dumped to specially allocated landfills, which results in environmental pollution. Processing such waste in order to produce either biological fodder supplements or fuel requires considerable investment and operating costs (Filonenko & Grishin, 1971; Sevastianov, 2013; Ma et al., 2018; Kliuchnikov, 2019). In European countries and the US, such processing is generally implemented in the form of water removal in decanter centrifuges (McKenna, 1986; Beránek & Kolařik, 2014; Altieri et al., 2020), dehydrating in vacuum driers or with the use of bioreactors (Atkinson & Mavituna, 1991; Tribuzi & Laurindo, 2014; Antal, et al., 2015). That said, the mechanical water removal with the use of the most common equipment, such as screw presses and decanter centrifuges, is unable to deliver a final moisture content of less than 74–76% in the processed waste, which implies need in its additional drying prior to using it as animal fodder or fuel and results in the considerable increase of the total power consumption rate of the work process (Panfilov et al., 2001; Sevostianov, 2013). With regard to biological reactors, it has to be noted that they are rather complex and bulky process systems, too expensive for the majority of the national food and processing industry companies. In the papers (Boyce, 1965; Bruce & Giner, 1993; Filonenko & Grishin, 1971; Hemis, et al, 2012; Giner, 2019), the high efficiency of the vibration impact water removal from the above-mentioned food by-products in process units with hydraulic-pulse drives is proved theoretically and experimentally. That technique ensures reducing the final moisture content in the food production waste from the initial value of $U_{n.o}$ = 90–95% to $U_{к.o}$ = 20–25% (moisture content after dehydration), the energy intensity of the process staying at about 7 (kW h) t^{-1} and a daily output reaching up to 1900 t of dehydrated waste (Sevostianov, 2013; Sevostianov et al., 2015). Nevertheless, even when applying the latter technique, the dehydrated waste still needs to be additionally dried to a moisture content level of about $U_{c.o}$ = 8% in order to provide for its long-term storage (Atkinson, 1979).

In view of the above-stated circumstances, it is a topical problem to improve the methods and equipment used for drying food production waste in order to provide it with the necessary properties at the minimum energy intensity and the targeted production rate.

According to the results of the investigations presented in a number of papers, the air-fluidised and vibration-fluidised bed apparatus are among the most efficient types of driers. In comparison with the drum, tunnel, tower, continuous-belt and roll driers, they maintain a continuous and higher-output work process, in which the targeted values of the final moisture content in the processed material are achieved (Sazhin, 1984; Daud, 2008; Ovchinnikov et al., 2009; Aboltins & Upits, 2012; Bulgakov et al., 2018). The air-fluidised bed and vibration-fluidised bed apparatus include atomizing (spray), convection, vibrating (shaker), spiral, cyclone and flash driers as well as pneumatic pipe driers (Filonenko & Grishin, 1971; Mujumdar, 2014).

In the paper (Ostrikov et al, 2006), various designs of atomizing driers are presented: with central involute heat carrier supply (direct-flow); with central heat carrier supply and separate removal of the gas and the product; with uniform distribution of the supplied gas over the cross-section via a gas-distributing grill; with radial (peripheral) heat carrier supply and central exhaust. The listed equipment delivers a sufficiently high productive capacity of the work process, but features a rather high energy intensity due to the fact that the motion of waste particles in the operating space is created with the use of the most energy-intensive method of pneumatic transport (design velocity of material particles is 6–12 m s^{-1}), while the removal of water from them is achieved by burning expensive organic heat carriers (Ostrikov et al., 2006). Moreover, its shortcomings include the frequent clogging of the pneumatic nozzles in the driers as well as their rapid abrasive wear (Sazhin, 1984).

During the operation of vibration driers (El Hor et al., 2005; Palamarchuk et al., 2018; Bulgakov et al., 2020), the material in the process chamber passes, as a result of the latter's oscillations, into the state of the fluidised bed or the vibratory fluidised bed (Goncharevich, 1977; Handayani et al., 2017; Hoffman et al., 2017; Lehmann et al., 2019), in which the particles mutually depart from each other, get thoroughly mixed, the heat carrier efficiently enters the space between particles and carries away the moisture. This type of the equipment under consideration is, in the authors' opinion, the most promising one, as it delivers the required values of the final moisture content $U_{c.o}$ = 8% with the minimum consumption of energy and time. However, the above equipment has a disadvantage of the complex and material-intensive design. Another drawback is that the majority of industrial vibration driers falls into the category of batch-type equipment, which implies great amounts of time being spent for the batch loading and unloading operations, while these operations are performed with the assistance of auxiliary machines outside the main process cycle, and that has a negative impact on the productivity of the process.

Also, (Panfilov et al., 2001; Wang, et al., 2011; Yogendrasasidhar & Setty, 2019) contains several designs of pneumatic driers, in which the fluidised or vibratory fluidised bed is created with the use of hot heat carrier streams passing through the material pulverized by a rotating disk: pneumatic transport with additional intensive heating (see the note above). The dispersal process alone consumes 50–60 kW per тon of pulverized material (Ostrikov et al., 2006). The gaseous heat carrier flow rate is 8,000 m^3 h^{-1} (Sazhin, 1984). Another drawback is the high possibility of the disk holes being clogged with particles of the material. Even lower expectations are with regard to the pneumatic driers, in which the processed material is transported in a continuous flow along the bearing surface of the process chamber. In these driers, the heat carrier is fed through the holes in the bearing surface, passes through the bed of the material bringing it into the fluidised or vibratory fluidised state (Mohseni et al., 2019).

The spray drier presented in (Panfilov et al., 2001; Ostrikov et al., 2006; Robaina-Mesa & Chanfrau, 2019; Wawrzyniak et al., 2020) in which mixed flows of the processed material and the heat carrier are used, features considerable design complexity, a high material intensity and large dimensions (unit comprises up to 20 separate apparatus), while the spraying requires the supply of pressure at a level of 10–20 MPa (Ostrikov et al., 2006). It is worth mentioning that the auxiliary equipment used for preparing the heat carrier, removing processed material particles from it and separating the liquid and gaseous phases of the used heat carrier is also employed in the other apparatus analysed earlier in this paper.

The driers discussed in the paper (Dufour, 2006), that is, the driers with spiral channels, through which the mixture of the processed material and the heat carrier passes, cyclone driers and two-stage pipe drier installations have specific areas of application and high energy consumption (drying medium flow rate - 12,000–15,000 m^3 h^{-1}), while the two latter types - large dimensions as well.

Moreover, the power input required for the removal of water from the waste under consideration with the use of the known designs of rotary drum driers amounts to about 2,500 kW h per ton of removed liquid, spray driers - 2,250 kW h t^{-1}, double-drum driers - 1,300 kW h t^{-1}, vacuum dryers - 740–760 kW h t^{-1}. The listed figures indicate that the energy consumption rates in the work processes of food production waste drying with the use of the known designs of driers are very high and, consequently, have to be reduced.

Overall, the analysis that has been carried out by the authors has brought them to a conclusion that the currently known drying machinery used in integrated process facilities for the recovery of food production waste needs improvement in the direction of cutting down the power intensity of the work process, reducing the dimensions and increasing the operational reliability of the equipment.

The aim of this research is to provide for achieving the minimum power intensity of the work process, in which the food production waste is dried for its further recycling, by means of developing a new design of the vibration drier with a fluidised bed and also theoretically and experimentally proving its rational design and process parameters.

MATERIALS AND METHODS

For the purpose of developing a high-efficiency vibration drier with fluidised bed and analysing its properties, the authors have applied the methods of comparison, criterion scores and optimisation, the principles and relations of the theoretical mechanics, fluid mechanics, heat engineering, the theory of food production process and apparatus engineering as well as the theory of vibration and vibratory percussion equipment.

The authors have developed a new fluidised bed drier, which provides for efficiently drying food production waste in batches.

In Fig. 1, the design and process schematic model is presented for the new vibration drier designed for processing food production waste. The work process of food production waste drying takes place as follows. The waste is fed into the drier under consideration immediately after its preliminary four-stage mechanical dehydration in the unit described in (Ward, 2002; Ruiz Celma et al., 2012; Sevostianov & Luchik, 2017), after

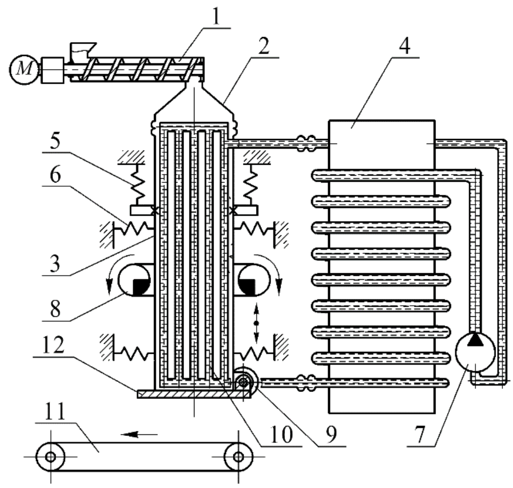

Figure 1. Design and process schematic model of vibration drier for processing food production waste: 1 – auger feeder; 2 – conical top; 3 – casing shell, 4 – heat exchanger on process tank of primary production process; 5 – vertical springs; 6 – horizontal springs; 7 – heat exchanger pump; 8 – unbalance vibration exciter; 9 – electric motor; 10 – heating pipes; 11 – belt conveyor; 12 – discharge slide valve.

which its moisture content does not exceed the earlier indicated target value of $U_{к.o}$ = 20–25% (Sevostianov & Luchik, 2017). In the process of feeding, the casing shell of the drying apparatus is filled with food by-products by the auger feeder 1, the slide valve 12 being closed.

The process of feeding the waste into the vibration drier´s in casing shell 3 continues until the pressure transducer installed on the inner surface of the slide valve 12 sends the signal that activates the respective relay switch, after which the auger feeder 1 stops operating. The heating pipes 10 form a rigid structure, which is connected via bellow rubber tubes to the heat exchanger on the process tank 4. The circulation of the heat carrier along the pipes 10 and the pipe coil is maintained by the pneumatic or hydraulic pump 7, hence, the preparation of the heat carrier for food production waste drying is performed virtually without any energy input. The direction of the heat carrier flow supplied by the pump 7 and guided into the pipes 10 is shown with the arrows. The heat energy is transferred from the pipes 10 to the batch of food production waste fed into the spaces between them, which ensures the efficient removal of the liquid phase as in the peripheral, so in the middle layers of the batch. Moreover, in order to intensify the drying process, the shell 3 with the food by-products is set in oscillatory motion with the use of the unbalance vibration exciters 8. For that purpose, the casing shell 3 is suspended on vertical springs 5 and horizontal springs 6, while its freedom of movement with respect to the auger feeder 1 is facilitated with the use of a bellow rubber pipe.

Due to the oscillatory motion of the casing shell 3, the particles of the food production waste batch inside the shell 3 become vibration-fluidised, which facilitates more active and less energy-intensive removal of the liquid phase from them. The said phase escapes outside the shell through the small holes in the walls of the casing shell 3 covered inside by filter gauze (not shown in the schematic model). When the electronic moisture meter senses that the pre-set value $U_{c.o}$ = 8% of the final moisture content in the food production waste batch in the casing shell is reached, it sends the command signal that starts the stepping motors 9, which turn and open the slide valves 12. The batch of dehydrated food by-products is poured out onto the conveyor belt 11, then the slide valves 12 are again closed and the auger feeder 1 is started. The casing shell 3 is filled with a new batch of food production waste and the next drying cycle begins.

Depending on the type of waste, its initial moisture content at the drier's inlet equal to $U_{к.o}$ = 20 – 25% and the temperature of the heat carrier in the pipes, in some instances the continuous mode of operation can be established, when the food production waste continuously passes through the casing shell 3 obtaining in this process the pre-set final moisture content of $U_{c.o}$ = 8%. For that purpose, by means of experiments with turning the slide valves 12, the area of the bottom passage in the casing shell is adjusted to the required size, which governs the time of the waste staying inside the shell.

VIBRATION DRIER MODEL

The advantages of the proposed vibration drier in comparison with the other earlier described equipment for drying with the use of the air-fluidised and vibration-fluidised bed are: the simplicity and compactness of its design, multipurpose application, absence of the danger of clogging the passage spaces in the casing shell, the efficient transfer of heat to the particles of the material throughout the whole cross-section of the shell, the simplicity and fail-safety of the auxiliary heat carrier preparation equipment, the absent need for cleaning the heat carrier and separating it into phases and the most important feature - the minimum input of energy for the drying process itself due to the utilisation of the heat output from the primary process.

It is necessary to analyse the principal efficiency parameters of the vibration drier operation and establish their relations with the operation and design parameters of the equipment under investigation as well as the physical and mechanical properties of the processed waste.

In order to ensure that the particles of the processed batch of food production waste situated in the casing shell of the vibration drier pass into the vibration-fluidised state, it is necessary to meet the following condition (Bezbakh & Bakhmutyan, 2006):

$$\ddot{x} \geq (2 \div 3)\mathrm{g}, \tag{1}$$

where $\ddot{x}$ – acceleration in the oscillatory motion performed by the vibration drier casing shell; g – acceleration of gravity.

The acceleration in the oscillatory motion of the vibration drier casing shell specified by (1) can be determined basing on the generation of a mathematical model for the shell's oscillations in the longitudinal and vertical plane. Within the framework of the said mathematical model, it is necessary to generate the differential equation of the vertical translational oscillations performed by the vibration drier casing shell suspended on the springs during the operation of the drier's unbalance vibration exciter, in order to obtain the relation between the above-mentioned acceleration and the design and kinematic parameters of the vibration drier under consideration.

For the development of the mathematical model, i.e. to obtain the required differential equation of motion for the vibration drier casing shell, it is necessary, first of all, to generate the equivalent schematic model.

In this process, the following tentative assumptions are made. First of all, the elastic forces generated by the bellow pipes that connect the vibration drier casing shell and the auger feeder are disregarded as negligible. Moreover, taking into account the fact that the eccentric weights of the vibration exciter have identical geometric and dynamic parameters, but rotate with mutually opposite senses, the oscillations of the vibration drier casing shell in the horizontal plane can be neglected. The above-mentioned equivalent schematic model is shown in Fig. 2.

In this instance, the vibration drier casing shell is considered in the form of a separate body mounted in the frame on several springs and capable of moving in the vertical plane up and down during the operation of the vibration exciters rigidly attached to it. In Fig. 2, the vibration drier casing shell is shown in the position at the random instant of time t during its translational vertical oscillation. It can be assumed that the vibration drier casing shell is shown in the equivalent schematic model in its uppermost position. In the equivalent schematic model, the vertical axis x is designated, which is aligned with the longitudinal symmetry axis of the casing shell and has its origin at the point O that coincides with the bottom end of the casing shell, when the latter is in its equilibrium position. Thus, it is assumed that the vibration drier's casing shell is in its equilibrium position, when its side springs $D_i L_i$ ($i = \overline{1,4}$) on both sides of it are aligned horizontally (that is, the points of attachment L_3, D_3, L_4 and D_4 of the lower lateral springs L_3D_3 and L_4D_4 are level with the point O to an accuracy of the static deformation of the said springs). Accordingly, when the vibration drier casing shell moves up or down from its equilibrium position, all the lateral springs $D_i L_i$ ($i = \overline{1,4}$) expand, then, when the casing shell moves back to the equilibrium position, they contract. The lateral spring attachment points L_1, L_2, L_3 and L_4 are situated on the frame.

Since the point O is designated as the origin of the Ox one-dimensional coordinate system, it can be stated that the vibration drier casing shell performs translational vertical oscillations along the above-mentioned axis.

In view of that, the position of the vibration drier casing shell at the random instant of time t is specified by the coordinate x that shows the displacement of the casing shell from the equilibrium position. In Fig. 2 the case is shown, when the vibration drier casing shell is situated at the position that is higher than the equilibrium position exactly by the x value. In this instance, $0 \leq x \leq x_{max}$, where x_{max} – amplitude of oscillations performed by the vibration drier casing shell. In the cases, when the vibration drier casing shell is situated below the equilibrium position, the following condition takes place: $-x_{max} \leq x \leq 0$.

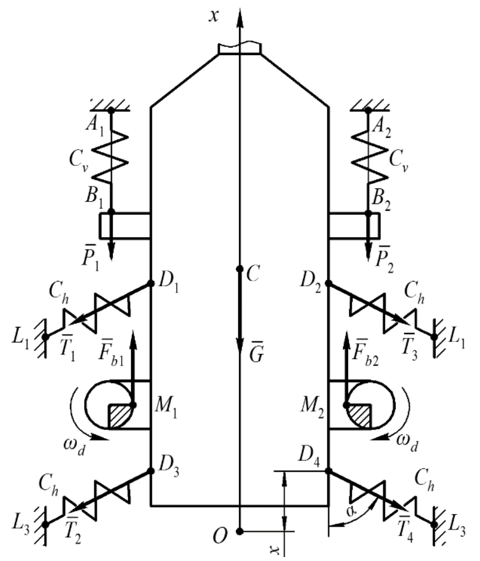

Figure 2. Equivalent schematic model of oscillations performed by vibration drier casing shell.

The vertical springs A1B1 and A2B2 (A1, A2 and B1, B2 – points of attachment of the vertical springs to the frame and the vibration drier casing shell, respectively) contract, when the casing shell moves up, during its down movement they expand. The maximum magnitude of their deformation is equal to two amplitudes of the casing shell oscillations, that is $2x_{max}$. The stiffness factors of the springs are assigned the following designations: C_{vi} $(i = \overline{1,2})$ for vertical and C_{hi} $(i = \overline{1,4})$ for horizontal springs.

Hence, the elastic forces generated by all the above-mentioned springs are restoring forces in the oscillatory process under consideration.

The oscillations of the vibration drier casing shell are performed under the action of the two unbalance vibration exciters generating centrifugal inertial forces, the vertical components of which act as the perturbing forces in the said oscillations.

The equivalent schematic model features the following forces:

$\bar{F}_{b1}, \bar{F}_{b2}$ – perturbing forces of the forced translational oscillations of the vibration drier casing shell (vertical components of the centrifugal inertial forces generated by the rotation of the vibration exciter eccentric weights and applied at the points M_1 and M_2, respectively);

$\bar{P}_1$, $\bar{P}_2$ – elastic forces generated by the longitudinal deformation of the vertical springs A_1B_1 and A_2B_2 and applied at the points B_1 and B_2, respectively;

$\bar{T}_i$ $(i = \overline{1,4})$ – elastic forces generated by the longitudinal deformation of the horizontal springs D_iL_i $(i = \overline{1,4})$ and applied at the points D_i $(i = \overline{1,4})$, respectively;

$\bar{G}$ – weight force of the vibration drier casing shell together with the processed food production waste applied at the centre of mass of the vibration drier casing shell (point *C*).

Fig. 2 also shows the vertical displacement *x* of the vibration drier casing shell from its equilibrium position at the random instant of time *t*.

Further, it is necessary to determine the magnitudes of all the forces shown in the equivalent schematic model (Fig. 2).

It is obvious that the forces F_{bi} (I = 1,2) that are the vertical components of the centrifugal inertial forces generated by the rotation of the vibration exciter eccentric weights can be found with the use of the following formula:

$$\bar{F}_{bi} = m_d \cdot r_d \cdot \omega_d \cdot k_d \cdot \cos\left(\hat{\omega_d} \cdot t\right), (i = 1{,}2), \tag{2}$$

where m_d – mass of the eccentric weight; r_d – radius of the circle described by the eccentric weight in its rotation; ω_d – angular velocity of rotation of the vibration exciter drive shaft; k_d– number of eccentric weights in the vibration exciter; *t* – current time.

In case the revolutions per minute of the eccentric weight are set at n_d, while the diameter of the circle described by the eccentric weight in its rotation is equal to d_d, also taking into account that:

$$\omega_d = \frac{\pi \cdot n_d}{30}, \tag{3}$$

the following formula is obtained for finding the magnitudes of the forces $\bar{F}_{bi}$:

$$F_{bi} = \frac{\pi^2 \cdot m_d \cdot d_d \cdot n_d^2 \cdot k_d}{1{,}800} \cdot \cos\left(\frac{\pi \cdot n_d}{30} \cdot t\right), (i = 1{,}2), \tag{4}$$

The forces P_i (i = 1,2) can be determined with the use of the following expression:

$$P_i = C_v \cdot n_{ts}\left(x + l_{ts}\right), (i = 1{,}2), \tag{5}$$

where C_v – coefficient of elastic stiffness of the vertical spring; n_{ts} – number of spring turns in one elastic suspension; *x* – amount of the longitudinal deformation of the vertical spring; l_{ts} – amount of the static longitudinal deformation of the vertical spring.

For the purpose of determining the magnitudes of the elastic forces $\bar{T}_i$ ($i = \overline{1,4}$) generated by the horizontal springs, it should be noted that their longitudinal deformations l_t at the random instant of time t, are, as can be seen in the equivalent schematic model (Fig. 2), equal to:

$$l_T = \sqrt{x^2 + \left(l_{hs} + l_{shs}\right)^2} - l_{hs}, \tag{6}$$

where l_{hs} – design length of the horizontal spring (in its load-free state); l_{shs} – static deformation of the horizontal spring.

Accordingly, the magnitude of the force T_i ($i = \overline{1,4}$) can be determined with the use of the following expression:

$$T_i = C_h \cdot n_{ss}\left(\sqrt{x^2 + \left(l_{hs} + l_{shs}\right)^2} - l_{hs}\right), (i = \overline{1,4}), \tag{7}$$

where C_h – coefficient of elastic stiffness of the horizontal spring; n_{ss} – number of horizontal springs in one elastic suspension.

At the same time, the vertical components of the forces T_i ($i = \overline{1,4}$), that is, their projections on the axis *Ox* are equal to:

$$T_i = C_h \cdot n_{ss}\left(\sqrt{x^2 + \left(l_{hs} + l_{shs}\right)^2} - l_{hs}\right)\cdot \cos\alpha \,,\ (i = \overline{1{,}4}), \tag{8}$$

where α – angle of inclination of the horizontal springs with respect to the axis O_x at the random instant of time t (Fig. 2).

Further, after the cosα value is determined and substituted into the expression (8), the following final expression is obtained for the magnitudes of the forces T_i $(i = \overline{1{,}4})$ that cause the translational vertical oscillations of the vibration drier casing shell:

$$T_i = C_s \cdot n_{ss}\left(\sqrt{x^2 + \left(l_{hs} + l_{shs}\right)^2} - l_{hs}\right)\cdot \frac{x}{\sqrt{x^2 + \left(l_{hs} + l_{shs}\right)^2}}\,,\ (i = \overline{1{,}4}), \tag{9}$$

The force of the weight G of the vibration drier casing shell together with the process material is equal to:

$$G = m \cdot g\,, \tag{10}$$

where m – total mass of the vibration drier casing shell, processed waste and all other vibrating members of the structure; g – acceleration of gravity.

Further, basing on the generated equivalent schematic model (Fig. 2), the following equation of motion in vector notation can be written for the oscillating vibration drier casing shell together with the processed waste:

$$m\overline{a} = \overline{F}_{b1} + \overline{F}_{b2} + \overline{P}_1 + \overline{P}_2 + \overline{T}_1 + \overline{T}_2 + \overline{T}_3 + \overline{T}_4 + \overline{G}\,, \tag{11}$$

where $\overline{a}$ – acceleration of the oscillating casing shell of the vibration drier.

Taking into account the expressions (4), (5), (9) and (10) as well as assuming that the respective forces from different springs are equal to each other, the following differential equation of the oscillations performed by the vibration drier casing shell is derived from the obtained vector Eq. (11) in its projection on the Ox axis:

$$\begin{aligned} m\ddot{x} = {} & \frac{\pi^2 \cdot m_d \cdot d_d \cdot n_d^2 \cdot k_d}{900} \cdot \cos\left(\frac{\pi \cdot n_d}{30} \cdot t\right) - 2C_s \cdot n_{ts}\,(x + l_{ts}) - \\ & -4C_s \cdot n_{ss}\left(\sqrt{x^2} + (l_{hs} + l_{shs})^2 - l_{hs}\right) \cdot \frac{x}{\sqrt{x^2 + (l_{hs} + l_{shs})^2}} - mG, \end{aligned} \tag{12}$$

from which, after the transformations, the following final expression is obtained:

$$\begin{aligned} \ddot{x} + \frac{2}{m}\Bigg[& C_s \cdot n_{ts}(x + l_{ts}) + 2C_s \cdot n_{ss}\left(\sqrt{x^2 + (l_{hs} + l_{shs})^2} - l_{hs}\right) \times \\ & \times \frac{x}{\sqrt{x^2 + (l_{hs} + l_{shs})}}\Bigg] + \mathrm{g} = \frac{\pi^2 \cdot m_d \cdot d_d \cdot n_d^2 \cdot k_d}{900m} \cdot \cos\left(\frac{\pi \cdot n_d}{30} \cdot t\right). \end{aligned} \tag{13}$$

In order to solve the differential Eq. (13) numerically, it is necessary to specify the design and kinematic parameters of the vibration drier. First of all, the mass parameters have to be defined.

The required parameters of the food production waste drying work process have to be examined and defined. For that purpose, as an example, the initial mass parameters used in a real food production waste processing plant (Sevostianov & Luchik, 2017) are taken under consideration.

First, the total waste mass m_o has to be determined proceeding from the daily mass m_c of the food by-products processed in the plant with the use of the vibration drier of the discussed design. m_o is the mass after the four-stage mechanical dehydration

(Tribuzi & Laurindo, 2014) to a moisture content of $U_{k.o} = 25\%$, i.e. the mass of the waste that enters the vibration drier. For the calculation, the following expression is used:

$$m_o = m_c - \frac{U_{n.o} - U_{k.o}}{100} = m_c - m_c \frac{95 - 25}{100} = 0.3 \cdot m_c, \tag{14}$$

where $U_{n.o} = 95\%$ – initial moisture content in the food by-products.

The total time t_z spent for feeding the food production waste with a mass of m_o into the vibration drier under consideration can be found taking into account the production rate Q_s of the auger feeder with the use of the following formula (Panfilov et al., 2001):

$$t_z = \frac{m_o}{Q_s} = \frac{m_o}{\left[\frac{m_s \cdot k_s}{4} \cdot \left(D_s^2 - d_s^2\right)\right] \cdot \left[t_s - \frac{b_1 - b_2}{2\cos\alpha}\right] \cdot n_s \cdot \rho_{o.o} \cdot k_1 \cdot k_2 \cdot k_3}, \tag{15}$$

where m_s, k_s, D_s, d_s, t_s, b_1, b_2, α, n_s – number of entries in the auger, number of augers, greater and lesser diameters of the auger, pitch of the auger, widths of the helical blade in the cross-section on the inner and outer radii of the auger, angle of helix on the pitch diameter of the auger, rotation speed of the feeder auger, respectively; k_1, k_2, k_3 – coefficients of interturn space filling ($k_1 = 0.9 – 1.0$), waste compression ($k_2 = 0.51 – 0.56$), feeding rate reduction ($k_3 = 0.9$), respectively; $\rho_{o.o}$ – density of the waste dehydrated to a moisture content of $U_{\kappa.o} = 25\%$.

The daily mass $m_{c.o}$ of the food production waste after drying it to a moisture content of $U_{c.o} = 8\%$ is calculated as follows:

$$m_{c.o} = m_o - m_o \frac{U_{k.o} - U_{c.o}}{100} = m_o \frac{25 - 8}{100} = 0.17 \cdot m_o = 0.051 \cdot m_c. \tag{16}$$

The time t_r spent for discharging the food by-products with a mass of $m_{c.o}$ from the vibration drier can be determined on the basis of the main parameters of the belt conveyor by the formula:

$$t_r = \frac{m_{c.o}}{\rho_{c.o} \cdot v_k \cdot B_k \cdot h_k}, \tag{17}$$

where $\rho_{c.o}$ – density of waste dehydrated to a moisture content of 8%; v_k – conveyor belt travel rate; B_k – working width of conveyor; h_k – thickness of the dried waste layer on the belt, which corresponds to the clearance between the end face of the slide valve in its open position and the surface of the belt.

Next, it is necessary to operate an experimental prototype of the vibration drier and establish experimentally the time $t_{s.p}$ spent for drying a batch of food by-products with a mass of $m_{p.e}$ to a moisture content of $U_{k.c} = 8\%$, when the casing shell is filled up and the slide valves are closed.

Taking into account $t_{s.p}$, it is possible to find the quantity n_p of the food production waste batches dehydrated in the unit:

$$n_p = \frac{[24 \cdot 3{,}600 - (t_z - t_r)]}{t_{c.p}}. \tag{18}$$

The mass $m_{p.p}$ of one food production waste batch with a moisture content of $U_{k.o}$, which the commercial vibration drier must dehydrate in the time $t_{s.p}$, can be found with the use of the formula:

$$m_{p.p} = \frac{m_o}{n_p}. \tag{19}$$

The required surface area $S_{t.p}$ of the heating pipes in the commercial unit is determined with the use of the following relation:

$$S_{t.p} = \frac{m_{p.p}}{m_{p.e}} S_{t.e}, \tag{20}$$

where $S_{t.e}$ – surface area of the heating pipes in the experimental prototype of the vibration drier.

The length of the heating pipes l_t is set on the basis of the ceiling height in the shop floor, where the vibration drier is planned to be installed, the height of the auger feeder, the height h_n of the conical top, the sizes of the clearances l_{zv}, l_{zn}, in accordance with the similar parameters of the experimental prototype, the working length l_z of the slide valve in its open position, the thickness h_k of the dried food production waste layer on the belt and the height of the conveyor.

Subsequently, the diameters of the heating pipes d_t in the middle of the casing shell can be calculated as follows:

$$d_t = \frac{S_{t.p}}{\pi \cdot l_t \cdot n_t}, \tag{21}$$

where n_t – number of heating pipes.

The height h_k and radius r_k of the vibration drier's casing shell is determined by the following formulae:

$$h_k = l_t + l_{zv} + l_{zn}; \quad r_k = \sqrt{\frac{\left[\frac{\pi d_t^2}{4} l_t n_t + \frac{m_{p.p}}{\rho_{o.o}}\right]}{\pi \cdot h_k}}. \tag{22}$$

Knowing the external dimensions of the heating pipes and the casing shell of the vibration drier, their thicknesses are determined following the design considerations; also, taking into account the practice of developing vibration driers (Panfilov et al., 2001), the material for constructing the said components is chosen, after which their masses can be calculated.

Proceeding from the radius r_k of the vibration drier casing shell and the design considerations, the dimensions and mass m of the slide valves, with provision for the masses of their attachment units, are determined.

After choosing the electric motors and unbalance vibration exciters, the mass m is calculated as follows:

$$m = m_{p.p} + m_t + m_k + 2m_z + n_v \cdot m_v + 2m_e + m_{tep}, \tag{23}$$

where m_t, m_k, m_v, m_e – masses of the heating pipes, casing shell (with provision for the masses of the spring holders), vibration exciter and motor, respectively; m_{tep} – mass of the heat carrier in the total volume of the heating pipes ($V_1 = \frac{\pi \cdot d_t^2}{4} l_t \cdot n_t$ – taken into account, when using liquid heat carrier for drying); n_v – number of vibration exciters.

After that, the horizontal and vertical springs that hold the casing shell in the frame are defined, then the differential Eq. (13) is solved with the use of the PC and numerical techniques.

Proceeding from the obtained results, the criterion that has to be met for the particles in the batch of food production waste in the casing shell to pass in the process of drying into the vibration-fluidised state is checked in accordance with the expression (1). In case the criterion (1) is not met, the parameters in the Eq. (13) have to be adjusted, then, solving the said equation again, the fulfilment of the criterion (1) has to be achieved.

The primary efficiency parameter of the drying process is the total heat input Q determined with the use of the methods (Mujumdar, 2014):

$$Q = Q_s + Q_o + Q_{pot}, \tag{24}$$

where Q_s, Q_o, Q_{pot} – amounts of heat consumed by the drying process itself, the heating of the solid phase of the waste and the heat losses into the ambient environment, respectively. The first term Q_s can be found with the use of the formula:

$$Q_s = \frac{(m_o - m_{c.o})\left[\left(r_p + c_p T_v\right) - c_v t_{o1}\right]}{\left[24 \cdot 3600 - \left(t_z + t_r\right)\right]}. \tag{25}$$

where r_p, c_p – heat of evaporation and the thermal capacity of vapour, respectively; T_v – temperature of the air around the drier; c_v – thermal capacity of water; t_{o1} – temperature of the waste at the inlet into the drier.

The heat input for heating the solid phase is found as follows:

$$Q_o = \frac{m_{s.o} \cdot c_{s.o}\left(t_{o2} - t_{o1}\right)}{\left[24 \cdot 3600 - \left(t_z + t_r\right)\right]}, \tag{26}$$

where $c_{s.o}$ – specific thermal capacity of dried waste; t_{o2} – final temperature of the waste approximately equal to the temperature T_T of the heat carrier in the heating pipes.

The last term in the formula (24) can be presented, in accordance with the results of experimental research found in (Sevostianov & Luchik, 2017), in the form of the following relation:

$$Q_{pot} = 0.1 \cdot Q_s, \tag{27}$$

When the value Q is known, it is possible to calculate the required heat-transfer surface area $S_{t.p.n}$ of the heating pipes:

$$S_{t.p.n} = \frac{Q}{K_p\left(T_T - t_{o1}\right)}, \tag{28}$$

where K_p – heat transfer coefficient (kinetic coefficient).

Thus, in order to ensure the efficient operation of the unit, the surface area $S_{t.p}$ of its heating pipes that corresponds to the targeted work process productivity (see the expression 20) has to be equal to or greater than the heat exchange surface area $S_{t.p.n}$ (see the expression 28):

$$S_{t.p} \geq S_{t.p.t}, \tag{29}$$

The required surface area $S_{t.p}$ of the heating pipes in the industrial vibration drier unit is determined in accordance with the expression (20). Obviously, it must be equal to or greater than the heat exchange surface area $S_{t.p.n}$ of the heating pipes.

That said, in case the criterion (29) is not met, the parameters n_t, r_t have to be selected in accordance with the heat-transfer surface area $S_{t.p.n}$ and the length l_t of the heating pipes.

Also, the value Q provides the basis for calculating the required mass $G_{t.t}$ of the heat carrier supplied into the heating pipes:

$$G_{t.t} = \frac{Q}{c_p \left(T_T - t_{o1} \right)}, \qquad (30)$$

which then can be compared with the actual mass G_t:

$$G_t = n_t \cdot \pi \cdot r_t^2 \cdot l_t \cdot \rho_t \geq G_{t.t}, \qquad (31)$$

where ρ_t – specific gravity of the heat carrier in the heating pipes.

When the mode of operation of the plant is the continuous drying of food production waste, the mean rate of travel v_o of the waste in the vibration drier casing shell is found, taking into account the specified daily output of the proposed equipment, as follows:

$$v_o = \frac{m_o}{24 \cdot 3{,}600 \cdot \rho_{o.o} \cdot S_p}, \qquad (32)$$

where S_p – passage area of the auger feeder.

Then, the required area S_z of the passage in the slide valves is equal to:

$$S_z = \frac{m_o}{\rho_{o.o} \cdot v_o}. \qquad (33)$$

RESULTS AND DISCUSSIONS

The heat input required for implementing the drying work process in the continuous mode of operation is determined by the formulae (24–27).

The next task is to calculate the relations between $S_{t.p.n}$ and varying K_p and t_{o2}, then to calculate and plot the relations between the principal design parameters of the pipes, i.e. r_t, l_t, n_t, at the fixed minimum values of $S_{t.p.n}$ and $G_{t.t}$. In the calculation, the formulae (14–17, 24–28) have been used together with the following initial parameters (see above): m_s = 10,000 kg; r_s = 0.4 m; D_s = 0.8 m; d_s = 0.7 m; n_s = 0.01 s^{-1}; t_s = 0.25 m; $\rho_{o.o}$ = 950 kg·m^{-3}; $\rho_{s.o}$ = 162 kg m^{-3}; m_s = 1; k_s = 2; b_1 = 0.02 m; b_2 = 0.025 m; α = 6.3°; k_1 = 0.95; k_2 = 0.52; k_3 = 0.9; r_p = 2,258 kJ g^{-1}; c_p = 2,135 J kg^{-1} K^{-1}; c_v = 1,877 J kg^{-1} K^{-1}; t_{o1} = 20 °C; T_v = 20 °C; $c_{s.o}$ = 1,100 J kg^{-1} K^{-1}; v_k = 1 m s^{-1}; B_k = 1.5 m; h_k = 0.1 m; t_{o2} = 50–100 °C; K_p = 10–60; n_t = 50–200; l_t = 1–5 m; r_t = 0.025–0.1 m.

For the purpose of PC-assisted calculation, a programme has been compiled in the Microsoft Excel 2016 environment, with the use of which the initial data for plotting the graphical relations have been obtained.

The data calculated with the use of the PC for plotting the relation between the heat transfer area $S_{t.p.n}$ and the temperature t_{o2} were first used together with the expression (28) for generating Table 1, which contained the initial data of the said relation at a fixed value of K_p = 10, i.e. at its minimum value.

After that, the numerical values presented in Table 1 were used for

Table 1. Heat transfer surface area of heating pipes in relation to final temperature of dried waste

t_{o2}, °C	50	60	70	80	90	100
$S_{t.p.n}$, m^2	2.57	2.22	2.01	1.87	1.77	1.69

plotting the diagram shown in Fig. 3, which represented the relation between the heat transfer area $S_{t.p.n}$ and the temperature t_{o2}. In this case, the heat transfer coefficient K_p with a value of K_p = 10 corresponded to hot air.

The analysis of the graphical relation shown in Fig. 3 proves that for transferring a greater amount of heat to the certain mass of waste by means of heating to a higher temperature t_{o2}, a smaller heat-transfer surface area $S_{t.p.n}$ is required. For example, for heating the food by-product to a temperature of t_{o2} = 100 ºC, the required heat-transfer surface area $S_{t.p.n}$ is equal to 1.69 m^2, which, in case of the specified level of productivity, does not imply increasing the mass and dimension parameters to a higher level, than that of the similar commercial machines used for drying food production waste. The obtained relation (Fig. 3) can be used for comparative analysis in view of the fact that for all the industrial designs of driers represented in reference books and advertising booklets the dimensions of the process chambers are always indicated and that allows to determine easily the respective heat-transfer surface areas (Sazhin, 1984; Ostrikov et al., 2006).

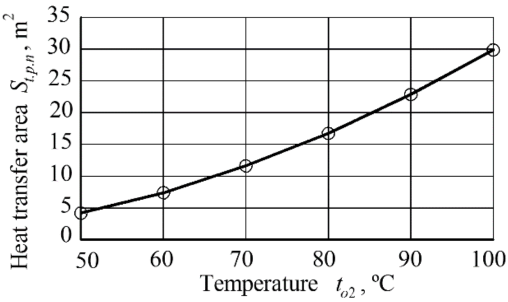

Figure 3. Relation between heat-transfer area $S_{t.p.n}$ and temperature t_{o2} at K_p = 10.

In Fig. 4, the graphical relation between the pipe length l_t and the pipe radius r_t is shown. The relation has also been obtained using the expression (28), at fixed values of Q, $T_T \approx$ 100 ºC, t_1 and the heat transfer coefficient K_p varying within the range of K_p = 10–60. As could be expected taking into account the appearance of the expression (28), the graphical relation $S_{t.p.n} = f(K_p)$ is a decreasing hyperbola, which means that the increase of the coefficient K_p results in the substantial decrease of the required heat-transfer surface area $S_{t.p.n}$ of the heating pipes, i.e. the said area depends to a significant extent on the type of heat carrier. Consequently, the dimensions of the vibration drier casing shell can be substantially reduced, which in itself is a very important point. Moreover, the diagram under consideration indicates that a sufficiently high efficiency of the vibration drier can be achieved by using hot air as the heat carrier, because the coefficient of the heat transfer from hot air to the liquid (the moisture evaporated from the waste) is equal to K_p = 10–60, that is, in case of its minimum guaranteed value of K_p = 10, the required heat-transfer surface area of the heating pipes

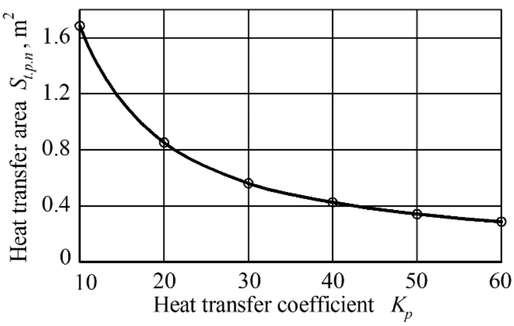

Figure 4. Relation between heat-transfer area $S_{t.p.n}$ and heat-transfer coefficient K_p at t_{o2} = 100 °C.

amounts to just $S_{t.p.n}$ = 1.69 m^2, which is an acceptable value and can be easily provided in actual practice for a practical vibration drier design.

Thus, it can be stated basing on the relation presented in Fig. 4, the area $S_{t.p.n}$ and, accordingly, the overall dimensions of the vibration drier casing shell depend to a significant extent on the type of the heat carrier passing in the heating pipes as well as the heat-transfer coefficient K_p of that heat carrier. That said, the highest efficiency of the vibration drier of the proposed design and its work process is reached in case condensing water steam is used as the heat carrier, as it has K_p = 70 (Mujumdar, A.S. 2014). The obtained graphical relation presented in Fig. 4 can reasonably be used for selecting the most acceptable heat carrier on the basis of the available workspace for installation of the unit.

The application of the obtained expression (21) has provided for plotting the graphical relation between the length of pipe l_t and the radius of pipe r_t. For that purpose, the expression (21) has been transformed into the functional relation of the following form: $l_t = S_{t.p.}.(2\pi \cdot r_t \cdot n_t)^{-1}$. The graph of the function $l_t = f(r_t)$ at fixed values of $S_{t.p.n}$, K_p = 30 (i.e. its mean value), t_{o2} = 70 °C, the number of pipes n_t and the increasing value of the pipe radius r_t is a decreasing hyperbola, as can be seen in Fig. 5.

As is obvious from the diagram shown in Fig. 5, at a fixed number of pipes of n_t = 7, which can be assumed acceptable in terms of the dimensions and the manufacturing complexity, when the radius r_t of the pipes increases from 0.025 to 0.060 m, their required length l_t becomes significantly reduced. In that context, values of l_t = 5–10 m acceptable for the majority of plants in the food industry are reached at $r_t \approx$ 0.055–0.08 m. The relation presented in Fig. 5 can be used in designing the unit on the basis of the pipe grades already available at the manufacturing plant or in order to achieve the conformance of the r_t value to the actual pipe cross-section in the already operated equipment (conformance to the company's internal standards).

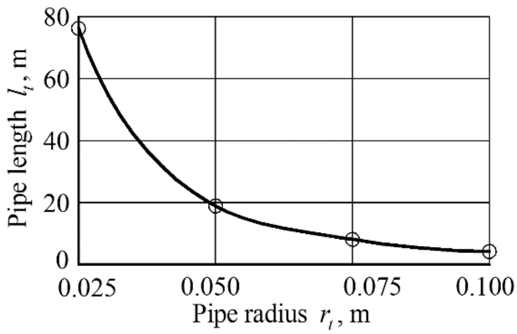

Figure 5. Relation between length of pipe l_t and its radius r_t at: t_{o2} = 70 °C; n_t = 7; K_p = 30.

The diagram that shows the relation between the pipe radius r_t and the number of pipes n_t presented in Fig. 6 has been obtained with the use of the expression (21) at fixed values of $S_{t.p.n}$, K_p = 30, t_{o2} = 70 °C, the length of pipe l_t = 5 m and the number of pipes varying within the range of n_t = 4–20 pieces. As is obvious from the expression (21), it is also a decreasing hyperbola.

The analysis of the graphical relation diagram presented in Fig. 6 shows that, in case of a value of l_t = 5 m, which is acceptable in the majority of cases, when the number of pipes n_t varies within the range from 4 to 20, the radius of pipe r_t stays within an acceptable range: r_t = 0.046–0.103 m. The diagrams in Fig. 5 and 6 give evidence of the fact that the length of pipe l_t has a greater impact on the required radius of pipe r_t, than the number of pipes n_t. The same as in case of the preceding graph, the relation shown in Fig. 6 can be used for the comparative analysis of several the unit design versions on the basis of the available pipe sizes in order to select the optimum solution.

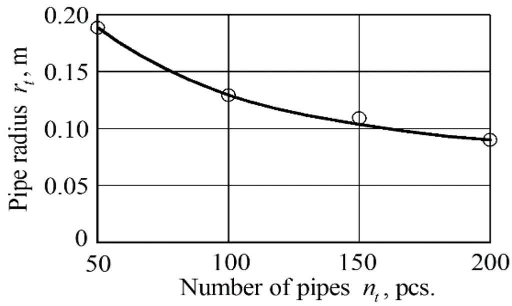

Figure 6. Relation between radius of pipe r_t and number of pipes n_t at: l_t = 5 m; K_p = 30; t_{o2} = 70 °C.

The graph that shows the relation between the number of pipes n_t and the length of pipe l_t presented in Fig. 7 has also been obtained with the use of the expression (21), at fixed values of $S_{t.p.n}$, K_p = 30, t_{o2} = 70 °C, the radius of pipe r_t = 0.05 m and the length of pipe l_t varying within the range of l_t = 1–5 m. The curve of the relation is, again, a decreasing hyperbola.

The obtained graphical relation indicates that, if the radius of pipe is constant: r_t = 0.1 m, the increase of the value l_t from 1 to 5 m (Fig. 7) results in the decrease of the number of heat-exchange pipes n_t to a level within the acceptable value of 200 pieces for the length of pipes within l_t = 4.4–5.0 m, that is, to the value, at which it is possible to select the principal design parameters of the pipes and, accordingly, the overall dimensions of the drier's casing.

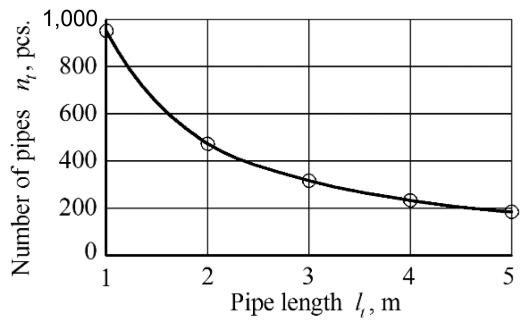

Figure 7. Relation between number of pipes n_t and length of pipe l_t at: r_t = 0.05 m; K_p = 30; t_{o2} = 70 °C.

Thus, the relation presented in Fig. 7 allows calculating the principal design parameters of the drying unit on the basis of the ceiling height in the shop, where the unit is to be installed and operated in the future.

In accordance with the diagrams shown in Fig. 5–7, the reasonable design and process parameters of the vibration drier type under consideration in terms of achieving the specified work process productivity and final moisture content in the dehydrated food production waste are as follows: r_t = 0.05–0.10 m; l_t = 3.0–5.0 m; n_t = 7–20, at K_p = 30–60 and t_{o2} = 60–80 °C.

In general, the obtained relations can be used as the basis for developing a computer-aided engineering technique for the design calculation of the proposed vibration drier.

CONCLUSIONS

1. The analysis completed by the authors has revealed that the air-fluidised and vibration-fluidised bed units are the most suitable equipment for food production waste drying. In comparison with other types of equipment for similar applications, these units ensure high productivity and energy efficiency, while having a simpler and more reliable design.

2. At the same time, the analysis has shown that the known designs of vibration driers are rather bulky and reducing their energy intensity also remains the order of the day.

3. The authors have proposed the improved design of the vibration drier, in which the heat energy output from the primary production work of the plant is utilised, which provides for bringing down the energy intensity of the drying process to a minimum as compared to the drying installations that operate with the use of organic fuels or electric power for heating. Moreover, the design of the drier eliminates the possibility of clogging the passage spaces, where the waste and heat carrier flow. The number of auxiliary components, dimensions and cost have been reduced as compared to the known equipment.

4. The equivalent schematic model of the forces acting on the casing shell of the vibration drier has been developed and on its basis the differential equation of the translational vertical oscillations of the casing shell together with the processed food production waste has been generated. The PC-assisted solving of the above-mentioned equation allows to determine the needed conditions of the vibratory fluidisation of the processed material.

5. The relations have been proposed for determining the main efficiency parameters of the developed new vibration drier - the required heat energy consumption rate Q proceeding from the specified and chosen physical and mechanical properties of the processed waste and design parameters of the equipment.

6. On the basis of the above-mentioned relations, the computer programme for calculation has been compiled and with its use the diagrams have been obtained for selecting the reasonable parameters of the drier and ensuring the specified work process productivity and final moisture content in the food production waste, without needing any additional heat input. The obtained relations can be used in the further theoretical and experimental investigations on the drier as well as the development of the technique for its design calculation.

REFERENCES

Aboltins, A. & Upitis, A. 2012. Experimental and theoretical investigation of agricultural material drying process. *Engineering for Rural Development* **11**, 93–98.

Atkinson, B. 1979. *Biochemistry reactors*. Moskow, Food Processing Industry, 280 pp. (in Russian)

Atkinson, B. & Mavituna, F. 1991. *Biochemical Engineering and Biotechnology Handbook*. 2nd Edition, Stockton Press, 1271 pp.

Altieri, G. 2020. Comparative trials and an empirical model to assess throughput indices in olive oil extraction by decanter centrifuge. *Journal of Food Engineering* **97**(1), 46–56. doi: 10.1016/j.jfoodeng.2009.09.014

Antal, T., Kerekes, B., Sikolya, L. & Tarek, M. 2015. Quality and Drying Characteristics of Apple Cubes Subjected to Combined Drying (FD Pre-Drying and HAD Finish-Drying). *Journal of Food Processing and Preservation* **39**(6), 994–1005. doi: 10.1111/jfpp.12313

Beránek, L. & Kolařik, K. 2014. Surface integrity analysis of duplex steel by design of experiment Approach. Procedia Engineering 69, 630–637. doi: 10.1016/j.proeng.2014.03.036

Bezbakh, I.V. & Bakhmutyan, N.V. 2006. Investigation of the drying process of fruits and berries in a suspended layer. *Scientific works of ONAHT*, Odessa, **28**, pp. 112–116.

Boyce, D.S. 1965. Grain moisture and temperature changes with position and time during through drying. *Journal of Agricultural Engineering Research* **10**(4), 333–341. doi: 10.1016/0021-8634(65)90080-6

Bruce, D.M. & Giner, S.A. 1993. Mathematical modelling of grain drying counter-flow beds: Investigation of crossover of air and grain temperatures. *Journal of Agricultural Engineering Research* **55**(2), 143–161. doi: 10.1006/jaer.1993.1039

Bulgakov, V., Bandura, V., Arak, M. & Olt, J. 2018. Intensification of rapeseed drying process through the use of infrared emitters. *Agronomy Research* **16**(2), 349–356. doi: 10.15159/AR.18.054

Bulgakov, V., Holovach, I., Kiurchev, S., Pascuzzi, S., Arak, M., Santoro, F., Anifantis, A.S. & Olt, J. 2020. The theory of vibrational wave movement in drying grain mixture. *Agronomy Research* **18**(2), 360–375. doi: 10.15159/AR.20.051

Daud, W.R.W. 2008. Fluidized Bed Dryers – Recent Advances. *Advanced Powder Technology* **19**(5), 408–418. doi: 10.1163/156855208X336675

Dufour, P. 2006. Control engineering in drying technology: Review and trends. *Drying Technology* **24**(7), 889–904. doi: 10.1080/07373930600734075

El Hor, H., Linz, S.J., Grochowski, R., Walzel, P., Kruelle, C.A., Rouijaa, M., Götzendorfer, A. & Rehberg, I. 2005. Model for transport of granular matter on vibratory conveyors. *Powders and Grains 2005 - Proceedings of the 5th International Conference on Micromechanics of Granular Media* **2**, 1191–1195.

Filonenko, G.K. & Grishin, M.A. 1971. *Drying of food plant materials*. Moscow, Food Processing Industry, 231 pp. (in Russian)

Giner, S.A. 2019. Estimation of the influence of variable boundary when using thin layer equations for grain dryer simulation. *Biosystems Engineering* **186**, 228–233. doi: 10.1016/j.biosystemseng.2019.08.004

Goncharevich, I.F., Uriev, I.B. & Taleysnik, M.A. 1977. *Vibration engineering in food industry*. Moscow: Food Industry, 279 pp. (in Russian).

Handayani, S.U, Utomo, Tony Suryo Utomo, M.S.K. & Yulianto, M.E. 2017. Performance evaluation of continuous vibrating fluidized bed dryer on green tea production. *Advanced Science Letters* **23**(3), 2530–2532. doi: 10.1166/asl.2017.8676

Hemis, M., Choudhary, R. & Watson, D.G. 2012. A coupled mathematical model for simultaneous microwave and convective drying of wheat seeds. *Biosystems Engineering* **112**(3), 202–209. doi: 10.1016/j.biosystemseng.2012.04.002

Hoffman, P., Pěnička, M. & Fořt, I. 2017. Effect of Fluidized Bed Stirring on Drying Process of Adhesive Particles. *Chemical and Biochemical Engineering Quarterly* **31**(1), 1–10. doi: 10.15255/CABEQ.2015.2335

Kliuchnikov, A. 2019. Development of new method of drying at energy-saving universal dryer to improve quality of crops used in fodder production. *Engineering for Rural Development* **18**, 105–111. doi: 10.22616/ERDev2019.18.N125

Lehmann, S.E., Hartge, E.-U., Jongsma, A., deLeeuw, I.-M., Innings, F. & Heinrich, S. 2019. Fluidization characteristics of cohesive powders in vibrated fluidized bed drying at low vibration frequencies. *Powder Technology* **357**, 54–63. doi: 10.1016/j.powtec.2019.08.105

Ma, J., Zhang, L., Mu, L., Zhu, K. & Li, A. 2018. Thermally assisted bio-drying of food waste: Synergistic enhancement and energetic evaluation. *Waste Management* **80**, 327-338. doi: 10.1016/j.wasman.2018.09.023

McKenna, J.V. 1986. Centrifuging citrus waste & juice. *Transactions of the Citrus Engineering Conference* **32**, 49–64. doi: 10.1115/cec1986-3205

Mohseni, M., Kolomijtschuk, A., Peters, B. & Demoulling, M. 2019. Biomass drying in a vibrating fluidized bed dryer with a Lagrangian-Eulerian approach. *International Journal of Thermal Sciences* **138**, 219–234, doi: 10.1016/j.ijthermalsci.2018.12.038

Mujumdar, A.S. 2014. *Handbook of Industrial Drying*, 4th Edition, CRC Press, 1348 p, eISBN: 9780429169762. doi: 10.1201/b17208

Ostrikov, A.N., Krasnovitskiy, J.V. & Petrov, S.M. 2006. *Processes and apparatus for food production*. Book 2, St. Petersburg: GIORD, 559 pp.

Ovchinnikov, N.L, Ovchinnikov, L.N. & Natareev, S.V. 2009. *Drying and baking in fluidized bed*. Ivanovo: GOUVPO Ivanov State Chemical Engineering University, 106 pp.

Palamarchuk, I.P., Kurchev, S.V. & Verkholantseva, V.A. 2018. Trends in the development of conveyor vibratory dryers. In: The development of technical sciences: problems and solutions: *Proceedings of the international research and practical conference (*April, 27–28, 2018), Brno, pp. 9–12.

Panfilov, V.A., Antipov, S.T., Kretov, I.T. & Ostrikov, A.N. 2001. *Technique and apparatus for food industry*. Moskow, Higher School, 703 pp. (in Russian)

Robaina-Mesa, M. & Chanfrau, J.E.R. 2019. Spray drying of pectin obtained from citrus sinensis waste. *Biointerface Research in Applied Chemistry* **10**(1), 4825–4828. doi: 10.33263/BRIAC101.825829

Ruiz Celma, A., Cuadros, F. & López-Rodríguez, F. 2012. Characterization of pellets from industrial tomato residues. *Food and Bioproducts Processin*g **90**(4), 700–706, doi: 10.1016/j.fbp.2012.01.007

Sazhin, B.S. 1984. *Foundations of the theory of drying*. Moskow, Chemistry, 320 pp.

Sevostianov, I.V. 2013. *Processes and equipment for vibro-blowing separation of food waste*, Saarbrücken: LAP LAMBERT Academic Publishing, 417 pp, ISBN: 978-3-659-47395-1.

Sevostianov, I.V., Polischuck, O.V. & Slabkiy, A.V. 2015. Elaboration and research of an installation for two-component vibro-blowing dehydration of waste food productions. Eastern-*European Journal of Enterprise Technologies* **5**(7), 40–46, doi: 10.15587/1729-4061.2015.49272

Sevostianov, I.V. & Luchik, V.L. 2017. Installation for multi-stage dehydration of food production waste. *Mechanical Engineering and Transport News* **1**, 105–113 (in Russian).

Tribuzi, G. & Laurindo, J.B. 2014. How to Adapt a Lab-Scale Freeze Dryer for Assessing Dehydrating Curves at Different Heating Conditions. *Drying Technology* **32**(9), 1119–1124. doi: 10.1080/07373937.2014.886258

Wawrzyniak, P., Jaskulski, M., Piatkowski, M., Sobulska, M., Zbicinski, I. & Egan, S. 2020. Experimental detergent drying analysis in a counter-current spray dryer with swirling air flow. *Drying Technology* **38**(1–2), 108–116. doi: 10.1080/07373937.2019.1626878

Wang, X., Zhang, Z. & Deng, Y. 2011. The harmonic response analysis on vibration system of disc vibration dryer. *Applied Mechanics and Materials* **84–85**, 209–213. doi: 10.4028/www.scientific.net/AMM.84-85.209

Ward, K. 2002. Drying out: Technology comes in from the cold. *Chemical Engineer* **734**, 26–27.

Yogendrasasidhar, D. & Setty, Y.P. 2019. Experimental studies and thin layer modeling of pearl millet using continuous multistage fluidized bed dryer staged externally. *Engineering Science and Technology, an International Journal* **22**(2), 428–438. doi: 10.1016/j.jestch.2018.10.010

Agronomy Research **18**(4), 2410–2424, 2020
https://doi.org/10.15159/AR.20.230

Pancakes for a healthy diet: low-carb, prebiotic, gluten-free

E.I. Kiprushkina, O.V. Golovinskaia*, E.A. Ovsyuk, V.V. Baklanova,
L.A. Alekseeva, A.K. Tulina, V.R. Beloded and I.A. Shestopalova

ITMO University, Faculty of Food Biotechnology and Engineering, 9 Lomonosova street, RU191002 St. Petersburg, Russia
*Correspondence: oksana2187@mail.ru

Abstract. The work aims to develop pancake recipes corresponding to the standards of a healthy diet by replacing traditional components with ingredients containing nutritional functional properties. Corn and rice flour are gluten-free and can be used to design gluten-free pancakes. Barley flour contains beta-glucans, a large amount of fiber, reduces the glycemic index of products, is useful not only for a healthy diet but also for people suffering from diabetes and obesity. Rye flour is low in calories, as millet flour contains dietary fiber, vitamins, and lowers cholesterol. Dietary fiber and inulin contribute to the regulation of intestinal microbiota. The results show the possibility of 100% replacement of wheat flour with other types of flour in the production of low-carb, prebiotic, and gluten-free pancakes. The water absorption capacity of flour, dough viscosity, humidity, texture of products, and sensory analysis of finished products were investigated. Replacing wheat flour with alternative types of flour can improve the nutritional value of products, increase the content of dietary fiber, and reduce the calorie content of pancakes.

Key words: pancakes, functional properties, dietary fiber, healthy nutrition.

INTRODUCTION

According to the World Health Organization, there is an increase in the number of patients with alimentary-dependent diseases (Smyth & Heron, 2006), which primarily include functional disorders and chronic digestive diseases, as well as obesity and diabetes, which are interrelated (Mayurnikova & Ashirova, 2011).

People with inflammatory bowel disease, type 2 diabetes (T2DM), and celiac disease have a decrease in bacterial diversity (Hiippala et al., 2018; Cancello et al., 2019; O'Callaghan & Corr, 2019). 'Musso et al. (2011) noted the interaction between intestinal microbiota and host metabolism predisposing to obesity and diabetes'. It has been shown that intestinal microbiota plays an important role in influencing the development of both T1DM and T2DM. This is confirmed by the results of studies in humans and animals (Baothman et al., 2016). Prebiotics nourish the intestinal microbiota, which is affected by dysbiosis, infectious diseases, as well as intestinal diseases, gradually reducing the amount of harmful and increasing the concentration of beneficial microflora (Sekirov et al., 2010; Duncan & Flint, 2013). The prebiotic potential of arabinoxylan, resistant starch, and inulin is well known; they modulate healthy bacteria such as *Bifidobacterium*, *Fecalibacterium*, and *Lactobacillus* (Yang et al., 2020). More than that, partially hydrolyzed guar gum and xanthan can act as a prebiotic and stimulate the growth of native intestinal microflora. An *in vivo* study showed that supplementation of mice with xanthan gum alters the susceptibility of mice to *C. difficile* colonization, maintaining the microbiota during antibiotic treatment. (Mudgil et al., 2018; Schnizlein et al., 2020). 'Tuohy et al. (2001) determined the prebiotic effect of buscuits containing partially hydrolyzed guar gum, which is retained in the final product, as evidenced by an increase in the number of bifidobacteria in human volunteers participating in the research'. It has been established that fructans such as inulin contribute to the development of bifidobacteria. Animal studies have shown that inulin or inulin-type fructan can alter intestinal microbial diversity and *Bifidobacterium sp.* (Licht et al., 2006; Catry E. et al., 2018). Inulin improves bowel function and selectively stimulates the growth of bifidobacteria (Bouhnik et al., 1999; Brighenti et al., 1999; Kruse et al., 1999).

Currently creating products for people with diabetes, lactase deficiency, who are overweight. The production of gluten-free products for people with celiac disease is also relevant (Bazhenova et al., 2018). Celiac disease is characterized by chronic inflammation of the intestinal mucosa, intestinal villous atrophy, which interferes with the absorption of nutrients from food (De la Hera et al., 2013) and several clinical manifestations (Niewinski, 2008). The nutrition of patients with celiac disease is based on the exclusion from the diet of products containing gluten; limiting the amount of easily digestible carbohydrates; the introduction of protein ingredients; microflora correction using products with probiotic and prebiotic factors (Mayurnikova & Ashirova, 2011). Thus, to prevent and reduce metabolic diseases, it is necessary to maintain a healthy lifestyle and proper nutrition. Treatment of people with obesity and diabetes involves dietary correction and the systematic use of functional foods with a low glycemic index, high fiber content, and the use of sweeteners (Skripleva & Arseneva, 2015). When developing gluten-free products, they must have high nutritional value (Sciarini et al., 2010), since removing the gluten-free ingredient from the products leads to loss of nutrients (Mariani et al., 1998; Dubrovskaya et al., 2017).

The mixture of rice, soy flour, and corn starch improved the sensory and nutritional qualities of gluten-free muffins (Man et al., 2014). Biscuits for celiac disease patients were made from a mixture of rice, corn flour, and sorghum flour and had high nutrition value and sensory characteristics similar to biscuts made from wheat flour (100% gluten) (Ali & Abol-Ela, 2019).

For traditional Russian pancakes known to a wide variety of recipes, including various additives that provide high sensory indicators and the attractiveness of the product for the consumers. However, there are practically no recipes for pancakes for dietary and preventive purposes.

Corn flour does not contain gluten, which allows its use in the development of gluten-free food products (Shi et al., 2016). Besides, cornmeal contains a large number of vitamins and minerals, including potassium, phosphorus, zinc, calcium, iron, thiamine, niacin, vitamin B6, and folate (Sabanis & Tzia, 2009; Makinde & Taibat, 2018). Cornmeal reduces blood cholesterol (Kahlon & Chow, 2000), normalizes sugar levels in diabetics (Granfeldt et al., 1995), improves intestinal function and normalizes lipid metabolism, which allows it to be used in the production of low-carbohydrate foods (Mahalko et al., 1984). Corn flour has a higher antioxidant ability compared to wheat, oat, and rice (Soong et al., 2014).

Barley flour contains a large amount of fiber 4.5 g per 100 g of product, potassium, calcium, phosphorus, iron, as well as copper, manganese, iodine, and others (Tipsina & Selezneva, 2011). Barley products are effective natural enterosorbents. They contribute to the elimination of various toxicants from the human body, in particular, organochlorine compounds of inorganic metal salts (Vybornov & Anisimova, 2013). Barley flour contains beta-glucans, a soluble dietary fiber. It was found that β-glucan and cereal products containing it perform useful physiological functions: they reduce the glycemic index of starch-containing products, serum lipids, and lower cholesterol (Miyamoto et al., 2018; Rieder et al., 2019), which makes barley flour is useful for patients with diabetes and obesity (Gapparov et al., 2009). Barley flour improves the physicochemical properties of bakery products, increases their nutritional value, as well as the content of dietary fiber, β-glucan, minerals, vitamins, and antioxidants (El-Taib et al., 2018).

Millet grain has a large number of nutrients, including proteins, sulfur-containing amino acids, minerals such as iron and calcium, carbohydrates and phenolic compounds that have antioxidant properties (Adebiyi et al., 2017). Millet has a positive effect on the cardiovascular system, helps lower blood pressure, cholesterol, and has a lipotropic effect (Truswell, 2002). Products from millet flour remove antibiotics and toxins from the body. Millet flour is a valuable source of vitamins, minerals, fiber, and is an excellent alternative to wheat flour (Kuvandykova & Vayskrobova, 2017).

Rye is characterized by the lowest calorie content of grain among all crops and at the same time contains much more trace elements, vitamins, and essential amino acids than wheat. Rye flour contains 3.5 times more dietary fiber compared to wheat flour. Also, rye flour contains large amounts of high molecular weight pentosans - mucus, which along with dietary fiber improve the functioning of the gastrointestinal tract, as well as adsorb and remove metabolic products and harmful substances from the body (Lapteva, 2012).

Rice flour can be used in the production of gluten-free products, as it has high nutritional value and digestibility and does not cause an allergic effect (Demirkesen et al., 2013). 'According to Pereira et al. (2016), rice flour can be used as a technological additive in a healthy diet, as an emulsifier and fat substitute in foods, and can also be used as a structuring agent for a wide group of products'.

Dietary fiber plays an important role in the prevention and treatment of overweight and obesity, reducing the risk of developing cardiovascular, gastrointestinal, oncological diseases, metabolic syndrome, contribute to lowering cholesterol, slowing down the absorption of carbohydrates, and regulating the intestinal microbiota (Khramtsov et al., 2018) and performs an immunoregulatory function (Zimmerman, 2013). Inulin was added to pancake recipes to obtain products with prebiotic properties. Inulin is a prebiotic and stimulates the growth of microflora in the intestines, which improves human health. 'The effect of inulin on the microbiota of the human intestine has been extensively studied both in vivo and in vitro by Shoaib et al. (2016)'. 'Morris C. & Morris G. (2012) concluded that inulin and oligofructose exhibit prebiotic properties when consumed 5–15 g per day for several weeks'.

The work aims to develop recipes and techniques for the preparation of pancakes (low-carb, prebiotic, and gluten-free) that correspond to the standards of a healthy diet by replacing traditional components with ingredients containing nutritional functional properties.

MATERIALS AND METHODS

Materials

For research using wheat, rice, corn, rye flour of the Kudesnitsa brand produced by the St. Petersburg Mill Plant, as well as barley and millet flour from the manufacturer Garnets. Dry whey curd milk with a protein content of 6% manufacturer Tagris Milk.

Salt, maltodextrin, inulin, dietary fiber, baking powder, dry egg melange, xanthan gum, vegetable oil for making pancake dough were purchased at local stores.

The technology of preparation of pancakes

Several healthy pancakes have been developed gluten-free, low-carb, and prebiotic formulations are presented in tables. Pancakes prepared using wheat flour were used as a control sample. All flour was sieved before use. Water and vegetable oil was added to the mixture of dry ingredients, mixed for 1 min with a mixer, and left for 30 min to swell the proteins. The 130–140 g batter was poured onto a pre-heated pan t = 190 °C and baked for 90 s, then the pancakes were turned on the other side and baked for 40–60 s. After baking, the pancakes were cooled to room temperature over 30 minutes, then the diameter, thickness, and weight of the pancakes were measured.

Weight and overall dimensions of pancakes

The diameter and thickness of each pancake were measured using a caliper. The mass of pancakes was determined using a high-precision electronic laboratory-scale VK II. The size and weight of the products were determined by measuring 5 pieces of products. The average value was taken for the final result.

Sensory evaluation of pancakes

For sensory analysis of pancakes, 12 participants from the Faculty of Food Biotechnology and Engineering of ITMO University (aged 22–65 years) were selected and trained, who were given plates with numbers of pre-cut samples and were asked to evaluate each sample by five sensory characteristics–appearance, texture, color, smell, and taste using a linear scale (ISO 4121:2003) from 1 (‘really dislike’) to 5 (‘really like’).

During the analysis, the quality of individual characteristics of taste, smell, and color, as well as the presence of extraneous odors and tastes, were evaluated. When establishing the appearance was evaluated the shape of the product and surface condition.

Analysis of indicators

The viscosity of the batter was determined on a Rheotest RV2.1 rotational viscometer (Messgerate Medingen GmbH, Germany), with a speed gradient of 5.4 s^{-1} and a temperature of 20 °C (Starshov et al., 2017). For each sample, two sequential determinations were performed. Kinematic viscosity was determined as the ratio of dynamic viscosity to batter density at the same temperature. All ingredients of batter were mixed for 1 min with a mixer and left for 30 min.

The water absorption capacity of flour was determined using a Chopin mixolab device (CHOPIN Technologies, France) (Xhabiri et al., 2016).

The mass fraction of moisture was determined by the accelerated weighing method on an Eleks-7 moisture meter (Technotest Group, Ukraine) at a temperature of 160 °C for 5 minutes.

The determination of soluble and insoluble fibers was carried out by the enzymatic gravimetric method. The method is based on the enzymatic hydrolysis of starch and non-starch compounds using enzymes to mono sugars and peptides. Dietary fiber is precipitated with ethanol and dried (McCleary et al., 2012).

The elasticity of pancakes was determined using a texture meter (Shimadzu, EZ test, Japan) using the basis for testing products for elasticity (346-52275-02) and equipment for assessing the elasticity of 5 mm (346-51687-02) at a speed of 100 mm min^{-1}. The measurements were performed 3 times on each sample, and the average value was taken for the final result (López-Mejía et al., 2019).

Energy value was calculated using conversion factors: proteins and carbohydrates– 4 kcal g^{-1}, fats - 9 kcal g^{-1} (Grigelmo-Miguel et al., 1999).

RESULTS AND DISCUSSION

To obtain products with high sensory characteristics, it is necessary to take into account the structural and mechanical properties of pancake dough (viscosity, plasticity, elasticity) from gluten-free flour.

The gluten-free flour dough does not contain gluten, which provides elastic properties, so the dough becomes less elastic, has a lower viscosity compared to wheat flour dough. The viscosity of pancake dough affects the appearance, texture, and sensory characteristics of the finished product. It was found that the dough made from rice and amaranth flour has a lower viscosity (Fig. 1).

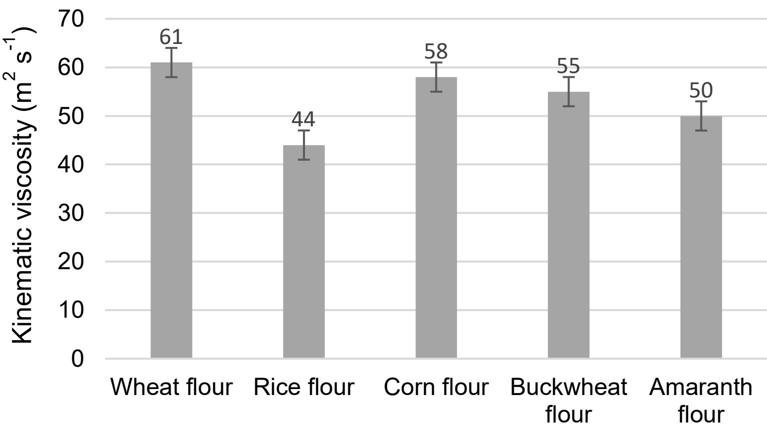

Figure 1. Kinematic viscosity of dough from different types of flour.

‘Shih et al. (2006) also report that the viscosity of rice flour dough is significantly lower than that of wheat dough. Besides, rice flour has a lower water-holding capacity and absorbs less water than wheat flour’. Thus, to obtain the necessary structural and mechanical properties, it is advisable to mix flour (buckwheat and corn), which has a high kinematic viscosity, with other types that have a lower kinematic viscosity (rice and amaranth). The possibility of developing pancake recipes from mixtures of rice and corn flour was investigated as a substitute for a standard of wheat flour. Amaranth flour has a high cost, and buckwheat gives the product a specific color and flavor, so it was decided to refuse to use them in further research.

Pancakes from gluten-free types of flour were prepared by replacing wheat flour with rice and corn in a different percentage ratio of 50 : 50, 70 : 30, 75 : 25, 85 : 15 (Table 1).

Table 1. Recipes for gluten-free pancakes with a different ratio of rice and corn flour

Name of raw materials	The ratio of rice : corn flour, %				
	0	50 : 50	70 : 30	75 : 25	85 : 15
	quantity of raw materials, g				
Wheat flour	100.0	-	-	-	-
Rice flour	-	50.0	70.0	75.0	85.0
Corn flour	-	50.0	30.0	25.0	15.0
Wheat fiber	-	3.0	3.0	3.0	3.0
Dry egg melange	14.0	14.0	14.0	14.0	14.0
Salt	1.0	1.0	1.0	1.0	1.0
Xanthan gum	0.1	0.1	0.1	0.1	0.1
Maltodextrin	5.0	5.0	5.0	5.0	5.0
Baking powder	4.0	4.0	4.0	4.0	4.0
Vegetable oil	5.0	5.0	5.0	5.0	5.0

Pancakes with increasing addition of cornmeal had a more pronounced yellow color, but they broke, were torn and had a crumbling texture. Zaitseva et al. (2020) recommend introducing various polysaccharides into the recipe as structural agents and thickeners to improve the structural and mechanical properties of gluten-free products. Xanthan gum was added to increase the elasticity of the finished products. Sample 85 : 15 received the highest sensory scores (Fig. 2).

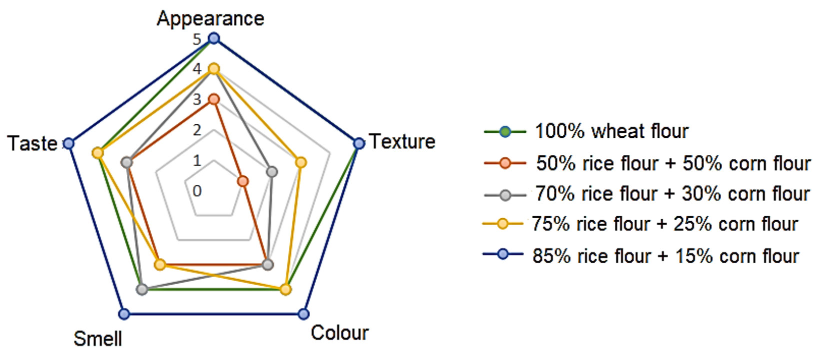

Figure 2. Sensory properties of gluten-free pancakes prepared with different ratio of rice flour to corn flour.

Low-carb and prebiotic pancakes were developed taking into account such an indicator as to the water absorption capacity of flour, which affects the viscosity of the dough and the quality of the finished products, this fact is also confirmed by the work of

Meleshkina & Popova (2011) and Anistratova et al. (2019). Water absorption was determined during the kneading dough (Fig. 3).

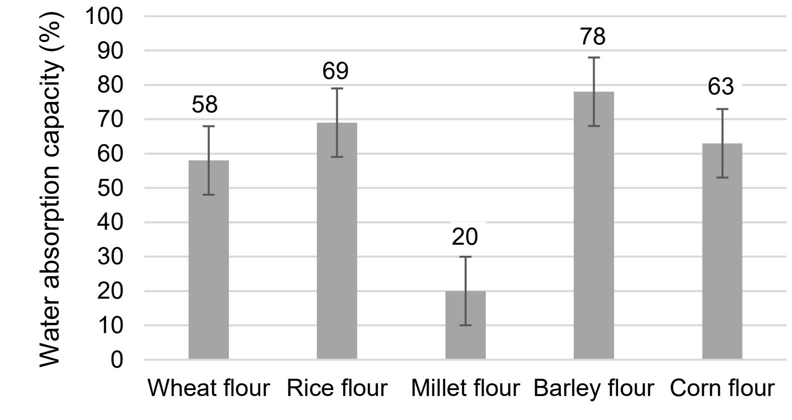

Figure 3. Water absorption capacity of various types of flour.

‘Rye and barley flour have a high water absorption capacity, similar data were obtained by Holtekjolen et al. (2008) and Stępniewska S. et al. (2018)’, therefore, it is advisable to use them with other types of gluten-free flour, which are characterized by low water absorption, such as millet and corn.

Prebiotic pancakes were prepared by replacing wheat flour with rye and millet in a different percentage ratio of 70 : 30, 60 : 40, 55 : 45, 50 : 50, 30 : 70. Furthermore, inulin was added to pancake recipes to give products prebiotic properties (Table 2).

Table 2. Recipes for prebiotic pancakes with a different ratio of rye and millet flour

Name of raw materials	The ratio of rye : millet flour, %						
	0	70 : 30	60 : 40	55 : 45	50 : 50	40 : 60	30 : 70
	quantity of raw materials, g						
Wheat flour	100.0	-	-	-	-	-	-
Rye flour	-	70.0	60.0	55.0	50.0	40.0	30.0
Millet Flour	-	30.0	40.0	45.0	50.0	60.0	70.0
Dry curd milk whey	26.0	26.0	26.0	26.0	26.0	26.0	26.0
Dry egg melange	14.0	14.0	14.0	14.0	14.0	14.0	14.0
Salt	1.0	1.0	1.0	1.0	1.0	1.0	1.0
Inulin	-	5.0	5.0	5.0	5.0	5.0	5.0
Maltodextrin	5.0	5.0	5.0	5.0	5.0	5.0	5.0
Baking powder	4.0	4.0	4.0	4.0	4.0	4.0	4.0
Vegetable oil	5.0	5.0	5.0	5.0	5.0	5.0	5.0

Kneading the dough, it was found that the gluten content in millet flour is less than in wheat and rye. Also, the gluten of millet flour has a low water absorption capacity, as a result of which the dough is more liquid and the water exfoliates. Due to the settling of millet flour, the dough is uneven, so it is necessary to sift the millet flour through sieves.

The quality of the finished products was determined by the amount of introduced millet and rye flour. With an increase in the amount of millet flour, the finished pancakes had a more pronounced yellow color, but they held their shape worse and acquired a crumbling texture. An increase in the content of millet flour over 50% led to a deterioration in the rheological properties of the dough and the appearance of the finished product. Finished products stuck to the pan and torn, and the excess humidity of the finished pancakes was noted.

With an increase in the amount of rye flour, the products had a dark color not typical for pancakes and denser consistency. Sample 55 : 45 received the highest sensory scores (Fig. 4).

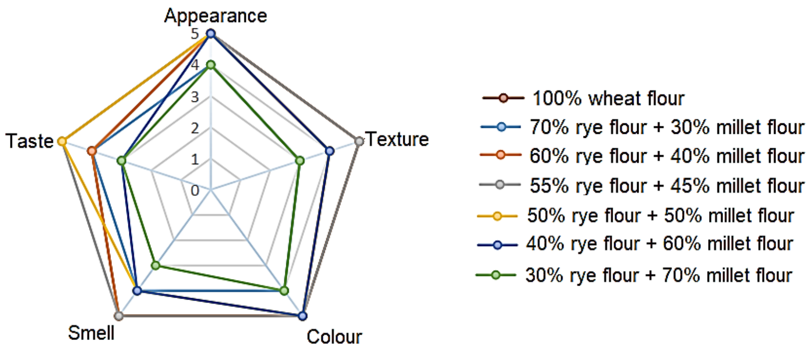

Figure 4. Sensory properties of prebiotic pancakes with a different ratio of rye and millet flour.

'A mixture of rye and millet flour (55 : 45) does not form gluten (although rye flour contains gliadin protein), but the elasticity of pancakes is similar to a control sample of wheat flour. This can be explained by the presence in rye flour of a large amount of mucus and water-soluble pentosans, which add viscosity to the dough and have a high water absorption capacity, similar results were obtained by Anistratova et al. (2019)'. It was found that the recipe composition for pancakes, consisting of a mixture of wheat, rye, and oatmeal, in comparison with the control sample (wheat flour), has higher viscosity and water absorption capacity.

Developing recipes for low-carb pancakes, wheat flour was replaced with barley and corn in various percentages (Table 3).

Table 3. Recipes for low-carb pancakes with a different ratio of barley and corn flour

Name of raw materials	The ratio of barley : corn flour, %				
	0	90 : 10	80 : 20	75 : 25	70 : 30
	quantity of raw materials, g				
Wheat flour	100.0	-	-	-	-
Barley flour	-	90.0	80.0	75.0	70.0
Corn flour	-	10.0	20.0	25.0	30.0
Dry curd milk whey	11.0	11.0	11.0	11.0	11.0
Wheat fiber	-	3.0	3.0	3.0	3.0
Dry egg melange	20.0	20.0	20.0	20.0	20.0
Baking powder	2.0	2.0	2.0	2.0	2.0
Xanthan gum	0.5	0.5	0.5	0.5	0.5
Vegetable oil	2.0	2.0	2.0	2.0	2.0

Beta-glucans contained in barley flour (2.5–11.3%) have a high water absorption capacity, i.e. bind a large amount of water, and make it less accessible for the development of gluten, which can adversely affect the quality of finished products. Holtekjolen et al. (2008), also noted that the quality of bakery products made from a mixture of wheat and barley flour is affected by the total content of β-glucan, which has a significant effect on the water absorption capacity of flour. Therefore, it is important to use barley flour in a mixture with other types of flour, which are characterized by low water absorption capacity (Rieder A. et al., 2012), such as corn.

With an increase in the amount of barley flour 80–100%, the viscosity of the dough increased significantly, which made it difficult to evenly distribute in the pan, the pancakes had an unusual pale-beige color, torn and acquired a more dense consistency. An increase in the content of corn flour over 30% led to a deterioration in the rheological properties of the dough and the appearance of the products. Pancakes were tough and crumbly.

To improve the rheological properties of the dough and consumer properties of the finished products, xanthan gum was introduced into the recipes. The addition of xanthan gum to the pancake dough gave the products a more elastic structure, the pancakes did not tear, did not crumble. Thus, a sample was selected with a ratio of barley and corn flour 75 : 25 (Fig. 5).

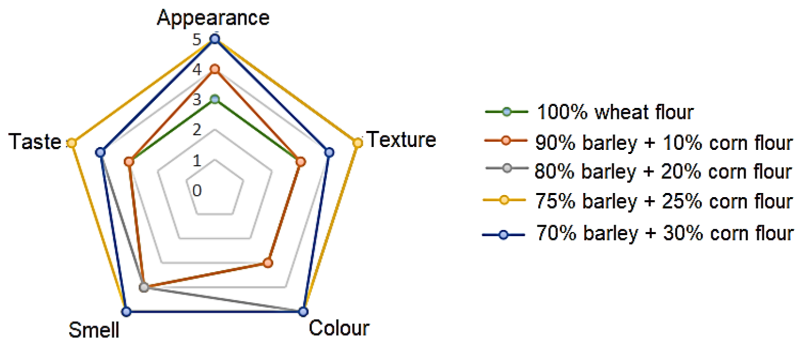

Figure 5. Sensory properties of low-carb pancakes with a different ratio of barley and corn flour.

Brennan & Cleary (2005), as a result of clinical trials, found that grain beta-glucans lower the glycemic index, cholesterol, and also slows the increase in blood sugar, which means they can be used to create dietary products.

Wheat dietary fiber and inulin were added to pancake recipes. 'The addition of inulin did not significantly change the structure and properties of the dough, which is also confirmed by Hager et al. (2011)'. Also, 'Rosell et al. (2010) note that inulin improves the structure of the dough and increases its stability'. 'The beneficial effects of dietary fiber on intestinal bifidobacteria and lactobacilli have been demonstrated in many works by Makki et al. (2018), Khramtsov et al. (2018), Pyryeva & Safronova (2019)'. 'However, Slavin et al. (2013) note that the consumption of wheat dietary fiber also leads to a decrease in the conditionally pathogenic microflora, for example, the content of bacteroids–Cl. Perfringens'.

Moisture content, weight, and overall dimensions of pancakes– diameter and thickness are presented in Table 4.

The difference in pancake thickness, weight, and diameter was insignificant and was almost the same for all samples.

The nutritional and energy value of pancakes was calculated. In each recipe, as a control sample for comparison, there were pancakes made from 100% wheat flour (instead of experimental) and without adding dietary fiber (Table 5).

Table 4. Moisture content, weight and overall dimensions of pancakes

Name of indicator	Results		
	gluten free	prebiotic	low carb
Weight, g	103.0	103.0	102.0
Diameter, cm	29.0	28.5	29.0
Thickness, mm	2.0	2.0	2.0
Moisture content, %	50.5	51.2	50.8

Table 5. Nutrition and energy value of pancakes per 100 g of product

Name of indicator	Results, g per 100 g					
	control for gluten free	gluten free	control for prebiotic	prebiotic	control for low carb	low carb
Proteins	8.62	6.18	6.37	7.18	9.58	10.71
Fats	5.27	5.60	4.90	4.62	6.70	1.34
Carbohydrates	38.70	36.35	34.20	30.81	29.68	24.46
Energy value, kcal / kJ	229 / 939	220 / 902	207 / 849	193 / 791	222 / 910	139 / 570

Table 5 shows that the developed recipes have insignificant differences in the content of protein and fat in comparison with samples from wheat flour. However, the introduction of pancake recipes rye, barley, millet, rice, and corn flour, instead of wheat, reduces the number of carbohydrates and calorie content.

The content of dietary fiber was determined in the developed products and for comparison, we used the recipe of pancakes from wheat flour without the additional introduction of dietary fiber (Fig. 6).

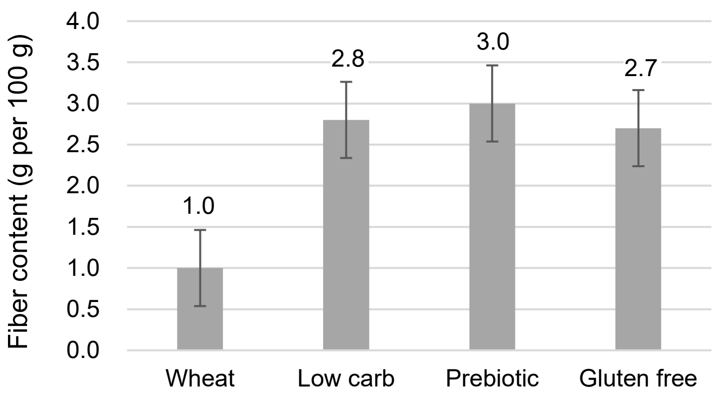

Figure 6. Dietary fiber content in pancake.

According to Fig. 6, the amount of dietary fiber per 100 g of developed products is 2.7–3.0 g, which is 3 times more compared to traditional pancakes (wheat). Thus, with the use of one such pancake, the daily need for dietary fiber will be satisfied by 14–15% with a norm of 20 g per day (Onishchenko, 2008).

As a result of measuring the elasticity of pancakes, it was found that the gluten-free pancakes had the lowest elasticity value, and the prebiotic and low-carb pancakes also had lower elasticity compared to their wheat flour pancakes (Fig. 7).

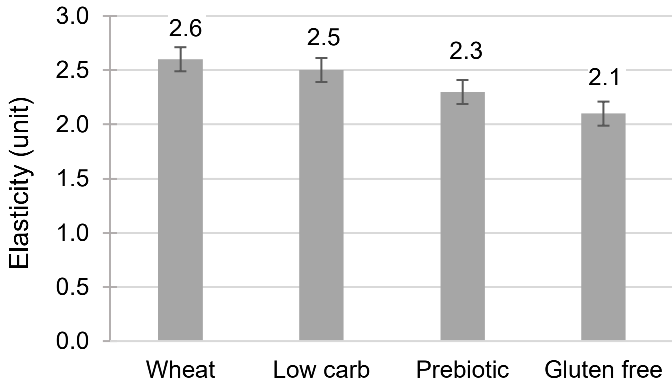

Figure 7. The value of elasticity of gluten-free, prebiotic, low-carb pancakes and pancakes from wheat flour (control).

The lack of gluten in the recipe helps to reduce the elasticity of products. Gluten with gelatinized starch forms a binder mass, which gives elasticity to products. 'Similar results were obtained by Vavilova (2020) in the production of pasta'. 'López-Mejía et al. (2019) showed that the elasticity of products is affected by the content of dietary fiber that was added to the product's recipes'.

CONCLUSION

Replacing wheat flour with alternative types can improve the nutritional value of products, increase the content of dietary fiber. As a result of the analysis of the sensory characteristics of the developed pancake recipes, the best formulation ratios of various types of flour (barley, rye, millet, corn, rice) were determined. These types of flour, unlike wheat flour, are characterized by a low glycemic index and a high fiber content, which makes it possible to use them in a healthy diet, as well as in a specialized one, for diseases such as celiac disease, obesity, diabetes mellitus, for the regulation of intestinal microbiota.

REFERENCES

Adebiyi, J.A., Obadina, A.O., Adebo, O.A. & Kayitesi, E. 2017. Comparison of nutritional quality and sensory acceptability of biscuits obtained from native, fermented, and malted pearl millet (Pennisetum glaucum) flour. *Food chemistry* **232**, 210–217.

Ali, J.B. & Abol-Ela, M.F. 2019. Effect of gluten-free flour on physical properties and quality characteristics of biscuits. *Research Journal of Applied Biotechnology* **5**(1), 1–14.

Anistratova, O.V., Serpunina, L.T. & Kobzareva, A.S. 2019. The rationale for the use of various types of flour in the formulation of the test shell for pancakes. *Proceedings of KSTU* **53**, 89–100 (in Russian).

Baothman, O.A., Zamzami, M.A., Taher, I., Abubaker, J. & Abu-Farha, M. 2016. The role of gut microbiota in the development of obesity and diabetes. *Lipids in health and disease* **15**(1), 108.

Bazhenova, T.S., Bazhenova, I.A. & Safonova, E.E. 2018. The study of grain and flour of breeding varieties of millet to create flour confectionery and culinary products for specialized purposes. *Polzunovsky Bulletin* **1**, 32 (in Russian).

Bouhnik, Y., Vahedi, K., Achour, L., Attar, A., Salfati, J., Pochart, P., Marteau, P., Flourie, B., Bornet, F. & Rambaud, J.C. 1999. Short-chain fructo-oligosaccharide administration dose-dependently increases fecal bifidobacteria in healthy humans. *The Journal of nutrition* **129**(1), 113–116.

Brennan, C.S. & Cleary, L.J. 2005. The potential use of cereal (1→3, 1→4)-β-D-glucans as functional food ingredients. *Journal of cereal science* **42**(1), 1–13.

Brighenti, F., Casiraghi, M.C., Canzi, E. & Ferrari, A. 1999. Effect of consumption of a ready-to-eat breakfast cereal containing inulin on the intestinal milieu and blood lipids in healthy male volunteers. *European Journal of Clinical Nutrition* **53**(9), 726–733.

Cancello, R., Turroni, S., Rampelli, S., Cattaldo, S., Candela, M., Cattani, L., Mai, S., Vietti, R., Scacchi, M. & Brigidi, P. 2019. Effect of short-term dietary intervention and probiotic mix supplementation on the gut microbiota of elderly obese women. *Nutrients* **11**(12), 3011.

Catry, E., Bindels, L.B., Tailleux, A., Lestavel, S., Neyrinck, A.M., Goossens, J.F. & Bouzin, C. 2018. Targeting the gut microbiota with inulin-type fructans: preclinical demonstration of a novel approach in the management of endothelial dysfunction. *Gut* **67**(2), 271–283.

De la Hera, E., Martinez, M. & Gomez, M. 2013. Influence of flour particle size on quality of gluten-free rice bread. *LWT-Food Science and Technology* **54**(1), 199–206.

Demirkesen, I., Sumnu, G. & Sahin, S. 2013. Image analysis of gluten-free breads prepared with chestnut and rice flour and baked in different ovens. *Food and Bioprocess Technology* **6**(7), 1749–1758.

Duncan, S.H. & Flint, H.J. 2013. Probiotics and prebiotics and health in ageing populations. *Maturitas* **75** (1), 44–50.

Dubrovskaya, N., Savkina, O., Kuznetsova, L. & Parakhina, O. 2017. Development of glutenfree bread with unconventional raw ingredients of high nutritional value and antimicrobial activity. *Agronomy Research* **15**(S2), 1276–1286.

El-Taib, H.I., Rizk, I.R.S.A., Yousif, E.I. & Hassan, A.A. 2018. Effect of barley flour on wheat bread quality. *Arab Universities Journal of Agricultural Sciences* **26**(Special issue (2A)), 1109–1119.

Gapparov, M.M., Kaganov, B.S., Plotnikova, O.A., Zykina, V.V., Shlelenko, L.A., Tyurina, O.E. & Sharafetdinov, Kh. Kh. 2009. The effect of bakery products using barley, buckwheat, oat flour and barley flakes on post-food glycemia in patients with type 2 diabetes. *Nutrition issues* **78**(4), 40–47 (in Russian).

Granfeldt, Y., Drews, A. & Björck, I. 1995. Arepas made from high amylose corn flour produce favorably low glucose and insulin responses in healthy humans. *The Journal of nutrition* **125**(3), 459–465.

Grigelmo-Miguel, N., Carreras-Boladeras, E. & Martín-Belloso, O. 1999. Development of high-fruit-dietary-fibre muffins. *European Food Research and Technology* **210**(2), 123–128.

Hager, A.S., Ryan, L.A., Schwab, C., Gänzle, M.G., O'Doherty, J.V. & Arendt, E.K. 2011. Influence of the soluble fibres inulin and oat β-glucan on quality of dough and bread. *European Food Research and Technology* **232**(3), 405–413.

Hiippala, K., Jouhten, H., Ronkainen, A., Hartikainen, A., Kainulainen, V., Jalanka, J. & Satokari, R. 2018. The potential of gut commensals in reinforcing intestinal barrier function and alleviating inflammation. *Nutrients* **10**, 988.

Holtekjolen, A.K., Olsen, H.H.R., Fergestad, E.M., Uhlen, A.K. & Knutsen, S.H. 2008. Variations in water absorption capacity and baking performance of barley varieties with different polysaccharide content and composition. *LWT-Food Science and Technology* **41**(10), 2085–2091.

ISO 4121:2003. 'Sensory analysis. Guidelines for the use of quantitative response scales'. International Organization for Standardization, Geneva, Switzerland.

Kahlon, T.S. & Chow, F.I. 2000. Lipidemic response of hamsters to rice bran, uncooked or processed white and brown rice, and processed corn starch. *Cereal chemistry* **77**(5), 673–678.

Khramtsov, A.G., Ryabtseva, S.A., Budkevich, R.O., Akhmedova, V.R., Rodnaya, A.B. & Marugina, E.V. 2018. Prebiotics as functional food ingredients: terminology, selection and comparative criteria, classification. *Nutrition Issues* **87**(1), 5–17 (in Russian).

Kruse, H.P., Kleessen, B. & Blaut, M. 1999. Effects of inulin on faecal bifidobacteria in human subjects. *British Journal of Nutrition* **82**(5), 375–382.

Kuvandykova, G.I. & Vayskrobova, E.S. 2017. Nutritional value of various types of flour. In Baryshnikova, N.I. (ed): *Product, Technology and Education Quality: Proceedings of the XII International Scientific and Practical Conference*. State technical university named G.I. Nosova, Magnitogorsk, pp. 115–121 (in Russian).

Lapteva, N.K. 2012. Assortment of bakery and flour confectionery products using rye raw materials and its role in the nutrition of modern man. *Achievements of science and technology APK* **6**, 75–78 (in Russian).

Licht, T.R., Hansen, M., Poulsen, M. & Dragsted, L.O. 2006. Dietary carbohydrate source influences molecular fingerprints of the rat faecal microbiota. *Bmc Microbiology* **6**(1), 98.

López-Mejía, N., Martínez-Correa, H.A. & Andrade-Mahecha, M.M. 2019. Pancake ready mix enriched with dehydrated squash pulp (Cucurbita moschata): formulation and shelf life. *Journal of food science and technology* **56**(11), 5046–5055.

Mahalko, J.R., Sandstead, H.H., Johnson, L.K., Inman, L.F., Milne, D.B., Warner, R.C. & Haunz, E.A. 1984. Effect of consuming fiber from corn bran, soy hulls, or apple powder on glucose tolerance and plasma lipids in type II diabetes. *The American journal of clinical nutrition* **39**(1), 25–34.

Makinde, F.M. & Taibat, A.A. 2018. Quality characteristics of biscuits produced from composite flours of wheat, corn, almond and coconut. *Annals. Food Science and Technology* **19**, 216–225.

Makki, K., Deehan, E.C., Walter, J. & Bäckhed, F. 2018. The impact of dietary fiber on gut microbiota in host health and disease. *Cell host & microbe* **23**(6), 705–715.

Man, S., Păucean, A., Muste, S. & Pop, A. 2014. Studies on the formulation and quality characteristics of gluten free muffins. *Journal of Agroalimentary Processes and Technologies* **20**(2), 122–127.

Mariani, P., Viti, M.G., Montouri, M., La Vecchia, A., Cipolletta, E., Calvani, L. & Bonamico, M. 1998. The gluten-free diet: a nutritional risk factor for adolescents with celiac disease?. *Journal of pediatric gastroenterology and nutrition* **27**(5), 519–523.

Mayurnikova, L.A. & Ashirova, N.N. 2011. Celiac disease. Problems and Solutions. *Food industry* **6**, 60–63 (in Russian).

McCleary, B.V., DeVries, J.W., Rader, J.I., Cohen, G., Prosky, L., Mugford, D.C. & Okuma, K. 2012. Determination of insoluble, soluble, and total dietary fiber (CODEX definition) by enzymatic-gravimetric method and liquid chromatography: collaborative study. *Journal of AOAC International* **95**(3), 824–844.

Meleshkina, L.E. & Popova, A.V. 2011. Investigation of the effectiveness of kneading and molding of gluten-free pasta. *Polzunovsky Bulletin* **3/2**, 77–81 (in Russian).

Miyamoto, J., Watanabe, K., Taira, S., Kasubuchi, M., Li, X., Irie, J. & Kimura, I. 2018. Barley β-glucan improves metabolic condition via short-chain fatty acids produced by gut microbial fermentation in high fat diet fed mice. *PLoS One* **13**(4), e0196579.
Morris, C. & Morris, G.A. 2012. The effect of inulin and fructo-oligosaccharide supplementation on the textural, rheological and sensory properties of bread and their role in weight management: A review. *Food chemistry* **133**(2), 237–248.
Mudgil, D., Barak, S., Patel, A. & Shah, N. 2018. Partially hydrolyzed guar gum as a potential prebiotic source. *International journal of biological macromolecules* **112**, 207–210.
Musso, G., Gambino, R. & Cassader, M. 2011. Interactions between gut microbiota and host metabolism predisposing to obesity and diabetes. *Annual review of medicine* **62**, 361–380.
Niewinski, M.M. 2008. Advances in celiac disease and gluten-free diet. *Journal of the American Dietetic Association* **108**(4), 661–672.
O'Callaghan, A.A. & Corr, S.C. 2019. Establishing boundaries: The relationship that exists between intestinal epithelial cells and gut-dwelling bacteria. *Microorganisms* **7**(12), 663.
Onishchenko, G.G. 2008. Rational nutrition. Norms of physiological requirements for energy and nutrients for various groups of the population of the Russian Federation: MP 2.3. 1.2432-08. Moscow, Russia (in Russian).
Pereira, J., Gh, Z. & Zhang, W.G. 2016. Effects of rice flour on emulsion stability, organoleptic characteristics and thermal rheology of emulsified sausage. *Journal of Food and Nutrition Research* **4**(4), 216–222.
Pyryeva, E.A. & Safronova, A.I. 2019. The role and place of dietary fiber in the nutritional structure of the population. *Nutrition Issues* **88**(6), 5–11 (in Russian).
Rieder, A., Holtekjolen, A.K., Sahlstrom, S. & Moldestad, A. 2012. Effect of barley and oat flour types and sourdoughs on dough rheology and bread quality of composite wheat bread. *Journal of Cereal Science* **55**(1), 44–52.
Rieder, A., Knutsen, S.H., Fernandez, A.S. & Ballance, S. 2019. At a high dose even partially degraded beta-glucan with decreased solubility significantly reduced the glycaemic response to bread. *Food & function* **10**(3), 1529–1539.
Rosell, C.M., Santos, E. & Collar, C. 2010. Physical characterization of fiber-enriched bread doughs by dual mixing and temperature constraint using the Mixolab. *European Food Research and Technology* **231**(4), 535–544.
Sabanis, D. & Tzia, C. 2009. Effect of rice, corn and soy flour addition on characteristics of bread produced from different wheat cultivars. *Food and Bioprocess Technology* **2**(1), 68–79.
Schnizlein, M.K., Vendrov, K.C., Edwards, S.J., Martens, E.C. & Young, V.B. 2020. Dietary xanthan gum alters antibiotic efficacy against the murine gut microbiota and attenuates Clostridioides difficile colonization. *Msphere*, **5**(1).
Sciarini, L.S., Ribotta, P.D., Leon, A.E. & Perez, G.T. 2010. Influence of gluten-free flours and their mixtures on batter properties and bread quality. *Food and Bioprocess Technology* **3**(4), 577–585.
Sekirov, I., Russell, S.L., Antunes, L.C.M. & Finlay, B.B. 2010. Gut microbiota in health and disease. *Physiological reviews* **90**(3), 859–904.
Shi, L., Li, W., Sun, J., Qiu, Y., Wei, X., Luan, G., Hu, Y & Tatsumi, E. 2016. Grinding of maize: The effects of fine grinding on compositional, functional and physicochemical properties of maize flour. *Journal of Cereal Science* **68**, 25–30.
Shih, F.F., Truong, V.D. & Daigle, K.W. 2006. Physicochemical properties of gluten-free pancakes from rice and sweet potato flours. *Journal of food quality* **29**(1), 97–107.
Shoaib, M., Shehzad, A., Omar, M., Rakha, A., Raza, H., Sharif, H.R. & Niazi, S. 2016. Inulin: Properties, health benefits and food applications. *Carbohydrate polymers* **147**, 444–454.
Skripleva, E. & Arseneva, T. 2015. Optimization of the recipe of yoghurt with additives and control of some quality attributes of new yoghurt recipe. *Agronomy Research* **13**(4), 1086–1095.
Slavin, J. 2013. Fiber and prebiotics: mechanisms and health benefits. *Nutrients* **5**(4), 1417–1435.

Smyth, S. & Heron, A. 2006. Diabetes and obesity: the twin epidemics. *Nature medicine* **12**(1), 75–80.

Soong, Y.Y., Tan, S.P., Leong, L.P. & Henry, J.K. 2014. Total antioxidant capacity and starch digestibility of muffins baked with rice, wheat, oat, corn and barley flour. *Food chemistry* **164**, 462–469.

Starshov, D.G., Sedelkin, V.M. & Starshov, G.I. 2017. Research and development of a vacuum kneading machine. *Food Engineering* **45**(2), 99–105 (in Russian).

Stępniewska, S., Słowik, E., Cacak-Pietrzak, G., Romankiewicz, D., Szafrańska, A. & Dziki, D. 2018. Prediction of rye flour baking quality based on parameters of swelling curve. *European Food Research and Technology* **244**(6), 989–997.

Tipsina, N.N. & Selezneva, G.K. 2011. The use of barley flour in the production of bakery products. *Bulletin of the Krasnoyarsk State Agrarian University* **10**, 204–208 (in Russian).

Truswell, A.S. 2002. Cereal grains and coronary heart disease. *European journal of clinical nutrition* **56**(1), 1–14.

Tuohy, K.M., Kolida, S., Lustenberger, A.M. & Gibson, G.R. 2001. The prebiotic effects of biscuits containing partially hydrolysed guar gum and fructo-oligosaccharides–a human volunteer study. *British Journal of Nutrition* **86**(3), 341–348.

Vavilova, M.A. 2020. Features of the production of gluten-free pasta for the tolerance of gluten. In Gulyaev G.U. (ed): *European Scientific Conference.* ICSN Science and Enlightenment, Penza, pp. 18–20 (in Russian).

Vybornov, A.A. & Anisimova, L.V. 2013. Development of barley flour technology of improved quality. In Glebova, A.A. (ed): *Modern problems of engineering and technology of food production:materials of the XIV international scientific-practical conference.* Altai State Technical University, Barnaul, pp. 27–31 (in Russian).

Xhabiri, G.Q., Durmishi, N., Idrizi, X., Ferati, I. & Hoxha, I. 2016. Rheological qualities of dough from mixture of flour and wheat bran and possible correlation between bra bender and mixolab chopin equipments. *MOJ Food Processing and Technology* **2**, 42.

Yang, Q., Liang, Q., Balakrishnan, B., Belobrajdic, D.P., Feng, Q.J. & Zhang, W. 2020. Role of dietary nutrients in the modulation of gut microbiota: A narrative review. *Nutrients* **12**(2), 381.

Zaitseva, L.V., Yudina, T.A., Ruban, N.V., Bessonov, V.V. & Mehtiev, V.S. 2020. Modern approaches to the development of gluten-free bakery product formulations. *Nutrition Issues* **89**(1), 77–85 (in Russian).

Zimmerman, Ya.S. 2013. Eubiosis and dysbiosis of the gastrointestinal tract: myths and realities. *Clinical Medicine* **91**(1), 4–11 (in Russian).

Agronomy Research **18**(4), 2425–2435, 2020
https://doi.org/10.15159/AR.20.210

Boron content and some quality features of potato tubers under the conditions of using sulphur fertilizer

H. Klikocka

University of Life Sciences in Lublin, Department of Economics and Agribusiness, Akademicka 13, PL20-950 Lublin, Poland
Correspondence: hanna.klikocka@up.lublin.pl

Abstract. The objective of the study was to investigate the impact of sulphur application on the content and uptake of boron (B) with the yield of potato tubers. A field experiment with potato was conducted in 2009–2011, with S applied in different forms (elemental and K_2SO_4) and at different rates (0, 25 and 50 kg ha^{-1}).
The content of B in tubers depended significantly on each fertilizer S rate and form. The uptake of boron with dry mass of tubers was equally advantageous in the application of each rate and form with sulphur fertilization compared to controls. No significant effect of weather on the content and uptake of boron tubers was found. The tuber yield and starch content were significantly increased by both the fertilizer S rate and form. A positive correlation was found between B content and B uptake of the yield of tubers. B uptake positively correlated with tuber yield and with a yield of DM and with the yield of starch.
Sulphur applied as sulphate increased the content of SO_4-S in the soil. Application of elemental S at a rate of 50 kg ha^{-1} decreased the pH of the soil. Soil content of total C depended on each rate and form of S applied. No correlation was found between B content and B uptake between the analysed soil parameters. The content of total C in the soil was positively correlated with tuber yield. The pH of soil negatively correlated with tuber yield.

Key words: sulphur fertilization, boron, potato.

INTRODUCTION

Boron is an essential component of plants for proper development and growth. It plays a part in carbohydrate metabolism, synthesis of nucleic acids (DNA and RNA) and phytohormones. Boron regulates the development of tissues and the structure of cell walls, promotes the development of buds and flowering, and also acts as a protective antioxidant (Cakmak & Römheld, 1997; Korzeniowska, 2008). Boron reduces the oxidation of phenols and prevents discolouration of tubers. Boron deficiency induces the internal breakdown of tubers in sugar beet, turnip and potatoes (Brown et al., 2002). Hopkins et al. (2007) studied the role of boron on tuberization and yield in potato and reported a non-significant increase due to soil or foliar application of boron. Boron does not have a direct influence on yield or related attributes; however, it plays a supplementary role when applied with sulphur (Bari et al., 2001; Singh et al., 2018).

Plants uptake boron from the soil solution as ions BO_3^{3-} and $B_4O_7^{2-}$. The concentration of boron in the soil solution is a characteristic of the high dynamics of changes. For the duration of one vegetation season boron concentration can indicate toxic and deficiency values. At the same time, the distinction between toxic and deficiency concentration levels are very fine (Zhu et al., 2007; Szulc & Rutkowska, 2013). The uptake of boron anions through the roots is partly limited in the presence of other anions: Cl^-, SO_4^{2-}, $PO^{3-}{}_4$. This element is most intensively taken from acidic soils. Plants that require a lot of boron include some *Fabaceae* (alfalfa), root crops (beets, potatoes), vegetables, (cauliflower, celery) and fruit trees (apple trees) (Singh et al., 2018).

Our earlier research also showed an increase in macro- and microelements in potato tubers and cereal grains fertilized with sulphur (Klikocka et al., 2005; Klikocka, 2010; Klikocka & Głowacka, 2013; Klikocka et al., 2017). Sulphur deficiency occurs in many European and other countries (Järvan et al., 2008; Klikocka, 2011a; Tabak et al., 2019). Particularly in Poland, some regions are characterized by low SO_2 emissions to the atmosphere and low soil element content. Sulphur dioxide emissions have also been significantly reduced in Estonia (Podkuiko et al., 2017). Research on sulphur fertilization shows that sulphur should be added to fertilization to increase plant production and improve the quality of agricultural products (Klikocka, 2011b; Siebielec et al., 2017).

Sulphur supplementation for mineral fertilization, mainly nitrogen, is a very significant and current problem in agriculture. The lack of wider scientific research on the fertilization of plants with sulphur results from the fact that, especially in Poland (which is mainly dependent on industry), the positive balance of this element in agroecosystems was maintained for many years, as a result of high SO_2 emissions to the atmosphere in the country. However, due to environmental protection initiatives aimed at reducing SO_2 emissions to the atmosphere in Western Europe a progressing negative sulphur balance in soil could be observed from the second half of the 1980s (Klikocka, 2011a). Studies concerning the content of sulphur in plants have shown that there is a group of plants particularly sensitive to deficiency of this element. These are *Brassicaceae* (rape), *Liliaceae* (garlic, onion), *Fabaceae* (bean), *Amaranthaceae* (sugar beet), *Solanaceae* (potato) and *Poaceae* (wheat) (Klikocka, 2011b).

Sulphur application has been found to increase the yield of potato tubers and improve tuber quality and resistance to *Streptomyces scabies* and *Rhizoctonia solani* (Klikocka et al., 2005; Klikocka, 2010). According to Wang et al. (2008), potato is not considered a high S-demanding crop, with S concentrations ranging from 1.2 to 2.8 g kg^{-1} in the dry matter of tuber and haulm, but considerable amounts of S can be removed from the soil over the long term when yields are high. In S-deficient soil, application of S fertilizer can significantly increase the tuber yield and starch content of potato, while contributing to a decrease in tuber N concentration due to increased dry matter production (Kołodziejczyk, 2014). Furthermore, Eppendorfer & Eggum (1994) found that S deficiency significantly influenced the amino acid composition of potato; the concentration of the S-containing amino acids methionine and cysteine decreased by 30% and 60%, respectively, in S-deficient soil.

Potato (*Solanum tuberosum* L.) is the fourth most important food crop in the world, providing more food than the combined world output of fish and meat. Potato tube yield depends on agrotechnical treatments, cultivars and environmental conditions (Barbaś & Sawicka, 2020). Potato tubers contain 1–1.2% mineral compounds, the most basic being potassium, magnesium, calcium and phosphorus (Gugała & Zarzecka; 2011, Klikocka & Głowacka; 2013). In the study by Wierzbicka (2012), the average boron content in potato tubers was 0.10 mg 100 g^{-1} fresh mass, which on average corresponds to 7% of the daily human demand for boron.

However, there is little information available concerning the influence of S supply on boron content in potato tubers. We therefore made an attempt to determine the effect of the form (sulphate or elemental) and rate (0, 25, 50 kg ha^{-1}) of sulphur application on the content and uptake of boron (B) in the dry mass of potato tubers.

MATERIALS AND METHODS

Field experiments were conducted in 2009–2011 in south-eastern Poland (50º42' N, 23º15' E). A two-factor experiment was carried in a randomized split-plot design (with four replications). The soil in the experiment was marked as Cambisols (WRB 2015) consisting of light silty sand (sand 68%, silt 31% and clay 1%). In the soil a high content of phosphorus (P) (53.5 mg kg^{-1}) was found, an average content of potassium (K) and magnesium (Mg) (respectively 85.2 and 33.7 mg kg^{-1}), and low total and available sulphur ($S\text{-}SO_4^{2-}$) (respectively 87.0 and 12.4 mg kg^{-1}). The soil reaction was slightly acidic (pH 5.7) and total C content amounted to 9.0 g kg^{-1}.

The object of the study was potato (*Solanum tuberosum* L.) of the medium-early edible Irga variety fertilized with sulphur in the amount of 0, 25 and 50 kg S ha^{-1} in the form of potassium sulphate (K_2SO_4) and elemental sulphur (S^0). The area of the plots was 30 m^2 for planting and observation, and 19.5 m^2 (3.0 m × 6.5 m) for harvesting.

After harvesting of spring Triticale, 3 t ha^{-1} of straw from spring Triticale (as organic fertilizer) and 46 kg N ha^{-1} (urea $CO(NH_2)_2$, for stabilization of the C:N ratio) was applied, and the soil was ploughed (20 cm, second or third week of August). Spring fieldwork was carried out in the third week of March, using shallow ploughing (15 cm). Each year mineral fertilizers were applied pre-planting (kg ha^{-1}): N - 100 (as ammonium nitrate); P - 40 (as mineral superphosphate - triple granular); and K - 140 (as potassium chloride in control plots and plots with elemental S, and as potassium chloride balanced with potassium sulphate in plots with sulphate sulphur - 116 kg of K as K_2SO_4 + 24 kg of K as KCl). Potato planting was carried out in the second third of April. Row-space was 67.5 cm with 44,000 tubers planted per ha. The distance between plants in a row was 30 cm.

Chemical application of fungicides and herbicides for the control of pests and potato diseases was carried out using the recommendations of the Institute of Plant Protection (IOR-Poland).

Table 1. Meteorological conditions in 2009–2011 and the long-term average from 1971–2005 (Zamość Research Station)

	Months (k)						Sum - Mean (IV-IX)		
Years	Apr	Mai	Jun	Jul	Aug	Sep	*k*	*p*	*t*
2009	0.46	2.39	2.06	0.39	0.78	0.68	1.10	350.1	3,122
2010	1.13	2.02	1.14	2.08	1.34	1.79	1.56	489.0	2,967
2011	1.14	0.75	0.95	2.39	2.27	0.05	1.33	404.2	2,923
1971–2005	1.85	1.50	1.56	1.72	0.99	1.35	1.44	393.5	2,690

p – precipitation (mm); *t* – temperature (°C); k – Selyaninov's hydrothermal coefficient [$k = (p \times 10)/\sum t$). The value of the Sielianinov's coefficient (Skowera, 2014): extremely dry $k \leq 0.4$, very dry $0.4 < k \leq 0.7$, dry $0.7 < k \leq 1.0$, rather dry $1.0 < k \leq 1.3$, optimal $1.3 < k \leq 1.6$, rather humid $1.6 < k \leq 2.0$, humid $2.0 < k \leq 2.5$, very humid $2.5 < k \leq 3.0$, extremely humid $k > 3.0$.

Table 1 presents rainfall and air temperature during the vegetation season (IV–IX) in 2009–2011. The hydrothermal coefficient of Selyaninov was analysed based on meteorological data. The 2009 growing season was rather dry (1.10), while the 2010 and 2011 seasons were optimum (respectively 1.56 and 1.33).

After potato harvest, the tuber yield in t ha^{-1} and the percentage starch content (using the Reiman-Parow hydrostatic balance) were determined. Tuber samples (from each plot) after drying were ground into particles smaller than 0.12 mm. Boron (B) was analysed in dry mass (DM) of potato tubers by colourimetry using diantrimide (Poulain & Al Mohammad, 1995) after digestion of the dried tubers at 550 °C and dissolution of the residue in hydrochloric acid solution. In soil samples taken annually from each plot in spring (before sowing fertilizers) and after the harvesting of potato tubers, the content of sulphate sulphur, total carbon and soil pH were determined using methods indicated in Table 2. The analyses were carried out in the Laboratory of the Institute of Plant Nutrition and Soil Science at FAL in Braunschweig (Germany) (Table 2).

Table 2. Analytical methods for plant tissue materials and soil

Parameter	Method
Plant tissue material	
Dry matter	Oven method (at 105 °C)
Starch	Specific gravity method using a Reimann-Parow hydrostatic balance
Boron	Determined by colourimetry with diantrimide (Poulain & Al Mohammad, 1995) after digestion of the dried potato tubers at 550 °C and dissolution of the residue in hydrochloric acid solution
Soil	
pH	Determined potentiometrically in 0.01 M $CaCl_2$ suspension using a Methrohm 605 pH-meter
Total C	Dry combustion; LECO EC-12®, model 752-100
SO_4^{2-}	Extracted using 0.025 m KCl and determined by ion-chromatography

The results were subject to an analysis of variance (ANOVA) using the Snedecor F test, and mean values were compared by the Tukey test using Statistica software, version 7.0 (StatSoft Inc.: Tulsa, OK, USA, 2007; StatSoft Polska Kraków, 2007) and Excel 7.0 (2007 Microsoft Office System). The significance level for rejection of the null hypothesis was 5% ($p < 0.05$). The relationships between the tested parameters were determined by Pearson's correlation.

RESULTS AND DISCUSSION

The analysis of variance showed that the differences in the content and uptake of boron with the yield of the tubers were statistically significant. The experimental factors had different effects on the analysed characteristics (Table 3). The content of B in tubers depended significantly on the rate and form of S fertilizer. In ascending order, the following combinations worked best: (1) 50 kg SO_4 ha^{-1} - 100%, (2) 25 kg S ha^{-1} - 96.2%, (3) 50 kg S ha^{-1} - 93.5%, (4) 25 kg SO_4 ha^{-1} - 90.9%, (5) 0 kg S ha^{-1} (Control) - 84.9%. In our own study potato tubers accumulated on average 9.11 mg kg^{-1} DM of boron. In the study of Hajduk et al. (2012), potato tubers accumulated much less boron (2.2–7.5 mg kg^{-1} DM).

Table 3. The influence of S fertilization on the content (mg kg^{-1}) and uptake (g ha^{-1}) of B in potato tubers and yield of tubers (t ha^{-1})

S rate (kg ha^{-1})	S form	Boron		Yield of tubers (t ha^{-1})
		Content (mg kg^{-1} DM)	Uptake (g ha^{-1})	
0 – Control		8.28 e	47.99 b	25.56 c
25	SO_4-S	8.86 d	55.63 a	28.06 a
25	S°	9.38 b	54.05 a	26.17 b
50	SO_4-S	9.75 a	56.44 a	27.02 ab
50	S°	9.12 c	55.54 a	27.44 ab
0 – Control		8.28 A	47.99 A	25.56 B
25	Mean	9.12 A	54.84 A	27.12 A
50		9.51 A	55.54 A	27.23 A
0 – Control		8.28 A	47.99 A	25.56 B
SO_4-S	Mean	9.30 A	56.03 A	27.54 A
S°		9.33 A	54.35 A	26.81 A
Years	2009	9.49 A	52.82 A	25.03 C
	2010	8.99 A	53.82 A	27.07 B
	2011	8.86 A	54.61 A	28.46 A
F-distribution	R	1.04	1.21	5.20
	F	0.50	1.46	6.55
	R × F	4.04	3.22	3.11
	Y	0.97	0.39	15.67
p-value	R	0.3683	0.3130	0.0123
	F	0.6125	0.2510	0.0048
	R × F	0.0069	0.0209	0.0241
	Y	0.1042	0.6822	0.0000
LSD	R	n.s.	n.s.	1.19
$P = 0.05$	F	n.s.	n.s.	1.19
	R × F	0.22	5.32	1.60
	Y	n.s.	n.s.	1.19

Explanations: Variable: R rate ($df_1 = 2$, $df_2 = 27$); F form ($df_1 = 2$, $df_2 = 27$); RF rate x form ($df_1 = 4$, $df_2 = 45$); Y years ($df_1 = 2$, $df_2 = 45$): where df_1 – variable degree of freedom; df_2 – error degree of freedom; F – distribution in analysis of variance, *p*-value of F variance ratio; LSD – least significant difference; n.s. – not significant.

Uptake of boron with a dry mass of tubers was equally advantageous for all rates and forms of sulphur fertilization compared to controls. In our own study, potato tubers have an uptake of boron on average 53.75 g ha^{-1}. No significant effect of weather on the content and uptake of boron tubers was observed (Table 3).

Sulphur application had a positive effect on the tuber yield. The application of each rate of sulphur, regardless of its form, had a significantly positive effect on tuber yield compared to the control group (in which sulphur was not used). However, the most favourable tuber yield was obtained after the application of 25 kg ha^{-1} of sulphate sulphur (SO_4-S) (Table 3). A less favourable result was achieved after using elemental sulphur. As reported by Klikocka et al. (2005), elemental sulphur must undergo some biochemical and microbiological processes in the soil before it becomes available to plants, so a rate of 25 kg ha^{-1} in the elemental form is not as effective as sulphate that is directly available to plants. A positive impact of sulphur fertilization (in the form of potassium sulphate, ammonium sulphate, single superphosphate, gypsum and elemental sulphur) on potato yields has been reported by numerous authors, such as Carew et al. (2009). The effect may result from a slight decrease in soil pH (pH) due to the use of sulphur, in conditions where the boron anion is better absorbed (Singh et al., 2018).

Kumar et al. (2007) reported that tuber dry-matter percentage was higher after the application of K in the form of potassium sulphate and nitrate than potassium chloride. In the presented studies, an inverse relationship was noted. This is because the addition of each rate and form of S to NPK fertilization caused a significant reduction in the percentage of dry matter. This content was highest on control plots where sulphur was not used (Table 4).

Wang et al. (2008) state that in S-deficient soil the application of S fertilizer can significantly increase tuber yield and the starch content of potato. A similar phenomenon was noted in the presented research. It was found that each rate and form of sulphur used significantly increased the starch content in potato tubers. It was noted that the most favourable rate was 25 kg ha^{-1} of sulphate sulphur (SO_4-S) (Table 4).

Table 4. The influence of S application on quality of potato tubers

S rate (kg ha^{-1})	S form	Dry Mass of tubers (%)	Dry Mass Yield (t ha^{-1})	Starch content (%)	Yield of starch (t ha^{-1})
0 – Control		22.75 a	5.81 b	14.63 c	3.74 b
25	SO_4-S	22.38 b	6.28 a	14.73 bc	4.14 a
25	S^o	22.10 b	5.78 b	14.97 a	3.92 ab
50	SO_4-S	21.50 c	5.80 b	14.85 ab	4.04 a
50	S^o	21.52 c	5.90 b	14.78 bc	4.06 a
0 – Control		22.75 A	5.81 A	14.63 B	3.74 B
25	Mean	22.24 B	6.03 A	14.85 A	4.03 A
50		21.51 C	5.85 A	14.82 A	4.05 A
0 – Control		22.75 A	5.81 A	14.43 B	3.74 C
SO_4-S	Mean	21.94 B	6.04 A	14.79 A	4.09 A
S^o		21.81 B	5.56 A	14.88 A	3.99 B
Years	2009	22.32 A	5.58 B	14.11 C	3.53 C
	2010	22.14 A	5.99 A	14.99 B	4.06 B
	2011	21.69 B	6.17 A	15.28 A	4.35 A
F-distribution	R	67.07	1.95	10.63	7.28
	F	56.42	2.43	6.14	8.94
	R × F	29.75	3.21	4.83	3.26
	Y	17.41	11.16	189.70	38.77
p-value	R	0.0000	0.1621	0.0004	0.0030
	F	0.0000	0.1069	0.0063	0.0010
	R × F	0.0000	0.0210	0.0025	0.0197
	Y	0.0000	0.0001	0.0000	0.0000
LSD	R	0.22	n.s.	0.10	0.19
P = 0.05	F	0.22	n.s.	0.10	0.19
	R × F	0.29	0.33	0.16	0.25
	Y	0.22	0.24	0.10	0.19

Explanations: as in Table 3.

The study of Singh et al. (2018) and Sharma et al. (2011) revealed that application of sulphur led to a significantly high yield and quality of potato tubers in terms of DM and starch content. According to Singh et al. (2018), Eppendorfer & Eggum (1994) the plants without the application of sulphur and boron might suffer from deficiency so dry matter and starch content was lowest. For yield of tubers, yield of dry mass, starch content and yield of starch the most favourable growing season was 2011. In this season July and August were humid (k = 2.39 and 2.27) and September was extremely dry (k = 0.05). In the study by Pszczółkowski et al. (2019) the highest content and yield of dry matter and starch were obtained in years with optimum and well-distributed rainfall, while the highest starch content was recorded in dry and sunny years. Makaraviciute (2003) observed in their research that the use of different rates and forms of fertilizers as well as changing weather during the potato growing season had an irregular effect on the content. In favourable meteorological conditions, the use of NP and K fertilizers in the form of potassium sulphate and the addition of microelements increased the amount of starch and dry matter in most of the studied varieties' mass in potato tubers.

Table 5 shows soil pH and soil content of total carbon and SO_4-S after the potatoes were harvested. Generally, the application of S significantly increased SO_4-S content in the soil. Soil content of SO_4-S depended more on the form of S than on the rate of application and was highest after the application of elemental S at 50 kg ha^{-1}.

Table 5. The influence of S application on the soil characteristics

S rate (kg ha^{-1})	S form	pH (0.01 M KCl)	Total C (g kg^{-1})	SO_4-S (mg kg^{-1})
0 – Control		5.28–5.30	8.00 c	24.88 b
25	SO_4-S	5.24–5.33	7.93 c	29.03 ab
25	S^o	5.16–5.37	9.74 a	26.03 b
50	SO_4-S	5.12–5.39	9.04 b	33.40 a
50	S^o	5.12–5.15	9.38 ab	26.79 b
0 – Control		5.28–5.30	8.00 C	24.88 A
25	Mean	5.22–5.35	8.84 B	27.53 A
50		5.12–5.27	9.21 A	30.10 A
0 – Control		5.28–5.30	8.00 C	24.88 B
SO_4-S	Mean	5.18–5.36	8.49 B	31.21 A
S^o		5.15–5.25	9.56 A	26.41 B
Years	2009	5.26–5.39	7.66 C	23.75 B
	2010	5.20–5.27	9.19 B	35.86 A
	2011	5.16–5.22	9.61 A	24.47 B
F-distribution	R	-	24.46	3.12
	F	-	67.22	6.31
	R × F	-	18.56	3.99
	Y	-	48.81	27.10
p-value	R	-	0.0000	0.0601
	F	-	0.0000	0.0056
	R × F	-	0.0000	0.0074
	Y	-	0.0000	0.0000
LSD P = 0.05	R	-	0.28	n.s.
	F	-	0.28	3.82
	R × F	-	0.54	4.80
	Y	-	0.28	3.82

Explanations: as in Table 3.

The application of elemental S noticeably reduced soil pH. The application of S in the form of sulphate generally increased the content of SO_4-S in the soil, while fertilization with elemental S at a rate of 50 kg ha^{-1} decreased soil acidity. Irrespective of the form of S, the rate of 50 kg ha^{-1} was more favourable to total C content in the soil. Sulphate applied with mineral fertilizers is more prone to leaching, and S sequestration depends on both the fertilizer type and the S application rate (Scherer et al., 2012).

The content of SO_4-S and content of total C in the soil and pH of soil did not correlate with the content and uptake of B by the yielsd of tubers (Table 5). The pH of soil negatively correlated with the yield of tubers and with starch content and yield of starch. There was a positive correlation between the pH of the soil and dry mass of tubers and with yield of DM and with starch content and yield of starch. The content of total C in the soil negatively correlated with the dry mass of tubers. No correlation was found between the content of SO_4-S and the analysed features. The pH of soil negatively correlated with total C content in the soil. Also, a positive correlation was noted between B uptake and yield of tubers. A positive correlation was found between B content and B uptake and between B uptake and yield of DM and yield of starch. Tuber yield negatively correlated with dry mass of tubers. A positive correlation was identified between tuber yield and yield of DM and starch content and yield of starch (Table 6).

Table 6. Significant correlation coefficients (r_{xy}) between elements in plants, soil properties and yield of potato tubers (mean values from 2009–2011)

Specification (n = 60)	No.	Number of features								
		2	3	4	5	6	7	8	9	10
B content (mg kg^{-1})	1	**0.774**	-0.132	-0.136	-0.200	-0.161	-0.162	0.075	-0.054	0.040
B uptake (g ha^{-1})	2	-	**0.473**	-0.171	**0.462**	0.052	**0.368**	-0.023	0.121	0.135
Yield of tubers (t ha^{-1})	3	-	-	**-0.435**	**0.929**	**0.365**	**0.902**	**-0.277**	**0.340**	0.150
Dry Mass of tubers (%)	4	-	-	-	-0.074	**-0.366**	**-0.496**	**0.436**	**-0.314**	-0.058
Yield of DM (t ha^{-1})	5	-	-	-	-	**0.249**	**0.793**	-0.141	**0.254**	0.154
Starch content (%)	6	-	-	-	-	-	**0.729**	**-0.357**	**0.327**	0.139
Yield of starch (t ha^{-1})	7	-	-	-	-	-	-	**-0.351**	**0.393**	0.171
pH of soil	8	-	-	-	-	-	-	-	**-0.335**	0.040
Total C content (g kg^{-1})	9	-	-	-	-	-	-	-	-	0.117
SO_4-S content (mg kg^{-1})	10	-	-	-	-	-	-	-	-	-

* Bold letters mean significant differences (P 0.05 = 0.250 and P 0.01 = 0.325).

As reported by Jaggi et al. (2005) and Scherer et al. (2012), sulphur deficiency in world soils has led to the supplementation of S fertilizer to enhance the production and improvement of quality of crops. Among S-containing fertilizers, elemental S (S^o) is becoming increasingly popular in field crops. The use of S^o helps to reduce leaching and run-off losses, leaving prolonged residual effects on the S nutrition of the succeeding crop.

The biochemical oxidation of S^o produces H_2SO_4, which decreases soil pH and makes soil conditions more favourable for plant growth (Jaggi et al., 2005; Safaa et al., 2013). Therefore, supplementation of mineral fertilization for potatoes with sulphur, and particularly its elemental form, should be recommended. Kalembasa & Kuziemska (2013) found that plants take up boron (B) in greater quantities from acidic and weakly acidic soils, and its uptake by plants decreases with increasing pH. This phenomenon can be referred to as the presented own research.

Based on the present study, an optimum rate of 50 kg ha^{-1} of elemental sulphur may be proposed for potato. This will introduce an additional 39.9 mg kg^{-1} SO_4-S into the soil (assuming that the average depth of the topsoil is 25 cm and soil density is 1.5 Mg m^{-3}). At present, 91.7% of soil profiles in Poland contain less than 10.0 mg kg^{-1} SO_4-S, so that they are classified as low-sulphur, which entails a possibility that such soils may be deficient in sulphur (Siebielec et al., 2017). The soil on which the experiment was carried out contained 10.1 mg kg^{-1} SO_4-S, which was very low content.

CONCLUSIONS

1. Fertilization with sulphate sulphur at 25 kg S ha^{-1} and elemental sulphur at 50 kg ha^{-1} proved most favourable for the yield of potato tubers and the yield of dry matter and starch. The content of starch was significantly increased by both rates of supplementation and both forms of sulphur fertilizer.
2. The application of sulphur increased B content and uptake irrespective of the rate or form of S fertilizer. Boron content was highest when sulphate (SO4-S) was applied at 50 kg S ha-1. Boron uptake by the yield of tubers was significantly increased by both rates and forms of the applied S fertilizer.
3. Fertilization with sulphur at 50 kg ha-1 and in its elemental form significantly increased the content of total carbon in the soil. On the other hand, the use of sulphate, regardless of the rate, fostered the content of total nitrogen in the soil.
4. A positive correlation was identified between B content and B uptake in the yield of tubers. B uptake positively correlated with tubers yield and with the yield of DM and yield of starch. No correlation was determined between B content and B uptake in the analysed parameters of the soil. The content of total C in the soil was positively correlated with tuber yield. The pH of soil negatively correlated with tuber yield.
5. Sulphur fertilization can also be recommended for organisational reasons because it has a generally positive biological effect.

REFERENCES

Barbaś, P. & Sawicka, B. 2020. Dependence of potato yield on weed infestation. *Agronomy Research* **18**(2), 346–359. doi.10.15139/AR.20.122

Bari, M.S., Rabbani, M.G., Rahman, M.S., Islam, M.J. & Hoque, A.T.M.R. 2001. Effect of zinc, boron, sulphur and magnesium on the growth and yield of potato. *Pak. J. Biol. Sci.* **4**, 1090–1093. doi: 10.3923/p.2001.1090.1093

Brown, P.H., Bellaloui, N., Wimmer, M.A., Bassil, E.S., Ruiz, J., Hu, H. & Römheld, V. 2002. Boron in plant biology. *Plant Biol.*, **4**, 205–223. https://-doi.org-10.1055/s-2002-25740

Cakmak, I. & Römheld, V. 1997. Boron deficiency-induced impairments of cellular functions in plants. *Plant Soil* **193**, 71–83. https://doi.org/10.1023/A:1004259808322

Carew, R., Khakbazan, M. & Mohr, R. 2009. Cultivar Developments, Fertilizer Inputs, Environmental Conditions, and Yield Determination for Potatoes in Manitoba. *Am. J. Potato Res*. **86**, 442–455.

Eppendorfer, W.H. & Eggum, B.O. 1994. Effects of sulphur, nitrogen, phosphors, potassium, and water stress on dietary fibre fractions, starch, amino acids and the biological value of potato protein. *Plant Food Hum. Nutr.* **45**, 299–313. https://doi.org/10.1007/BF01088079

Gugała, M. & Zarzecka, K. 2011. Effect of insecticides on phosphorus and potassium content in tubers of three potato cultivars. *J. Elem.* **16**(1), 43–50. doi: 10.5601/jelem.2011.16.1.43-50

Hajduk, E., Gąsior, J., Właśniewski, S., Nazarkiewicz, M. & Kaniuczak, J., 2017. Influence of liming and mineral fertilization on the yield and boron content of potato tubers (*Solanum tuberosum* L.) and green mass of fodder sunflower (*Helianthus annuus* L.) cultivated in loess soil. *J. Elem*. **22**(2), 411–426. doi: 10.5601/jelem.2016.21.2.1101

Hopkins, B., Jolley, V.D., Webb, B.L., Ellsworth, J. & Callahan, R. 2007. Boron fertilization in Potato. In: *Western Nutrient Management Conference*. Vol. **7**, pp. 215–218.

Jaggi, R.C., Aulakh, M.S. & Sharma, R. 2005. Impacts of elemental S applied under various temperature and moisture regimes on pH and available P in acidic, neutral and alkaline soils. *Biology Fert. Soils* **41**, 52–58. doi: 10.1007/s00374-004-0792-9

Järvan, M., Edesi, L., Adamson, A., Lukme, L. & Akk, A. 2008. The effect of sulphur fertilization on yield, quality of protein and baking properties of winter wheat. *Agronomy Research* **6**(2), 459–469.

Kalembasa, S. & Kuziemska, B. 2013. Effect of varied content of molybdenum and boron in soil on urease activity. *Ecol. Chem. Eng. A.* **20**(6), 611–620. doi: 10.2428/ecea. 2013.20(06)056

Klikocka, H., Haneklaus, S., Bloem, E. & Schnug, E. 2005. Influence of sulphur fertilization on infestations of potato tubers (*Solanum tuberosum* L.) with *Rhizoctonia solani* and *Streptomyces scabies*. *J. Plant Nutr*. **28**, 819–833. https://doi.org/10.1081/PLN-200055547

Klikocka, H. 2010. The sulphur status in biosphere and plant fertilization. *Przem. Chem*. **89**, 903–908.

Klikocka, H. 2011a. The effect of sulphur kind and dose on content and uptake micro-nutrients by potato tubers (*Solanum tubersosum* L.). *Acta Sci. Pol.-Hortoru*. **10**, 137–151.

Klikocka, H. 2011b. Resources of sulphur in Poland and its importance in industry and agriculture. *Przem. Chem.* **90**, 1728–1737.

Klikocka, H. & Głowacka, A. 2013. Does the sulphur fertilization modify magnesium and calcium content in potato tubers (*Solanum tuberosum* L.)? *Acta Sci. Pol.-Hortoru*. **12**, 41–53.

Klikocka, H., Cybulska, M. & Nowak, A. 2017. Efficiency of Fertilization and Utilization of Nitrogen and Sulphur by Spring Wheat. *Pol. J. Environ. Stud.* **26**, 2029–2036. doi: 10.15244/pjoes/69942

Kołodziejczyk, M. 2014. Effectiveness of nitrogen fertilization and application of microbial preparations in potato cultivation. *Turk. J. Agric. For*. **38**, 299–310. doi:10.3906/tar-1305-105

Korzeniowska, J. 2008. Response of ten winter wheat cultivars to boron foliar application in a temperate climate (South-West Poland). *Agronomy Research* **6**(2), 471–476.

Makaraviciute, A. 2003. Effect of organic and mineral fertilizers on the yield and quality of different potato varieties. *Agronomy Research* **1**(2), 197–209.

Podkuiko, L., Olt, J. & Kikas, T. 2017. Growth of *Scenedesmus obliquus* under artificial flue gas with a high sulphur concentration neutralized with oil shale ash. *Proceedings of the Estonian Academy of Sciences* **66**, 2, 151–158. doi. 10.3176/proc.2017.2.03

Poulain, D. & Al Mohammad, H. 1995. Effects of boron deficiency and toxicity on faba bean (*Vicia faba* L.). *Eur. J. Agron.* **4**(1), 127–134. https://doi.org/10.1016/S1161-0301(14) 80024-5

Pszczółkowski, P., Sawicka, B. & Danilčenko, H. 2019. Effect of biopreparates on the dry matter, starching and vitamin C in potato tubers. *Agronomy Science* **74**(3), 47–56 (in Polish). https://doi.org/10.24326/as.2019.3.4

Safaa, M.M., Khaled, S.M. & Hanan, S.S. 2013. Effect of elemental sulphur on solubility of soil nutrients and soil heavy metals and their uptake by maize plants. *J. Am. Sci.* **9**(12), 19–24. ISSN: 1545-1003

Scherer, H.W., Főrster, S. & Welp, G. 2012. Sulphur fractions in particle-size separates as influenced by long-term application of mineral and organic fertilizers. *Plant Soil Environ.* **58**(5), 242–248. doi: 10.17221/78/2012-PSE

Siebielec, G., Smereczak, B., Klimkowicz-Pawlas, A., Kowalik, M., Kaczyński, R., Koza, P., Ukalska-Jaruga, A., Łysiak, M., Wójtowicz, U., Poręba, L & Chabros, E. 2017. Report from the third stage of the contract implementation. In Monitoring of Chemistry of Arable Soils in Poland in 2015–2017; IUNG-PIB Puławy, pp. 1–170 (in Polish).

Sharma, D.K., Kushwah, S.S., Nema, P.K. & Rathore, S.S. 2011. Effect of sulphur on yield and quality of potato. *Int. J. Agric. Res.* **6**, 143–148. doi: 10.3923/ijar.2011.143.148

Singh, S.K., Sharma, M., Reddy, K.R. & Venkatesh, T. 2018. Integrated application of boron and sulphur to improve quality and economic yield in potato. *J. Envin. Biol.* **39**, 204–210. doi: http://doi.org/10.22438/jeb/39/2/MRN-395

Skowera, B. 2014. Changes in hydrothermal conditions in Poland (1971−2010). *Fragm. Agron.* **31**(2), 74–87 (in Polish).

Szulc, W. & Rutkowska, B. 2013. Diagnostics of boron deficiency for plants in reference to boron concentration in the soil solution. *Plant Soil Environ.* **59**(8), 372–377. doi: 10.17221/306/2013-PSE

Tabak, M., Lepiarczyk, A., Filipek-Mazur, B. & Bachara, P. 2019. The effect of fertilization with ammonium nitrate enriched with ammonium sulfate on the quantity and quality of winter wheat grain yield as well as on soil properties. *Plant Soil Environ.* **65**, 211–217. doi:10.17221/44/2019-PSE

Wang, Zhao-Hui., Li, Sheng-Xiu. & Malhi, S. 2008. Effects of fertilization and other agronomic measures on nutritional quality of crops. *J. Sc. Food Agric*. **88**, 7–23. doi. 10.1002/jsfa.3084

Wierzbicka, A. 2012. Mineral content of potato tubers grown in the organic system, Their nutritional value and interaction. *J. Res. Applic. Agric. Eng*. **57**(4), 288–292.

Zhu, D., Wang, J., Liao, S. & Liu, W. 2007. *Relationship between plant availability of boron and the physico-chemical properties of boron in soils*. In: Xu, F., Goldbach, H.E., Brown, P.H., Bel, R.W., Fujiwara, T., Hunt, C.D., Goldberg, S. & Shi, L. (eds.): *Advances in Plant and Animal Boron Nutrition.* Springer, Dordrecht, pp. 345–354.

Agronomy Research **18**(4), 2436–2448, 2020
https://doi.org/10.15159/AR.20.206

The effectiveness of biopreparations in soft wheat cultivation and the quality assessment of the grain by the digital x-ray imaging

L.E. Kolesnikov[1,*], I.I. Novikova[2], E.V. Popova[2], N.S. Priyatkin[3], E.V. Zuev[4], Yu.R. Kolesnikova[4] and M.D. Solodyannikov[1]

[1]Saint-Petersburg State Agrarian University, Faculty of Agrotechnologies, Soil science and Ecology, Department of Plant Protection and Quarantine, Petersburgskoe Shosse (highway), 2, RU196601 St. Petersburg, Pushkin, Russia
[2]All-Russian Institute of Plant Protection (VIZR), Laboratory of microbiological plant protection, shosse Podbel'skogo highway, 3, RU196608 S. Petersburg, Pushkin, Russia
[3]Agrophysical Research Institute (ARI), plant biophysics division, Grazhdanskiy ave. 14, RU195220 St. Petersburg, Russia
[4]Federal Research Center N.I. Vavilov All-Russian Institute of Plant Genetic Resources (VIR), genetic resource of wheat department, plant introduction department, Bolshaya Morskaya street, 42–44, RU190000 St. Petersburg, Russia
[*]Correspondence: kleon9@yandex.ru

Abstract. The main trend of modern crop production is the expansion of the use of plant protection solutions and technologies, that ensure not only effective management of the number of populations of harmful organisms, but also the production of environmentally safe agricultural products with minimal anthropogenic impact on agro-ecosystems. One of our priorities is to develop new environmentally sound polyfunctional biopreparations, that combine useful properties of microbial strains such as phytopathogen antagonists and chitosan compositions that increase disease resistance. The introscopic analysis of the seed material quality realized with the non–destructive express techniques application was used for evaluation the effectiveness of the compositions' complex influence on plants. The research studies the effectiveness of the influence of *Bacillus subtilis* strains and chitosan compositions, including their combined effect, on soft wheat productivity and its damage by disease agents. Data on the quality assessment of the grain using microfocus x-ray radiography and gas-discharge visualization (electrophotography) are also provided. The complex of more than 20 structural elements of wheat productivity was analysed during the research. Assessment of the plant damage intensity according to the standard criterion - the disease development, and additional phytopathological indicators was carried out. The evaluation of the grains' introscopic characteristics was carried out by the microfocus x-ray radiography techniques combined with the digital x-ray image analysis. It is shown that the biopreparation complexes, containing *B. subtilis* strains and Chitosan, have a combined biological activity manifested in the optimization of wheat plants' physiological state, increasing productivity, diseases resistance.

Key words: *Bacillus subtilis,* biopreparations, Chitosan, microfocus x-ray radiography, polyfunctional complex, soft wheat, wheat diseases, yield structure.

INTRODUCTION

Wheat is one of the most important cereal crop that provides food for more than a half of the world's population (Reynolds et al., 2009; Falcone et al., 2019). One of the reasons for the decline in wheat productivity is the deterioration of the phytosanitary condition of the crops, that is highly dependent on the technologies of its cultivation.

Recently, the world has been most in demand for green farming strategies based on the use of natural alternatives to chemical plant protection products. Some alternative methods of dealing with common plant diseases are based on the use of natural compounds that not only induce resistance through the priming mechanism, but also help to uncover the complex mechanisms underlying the phenomenon of induced resistance. These include chitosans, oligogalacturonides, volatile organic compounds, azelaic and pipecolic acids and others (Aranega-Bou et al., 2014).

Chitosan is a natural polyaminosaccharide, which is a copolymer of glucosamine and acetylglucosamine, which has a number of valuable properties (nontoxicity, biocompatibility, hypoallergenicity, biodegradability) and widely used in agriculture to increase the resistance of plants to diseases (El Hadrami et al., 2010, Aranega-Bou et al., 2014). The organic polymers (chitosan and others) can be used as a prospective eco-friendly carrier for bacteria in the creation of immobilized preparative forms of microorganisms in biofertilizers (Shcherbakova et al., 2018). Chitosan has been shown to be able to efficiently induce phytochemicals in plants, is an effective elicitor, and serves as an alternative to plant genetic modification (Kim et al., 2005). In addition, according to existing data, chitosan affects the growth and productivity of plants (Reddy et al., 1999; Kim et al., 2005; Cho et al., 2008; Aranega-Bou et al., 2014). The treatment of wheat seeds with chitosan (2–8 mg mL^{-1}) significantly improved seed germination to recommended seed certification standards (> 85%) and germination energy at concentrations > 4 mg mL^{-1} in spring wheat varieties by combating *Fusarium graminearum* seed infection (Reddy et al., 1999). In a number of experiments with various host plants and pathogens (Iriti et al., 2010), it was shown that chitosan can directly activate systemic resistance or induce a more effective protective response to a call, depending on the dose, taking into account different cytotoxicity thresholds for each chitosan derivative and plants. (Iriti, & Faoro, F., 2009; Aranega-Bou et al., 2014). An important role in creating natural plant protection systems is played by microbial antagonists of plant pathogens. Compounds that are released from the cell wall of phytopathogens as a result of the action of antagonist hydrolases can function as resistance elicitors, causing protective reactions in a plant: phytoalexin synthesis, activation of hydrolytic enzymes, lignification, etc. (Sidorova et al., 2018). The group of strains of *Bacillus subtilis* is recognized as a powerful biocontrol tool, because it has suppressive activity against a wide range of phytopathogens due to its ability to produce many secondary metabolites of various chemical nature: cyclic lipopeptides, polypeptides, proteins and non–peptide compounds, among others (Stein, 2005; Sidorova et al., 2018). The ability of bacteria to synthesize compounds of a certain structure suggests the presence of a specific mechanism of action on a phytopathogenic object, and also explains the biological activity of a particular strain against specific microorganisms (Sidorova et al., 2018).

Thus, the researchers showed the influence of two strains of *B. fortis* IAGS162 and *B. subtilis* IAGS174, which not only provided maximum control of Fusarium wilt of tomatoes, but also significantly increased the growth and yield of plant fruits in the field (Akram et al., 2013). The effect of six strains of *Bacillus pumilus* INR7, *B. megaterium* P2, *B. subtilis* GB03*, B. subtilis* S, *B. subtilis* AS and *B. subtilis* BS and four native strains of *Achromobacter* sp. B124, *Pseudomonas geniculate* B19, *Serratia marcescens* B29 and *B. simplex* B21 to suppress all wheat diseases by inducing plant defense mechanisms. Most treatments were equally effective against all diseases, both when watering the soil and when spraying plants. Bacterial strains not only suppressed diseases, but also enhanced plant growth, whereas when treated with chemical inductors, it decreased (Jasem et al., 2018). According to some studies, *B. subtilis* is preventive and has curative properties in the early stages of the yellow rust development. The pathogen's urediniospore germination significantly inhibited by spraying *Bacillus subtilis* strain E1R-j on leaf surface before inoculation (Li et al., 2013). The possibilities for the biological control of yellow rust was investigated by winter wheat treatments with the biological products that contained *Bacillus* spp., *Pseudomonas aurantiaca*, *Brevibacillus* spp., *Acinetobacter* spp., and chitosan. However, after two years of researches, the results were not convincing (Feodorova-Fedotova et al., 2019). The effect of preliminary inoculation of *Triticum aestivum* seeds with endophytic *B. subtilis* 26D strain cells on the growth of shoots and the activity of antioxidant enzymes when exposed to heavy metals - cadmium and lead was established. Inoculation of seeds with *B. subtilis* bacteria cells contributed to better growth of wheat plants in the soil, a decrease in the intensity of lipid peroxidation in plant tissues, both with the combined action of metals and with separate action. The protective effect of *B. subtilis* 26D was due to the biological activity of bacteria that produce a large number of biologically active substances (Smirnova et al., 2016). Inoculation of plant seeds with bacteria contributed to a decrease in the metal content in shoots (Kuramshina et al., 2016). Under conditions of moisture deficiency in plants inoculated with *B. subtilis*, an increase in mycorrhization was found, it was revealed that *B. subtilis* bacteria reduced stress caused by drought in plants (Kuramshina et al., 2015).

One of the highest priority areas in the practice of ecologic adaptive agriculture today is the use of multifunctional biological products in order to obtain high–quality agricultural products. Biological products, such as chitosan and its derivatives, which are a combination of microbes antagonists of pathogens with activators of plant disease resistance, can be promising plant protection products. The high protective effect of complex biologics is associated with a combination of the antagonistic properties of the microbe antagonist with the ability of chitosan, together with biologically active substances, to stimulate the mechanisms of phytoimmunity (Kolesnikov et al., 2018).

The soft-ray microfocus radiography method has been successfully used for many years in Russia (Arkhipov et al., 2019) and in other countries (Burg et al., 1995; Gomes-Junior et al., 2012; Silva et al., 2013). Since 1976, the method has been included in international and national standards, primarily for assessing of grain infestation and damage by pests. It can be used to detect various structural defects of seeds, such as fracturing, enzymomycosis depletion (EMIS), internal germination, hidden pest population, damage by the bug 'harmful turtle', mechanical injuries and defects of the germ, empty seed. The methodology can be used for evaluation of seeds of various densities and sizes (Priyatkin et al., 2018). Developing and application of new software for seed images' automatic analysis is promising direction of modern scientific and practical elaborations. In particular, the measurement of morphometric as well as optical parameters of radiographs that characterize the endosperm density degree can be performed, for example, by the use of software for images' morphometric analysis produced by Argussoft LLC, Saint Petersburg, Russia (Priyatkin et al., 2018).

The purpose of the work is to justify the prospect of using multifunctional preparations based on strains of microorganisms antagonists of pathogens and activators of plant disease resistance - chitosan complexes in the cultivation of common wheat.

MATERIALS AND METHODS

The location of the research - Laboratory of Microbiological Plant Protection VIZR, Department of Plant Protection and Quarantine, St. Petersburg State Agrarian University, Plant Biophysics Sector of Agrophysical Research Institute.

The experimental studies were implemented in the experimental field of Pushkin laboratories of the Federal State Budgetary Institution of Higher Education FIC N.I. Vavilov All–Russian Institute of Plant Genetic Resources (VIR). The plant material of the study was the spring soft wheat variety Leningradskaya 6, k–64900, which was provided for the research by the VIR wheat genetic resources department.

The experimental design provided for the following options:

• without treatments (control);

• 'Vitaplan, CL' - the culture liquid of *B. subtilis* strain VKM B-2604D and *B. subtilis* strain VKM B-2605D at a ratio of 1: 1 with a titer of living cells and spores / g *B. subtilis* - 1010;

• 'Vitaplan, CL + 0.1% Chitosan' (chitosan salicylate). Chitosan salicylate was added to the concentration of 0.1% to the Vitaplan culture fluid diluted with distilled water 10 times (cell titer 1010 CFU mL^{-1}). To obtain chitosan salicylate, chitosan with a mM of 60 kDa obtained by oxidative degradation (Muzzarelli Riccardo, 1977) from chitosan with a molecular mass of 150 kDa and a degree of deacetylation of 85% (Bioprogress, RF) was used. Based on it, a chitosan derivative was synthesized: Chit + SC, containing ion–bound fragments of salicylic acid (SC), comprising 25%.

• 'Vitaplan CL + colloidal chitin (0.1%)' During the deep cultivation of Vitaplan, 0.1% of colloidal chitin was added to the standard nutrient medium (calculated on the dry weight of chitin). Then the culture fluid with a titer of 1011 CFU $mL^{-1}$was diluted 10 times. The preparation of colloidal chitin was implemented according to the method of Roberts & Selitrennikoff (1988) from chitin with mM 100 kDa (by dissolving chitin in concentrated hydrochloric acid and subsequent precipitation of colloidal chitosan with acetone.

• 'Vitaplan CL + colloidal chitin (0.1%) + 0.1% Chitosan' (chitosan salicylate). During the deep cultivation of Vitaplan, 0.1% of colloidal chitin (calculated on the dry weight of chitin) was added to the standard nutrient medium, the titer of the culture fluid was 1011 CFU mL^{-1}. Then the culture fluid was diluted 10 times and 0.1% chitosan salicylate was added.

• 'Vitaplan, WP' (standard), containing cells of the strains of *Bacillus subtilis* VKM B-2604D and *B. subtilis* VKM B-2605D. The *B. subtilis* strain VKM–2604D synthesizes antibiotics of various structures (the polypeptide antibiotic from the bacteriocin group and the polyene antibiotic), and the *B. subtilis* strain VKM B-2605D forms a polypeptide close to bacillin and hexaene antibiotics, one of which is assigned to the subgroup of mediocidin.

In the experiment the seeds of spring soft wheat Leningradka 6, k-64900 were treated with the biopreparations before sowing and vegetating plants later were sprayed three times.

During the tillering stage of wheat, the number, length, and weight of the roots (main germinal root, germinal and coleoptile roots) originating from the epicotyl were determined. The number and length of the nodal roots of wheat were taken into account. The calculation of the phases of ontogenesis of soft wheat during processing with biological products was implemented on the Eukarpia (Zadox) scale.

When examining the wheat yield structure, the data on field germination, productive and total bushiness, plant height, spike length, number of spikelets per spike, number of grains per spike, spike weight, and the 1,000 grains weight were analyzed. The weight of the vegetative part of plants and the area of flag and pre–flag leaves were determined.

The degree of damage to plants by root rot was assessed in the field on a generally accepted scale.

The intensity of wheat damage by the pathogen of powdery mildew (*Blumeria graminis* Speer.) was taken into account during the phases of tillering of wheat, going into the tube, ripening (milk ripeness of grain) according to the indicators: the conditional value of the development of the disease, the number and area of spots with plaque. The brown rust development (*Puccinia recondita* Rob. Ex Desm. F. Sp. Tritici Eriks.) on flag leaves was taken into account during the stem extension stage and milk stage, according to the standard criterion - the disease development and additional parameters: the pustules number, the pustule area. The intensity of the defeat of the samples by wheat leaf blotch (*Stagonospora nodorum* Castell. et Germano) was determined in the phases of milk and wax ripeness of grain according to the conditional development of the disease on the flag and pre–flag leaf surface in accordance with the James scale. The intensity of wheat damage by yellow rust was determined both by using a generally accepted indicator - the conditional intensity of the pathogen development (according to the Manners scale), and by using additional parameters: the number of pustules (total per sheet), the number of strips with pustules, the length of strips with pustules, the area of the pustule and their numbers in the band (Kolesnikov et al., 2018).

X-ray analysis was performed using a mobile X-ray diagnostic unit PRDU-02 and the Argus-BIO software, according to the method described previously (Kolesnikov et al., 2019).

Descriptive statistics methods were used to assess the biological effectiveness of biological products and multifunctional complexes (based on standard errors of the mean ± SEM, 95% confidence intervals, and Student t-test), factor analysis, and Spearman rank correlation calculation. Statistical analysis was performed in SPSS 21.0, Excel 2016.

RESULTS AND DISCUSSION

In the control variant, the following development of pathogens was recorded on cultivar Leningradskaya 6, k-64900 experiment (without treatment): helminthosporious root rot - 38.9 ± 7.1% (2016–2019 - 39.4 ± 3.1%) yellow rust - 24.2 ± 5.6% (2016–2019 - 11.2 ± 2.4%), leaf blotch - 47.0 ± 15.4% (2016–2019 - 41.4 ± 4.2%); brown rust - 29.3 ± 7.2% (2016–2019 - 20.9 ± 4.2%), powdery mildew - 18.2 ± 2.1% (2016–2019 - 18.8 ± 4.8%). When applying multifunctional complexes on soft wheat: ‘Vitaplan, CL + 0.1% Chitosan’ and ‘Vitaplan, CL + colloidal chitin (0.1%) + 0.1%

Chitosan', a statistically significant decrease ($P < 0.05$) development of root rot - by 22–31%, leaf blotch - by 41–47% (Fig. 1).

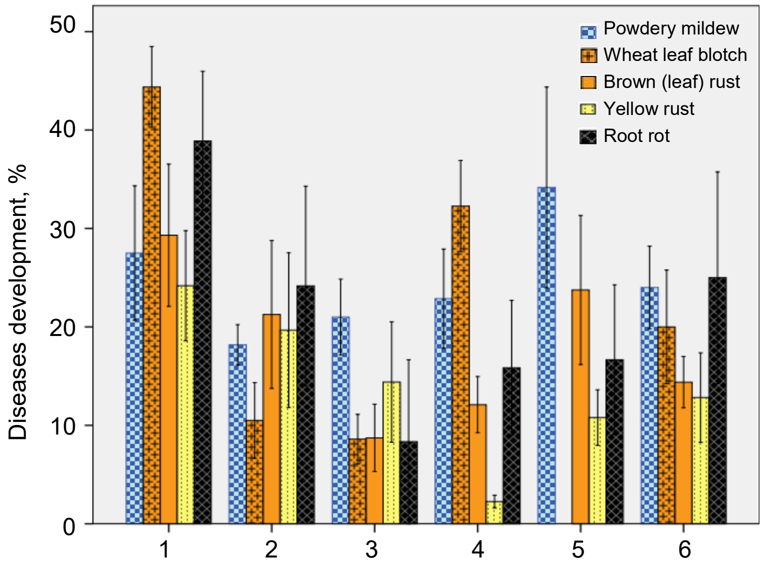

Figure 1. Change in the intensity of the development of wheat diseases with the use of biological products and multifunctional complexes in comparison with the control. 2019 year. Explanation: 1 – Control (water); 2 – Vitaplan, CL; 3 – Vitaplan, CL + 0.1% Chitosan; 4 – Vitaplan, WP; 5 – Vitaplan, CL + colloidal chitin (0.1%) + 0.1% Chitosan; 6 – Vitaplan, CL + colloidal chitin (0.1%) (95% confidence intervals for means).

According to the literature data, it is known that chitosan induces the synthesis of various phytoalexins that can start-up plant phytoimmunity reactions and suppress infections (Gamzazade et al., 1999). At the same time, any activity in the polymer (fungicidal, antibacterial, growth-stimulating) can be increased by its chemical modification with appropriate biologically active substances (BAS).

The use of the Vitaplan, CL + 0.1% Chitosan complex reduced wheat damage by brown rust by 20.6%, and the Vitaplan, CL + colloidal chitin (0.1%) + 0.1% Chitosan complex reduced yellow rust by 13.4%. On the flag leaves of wheat in the indicated experimental variants, the decrease in the total number of yellow rust pustules (Fig. 2) - by 37.6% and 55.3%

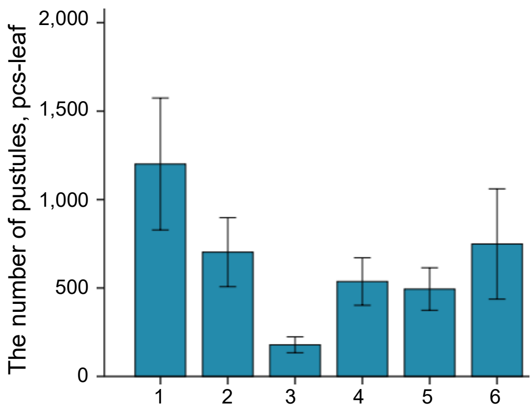

Figure 2. Change in the number of pustules of wheat rust species when using biological products and multifunctional complexes compared to the control. 2019 year.

Explanation: 1 – Control (water); 2 – Vitaplan, CL; 3 – Vitaplan, WP; 4 – Vitaplan, CL + colloidal chitin (0.1%) + 0.1% Chitosan; 5 – Vitaplan, CL + colloidal chitin (0.1%); 6 – Vitaplan, CL + 0.1% Chitosan (95% confidence intervals for means).

(the number of bands by 37.8% and 34.9%) was determined; brown rust - by 20.6% and 5.6%, respectively.

An important indicator that characterizes the wheat resistance or susceptibility to types of rust is the area of the pustule. To the greatest extent, the area of yellow rust pustule decreased in comparison with the control in the experimental variant: 'Vitaplan, CL + colloidal chitin (0.1%) + 0.1% Chitosan' - by 22.8%. No statistically significant effect of biological products on the area of wheat rust pustule was revealed.

A significant decrease in the development of major wheat diseases has affected its potential yield. In the experiment, where the Vitaplan, CL + colloidal chitin (0.1%) + 0.1% Chitosan multifunctional complex was used), the wheat yield statistically significantly increased by 50.3% compared to the control (Fig. 3). The use of the multifunctional complex 'Vitaplan, CL + 0.1% Chitosan' increased the yield of wheat by 24.4%. According to researchers, chitosan inhibits the phytopathogens development: it suppresses the growth of fungal mycelium spores, has antiviral activity, and in addition, it stimulates seed germination, plants growth and development, and increases their productivity (Gamzazade et al., 1999; Yakushkina & Bakhtenko, 2005).

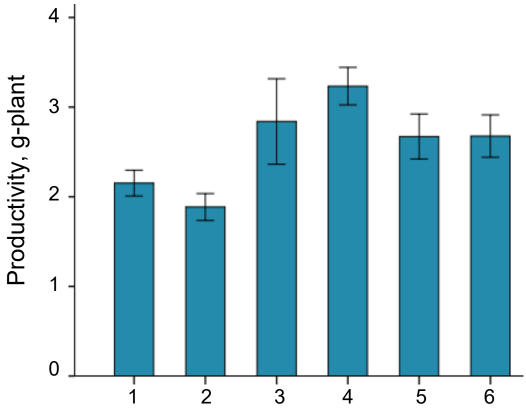

Figure 3. The potential yield of soft wheat when using biological products and multifunctional complexes. 2019 year.

Explanation: 1 – Control (water); 2 – Vitaplan, CL; 3 – Vitaplan, WP; 4 – Vitaplan, CL + colloidal chitin (0.1%) + 0.1% Chitosan; 5 – Vitaplan, CL + colloidal chitin (0.1%); 6 – Vitaplan, CL + 0.1% Chitosan (95% confidence intervals for means).

Numerous experimental data have been published on the ability of useful microorganisms of the rhizo - and phyllosphere to synthesize metabolites that affect the plants resistance and growth and have signaling and hormonal functions. Thus, natural growth regulators are auxins, gibberellins, cytokinins, abscisic (ABC), salicylic, and jasmonic acids (Forchetti et al., 2007; Dodd et al., 2010; Sivasakthi et al., 2013; Kudoyarova et al., 2014). Many strains of bacteria of the genera Bacillus, Azospirillium, Pseudomonas, etc. have the ability to synthesize auxins, which leads to stimulation the root system development, and, as a result, to more active absorption of water and nutrients by plants. These processes together increase the plants resistance to diseases and allow them to pass faster the development stages, when they are most susceptible to pathogens (Kumar et al., 2012). It was revealed that gibberellin can synthesize by many strains of the genus Bacillus bacteria (Kilian et al., 2000). The Bacillus, Rhizobium, Arthtrobacter, Azotobacter, Azospirillium, Pseudomonas bacteria can produce cytokinins. For example, the chlorophyll and cytokinins content increased in plants when they were inoculated with cytokinin-producing strains of *B. subtilis*, which subsequently caused an increase in the biomass of the root system and the vegetative part (Cohen et al., 2009).

When using the multifunctional complex 'Vitaplan, CL + 0.1% Chitosan', a significant increase in the length of nodal roots was noted by 49.2%, and the total bushiness - by 50.4%. In the experiment, where the Vitaplan, CL + colloidal chitin (0.1%) + 0.1% Chitosan complex was used, a significant increase in productive bushiness - by 32.3%, total bushiness - by 74.4% was revealed (Fig. 4), spike weight - by 66.8%, as well as root lengths by 30.9%, number of nodal roots - by 25%, length of nodal roots - by 18.6%.

Plant growth and formation processes are regulated by a certain proportion of phytohormones. At the same time, each morphogenetic process does not require its own hormone; from 2-3 substances can be created many different proportions. In this way the direction and rate of growth, the appearance of each organ will depend on the certain proportion. (Yakushkina & Bakhtenko, 2005).

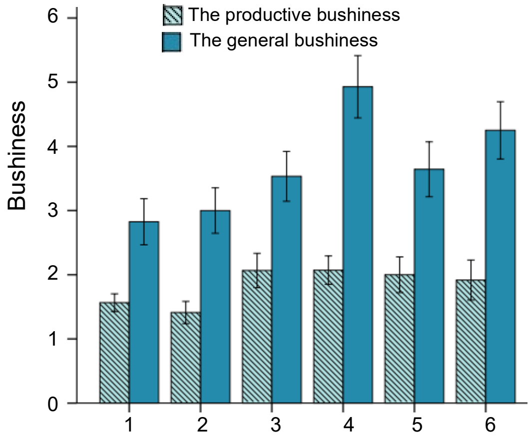

Figure 4. Change in the productive and general bushiness of soft wheat when using biological products and multifunctional complexes. 2019 year.

Explanation: 1 – Control (water); 2 – Vitaplan, CL; 3 – Vitaplan, WP; 4 – Vitaplan, CL + colloidal chitin (0.1%) + 0.1% Chitosan; 5 – Vitaplan, CL + colloidal chitin (0.1%); 6 – Vitaplan, CL + 0.1% Chitosan (95% confidence intervals for means).

The relationship between the elements of wheat productivity when using the multifunctional complexes 'Vitaplan, CL + colloidal chitin (0.1%) + 0.1% Chitosan' and 'Vitaplan, CL and 0.1% Chitosan' were studied by factor analysis. The cumulative percentage of variance in the measurements of productivity indicators, due, in particular, to factors F1 and F2, was 54% and 49.7%, respectively. To simplify the interpretation of factors, the varimax rotation method is used.

It was shown that six indicators turned out to be the most sensitive to the action of the multifunctional complex 'Vitaplan, CL + colloidal chitin (0.1%) + 0.1% Chitosan': plant phase, number and length of roots, plant height, productive bushiness, flag area leaf, and when applying 'Vitaplan, CL and 0.1% Chitosan' - five indicators: root length, number of nodal roots, productive and total bushiness, root weight (described by F1). Between the values of these indicators revealed strong positive correlation. In addition (factor F2), 'Vitaplan, CL + colloidal chitin (0.1%) + 0.1% Chitosan' had some effect on the spike weight, the number of spikelets per spike, the number of grains per spike, the weight of grains in one spike, and 'Vitaplan, CL and 0.1% Chitosan' - on spike weight, number of spikelets per spike, weight of grains of one spike and the 1,000 grains weight. Moreover, the number of spikelets per spike correlated, in particular, with the 1,000 grains weight.

X-ray analysis data are presented in Fig. 5. It was found that the area of the x-ray projection and the length of the projection of the grains was significantly increased with the use of the multifunctional complexes Vitaplan CL + 0.1% Chitosan and Vitaplan CL + colloidal chitin (0.1%). It was also revealed that the use of multifunctional complexes significantly affected the values of the 'X-ray projection elongation' in the

‘Vitaplan, CL’ and ‘Vitaplan, CL + colloidal chitin (0.1%) + 0.1% Chitosan’ options, in other cases we can talk about the tendency of increase of this indicator. Thus, in a number of test variants, the seeds became larger, the shape of the seeds also changed - they became more elongated. The greatest impact of the multifunctional complexes was noted on the brightness parameters of X-ray diffraction patterns of the grains. In all cases, in comparison with the control, a statistically significant decrease in the values of the mean square deviation of brightness (the largest decrease in the ‘Vitaplan CL + 0.1% Chitosan’ variant) and the Interval of brightness (the largest decrease in the ‘Vitaplan WP’) was found. This fact may indicate a more optically uniform x-ray projection of the caryopsis, and possibly a reduced percentage of latent defects, manifested in the form of various kinds of blackouts on the x-ray.

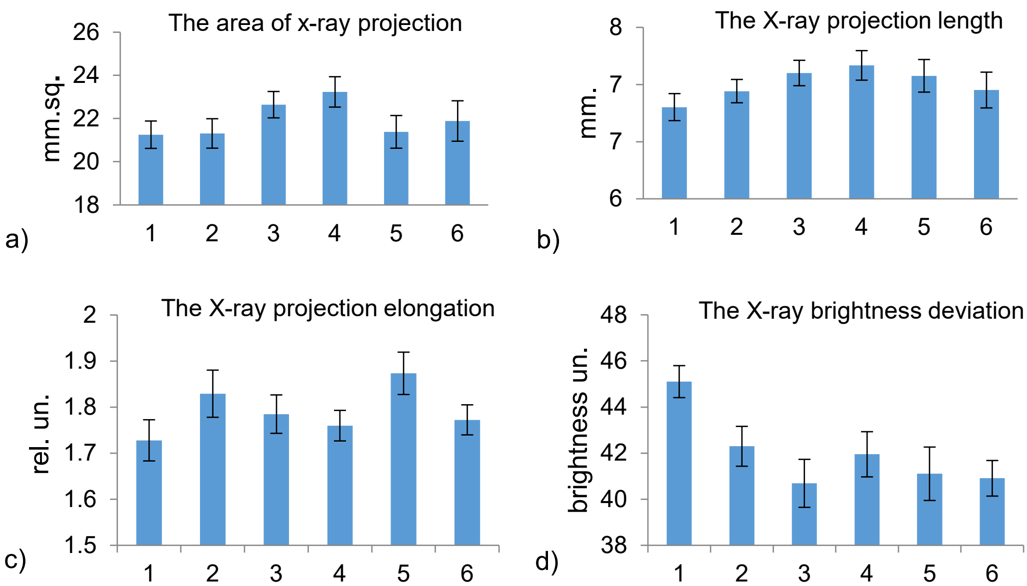

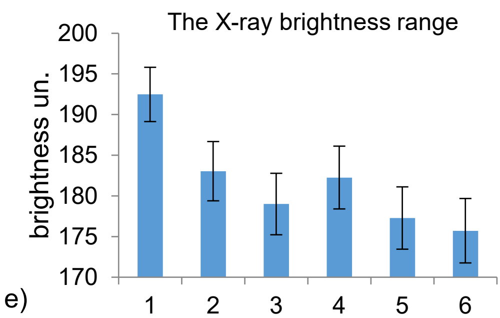

Figure 5. X-ray analysis of soft wheat grains in various experimental variants. 2019.

Explanation: 1 – Control (water); 2 – Vitaplan, CL; 3 – Vitaplan, CL + 0.1% Chitosan; 4 – Vitaplan, CL + colloidal chitin (0.1%); 5 – Vitaplan, CL + colloidal chitin (0.1%) + 0.1% Chitosan, 6 – Vitaplan, WP (95% confidence intervals for means).

CONCLUSIONS

Thus, as a result of the studies, a high biological effectiveness of multifunctional biological products was noted, which manifested itself in a decrease in the intensity of diseases and an increase in the productivity of wheat. It is shown that the *B. subtilis* strains contained as part of the Vitaplan biopreparation and the ‘Vitaplan, QL + Chitosan II’ and ‘Vitaplan, CS + Chitosan II’ biopreparation complexes have a combined biological activity associated with the synthesis of various BAS and manifested in the optimization of wheat plants’ physiological state, increasing productivity, diseases resistance and reducing diseases incidence. The use of the multifunctional complex ‘Vitaplan, CL + 0.1% Chitosan’ statistically significantly reduced the value of 5 phytopathological indicators (development of root rot, spots with powdery mildew, development and number of brown rust pustules, number of yellow rust strips), and ‘Vitaplan, CL + colloidal chitin (0.1%) + 0.1% Chitosan’ - 3 indicators (root rot development, development and area of yellow rust pustule. Use of the multifunctional complex ‘Vitaplan CL + colloidal chitin (0.1 %) + 0.1% Chitosan’ to the greatest extent *UV* increased potential yield of wheat (by 50.3%), which was mainly due to an increase in productive bushiness of plants (by 32.3%). It was shown by the method of x-ray analysis of digital x-ray images that the use of multifunctional complexes to one degree or another influenced the characteristics of grain x-ray (dimensional indicators, shape indicators, as well as brightness indicators). The digital x-ray image analysis has shown that the implementation of polyfunctional complex has increased the average brightness of the digital x-ray images of the grain and the modification of their size and density. It was revealed that the area of the x-ray projection and the length of the projection of the grains was significantly increased with the use of the multifunctional complexes Vitaplan CL + 0.1% Chitosan and Vitaplan CL + colloidal chitin (0.1%). It was also revealed that the use of multifunctional complexes significantly affected the values of the ‘X-ray projection elongation’ in the ‘Vitaplan, CL’ and ‘Vitaplan, CL + colloidal chitin (0.1%) + 0.1% Chitosan’ options, in other cases we can talk about the tendency of increase of this indicator. Thus, in a number of test variants, the seeds became larger, the shape of the seeds also changed - they became more elongated. The greatest impact of the multifunctional complexes was noted on the brightness parameters of X-ray diffraction patterns of the grains. In all cases, in comparison with the control, a statistically significant decrease in the values of the mean square deviation of brightness (the largest decrease in the ‘Vitaplan CL + 0.1% Chitosan’ variant) and the Interval of brightness (the largest decrease in the ‘Vitaplan WP’) was found. This fact may indicate a more optically uniform x-ray projection of the caryopsis, and possibly a reduced percentage of latent defects, manifested in the form of various kinds of blackouts on the x-ray.To establish a relationship between the indicators of x-ray of grains and their sowing qualities, a further test for the energy of germination is promising germination, germination and additional growth indicators (root and sprout length). The results of the work can be used to develop environmentally friendly technologies for wheat cultivation and optimize the phytosanitary condition of crops.

ACKNOWLEDGEMENTS. The research was performed within the framework of the State Task according to the theme plan of VIR, Project No. 0662-2019-0006 ‘Search For and Viability Maintenance, and Disclosing the Potential of Hereditary Variation in the Global Collection of Cereal and Groat Crops at VIR for the Development of an Optimized Genebank and Its Sustainable Utilization in Plant Breeding and Crop Production’.

REFERENCES

Akram, W., Anjum, T., Ali, B. & Ahmad, A. 2013. Screening of native bacillus strains to induce systemic resistance in tomato plants against fusarium wilt in split root system and its field applications. *International journal of agriculture and biology* **15**, 1289–1294.

Aranega-Bou, P., de la O Leyva, M., Finiti, I., García-Agustín, P. & González-Bosch, C. 2014. Priming of plant resistance by natural compounds. Hexanoic acid as a model. *Frontiers in plant science* **5**, 488. doi: 10.3389/fpls.2014.00488

Arkhipov, M.V., Priyatkin, N.S., Gusakova, L.P., Potrakhov, N.N., Gryaznov, A.Y., Bessonov, V.B., Obodovskii, A.V. & Staroverov, N.E. 2019. X-Ray computer methods for studying the structural integrity of seeds and their importance in modern seed science. *Technical Physics. The Russian Journal of Applied Physics* **64**(4), 582–592. doi: 10.1134/S1063784219040030

Burg, W.J. van der, Jalink, H., Zwol, R.A. van, Aartse, J.W. & Bino, R.J. 1995. Non-destructive seed evaluation with impact measurements and X-ray analysis. *Acta Horticulturae* **362**, 149–157.

Cho, M.H., No, H.K. & Prinyawiwatkul, W. 2008. Chitosan treatments affect growth and selected quality of sunflower sprouts. *Journal of food science* **73**, 70–77. doi: 10.1111/j.1750-3841.2007.00607.x

Cohen, A.C., Travaglia, C.N., Bottini, R. & Piccoli, P.N. 2009. Paticipation of abscisic acid and gibberellins produced by endophytic Azospirillum in the alleviation of drought effects in maize. *Botany* **87**, 455–462. doi: 10.1139/B09-023

Dodd, I.C., Zinovkina, N.Y., Safronova, V.I. & Belimov, A.A. 2010. Rhizobacterial mediation of plant hormone status. *Annals of Applied Biology* **157**, 361–379. doi: 10.1111/j1744-7348.2010.00439.x

El Hadrami, A., Adam, L.R., El Hadrami, I. & Daayf, F. 2010. Chitosan in Plant Protection. *Marine Drugs* **8**(4), 968–987. doi: 10.3390/md8040968

Falcone, G., Stillitano, T., Montemurro, F., De Luca, A.I., Gulisano, G. & Strano, A. 2019. Environmental and economic assessment of sustainability in Mediterranean wheat production. *Agronomy Research* **17**(1), 60–76. https://doi.org/10.15159/AR.19.011

Feodorova-Fedotova, L., Bankina, B. & Strazdina, V. 2019. Possibilities for the biological control of yellow rust (*Puccinia striiformis f. sp. tritici*) in winter wheat in Latvia in 2017–2018. *Agronomy Research* **17**(3), 716–724. https://doi.org/10.15159/AR.19.137

Forchetti, G., Masciarelli, O., Alemano, S., Alvarez, D. & Abdala, G. 2007. Endophytic bacteria in sunflower (*Helianthus annuus L.*): isolation, characterization, and production of jasmonates and abscisic acid in culture medium. *Applied Microbiology and Biotechnology* **76**(5), 1145–1152. (doi: 10.1007/s00253-007-1077-7)

Gamzazade, A.I., Ismailov, E.Ya. & Tyuterev, S.L. 1999. New modification of plant disease resistance inductor and growth regulator. In: *Materials of the V all-Russian conference "New perspectives in the study of chitin and chitosan".* Moscow-Shchelkovo, pp. 83–87 (in Russian).

Gomes-Junior, F.G., Yagushi, J.T., Belini, U.L., Cicero, S.M. & Tomazello-Filho, M. 2012. X-ray densitometry to assess internal seed morphology and quality. *Seed Science and Technology* **40**(1), 102–107.

Iriti, M. & Faoro, F. 2009. Chitosan as a MAMP, searching for a PRR. *Plant signaling and behavior* **4**, 66–68. doi: 10.1016/j.plaphy.2008.08.002

Iriti, M., Giulia, C., Sara, V., Ilaria, M., Soave, C., Fico, G. & Faoro, F. 2010. Chitosan-induced ethylene-independent resistance does not reduce crop yield in bean. *Biological Control* **54**, 241–247. doi: 10.1016/j.biocontrol.2010.05.012

Jasem, A.M., Sharifi, R. & Abbasi, S. 2018. Induced systemic resistance to wheat take-all disease by probiotic bacteria. *Journal of Plant Protection Research* **58**(3), 304–310. https://doi.org/10.24425/jppr.2018.124639

Kilian, M., Steiner, U., Krebs, B., Junge, H., Schmeiedeknecht, G. & Hain, R. 2000. FZ B 24® Bacillus subtilis – mode of action of microbial agent enhancing plant vitality. *Pflanzenschutz-Nachrichten Bayer* **1**, 72–93.

Kim, H.J., Chen, F., Wang, X. & Rajapakse, N.C. 2005. Effect of chitosan on the biological properties of sweet basil (*Ocimum basilicum* L.). *Journal of agricultural and food chemistry* **53**, 3696–3701. doi: 10.1021/jf0480804

Kolesnikov, L.E., Popova, E.V., Novikova, I.I., Priyatkin, N.S., Arkhipov, M.V., Kolesnikova, Yu.R., Potrakhov, N.N., van Duijn, B. & Gusarenko, A.S. 2019, Multifunctional biologics which combine microbial anti-fungal strains with chitosan improve soft wheat (*Triticum aestivum L.*) yield and grain quality. *Sel'skokhozyaistvennaya Biologiya [Agricultural Biology]* **54**(5), 1024–1040 (in Russian). doi: 10.15389/agrobiology.2019.5.1024eng

Kolesnikov, L.E., Novikova, I.I., Surin, V.G., Popova, E.V., Priyatkin, N.S. & Kolesnikova, Yu.R. 2018. *Applied Biochemistry and Microbiology* **54**, 540–546 (in Russian). https://doi.org/10.1134/S0003683818050083

Kudoyarova, G.R., Melentiev, A.I., Martynenko, E.V., Timergalina, L.N., Arkhipova, T.N., Shendel, G.V., Kuz'mina, L.Y., Dodd, I.C. & Veselov, S.Y. 2014. Cytokinin producing bacteria stimulate amino acid deposition by wheat roots. *Plant Physiology and Biochemistry* **83**, 285–291. doi: 10.1016/j.plaphy.2014.08.015

Kumar, P., Dubey, R.C. & Maheshwari, D.K. 2012. Bacillus strains isolated from rhizosphere showed plant growth promoting and antagonistic activity against phytopathogens. *Microbiological Research* **167**, 493–499. doi: 10.1016/j.micres.2012.05.002

Kuramshina, Z.M., Khairullin, R.M. & Sattarova, L.R. 2015. The influence of endophytic bacteria strains Bacillus subtilis on mycorhization of roots of cereals in the imitation of a soil drought. *Agrochemistry* **5**, 69–73 (in Russian).

Kuramshina, Z.M., Smirnova, Y.V. & Khairullin, R.M. 2016. Increasing *Triticum aestivum* tolerance to cadmium stress through endophytic strains of *Bacillus subtilis*. *Russian Journal of Plant Physiology* **63**(5), 636–644 (in Russian).

Muzzarelli Riccardo, A.A. 1977. *Chitin*. Pergamon Press, Oxford, 309 pp.

Li, H., Zhao, J., Feng, H., Huang, L. & Kang, Z. 2013. Biological control of wheat stripe rust by an endophytic *Bacillus subtilis* strain E1R-j in greenhouse and field trials. *Crop Protection* **43**, 201–206. doi: 10.1016/j.cropro.2012.09.008

Priyatkin, N.S., Arkhipov, M.V., Gusakova, L.P., Potrakhov, N.N., Kropotov, G.I., Tzibizov, I.A. & Vinerov, I.A. 2018. Introscopic methods of seed quality evaluation: state of problem and prospects of realization. *Agrophysica* **2**, 29–39. doi: 10.25695/FGRPH.2018.02.05. (in Russian)

Reddy, M.V.B., Arul, J., Angers, P. & Couture, L. 1999. Chitosan treatment of wheat seeds induces resistance to *Fusarium graminearum* and improves seed quality. *Journal of agricultural and food chemistry* **47**, 1208–1216. doi: 10.1021/jf981225k

Reynolds, M., Foulkes, M.J., Slafer, G.A., Berry, P., Parry, M.A.J., Snape, J.W. & Angus, W.J. 2009. Raising yield potential in wheat. *Journal of Experimental Botany* **60**(7), 1899–1918. https://doi.org/10.1093/jxb/erp016

Roberts, W.K. & Selitrennikoff, C.P. 1988. Plant and Bacterial Chitinases Differin Antifungal Activity. *Journal of General Microbiology* **134**, 169–176.

Shcherbakova, E.N., Shcherbakov, A.V., Rots, P.Yu., Gonchar, L.N., Mulina, S.A., Yahina, L.M., Lactionov, Yu.V. & Chebotar, V.K. 2018. Inoculation technology for legumes based on alginate encapsulation. *Agronomy Research* **16**(5), 2156–2168. https://doi.org/10.15159/AR.18.186

Sidorova, T.M., Asaturova, A.M. & Homyak, A.I. 2018. Biologically active metabolites of bacillus subtilis and their role in the control of phytopathogenic microorganisms. *Sel'skokhozyaistvennaya biologiya [Agricultural Biology]* **53**(1), 29–37 (in Russian) doi: 10.15389/agrobiology.2018.1.29eng

Silva, V.N., Cicero, S.M. & Bennett, M. 2013. Associations between X-ray visualised internal tomato seed morphology and germination. *Seed Science and Technology* **41**(2), 225–234.

Sivasakthi, S., Kanchana, D., Usharani, G. & Saranraj, P. 2013. Production of plant growth promoting substance by *Pseudomonas fluorescens* and *Bacillus subtilis* isolates from paddy rhizosphere soil of Cuddalore district, Tamil Nadu, India. *International Journal of Microbiological Research* **4**(3), 227–233. doi: 10.5829/idosi.ijmr.2013.4.3.75171

Smirnova, J.V., Kuramshina, Z.M., Horohorina, E.E. & Khairullin, R.M. 2016. Influence of bacteria *Bacillus subtilis* antioxidant enzymes *Triticum aestivum* under the joint action of cadmium and lead. *Modern problems of science and education* **6**, 541. http://www.science-education.ru/ru/article/view?id=25757

Stein, T. 2005. Bacillus subtilis Antibiotics: Structures, Synthesis and Specific Functions. *Molecular Microbiology* **56**, 845–857. http://dx.doi.org/10.1111/j.1365-2958.2005.04587.x

Yakushkina, N.I. & Bakhtenko, E.Yu. 2005. *Plant physiology*. Moscow. Vlados, pp. 342–368 (in Russian).

Agronomy Research **18**(4), 2449–2464, 2020
https://doi.org/10.15159/AR.20.211

Advantages of electric resistance method for baking bread and flour confectionery products of functional purpose

B. Kulishov[1,*], K. Kulishova[1,2], N. Rudometova[1,2], A. Fedorov[1] and A. Novoselov[1]

[1]ITMO University, Saint-Petersburg, Faculty of Food Biotechnologies and Engineering, School of Biotechnology and Cryogenic Systems, Kronverkskiy ave. 49, RU 197101 St. Petersburg, Russia
[2]All-Russian Research Institute for Food Additives – Branch of V.M. Gorbatov Federal Research Center for Food Systems of RAS, Liteyniy ave. 55, RU 191014 St. Petersburg, Russia
[*]Correspondence: kulishov.b@list.ru

Abstract. In this paper we studied the effect of the baking method on the preservation of beta-carotene in two types of products: pan wheat bread and sponge cake. Five sources of beta-carotene were used in the study, three of which are commercially available samples, and the two others are experimental samples of supramolecular complexes of beta-carotene with alpha- and beta-cyclodextrins in powder form (molecular ratio 1: 1). Bread and sponge cake were baked by convective and electric resistance methods. The values of temperature and current flowing through the dough were monitored during electric resistance baking. The beta-carotene content was measured in the dough after kneading, in the cake batter after mixing and in the finished products after baking and cooling. The beta-carotene content was evaluated by spectrophotometry after extraction. The control samples of bread and sponge cake were baked without adding beta-carotene. Different sources of beta-carotene exhibited varying stability in bread and sponge cake. Bread samples baked by the electric resistance method with addition of supramolecular complexes had minimum losses of beta-carotene. Electric resistance baking ensured lower losses of beta-carotene in bread and sponge cake samples.

Key words: beta-carotene, bread, electric resistance baking, sponge cake, supramolecular chemistry.

INTRODUCTION

The development of the modern food industry is characterized by the creation of new types of products with high nutritional value intended for dietary and functional purposes. It explains an interest in methods of processing raw materials that allow to preserve the maximum possible amount of useful nutrients and to obtain a high-quality product that meets modern safety standards.

Integrity of functional ingredients in consumer products can be achieved in several ways. One of them is microencapsulation. It is used to reduce the loss of nutritional value of food, to increase the stability of the properties of microingredients, etc. (Gonçalves et al., 2016; Sepelevs & Reineccius, 2018; Baranenko et al., 2019) Starches, sugars, cellulose, lipids, animal and vegetable proteins, surfactants are mainly used as encapsulating materials (Nik et al., 2011; Trentin A.et al., 2011; Zabodalova et al., 2014; Yi et al., 2015). Another method is creation of supramolecular inclusion complexes. Formation of an inclusion complex affects physicochemical properties of the embedded molecule. Therefore, supramolecular complexes are obtained in order to enhance or alter any of the physicochemical properties of so-called guest substances (Mercader-Ros et al., 2010; Jin Z.-Y., 2013; Kurkov & Loftsson, 2013; Mangolim et al., 2014; Rudometova & Nikiforova, 2016).

Degradation of labile substances can also be reduced by the use of gentle technological processing modes (Strizhevskaya et al., 2019). One of these methods of bread baking is based on the use of the electric resistance (ER) heating method instead of the traditional convective heating (C) method. ER baking is characterized by a high heating rate and a lower maximum process temperature, reaching up to 100 °C (Derde et al., 2014), while C baking is carried out at a temperature of the air in the oven up to 180–240 °C (Sidorenko et al., 2012). Due to the lower temperatures and the shorter duration of the ER process baking allows to preserve useful nutrients of bread to a greater extent (Popov et al., 2012; Javkina et al., 2014), as well as to obtain functional products, reducing the loss of functional ingredients (Yalaletdinova, 2010).

An increased preservation of functional microingredients can be achieved by combining several technological methods simultaneously. A special case of such combination is the use of various stabilized forms of functional ingredients and ER baking. Such a combined method can be used, for example, to reduce the beta-carotene loss in bread and flour confectionery products.

Beta-carotene is a food supplement, used in the food industry as food dye E160a, it is also included in the list of functional food ingredients. Beta-carotene has great potential for use in functional foods as a precursor of vitamin A (retinol) (Rodriguez-Amay et al., 2011; Kumar & Kumar, 2012; Naumova & Kozubtsev, 2016). However, a significant disadvantage of beta-carotene is its liability to collapse under the influence of light, oxygen and high temperatures (Rudometova et al., 2018; Mérillon, 2019).

The aim of this paper was to study the influence of the baking method and stabilizing additives on the loss of beta-carotene during baking. In order to achieve this goal a series of experiments in C and ER baking with various types of beta-carotene was set up.

MATERIALS AND METHODS

Beta-carotene

In this paper the following sources of beta-carotene were used:

– water-dispersible suspension of beta-carotene with the content of coloring substances 1.6%;

– fat-soluble suspension of beta-carotene with the content of coloring substances 2.0%;

– water-soluble food-grade beta-carotene with the content of coloring substances 2.0%;

– experimental supramolecular complex of beta-carotene: beta-cyclodextrin (β-CD) with a molecular ratio of 1:1 and with the content of coloring substances 30% (Rudometova et al., 2018; Rudometova & Kulishova, 2018);

– experimental supramolecular complex of beta-carotene: alpha-cyclodextrin (α-CD) with a molecular ratio of 1:1 and with the content of coloring substances 25% (Rudometova et al., 2018; Rudometova & Kulishova, 2018).

Beta-carotene dosage selection

Beta-carotene dosage selection was based on the recommended daily allowance and the color intensity of the end product acceptable for consumer (MR 2.3.1.2432-08, 2008).

We have chosen a dosage of 20 mg of beta-carotene which, taking into account the inaccuracy and baking losses, will be 25–35% of the daily intake in the finished product. Along with that the product will be classified as fortified food (European Commission, 2006; Watson, 2017), and according to the results of preliminary experiments its coloration will not be excessive.

Bread making technology

A straight-dough preparation method was used. The processes were carried out in the following sequence:

– weighing components, heating water to 36 °C;

– mixing yeast with flour, dissolving salt in a portion of water, embedding beta-carotene;

– dosing components into the bowl of the dough mixing machine;

– kneading dough in a dough mixing machine (Bear Varimixer Teddy);

– fermentation of the dough for 2 hours, at 35 °C, with manual punching after 1 hour and 20 minutes (proofing cabinet Miwe Aero, model AE 6.06.04, Germany);

– cutting dough and forming dough pieces;

– proofing dough in a proofing cabinet at temperature of 40 °C and at relative humidity of 80% for 1 hour (Miwe Klima, type MGT, Germany);

– baking dough using two methods, namely, the convective one in the oven (Miwe Aero, model AE 6.06.04, Germany) and the electric resistance method in the laboratory ER oven;

– cooling the bread.

The dough formula is shown in Table 1.

Table 1. The dough formula

Ingredients	The mass of ingredients, g
Wheat flour 1st grade	500.0 ± 1.00
Salt	5.0 ± 0.10
Instant yeast	2.5 ± 0.10
Water	315.0 ± 2.00
Beta-carotene	20×10^{-3} ± 0.01

The list of used sources of beta-carotene, as well as the method of their embedding in the bread formula is shown in Table 2.

Table 2. The used sources of beta-carotene

Type of additive	Beta-carotene dosage, mg	Application method	Sample name
Water-dispersible suspension, 1.6%	20	water dispersion	B1
Fat-soluble suspension, 2.0%			B2
Liquid Water-Soluble Beta-Carotene, 2.0%			B3
Supramolecular complex α-CD: beta-carotene (molecular ratio 1:1)			B4
Supramolecular complex β-CD: beta-carotene (molecular ratio 1:1)			B5

For successful baking a round piece of dough with a mass of 230 ± 1 g was formed, its edges were cut off so that to obtain area of 50 mm that will ensure close contact of the piece of dough with electrodes. The forming scheme is shown in Fig. 1. The dough sample had a mass of 150 ± 5 g. The inaccuracy is explained by the difficulty of simultaneously observing the weight of the dough sample and the required distance between the vertical edges.

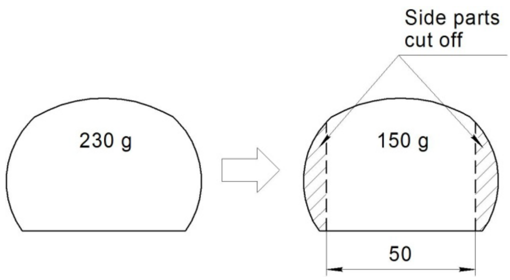

Figure 1. The forming scheme of the dough sample.

The dough sample was placed in the electric resistance oven so that the cut edges had close contact with electrodes.

In parallel with ER baking a bread sample from the same dough of the same mass was baked by C baking method at a temperature of 210 °C for 25 minutes.

After baking, bread samples were cooled at room temperature for 1 hour.

Sponge-cake baking technology

The sponge cake batter formula is shown in Table 3.

The sponge cake batter was prepared as follows. The mixture of salt, eggs and sugar was whipped for 10 minutes using stand mixer KitchenAid Artisan; in the process of whipping the mixture increased in volume by 2–3 times. Egg whites and egg yolks were not separated before whipping. In order to increase the batter conductivity and to speed up the ER baking process some amount of salt was added to the formula.

Table 3. The sponge cake batter formula

Ingredients	The mass of ingredients, g
Eggs	253 ± 5.00
Sugar	150 ± 1.00
Premium wheat flour	160 ± 1.00
Salt	1.0 ± 0.100
Beta-carotene	$20\times10^{-3} \pm 0.01$

After whipping, the flour was added evenly into the mixture so that to avoid formation of lumps.

The list of used sources of beta-carotene, as well as the way of their embedding in the sponge cake batter formula, is shown in Table 4.

Table 4. The list of sources of beta-carotene used in the sponge cake batter

Type of additive	Beta-carotene dosage, mg	Application method	Sample name
Water-dispersible suspension, 1.6%	20	mixing with eggs	SC1
Fat-soluble suspension, 2.0%			SC2
Liquid Water-Soluble Beta-Carotene, 2.0%			SC3
Supramolecular complex α-CD: beta-carotene (molecular ratio 1:1)			SC4
Supramolecular complex β-CD: beta-carotene (molecular ratio 1:1)			SC5
Supramolecular complex β-CD: beta-carotene (molecular ratio 1:1)		mixing with flour	SC6

Beta-carotene and eggs were whipped until the beta-carotene sample was evenly mixed.

The viscous medium of eggs prevents even distribution of the supramolecular complex in powder form, while there is no such problem when dispersing complex in water (as in the case of bread dough). It can cause a decrease in intensity and uniformity of color in the finished product. In order to compare two different ways of complex embedding, the sample SC6 was added to the sponge cake experiment plan.

Embedding of beta-carotene into the flour in the sample SC6 was carried out in several stages before mixing. Initially, beta-carotene in powder form was mixed with part of the flour with the same volume ratio, and the mixing was carried out until the mixture was evenly colored. At the next stage, a double volume of flour was added to the mixture, and the mixing was carried out again until color was even, and so on until the beta-carotene sample was completely mixed with flour.

After mixing, the baking mold for the ER baking method and the one for the C baking method were filled with batter. The weight of batter in the ER baking mold was 107 g.

Convective baking was carried out in a Miwe Aero oven, model AE 6.06.04, Germany, at a temperature of 180 °C for 19 minutes in a mold with a diameter of 300 mm and a height of the sponge layer of 30 mm.

After baking, the sponge cake was cooled at room temperature.

Electric resistance oven used for experiments

Baking samples of bread and sponge cake was carried out in a specially designed installation. The installation casing is a box, open at the top and equipped with a hinged bottom. The casing is made of monolithic sheet polycarbonate with a thickness of 8 mm. Two electrodes from sheet stainless steel AISI 304 with a thickness of 2 mm are installed in the grooves inside the casing. Dimensions of the internal chamber of the installation are 100×50×100 mm (L: W: H). The hinged bottom allows to remove the baked sample from the bottom without deformation, which is very important, because crustless bread and sponge cake are easily deformed. The installation drawing is shown in Fig. 2.

Baking of bread dough and sponge cake samples after proofing was carried out at a voltage of 220 V, a frequency of 50 Hz. During baking current flowing through the dough sample was measured using an IEK 266 C ammeter and the dough and the batter temperature was measured using a chromel-alumel DTPK011-07 / 1.5 thermocouple. The thermocouple was connected to an analog input module, which was connected to a personal computer via the RS-485 - USB interface. Data from the input module was processed in MasterScada in real time. The thermocouple was installed in the dough sample at a certain point, in the center, at a height of 45 ± 5 mm from the chamber bottom. Baking was stopped at the moment when current reached a minimum and remained constant for 10 s. According to the data obtained, the duration of bread baking was about 120 seconds and the duration of sponge cake baking was about 600 s.

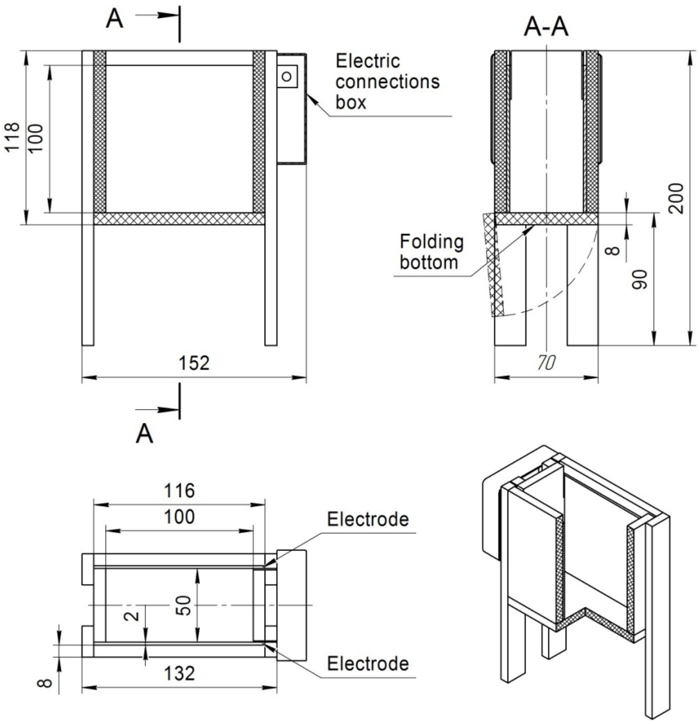

Figure 2. Drawing of the installation for electric resistance baking.

Extraction of beta-carotene from bread

5 g of sample (with an accuracy of 0.001 g) were mixed with quartz sand in a 1:1 mass ratio. The resulting mixture was ground in a ceramic mortar for 10 minutes, with addition of 10 cm^3 of solvent (chloroform). Then the mixture was filtered into a 250 cm^3 conical flask; the resulting precipitate was transferred to the mortar. The procedure was repeated until the sample was completely discolored.

Extraction of beta-carotene from sponge cake

2 g of the sample (with an accuracy of 0.001 g) were placed in a 100 cm^3 conical flask, where 30 cm^3 of solvent (chloroform) were added. Extraction was performed in a Bandelin Sonorex ultrasonic bath at room temperature at an installed power of 128 W for 30 minutes. The mixture was then filtered into a 250 cm^3 conical flask, and the resulting precipitate was transferred back. The procedure was repeated until the sample was completely discolored.

Determination of beta-carotene content

The optical density of the resulting combined solutions was determined. The measurement was carried out on a SHIMADZU UV-1800 double-beam scanning spectrophotometer in the wavelength range of 300–700 nm against the solvent.

Mass fraction of beta-carotene in the object of study (in mg g^{-1}) was calculated according to the formula, referred to in the reference source (Socaciu, 2007; European Commission, 2012).

Organoleptic analysis of bread and sponge cake

The organoleptic parameters were evaluated by a group of three tasters in accordance with GOST R 58233 (State Standard of the Russian Federation, 2018). The organoleptic properties of bread and sponge cake baked by C and ER methods were evaluated on a 5-point scale, the accuracy of the point evaluation was 0.1 points.

Evaluation of bread samples was carried out according to the following parameters: the state of the bread surface (smoothness, presence of tears, lumps, etc.), the color of the crumb (taking into account the introduction of beta-carotene as a dye), porosity (thin-walled or thick-walled, uniform, etc.), crumb consistency (tenderness, mellowness, dryness, etc.), bread aroma, crumb taste (State Standard of the Russian Federation, 2018).

Evaluation of sponge cake samples was carried out according to the following parameters: external appearance (smoothness, presence of tears, cracks, etc.), crumb color (taking into account the introduction of beta-carotene as a dye), consistency (softness, elasticity, dryness), crumb taste, aroma (Popov et al., 2014).

Since bread and sponge cake samples prepared by ER baking lacked a crust, the taste and color of samples obtained by different baking methods were evaluated only by crumb.

Statistical data processing

All experimental measurements were performed three times. Analysis of variance (one-way ANOVA) of the obtained data was carried out by Microsoft Excel with a significant difference at $P \leq 0.05$. Some of the parameters were compared using the Fisher test. Graphical dependencies were obtained using Microsoft Excel software.

RESULTS AND DISCUSSION

Dynamics of changes in the current strength and temperature during ER baking of bread and sponge cake

Fig. 3 shows experimental data on changes in the current strength and temperature when baking bread. Dynamics of the current strength is complex, which can be explained by thermal and physicochemical processes occurring in the dough during baking. At the beginning of bread baking, an increase in the current strength occurs due to an increase in the degree of dissociation of salts and acids and transition of soluble substances to the liquid phase. Subsequently, the current strength decreases somewhat, which the authors attribute to the swelling of the protein and carbohydrate components of the dough. Insignificant repeat increase in the current strength can be caused by denaturation of proteins and release of moisture, resulting in a short-term increase of conductivity. Further decrease in the current strength is associated with the evaporation of moisture from the dough and the decrease in conductivity, which is confirmed by the data from the authors (Sidorenko et al., 2012).

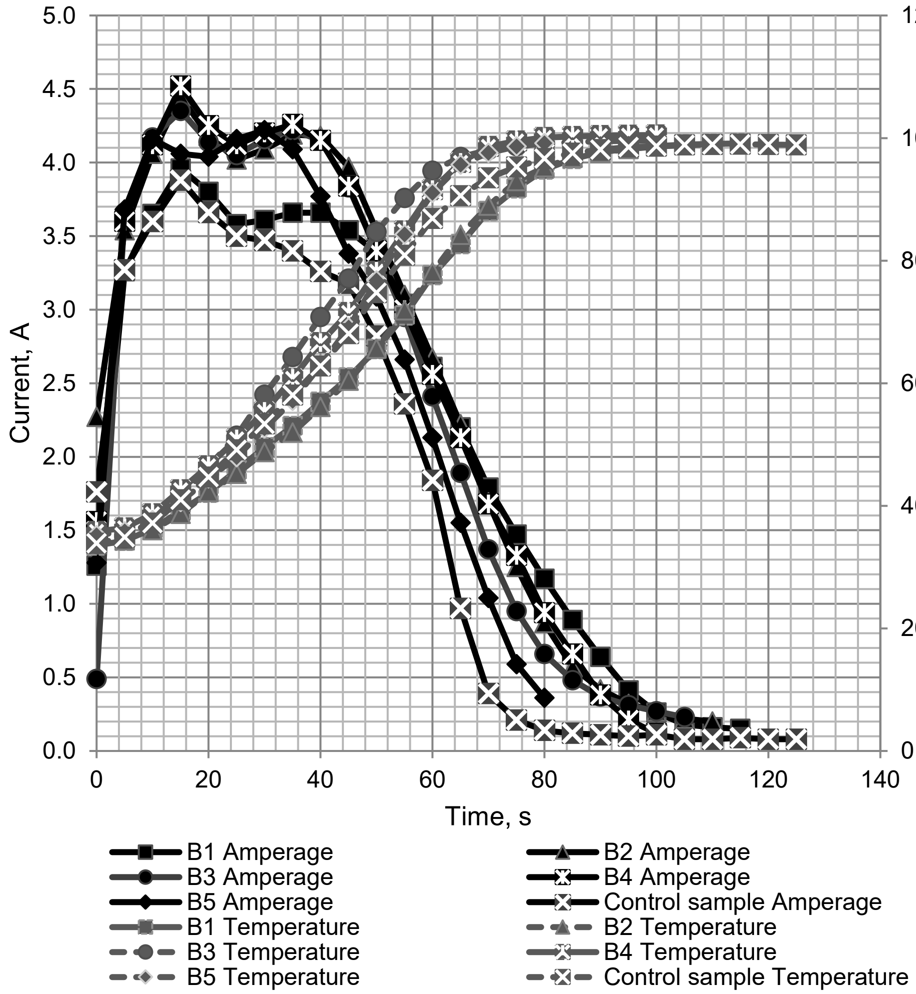

Figure 3. Experimental data on changes in current strength and temperature during ER baking of bread

The sample is heated almost linearly up to a temperature of 80–90 °C, smoothly going to a plateau at 98–99 °C. Analysis shows that experimental curves are similar and generally vary slightly. The scatter of current strength values can be explained by an inaccuracy in the current measurements, as well as by inevitable fluctuations in humidity, the mass of dough samples, the contact area between the dough and electrodes and the degree of proofing of dough samples. The combined influence of these factors, however minor they are, can lead to differences in the maximum current strength among experiments. Consequently, differences in the dynamics of changes in the current strength affect the heating rate of the dough sample in various experiments.

Figs 4 and 5 show experimental data on changes in the current strength and temperature during baking of sponge cake. It should be noted that, compared with bread, the dynamics of changes in the current strength during baking of sponge cake are less complex.

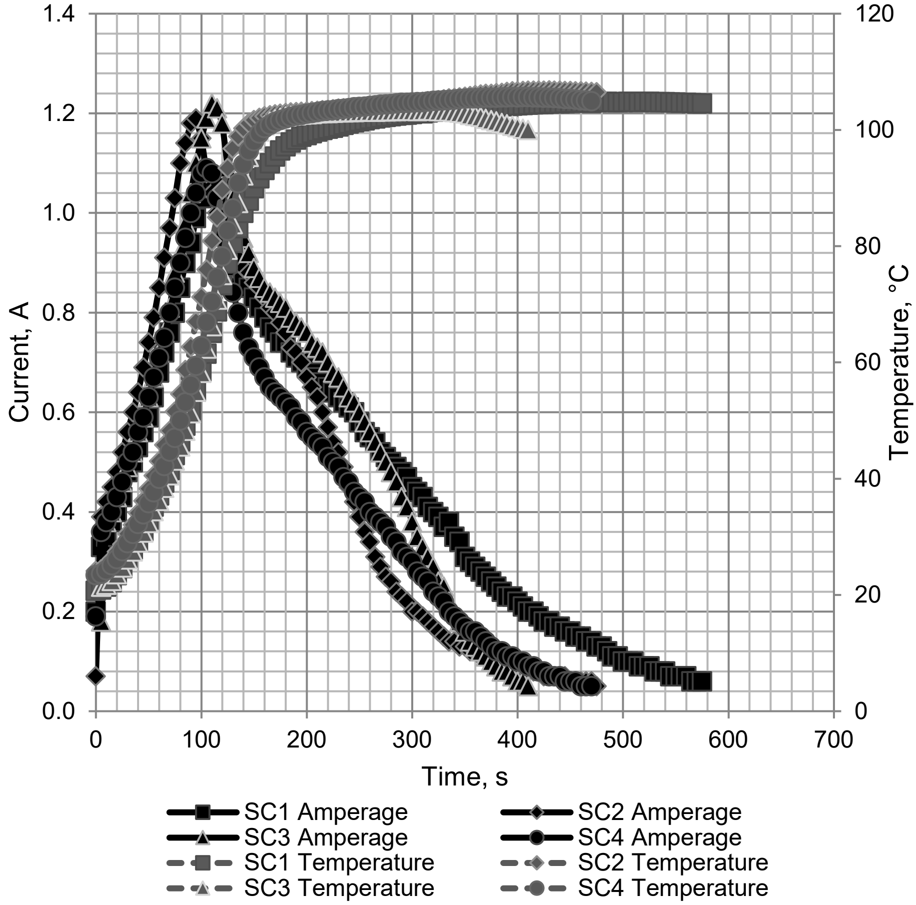

Figure 4. Experimental data on changes in current strength and temperature during ER baking of sponge cake, samples SC1–SC4.

The curve is a single peak function. The initial increase in the current strength to a maximum can be caused by an increase in conductivity due to an increase in temperature of the sponge cake batter. Upon reaching a temperature close to 100 °C, a decrease in the current strength is presumably caused by the evaporation of moisture from sponge cake and a decrease in the overall conductivity of the sponge cake batter.

The dynamics of changes in the temperature of sponge cake is close to the ones of yeast dough, with the exception of the maximum process temperature, which reaches 105 °C in sponge cake. Scatter of the maximum current strength during baking observed in experiments can be explained by the ammeter error, as well as by the difference in the composition of the eggs in different batches, whose intrinsic conductivity significantly affects the overall conductivity of sponge cake.

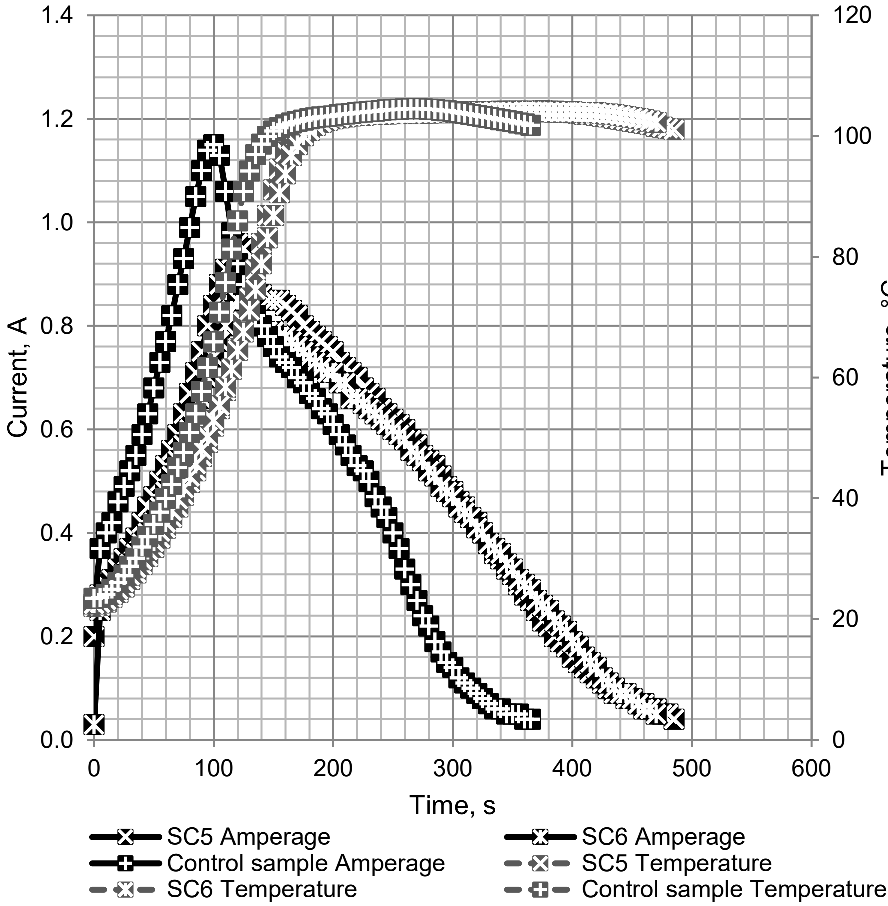

Figure 5. Experimental data on changes in current strength and temperature during ER baking of sponge cake, samples SC5–SC6 and control sample.

Selection of the extraction method

Beta-carotene extraction methods based on literature sources (Schierle et al., 2004; State Standard of the Russian Federation, 2010) require either a complex process or a large amount of equipment. Some studies have been conducted to develop a rapid method of extracting beta-carotene. Those are methods of Quı'lez (method 1) and U. Schweiggert (method 2) (Quílez et al., 2003; Schweiggert et al., 2005). We have tested these methods of sample preparation on sample B1 (Table 5).

Table 5. Efficiency of beta-carotene extraction by two methods

Method	The initial amount of beta-carotene, mg	The content of beta-carotene in the finished product, mg
1	20.10 ± 0.1	2.22 ± 0.2
2	20.00 ± 0.1	7.31 ± 0.1

However, as can be seen from the results obtained, these extraction methods do not provide complete extraction of coloring substances from the samples, which leads to unreliable results of the beta-carotene content. Therefore, we have developed the extraction methods described in the Materials and Methods section.

Beta-carotene content in bread and sponge cake samples

Fig. 6 shows data on the content of beta-carotene in mg g^{-1} of the final product in samples of bread obtained by two baking methods. It should be noted that in the control samples (prepared without adding beta-carotene) no significant amount of beta-carotene was found.

Data analysis shows that beta-carotene is lost in all bread samples during baking. However, these losses are less than those recorded by the authors (Rogers et al., 1993; Ranhotra et al., 1995). This significant difference can be explained by the fact that the authors used samples of stabilized beta-carotene developed more than 30 years ago, and during this time progress in improving the stability of beta-carotene has stepped forward.

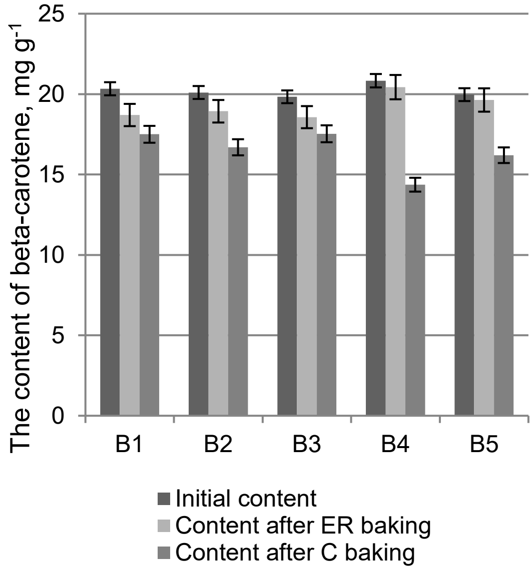

Figure 6. Beta-carotene content in bread samples.

Statistically significant differences in the samples prepared by different baking methods were observed in the samples with the addition of supramolecular complexes and fat-soluble beta-carotene. Close values of beta-carotene losses were observed for samples B1, B2 and B3 obtained using emulsified forms of beta-carotene, which are more stable during convective baking than supramolecular complexes. Perhaps this is due to the presence of an emulsifier and a fatty phase in carotene-containing additives.

The higher preservation of beta-carotene in the samples obtained by ER baking can be explained by the different temperatures and duration of baking of the samples: during ER baking, the product temperature did not exceed 100 °C, while C baking was carried out at a temperature of 210 °C. In addition, only the outer layers of bread were exposed to higher temperatures during C baking. Thus, the difference in beta-carotene losses between the samples is explained only by the losses in the crust, and taking into account the fact that the fraction of crust in the mass of the product is relatively small and does not exceed 30%, a slight difference fits completely into these facts.

According to the experimental data obtained, it can therefore be concluded that the greatest stability of beta-carotene during baking can be achieved by combining technological parameters and using a stabilized form of beta-carotene, for example, supramolecular forms of beta-carotene and ER baking.

Fig. 7 shows data on beta-carotene content in mg g^{-1} of the final product in sponge cakes prepared by two baking methods.

Statistically significant differences in sponge cake samples prepared by different baking methods were observed when adding supramolecular complexes and fat-soluble beta-carotene (samples SC4, SC5, SC6. SC2, respectively).

The same as bread samples, sponge cake samples with supramolecular complexes were characterized by greater losses than samples with emulsified sources of beta-carotene during convective baking.

Comparison of losses in samples SC5 and SC6, in which the same source of beta-carotene is used, but the application method is different, allows us to conclude that, in addition to the baking method and to the form of carotene, the method of introduction of additives also affects the preservation.

The influence of the baking method as a whole can be explained by the same factors as those in bread baking process: lower temperature, process duration and a decrease in losses in the surface layer due to the absence of crust.

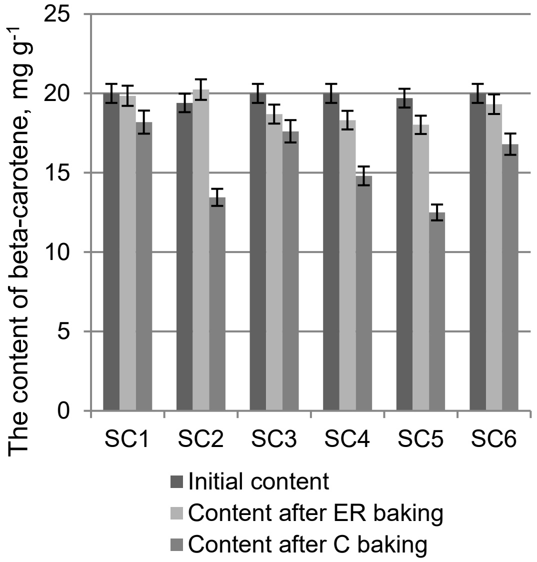

Figure 7. Beta-carotene content in sponge cake samples.

Organoleptic analysis of bread and sponge cake

Organoleptic parameters of bread are shown in the Table 6.

Table 6. Sensory characteristics of bread

Sample		State of the bread surface	Color of the crumb	Porosity	Crumb consistency	Bread aroma	Crumb taste
B1	ER	4.80 ± 0.16	4.77 ± 0.05	4.00 ± 0.08	4.17 ± 0.09	3.27 ± 0.05	3.87 ± 0.05
	C	4.73 ± 0.12	4.80 ± 0.16	4.47 ± 0.09	4.13 ± 0.05	4.80 ± 0.08	3.70 ± 0.12
	F	0.21	0.08	28.00*	0.20	529.00*	4.50
B2	ER	4.80 ± 0.16	4.83 ± 0.12	3.97 ± 0.21	4.17 ± 0.05	3.33 ± 0.12	4.63 ± 0.17
	C	4.77 ± 0.09	4.87 ± 0.09	4.47 ± 0.12	4.20 ± 0.16	4.83 ± 0.05	4.53 ± 0.12
	F	0.06	0.09	8.65*	0.08	253.00*	0.45
B3	ER	4.83 ± 0.12	4.87 ± 0.19	3.93 ± 0.12	4.30 ± 0.08	3.17 ± 0.17	3.73 ± 0.17
	C	4.77 ± 0.12	4.93 ± 0.09	4.47 ± 0.09	4.27 ± 0.12	4.87 ± 0.12	3.77 ± 0.09
	F	0.29	0.20	23.30*	0.10	130.00*	0.06
B4	ER	4.73 ± 0.19	3.90 ± 0.08	4.17 ± 0.05	4.27 ± 0.09	3.40 ± 0.08	4.83 ± 0.12
	C	4.83 ± 0.17	3.83 ± 0.12	4.37 ± 0.05	4.43 ± 0.09	4.83 ± 0.05	4.87 ± 0.05
	F	0.31	0.40	18.00*	3.10	462.00*	0.13
B5	ER	4.93 ± 0.09	3.73 ± 0.19	3.80 ± 0.14	4.33 ± 0.12	3.23 ± 0.09	4.83 ± 0.09
	C	4.73 ± 0.12	3.70 ± 0.08	4.53 ± 0.09	4.40 ± 0.08	4.73 ± 0.05	4.80 ± 0.08
	F	3.30	0.05	37.20*	0.40	405.00*	0.14

* means unacceptance of the hypothesis (a significant difference in the results at the level of 0.05); calculated value of the *F-criterion*. The tabular value of the *F-criterionis* 7.71.

There were no statistically significant differences in crumb shape, taste and consistency between samples of different baking methods. However, there is a statistically significant difference in the aroma indices, which may be due to the fact that during ER baking the temperature of the dough does not reach sufficient values for the Maillard reactions to occur.

Nature of porosity is conditioned by the geometric shape of the bread prepared by two baking methods and having the same weight: the form for ER baking is narrower and higher than the standard baking form.

Also there is a significant difference in the color intensity between the samples with different sources of beta-carotene: the samples with the addition of supramolecular complexes are less colored, which is caused by their physicochemical properties (Rudometova et al., 2018; Rudometova & Kulishova, 2018).

Organoleptic parameters of sponge cake are shown in the Table 7.

Table 7. Sensory characteristics of sponge cake

Sample		External appearance	Crumb color	Consistency	Crumb taste	Aroma
SC1	ER	4.83 ± 0.09	4.80 ± 0.08	4.63 ± 0.05	4.43 ± 0.05	3.90 ± 0.14
	C	4.93 ± 0.05	4.9 ± 0.08	4.53 ± 0.12	4.47 ± 0.12	4.9 ± 0.08
	F	1.80	1.50	1.13	0.13	75.00*
SC2	ER	4.80 ± 0.14	4.80 ± 0.08	4.53 ± 0.05	4.77 ± 0.09	4.17 ± 0.05
	C	4.83 ± 0.09	4.87 ± 0.05	4.40 ± 0.08	4.67 ± 0.05	4.83 ± 0.05
	F	0.08	1.00	4.00	1.80	200.00*
SC3	ER	4.70 ± 0.08	4.73 ± 0.09	4.73 ± 0.09	4.77 ± 0.12	3.93 ± 0.12
	C	4.83 ± 0.12	4.87 ± 0.05	4.60 ± 0.08	4.80 ± 0.08	4.87 ± 0.05
	F	1.60	3.20	2.29	0.10	98.00*
SC4	ER	4.80 ± 0.08	3.50 ± 0.08	4.67 ± 0.12	4.83 ± 0.05	4.00 ± 0.14
	C	4.90 ± 0.08	3.37 ± 0.05	4.40 ± 0.08	4.73 ± 0.12	4.87 ± 0.09
	F	1.50	4.00	6.40	1.13	52.00*
SC5	ER	4.73 ± 0.05	3.27 ± 0.12	4.67 ± 0.12	4.77 ± 0.12	4.03 ± 0.12
	C	4.77 ± 0.09	3.23 ± 0.12	4.63 ± 0.12	4.80 ± 0.08	4.97 ± 0.05
	F	0.20	0.07	0.07	0.10	98.00*
SC6	ER	4.77 ± 0.12	4.27 ± 0.12	4.60 ± 0.14	4.73 ± 0.12	4.03 ± 0.12
	C	4.83 ± 0.12	4.20 ± 0.16	4.70 ± 0.08	4.83 ± 0.09	4.93 ± 0.09
	F	0.29	0.21	0.75	0.83	66.28*

* means unacceptance of the hypothesis (a significant difference in the results at the level of 0.05); calculated value of the *F-criterion*. The tabular value of the *F-criterionis* 7.71.

According to the results of the organoleptic evaluation of sponge cake samples prepared by different baking methods, no statistically significant differences were found in the external appearance, crumb color, crumb consistency and taste. A significant difference is observed in the aroma of the samples, which is due to the absence of melanoid-forming products in the sponge cake prepared by ER baking.

There is a difference in color saturation between samples with different sources of beta-carotene; samples with supramolecular complexes are less intensely colored. It should be noted that the color intensity is influenced by the method of beta-carotene addition, which is confirmed by the different mean values of the color intensity in samples SC5 and SC6.

CONCLUSION

The use of electric resistance baking in the production of crustless bread and sponge cakes allows for better preservation of the embedded beta-carotene in bread and sponge cake batter samples. Thus, combination of the ER baking method and the use of stabilized forms of beta-carotene, such as supramolecular complexes, for example, allow to obtain functional bread and flour confectionery products with minimal loss of useful nutrients. Furthermore, the use of ER baking instead of the traditional method does not significantly affect the organoleptic characteristics of crumb in the finished products.

REFERENCES

Baranenko, D., Bespalov, V.G., Nadtochii, L., Shestopalova, I., Chechetkina, A., Lepeshkin, A. & Ilina, V. 2019. Development of encapsulated extracts on the basis of meadowsweet (Filipendula ulmaria) in the composition of functional foods with oncoprotective properties. *Agronomy Research* **17**(5), 1829–1838. doi:10.15159/ar.19.155

Derde, L.J., Gomand, S.V., Courtin, C.M. & Delcour, J.A. 2014. Moisture distribution during conventional or electrical resistance oven baking of bread dough and subsequent storage. *Journal of Agricultural and Food Chemistry* **62**, 6445–6453. doi:10.1021/jf501856s

European Commission. 2006. Regulation (EC) No. 1925/2006 of the European Parliament and of the Council of 20 December 2006 on the addition of vitamins, minerals and of certain other substances to foods (2006). *Official Journal of the European Union*, L404/26.

European Commission. 2012. Regulation (EU) No. 231/2012 of 9 March 2012 laying down specification for food additives listed in Annexes II and III to Regulation (EC) № 1333/2008 of the European Parliament and of the Council. Official Journal of the European Union, L 83/1. pp. 1–295.

Gonçalves, A., Estevinho, B.N. & Rocha, F. 2016. Microencapsulation of vitamin A. *Trends in Food Science & Technology* **51**, 76–87. doi: 10.1016/j.tifs.2016.03.001

GOST R 54059-2010. 2010. 'Functional foods. Functional food ingredients. Classification and general requirements'. Moscow State University of Food Production, Moscow, Russia (in Russian).

GOST R 58233-2018. 2018. 'Wheat bread. Specifications'. Scientific Research Institute of the Bakery Industry, Moscow, Russia (in Russian).

MR 2.3.1.2432-08. 2008. 'Balanced diet. Norms of physiological needs for energy and nutrients for various groups of the population of the Russian Federation'. Scientific Research Institute of Nutrition of the Russian Academy of Medical Sciences, Moscow, Russia (in Russian).

Javkina, D.I. Sidorenko, G.A., Popov, V.P., Zinjuhin, G.B. & Krasnova, M.S. 2014. Influence of technological parameters on the quality of grain bread baked by the electric resistant method. *Vestnik OGU* **164**(3), pp. 187–194.

Jin, Z.-Y. 2013. *Cyclodextrin Chemistry: Preparation and Application.* World Scientific Publishing Co. Pte. Ltd., 290 pp.

Kumar, K. & Kumar, N. 2012. Development of Vitamin and Dietary Fibre Enriched Carrot Pomace and Wheat Flour based Buns. *Journal of Pure and Applied Science & Technology* **2**(1), 107–115.

Kurkov, S. & Loftsson, T. 2013. Cyclodextrins. *International Journal of Pharmaceutics* **453**(1), 167–180.

Kodentsova, V.M. 2016. About food fortification with vitamins. *Voprosy pitaniia* **85**(4), 87–90 (in Russian).

Mangolim, C.S., Moriwaki, C., Nogueira, A.C., Sato, F., Baesso, M.L., Neto, A.M. & Matioli, G. 2014. Curcumin–b-cyclodextrin inclusion complex: Stability, solubility, characterization by FT-IR, FT-Raman, X-ray diffraction and photoacousticspectroscopy, and food application. *Food Chemistry* **153**, 361–370. doi: 10.1016/j.foodchem.2013.12.067

Mercader-Ros, M.T. Lucas-Abellan, C., Fortea, M.I., Gabaldón, J.A. & Núñez-Delicado, E. 2010. Effect of HP-β-cyclodextrins complexation on the antioxidant activity of flavonols. *Food Chemistry* **118**(3), 769–773. doi: 10.1016/j.foodchem.2009.05.061

Mérillon, J.-M. 2019. *Bioactive Molecules in Food*. Springer International Publishing, 2370 pp.

Naumova, N.L. & Kozubtsev, M.V. 2016. Functional and fortified foods containing minerals and vitamins. *Proceedings of 1-st International Conference "Innovative food technology and quality assessment: science, education, production"*. ESSUTM, Ulan-Ude, pp. 28–33 (in Russian).

Nik, A.M., Wright, A.J. & Corredig, M. 2011. Micellization of Beta-Carotene from Soy-Protein Stabilized Oil-in-Water Emulsions under In Vitro Conditions of Lipolysis. *Journal of the American Oil Chemists' Society* **88**, 1397–1407. doi: 10.1007/s11746-011-1806-z

Popov, V.P., Sidorenko, G.A., Biktimirova, G.I., Zinyukhin, G.B. & Krakhmaleva, T.M. 2014. Electric resistance baking of sponge cake with a partial replacement of flour by starch. *Vestnik OGU* **167**(6), pp. 233–238. (in Russian)

Popov, V.P., Sidorenko, G.A., Zinyukhin, G.B. & Korotkov, V.G. 2012. *Development of bread production technologies using an electric resistance baking method.* OGU, Orenburg. 124 pp. (in Russian).

Quílez, J., Rafecas, M., Brufau, G., Garcia-Lorda, P., Megias, I., Bullo, M., Ruiz, J.A. & Salas-Salvado, J. 2003. Bakery Products Enriched with Phytosterol Esters, a-Tocopherol and -Carotene Decrease Plasma LDL-Cholesterol and Maintain Plasma -Carotene Concentrations in Normocholesterolemic Men and Women. *The Journal of Nutrition* **133**(10), 3103–3109. doi: 10.1093/jn/133.10.3103

Ranhotra, G.S., Gelroth, J.A., Langemeier, J. & Rogers, D.E. 1995. Stability and Contribution of Beta Carotene Added to Whole Wheat Bread and Crackers. *Cereal Chemistry* **72**(2), 139–141.

Rodriguez-Amaya, B.D., Nutti, M.R. & de Carvalho, J.L.V. 2011. *Flour and Breads and their Fortification in Health and Disease Prevention*. Elsevier Inc., 542 pp.

Rogers, D.E., Malouf, R.B., Langemeier, J., Gelroth, J.A. & Ranhotra, G.S. 1993. Stability and nutrient contribution of β-carotene added to selected bakery products. *Cereal Chemistry* **70**(5), 558–561.

Rudometova, N.V. & Kulishova, K.E. 2018. Stabilization of coloring substances in the composition of inclusive nanocomplexes based on starch products. *Scientific journal NRU ITMO. Series Processes and equipment for food production* **4**, pp. 15–21 (in Russian). doi: 10.17586/2310-1164-2018-11-4-15-21

Rudometova, N.V., Kulishova, K.E. & Kim, I.S. 2018. The influence of cyclodextrin and modified starches on the beta-carotene light fastness in inclusion complexes. *Scientific journal NRU ITMO. Series Processes and equipment for food production* **3**, pp. 3–11 (in Russian). doi: 10.17586/2310-1164-2018-11-3-3-11

Rudometova, N.V. & Nikiforova, T.A. 2016. Obtaining supramolecular complexes of indigo carmine with beta-cyclodextrin. *Storage and Processing of Farm Products* **3**, pp. 13–16 (in Russian).

Schweiggert, U., Kammerer, D.R., Carle, R. & Schieber, A. 2005. *Rapid communications in mass spectrometry* **19**(18), 2617–2628. doi: 10.1002/rcm.2104

Sepelevs, I. & Reineccius, G.A. 2018. Encapsulation of Gallic acid in solid lipid core surrounded with maltodextrin shell. *Agronomy Research* **16**(S2), 1475–1485. doi: 10.15159/AR.18.052

Schierle, J., Pietsch, B., Ceresa, A., Fizet, C. & Waysek, E.H. 2004. Method for the Determination of b-Carotene in Supplements and Raw Materials by Reversed-Phase Liquid Chromatography: Single Laboratory Validation. *Journal of AOAC international* **87**(5), 1070–1082.

Sidorenko, G.A., Popov, V.P., Zinyukhin, G.B., Yalaletdinova, D.I. & Zinyukhina, A.G.2012. Electric contact energy supply for baking bread. *Vestnik OGU* **137**(1), pp. 214–221 (in Russian).

Socaciu, C.2007. *Food Colorants: Chemical and Functional Properties*. CRC Press, 648 pp.

Strizhevskaya, V., Pavlenkova, M., Nemkova, S., Nosachyova, N., Simakova, I. & Wolf, E. 2019. Possibility and prospects of preservation of minor components in technology of fruit raw materials conservation. *Agronomy Research* **17**(5), 2082–2088. https://doi.org/10.15159/AR.19.139

Trentin, A., De Lamo Castellvi, S., Güell, C., López, F. & Ferrando, M. 2011. Protein-stabilized emulsions containing beta-carotene produced by premix membrane emulsification. *Journal of Food Engineering* **106**(4), 267–274. doi: 10.1016/j.jfoodeng.2011.03.013

Watson, R.R. 2017. *Nutrition and Functional Foods for Healthy aging*. Academic Press, 386 pp.

Yalaletdinova, D.I. 2010. Comprehensive indicators for determining the quality of grain bread of an electric resistance baking method. *Vestnik OGU* **116**(10), pp. 179–183 (in Russian).

Yi, J., Zhang, Y., Liang, R., Zhong, F. & Ma, J. 2015. Beta-Carotene Chemical Stability in Nanoemulsions Was Improved by Stabilized with Beta-Lactoglobulin–Catechin Conjugates through Free Radical Method. *Journal of Agricultural and Food Chemistry* **63**(1), 297–303. doi: 10.1021/jf5056024

Zabodalova, L., Ishchenko, T., Skvortcova, N., Baranenko, D. & Chernjavskij, V. 2014. Liposomal beta-carotene as a functional additive in dairy products. *Agronomy Research* **12**(3), 825–834.

Agronomy Research **18**(4), 2465–2477, 2020
https://doi.org/10.15159/AR.20.194

Open windrow composting of fish waste in Estonia

M. Lanno[1,*], M. Silm[2], M. Shanskiy[1], A. Kisand[2], K. Orupõld[3] and M. Kriipsalu[4]

[1]Estonian University of Life Sciences, Institute of Agricultural and Environmental Sciences, Chair of Soil Science, Fr.R. Kreutzwaldi 5, EE51006 Tartu, Estonia
[2]Estonian University of Life Sciences, Institute of Agricultural and Environmental Sciences, Chair of Hydrobiology and Fishery, Fr.R. Kreutzwaldi 5, EE51006 Tartu, Estonia
[3]Estonian University of Life Sciences, Institute of Agricultural and Environmental Sciences, Chair of Environmental Protection and Landscape Management, Fr.R. Kreutzwaldi 5, EE51006 Tartu, Estonia
[4]Estonian University of Life Sciences, Institute of Forestry and Rural Engineering, Chair of Rural Building and Water Management, Fr.R. Kreutzwaldi 5, EE51006 Tartu, Estonia
[*]Correspondence: marge.lanno@emu.ee

Abstract. By-catch fish is caught unintentionally during the fishing and is currently thrown back in water bodies to cause the water pollution. Currently fishermen does not have a motivation to bring the by-catch fish to the shore, as it needs to be sorted by fish species, causing fishermen extra work without additional income. Estonian Ministry of Rural Affairs decided to give funding to present study with purpose to find solution to this matter. One possible solution for by-catch fish utilization is to produce high value nutrient rich fertilizer in order to close nutrient cycle and return valuable nutrients into soil. The adaptive study of outdoor windrow composting was conducted with consecutive treatments, rather than simultaneously, in order to make adaptive improvements to the set-up of each consecutive treatment. The consecutive treatments showed that fish waste composting is manageable from a technical perspective, feasible in a temperate climate, and that this type of compost holds high potential as an organic fertiliser or soil improver. Composting process started rapidly and, as required by the EU Commission regulation EU 142/2011, temperatures exceeded 70 °C for at least 1 h in all windrows. While initial treatments suffered from odours, as well as events inhibitive to the composting process, these disadvantages were successfully avoided in later treatments by adding a biofilter and inoculant from previous composting windrows, as well as lake sediments. Rather than disposing of low-value fish, these can be recycled into stable and nutrient-rich compost on-site, near fishing harbours.

Key words: by-catch, biofilter, clay minerals, lake sediment, organic fertiliser, wheat straw.

INTRODUCTION

Composting is an aerobic microbial process that turns organic material into stable humus-like material that can be used to improve soil texture and nutrient content for agricultural use. Composting is suitable for treating different kinds of organic wastes such as food waste, manure, green wastes or municipal solid wastes (Rynk, 1992;

Awasthi et al., 2020). Composting can be performed with different technologies, and at different scales (Rynk, 1992; Hobson et al., 2005). In Estonia, composting is mostly done in open windrows, which are periodically mixed in order to improve porosity and oxygen supply. Mainly source-separated municipal biowaste is composted in Estonia (BEU, 2020), sometimes in combination with garden waste and animal by-products. National end-of-waste regulations for biowaste compost (BEU, 2020) and sewage sludge compost quality (Regulation, 2017) have been enforced since 2013 and 2017, respectively.

Nutrient rich compost holds high potential as an organic fertiliser or soil improver, offering the possibility to reduce the use of synthetic fertilisers. Although fish waste composting is not yet included in local waste management plans in Estonia, there is growing interest for fish waste valorisation and associated nutrient recycling. The topic was also prioritised by the Estonian Ministry of Rural Affairs, through the decision to fund the present study, with the aim of finding new solutions regarding fish waste management. Both the waste from fish processing, as well as by-catch, could represent inputs for composting. For example, Lake Võrtsjärv represents approximately 8% of commercial fishing in Estonian lakes and rivers. In 2018, it was estimated that, for each kg of commercial catch, there were approximately 1.45 kg of by-catch, resulting in 6,300 tons of by-catch per year (Bernotas et al., 2018). During the years 2008–2017, the yearly average commercial catch for Estonian lakes and rivers was 2,800 tons, 65,000 tons for the Baltic Sea and 12,500 tons for the Atlantic Ocean (Quarterly bulletin…., 2018). In Estonia, similar to Baltic region as a whole, fisheries represent an important part of the economy; thus, fish waste composting should be included in local waste management plans.

Besides leftovers from the fish industry, a significant source of unwanted fish is by-catch. By-catch includes fish caught of unusable size, damaged fish and species without economic value (Clucas, 1997). Rather than being revalued, by-catch in Estonia is often thrown back into the aquatic environment, where it results in pollution.

Long-term cultivation and fertilisation both affect the humus content in soils (Hospodarenko et al., 2018). Also, mineral sources for phosphorus (P) fertilisers are located in sensitive regions, or generate a large ecological footprint during transportation to agricultural fields (Roy et al., 2005). Therefore, the available of local P nutrient sources is vital. Compost can add humus to soils over a longer period, and reduce the need for using synthetic fertilisers (Epstein, 2017). Compost represents a slow-release fertiliser, as nutrients from composted material are released slowly yet consistently, thus building up a stable reserve of soil nutrients (Hepperly et al., 2009).

It has been claimed that fish-derived amendments behave like slow-release nitrogen (N) fertilisers, and hold higher P release capacities, as well as being rich in calcium (Ca) (Laos et al., 2000). Therefore, fish waste could be processed into a nutrient-rich soil amendment. There have been different composting trials indicating that fish waste compost represents a suitable fertiliser for agricultural use, and can increase crop yield (Laos et al.,1998; López-Mosquera et al., 2011; Illera-Vives et al.,2015; Radziemska et al., 2018).

Due to problematic odour emission, fish waste must be stabilised rapidly. One key factor may be choosing an appropriate compost mixture. In addition to organic wastes, different substrates such as bulking agents and other additives must be used while creating compost windrows. Shredded wood and straw are porous and rich in carbon

(C), and can improve aeration and moisture regulation, as well as improve odour absorption (Rynk, 1992). Sufficient aeration is necessary, as a limited oxygen (O_2) supply during the active composting period decreases microbial activity, inhibiting the composting process (Avnimelech et al., 2004). To understand the progression of composting, O_2 consumption must be measured. Respiration rate reflects microbial activity and the decomposition of organic matter. Accordingly, higher O_2 consumption is associated with higher microbial activity. In stable or mature compost, easily degradable organic matter is decomposed, and the resulting compost is safe to use (Wichuk & McCartney, 2013). Moisture content is also important, as water transports dissolved nutrients to microorganisms, resulting in greater microbial activity, which is essential for the decomposition process.

Straw as a bulking agent is light and fluffy, making the windrows porous. Also, it biodegrades more easily than wood chips. This may be the result of higher undesirable ammonia (NH_3) emission; but at the same time, it has been demonstrated that composts with straw amendments contain higher nutrient concentrations than those with wood chips (Sardá et al., 2019).

In order to improve the composting process, different additives such as biochar, peat, clay minerals and mature compost can be added into fresh composting mixtures, with the purpose of reducing gas- and odour emissions, as well as to increase the nutrient content of the final product, thus influencing microbial activity. As a result, the degradation process starts earlier and the thermophilic phase lasts longer (McCrory & Hobbs, 2001; Gabhane et al., 2012; Sánchez-García et al., 2015; Barthod et al., 2018). Additives such as clay minerals can also limit water loss and reduce greenhouse gas emissions (Barthod et al., 2016). It has been shown that an adequate moisture content has have a greater influence than temperature on the decomposition process (Liang et al., 2003); an adequate moisture level in compost is approximately 40–60% (Rynk, 1992). Clay minerals can also influence microbial activity, as clay provides a pH suitable for sustainable microbial growth (Stotzky & Rem, 1966).

Temperature is an important indicator for the composting process, reflecting both the degradation of organic matter and microbial activity (Eklind et al., 2007). The thermophilic phase occurs when temperatures inside compost windrows exceed 40 °C; where the organic matter decomposition process is the fastest at 55 °C (Eklind et al., 2007; Rynk, 1992), when microbial activity is highest (Miyatake & Iwabuchi, 2005).

Compost must be safe for humans and the environment, and therefore it must be free of pathogens. Because of its status of being animal by-products (ABPR), temperatures must exceed 70 °C for 1 h for sanitation purposes, as required by the EU Commission regulation EU 142/2011 (European Commission, 2011). After the active composting period, it is necessary to let compost mature, as immature compost may inhibit plant growth (Ozores-Hampton et al., 2002).

The aim of this study was to develop a practical technological solution for composting, whereby fishermen can use nearby fishing harbours to revalue by-catch fish, allowing this resource to be converted into nutrient rich fertiliser suitable for agricultural use. We focused particularly on solutions for reducing odours and meeting sanitation requirements.

MATERIALS AND METHODS

Composting experiment

The composting experiment was conducted in Taali, Pärnu County, Estonia. Five batches of fish compost (corresponding to treatments F1–5), each having different raw material ratios, were composted from spring 2018 to autumn 2019 (Table 1). Treatments were performed consecutively, rather than simultaneously, in order to make adaptive improvements to the set-up of each consecutive treatment. The composting site was on a concrete surface, in order to prevent soil- and groundwater pollution. All windrows were covered with the semi-permeable geotextile KSV 200 (Compost Systems, Austria), in order to reduce the weather impact, maintain the in-compost microclimate, and protect the windrows from animals. All treatments were carried out at a scale 10 m^3 (12–16 m long and 1.5 m wide windrows). The main component in each compost mixture was low-value by-catch fish from Lake Võrtsjärv, followed by wheat straw as bulking material, as it is considered easily available.

Table 1. Initial ingredients of compost mixtures (kg). F1–5 represent different treatments (windrows). An asterisk (*) indicates that the straw was shredded

Windrow	By-catch fish	Straw	Water	Peat	Mature compost (horse manure)	Mature compost (fish, F1 treatment)	Lake sediment
F1	4,406	1,125	0	0	0	0	0
F2	1,705	1,312	1,860	0	0	0	0
F3	930	943	1,996	960	913	545	0
F4	905	1,155*	1,150	0	0	0	355
F5	960	1,347*	1,200	0	0	460	180

For treatments F1, F2 and F3, unshredded wheat straw was used; whereas in treatments F4 and F5, wheat straw was shredded with the trailed straw chopper PRIMOR 5570 M (KUHN Group, Austria).

Additives such as peat, mature compost (used as inoculant), and lake sediment rich in clay minerals, containing 6 g of clay material per 100 g dry matter (DM), were used in different treatments. All by-catch and lake sediment originated from Lake Võrtsjärv. Straw was collected in 2017 from the surrounding agricultural fields in in Taali, Pärnu County, Estonia. The straw was subsequently dried and pressed into 250 kg rolls. The by-catch fish samples, and straw, were analysed for total C and N in order justify an appropriate balance of material inputs. The calculations were based on the assumption, that efficient composting process takes place, when C/N is (20–30)/1. Composting materials were mixed together using a BVL van Lengerich feed mixer V-Mix 13 2S plus (BVL Group, Germany).

Different treatments lasted for different lengths of time, as treatments F2 and F3 were conducted during autumn, resulting in shorter period of time suitable for maturation process (Table 2).

Table 2. Composting treatments. F1–5 represent different treatments (windrows)

Windrow	Composting duration (d)	Moisture adjustment	Moisture adjustment	Turning frequency
F1	185	No	No	Day 35
F2	70	Yes	Days 1, 9	Days 9, 11, 14, 16 and 19
F3	50	Yes	Day 1	Days 5, 8, 11 and 22
F4	135	Yes	Days 1, 9	Days 6, 9, 15, 18, 25 and 40
F5	135	Yes	Days 1, 9	Days 6, 9, 15, 18, 25 and 40

Temperature was measured automatically from windrows F2, F3, F4 and F5, using thermocouple wires (type K, min -10 °C, max 105 °C, 2-Core, Unscreened, PVC-insulated, 100 m; Thermosense, UK). Depending on treatment, 2 or 3 sensors were inserted into each windrow, approximately 20 cm up from concrete surface. Carbon dioxide (CO_2) concentration was measured manually twice a day, using a Brigon Testoryt CO_2 detector (0–20%; Brigon Messtechnik, Germany). When temperatures exceeded 70 °C for several days, or CO_2 concentration rose above 10%, windrows were mixed using either a Backhus 16.30 windrow turner (Eggersmann, Germany) or an ST 300 windrow turner (COMPOST and WASTE technology, Austria).

To prevent odours, a biofilter was associated with each treatment (Fig. 1). The biofilter was made from a 1 m^3 container filled with a 4:1:1 ratio of shredded wood, coal and mature compost of horse manure, respectively; and was connected to its respective windrow via a 75 mm polyethylene aeration pipe perforated with 5 mm diameter holes spaced 10 cm apart, the holes forming two shifting lines. Negative pressure via fan was used for ventilation. Biofilters were turned on twice a day for 15 min, until problematic odours discontinued (4 to 5 days). The same biofilter was used for each treatment.

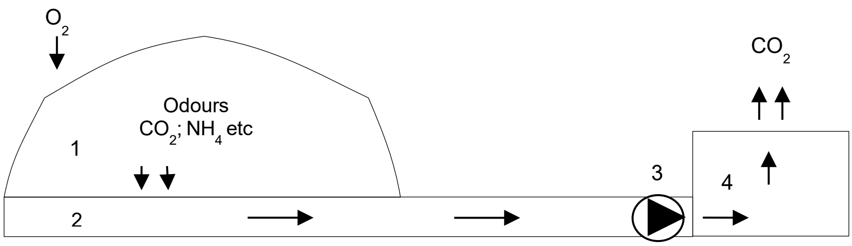

Figure 1. Biofilter- and windrow schematic: 1 – compost windrow; 2 – perforated pipe under the windrow; 3 – fan; 4 – biofilter.

Chemical analyses

Compost samples were collected from all treatments, from three different locations approximately 20–30 cm into the windrow. From each sample, approximately 250 g was homogenised, dried at 105 °C and ball-milled prior to analysis. DM- and ash concentrations were measured. P, potassium (K), Ca and magnesium (Mg) content was determined using the ammonium lactate (AL) method from Egnér et al. (1960); and C and N content was analysed using a VarioMAX CNS analyser (ELEMENTAR, Germany).

Compost stability

Four-day cumulative oxygen consumption was determined via manometric respirometry (OxiTop, WTW, Germany) according to the manufacture´s recommendations. Measurements were collected in 1 L air-tight containers with 50–60 g of fresh sample. Since produced CO_2 was removed by absorber (2 M NaOH), the oxygen consumption of samle could be calculated from the pressure drop in the container. Measurements were collected in triplicate at 20 °C in a climate chamber (Sanyo MLR-351H, Osaka, Japan), in total darkness.

Statistical analyses

A three-way analysis of variance (ANOVA) was performed in order to examine the effect of treatment, ambient temperature, duration of composting, and the interactions between these factors, on composting temperature. A one-way ANOVA was used to study the effect of treatment on mean temperature. A post-hoc Tukey *HSD* analysis was performed for pairwise comparisons, using the package 'agricolae' (Mendiburu, 2015) in R.

RESULTS AND DISCUSSION

Composting process

In all treatments, the thermophilic phase was reached in 1 to 2 days, and temperatures exceeded 70 °C, as required by the EU Commission regulation EU 142/2011 on animal by-products. The duration of thermophilic phase was treatment-dependent. After the thermophilic phase, temperatures decreased rather quickly, and ambient levels were reached within days (Table 3).

Table 3. Temperature characteristics: n.d. – data not determined; * – temperature fluctuation. In F2 treatment temperature decreased < 35 °C several times since day 6 and rised again after mechanical mixing with windrow turner

Batch Windrow	Time to reach > 45 °C	Number of days temp > 45 °C	Number of days temp > 70 °C	Peak temp °C	Time to reach the peak temp	Time to drop to ambient level < 35 °C
F1	n.d	n.d	n.d	n.d	n.d	n.d
F2	Day 1	14	1	72.9	Day 1	Day 6*
F3	Day 2	21	7	76.4	Day 6	Day 23
F4	Day 1	63	18	75.0	Day 7	Day 63
F5	Day 2	69	21	78.6	Day 8	Day 73

In treatment F1, a windrow turner was used for mixing the compost ingredients. We do not recommend this method for preparing compost mix with fish, as whole fish were thrown from the windrow.

In deeper layers of the F1 windrow, fish started to slow-cook as a result of high temperatures; and in outer layers of this windrow, fish became either dried or rotted. To prevent the spread of odours, the F1 windrow was covered with peat for 2 weeks, starting on day 7. It was concluded that the wheat straw is suitable as bulking material, but as it is too dry, water should be added at the beginning of the composting process. Also, shredding of fish would speed up degradation. As the feed mixer later partly shredded the fish, it made the compost mixture more homogeneous.

When compiling the F2 treatment, water was added to the compost mixture. Since, due to fish decomposition, there was a considerable problem with fish odour emission from treatment F1, a biofilter was implemented in treatment F2. Initially, the biofilter was turned on for 15 min every 2 h, which caused the temperature drop in the windrow. It was concluded that the optimal biofilter working mode was twice a day for 15 min. The biofilter also provided a sufficient O_2 supply to windrow, thus reducing the need for mechanical mixing of windrows during the first days.

In treatment F2, the thermophilic phase was reached at the end of the day 1. For unknown reasons, the temperature started to decrease after day 5 (Fig. 2). After the temperature decreased, the windrow was mixed with the windrow turner. This resulted in a temporary rise in temperature. Temperatures in the treatment F2 windrow exceeded the thermophilic phase threshold for 16 days (Table 3). These high temperatures in compost are associated with microbial activity, and therefore temperature decreases are frequently influenced by low microbial activity (Alves et al., 2019; Wichuk & McCartney, 2013). This may have been the cause of temperature fluctuation in the treatment F2 windrow. However, the cause of low microbial activity is unclear, as easily-biodegradable substrate was not consumed until the end of the active composting period, and neither O_2 supply nor moisture content were not considered to be limiting factors. Further research is needed to conclude what causes these types of temperature fluctuations.

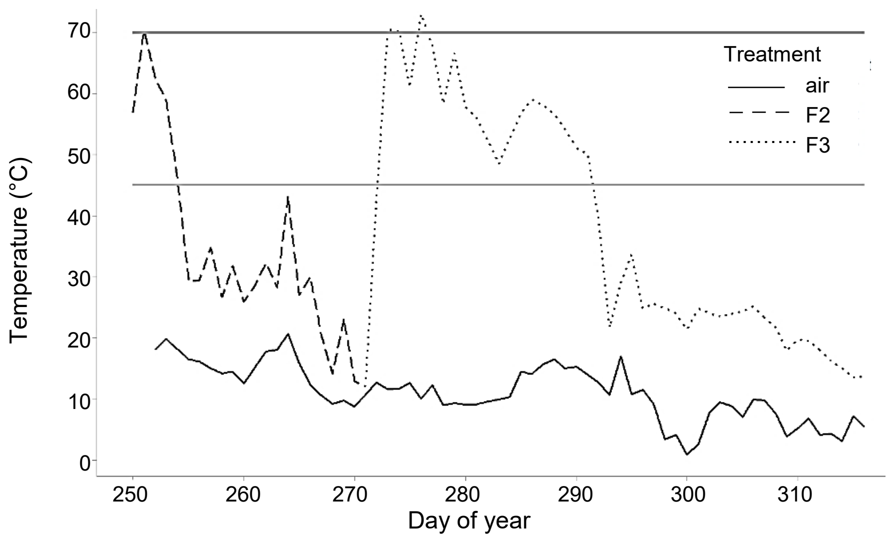

Figure 2. Windrow F2 and F3 temperature graphs from year 2018.

It was previously shown that the addition of mature compost can slightly increase temperature in the thermophilic phase (Maeda et al., 2009). For the purpose of stabilising temperatures during the active composting period, as well as to add more beneficial bacteria necessary for the decomposition process, peat and mature compost were added to treatment F3. The thermophilic phase for this treatment was reached by day 3, and temperatures were stable during the active composting period, which lasted for 23 days. As temperatures inside compost are not uniform (Avnimelech et al., 2004), the treatment

F3 windrow was mixed during days 5 and 8, in order to homogenise temperature and moisture. After turning the compost, temperatures inside the F3 windrow decreased for an hour, but then started to increase again. Similar behaviour has registered by Marešová & Kollárová, (2010). In their study they also noticed, that after mechanical mixing temperature decreased in the windrow, but after some time temperature started to increase, exceeding the previous level.

For treatments F4 and F5, both windrows contained by-catch fish, shredded straw and lake sediment; but in treatment F5, mature compost was also added. The mean in-windrow temperatures, between treatments F4 and F5, were not statistically different, even though the temperatures in F5 were slightly higher than in F4 (Fig. 3). In windrows of both F4 and F5, the thermophilic phase was reached by the end of day 1. Furthermore, temperatures > 65 °C lasted longer than in the previous treatments. In treatment F2 and F3, the thermophilic period lasted 14 and 21 days, respectively; while in treatments F4 and F5, the thermophilic period lasted 63 and 69 days, respectively (Table 3). Temperatures decreased to ambient levels in treatment F4 after day 63, and in F5 after day 73. While it has been reported that the decomposition process is most efficient at 55 °C (Eklind et al., 2007), our temperatures exceeded 70 °C for a long period, yet decomposition was still efficient. However, it should be considered that gas emissions can be more intense at higher temperatures (Eklind et al., 2007), and the metabolic activity of many microorganisms will decrease when temperatures exceed 60 °C (Miyatake & Iwabuchi, 2005).

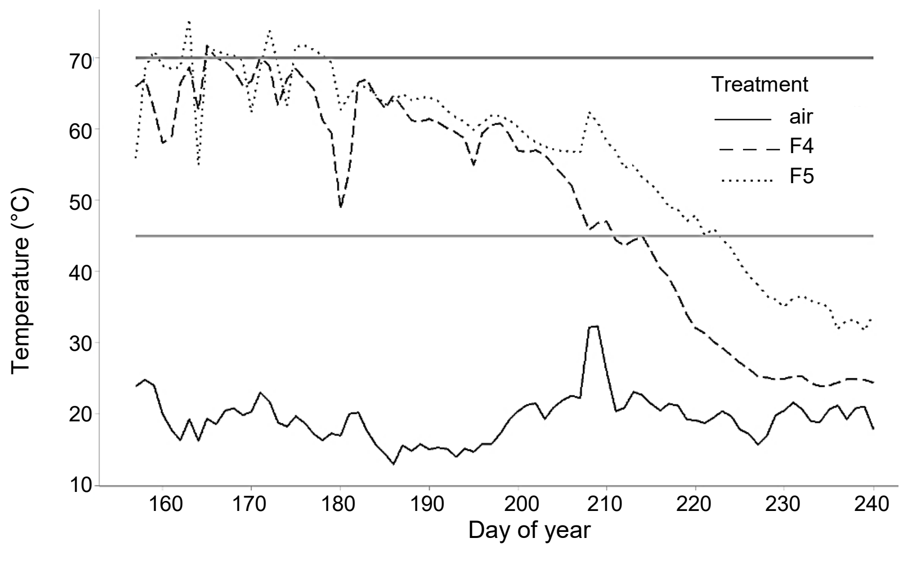

Figure 3. Windrow F4 and F5 temperature graphs from year 2019.

A more efficient composting process in treatments F4 and F5 can be attributed to the addition of shredded straw, which is readily degradable. In the first treatments (F1, F2 and F3), unshredded straw did not completely degrade, and was visible in the final compost product. Straw contains a large fraction of cellulose (29–35%), hemicellulose (26–32%) and lignin (16–21%) (Kapoor et al., 2016), for which decomposition is relatively slow (Eklind et al., 2007). Another explanation for more active composting process can be explained with the addition of clay minerals from lake sediments. Compost constituents were better bound together, making the mixture more homogeneous and providing better conditions for decomposition. It has been shown that the addition of clay minerals can increase water retention capacity and binding the organic material of composting mass (Chen et al., 2018). Therefor adding clay minerals assures the better conditions for microbial activity, resulting in higher temperatures and a longer duration of the thermophilic phase.

Compost stability

According to the Estonian regulation for sewage sludge compost, compost is referred as stable if O_2 consumption over 4 days is less than 10 mg O_2 g^{-1} DM (Regulation, 2017). These values in treatments F2 and F3 remained slightly over the given limit (Fig. 4). Unstable compost can produce odours, generate harmful compounds and, depending on the plant variety, reduce seed germination and inhibit plant growth (Mathur et al., 1993; Emino & Warman, 2004; Harrison, 2008). Temperature fluctuation in the treatment F2 windrow indicated unstable microbial activity during the composting process, resulting in a higher amount of undecomposed organic matter, as well as a higher respiration rate. Treatment F1, F4 and F5 windrows were very stable; their oxygen consumption was less than 5 mg O_2 g^{-1} DM, indicating that composts with longer maturation periods are more stable and safe to use.

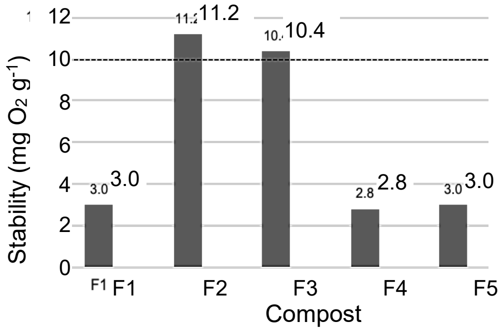

Figure 4. Compost stability determined as 4-days oxygen consumption. Values < 10 mg O_2 g^{-1} DM indicate stabile compost according to Estonian regulation for sewage sludge compost (Regulation, 2017).

Quality of composting process

The effect of treatment, ambient temperature and composting duration on composting temperature was significant (P < 0.05) (Table 4).

Table 4. Results of the three-way analysis of variance (ANOVA), testing the effect of treatment (TR), ambient temperature (AT), length of the composting duration (TIME), and the interactions between these factors, on composting temperatures

	Df	Sum of Square	Mean Square	F value	Pr (>F)	
TR	3	1,154,750	384,917	3,891.97	$< 2e^{-16}$	***
TIME	1	1,732,648	1,732,648	17,519.15	$< 2\times10^{-16}$	***
AT	1	27,913	27,913	282.23	$< 2e^{-16}$	***
TR × TIME	3	195,880	65,293	660.19	$< 2e^{-16}$	***
TR × AT	3	41,251	13,750	139.03	$< 2e^{-16}$	***
TIME × AT	1	17,517	17,517	177.12	$< 2e^{-16}$	***
TR × TIME × AT	3	5,178	1,726	17.45	$2.66e^{-11}$	***
Residuals	11,465	1,133,890	99			

Stars indicate significance: *** – 0.001.

Properties of compost

There were significant differences in P, K and Mg concentrations between treatments ($\alpha = 0.05$). Treatment F4 and F5 windrows had significantly different nutrient contents of P and Mg, compared to other treatments. Compared to other types of compost (e.g. made from horse manure, sewage sludge and green waste), fish compost contains considerably more P (488–918 mg 100 g^{-1}; author's unpublished data; Table 5. This could support the argument that clay minerals bind nutrients together, increasing nutrient content in the final product. It has been shown that fish waste is rich in nutrients such as P and Ca. Fish-derived amendments behave as slow-release N fertilisers, and have high P release capacity (Laos et al., 2000). Therefore, fish compost can be an important source of P based on excavated non- renewable mineral resources.

Table 5. Nutrient concentration (mg 100 g^{-1}) of fish (F1-F5), horse manure (HM), sewage sludge (SS) and green waste (GW) composts. Different letters indicate different groups according to Tukey *HSD* test ($\alpha = 0.05$)

Compost	P	K	Ca	Mg
F1	639^{b}	791^{cd}	$4,471^{ab}$	703^{a}
F2	593^{bc}	$1,329^{bc}$	$4,626^{ab}$	664^{a}
F3	488^{c}	$1,676^{b}$	$3,166^{ab}$	680^{a}
F4	802^{a}	668^{cd}	$2,680^{ab}$	291^{c}
F5	919^{a}	$1,031^{cd}$	$2,927^{ab}$	301^{c}
HM	136^{d}	$2,551^{a}$	$2,986^{ab}$	649^{a}
SS	118^{d}	552^{d}	$1,170^{b}$	518^{b}
GW	115^{d}	552^{d}	$6,682^{a}$	224^{c}

Table 6. Total C and N concentration (%) and C:N ratios of fish (F1-F5)-, horse manure (HM)-, sewage sludge (SS)- and green waste (GW) composts

Compost	C%	N%	C:N
F1	30.22	2.43	12.44
F2	33.04	2.75	12.01
F3	35.66	2.73	13.06
F4	27.92	2.77	10.08
F5	27.64	2.74	10.09
HM	30.99	2.47	12.55
SS	27.02	3.74	7.22
GW	13.35	0.60	22.25

Total N concentration in treatment windrows varied from 2.43–2.77%, while total N in alternative composts varied from 0.6–3.74%. Fish composts and horse manure compost had the most similar total N concentrations (Table 5). Brinton & Seekins (1994) have stated previously, that total N concentration of fish compost is 1.29% after 60 days of composting and 1.15% when compost was mature over-winter.

One possibility for assessing potential N availability is to observe the C:N ratio of the compost, as it has been shown that available N should be present if the C:N ratio is less than 20:1 (Harrison, 2008). The C:N ratios in various composts were less than 20:1, with the exception of green waste compost (Table 6). Our results are in agreement with the idea that composts made primarily from green waste are nutrient-poor (Harrison, 2008).

CONCLUSIONS

Fish waste can be processed into nutrient-rich soil amendments via the simple method of composting in windrows, which can be performed near fishing harbours. Fish compost is particularly rich in P and Ca. We suggest mixing fish compost ingredients with a feed mixer or similar mixing equipment, and to use a biofilter with negative aeration in order to reduce odours. Different additives, especially lake sediment with clay minerals, enhances the efficiency of the composting process. The thermophilic phase was reached in treatment windrows within 1–2 days, and temperatures exceeded 70 °C for at least 1 h, as required by the biofilter EU Commission regulation EU 142/2011 on animal by-products. Our work indicates that nutrient rich compost holds high potential as an organic fertiliser and soil improver, offering the possibility to reduce the use of synthetic fertilisers.

ACKNOWLEDGEMENTS. Research was funded by 'European Maritime and Fisheries Fund 2014–2020' project nr. 811017780003, and by projects PM180261 and PM180259. We appreciate the cooperation, support and experience of Matogard OU.

REFERENCES

Alves, D., Villar, I. & Mato, S. 2019. Thermophilic composting of hydrocarbon residue with sewage sludge and fish sludge as cosubstrates: Microbial changes and TPH reduction. *Journal of Environmental Management* **239**, 30–37.

Avnimelech, Y., Eilat, R., Porat, Y. & Kottas, P.A. 2004. Factors affecting the rate of windrowcomposting in field studies. *Compost Science & Utilization* **12**(2), 114–118. doi:10.1080/1065657x.2004.10702169

Awasthi, S.K., Sarsaiya, S., Awasthi, M.K., Liu, T., Zhao, J., Kumar, S. & Zhang, Z. 2020. Changes in global trends in food waste composting: Research challenges and opportunities. *Bioresource Technology* **299**, 1–12.

Barthod, J., Rumpel, C. & Dignac, M. 2018. Composting with additives to improve organic amendments. A review. *Agronomy For Sustainable Development* **38**(2). doi: 10.1007/s13593-018-0491-9

Barthod, J., Rumpel, C., Paradelo, R. & Dignac, M. 2016. The effects of worms, clay and biochar on CO_2 emissions during production and soil application of co-composts. *SOIL*, *2*(4), 673–683. doi: 10.5194/soil-2-673-2016

BEU. 2020. Bio-waste in Europe – turning challenges into opportunities (2020). European Environment Agency Report No 04/2020.

Bernotas, P., Silm, M. & Järvalt, A. 2018. Status of fish stocks in Estonia and Estonia analysis of the implementation of the eel management. Report. In Estonian. 37 pp. https://www.eea.europa.eu/publications/bio-waste-in-europe, access 18.06.2020

Brinton, W. & Seekins, M. 1994. Evaluation of farm plot conditions and effects of fish scrap compost on yield and mineral composition of field grown maize. *Compost Science & Utilization* **2**(1), 10–16. doi: 10.1080/1065657x.1994.10757912

Chen, H., Awasthi, M., Liu, T., Zhao, J., Ren, X., Wang, M., Duan, Y., Kumar, A. & Zhang, Z. 2018. Influence of clay as additive on greenhouse gases emission and maturity evaluation during chicken manure composting. *Bioresource Technology* **266**, 82–88. doi: 10.1016/j.biortech.2018.06.073

Clucas, I.J. 1997. The utilization of bycatch/discards. In Papers Presented at the Technical Consultation on Reduction of Wastage in Fisheries, Tokyo, Japan, 28 October-1 November 1996, pp. 25–44; 338 pp. FAO Fisheries Report 547 (Suppl.).

Egnér, H., Riehm, H. & Domingo, W. R. 1960. Investigations on the chemical soil analysis as a basis for assessing the soil nutrient status. II: Chemical extraction methods for phosphorus and potassium determination. *Kungliga Lantbrukshügskolans Annaler* **26**, 199–215.

Eklind, Y., Sundberg, C., Smårs, S., Steger, K., Sundh, I., Kirchmann, H. & Jönsson, H. 2007. Carbon turnover and ammonia emissions during composting of biowaste at different temperatures. *Journal of Environmental Quality* **36**(5), 1512–1520. doi: 10.2134/jeq2006.0253

Emino, E. & Warman, P. 2004. Biological assay for compost quality. *Compost Science & Utilization* **12**(4), 342–348. doi: 10.1080/1065657x.2004.10702203

Epstein, E. 2017. *The science of composting*. Routledge. doi: 10.1201/9780203736005

European Commission. 2011. Commission Regulation (EU) No 142/2011 of 25 February 2011implementing Regulation (EC) No 1069/2009 of the European Parliament and of the Council laying down health rules as regards animal by-products and derived products not intended for human consumption and implementing Council Directive 97/78/EC as regards certain samples and items exempt from veterinary checks at the border under that Directive. *Off J Eur Commun* **50**, 1–254.

Gabhane, J., William, S., Bidyadhar, R., Bhilawe, P., Anand, D., Vaidya, A. & Wate, S. 2012. Additives aided composting of green waste: Effects on organic matter degradation, compost maturity, and quality of the finished compost. *Bioresource Technology* **114**, 382–388. doi: 10.1016/j.biortech.2012.02.040

Harrison, R.B. 2008. *Composting and Formation of Humic Substances. Encyclopedia of Ecology* 713–719. doi:10.1016/b978-008045405-4.00262-7

Hepperly, P., Lotter, D., Ulsh, C., Seidel, R. & Reider, C. 2009. Compost, manure and synthetic fertilizer influences crop yields, soil properties, nitrate leaching and crop nutrient content. *Compost Science & Utilization* **17**(2), 117–126. doi: 10.1080/1065657x.2009.10702410

Hobson, A., Frederickson, J. & Dise, N. 2005. CH4 and N2O from mechanically turned windrow and vermicomposting systems following in-vessel pre-treatment. *Waste Management* **25**(4), 345–352. doi: 10.1016/j.wasman.2005.02.015

Hospodarenko, H., Prokopchuk, I., Prokopchuk, S. & Trus, A. 2018. Humus content in achernozem after a long-term application of fertilizers in a field crop rotation. *Agronomy Research* **16**(3), 728–736. doi: 10.15159/AR.18.080

Illera-Vives, M., Labandeira, S.S., Brito, L., López-Fabal, A. & López-Mosquera, M. 2015. Evaluation of compost from seaweed and fish waste as a fertilizer for horticultural use. *Scientia Horticulturae* **186**, 101–107. doi: 10.1016/j.scienta.2015.02.008

Kapoor, M., Panwar, D. & Kaira, G.S. 2016. *Bioprocesses for Enzyme Production Using Agro-Industrial Wastes. Agro-Industrial Wastes as Feedstock for Enzyme Production,* pp. 61–93. doi:10.1016/b978-0-12-802392-1.00003-4

Laos, F., Mazzarino, M., Walter, I. & Roselli, L. 1998. Composting of fish waste with wood by-products and testing compost quality as a soil amendment: Experiences in the Patagonia Region of Argentina. *Compost Science & Utilization* **6**(1), 59–66. doi: 10.1080/1065657x.1998.10701910

Laos, F., Satti, P., Walter, I., Mazzarino, M.E.J. & Moyano, S. 2000. Nutrient availability of composted and noncomposted residues in a Patagonian Xeric Mollisol. *Biology and Fertility of Soils* **31**(6), 462–469. doi: 10.1007/s003740000192

Liang, C., Das, K. & McClendon, R. 2003. The influence of temperature and moisture contents regimes on the aerobic microbial activity of a biosolids composting blend. *Bioresource Technology* **86**(2), 131–137. doi: 10.1016/s0960-8524(02)00153-0

López-Mosquera, M., Fernández-Lema, E., Villares, R., Corral, R., Alonso, B. & Blanco, C. 2011. Composting fish waste and seaweed to produce a fertilizer for use in organic agriculture. *Procedia Environmental Sciences* **9**, 113–117. doi: 10.1016/j.proenv.2011.11.018

Maeda, K., Morioka, R., Hanajima, D. & Osada, T. 2009. The impact of using mature compost on nitrous oxide emission and the denitrifier community in the cattle manure composting process. *Microbial Ecology* **59**(1), 25–36. doi: 10.1007/s00248-009-9547-3

Marešová, K. & Kollárová, M. 2010. Influence of compost covers on the efficiency of biowaste composting process. *Waste Management* **30**(12), 2469–2474. doi: 10.1016/j.wasman.2010.06.014

Mathur, S., Owen, G., Dinel, H. & Schnitzer, M. 1993. Determination of Compost Biomaturity. I. Literature Review. *Biological Agriculture & Horticulture* **10**(2), 65–85. doi: 10.1080/01448765.1993.9754655

McCrory, D. & Hobbs, P. 2001. Additives to Reduce Ammonia and Odor Emissions from Livestock Wastes: A Review. *Journal Of Environmental Quality* **30**(2), 345–355. doi: 10.2134/jeq2001.302345x

Mendiburu, F.D. 2015. *Agricolae: Statistical Procedures for Agricultural Research;* R Package Version 1.2-3; The Comprehensive R Archive Network: Vienna, Austria

Miyatake, F. & Iwabuchi, K. 2005. Effect of high compost temperature on enzymatic activityand species diversity of culturable bacteria in cattle manure compost. *Bioresource Technology* **96**(16), 1821–1825. doi: 10.1016/j.biortech.2005.01.005

Ozores-Hampton, M., Obreza, T.A., Stoffella, P.J. & Fitzpatrick, G. 2002. Immature compost suppresses weed growth under greenhouse conditions. *Compost Science & Utilization* **10**(2), 105–113. doi:10.1080/1065657x.2002.10702071

Quartely bulletin of Statistics Estonia 2/18. 2018. https://www.stat.ee/valjaanne-2018_eesti-statistika-kvartalikiri-2-18

Radziemska, M., Vaverková, M., Adamcová, D., Brtnický, M. & Mazur, Z. 2018. Valorization of fish waste compost as a fertilizer for agricultural use. *Waste and Biomass Valorization* **10**(9), 2537–2545. doi: 10.1007/s12649-018-0288-8

Regulation of the Minister of the Environment. 2017. Reoveesettest toote valmistamise nõuded (Requirements for the production of a product from sewage sludge) RT I, 18.02.2020, 5. https://www.riigiteataja.ee/akt/128072017004 (in Estonian).

Roy, R.N., Finck, A., Blair, G.J. & Tandon, H.L.S. 2006. Plant nutrition for food security. *A guide for integrated nutrient management.FAO Fertilizer and Plant Nutrition Bulletin* **16**, 368.

Rynk, R. 1992. *On-farm composting handbook*. Ithaca, NY: Natural Resource, Agriculture, and Engineering Service, pp. 6–18.

Sardá, L., Higarashi, M., de Oliveira, P. & Comin, J. 2019. Ryegrass straw and wood shavings as bulking agents on swine slurry co-composting: a case study in Southern Brazil. *International Journal of Recycling of Organic Waste in Agriculture* **8**(S1), 55–63. doi: 10.1007/s40093-019-0269-3

Sánchez-García, M., Alburquerque, J., Sánchez-Monedero, M., Roig, A. & Cayuela, M. 2015. Biochar accelerates organic matter degradation and enhances N mineralisation during composting of poultry manure without a relevant impact on gas emissions. *Bioresource Technology* **192**, 272–279. doi: 10.1016/j.biortech.2015.05.003

Stotzky, G. & Rem, L. 1966. Influence of clay minerals on microorganisms: I. Montmorillonite and Kaolinite on Bacteria. *Canadian Journal of Microbiology* **12**(3), 547–563. doi: 10.1139/m66-078

Wichuk, K. & McCartney, D. 2013. Compost stability and maturity evaluation - a literature review. *Journal of Environmental Engineering and Science* **8**(5), 601–620. doi: 10.1680/jees.2013.0063

WTW Field Report, 2007. AT_4 Respiration. Biodegradability of the dry residue of the original substance. WTW, German. doi: AR_BOD_AT4_lab_01_E

Agronomy Research **18**(4), 2478–2488, 2020
https://doi.org/10.15159/AR.20.177

Comparative economic efficiency of using pharmacological agents for the stress prevention in the course of immunization of birds against reovirus tenosynovitis

A. Miftakhutdinov, N. Zhuravel and I. Dikhtyaruk*

South Ural State Agrarian University, 13 Gagarina Str., RU457100 Troitsk, Chelyabinsk Region, Russia
*Correspondence: nirugavm@mail.ru

Abstract. This article describes the results of studies on the definition and comparative evaluation of the effectiveness of using SPAO-FA (stress protector antioxidant - feed additive) and SPAO-complex pharmacological preparation (stress protector antioxidant - complex preparation for birds) for the prevention of vaccine stress during immunization of birds against reovirus tenosynovitis. These preparations were used during 5 days (3 days before vaccination, on the day of vaccination and one day after vaccination) at the dose of 185 mg kg^{-1} body weight: SPAO-FA was given as a part of compound feed, SPAO-complex - with water. Stress prevention in chickens of the parent flock provides equally high level of protection of birds from a field virus, a causative agent of reovirus tenosynovitis: it reduces the development of a protective level of antibodies by 7 days. Using SPAO-complex contributed to the increase in antibody titers by a factor of 2.6, and to the decrease in the coefficient of variation by the term of monitoring immunity stress by 25.7%. Using SPAO-FA increased antibody titers by 1.6 times, but had no significant effect on vaccination homogeneity. Vaccination index that should be high in the case of successful vaccination was 3.5 times higher for SPAO-complex in comparison with the basic diet; this for SPAO-FA was 1.6 times higher. Positive effect of anti-stress therapy influences the livability of chickens which was 3.5% higher with SPAO-complex, 0.79% higher - with SPAO-FA; bird live weight and the yield of day-old chicks were also higher in comparison with the basic diet by 6.44 and 0.88%, and 4.22 and 0.55%, respectively. Cost-effectiveness of using SPAO-FA per RUR of costs amounted to 180.09 RUR, for SPAO-complex, this parameter amounted to 435.86 RUR.

Key words: poultry farming, vaccination, reovirus tenosynovitis, antibody titers, coefficient of variation, vaccination index, cost-effectiveness, yield of chicks.

INTRODUCTION

Key concepts for the development of agro-industrial complex, including poultry farming today and for long term, are efficiency (Skripleva & Arseneva, 2015), quality (Zinina et al., 2018) and biosafety (Surai et al., 2017). High productivity and product quality parameters (Surai & Fisinin, 2016a) can only be obtained from healthy birds (Surai et al., 2016b). Growing chickens on an industrial basis is accompanied by a serious risk of infectious diseases of viral or bacterial origin (Zhuravel & Miftakhutdinov, 2016), vaccination is the basis for protecting poultry stock. When carrying out preventive vaccination, numerous factors should be taken into account that may reduce the effectiveness of vaccination, including immunosuppressive conditions which can be caused by stress (Djavadov & Dmitrieva, 2012).

Reaction to physiological stress starts when brain detects a homeostatic problem and activates sympathetic nervous system which secretes catecholamines, adrenaline and norepinephrine. This is followed by a slower activation of hypothalamic-pituitary-adrenal axis. A variety of regulatory systems and mechanisms cannot lead to an entirely predictable effect; moreover, functioning of hypothalamic-pituitary-adrenal axis demonstrates significant individual variability (Sorrells et al., 2009). In regard to this study, the primary focus in theoretical and especially in practical aspects of this process should be on the effect of glucocorticoid hormones and stress on immune system and on inflammatory response (Sapolsky, 2004). Chronic exposure to glucocorticoids suppresses both innate and adaptive immunity; prolonged exposure to glucocorticoid hormones was proved to decrease the number of circulating WBC (Reichardt et al., 2001) and to reduce the production of a large number of pro-inflammatory cytokines, including IL-1β – interleukin 1 beta and TNF-α – tumor necrosis factor-alpha (De Bosscher et al., 2003). Although vaccination of birds is essential (Anosov et al., 2015; Kuklenkova et al., 2018b; Javadov et al., 2019) it remains a stress factor in poultry industry (Fisinin & Kavtarashvili, 2015b; Surai & Fisinin, 2016b; Zhuravel et al., 2017). This leads to a decrease in the level and homogeneity of immune response (Ponomarenko, 2015). Currently, one tries to develop different methods and tools to enhance the immune response during vaccination, as demonstrated by increased titer of antibodies to avian viral pathogens (Ali et al., 2013; Xu et al., 2018, Eladl et al., 2019; Semenov et al., 2019; Walaa & Awadin, et al., 2020). There are specific studies that prove the positive effect of pharmacological anti-stress drugs during immunization of birds (Miftakhutdinov & Amineva, 2019). Stress prevention in the vaccination process is a new scientific field, which can ensure efficiency increase of poultry industry (Miftakhutdinov & Amineva, 2019). Aside of efficiency, the economic effect of measures carried out has a significant value for the poultry industry.

SPAO-complex (stress protector antioxidant - complex preparation for birds) and SPAO.

These preparations contain an active complex of micro elements, vitamins, vitamin-like and other substances that have an effect on metabolism (Miftakhutdinov et al., 2019; Zhuravelet al., 2019a; Zhuravel et al., 2019b).

In connection with the above matter, the aim of our research was to determine and comparatively evaluate the effectiveness of using SPAO-FA feed additive and SPAO-complex pharmacological preparation for the prevention of vaccine stress during immunization of birds against reovirus tenosynovitis.

MATERIALS AND METHODS

The studies were carried out in a poultry farm of industrial type. **The object** of this study was chicken parent flock; **the subject** - parameters of humoral response to the injected live vaccine against reovirus tenosynovitis, strain 1133, with underlying giving SPAO-FA (stress protector antioxidant - feed additive) and SPAO-complex (stress protector antioxidant - complex preparation for birds) to the birds.

Drugs are developed to be used for animals and are experimentally applied in the conditions of industrial-grade poultry farms to prevent preslaughter and transportation stresses. Preliminary tests have shown capabilities of the drugs studied to cause mediated impact on humoral immunity formation processes in vaccinations; it is proven that under the effect of SPAO-complex the protective antibodies level in terms of vaccinal prevention of rednose, infectious bronchitis, bursal disease, Newcastle disease are reliably higher than control values (Ponomarenko, 2015; Miftakhutdinov & Amineva, (2019).

Study scheme

Birds were vaccinated with a live vaccine for reovirus tenosynovitis from strain 1133 at the age of 7 and 28 days, followed by re-vaccination with an inactivated vaccine at the age of 9–11 weeks. Baseline livestock of 32,000 birds was divided into three groups. Birds of experimental group 1 received basic diet and were a control group. Birds of experimental group 2 received SPAO-FA feed additive as a part of their diet. Birds of experimental group 3 were given SPAO complex pharmacological preparation with water. Feed additive and pharmacological preparation were used for 5 days: 3 days before vaccination, day of vaccination and one day after vaccination at the dose of 185 mg kg^{-1} of body weight.

Study results evaluation

Vaccination results were interpreted by the level of specific antibodies formation and homogeneity in titers, as well as by vaccination index (Olson,1978). Humoral immunity was evaluated 7 and 14 days after the first vaccination and 14 and 21 days after the second one.

Blood serum was used as the material studied. Antibodies generation evaluation, analysis and statistical processing were performed using BioChek (the Netherlands) test systems and BioChek II software. Results recording was done using Tecan (Austria) spectrophotometer with 405 nm wave length (The Avian Reovirus Antibody test kit). Vaccination index was set by the ratio of antibodies average titre and variation coefficient.

Cost-effectiveness was evaluated according to the method developed for poultry farming (Zhuravel & Miftakhutdinov, 2015; Fisinin et al., 2018; Zhuravel & Miftakhutdinov, 2019), thus, defining the following parameters: cost-effectiveness per RUR of expenses (ratio of benefit to veterinary expenses), benefit from veterinary measures (the difference between benefit, including prevented damage and the additional cost of production, and veterinary expenses), prevented damage (based on livability of chickens in parent flock), the cost of products obtained further by increasing its amount or quality (day-old chicks and chicken meat), veterinary expenses (material and labor costs).

RESULTS AND DISCUSSION

The level of specific antibodies indicates the level of response to vaccination (Table 1).

So, 7 days after the first vaccination, that is, at the initial stage of immunity development, antibody titer was several times lower in comparison with both a protective level and expected, or baseline. At the same time, antibody titer in birds that received

SPAO-FA and SPAO-complex was 1.91 times higher. This may indicate increased priming.

Table 1. Average titer of antibodies and coefficient of variation for vaccination of chickens against reovirus tenosynovitis

Age of bird, days	Post vaccination period	Expected		Basic diet		SPAO-FA		SPAO complex	
		titer	CV	average titer	CV	average titer	CV	average titer	CV
14	7_1	2,000–5,000	40–80	331 ± 304.8	92	631 ± 375.7	60	621 ± 294.22	47
21	14_1	2,000–5,000	40–80	377 ± 305.7	81	716 ± 388.2	54	1,088 ± 420.2	39*
42	14_2	2,000–5,000	40–80	1,505 ± 707.8	47	2,453 ± 1,047.3	45*	4,554 ± 1,255.4	28*
49	21_2	2,000–5,000	40–80	1,749 ± 603.4*	35*	2,836 ± 986.2*	35*	4,603 ± 1,177.9*	26*

Note: * Level corresponding to 'protective' one.

14 days after immunization, values in the groups of SPAO-FA and SPAO-complex were also higher in comparison with antibody titer in the group with basic diet and also higher than the level of antibodies in an earlier period, at the initial stage of immunity development, i.e. 7 days after vaccination. In group 1, this difference was insignificant and amounted to 1.81%, in group 2 - 13.47%, in group 3 - 75.2%. This demonstrates a response to vaccination at the first stage of immunization. Positive effect of SPAO-FA and SPAO-complex on the decreasing level of immunosuppression is confirmed with the relatively high titer of antibodies on the 14^{th} day after vaccination in comparison with experimental group 1 - in 2.12 and 3.23 times.

After the second vaccination, antibody titer in blood serum of the studied chickens changed. So, 14 days after the second vaccination, the average titer in experimental group 1 increased by 4.47 times, after 21 days - by another 1.16% and reached 'protective' level, although it was lower than expected. Apparently, this was due to the immunosuppression that occurred as a result of activated stress-triggering mechanisms during vaccination (Ponomarenko, 2015).

Using feed additives and drugs aimed at stress prevention contributed to a more intensive development of antibodies.

So, with adding SPAO-FA 14 days after vaccination, antibody titer was 62.99% higher than this in the blood of chickens of group 1, and reached the expected level (slightly above the minimum) and became higher than the protective one. 21 days after vaccination (term for monitoring immunity level), it increased by 16.7% and became 62.15% higher in comparison with the same parameter in the control group.

It should be noted that the level of antibodies corresponding to the protective one was not reached after the first vaccination. Immunity level that protects birds against the infection caused by a field strain of the causative agent of reovirus tenosynovitis, should be considered with an antibody titer more than 1:800 (Kuklenkova et al., 2018a). Therefore, using SPAO-complex helps to achieve this value by 21 days after the first vaccination with a live vaccine. In addition, the level of antibodies reached during an experimental test of live vaccines containing virus strains (Radyush et al., 2013) to different extents corresponded to the parameters obtained in experimental groups 2 and 3 that demonstrated immune response.

Using SPAO-complex contributed to a more intensive immunity development. 14 days after the second vaccination, antibody titers were close to the maximum expected level and were higher than in blood serum of chickens of experimental groups 1 and 2 by 3.06 and 1.86 times, respectively. By the 21st day after the second vaccination, this value increased slightly and was also higher by 2.6 and 1.6 times, respectively. This shows that SPAO complex contributes to seroconversion and accelerates the production of antibodies.

The degree of titer homogeneity is proved by the coefficient of variation; we can judge about the quality of vaccination in the batch of birds by its level. So, vaccination being a technological stress reduces the activity of specific humoral immunity, as demonstrated by the value of the coefficient of variation. 7 days after the first vaccination, this value was maximal, in control group - above the expected level. Using SPAO-FA and SPAO-complex allowed achieving a higher level of homogeneity - coefficient of variation in groups 2 and 3 was lower than in group 1 by 65.22% and 48.91%, respectively, and was within the expected range.

14 days after the first vaccination, a decrease in the coefficient of variation in each group was noted.

The smallest value was in the group of SPAO-complex; it was lower in comparison with vaccination according to the scheme adopted at the farm by 2.08 times; coefficient of variation in the group of SPAO-FA was 1.5 times lower than in experimental group 1. Moreover, vaccination homogeneity was achieved only in group 3 (coefficient of variation was lower than 45%).

Therefore, SPAO-FA and SPAO-complex contribute to vaccination homogeneity to a greater extent. At the same time, the effect of SPAO-FA is less pronounced than that of SPAO-complex. Both drugs shorten the time to reach the level of coefficient of variation that indicates homogeneity (< 45) - to 14th day after the second vaccination. In addition, using SPAO-complex helps to reduce the coefficient by the term of monitoring immunity level, i.e. to 21st day after the second vaccination, by 25.7%. Using SPAO-KD in comparison with basic diet has no effect on the coefficient of variation by 21st day after the second vaccination.

A sign of successful vaccination is the ratio of analyzed parameters: average antibody titer and coefficient of variation, i.e. vaccination index (van Lirdam & Bosman, 2011).

Vaccination index is a logical parameter that demonstrates high values with a successful vaccination. Data in Table 2 allow concluding that immunity level gradually increases reaching its maximum to the checkpoint - 21 days after the second vaccination (Table 2).

Table 2. Reovirus tenosynovitis vaccination index

Post vaccination period	Vaccination	Vaccine + SPAO-FA	Vaccine + SPAO complex
7_1	3.60	10.52	13.21
14_1	4.16	13.26	27.90
14_2	32.02	54.51	162.64
21_2	49.97	81.03	177.04

At the same time, better seroconversion was noted in the group of SPAO-complex; vaccination index in the blood of chickens of experimental group 3 is 3.5 times higher than in experimental group 1 and 2.18 times higher than in experimental group 2.

Study results - titer level and homogeneity - confirmed by vaccination index allow concluding that the development of antibodies occurred as a result of the action of vaccine; no information for the development of infectious process was found.

With strict compliance with the requirements for immunization and adequate immune status of birds, coefficient of variation will be low within normal limits. A high value of the coefficient of variation is due to both a low antibody titer, for example, if treatment plan was not followed, and high antibody titer that may be associated with the circulation of a field virus (Miftakhutdinov & Amineva, 2019).

Considering specific features of the technological process in poultry farming, a contradiction should be noted. On the one hand, vaccination is aimed at creating the immunity of poultry flocks to infectious diseases including reovirus tenosynovitis and on the other hand, it, as a stress factor, triggers the inhibition of antibody production what leads to decreased activity of specific humoral immunity. Negative association between stress and antibody response that confirms these studies is described in the number of works (Burns et al., 2003; Segerstrom & Miller, 2004; Auerbach et al., 2014). Effect of antistress drugs on achieving a high immune response during vaccination was also proven (Ponomarenko, 2015; Miftakhutdinov & Amineva, 2019).

Production parameters allow concluding about positive effects of the pharmacological complex and the feed additive that were used for anti-stress treatment.

So, by the time of reaching 140 days of age, that is, during the period when birds undergo intensive immunization, also against reovirus theosinovitis, the livability of birds in experimental group 1 was 97.2%, in experimental group 2–97.6%, in experimental group 3–97.8%. In the period of egg production (from 140 days of age to slaughtering at the age of 61 weeks) characterized with a relatively lower immunological load, the livability of laying hens also differed and amounted to 90.9, 91.2 and 93.5%, respectively. In general, over the period of growing and egg production, the livability of laying hens was higher with using the feed additive and the pharmacological complex. So, livability in experimental group 2 was 89.1% what is higher than in experimental group 1 by 0.79%. In experimental group 3, livability amounted to 91.5% what is higher than in experimental group 1 by 3.5% (Table 3).

In the group that received SPAO-complex, production of hatching eggs per hen increased by 3.24%, the number of day-old chicks - by 4.22%. In the group of SPAO-FA, the increase in production parameters was less significant: production of hatching eggs was higher by 0.22%, of day-old chicks - by 0.55%

Therefore, using feed additive and pharmacological preparation as an anti-stress treatment helps to reduce mortality and to increase the livability of livestock, as well as to increase final production parameters - hatching eggs, and, consequently, the number of day-old chicks.

In second-order breeding units, birds after using are slaughtered; the meat is used for preparing ground meat, or carcasses are sold, therefore, the weight of birds before slaughtering and meat yield are important parameters. Using feed additive and preparation had no effect on meat yield but at the same time, the live weight of chickens that received SPAO-FA was higher than the live weight of chickens received basic diet by 23 g, or 0.88%; and the live weight of chickens received SPAO-complex - by 167 g, or 6.44%. It was proved that live weight of birds immunized against reovirus tenosynovitis was significantly lower than that of non-immunized ones (Lazovskaya & Prudnikov, 2015). Vaccination being a technological stress reduces the gain in live weight while using feed additive and pharmacological complex reduces the negative impact of stress factor and contributes to an increase in production parameters. In this case, the feed additive has less effect than the pharmacological complex.

Table 3. Production parameters of chickens with using SPAO-complex and SPAO-FA

Parameter	Basic diet	SPAO-FA	SPAO complex
Baseline number of housed chickens, birds	32,000	32,000	32,000
Number of laying hens (140 days), birds	31,110	31,250	31,310
Number of laying hens at the end of technological cycle, birds	28,279	28,500	29,275
Gross egg production, thousand pcs.	5,913	5,959	6,119
including hatching eggs, thousand pcs.	5,644	5,697	5,879
Yield of hatching egg,%	95.5	95.6	96.1
Eggs obtained from laying hen, total, pcs.	190.2	190.7	195.4
including hatching eggs, pcs.	181.9	182.3	187.8
Chickens obtained from laying hen, birds	144.3	145.1	150.4
Hatching rate, %	79.3	79.6	80.1
Livability of laying hens during egg production, %	90.9	91.2	93.5
Livability of laying hens during technological cycle, %	88.4	89.1	91.5
Weight of a bird at the end of the technological cycle, g	2,590	2,613	2,757
Meat yield, %	75.1	75.1	75.2
Feed consumption for the production of hatching eggs, kg/10 pcs.	2.68	2.67	2.62

Using SPAO-FA feed additive and SPAO-complex pharmacological preparation for chickens of the parent flock in the course of their vaccination against reovirus infection reduces the negative effect of vaccination as a stress factor and stimulates immune response.

During this experiment, 10.09 kg of SPAO-FA and 10.09 kg of SPAO-complex were consumed. Considering the cost of preparations, material expenses for SPAO-FA (experimental group 2) amounted to 18,168.48 RUR, for SPAO-complex (experimental group 3) - 37,346.32 RUR. SPAO-complex was given with water, with the help of a medicator; time spent on preparing the drug for use (weighing, putting in a drinking system) was about 10 minutes per day, i.e. 100 minutes, or 1.67 hours for the whole study period. SPAO-FA was given with mixed feed; time spent was slightly less and amounted to 90 minutes, or 1.5 hours for the whole study period. Average salary of a veterinarian at the poultry farm was 50,000 RUR per month; taking into account its size per year (600,000 RUR) and annual working hours (1761.4 hours), salary per hour amounted to 340.64 RUR. Therefore, the cost of labor when using SPAO-complex amounted to 568.87 RUR, SPAO-FA - 510.96 RUR, the charges were 154.31 and 171.80 RUR, respectively. Thus, veterinary expenses for experimental group 2 amounted to 18,833.75 RUR, for experimental group 3 - 38,086.99 RUR.

Prevented damage amounted to 163,540 RUR for experimental group 2, and 737,040 RUR for experimental group 3. The cost of additionally obtained chicks in experimental group 2 was 3,164,140 RUR, in experimental group 3 - 15,389,570 RUR.

Taking into account the livestock by the end of hatching egg production cycle for one batch, the average weight of birds before slaughter, as well as meat yield, 55,005.2 kg of meat were obtained in experimental group 1, 55,927.3 kg - in experimental group 2, and 60,694.8 kg - in experimental group 3. Therefore, the cost of additionally obtained poultry meat amounted to 82,989 RUR in experimental group 2, and 512,064 RUR in experimental group 3.

In general, the additional value in experimental group 2 was 3,247,129.0 RUR, in experimental group 3 - 15,901,634.0 RUR.

Benefit in experimental groups 2 and 3 amounted to 3,391,835.25 RUR and 16,600,587.01 RUR. Cost-effectiveness per RUR of costs was 180.09 RUR and 435.86 RUR, respectively. Therefore, the effectiveness of SPAO-complex is 2.4 times higher in comparison with SPAO-FA.

As a result of the positive influence of SPAO-FA and SPAO-complex on bird organism during exposure to technological stresses, a high economic benefit was achieved due to the livability of the livestock and increased productivity. Therefore, the pronounced immunotropic effect of SPAO-complex and the less pronounced immunotropic effect of SPAO-FA during the development of stress is confirmed by the high level of production parameters and, as a result, level of cost-effectiveness of introducing anti-stress treatment into the hatching egg production cycle.

To prevent post-vaccination stress in order to ensure a homogeneous and high level of bird protection from the causative agent of reovirus tenosynovitis and to increase production parameters, we recommend using SPAO-complex (stress protector antioxidant - complex preparation for birds) and SPAO-FA (stress protector antioxidant - feed additive) for 5 days: 3 days before vaccination, on the day of vaccination and one day after vaccination at the dose of 185 mg kg^{-1} of body weight.

CONCLUSION

1. Stress prophylaxis in chickens of parent flock through the use of SPAO-FA and SPAO-complex during vaccination against reovirus infection provides a homogeneous and high level of bird protection against field virus: it reduces the time required for development of protective antibody level, contributes to more intensive achievement of vaccination homogeneity, as demonstrated by an increase in production parameters. A more significant effect was achieved when using SPAO-complex.

2. During using SPAO-FA and SPAO-complex, antibody titers reached the expected level and were higher than the protective level by the 14^{th} day after the second vaccination, in the birds that received basic diet - by the 21^{st} day after the second vaccination. By the 21^{st} day after the second vaccination, antibody titers in animal that were given SPAO-FA were 1.6 times higher than in animal that received basic diet; and in group of SPAO-complex - 2.6 times higher.

3. SPAO-FA and SPAO-complex used during vaccination shorten the time of reaching the level of coefficient of variation that indicates homogeneity (< 45) by the 14^{th} day after the second vaccination. Using SPAO-complex helps to reduce coefficient of variation by the time of monitoring immunity level, i.e. by 21^{st} day after the second vaccination, by 25.7%. Using SPAO-FA in comparison with basic diet had no effect on the coefficient of variation by this time.

4. Vaccination index that should be of high values during successful vaccination was 3.5 times higher when using SPAO-complex in comparison with basic diet; that of SPAO-FA was 1.6 times higher.

5. When using SPAO-complex, livability of chickens was higher by 3.5%, live weight of poultry - by 6.44%, number of day-old chicks - by 4.22%; these parameters with using SPAO-FA were higher by 0.79%, 0.88% and 0.55%, respectively.

6. Cost-effectiveness of using SPAO-FA per 1 RUR of expenses amounted to 180.09 RUR, for SPAO-complex it amounted to 435.86 RUR.

REFERENCES

Ali, A., Ibrahim, M., Eladl, A.E., Saif, Y.M. & Lee, C.W. 2013. Enhanced replication of swine influenza viruses in dexamethasone treated juvenile and layer turkeys. *Vet. Microbiol.* **162**, 353–359.

Auerbach, M.I., Glunder, G., Beyerbach, M. & Weber, M. 2014. Varying antibody responses of laying hens housed in an aviary system and in furnished cages. *Berliner Und Munchener Tierarztliche Wochenschrift* **127**, 267–273.

Burns, V.E., Carroll, D., Ring, Ch.J & Drayson, M.T. 2003. Antibody response to vaccination and psychosocial stress in humans: relationships and mechanisms. *Burns* **21**(Issue 19–20), 2523–2534.

De Bosscher, K., Berghe, W.V. & Haegemanuy, G. 2003. The interplay between the glucocorticoid receptor and nuclear factor-kappaB or activator protein-1: molecular mechanisms for gene repression. *Endocr. Rev*. **24**, 488–522.

Djavadov, E.D. & Dmitrieva, M.E. 2012. Effective Vaccinal Prevention as Epizootic Pledge of Wellbeing Industrial Enterprise of Poultry Farming. *Russian Veterinary Journal. Farm animals*(**3**), 6–7 (in Russian).

Eladl, A.H., Arafat, N., El-Shafei, R.A., Farag, V.M., Saleh, R.M. & Awadin,, W.F. 2019. Comparative immune response and pathogenicity of the H9N2 avian influenza virus after administration of Immulant®, based on Echinacea and Nigella sativa, in stressed chickens. Comp. *Immunol. Microbiol. Infect. Dis*. **65**, 65–175.

Fisinin, V.I. & Kavtarashvili, A.Sh. 2015. Heat stress in poultry. I. Danger, related physiological changes and symptoms. *Agricultural Biology* **50**(2), 162–171 (in Russian).

Fisinin, V.I. & Kavtarashvili, A.Sh. 2015. Heat stress in poultry. II. *Methods and techniques for prevention and alleviation Agricultural Biology* **50**(4), 431–433 (in Russian).

Fisinin, V.I., Zhuravel, N.A. & Miftakhutdinov, A.V. 2018. Methodology for determining the effectiveness of introducing new veterinary methods and tools in poultry farming. *Veterinary medicine* **6**, 14–20 (in Russian).

Javadov, E., Khokhlachev, O., Kozyrenko, O., Vikhreva, I. & Polyakova, O. 2019. Antigenic activity of an experimental inactivated vaccine against chicken infectious bronchitis. *International Transaction Journal of Engineering, Management and Applied Sciences and Technologies* **10**(11), 10A15J.

Kuklenkova, I.V., Samodelkin, A.G., Pashkin, A.V.C., Avilov, V.M., Sochnev, V.V., Kozyrenko, O.V. & Usenkov, A.V. 2018a. Immunogenic activity of the viral polyvalent inactivated vaccine against the Newcastle disease, infectious bronchitis, egg drop syndrome, reoviral and metapneumoviral infection in poultry. *International Journal of Pharmaceutical Research* **10**(4), 675–679.

Kuklenkova, I.V., Zhavoronkova, T.S., Pashkin, A.V., Sochnev, V.V., Avilov, V.M., Grigorieva, G.I., Pashkina, Yu.V., Kozyrenko, O.V., Usenkov, A.V., Filippov, N.V. & Gusev, A.A. 2018b. Development (optimization) of the scheme of immunization of birds of parent flocks against viral diseases. *Issues of Legal Regulation in Veterinary Medicine* **4**, 51–55 (in Russian).

Lazovskaya, N.O. & Prudnikov, V.S. 2015. Morphology of the bone marrow of chickens vaccinated against reovirus tenosinovitis. Transactions of the educational institution awarded the Badge of Honor Order ‘Vitebsk State Academy of Veterinary Medicine’, **51**(2), 52–54 (in Russian).

Lirdam, B. van & Bosman, G. 2011. Vaccination index: a new parameter for evaluating vaccination results using ELISA [electronic resource]. BIO 6 (129), June 2011. – Access mode: *http://www.vetmagazines.ru/* (in Russian).

Miftakhutdinov, A.V. & Amineva, E.M. 2019. Development and testing of anti-stress pharmacological agents aimed at increasing the immunological effectiveness of chickens’ vaccination. *Agro-Industrial Complex of Russia* **26**(5), 857–863 (in Russian).

Miftakhutdinov, A.V., Saifulmulyukov, E.R., Nogovitsina, E.A. & Miftakhutdinova, E.A. 2019. Meat productivity of chicken broilers when using stress protectors during the pre-slaughter period. *IOP Conference Series: Earth and Environmental Science. Proceedings of the conference AgroCON-2019*, 012050.

Olson, N.O. Reovirus Infection. 1978. *Diseases of Poultry*. 7th edition (edited by M.S. Hofstad, et al.) ames, Iowa, Iowa State University Press, 641 pp.

Ponomarenko, V.V. 2015. Effect of lithium-containing pharmacological agents on seroconversion rates during chicken vaccination. Development of scientific, creative and innovative activity of youth: materials of the VII All-Russian scientific and practical correspondence conference of young scientists. *Kurgan: Publishing House of the Kurgan State Agricultural Academy* **99**, 185–187 (in Russian).

Radyush, I.S., Gusev, A.A., Gulyako, A.A. & Nasonov, I.V. 2013. Immunogenicity of live vaccines against avian reovirus infection produced using spf-embryos, chicken embryo fibroblasts and vero cell culture. *Proceedings of the Federal Center for Animal Health* **11**(1), 124–134 (in Russian).

Reichardt, H.M., Tuckermann, J.P., Gottlicher, M., Vujic, M., Weih, F., Angel, P., Herrlich, P. & Schutz, G. 2001. Repression of inflammatory responses in the absence of DNA binding by the glucocorticoid receptor. *EMBOJ* **20**(24), 7168–7173.

Sapolsky, R. 2004. Stress and cognition. In the Cognitive Neurosciences. Cambridge, Massachusetts: MIT Press, 1031–1042.

Segerstrom, S.C. & Miller, G.E. 2004. Psychological Stress and the Human Immune System: A Meta-Analytic Study of 30 Years of Inquiry. *Psychological Bulletin* **130**(4), 601–630.

Semenov, V.G., Baimukanov, A., Ivanov, N.G., Tadzhiyeva, A.K., Karynbayev, A.K. & Karibayeva, D.K. 2019. Bird biopotential against the correction of non-specific resistance and specific immunogenesis. *Bulletin of the National Academy of Sciences of the Republic of Kazakhstan* **6**, 111–119.

Skripleva, E. & Arseneva, T. 2015. Optimization of the recipe of yoghurt with additives and control of some quality parameters of new yoghurt recipe. *Agronomy Research* **13**(4), 1086–1095.

Sorrells, S.F., Caso, J.R., Munhoz, C.D. & Sapolsky, R.M. 2009. The stressed CNS: when glucocorticoids aggravate inflammation. *Neuron* **64**(1), 33–39.

Surai, P.F. & Fisinin, V.I. (2016a). Vitagenes in poultry production: Part 1. Technological and environmental stresses. *Worlds Poultry Science Journal* **72**(4), 721–733.

Surai, P.F. & Fisinin, V.I. (2016b). Vitagenes in poultry production: Part 2. Nutritional and internal stresses. *Worlds Poultry Science Journal* **72**(4), 761–772.

Surai, P.F., Kochish, I.I. & Fisinin, V.I. 2017. Antioxidant systems in poultry biology: Nutritional modulation of vitagenes. *European Poultry Science* **81**. doi: 10.1399/eps.2017.214

The Avian Reovirus Antibody test kit // BioChek: Smart Veterinary Diagnostics. – URL: https://www.biochek.com/poultry-elisa/avian-reovirus-antibody-test-kit/

Walaa, F. Awadin, Eladl Abdelfattah, H., El-Shafei Reham, A., El-Adl Mohamed, A., Aziza Abeer, E., Hanaa, S. Ali, Mohamed, A. Saif. 2020. Effect of omega-3 rich diet on the response of Japanese quails (Coturnix coturnix japonica) infected with Newcastle disease virus or avian influenza virus H9N2. *Comparative Biochemistry and Physiology*, Part **C** **228**, 108668.

Xu, Y.Q., Guo, Y.W., Shi, B.L., Yan, S.M. & Guo, X.Y. 2018. Dietary arginine supplementation enhances the growth performance and immune status of broiler chickens. *Livestock Science* **209**, 8–13.

Zhuravel, N.A. & Miftakhutdinov, A.V. 2015. Features of Calculation of Cost-effectiveness of Stress Prevention in the Parent Flock of Chickens. *Achievements of Science and Technology of AIC* **29**(11), 25–27 (in Russian).

Zhuravel, N.A. & Miftakhutdinov, A.V. 2016. Evaluation of Veterinary and Sanitary Control Efficacy in the Production of Poultry Products. *Achievements of Science and Technology of AIC* **30**(5), 25–29 (in Russian).

Zhuravel, N.A. & Miftakhutdinov, A.V. 2019. Digitalization of the Method for Economic Evaluation of the Implementation of Innovative Veterinary Methods and Means into Poultry Farming. *Achievements of Science and Technology of AIC* **33**(11), 91–94 (in Russian).

Zhuravel, N.A., Anosov, D.E. & Miftakhutdinov, A.V. 2017. Economical Efficiency of Pharmacological Stress Prevention during Growing of Rearing Birds and Keeping of Parent-Stock Meat-Type Chickens. *Achievements of Science and Technology of AIC* **31**(1), 44–48 (in Russian).

Zhuravel, N.A., Miftakhutdinov, A.V. & Suchanova, S.F. 2019a. Economic assessment of stress prevention in broiler chickens in the pre-slaughter period. *IOP Conference Series: Earth and Environmental Science. Proceedings of the conference AgroCON-2019*, 012056.

Zhuravel, N.A., Miftakhutdinov, A.V. & Zhuravel, V.V. 2019b. Economic analysis of factors causing the effective implementation of innovative methods and means in industrial poultry. *Ecological Agriculture and Sustainable Development Editors*: Prof. Dr. Viktor G. Litovchenko, Rector of South Ural State Agrarian University; Prof. Dr. Mirjana Radovic Markovic, South Ural State University, pp. 117–124.

Zinina, O., Merenkova, S., Soloveva, A., Savostina, T., Sayfulmulyukov, E., Lykasova, I. & Mizhevikina, A. 2018. Effect of starter cultures on the qualitative parameters of dry fermented sausages made from poultry meat. *Agronomy Research* **16**(5), 2265–2281. https://doi.org/10.15159/AR.18.199

Agronomy Research **18**(4), 2489–2500, 2020
https://doi.org/10.15159/AR.20.217

Morphological variability of phenotypic traits in of *oregano* samples

E.F. Myagkikh[1,*], S.S. Babanina[1], V.S. Pashtetsky[1] and M.Yu. Karpukhin[2]

[1]Research Institute of Agriculture of Crimea, Kievskaya Str., 150, RU295453 Simferopol, Republic of Crimea, Russia
[2]Ural State Agrarian University, Karla Libknekhta Str., 42, RU620075 Yekaterinburg, Russia
[*]Correspondence: myagkih_e@niishk.ru

Abstract. The purpose of the research was to study the morphological variability of collection samples of *oregano* of the Crimean Peninsula. The experiments were carried out in 2016–2018 in the Foothill Zone of Crimea. The plant material consisted of 41 samples of *origanum* collected on the Crimean Peninsula territory. The degree of identification reliability of *oregano* collection samples by morphological traits was checked. The construction of relationship dendrograms was carried out by the Ward's method based on the Manhattan distances. It was found that qualitative traits (coloration of corolla, leaf, bract, stalk and male fertility) showed themselves more consistently than quantitative ones. It was recommended to use the most polymorphic traits (entropy, $H > 1.50$ bits) for reliable identification of *oregano* samples from the Crimean peninsula: coloration of bract, stem, leaf and corolla, as well as the number of shoots and mass fraction of essential oil. The structure of the association differed by the years of study when constructing dendrograms ($r = 0.58$).Nevertheless, a fairly clear correspondence of the clusters of different years' clusters to each other was established (78% of the samples). The established correspondence indicates the reliability of the genotypes combination into separate groups (clusters) and their similar reaction to environmental conditions. The most interesting combinations of samples for further breeding work were identified - these are clusters 2 and 5 (according to the 2018 data). In 42.7% of genotypes from the second cluster, the mass fraction of essential oil was at the level of 0.25–0.55% of the absolute dry mass (4–6 points). The samples from the second cluster could be used as high-oil sources, whereas samples from fifth cluster - as sources of high productivity of 'green' raw materials (up to 1,200 g plant^{-1}). It is advisable to select parental forms from these two clusters for hybridization. The grouping of *origanum* samples used in the work divides the samples quite accurately separated them not only on qualitative, but also on economically valuable traits.

Key words: breeding, Crimea, morphological trait, *oregano*, polymorphy.

INTRODUCTION

The formation and comprehensive study of collection funds are the main tasks in the conservation of plant genetic resources (Pagnotta et al., 2013).

Origanum (*Origanum vulgare* L.) is a valuable essential oil, spice, green and medicinal plant (Ibrahim et al., 2012; Sivicka et al., 2019). The distribution area in

Europe is from south to north from the Mediterranean to Norway, in the Southwest Asia– reaches the Himalayas (Bussmann et al., 2020). *Origanum* grows throughout the Russian Federation, with the exception of the Arctic regions (Bokov et al., 2013; Pashetsky et al., 2018). The preparations derived from the plant raw materials *O. vulgare* are actively used in many fields of medicine (Vale-Silva et al., 2012; Myagkikh, 2015; Masoudi & Saiedi, 2017; Sivicka et al., 2019).

Crimea is an important breeding center of essential oil and medicinal crops in Russia (Khlipenko & Rabotyagov, 2005; Pashetsky et al., 2018).

Polymorphism of herbaceous plants is manifests itself in the variability of such morphological traits as the coloration of plant organs, morphometric parameters of both individual parts and the plant as a whole, etc. It is possible to observe a significant variation of morphological traits due to the presence of many morphotypes within the species (Andi et al., 2011; Ibrahim et al., 2012).

At the All-Russian Scientific Research Institute of Medicinal and Aromatic Plants has developed a technology for reproduction of oreganum by rhizomes (Korotkikh & Khaziyeva, 2016). The breeding is carried out by the method of green cuttings in the Scientific Research Institute of Agriculture of Crimea (Myagkikh, 2015), and valuable collection material is obtained by clonal micropropagation methods (Yakimova & Yegorova, 2015; Yegorova & Yakimova, 2019).

The International Union for the Protection of New Varieties of Plants (UPOV) has developed tests to assess the differences, homogeneity and stability (DHS) of many plant species (Pagnotta et al., 2013). However, on the website of this organization it is noted that there is no guide for UPOV testing guide for the plant species of interest (*Origanum* L. (ORIGA). Dus Guidance and Cooperation). A technique has been developed for testing for DHS test when introducing new varieties of *origanum* are added to the the State Register in Russia (*Origanum* L. (ORIGA). Dus Guidance and Cooperation) has been developed. This technique includes qualitative (discrete) and quantitative (morphometric) plant traits. All of them are subject to genotype-environmental interactions, however the degree of environmental influence varies on them (Tétard-Jones et al., 2011).

The success of breeding work depends on the polymorphism of the source material and its quantity. But at the same time, this material requires a certain classification. The multi-approach, which includes estimation the assessment of not only of individual economically valuable traits, but also of all indicators available for visual morphometricassessment, allows the researcher to group the original collection material bymorphotypes.

The purpose of this work is to study the morphological variability of collection samples of *origanum* fromthe Crimean Peninsula in order to identify their phylogenetic relationships.

The objectives of the study included:

– assessment of morphological traits according to the marking scales developed by researchers;

– verification of the identification reliability degree of *origanum* collection samples by morphological traits;

– construction of relationship dendrograms;

– construction verification.

MATERIALS AND METHODS OF THE RESEARCH

The research was carried out in 2016–2018 in the Foothill zone of the Crimea (Krymskaya Roza settlement, Belogorsky District), coordinates: 45.053442, 34.361665.

The soil in the research site was southern carbonate heavy loam chernozem with the following agrochemical characteristics: pH - 7.0–7.2, humus content in the arable layer - 2.7–3.0%, total nitrogen - 0.12%, phosphorus - 0.10%, potassium - 1.0%).

The experiments were performed in the field. Planting was carried out in 2016, a comprehensive study was carried out in 2017–2018. The area of the plot was 3 m^2 (in total there were 15 plants on the plot, accounting - 10 plants), the repetition is double; placement-randomized blocks.

The meteorological conditions of the years of the study were favorable for the development of *origanum* plants.

In 2017, significant deviations from the average annual temperature indicators were noted in March and August (the average air temperature exceeded the average annual temperature by 4.0 and 2.1 °C respectively). The spring-summer period was characterized byabundant precipitation - only in March precipitation was less than the average annual norm by 11%, while in April, May and July they were extremely higher - 215, 212 and 117% of the norm respectively. The 2018 vegetation season was characterized by increased average monthly temperatures, which differed from the average long-term indicators by 0.5–3.8 °C. Rainfall since January has been well significantly below normal. In April, when intensive growth and development of the *origanum* plants began, only 4.2 mm of precipitation fell, which is 12.4% of the average multi-year value. The amount of precipitation in May and June was 98.8 and 39.3% of the norm. Only in July there was excessive moisture (169.8% of rain precipitation). The weather conditions caused faster passage of the growing phases and consequently lower *origanum* productivity rates.

The material for the study was 41 samples of *origanum* collected in different years on the territory of the Crimean Peninsula.

The area of the plot was 3 m^2, the repetition is double; placement–randomized blocks 13 traits were assessed in actual terms and converted into a point score proposed by the authors, which were divided into two groups - quantitative and qualitative in the course of the study. The color of the corolla, leaf, bract, stalk and male fertility were attributed to qualitative traits. Quantitative traits were as follows: height and diameter of the plant, the length and width of the leaf, the number of shoots, the mass of the bush, the mass fraction of essential oil (EOMF) from the absolute dry mass (adm) and the collection of oil per unit of area, which practically also covered the yield. Each trait was taken as a polymorphic system and its level of manifestation - as an alternate state of the traits. The scales of traits manifestation were developed by the authors independently, adapting the methodology on the DHS for the material, uniformly covering the entire studied sample studied (*Origanum vulgare* L., 2020) (Table 1).

To determine the informativity of individual phenotypic traits in the definition of polymorphism, entropy H (Dud´ık et al., 2007; Straszak & Vishnoi, 2020) is calculated:

$$\mathrm{H} = -\sum_{i=1}^{k}(\mathrm{p_i} \times \log_2 \mathrm{p_i}), \qquad (1)$$

where $\mathrm{p_i}$ is the probability (or frequency) of the system taking the i-th position among k possible. We calculated p as ratio number of all the samples to number of samples with a specific assessment, using table (Fig. 1). Each trait was taken as a polymorphic system and its level of manifestation - as an alternate state of the traits. For example, in total, according to the UPOV classifier, 4 possible options for the color of the corolla are noted. In our collection, sample 1 has 4 points. That is, when composing a binary matrix, the corolla color is considered as a polymorphic system, and sample 1 receives 0 points for coloring at 1, 2 and 3 points, and 1 point for coloring at 4 points.

Table1. Scales of *origanum* phenotypic traits manifestation

Trait	Marking											
	1		2		3		4		5		6	
	min	max	min	max	min	max	min	max	min	max	min	max
Corolla color	light pink		light lilac		lilac		white		-		-	
Leaf color	glaucous-green		yellow-green		dark green		green		-		-	
Bract color	weak pigmentation		medium pigmentation		strong pigmentation		no pigmentation		-		-	
Stalk color	weak pigmentation		medium pigmentation		strong pigmentation		no pigmentation		-		-	
Male sterility	fertile androecium		sterile androecium		semi-fertile androecium		reduced androecium		-		-	
Plant height, cm	0	45	46	65	66	85	85	105	-		-	
Plant diameter, cm	0	45	46	65	66	85	86	105	106	125	-	
Leaf length, mm	15.0	25.0	25.1	35.0	35.1	45.0	-		-		-	
Leaf width, mm	10.0	15.0	15.1	20.0	20.1	25.0	25.1	30.0	-		-	
Number of shoots, pcs.	0	50	51	100	101	150	151	200	251	300		
Mass of bush, g	0	300	301	600	601	900	901	1,200	-		-	
Essential oil mass fraction, % adm.	traces		0.050	0.149	0.150	0.249	0.250	0.349	0.350	0.449	0.450	0.549
Yield of oil, g m^{-2}	0.0	2.0	2.1	4.0	4.1	6.0	6.1	8.0	-		-	

1 Sample	2 Corolla color 1	3 Corolla color 2	4 Corolla color 3	5 Corolla color 4	6 Leaf color 1	7 Leaf color 2	8 Leaf color 3	9 Leaf color 4	10 Bract color 1	11 Bract color 2	12 Bract color 3	13 Bract color 4
1	0	0	0	1	0	0	1	0	0	0	0	1
2	0	0	1	0	0	0	0	1	1	0	0	0
5	0	0	1	0	1	0	0	0	1	0	0	0
7	1	0	0	0	1	0	0	0	0	0	0	1
8	0	0	0	1	1	0	0	0	1	0	0	0
9	0	1	0	0	0	1	0	0	1	0	0	0
10	0	0	1	0	0	0	0	1	0	0	0	1
11	0	0	1	0	0	0	0	1	0	0	0	1
16	0	0	1	0	0	0	0	1	0	0	0	1
17	0	1	0	0	0	0	0	1	1	0	0	0
20	1	0	0	0	1	0	0	0	0	0	0	1
22	0	0	1	0	0	0	1	0	0	0	1	0
24	0	1	0	0	0	0	0	1	0	1	0	0
25	1	0	0	0	0	0	0	1	1	0	0	0
30	0	0	0	1	1	0	0	0	1	0	0	0
31	0	0	0	1	1	0	0	0	0	1	0	0
32	0	1	0	0	0	0	0	1	1	0	0	0
33	0	0	0	1	1	0	0	0	1	0	0	0
34	0	0	0	1	1	0	0	0	1	0	0	0
35	0	0	0	1	1	0	0	0	0	1	0	0
38	1	0	0	0	0	0	0	1	1	0	0	0
39	1	0	0	0	0	0	0	1	1	0	0	0
42	0	0	0	1	0	1	0	0	1	0	0	0
64	0	1	0	0	0	0	0	1	0	1	0	0
65	0	0	0	1	1	0	0	0	0	1	0	0
70	0	0	0	1	1	0	0	0	1	0	0	0

Figure 1. The example of a binary matrix of morpho-biological traits of collection samples of *oregano*.

The degree of polymorphism of traits was assessed by comparing the calculated H with the maximum possible entropy H_{max} (Straszak & Vishnoi, 2020; Dud´ık et al., 2007).

$$H_{max} = \log_2 k \qquad (2)$$

The limits of variation of the calculated entropy are $0 \leq H \leq H_{max}$.

Entropy as a measure of the diversity and organization of the system, first of all, characterizes the degree of its uncertainty or determinism.

Clustering was carried out by the Ward's method based on Manhattan distances in the statistical analysis package Statistics 10. The correlation of the two matrices (matrices of distances (relations) between collection samples of *oregano* in two year investigation) were determined using the Mantel test in the Excel add-in system - XLSTAT.

RESULTS AND DISCUSSION

The manifestation of qualitative traits was stable over sthe years (Table 2) with a relatively even distribution of *oregano* samples in groups (marking scale for example '1' or '2' point), as evidenced by the calculated value of entropy. In almost all qualitative traits it was quite tightly close to the maximum possible entropy (2.00 bits) (Table 3, 4).

There is a clear affiliation of most of the samples to some single modal class in terms of quantitative traits. For example, 65.9% of the samples in 2017 and 63.4% in 2018 were characterized by a mark of 3 points.

An interesting pattern can be traced by the number of shoots: if in the first year of life mostly all the samples (85.4%) had the number of shoots marked at 1 and 2 points, then in the second year of life 56.2% of genotypes had a score on this trait from 3 to 5 points. The same trend in the mass of the bush - in 2017 modal class was 2 points, in 2018 - 3 points, with 29.3% of the samples were characterized by the mass of the bush at the level of 4 points. This is explained by the active growth and development of origanum plants with age and the fact that the conditions for full growth are optimal enough to accumulate vegetative mass and realize its productivity potential.

Table 2. The result of two way ANOVA of *oregano* qualitative traits

Source of variation	SS	df	MS
Corolla color			
Sample	104.7805	40	2.6195
Year	0.0000	1	0.0000
Sample*Year	0.0000	40	0.0000
Error		0	
Leaf color			
Sample	136.3902	40	3.4098
Year	0.0000	1	0.0000
Sample*Year	0.0000	40	0.0000
Error		0	
Bract color			
Sample	106.2439	40	2.6561
Year	0.0000	1	0.0000
Sample*Year	0.0000	40	0.0000
Error		0	
Stalk color			
Sample	61.7561	40	1.5439
Year	0.0000	1	0.0000
Sample*Year	0.0000	40	0.0000
Error		0	
Male sterility			
Sample	17.60976	40	0.44024
Year	0.01220	1	0.01220
Sample*Year	0.48780	40	0.01220
Error		0	

Table 3. Distribution of origanum samples by levels of qualitative traits manifestation, *n* = 41, 2017 (first year of life)

Trait	Distribution of samples by trait manifestation level, %						H, bit	H_{max}, bit
	1	2	3	4	5	6		
Qualitative traits								
Corolla color	17.1	19.5	22.0	41.5	-	-	1.90	2.00
Leaf color	34.1	14.6	14.6	36.6	-	-	1.87	2.00
Bract color	56.1	19.5	7.3	17.1	-	-	1.64	2.00
Stalk color	12.2	22.0	51.2	14.6	-	-	1.75	2.00
Male fertility	56.1	31.7	9.8	2.4	-	-	1.45	2.00
Quantitative traits								
Plant height, cm	2.4	26.8	65.9	4.9	-	-	1.25	2.00
Plant diameter, cm	2.4	24.4	31.7	36.6	4.9	-	1.90	2.32
Leaf length, mm	14.6	75.6	9.8	-	-	-	1.04	1.58
Leaf width, mm	4.9	56.1	36.6	2.4	-	-	1.42	2.00
Number of shoots, pcs.	36.6	48.8	9.8	4.9	0.0	-	1.58	2.32
Mass of bush, g	24.4	53.7	22.0	0.0	-	-	1.46	2.00
Essential oil mass fraction $_{a.d.m.}$, %	17.1	29.3	17.1	26.8	7.3	2.4	2.31	2.58
Yield of oil, g m^{-2}	58.5	26.8	14.6	0.0	-	-	1.37	2.00

Quantitative traits by the year were also not variable and depended only by genotype (Table 4).

Table 4. The result of two way ANOVA of *oregano* quantitative traits

Source of variation	SS	df	MS	Source of variation	SS	df	MS
Plant height				Number of shoots			
sample	8745.1	40	218.6	sample	1.0492	40	0.0262
year	1.7	1	1.7	year	0.0399	1	0.0399
sample*year	1607.7	40	40.2	sample*year	1.4412	40	0.0360
Error		0		Error		0	
Plant diameter				Essential oil mass fraction			
sample	15029.7	40	375.7	sample	1.170269	40	0.029257
year	489.3	1	489.3	year	0.101644	1	0.101644
sample*year	5324.0	40	133.1	sample*year	0.406013	40	0.010150
Error		0		Error		0	
Leaf length				Mass of bush			
sample	1033.81	40	25.85	sample	2833057	40	70826
year	36.46	1	36.46	year	1599370	1	1599370
sample*year	313.11	40	7.83	sample*year	819021	40	20476
Error		0		Error		0	
Leaf width				Yield of oil			
sample	377.88	40	9.45	sample	180.4074	40	4.5102
year	29.91	1	29.91	year	2.0613	1	2.0613
sample*year	194.89	40	4.87	sample*year	67.7679	40	1.6942
Error		0		Error		0	

In terms of the mass fractions of essential oil from absolute dry raw materials, the reverse trend can be noted: in the year 2017, which was hot and normally moisturized during the flowering period, as well as favorable for essential oil accumulation, high oil content (from 4 to 6 points) was seen in 36.5% of the samples, and in rainy 2018 - only 14.6% (Table 5). That is, on this trait the genotype-environment interactions and the strong influence of weather conditions on the formation of this valuable economic trait were clearly visible, which is well consistent with the correlation coefficients of the mass fraction of essential oil and yield of oil varyied between $r = 0.81–0.87$ depending on the year.

Table 5. Distribution of origanum samples by levels of traits manifestation, $n = 41$, 2018 (second year of life)

Trait	Distribution of samples by trait manifestation level, %						H, bit	H_{max}, bit
	1	2	3	4	5	6		
Qualitative traits								
Corolla color	17.1	19.5	22.0	41.5	-	-	1.90	2.00
Leaf color	34.1	14.6	14.6	36.6	-	-	1.87	2.00
Bract color	56.1	19.5	7.3	17.1	-	-	1.64	2.00
Stalk color	12.2	22.0	51.2	14.6	-	-	1.75	2.00
Male fertility	51.2	34.1	14.6	0.0	-	-	1.43	2.00
Quantitative traits								
Plant height, cm	2.4	29.3	63.4	4.9	-	-	1.28	2.00
Plant diameter, cm	0.0	17.1	61.0	22.0	-	-	1.35	2.32
Leaf length, mm	14.6	82.9	2.4	-	-	-	0.76	1.58
Leaf width, mm	9.8	75.6	14.6	0.0	-	-	1.04	2.00
Number of shoots, pcs.	4.9	39.0	41.5	4.9	9.8	-	1.81	2.32
Mass of bush, g	4.9	19.5	46.3	29.3	-	-	1.71	2.00
Essential oil mass fraction $_{a.d.m.}$, %	39.0	41.5	4.9	4.9	2.4	7.3	1.89	2.58
Yield of oil, g m^{-2}	65.9	29.3	2.4	2.4	-	-	1.18	2.00

Thus, comparing two years of trials, qualitative traits were shown more consistently than the quantitative ones. However, for identification it is interesting to use the most polymorphic traits with the highest entropy. In our experiments, it is ranged from 1.04 to 2.31 bits in 2017 and from 0.76 to 1.90 bits in 2018. The lower polymorphism of traits can be explained by the age of plants - in the second year, varietal traits are more stable and less susceptible to the environmental influence. Nevertheless, for reliable identification it is advisable to use the most polymorphic traits in both years. As a reference value, an empirical value of 1.50 bits was taken as a reference value. Such traits include the coloration of the bract, stalk, leaf and corolla, as well as the number of shoots and the mass fraction of essential oil.

The next stage of the work was the construction of dendrograms demonstrating the relationship of the collection samples of origanum with each other according to phenotypic traits (Figs 1, 2).

The structure of the construction differed over the years of the study, so the Mantel test was involved in addition to visual comparison, which allows one to compare two matrices (in this case - the distance matrices, along which the dendrograms were built) with each other. This test showed that the correlation coefficient had a reliable average $r = 0.58$.

For convenience (optimal number of clusters) a combined distance of 30 units for division into clusters was taken. As a result, in both years the collection samples of origanum are combined into five clusters (clusters were counted starting from the top).

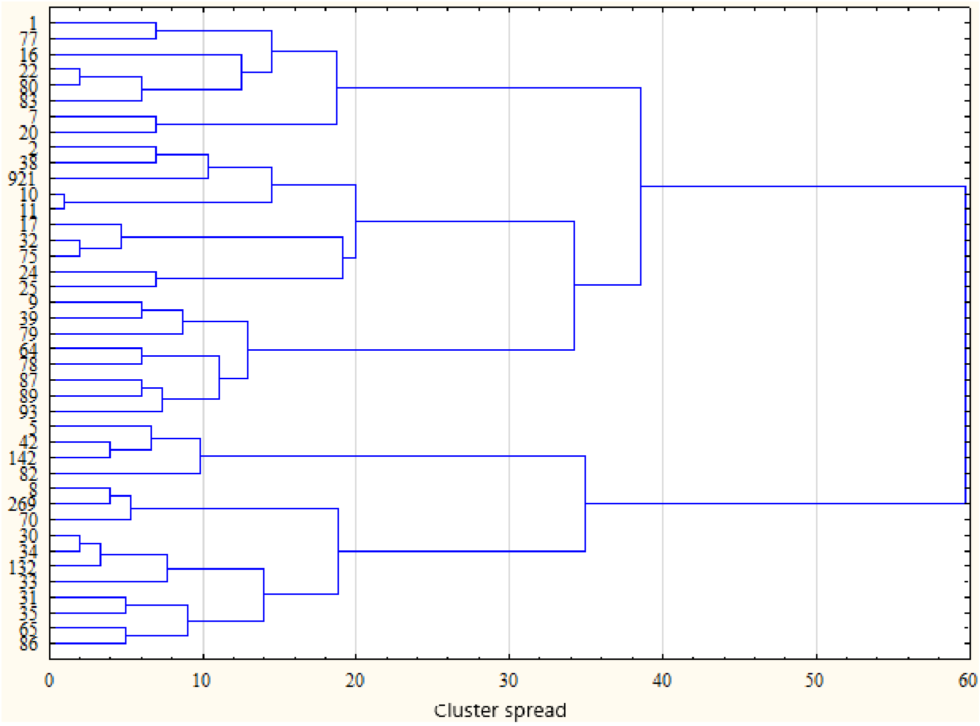

Figure 1. Dendrogram constructed on the phenotypic traits reflecting the relationship degree of origanum collection samples, 2017.

It is interesting to note that the first and fifth clusters of samples in both years coincided, and the second cluster of 2017 corresponded to the third cluster of 2018, the third cluster of 2017 - to the fourth of 2018, the fourth of 2017 - to the second of 2018. There are 78% of the samples (32 pieces) retained similarity in the construction over the years.

The occupancy of the clusters was quite similar over the years of the study. A stable grouping (the first cluster in 2017 and 2018) was formed by samples 1, 7, 20, 22, 77, 80, 83. They were characterized by an average mass of a bush (600–900 g), a low mass fraction of essential oil (from trace amounts to 0.15% of the adm) and low collection of essential oil per unit of area (up to 2.0 g m^{-2}).

The next resistant group (the second cluster in 2017 and the third in 2018) included genotypes 2, 10, 11, 17, 32, 75, distinguished by light lilac or lilac coloration of the corolla, green leaves, pigmented stalk, fertile flowers, a small number of shoots in a bush (up to 100 pcs.) and low mass of plants (up to 600 g $plant^{-1}$).

The third cluster of 2017 (fourth in 2018) was formed by samples 9, 39, 78, 79, 89. They were characterized by varying intensity lilac coloration of the corolla, lightly colored bracts, plants of medium height 66–65 cm, bush diameter - 66–85 cm, leaves

25–35 mm long and width 15–20 mm wide, low EOMF (0.05–0.25% of the adm), high bush mass (up to 1,200 g).

Sustainable construction was provided by genotypes 5, 8, 42, 70, 142, 269, which formed the fourth cluster in 2017 or the second in 2018. They were characterized by the presence of weakly pigmented stalks, leaves of medium length (25–35 mm), a rather high mass of the bush (up to 900 g).

The fifth cluster in both years was filled with samples 30, 33, 34, 35, 65, 86, 132. They were characterized by white coloration of the corolla, glaucous-green coloration of the leaf and generally intense coloration of the stalk, sprawling bushes (diameter of plants 86–105 cm), narrow (10–15 mm) and medium length (25–35 mm) leaves, high mass of plants (up to 1,200 g).

Thus, it may be concluded that clusters 3 and 5 are the most productive in terms of green mass yield.

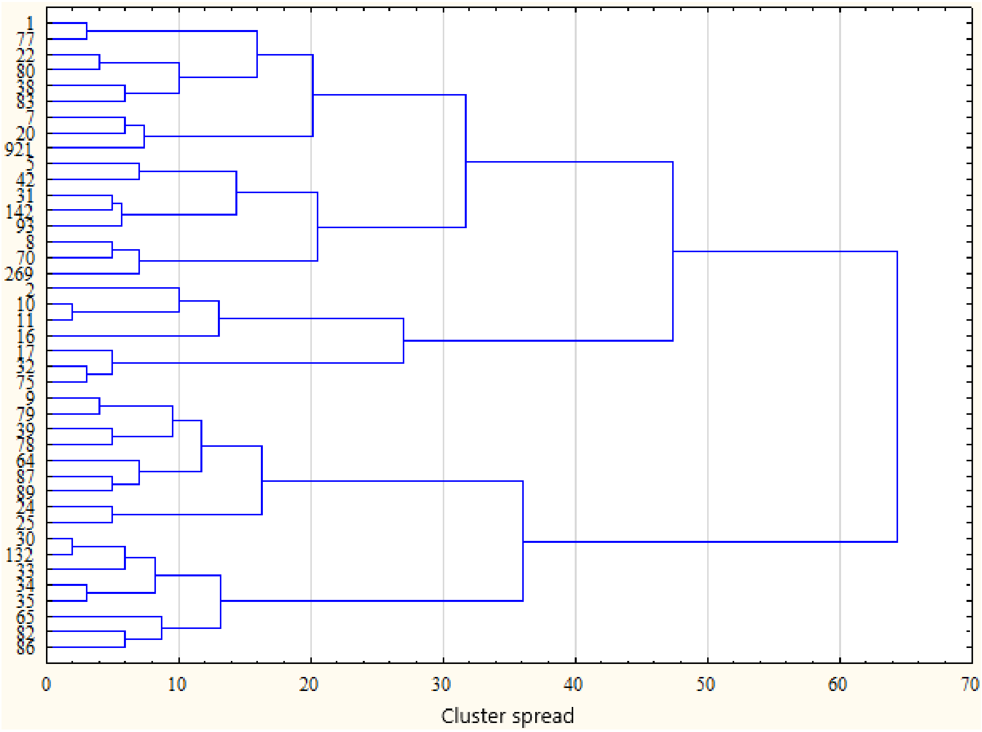

Figure 2. Dendrogram constructed on the phenotypic traits reflecting the relationship degree of origanum collection samples, 2018.

According to the authors, in the second year of plant life (the third after planting in open soil), the manifestation of quantitative phenotypic traits was more differentiated compared to qualitative ones. Therefore, it is interesting to consider the construction and grouping of samples in this year. The the first cluster was formed by samples 1, 7, 20, 22, 38, 77, 80, 83, 921 in 2018, which are characterized by large plants (up to 85 cm in height and a yield of green mass up to 900 g plant^{-1}) with a low essential oil mass fraction (from trace amounts up to 0.15% of the adm) and low a collection of essential oil (up to 2.0 g m^{-2}).

The second cluster was formed by samples 5, 8, 31, 42, 70, 93, 142, 269, having a painted corolla (light lilac or lilac), green leaves, pigmented stalks, low bush mass (up to 600 g) due to the low plant height (50% of samples - up to 65 cm) and the small number of shoots in the bush (up to 100 pcs.). However, this cluster was characterized by the presence of 42.7% of samples with EOMF at the level of 0.25–0.55% of the adm (4–6 points), which could be used as high-oil sources.

The third cluster was formed by samples 2, 10, 11, 16, 17, 32, 75, which was characterized mainly by white-flowered forms (7 samples out of 8) having intense anthocyanic coloration of stalks and bracts. The height of the bush is 2–3 points, 3 samples showed traces of essential oil (1 point), 1–2 points. In addition, this cluster included samples 10 and 11, which had EOMF of 0.490 and 0.420% of the adm or corresponding to 6 and 5 points.

Samples 9, 24, 25, 39, 64, 78, 87, 79, 89 included in the fourth cluster were characterized by tall (up to 85 cm) most yielding plants (bush mass up to 1,200 g).

The representatives of the fifth cluster (samples 30, 33, 34, 35, 65, 82, 86, 132) were characterized by the presence of exclusively high (66–85 cm) white flowered high-yield (up to 1,200 g plant^{-1}) samples with an average EOMF (up to 0.15% of the adm) and an average essential yield of oil, (up to 4.0 g m^{-2}), excluding sample 82 which had high oil content (up to 0.55% of the adm), which determines a high essential yield of oil (up to 8.0 g m^{-2}) along with high yield.

Thus, for breeding work, the contrasting clusters 2 and 5 (according to the 2018's data) were interesting for economically useful traits. For hybridization it is advisable to select parental forms from these two clusters for hybridization.

CONCLUSIONS

It was found that the qualitative traits showed themselves more consistently than the quantitative ones. For reliable identification of origanum samples of Crimean Peninsula, it is recommended to use the most polymorphic traits ($H > 1.50$ bits): coloration of the bract, stalk, leaf and corolla, as well as the number of shoots and mass fraction of essential oil.

When constructing dendrograms, the structure of the association differed in the years of study: according to the Mantel's test, the correlation coefficient was a reliable average $r = 0.58$. However, a fairly clear correspondence of the different years' clusters to each other was established (78% of the samples). This indicated genotype-environmental interactions in the manifestation of the studied phenotypic traits. Yet, the established correspondence of different years' clusters indicates the reliability of combining genotypes into separated groups (clusters) and their similar reaction to environmental conditions.

The most interesting combinations of samples for further breeding work were clusters 2 and 5 (according to the 2018 data). In 42.7% of genotypes from the second cluster, the mass fraction of essential oil was at the level of 0.25–0.55% of absolute dry mass (4–6 points). The samples from the second cluster could be used as high-oil sources, whereas samples from the fifth cluster - as sources of high productivity of 'green' raw materials (up to 1,200 g plant^{-1}). It would be advisable to select parental forms from these two clusters for hybridization.

Grouping of origanum samples used in the work quite accurately separated them not only on qualitative, but also on economically valuable traits.

It has been established that the grouping of origanum samples quite accurately divided samples not only on qualitative traits, but also on economic valuable traits. This may be offered to the breeders as one of the additional methods for classifying the source material and be further introduced into breeding and botanical practice.

REFERENCES

Andi, S.A., Nazeri, V., Zamani, Z. & Hadian, J. 2011. Morphological diversity of wild *Origanum vulgare* (Lamiaceae) in Iran.*The Iranian journal of botany* **17**(1), 88–97.

Bokov, D.O., Morokhina, S.L., Pyatigorskaya, N.V. & Popov, D.M. 2013. Modern approaches to the study of chemical composition of medicinal plant raw materials of Origanum L. genus representatives and development methods of its standardization. *Butlerov Communications* **35**(7), 94–101.

Bussmann, R. W., Batsatsashvili, K. & Kikvidze, Z. 2020. Origanum vulgare L. Lamiaceae: In book: Ethnobotany of the Mountain Regions of Central Asia and Altai. *Springer*, 1–7. doi: 10.1007/978-3-319-77087-1_95-1

Dud´ık, M., Phillips, S.J. & Schapire, R.E. 2007. Maximum entropy density estimation with generalized regularization and an application to species distribution modeling. *Journal of Machine Learning* **8**, 1217–1260.

Ibrahim, L., Bassal, A., Elezzi, A., El Ajouz, N., Ismail, A., Karaky, L., Kfoury, L., Sassine, Y., Zeineddine, A. & Ibrahim, S.K. 2012. Characterization and identification of Origanum Spp. from Lebanon using morphological descriptors. *World Research Journal of Agricultural Biotechnology* **1**(1), 4–9.

Khlipenko, L.A., Rabotyagov, V.D. & Orel, T.I. 2005 Study of Origanum L. genus in the conditions of the southern shore of Crimea, *Black sea Bot. Journ*. **1**(2), 63–66.

Korotkikh, I.N. & Khaziyeva, F.M. 2016. The features of vegetative reproduction by dividing rhizome method for Origanum vulgare L. *Taurida herald of the agrarian sciences* **3**(7), 16–28.

Masoudi, M. & Saiedi, M. 2017. Anti-inflammatory, antioxidant, anticancer and anti-microbial effect of Origanum vulgare: a systematic review. *Der Pharmacia Lettre* **9**(4), 85–94.

Methods of conducting tests for distinguishability, homogeneity and stability of common origanum (Origanum vulgare L.). URL: http://gossortrf.ru/22-metodiki-ispytaniy-na-oos.html (access date: 21.05.2020).

Myagkikh, E.F. 2015. Morpho-biological traits and economical traits of Origanum vulgare L. in the Foothill Zone of Crimea in connection with the problems of breeding: synopsis of thesis. Candidate of Biol. Sciences: 06.01.05 – breeding and seed production of agricultural plants, Krasnodar, 24.

Origanum, L. (ORIGA). Dus Guidance and Cooperation. URL: https://www.upov.int/genie/details.xhtml?cropId=3950 (access date: 21.05.2020).

Pagnotta, M.A., Rey, N.A., Ciancolini, A. & Crinò, P. 2013. Are UPOV descriptors a useful and feasible tool. *Acta Horticulturae* **983**, 145–149. doi: 10.17660/ActaHortic.2013.983.19

Pashetsky, V.S., Nevkrytaya, N.V., Mishnev, A.V. & Nazarenko, L.G. 2018. Essential oil industry of Crimea. Yesterday, today, tomorrow. Ministry of Science and Higher Education of the Russian Federation, Russian Academy of Sciences, Federal State Budget Institution of Science “Agriculture Research Institute of the Crimea”. 2nd ed., enl. Simferopol: ARIAL, 317. ISBN 978-5-907118-16-4

Sivicka, I., Adamovics, A., Ivanovs, S. & Osinska, E. 2019. Some morphological and chemical characteristics of oregano (Origanum vulgare L.) in Latvia. *Agronomy Research* **17**(5), 2064–2070. doi: 10.15159/AR.19.153

Straszak, D. & Vishnoi, N.K. 2020. Maximum Entropy Distributions: Bit Complexity and Stability. URL: https://arxiv.org/pdf/1711.02036.pdf (access date: 21.05.2020).

Tétard-Jones, C., Kertesz, M.A. & Preziosi, R.F. 2011. Quantitative trait loci mapping of phenotypic plasticity and genotype–environment interactions in plant and insect performance. *Phil. Trans. R. Soc. B*. **366**, 1368–1379. doi:10.1098/rstb.2010.0356

Yakimova, O.V. & Yegorova, N.A. 2015. Clonal micropropagation of origanum in vitro. *Taurida herald of the agrarian sciences* **2**(4), 39–44.

Yegorova, N.A. & Yakimova, O.V. 2019. The effect of long-term subcultivation on clonal Micropropagation of Melissa officinalis L. and Origanum vulgare L. Vestnic Tomskogo gosudarstvennogo universiteta. *Biologiya, Tomsk State University Journal of Biology* **47**, 22–39. doi:10.17223/19988591/47/2

Vale-Silva, L., Silva, M., Oliveira, D., Gonc`alves, M., Cavaleiro, C., Salgueiro, L. & Pinto, E. 2012. Correlation of the chemical composition of essential oils from Origanum vulgare subsp. virens with their in vitro activity against pathogenic yeasts and filamentous fungi. *Journal of Medical Microbiolog* **61**, 252–260.

Agronomy Research **18**(4), 2501–2511, 2020
https://doi.org/10.15159/AR.20.192

Biochar dosage impact on physical soil properties and crop status

V. Novák[1,*], K. Křížová[1,2] and P. Šařec[1]

[1]Czech University of Life Sciences Prague, Faculty of Engineering, Department of Machinery Utilization, Kamýcká 129, CZ16500 Prague, Czech Republic
[2]Crop Research Institute, Division of Crop Protection and Plant Health, Drnovská 507/73, CZ16106 Prague, Czech Republic
[*]Correspondence: novakvaclav@tf.czu.cz

Abstract. In the context of climate change and the ongoing population growth, current agriculture inevitably faces many challenges. Long periods of drought are often followed by shorter periods of heavy precipitation and degraded soil is often unable to retain the rainfall water properly. Apart from common organic fertilizers, soil amendments are currently considered a promising solution that might improve soil quality. The most discussed one is biochar, a natural soil conditioner that might under certain conditions improve soil properties. This study is based on the experiment that was established in 2017 in order to determine the impact of biochar dosage and it's effect over time. Four parcels approximately 15×30 m were designed in Rapotín, Czech Republic. Each of them was treated with a specific dose of biochar (15, 30, 45, 60 t ha^{-1}), and selected soil physical properties such as penetration resistance and reduced bulk density were then measured at the beginning of the cropping season 2019. In addition, vegetation properties were investigated with the use of handheld sensors repeatedly during the season on winter wheat. The dataset contained information about chlorophyll and nitrogen content as well as Normalized Difference Vegetation Index estimations. Acquired values were later compared with the results obtained from the fifth variant founded in 2014 with a 15 t ha^{-1} dose and from the control variant. Although the dosage levels applied were quite substantial, no significant difference was found when evaluating selected soil properties. Crop response gave similar results. Any of the examined characteristics differed among the 2017 variants and control. Nevertheless, when compared to the 2014 variant, clearly different results were detected. Thus, this study concluded that the effect of biochar dosage is might not be as significant factor, however, the time effect likely is. Therefore, the study has to continue and soil/crop properties will be observed in the upcoming season as well.

Key words: soil conditioner, penetration resistance, reduced bulk density, handheld sensor, vegetation index.

INTRODUCTION

Ensuring sufficient quantity and quality of foodstuff while protecting the environment is one of today's agricultural dilemmas. Today, the situation is dire due to various constraints related to soil properties such as soil degradation, soil compaction or carbon losses, all of which are often mentioned topics not only among scientific literature. Essentially, compacted soil has low water infiltration capacity, which is a crucial fact in terms of agricultural drought mitigation (Chyba et al., 2014). Consequently, there are significant constraints in nutrients uptake under soil compaction, namely nitrogen uptake might decrease by 30% by spring wheat (Kuht & Reintam, 2004). Moreover, the infiltration capacity is jeopardized even more during long drought periods or large amounts of precipitation in short periods of time. Due to reduced infiltration capacity, floods may occur, affecting the surrounding landscape. These negative changes are very often strengthened by anthropogenic activities, here in particular by the intensification of the agricultural practice (Kopittke et al., 2019). Also, the impact of ongoing climate change must be considered. Despite the undeniable progress in crop breeding and field management, drought still causes significant fluctuations which affect crop growth during the whole cropping season resulting in yield losses (Potopová et al., 2015).

Biochar is a carbon-rich material referred to as a soil conditioner. Its potential in terms of drought-related agricultural issues is an ongoing discussion in recent scientific studies. Primarily, the carbon content of this material is considered apparently beneficial. Depending on the properties of biomass as the input for the pyrolysis process as well as the pyrolysis conditions, the carbon content can reach up to 90%. Therefore, this material is believed to increase carbon sequestration application activities (Ippolito et al., 2017). Moreover, biochar processing can provide an efficient treatment of residual waste from food production, when taken as an input biomass (Tamelová, et al., 2019). Utilizing the waste biomass in this manner is a promising instrument for reducing greenhouse gases produced by agricultural practice (Lehmann et al., 2006).

The intrinsic links between soil and plants are undeniable facts. By means of the vegetation state, soil properties can be indirectly determined. With developments in the field of technology in recent decades, various non-destructive methods can be used to determine vegetation properties. While using the satellite imagery is suitable for larger areas, for smaller plots UAV (Unmanned Aerial Vehicles) or a variety of handheld devices is more appropriate (Tunca et al., 2018). The major difference between these two methods is the form of information which the devices provide. Apparently, the latter is used rather for direct measurement, while gathering mainly the point information. Those can be interpolated through various algorithms to acquire the spatial information about the plot as a whole. However, when requiring such data, UAVs are more recommended to be used, since today a very high resolution can be achieved by most of the sensors on the market. Spectral responses of different kinds of surface materials has been studied extensively and the achievements resulted in the development of Remote Sensing practices. Based on source imagery, hundreds of spectral indices are not only used describe plant properties. The NDVI (Normalized Difference Vegetation Index) was one of the first indices describing the vegetation biomass and health and it is one of the most widespread used even till today (Li et al., 2019). Furthermore, the nitrogen content in a plant material is one of the key indicators for predicting yields and vegetation status (Cartelat et al., 2005), since closely correlated with the chlorophyll content (Yoder & Pettigrew-Crosby, 1995).

As mentioned above, many studies look at biochar, however, the subject is often focused on physical or chemical properties of the biochar itself (de la Rosa et al., 2014; Yargicoglu et al., 2015; Yuan et al., 2015; Conti et al., 2016) or its general behaviour when applied to the soil profile respectively (Lehmann et al., 2006; Rasa et al., 2018; Razzaghi et al., 2019). The question of potential ecotoxicity is being also discussed

(Zhang et al., 2020). Nevertheless in terms of its effect, other biochar-based studies suggest that it may be responsible for reducing the soil bulk density and increase water infiltration and later availability for plants (Razzaghi et al., 2019; Tanure et al., 2019). It has been shown that the effect on reducing bulk density of the soil as well as on water-holding capacity is strongly correlated with the particle size. However, the entire effect may vary depending also on the soil type (Verheijen et al., 2019).

Although there have been many studies published on the subject of biochar, the experiment described in this paper is focused on its dosage rather than the effect itself. The objective here is to determine the potential differences in soil and crop performance based on the specific levels of biochar dose. Its impact on soil physical properties and related crop growth are about to be evaluated.

MATERIALS AND METHODS

Site and crop management

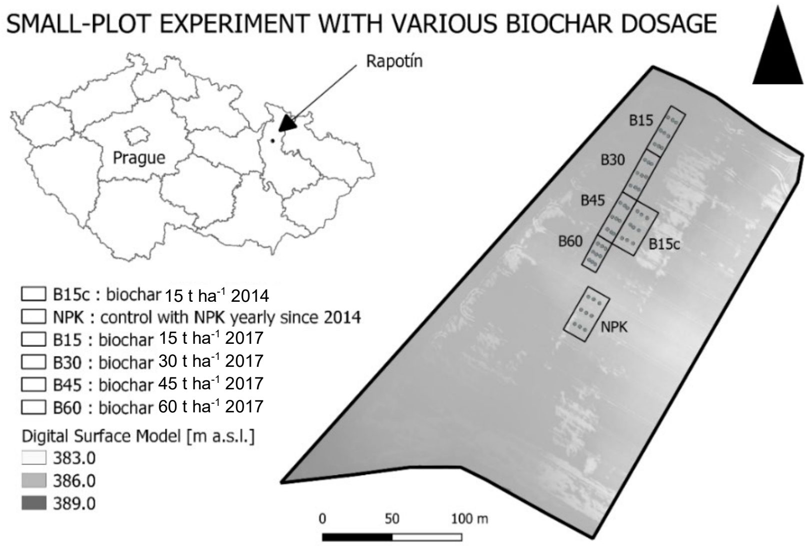

Figure 1. Experimental plot location and small-plots treatment specification.

This study was undertaken in the Czech Republic on agricultural plot located near the town of Šumperk in the Olomouc region (49° 59' 8.8296" N, 16° 59' 47.0904" E). The 13.24 ha field was divided into smaller plots with a variable area and also varying agricultural management. Five small-plots approximately 30×15 m treated by biochar in specific doses have been chosen for this study (Fig. 1). A control has also been included and marked as 'NPK' since the whole area was, besides investigated soil conditioners and fertilizers, treated by standard complex fertilizers (N, P, K) in a dose of 280'kg'ha^{-1} that is in accordance with the common practice. According to the FAO Soil Units, the soil type was classified as Gleyic Luvisols, which usually develops on flat surfaces. Complex soil analysis was undertaken before biochar application to obtain information about initial soil conditions (Table 1). Practically no sloping of the plot enables a wide-row crops cultivation without any erosion exposure. Crop rotation in recent years started with maize (2015) followed by in growing season 2019. *Proteus* (Soufflet Agro) wheat variety was sown on the 24th October 2018 and cultivated till the harvest date 10th August 2019. According to the producer it is semi-early to mid-late wheat with excellent resistance to laying flat and healthy leaf development. Disc harrow was used in 2014–2016 and 2018 at depths 9–12 cm, while in 2017 reversible plough at a depth of 25 cm was used during the soil tillage.

Table 1. Results of soil analysis that has been undertaken by the research company Agrovýzkum Rapotín in 2014

	Soil profile [cm]		
	0–30	30–60	
Clay (< 0.002 mm)	27	22	[%]
Clay particles (< 0.01 mm)	40	34	[%]
Silt (0.01–0.05 mm)	40	38	[%]
Fine sand (0.05–0.1 mm)	3	5	[%]
Sand (0.1–2 mm)	17	23	[%]
Bulk density	1.38	1.66	[g cm^{-3}]
Total porosity	47.72	38.91	[%]
Volumetric moisture	34.35	29.95	[%]
Humus content	1.93	1.09	[%]
pH (KCl)	5.13	5.4	–

Table 2. Technical specifications of biochar used for the study as provided by the BIOUHEL.CZ company

Total C in dry matter	min 45	[%]
Total N in dry matter	min 1	[%]
Total P (P_2O_5) in dry matter	16	[%]
Total K (K_2O) in dry matter	17	[%]
pH	9–11	–
Particle size < 2 mm	min 40	[%]
Particle size > 10 mm	max 10	[%]

Biochar used for this study was produced from plant biomass and wood waste in the Czech Republic by the company BIOUHEL.CZ. Table 2 gives its technical specifications more in detail. The dosage levels were designed intentionally high to assure the substantial difference in an effort to establish some threshold that defines the biochar effectivity. Since the common practice works with 10–15 t ha^{-1}, the doses for this experiment were 15, 30, 45 and 60 t ha^{-1}.

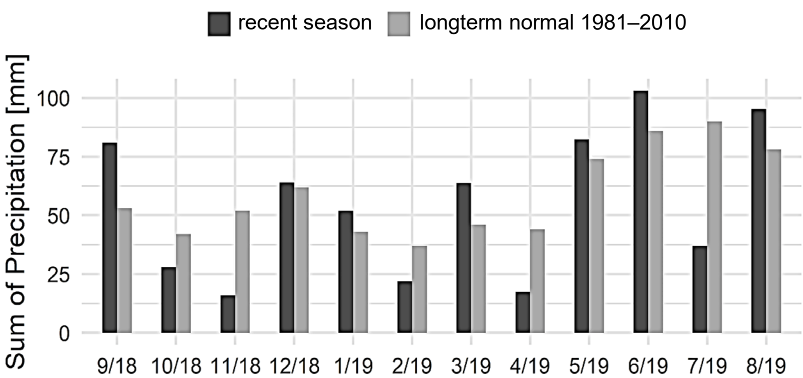

Figure 2. Precipitation condition in cropping season 2019 in comparison with the long term normal according to the Czech Hydrometeorological Institute.

Figs 2, 3 Represent meteorological conditions of the investigated cropping season. As shown on Fig. 2, the rainfall varied considerably in comparison with the long-term normal. In general, the total amount of precipitation in 2019 was 45.1 mm lower. The especially low amount of precipitation during April must have had a critical impact on the crop development. Furthermore, the temperature during this period exceeded the long-term normal during the entire season, excluding the month of May (Fig. 3). The range of temperature differences varied from -2.2 °C to 4.7 °C, however, the overall average temperature resulted in 1.6 °C higher than normal.

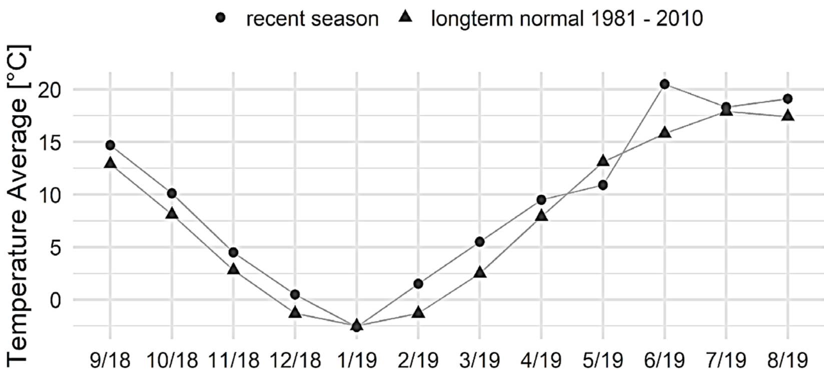

Figure 3. Monthly average temperature in cropping season 2019 in comparison with the long term normal according to the Czech Hydrometeorological Institute.

Data Acquisition and Processing

Field visits and in-situ terrestrial measurements were undertaken on the 18th April (term I; BBCH 30), 8th May (term II; BBCH 34) and 24th May 2019 (term III; BBCH 37) to obtain the terrestrial data. Soil physical properties were measured solely at the beginning of the cropping season (term I) in a period when the soil profile was saturated with water, as it is a common practice. For the information regarding Reduced Bulk Density, (BD) standard Kopecky's cylinders were used. Furthermore, Penetration Resistance (PR) of the soil profile was investigated. Using the instrument PEN 70, developed by Czech University of Life Sciences in Prague exclusively for these kinds of measurements. PR values in depths 4, 8, 12, 16 and 20 cm were recorded. Crop status data was monitored within all field visit terms. Namely it was Leaf Chlorophyll Content (LCC) measured by the CCM-300 sensor (OptiSciences), nitrogen content (N) and derived Normalized Difference Greenness Index (NDGI) measured by N-Pen (Photon Systems Instruments) and last Normalized Difference Vegetation Index (NDVI) acquired by GreenSeeker sensor (Trimble). 9 sampling points were established within each small-plot. Its GPS coordinates were recorded and the exact spot was marked by the red plastic pin to ensure the consistency of measurements in the exact spot.

The whole dataset was then processed in an open-source environment of R Studio (R Core Team, 2019) using packages tidyverse (Wickham et al., 2019), readxl (Wickham and Bryan, 2019), reshape2 (Wickham, 2007), pgirmess (Giraudoux, 2018) and multcompView (Graves et al., 2019).

The distribution of data was tested using the Shapiro-Wilk normality test in order to choose an appropriate statistical test. Since the data was not confirmed to be normally distributed, non-parametric statistical testing had to be utilized. To determine potential differences among investigated variables based on the biochar dose, the Kruskal-Wallis test was used instead of ANOVA.

RESULTS AND DISCUSSION

First of all, BD has been used to describe soil profile conditions. Since the process of collecting such data is time-consuming, the amount of information has been used for initial description of soil environment rather than for statistical testing. As shown by Fig. 4, the control (NPK) has the lowest values, while the B60 has the highest. According to the United States Department of Agriculture, the ideal bulk densities for plant growth related to present soil texture is lower than 1.10 g cm^{-3}. The bulk density which affects root growth is 1.49 g cm^{-3} and bulk densities that restrict root growth are higher than 1.58 g cm^{-3} (United States Department of Agriculture, 2019). Based on this recommendation, NPK performed the best, while by B60 the volume density limit was exceeded and the root growth was likely restricted. Variant B15c is still below USDA limit which on one hand affects the root growth, but still there is no root growth restriction. While a large number of studies have reported positive effects of biochar on soil bulk density (Walters & White, 2018; Alotaibi & Schoenau, 2019; Oni et al., 2020), there was no improvement observed in this study after two years from biochar application.

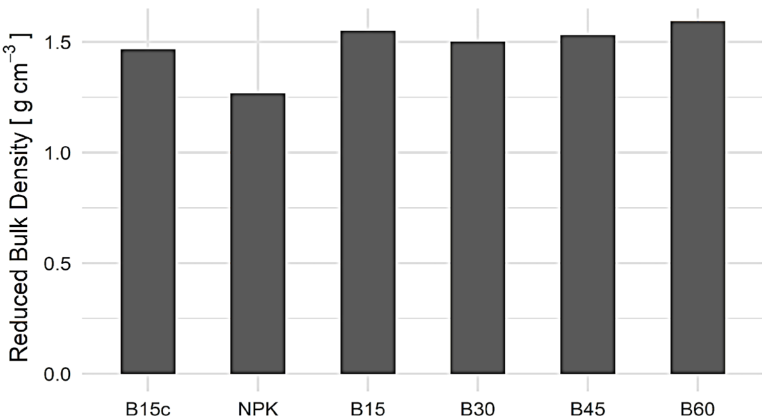

Figure 4. Values of reduced soil bulk density (0–0.05 m) - 18th April 2019.

PR results are illustrated by Fig. 5, where all investigated depths are represented. Nonetheless, neither here statistically significant difference has been observed among the variants (see also Table 3). Based on the results of other studies conducted on changes in PR, biochar is considered to reduce penetration resistance in the upper layers of the soil without increasing it in the deeper layers (Ahmed et al., 2017; Šařec et al., 2019). This is in accordance also with another study, where PR was reduced in the upper part of the sandy loam soil, but by loamy fine sand soil any influence of biochar on penetration resistance was observed (Obia et al., 2017). The measurement of soil physical parameters was undertaken in the springtime (term I) when higher water saturation of soil profile is expected. However, the precipitation in April 2019 was lower more than 50% less the normal precipitation rate. For this reason, the potential of biochar could not be sufficiently demonstrated. Otherwise, this would probably result in a decrease of PR, mainly due to the porosity of the biochar and thus its ability to retain water.

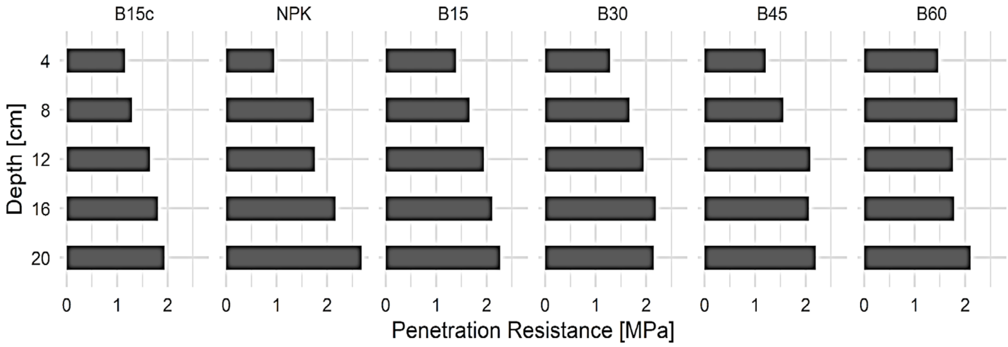

Figure 5. Soil penetration resistance values recorded during the term I in selected depth levels.

Regarding the crop growth indicators, results have been rather homogeneous as well. Table 3 provides the complex overview of Kruskal-Wallis analysis results. As shown here, only the LCC has indicated some significant differences, namely in term II and term III (see also Fig. 6).

Table 3. Kruskal-Wallis test of variance describing the variability of LCC (Leaf Chlorophyll Content), N (nitrogen content), NGDI (Normalized Difference Greenness Index) and PR (soil Penetration Resistance) in relation to small-plots treated by different dose of biochar

	Term	*p*-value	B15c	NPK	B15	B30	B45	B60
LCC	I	0.062	a	a	a	a	a	a
	II	0.023	ab	ab	a	ab	ab	b
	III	< 0.001	a	b	b	b	b	ab
N	I	0.235	a	a	a	a	a	a
	II	0.494	a	a	a	a	a	a
	III	0.344	a	a	a	a	a	a
NDGI	I	0.234	a	a	a	a	a	a
	II	0.489	a	a	a	a	a	a
	III	0.344	a	a	a	a	a	a
NDVI	I	0.035	a	a	a	a	a	a
	II	0.570	a	a	a	a	a	a
	III	0.192	a	a	a	a	a	a
	depth							
PR	4	0.129	a	a	a	a	a	a
	8	0.155	a	a	a	a	a	a
	12	0.740	a	a	a	a	a	a
	16	0.536	a	a	a	a	a	a
	20	0.230	a	a	a	a	a	a

First of all, there is apparently a difference in sensitivity of the sensors used. Although they are designed to indicate different properties, LCC are trusted to be highly correlated with the nitrogen content in a biomass (Evans, 1983). Therefore, similar results among those variables were expected. While the CCM 300 sensor measures the LCC as the chlorophyll fluorescence ratio utilizing the wavelengths assigned to the Red Edge region (CFR = 735 nm /700 nm), the N-Pen calculates the NDGI index according to the information in wavelengths of 560 nm (Green) and 780 nm (NIR). Secondly, the influence of meteorological conditions may explain the LCC data variability. As mentioned above, April was a significantly warm and dry period, which very likely affected the results recorded during the term I. During the month of May, when term II and III measurements taken, precipitation was rich and the recorded temperatures were lower. Such a combination very likely restored the suitable conditions for crop growth and therefore, the differences among the plots could be observed. The study of Tanureet al. (2019) suggest that the impact of biochar on crop growth parameters is strongly influenced by the level of drought. While under the regular conditions, biochar-enriched soils promote the photosynthesis and stomatal conductance, drought conditions cause the slowing down of these processes even more than seen in a control.

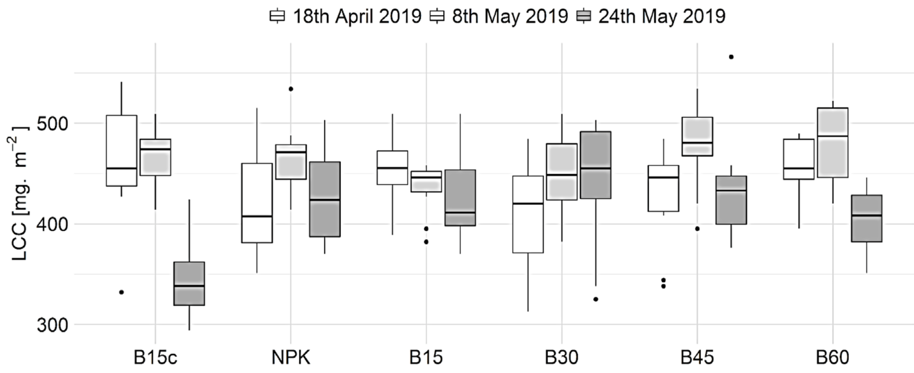

Figure 6. Leaf Chlorophyll Content obtained by CCM 300 handheld sensor during the term I, II and III among investigated small-plot variants.

During term II a significant difference was observed between B15 and B60. However, the situation became clearer in term III, when the chlorophyll content levels were significantly different by B15c compared to all variants with biochar established in 2017, excluding B60, and the control. This trend is in accordance with the previous study conducted on this small-plot experiment in 2018 (Novák et al., 2019). The conclusion of that study conducted on maize crops described the relation of crop growth parameters on variant with the longer biochar effect (B15c) and the largest dose (B60). The results of the term III confirm this conclusion, since B15c is related with the B60 only. Overall the results do not prove any other significant difference between the control NPK and any of the biochar amended variants in regard to the chlorophyll content. A similar conclusion was described by Li et al. (2020), where anatomical traits such as plant height or leaf area reflected the biochar amendment rather than the physiological parameters.

CONCLUSIONS

Based on the results of this study as well as of those from the previous year, the conclusion was drawn that so far the examined substantially different doses do not have any significant influence on i) soil penetration resistance as one of the staple soil physical properties ii) neither on crop growth physiological parameters. The sole observable differences may be found by LCC when comparing the four-year biochar effect to the control and lower-doses two-year biochar variants. Thus, the time effect seems to be more staple factor compared to dosage. Since it is so, this experiment will be observed also in the following seasons to confirm this statement.

ACKNOWLEDGEMENTS. This study was supported by the Faculty of Engineering, Czech University of Life Sciences in Prague under internal grant IGA 2019:31180/1312/3104, and by the Technology Agency of the Czech Republic in the framework of project TAČR TH02030169. Furthermore, the authors would like to kindly thank Pikola (Šumperk) for their extraordinary support.

REFERENCES

Ahmed, A., Gariepy, Y. & Raghavan, V. 2017. Influence of Wood-Derived Biochar on the Compactibility and Strength of Silt Loam Soil. *Int Agrophys* **31**(2), 149–55.

Alotaibi, K.D. & Schoenau, J. 2019. Addition of Biochar to a Sandy Desert Soil: Effect on Crop Growth,Water Retention and Selected Properties. *Agronomy* **9**(6), 273. Retrieved from https://doi.org/10.3390/agronomy9060327

Cartelat, A., Cerovic, Z.G., Goulas, Y., Meyer, S., Lelarge, C., Prioul, J.-L., … Moya, I. 2005. Optically assessed contents of leaf polyphenolics and chlorophyll as indicators of nitrogen deficiency in wheat (Triticum aestivum L.). *Field Crops Res*. **91**(1), 35–49. Retrieved 5 January 2020 from https://doi.org/10.1016/J.FCR.2004.05.002

Chyba, J., Kroulík, M., Krištof, K., Misiewicz, P.A. & Chaney, K. 2014. Influence of soil compaction by farm machinery and livestock on water infiltration rate on grassland. *Agron Res*. **12**(1), 59–64.

Conti, R., Fabbri, D., Vassura, I. & Ferroni, L. 2016. Comparison of chemical and physical indices of thermal stability of biochars from different biomass by analytical pyrolysis and thermogravimetry. *J. Anal. Appl. Pyrol*. **122**, 160–168. Retrieved from https://doi.org/10.1016/j.jaap.2016.10.003

de la Rosa, J.M., Paneque, M., Miller, A.Z. & Knicker, H. 2014. Relating physical and chemical properties of four different biochars and their application rate to biomass production of Lolium perenne on a Calcic Cambisol during a pot experiment of 79 days. *Sci. Total Environ* **499**, 175–184. Retrieved from https://doi.org/10.1016/j.scitotenv.2014.08.025

Evans, J.R. 1983. Nitrogen and Photosynthesis in the Flag Leaf of Wheat (Triticum Aestivum L.). *Plant Physiol* **72**(2), 297–302.

Giraudoux, P. 2018. pgirmess: Spatial Analysis and Data Mining for Field Ecologists. R package version 1.6.9. https://CRAN.R-project.org/package=pgirmess

Graves, S., Piepho, H.P., Selzer, L. & Dorai-Raj, S. 2019. multcompView: Visualizations of Paired Comparisons. R package version 0.1-8. https://CRAN.R-project.org/package=multcompView

Ippolito, J.A., Bjorneberg, D., Stott, D. & Karlen, D. 2017. Soil quality improvement through conversion to sprinkler irrigation. *Soil Sci. Soc. Am. J*. **81**(6), 1505–1516. Retrieved from https://doi.org/10.2136/sssaj2017.03.0082

Kopittke, P.M., Menzies, N., Wang, P., McKenna, B. & Lombi, E. 2019. Soil and the intensification of agriculture for global food security. *Environ Int*. **132**, 105078. Retrieved 2 January 2020 from https://doi.org/10.1016/j.envint.2019.105078

Kuht, J. & Reintam, E. 2004. Soil compaction effect on soil physical properties and the content of nutrients in spring barley (Hordeum vulgare L.) and spring wheat (Triticum aestivum L.). *Agron Res*. **2**(2), 187–194.

Lehmann, J., Gaunt, J. & Rondon, M. 2006. Bio-Char Sequestration in Terrestrial Ecosystems - A Review. *Mitig. Adapt Strat Gl.* **11**(2), 403–27.

Li, Y., Song, H., Zhou, L., Xu, Z. & Zhou, G. 2019. Tracking chlorophyll fluorescence as an indicator of drought and rewatering across the entire leaf lifespan in a maize field. *Agr. Water Manage* **211**, 190–201. Retrieved 23 January 2019 from https://doi.org/10.1016/J.AGWAT.2018.09.050

Li, Q., Li, H., Fu, Q., Li, T., Liu, D., Hou, R., Cui, S., Ji, Y. & Cai, Y. 2020. Effects of Different Biochar Application Methods on Soybean Growth Indicator Variability in a Seasonally Frozen Soil Area. *CATENA* **185**, 104307. https://www.sciencedirect.com/science/article/pii/S0341816219304497 (January 17, 2020).

Novák, V., Křížová, K., Šařec, P. & Látal, O. 2019. "EFFECTIVE DOSE OF BIOCHAR WITHIN THE FIRST YEAR AFTER APPLICATION." *7th International Conference on Trends in Agricultural Engineering*: 422–28.

Obia, A., Børresen, T., Martinsen, V., Cornelissen, G. & Mulder, J. 2017. Effect of Biochar on Crust Formation, Penetration Resistance and Hydraulic Properties of Two Coarse-Textured Tropical Soils. *Soil Till. Res.* **170**, 114–21. https://www.sciencedirect.com/science/article/pii/S0167198717300636 (January 17, 2020).

Oni, B.A., Oziegbe, O. & Olawole, O.O. 2020 (in press). Significance of Biochar Application to the Environment and Economy. *Ann. Agric. Sci*. https://www.sciencedirect.com/science/article/pii/S0570178319300405#bb0295 (January 25, 2020).

Potopová, V., Štěpánek, P., Možný, M., Türkott, L. & Soukup, J. 2015. Performance of the standardised precipitation evapotranspiration index at various lags for agricultural drought risk assessment in the Czech Republic. *Agr. Forest Meteorol*. **202**, 26–38. Retrieved 2 January 2020 from https://doi.org/10.1016/j.agrformet.2014.11.022

R Core Team. 2019. R: A language and environment for statistical computing. R Foundation for Statistical Computing, Vienna, Austria. URL https://www.R-project.org/.

Rasa, K., Heikkinen, J., Hannula, M., Arstila, K., Kulju, S. & Hyväluoma, J. 2018. How and Why Does Willow Biochar Increase a Clay Soil Water Retention Capacity? *Biomass Bioenerg* **119**, 346–53. https://www.sciencedirect.com/science/article/pii/S0961953418302708 (January 13, 2020).

Razzaghi, F., Obour, P.B. & Arthur, E. 2019. Does Biochar Improve Soil Water Retention? A Systematic Review and Meta-Analysis. *Geoderma* **361**, 114055. https://www.sciencedirect.com/science/article/pii/S0016706119322153 (January 6, 2020).

Šařec, P., Novák, V. & Křížová, K. 2019. EFFECT OF ORGANIC FERTILIZERS, BIOCHAR AND OTHER CONDITIONERS ON MODAL LUVISOL. *7th International Conference on Trends in Agricultural Engineering*, pp. 494–99.

Tamelová, B., Malaťák, J. & Velebil, J. 2019. Hydrothermal carbonization and torrefaction of cabbage waste. *Agron. Res*. **17**(3), 862–871. Retrieved from https://doi.org/10.15159/AR.19.098

Tanure, M.M.C., da Costa, L.M., Huiz, H.A., Fernandes, R.B.A., Cecon, P.R., Pereira Junior, J.D. & da Luz, J.M.R. 2019. Soil Water Retention, Physiological Characteristics, and Growth of Maize Plants in Response to Biochar Application to Soil. *Soil Till. Res.* **192**, 164–73. https://www.sciencedirect.com/science/article/pii/S0167198718311978 (January 6, 2020).

Tunca, E., Köksal, E.S., Çetin, S., Ekiz, N.M. & Balde, H. 2018. Yield and leaf area index estimations for sunflower plants using unmanned aerial vehicle images. *Environ Monit. Assess*. **190**(11), 682. Retrieved from https://doi.org/10.1007/s10661-018-7064-x

United States Department of Agriculture. 2019. Soil Bulk Density/Moisture/Aeration. Retrieved from https://www.nrcs.usda.gov/Internet/FSE_DOCUMENTS/nrcs142p2_050936.pdf

Verheijen, F.G.A., Zhuravel, A., Silva, F.C., Amaro, A., Ben-Hur, M. & Keizer, J.J. 2019. The Influence of Biochar Particle Size and Concentration on Bulk Density and Maximum Water Holding Capacity of Sandy vs Sandy Loam Soil in a Column Experiment. *Geoderma* **347**, 194–202. https://www.sciencedirect.com/science/article/pii/S0016706118315702 (January 13, 2020).

Walters, R.D. & White, J.G. 2018. Biochar in Situ Decreased Bulk Density and Improved Soil-Water Relations and Indicators in Southeastern US Coastal Plain Ultisols. *Soil. Sci.* **183**(3), 99–111.

Wickham, H. 2007. Reshaping Data with the reshape Package. Journal of Statistical Software, **21**(12), 1–20. URL http://www.jstatsoft.org/v21/i12/

Wickham, H., Averick, M., Bryan, J., Chang, W., D'Agostino McGowan, L., Francois, R., Grolemund, G., Hayes, A., Henry, L., Hester, J., Kuhn, A., Pedersen, T.L., Miller, E., Bache, S.M., Müller, K., Ooms, J., Robinson, D., Seidel, D.P., Spinu, V., Takahashi, K., Vaughan, D., Wilke, C., Woo, K. & Yutani, H. 2019. Welcome to the tidyverse. *Journal of Open Source Software* **4**(43), 1686 https://doi.org/10.21105/joss.01686

Wickham, H. & Bryan, J. 2019. readxl: Read Excel Files. R package version 1.3.1. https://CRAN.R-project.org/package=readxl

Yargicoglu, E.N., Sadasivam, B.Y., Reddy, K.R. & Spokas, K. 2015. Physical and chemical characterization of waste wood derived biochars. *Waste Manage* **36**, 256–268. Retrieved from https://doi.org/10.1016/j.wasman.2014.10.029

Yoder, B.J. & Pettigrew-Crosby, R.E. 1995. Predicting nitrogen and chlorophyll content and concentrations from reflectance spectra (400-2500 nm) at leaf and canopy scales. *Remote Sens Environ* **3**(3), 199–211. Retrieved from https://doi.org/10.1016/0034-4257(95)00135-N

Yuan, H., Lu, T., Huang, H., Zhao, D., Kobayashi, N. & Chen, Y. 2015. Influence of pyrolysis temperature on physical and chemical properties of biochar made from sewage sludge. *J Anal. Appl. Pyrol*. **112**, 284–289. Retrieved from https://doi.org/10.1016/j.jaap.2015.01.010

Zhang, P., Zhang, X., Li, Y. & Han, L. 2020. Influence of Pyrolysis Temperature on Chemical Speciation, Leaching Ability, and Environmental Risk of Heavy Metals in Biochar Derived from Cow Manure. *Bioresource Technol*. **302**, 122850. https://linkinghub.elsevier.com/retrieve/pii/S096085242030119X

Agronomy Research **18**(4), 2512–2519, 2020
https://doi.org/10.15159/AR.20.203

Effect of seed inoculation and foliar fertilizing on structure of soybean yield and yield structure in Western Polissya of Ukraine

N. Novytska[1], G. Gadzovskiy[1], B. Mazurenko[1,*], S. Kalenska[1], I. Svistunova[2] and O. Martynov[3]

[1]National University of Life and Environmental Science, Department of Plant Science, Heroiv Oborony street 15, UA03041 Kyiv, Ukraine
[2]National University of Life and Environmental Science, Department of Fodder production, melioration, and meteorology, Heroiv Oborony street 13, UA03041 Kyiv, Ukraine
[3]Ukrainian Institute for Plant Variety Examination, Generala Rodimceva street 15, UA03041 Kyiv, Ukraine
[*]Correspondence: mazurenko.bohdan@nubip.edu.ua

Abstract. Growing soybeans requires adjustment of micronutrient nutrition on poorly fertile soils. Foliar fertilization can overcome the deficiency of micronutrients in plants in the most important period. Three factorial field experiment to study foliar fertilization with complex micronutrients, seed inoculation by *Bradyrhizobium japonicum* in two soybean varieties (Kassidy and ES Mentor) was conducted. Foliar fertilization with Quantum oil and WUXAL Oilseed significantly increased certain elements in soybean yield structure. Fertilizer WUXAL Oilseed with a higher concentration of Mo, Mn and B more effectively increased the number of pods and seeds from the plant and formed a higher yield in soybeans. Foliar fertilization with WUXAL Oilseed and Quantum oil increased seed yield to 3.00 t ha^{-1} and 2.94 t ha^{-1}, respectively in regard to variant without fertilizing, where yield was 2.71 t ha^{-1}. Variety Kassidy had greater number of pods and seeds, seed weight in comparison to foliar fertilizing ES Mentor. Seed inoculation gaves a stable increase in yield under different foliar fertilizations in varieties Kassidy and ES Mentor.

Key words: *Bradyrhizobium japonicum*, micronutrients, variety.

INTRODUCTION

Symbiosis of nodule bacteria and the soybean root system is an important element in increasing productivity. Nodule bacteria *Bradyrhizobium japonicum* can persist in the soil for a long time, but inoculation of seeds is guaranteed to form enough nodes (Shcherbakova et al., 2018). Inoculation is an important source of nitrogen for soybean plants, but nodule bacteria can provoke a deficiency of micronutrients for soybean plant (Pacovsky, 1986). Deficiency of certain micronutrients can adversely affect the process of bud formation, flowering and soybean formation. Application of micronutrients before flowering is an effective way to compensate soil deficit of these elements in (Yasari & Vahedi, 2012).

Foliar fertilizing with H_3BO_3 solution is inefficient, so application of available forms of complex micronutrients is more justified (Reinbott & Blevins, 1995). Complex fertilizers for foliar fertilization contain available forms of Mn, Mo, B and Zn (Hänsch & Mendel, 2009). Modern soybean genotypes are greater branched, so the B role in pod and seed formation is growing (Devi et al., 2012).

Positive effect of foliar Mo-fertilizing on yield is maximal in the flowering phase and decreases with late application (Campo et al., 2009). Soybean plants have varietal sensitivity to Mn, and foliar fertilization is more effective than soil application (Loecker et al., 2010).

Establishing the varietal sensitivity of soybean plant to foliar fertilizers with different concentrations of micronutrients allows to obtain stable soybean yields. Foliar fertilizing of inoculated and non-inoculated soybean plants can affect formation of elements of yield structure in different ways, what was tested on two soybean genotypes in a field conditions.

MATERIALS AND METHODS

Field experiment was carried out in 2017–2019 in Kovel district Volyn region, Ukraine (51° 14’ N; 24° 57’ E) conditions of Ukrainian Western Polissya. Physical and chemical characteristics of sod-podzolic soil are: humus content - 1.2%; pH_{KCl} - 7.2, available nitrogen - 72.8 mg kg^{-1}; P_2O_5 in acetic acid extract - 26.0 mg kg^{-1}; exchangeable potassium - 54.0 mg kg^{-1}; B - 0.16 mg kg^{-1}; Mo - 0.03 mg kg^{-1}; Mn - 2.5 mg kg^{-1} of soil; soil density 1.58 g cm^{-3}. Soil characteristics were established by state institution ‘Soil protective institute of Ukraine’ (Volyn department).

Climate conditions

Field experiment was conducted in 3 vegetation seasons (2017–2019). The average daily temperature of 1st vegetation season was 17.9 °C with maximum noticed in August (20 °C); precipitations sum was 311.4 mm. Second year (2018) of research was warmer than previous year. Average daily temperature was 19.2 °C with maximum in August (20.5 °C); precipitations sum was 429.2 mm. The last year (2019) of research was characterized by following parameters: daily average temperature was 18.6 °C with maximum obtained in June (21.8 °C), precipitations sum was 453.3 mm. All meteorological information collected from WMO #33173.

Experiment design

The experimental design was Randomized Complete Block with four replications. Its included 3 factors. Factor A was soybean cultivars: ES Mentor (early maturity, thousand seed weight 195–215 g, semi-determinate) and Kassidy (mid-early maturity, thousand seed weight 165–185 g, indeterminate). Factor B was seed inoculation (‘Legume Fix’, *Bradyrhizobium japonicum 532c*, 2×10^9 colony-forming units per 1 g) and variant without inoculation. Factor C was foliar fertilization by ‘Quantum Oil’ (P_2O_5 - 5%, K_2O - 9%, SO_3 - 3%, B - 0.6%, Zn - 1.2%, Cu - 1.2%, Mn - 1.2%, Mo - 0.015%, Ni - 0.01%, Co - 0.003%); WUXAL Oilseed (B - 6%, Mn - 5%, Mo - 0.25%, S - 3%); and variant without foliar fertilizing.

The size of elementary plot was 50 m^2 (25 m^2 was used for harvesting). Previous crop is winter wheat. Soybean was sown with 12.5-cm inter-row spacing with rate

65 seeds per square meter. Sowing time depended on soil temperature in 5 cm depth (sowing began at 10–12 °C). Seed was inoculated in the same day before sowing by 'Legume Fix' © (*Bradyrhizobium japonicum 532c*) with rate 2.5 kg t^{-1} seed. Fertilizing system included 100 kg ha^{-1} Azofoska ($N_{16}P_{16}K_{16}$) before ploughing, 150 kg ha^{-1} ammonium nitrate (N_{52}) and 110 kg ha^{-1} ammonium sulphate(N_{23}) before sowing. Foliar fertilizers were applied due recommendations: WUXAL oilseed was applied in BBCH 60-66 with rate 2 L ha^{-1}; Quantum Oil was applied in two terms - 2 L ha^{-1} in BBCH 50-59 and 1 L ha^{-1} in BBCH 71-73. Plant protection included application herbicide Bazagran (benthazone 480 g L^{-1}) in BBCH 11-13(soybean) and Haruma (Quizalofop-p-ethyl, 125 g L^{-1}) in BBCH 12-14 (cereal weeds).

Sampling

30 plants from each variant were analyzed to establish elements of yield structure of soybean. The number of pods per plants, seeds per plants, seed weight per plant and thousand seed weight for each variant were measured. Soybean yield was established by harvesting and seed yield, seed weight per plant and thousand seed weight was calculated to 14% moisture.

Statistical analysis

Fisher LSD was conducted for establishing significant difference between variants in yield structure (pods and seeds per plant, seed weight and thousand seed weight). *Analysis of variance* and *Tukey HSD* were conducted by Statistica 13.3 for year and average seed yield. Means of yield structure were presented with standard error (SE).

RESULTS AND DISCUSSION

Elements of soybean productivity

Varieties had a significant difference in terms of productivity. Foliar fertilizing and seed inoculation increased the average value of pods per plant and seed weight of each variety (Fig. 1), but some variants had no significant difference.

Variety Kassidy formed significantly more pods per plant than ES Mentor in all variants (Fig. 1, a). Seed inoculation had no significant effect 'number of pods per plant' in each cultivar, but number of pods increased by 4.8% at Kassidy and 3.1% at ES Mentor, compared to variants without innoculation. Foliar fertilizing significantly increased number of pods in the variety Kassidy in inoculated and non-inoculated variants.

Application of fertilizer with a higher B content (WUXAL Oilseed, B - 6%) also significantly increased the number of pods per plant compared with Quantum Oil (B - 0.6%) in the variants without seed inoculation. Increasing boron rateand time of application may influence on number of pods per plant. Foliar fertilizing with boron at a rate of 0.5 kg ha^{-1} compared to variant witout fertilizing significantly increased the number of pods, but a multiple increase in rate had less effect in this parameter (Devi et al., 2012). Apllied boron rate in this research is low (0.018 kg ha^{-1} in Quantum Oil, 0.12 kg ha^{-1} in WUXAL Oilseed), so increasing the rate of boron by few times had a strong effect on the number of pods in variety ES Mentor. In other side, variety Kassidy had no significant difference between variants of different foliar fertilizing. Certain varieties may not respond to fertilization of boron by increasing the number of pods

(Rerkasem et al., 1993) or boron fertilization have a less effect in some varieties (Ross et al., 2006).

Seed inoculation has a less effect on number of pods per plant, but it can improve this parameter in combination with foliar fertilizing by micronutrients (Jarecki et al., 2016). From the other side, seed inoculation can have a significant effect on number of pods per plant, but it needs a specific condition (Afzal et al., 2010; Ntambo et al., 2017). The maximum efficiency of nodule bacteria occurs during flowering, while the boron content in the plant is significantly reduced at that moment (Yamagishi & Yamamoto, 1994). Foliar fertilizing with boron should compensate deficit and promote the normal development of pods.

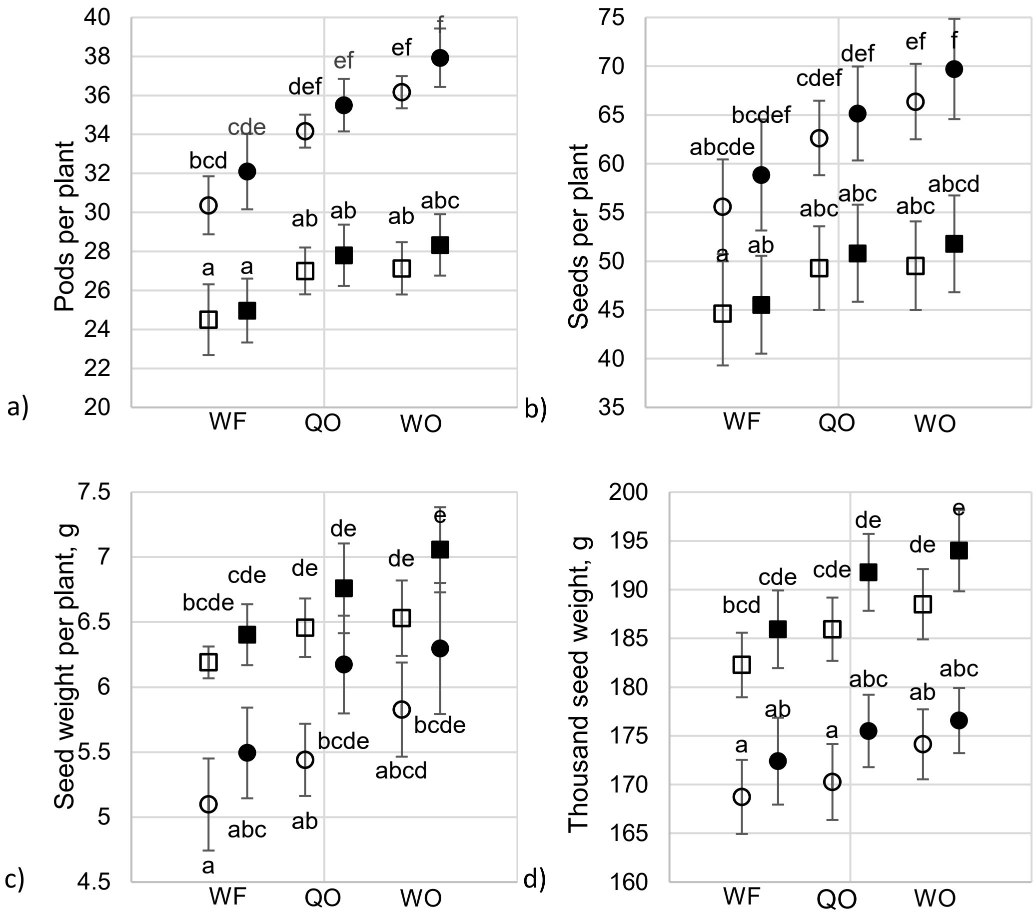

Figure 1. Elements of soybean yield structure depend on foliar fertilization and seed inoculation (□ – Kassidy, non-inoculated; ■ – Kassidy, inoculated; ○ – ES Mentor, non-inoculated; ● – ES Mentor, inoculated; WF – without fertilizing; QO – Quantum Oil; WO – WUXAL Oilseed, different superscripts denote statistical significance at $p \leq 0.05$ by Fisher`s post-hoc test).

Number of seeds per plants had same trend as the number of pods, but it had a greater variation of the average mean (Fig. 1, b). Number of seeds per plant did not differ significantly from the studied factors in variety ES Mentor. Seed inoculation did not have significant effect on seeds per plant in variety Kassidy, but foliar fertilizers was effective in this variety. Foliar fertilizing by WUXAL Oilseed significantly increased the number of seeds per plant compared to variant without fertilizers in inoculated and non-inoculated variants in both cultivars. Seed inoculation has a low effect on number of seeds per plant (Nyoki & Ndakidemi, 2018). Number of seed per plant has a large variation, but seed inoculation can improve number of seeds and decrease variation (Adeyeye et al., 2017).

Seed weight per plant of ES Mentor was much higher than its in variety Kassidy (Fig. 1, c). Foliar fertilization significantly increased seed weight in variety Kassidy by the treatment with WUXAL Oilseed. Fertilizing with Quantum oil had a same effect in innoculated variant in this variety, but efficiency was significantly lower in non-inoculated variant. Foliar fertilization increased seed weight per plant in variety ES Mentor, but this effect was without significant differences between variants. Seed inoculation increased the grain weight of the plant more than the number of beans, because it optimized the accumulation of dry matter, but did not affect the quantitative elements of yield structure. The same effect of seed inoculation is typical for other legumes, too (Shcherbakova et al., 2017).

Thousand seed weight varied the least depend on studied factors (Fig. 1, d). Variety ES Mentor formed larger seeds than Kassidy on average, which was manifested through seed weight per plant. Seed inoculation and foliar fertilizing had insignificant effect on this parameter, but they increase average means. Effect of foliar fertilizing by Mo has almost no effect on thousand seed weight, but affects its chemical content (Galindo et al., 2017). Inoculation has a low impact on thousand seed weight but improve efficiency of N accumulation in seed (Htwe et al., 2019).

Grain yield

All studied factors significantly affected soybean yield (Table 1). The largest participation (85.7%) in yield variation was due to weather conditions (year). Seed inoculation and foliar fertilization was due to only 6.5 and 6.1% variation, respectively. Interaction 'seed inoculation - foliar fertilizing' and 'seed inoculation - weather conditions (year)' had the significant effects, and other interactions were statistically insignificant.

Table 1. ANOVA for soybean yield (average 2017–2019)

Effect	MS	*p*	Participance, %	Significance
Cultivar(A)	0.247	< 0.001	1.3	*
Seed inoculation(B)	1.262	< 0.001	6.5	*
Foliar fertilization (C)	1.167	< 0.001	6.1	*
Year (Y)	16.542	< 0.001	85.7	*
B x C	0.013	0.009	0.1	*
B x Y	0.039	< 0.001	0.2	*
Others	< 0.01	> 0.05	0.1	ns

Soybean yields varied over the years, but the effect of the studied factors was through. Yield of variety ES Mentor significantly exceeded variety Kassidy (Table 2). Difference in yield between inoculated and non-inoculated variants was greater than between varieties in 2017. Foliar fertilization also had a significant effect on yield compared to variant without fertilization. There was no significant difference between the type fertilizers in 2017, but foliar fertilizing by WUXAL Oilseed significantly increased the yield of soybeans compared to variant without fertilization and Quantum Oil treated in 2018 and 2019. Application of WUXAL Oilseed insignificantly increased yield by 0.04 t ha^{-1} more than Quantum Oil in 2017. Difference between the type fertilizers was significantly in years with high amount of precipitations, foliar application by WUXAL Oilseed additionally increased yield by 0.09 and 0.07 t ha^{-1} compared to treatment with Quantum Oil in 2018 and 2019 accordingly.

Table 2. Grain yield of soybean, t ha^{-1}

Cultivar (A)	Inoculation (B)	Foliar fertilizing (C)			Average		
		Without fertilizing	Quantum Oil	WUXAL Oilseed	A × B	A	B
			2017				
ES Mentor	–	2.05	2.25	2.28	2.19^{b}	2.25^{b}	2.14^{a}
	+	2.17	2.39	2.37	2.31^{c}		2.27^{b}
Kassidy	–	1.92	2.15	2.21	2.09^{a}	2.17^{a}	
	+	2.05	2.30	2.36	2.24^{b}		
Average C		2.05^{A}	2.27^{B}	2.31^{B}			
			2018				
ES Mentor	–	2.93	3.08	3.25	3.09^{b}	3.21^{b}	3.05^{a}
	+	3.11	3.43	3.45	3.33^{d}		3.29^{b}
Kassidy	–	2.81	3.05	3.17	3.01^{a}	3.13^{a}	
	+	3.07	3.32	3.37	3.25^{c}		
Average C		2.98^{A}	3.22^{B}	3.31^{C}			
			2019				
ES Mentor	–	3.07	3.25	3.35	3.22^{b}	3.32^{b}	3.18^{a}
	+	3.22	3.48	3.52	3.41^{d}		3.37^{b}
Kassidy	–	2.95	3.18	3.27	3.13^{a}	3.23^{a}	
	+	3.14	3.39	3.45	3.33^{c}		
Average C		3.10^{A}	3.33^{B}	3.40^{C}			
Average 2017–2019							
ES Mentor	–	2.68	2.86	2.96	2.83^{b}	2.93^{b}	2.79^{a}
	+	2.83	3.10	3.11	3.02^{d}		2.98^{b}
Kassidy	–	2.56	2.79	2.88	2.75^{a}	2.84^{a}	
	+	2.75	3.00	3.06	2.94^{c}		
Average	C	2.71^{A}	2.94^{B}	3.00^{C}			

Different superscripts ($^{a, b, c \cdots}$ in column and $^{A, B, C}$ in rows) denote statistical significance at $p \leq 0.05$ by Tukey's post-hoc test.

Weather conditions were more favourable in 2018, so soybean formed a significantly higher yield. Inoculation increased the yield by 0.24 t ha^{-1} on average, which almost reached the effect of foliar fertilizing.

Variations in yield across treatments and genotypes, had a significant difference in 2019, compared with other years but exceeded yield in 2018 by only 0.1 t ha^{-1}. Difference between the varieties was similar to 2017 and 2018, but the efficiency of inoculation and foliar fertilizing decreased compare to 2018.

Inoculation increased yields by 0.19 t ha^{-1} on average over 3 years. Low efficiency of inoculation may be due to large rate of nitrogen fertilizers (N_{75}) applied before sowing. Formation the high yield of soybeans on poorly fertile soils is possible only with high rates of nitrogen fertilizers, and nitrogen fixation by nodule bacteria is only an additional source of nitrogen. Nodule bacteria may consume soil nitrogen instead of nitrogen fixation when applying nitrogen fertilizers, so the effect of inoculation on yield may be low or absent (Hungria et al., 2006).

Foliar fertilizing allowed significant increase of the soybean yield, and WUXAL Oilseed had a significantly higher effect than Quantum Oil treatment. Higher yield of fertilized varieties is due to the increase in the number of pods, seeds and, accordingly seed weight per plant. Foliar application with Mn an Zn microfertilizers can have a variety effect and responses to seed yield (Zolfaghari Gheshlaghi et al., 2019). Deficiency of certain micronutrients significantly reduce yields, even with a sufficient of others. Zn deficiency has a large impact on yield formation (Dimkpa et al., 2019). Application of micronutrient fertilizers has a positive effect on the formation of pods and seeds, and the rate of boron may play a key role in realizing yield potential (Sutradhar et al., 2017).

CONCLUSIONS

Seed inoculation is an effective way to increase soybean yields. Inoculation had different effects on the formation of yield parameters, but its effect on seeds yield was the same in both varieties. Inoculation had a greater effect on the number of pods, seeds, and seed weight per plant in variety Kassidy. Foliar fertilizing by WUXAL Oilseed had a significant effect on the number of pods and seeds compared to variant without foliar fertilizing. Inoculation and foliar fertilizing increased some yield elements insignificantly, but they had a significant impact on yield in general. Application of Quantum Oil increased the yield of soybeans by 8.5%, but fertilizer with greater boron concentration (WUXAL Oilseed) increased yield on 10.7%. Inoculation increased yield on 6.8%. Fertilizers with high boron content allowed to form more pods and seeds, which led to an increase in seed weight and yield in both studied varieties.

REFERENCES

Adeyeye, A.S., Togun, A.O., Olaniyan, A.B. & Akanbi, W.B. 2017. Effect of fertilizer and rhizobium inoculation on growth and yield of soyabean variety (Glycine max L. Merrill). *Advances in Crop Science and Technology* **5**(01), 1–9.

Afzal, A., Bano, A. & Fatima, M. 2010. Higher soybean yield by inoculation with N-fixing and P-solubilizing bacteria. *Agronomy for sustainable development* **30**(2), 487–495.

Campo, R.J., Araujo, R.S. & Hungria, M. 2009. Molybdenum-enriched soybean seeds enhance N accumulation, seed yield, and seed protein content in Brazil. *Field Crops Research* **110**(3), 219–224.

Devi, K.N., Singh, L.N.K., Singh, M.S., Singh, S.B. & Singh, K.K. 2012. Influence of sulphur and boron fertilization on yield, quality, nutrient uptake and economics of soybean (Glycine max) under upland conditions. *Journal of Agricultural Science* **4**(4), 1.

Dimkpa, C.O., Singh, U., Bindraban, P.S., Adisa, I.O., Elmer, W.H., Gardea-Torresdey, J.L. & White, J.C. 2019. Addition-omission of zinc, copper, and boron nano and bulk oxide particles demonstrate element and size-specific response of soybean to micronutrients exposure. *Science of the Total Environment* **665**, 606–616.

Galindo, F.S., Teixeira Filho, M., Buzetti, S., Santini, J.M., Ludkiewicz, M.G. & Baggio, G. 2017. Modes of application of cobalt, molybdenum and Azospirillum brasilense on soybean yield and profitability. *Revista Brasileira de Engenharia Agrícola e Ambiental* **21**(3), 180–185.

Hänsch, R. & Mendel, R.R. 2009. Physiological functions of mineral micronutrients (cu, Zn, Mn, Fe, Ni, Mo, B, cl). *Current opinion in plant biology* **12**(3), 259–266.

Htwe, A.Z., Moh, S.M., Soe, K.M., Moe, K. & Yamakawa, T. 2019. Effects of biofertilizer produced from Bradyrhizobium and Streptomyces griseoflavus on plant growth, nodulation, nitrogen fixation, nutrient uptake, and seed yield of mung bean, cowpea, and soybean. *Agronomy* **9**(2), 77.

Hungria, M., Franchini, J.C., Campo, R.J., Crispino, C.C., Moraes, J.Z., Sibaldelli, R.N., Mendes, I. & Arihara, J. 2006. Nitrogen nutrition of soybean in Brazil: contributions of biological N2 fixation and N fertilizer to grain yield. *Canadian Journal of Plant Science* **86**(4), 927–939.

Jarecki, W., Buczek, J. & Bobrecka-Jamro, D. 2016. Response of soybean (Glycine max (L.) Merr.) to bacterial soil inoculants and foliar fertilization. *Plant, Soil and Environment* **62**(9), 422–427.

Loecker, J.L., Nelson, N.O., Gordon, W.B., Maddux, L.D., Janssen, K.A. & Schapaugh, W.T. 2010. Manganese response in conventional and glyphosate resistant soybean. *Agronomy journal* **102**(2), 606–611.

Ntambo, M.S., Chilinda, I.S., Taruvinga, A., Hafeez, S., Anwar, T., Sharif, R., Chambi, C. & Kies, L. 2017. The effect of rhizobium inoculation with nitrogen fertilizer on growth and yield of soybeans (Glycine max L.). *International Journal of Biological Sciences* **10**(3), 163–172.

Nyoki, D. & Ndakidemi, P.A. 2018. Selected chemical properties of soybean rhizosphere soil as influenced by cropping systems, rhizobium inoculation, and the supply of phosphorus and potassium after two consecutive cropping seasons. *International Journal of Agronomy* **2018**. https://doi.org/10.1155/2018/3426571

Pacovsky, R.S. 1986. Micronutrient uptake and distribution in mycorrhizal or phosphorus-fertilized soybeans. *Plant and Soil* **95**(3), 379–388.

Reinbott, T.M. & Blevins, D.G. 1995. Response of soybean to foliar-applied boron and magnesium and soil-applied boron. *Journal of Plant Nutrition* **18**(1), 179–200.

Rerkasem, B., Bell, R.W., Lodkaew, S. & Loneragan, J.F. 1993. Boron deficiency in soybean [Glycine max (L.) Merr.] peanut (Arachis hypogaea L.) and black gram [Vigna mungo (L.) Hepper]: Symptoms in seeds and differences among soybean cultivars in susceptibility to boron deficiency. *Plant and Soil* **150**(2), 289–294.

Ross, J.R., Slaton, N.A., Brye, K.R. & DeLong, R.E. 2006. Boron fertilization influences on soybean yield and leaf and seed boron concentrations. *Agronomy Journal* **98**(1), 198–205.

Shcherbakova, E.N., Rots, P.Y., Mulina, S.A., Shcherbakov, A.V., Lactionov, Y.V., Yahina, L.M., Gonchar, L.N. & Chebotar, V.K. 2018. Inoculation technology for legumes based on alginate encapsulation. *Agronomy research* **16**(5), 2156–2168. https://doi.org/10.15159/AR.18.186

Shcherbakova, E.N., Shcherbakov, A.V., Andronov, E.E., Gonchar, L.N., Kalenskaya, S.M. & Chebotar, V.K. 2017. Combined pre-seed treatment with microbial inoculants and Mo nanoparticles changes composition of root exudates and rhizosphere microbiome structure of chickpea (*Cicer arietinum* L.) plants. *Symbiosis* **73**(1), 57–69.

Sutradhar, A.K., Kaiser, D.E. & Behnken, L.M. 2017. Soybean response to broadcast application of boron, chlorine, manganese, and zinc. *Agronomy Journal* **109**(3), 1048–1059.

Zolfaghari Gheshlaghi, M., Pasari, B., Shams, K., Rokhzadi, A. & Mohammadi, K. 2019. The effect of micronutrient foliar application on yield, seed quality and some biochemical traits of soybean cultivars under drought stress. *Journal of Plant Nutrition* **42**(20), 2715–2730.

Yamagishi, M. & Yamamoto, Y. 1994. Effects of boron on nodule development and symbiotic nitrogen fixation in soybean plants. *Soil Science and Plant Nutrition* **40**(2), 265–274.

Yasari, E. & Vahedi, A. 2012. Micronutrients impact on soybean (Glycine max (Merrill)) qualitative and quantitative traits. *International Journal of Biology* **4**(2), 112.

Agronomy Research **18**(4), 2520–2534, 2020
https://doi.org/10.15159/AR.20.193

Production of cellulose nanostructures from Chilean bamboo, *Chusquea quila*

P.E. Oliveira[1,*], X. Petit-Breuilh[2], O.J. Rojas[3] and W. Gacitúa[4]

[1]Department of Industrial Process Engineering, Nucleus of Research in Bioproducts and Advanced Materials, Catholic University of Temuco, Manuel Montt Street, Postal Code CL4813302 Temuco, Chile
[2]School of Engineering and Business, Viña del Mar University, Diego Portales Street, Postal Code CL2580022, Chile
[3]Department of Bioproducts and Biosystems, Aalto University School of Chemical Engineering, P.O. Box 16300, 00076 Aalto, Finland
[4]Postgraduate Department of Wood Engineering, Biomaterials and Nanotechnology Center, Bío-Bío University, Collao Avenue 1202, Postal Code CL4051381 Concepción, Chile
[*]Correspondence: poliveira@uct.cl

Abstract. In Chile, bamboo bushes of *Chusquea quila* genus (or popularly known as 'quila') have brought economic and ecological problems for decades in the south-central part of this country. On the other hand, this plant species was studied as a raw material for the production of nanofibrillated cellulose (CNF) and nanocrystalline cellulose (CNC), presenting an opportunity for sustainable and environmentally friendly management, positioning Chile as a Latin American country at the forefront of studies with nanotechnological approaches. The methodology applied to generate these nanostructures contemplated hydrolysis with sulfuric acid and oxalic acid, in addition to an intermediate stage of microfluidization to generate nanofibrillated cellulose. The products obtained showed morphological and topographic homogeneity in the scanning electron microscopy (SEM) and atomic force microscopy (AFM) images. The diameter values of the particles ranged from 10 to 20 nanometers for the CNCs. Through Fourier transformed spectrophotometry (FTIR) it was found that the processes of microfluidization and acid hydrolysis did not affect the molecular shape of the nanostructures and X-ray diffraction (XRD) was important to determine crystallinity index (IC), presenting values higher than 80%.

Key words: *Chusquea quila*, Chilean bamboo, cellulose nanofibrils, cellulose nanocrystals, acid hydrolysis.

INTRODUCTION

Bamboo is a naturally occurring composite material which grows abundantly in most tropical countries and has been used widely for household products and industrial applications, thanks to advances in processing technology and increased market demand. In Asian countries, bamboo has been used for a multitude of household utilities such as containers, chopsticks, woven mats, fishing poles, cricket boxes, handicrafts, chairs, etc.

It also finds a role in a variety of building applications, such as flooring, ceiling, walls, windows, doors, fences, roofs and trusses (Banga et al., 2015).

This species is considered a composite material because it consists mainly of cellulose fibres imbedded in a lignin matrix. Apart from these two constituents, hemicelluloses and other minor components are also present. In this composite system, cellulose fibres are aligned along the length of the bamboo, providing maximum tensile and flexural strength and rigidity in that direction (Wang & Shen, 1987). So far, over 1,200 bamboo species have been identified globally (Banga et al., 2015). Bamboo offers several advantages as a promising alternative feedstock to substitute for wood: fast growth and development, high productivity per hectare, low management costs and capital investment, and minimal energy expenditure in processing (Canilha et al., 2012). Based on these advantages, it is already being used in more than 4,000 different areas. Bamboo does not suffer from cracks or knots, which leads to far more evenly distributed stresses throughout the length of pieces.

In Chile, the genus Chusquea is represented by 11 species, of which *Chusquea quila* is among those with the greatest potential as a source of cellulose (Oliveira et al., 2016). Traditionally, this native species has been regarded as brush-wood. Its main habitat is the forest of the provinces of Cautín, Valdivia, Llanquihue and Chiloe, with an altitude distribution from sea level up to 800–900 m.

Oliveira et al., 2018 reports a delignification process which can be applied to 'quila' to produce crystalline cellulose, an important resource for obtaining cellulose nanofibres or nanocrystals. Alternatively, the crystalline cellulose can then be subjected to fermentation processes, making it a useful raw material for biofuel production. The treatment studied is an oxidative treatment at low concentration (15% v/v), for short time periods (10, 20 min) and at temperatures between 100 and 140 °C, which produces alpha-cellulose fibres with high crystallinity (over 70%) and low residual lignin content (< 2%). The morphology of the cellulose fibres was analysed by scanning electron microscope, revealing a smooth surface containing many fibrils. Infrared spectroscopy was used to identify functional groups, showing that almost 99% of the lignin was removed.

Biodegradable plastics and biocompatible compounds from lignocellulosic sources are promising materials which could replace synthetic polymers and reduce dependence on fossil fuels (González et al., 2013). Among these, nanostructured cellulose has unique characteristics which are of interest for the development of new materials, including high strength and rigidity; mechanical and barrier properties, biocompatibility and low density (Lin et al., 2015).

In Federal University of Lavras (Department of Agricultural Engineering), Ferraz et al (2020) study use of lignocellulosic materials residue in cement composites has one of the rises as sustainable building materials in most developing countries. Besides, this alternative is seen as a good option for new cement panels formulations for indoor applications. In this case, the research aims to evaluate de chemical properties of five potential lignocellulosic materials residues to be used for cement panels reinforcement: Eucalyptus, sugarcane bagasse, coconut fibre, coffee rusk, and banana pseudostem. The physical properties of the lignocellulosic materials were evaluated such as lignin, extractives, ash, and holocellulose.

Today, the most frequently source of cellulose nanocrystals is wood. However, there is growing interest in alternative sources with rich lignocellulosic composition. In the last 10 years, there has been an increase in the number of reports using other resources, for example, from biomass derived from the agri-food industry. Meanwhile in tropical countries (in Asia, Africa and the Americas) interest has focused on non-wood forest species such as shrubs and bamboos.

Some of the common non-wood resources used to produce cellulose nanofibers include bamboo (Li et al., 2015), wheat straw (Chen et al., 2011), New Zealand flax *Phormium tenax* (Fortunati et al., 2013), banana skins (Khawas & Deka, 2016), orange peel (Hideno et al., 2014) and palm oil industry waste (Fatah et al., 2014). Bamboo, the species selected for this study, grows in abundance in most tropical countries and is a material with a complex cell structure. It has been widely used in products for home use and industrial applications, owing to advances in processing technologies and increased market demand (Banga et al., 2015).

Among these, *Chusquea* is a genus of bamboo found in Chile, with eleven species, with *Chusquea quila,* or simply quila, being one of the most abundant. For years, quila has created environmental and economic problems for farmers in southern Chile. During flowering, it promotes an increase in the mouse population (Schlegel, 1993) and in summer it presents a high fire risk due to the accumulation of dry biomass (CONAF, 2012). In addition, it forms a dense scrub which occupies land that could otherwise be used for farm production (Pinto & Barrientos, 1993).

According to preliminary studies by Oliveira et al., 2016, its chemical composition, bamboo, quila, contains 54.7% cellulose; 13.8% lignin; 4.6% extractable compounds and 2.2% ash. Its particularly high cellulose content, together with the structural characteristics of the lignocellulosic matrix, is a promising resource from which cellulose nanomaterials can be obtained. The objective of the present study was to investigate the potential of *Chusquea quila* as a source of cellulose nanofibrils, CNF and cellulose nanocrystals. CNCs were obtained following two protocols: via acid hydrolysis to produce nanocrystals directly using the quila cellulose and physical microfluidization to obtain CNF which was then finally hydrolysed to CNC.

MATERIALS AND METHODS

Preparation of cellulose nanostructures from Chusquea quila

Quila samples presented colour variations from opaque to shiny green; and were generally covered with algae, lichens and mosses. According to previous studies, the best age to harvest the canes is 1.5 to 2 years, when they are mature, and their structure is strongest. Samples were selected following the methodology of Campos et al. (2003). The bamboo was collected from local farmers in Temuco and Freire (towns in the Araucanía Region, Chile). Samples approximately 2 metres in height were cut 20 cm above ground level. They were prepared by eliminating impurities from the surface by washing (maintaining the outer skin) and then converted to chips for analyses and reactive oxidation.

The process for obtaining cellulose fibres from quila followed Oliveira et al., 2018. Briefly, the bamboo was oxidised with a low concentration of peracetic acid (15% v/v) for short periods of time (10 and 20 minutes) at 100 and 120 °C. The produced cellulose fibres had an apparent crystallinity index of alpha-cellulose of 78% and residual lignin content less than 2% (Kappa number 12.34).

The proposed methods for isolation of cellulose nanostructures is shown in Fig. 1. Quila cellulose fibres were first reduced to particles (150 to 80 µm) in an ultra-centrifugal mill (ZM200 Ultra-Centrifugal Mill, Retsch GmbH, Haan, Germany). The first method for obtaining nanocrystalline cellulose followed Brinchi et al., 2013 for obtaining cellulose nanocrystals using sulphuric acid. The second method used involved acid hydrolysis with oxalic acid, following Abraham et al., 2011.

Treatments were divided into the following stages: (1) Acid hydrolysis of pure cellulosic material (15 g of quila cellulose) under strictly controlled conditions which included temperature in a thermo-regulated bath (45 °C), time (45min), shaking (35 rpm), acid concentration 55% v/v sulphuric acid and 5% w/v oxalic acid hydrolysis. The same ratio of acid solution/cellulose, 1:20 (gm L^{-1}), was used in both cases; (2) Dilution with distilled water to stop the reaction and repeated washing by successive centrifugation; (3) Extensive dialysis to eliminate any free acid (72 hours repeated exchange with distilled water); (4) Mechanical sonication (20 minutes) to disperse the nanocrystals as a stable, uniform suspension; (5) Ultra-centrifugation to obtain a concentrated CNC suspension.

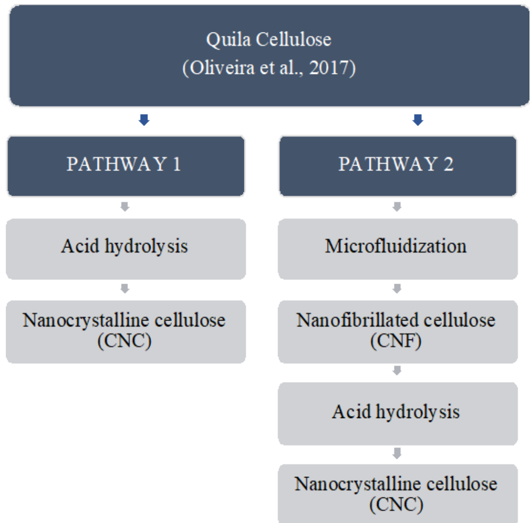

Figure 1. Synthesis methods to obtain nanostructures (nanocrystals and nanofibrillated cellulose) from *Chusquea quila*.

The second method to obtain CNC included an intermediate quila cellulose fibre microfluidization stage (Junka et al., 2014). In this stage, cellulose was diluted in ultra-pure water (Water for chromatography, LC-MS Grade, LiChrosolv®. CAS 7732-18-5), at a concentration of 1% w/v, for 24 hours. Then the suspension was subjected to high pressure fluidization (Microfluidics Corporation, model M-110P, Newton, Massachusetts, USA) at operating pressures of 69 MPa (10,000 psi), 138 MPa (20,000 psi) and 207 MPa (30,000 psi). The suspension obtained was centrifuged to eliminate excess water and then stored as a hydrogel (5% dry weight). Finally, the quila CNF was subjected to acid hydrolysis under the same conditions as in the first method to obtain quila CNC.

Final yield (Y) of CNC was determined by calculating the total nanocrystalline cellulose mass obtained compared to the initially hydrolyzed fiber mass as demonstrated in Eq. 1 (Beltramino, 2016). In brief, 25 mL (in triplicate) of each suspension was measured in tared beakers. The CNC suspensions were evaporated at 50 °C until constant weight; and, after cooling in a desiccator, total mass was determined.

$$Yield\ (\%) = \left(\frac{(a-b)\cdot total\ volume(mL)}{dried\ volume\ (mL)\cdot fibers\ mass(g)}\right)\cdot 100 \qquad (1)$$

Characterization of the cellulose nanostructures

Concentration of carboxyl groups in CNC was determined by conductimetric assessment following Katz et al. (1984). Briefly, a dry sample was dispersed in 15 mL HCl (0.01M) to exchange the sodium cations bound to the COO^- groups for protons (H^+). This suspension was shaken for 10 minutes and conductivity was determined in a nitrogen atmosphere. The assessment was completed by adding 0.1 mL of a solution of NaOH (0.01M) and recording the conductivity value. This operation was repeated until constant conductivity was reached. The titration profile revealed the presence of a strong acid (HCl) and a weak acid, the carboxyl content.

Morphology of the nanofibrillated structures derived from the quila fibres was characterised by scanning electron microscopy (SEM, Zeiss Sigma VP, Carl Zeiss Microscopy Ltd, Cambridge, UK). Operating voltage was 2 kV to 3 kV, and the working distance was between 2.5 mm and 2.6 mm. Sample drops of CNF at a consistency of approximately 0.1% were dried on polished aluminium supports and gold-coated to provide the required conductivity.

Fourier transform infra-red spectrophotometry (FTIR) was used to identify the characteristic functional groups of quila CNC and CNF. Samples were measured using a Bio-Rad FTS 6000 spectrophotometer (Cambridge, MA, USA) with a photo-acoustic detector and a constant mirror velocity of 5kHz, resolution 8 cm^{-1} and 1.2 kHz filter.

X-ray diffraction (XRD) was used to determine the crystallinity of the nanocrystalline cellulose. X-ray diffraction analysis was carried out on fibres dried at 60 °C for 24 h in an ED53 chamber stove (Binder GmbH, Germany). Samples weighing approximately 1 g were compressed in a 25 mm diameter matrix at 4 kPa for 5 min. The discs were mounted on the rotating sample holder (15 rpm) of a D2 Phaser diffractometer (Bruker, Germany). The equipment used filtered Ni-Cu radiation (30 kV and 10 mA), 1 mm divergence slit, 1 mm anti-dispersion slit, 2.5° Soller slits and a LYNXEYE™ detector. The alignment was checked regularly with the NIST SRM1976 alumina plate standard. The patterns were collected over a range of 5–45°, counting 5 seconds per 0.01° pass. The crystallinity index (CI) was calculated according to the method of Segal et al., 1959. In order to ensure minimum statistical validity, each analysis was repeated with at least three different samples.

Atomic force microscopy (AFM, NanoScope IIIa Multimode, Digital Instruments Inc., Santa Barbara, CA, USA) was udrf to assess nanoscale topography of the fibrils and crystals. The recorded images were adjusted using NanoScope Analysis 1.2 software.

RESULTS AND DISCUSSION

We tested hydrolysis reactions with a mineral acid (sulphuric acid - H_2SO_4), and an organic acid (oxalic acid). Fig. 2 includes a schematic illustration of both methods.

Method 1, acid hydrolysis with oxalic acid, yielded no nanocrystals. This result was due to the format of the molecular structure of cellulose, which is characteristic of bamboo, i.e., oriented along the length of the bamboo fibre, giving strength, flexion and rigidity in that direction (Chattopadhyay et al., 2011).

The CI obtained was 75.56%, close to the value for cellulose fibre prior to hydrolysis. The X-ray diffraction pattern in Fig. 3 shows the similarity between the structures of hydrolysed and unhydrolyzed cellulose. The amorphous cellulose predominates close to the macrofibrillated surface, leading to the exposure of the bundles of microfibrils (Zhao et al., 2007). The loss of this amorphous cellulose surface did not significantly alter the apparent crystallinity of the cellulose, since the amount was very small (CI almost 15%) when compared with the volume of amorphous cellulose.

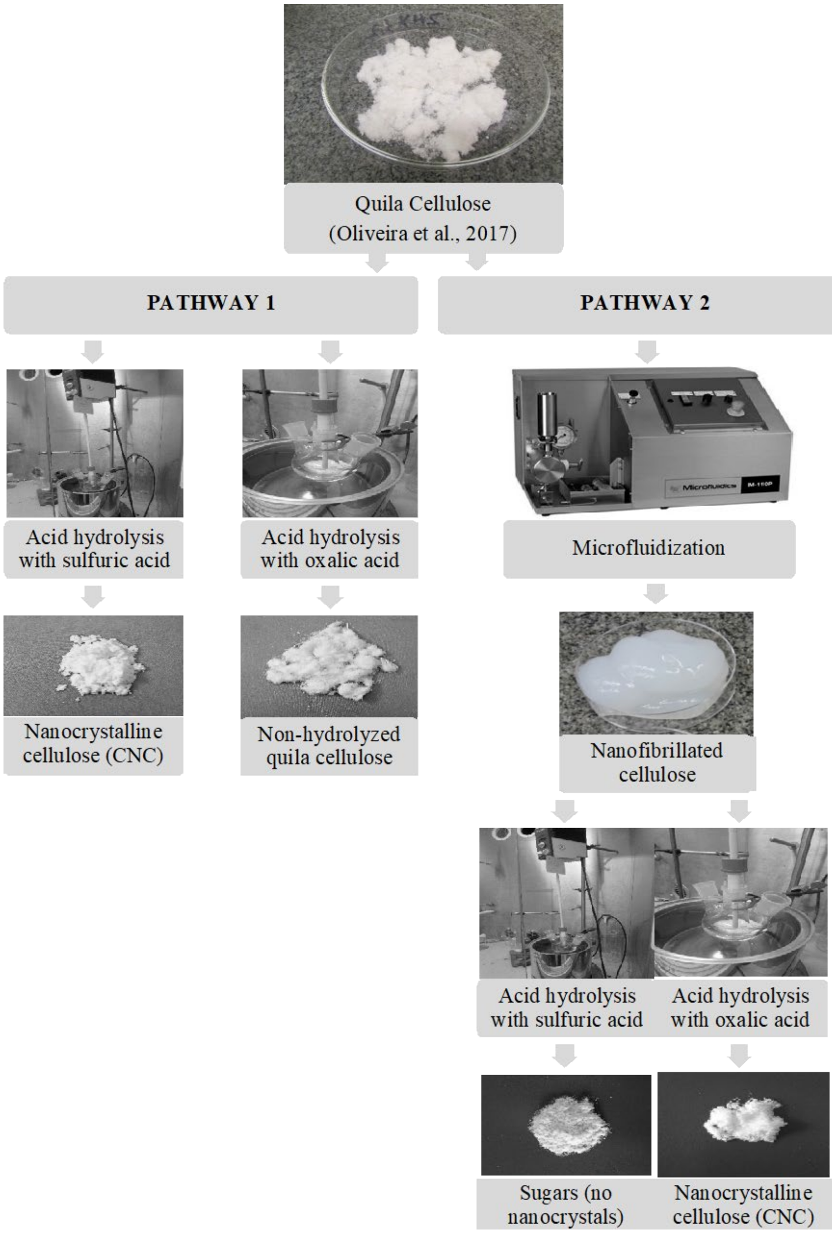

Figure 2. Photographic diagram of pathways 1 and 2 used in this study.

Most cellulosic materials consist of crystalline and amorphous domains, in varying proportions, depending on both source and history. The physical properties of cellulose, as well as their chemical behavior and reactivity, are strongly influenced by the arrangement of the cellulose molecules with respect to each other and to the fiber axis, as well. Most of the reactants penetrate only the amorphous regions and it is only in these regions with a low level of order and on the surface of the crystallites that the reactions can take place, leaving the intracrystalline regions unaffected (Ciolacu et al., 2011).

After dialysis and sonication, the supernatant of the hydrolysed sample was examined by atomic force microscopy (AFM) to identify the presence of nanoparticles, however no nanocrystals were found.

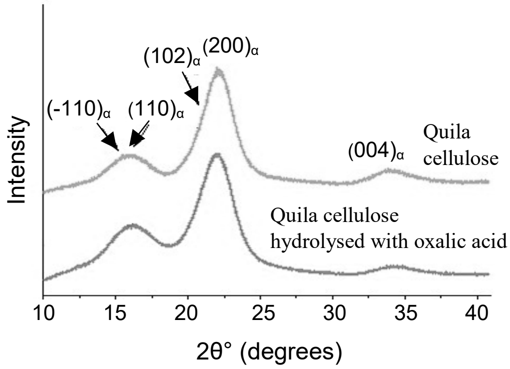

Figure 3. XRD diffractogram of the sample hydrolysed by oxalic acid (Method 1).

Were found no nanocrystals in the product obtained by hydrolysis of nanofibrillated cellulose with sulphuric acid (Method 2). According to Kumar et al. (2009), this process may have generated mainly monomers from fermentable sugars. Minerals acids first attack the amorphous regions in cellulose and nanocellulose, since they are more susceptible to degradation. In the methodology applied, we considered the possibility that sugars were generated (degradation of nanofibers).

In the event that in the future is necessary to determine what types of sugars were formed as a result of this hydrolysis process, the study by Meile et al., 2018 could be used as a guide. Their work consisted of obtaining quantitative results from the determination of sugar in birch wood hydrolyzates using two iodometric titration methods and UPLC-ELSD. Both analytical methods showed acceptable precision with a relative standard deviation < 5% and xylose recovery from an enriched sample of approximately 90% and could be used to control the performance of sugars in the wood pretreatment process.

After the hydrolysis stage, we recovered the supernatant from the hydrolysed sample for examination via atomic force microscope (AFM), however no suspension could be recovered from the dialysis process. The alternative was to bring the solution to neutral pH and lyophilise the mixture.

Table 1. Yields of CNC and CNF

Raw material	CNC (Y%)	References	Raw material	CNF (Y%)	References
Banana waste	27	Bolio-López et al., 2011	Bleached eucalyptus pulp	> 95	Beltramino, 2016
Residues of *Furcraea bedinghausii*	2	Espitia, 2010	Banana waste	64	Bolio-López et al., 2011
Bamboo pulp	21.8	Hong et al., 2013	Poplar cellulose kraft pulp	86	Qinghua et al., 2013
C. quila Route 1	32 ± 0.3	This work	Hibiscus cannabinus (kenaf)	67	Safwa et al., 2015
C. quila Route 2	1.2 ± 0.3	This work	C. quila cellulose	91 ± 0.5	This work

The treatments which formed cellulose nanocrystals, Method 1, included acid hydrolysis with sulphuric acid, and Method 2, acid hydrolysis of nanofibrillated cellulose with oxalic acid. Table 1 shows, in the first column, the empirical results obtained in this Chusquea quila study compared with other lignocellulosic sources reported in different manuscripts. It can be seen that, related to yields, the treatment with Chilean bamboo has better yields, which can be verified by the study by Abraham et al., 2011 when it refers to the need to study different raw materials.

Concentrations of the carboxyl groups were determined by conductivity titration of the CNC samples. Results for the product of hydrolysis with sulphuric acid (Method 1) was 1.47 mmol g^{-1}, indicating that the carboxyl groups on the CNC surfaces were not affected by acid hydrolysis with H_2SO_4 (reference value, 1.50 mmol g^{-1}, Salajková et al., 2016). The nanocrystalline cellulose produced by hydrolysis with sulphuric acid was accompanied by the formation of sulphate esters on the surface. One of the main problems was that the sulphate remnants on the surfaces of the nanocrystals were very unstable, however they were able to be eliminated by alkaline treatment. To improve dispersion in water, oxidation reactions were used to convert primary hydroxyls (C6) into carboxylic acid groups, which are more chemically stable than sulphate esters (Habibi et al., 2010). The product of acid hydrolysis of CNFs by oxalic acid (Method 2) presented a concentration of 1.63 mmol g^{-1}.

The morphology and topography of cellulose nanofibers were investigated with scanning electron microscopy (SEM) and atomic force microscopy (AFM). Fig. 4 shows that microfluidization produced a fine, homogeneous, uniform CNF network structure. Although it is difficult to measure the width and length of the nanofibers, 10–30 nm and 2,000–3,000 nm were estimated in the present case, respectively.

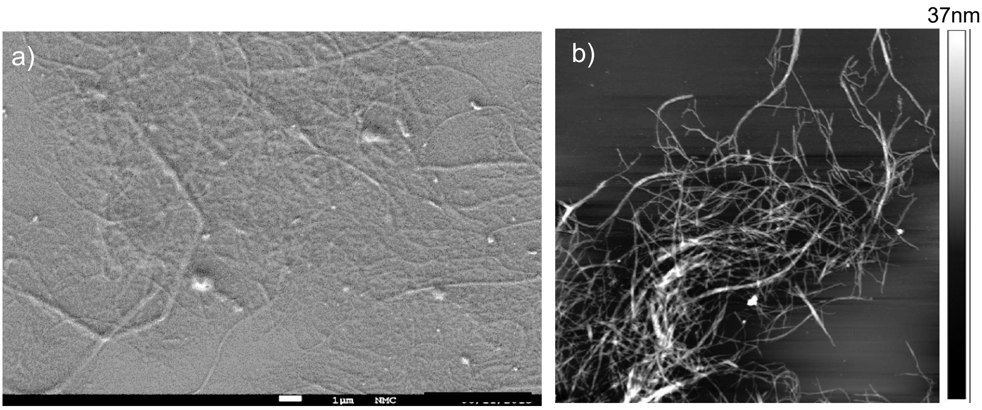

Figure 4. a) Scanning electron microscopy (SEM) and b) atomic force microscopy (AFM) of CNF from quila cellulose.

Fig. 5 shows size differences of the crystals isolated by Method 1 (acid hydrolysis with sulphuric acid) and Method 2 (acid hydrolysis of CNF with oxalic acid). The crystals in Fig. 5, a are heterogeneous in both size and shape (more sharply pointed). Meanwhile, the crystals in Fig. 5, present a more homogeneous form and suggest a trend towards regular size. It should be noted that CNC produced with mineral acids have a greater tendency of degradation, depending on the type of cellulose used and reaction time, suggesting the formation of smaller crystals (Wang et al., 2014). In fact, the presence of sulphate groups on the NCC results in negatively charged surfaces that repel each other and do not allow the aggregation of the NCC by hydrogen bonding (Marchessault et al., 1961).

The sulphate esters produced during acid hydrolysis can decompose as the temperature increases, forming an organic sulphate that causes the dehydration of the cellulose due to the low energy required to remove the acid sulphate from the sulphated anhydroglucose units, then the sulfuric acid considered as a catalyst for dehydration. Then, the decomposition involves both the dehydration reaction and the increase in the formation of gas, carbonyl compounds, carboxyl and carbon residues (Wei et al., 1017).

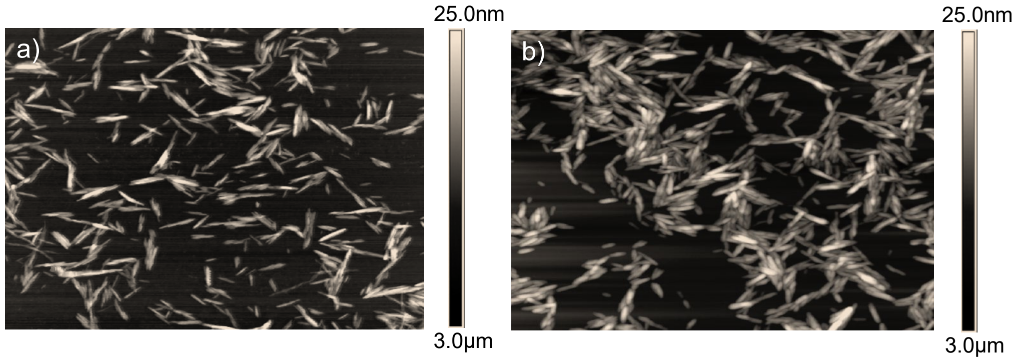

Figure 5. Atomic force microscopy images of CNC obtained by Methods 1 and 2.

Width of the cellulose nanocrystals was measured with ImageJ processing software (IJ 1.46) using images obtained AFM. Twelve AFM images were used to measure the size distribution. Histograms for width distribution are presented in Fig. 6. The diameters of the product of Method 1, Fig. 6, a presented variable frequency, with a maximum distribution range between 10 and 15 nm. Fig. 6, b shows a more uniform diameter distribution, between 10 and 25 nm.

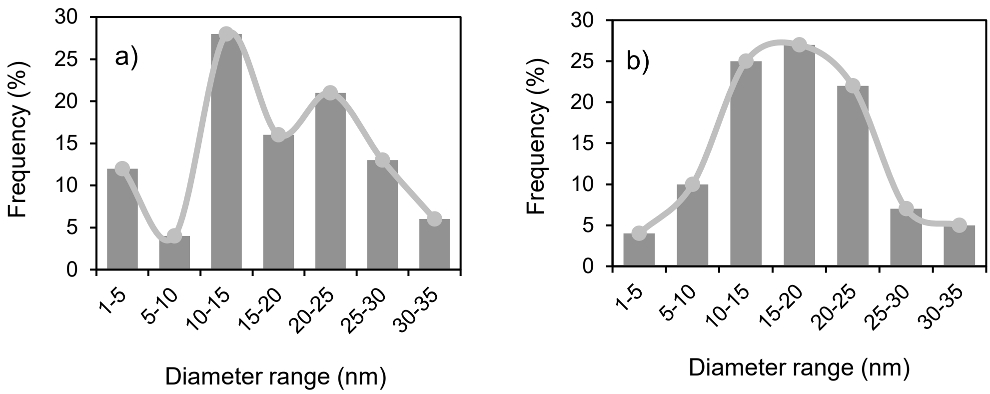

Figure 6. Width distribution histograms for nanocrystalline cellulose produced by Methods 1 (a) and 2 (b).

The study carried out by Oliveira et al. (2018), the processes of delignification and bleaching of cellulose used in this research are considered in detail. The methodology details the oxidation reactions using 15% (v/v) peracetic acid. During the acid hydrolysis that we estimate here, most of the amorphous part of cellulose was eliminated, remembering the successful processes: Method 1 hydrolysis using sulfuric acid and Method 2 using oxalic acid.

The crystalline parts of cellulose have a high resistance to acid hydrolysis (Vanhatalo & Dahl, 2014). Fig. 7 shows the FTIR spectrum of nanofibrillated quila cellulose and the nanocrystalline cellulose of the two proposed Methods. As indicated by Rosli et al. (2013), the peak 1,735 cm^{-1} belonged to C = O and C-O of the acetyl groups, uronic ester and the aryl group in hemicellulose and lignin, respectively. During the delignification phase, carbohydrates are very stable and in the bleaching phase, there was an increase in carbohydrate degradation when about 90% of the lignin was oxidized (Zimmermann et al., 1992). The peaks 3,440–3,300 cm^{-1} belong to the free stretch of OH of the hydroxyl group in the cellulose molecules. In addition, the peak at 2,887 cm^{-1} belongs to the C-H stretch (Wang et al., 2007).

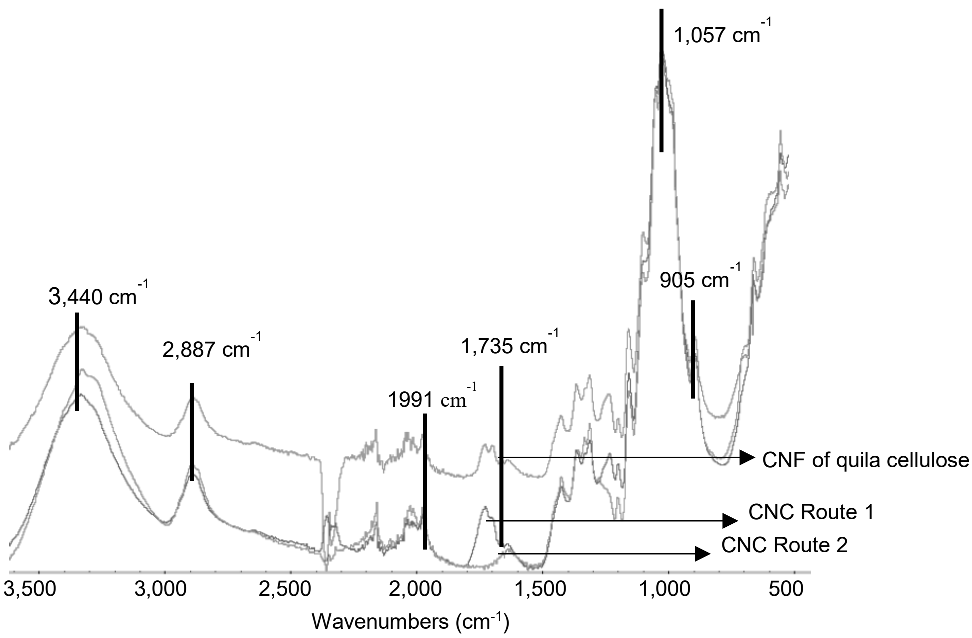

Figure 7. FTIR spectrum of CNC and CNF from quila cellulose.

The C-O-C bond of the pyranose skeletal ring can be observed at 1,057 cm^{-1}, which increases the intensity of this bond due to the increases in the crystallinity of the samples. The most significant absorption bond of 905 cm^{-1} has been related to the CH bond of glycoside deformation and OH flexion, these properties are characteristic of the β-glycosidic bond between the anhydroglucose units in cellulose (Razalli et al., 2017). No significant difference was found in the FTIR spectrum between CNF and CNC, suggesting that their molecular chemical structures remained practically unaltered during microfluidization and acid hydrolysis.

Cellulose nanofibers presented a clear, characteristic peak at diffraction angle 2θ = 22.7° (Fig. 8). X-ray diffraction analysis showed that the nanofibers analysed in this study had a crystallinity index > 80%. The CI value for nanofibrillated quila cellulose was 85%, while the nanocrystals isolated by Methods 1 and 2 presented indices of 92 and 88%, respectively. The slightly lower crystallinity in the sample from Method 2 could be explained by the fact that the size reduction of the crystalline cellulose structure (CNF) leads to a lower volume of crystals (Method 2, acid hydrolysis of nanofibrillated cellulose using oxalic acid), and therefore, a reduction in crystallinity (Qinghua et al., 2013).

It is important to remember that hemicellulose and lignin exist naturally in an amorphous form in the biomass, while the cellulose macromolecule is a pure crystalline structure. For cellulose, changes in crystallinity reflect changes in the composition and structure of plant fibers (Li et al., 2014). This study showed that the crystalline form of cellulose did not change during the treatment, but the crystallinity of the fiber was substantially improved. From the raw material (quila cellulose) the crystallinity index increased regardless of the treatment method since the non-crystalline region in the cellulose was gradually eliminated in each stage. It is noted that the bleaching process did not destroy the cellulose structure by fractionating hemicellulose and lignin.

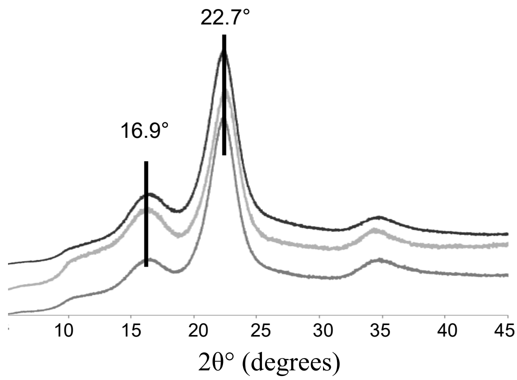

Figure 8. XRD diffractogram of quila cellulose CNC and CNF.

From the diffraction pattern obtained from CNC, the high-intensity peak was noted at 2θ reflection assigned to the crystallographic plane = 22.7° (arising due to diffraction from the plane (200)), with additional double peak signals at = 15° and 16.9° due to the reflections of (110) and (110) diffraction, respectively. The higher value of the given index shows that the test material has a high degree of crystallinity with an adequate order structure. The treatments with chemical products can alter the order in the structure and, in the case of CNC, reach a higher value due to the elimination of the amorphous state of cellulose (Theivasanthi et al., 2018).

From another perspective, prior milling can help the action of hydrolysis in amorphous regions of cellulose fibres, leading to crystal separation. This process has been reported with positive results in fibres of *Pinus banksiana* (jack pine) (Rambabu et al., 2016).

CONCLUSIONS

Chilean bamboo *Chusquea quila* was used as source of nanocrystalline and nanofibrillated cellulose. Two alternative methods were introduced for obtaining these nanostructures. Methods involved acid hydrolysis of the cellulosic fibres with an intermediate microfluidization stage. Method 1 used direct hydrolysis of quila cellulose fibre using sulphuric acid; and Method 2 involved an alternative stage of fibre microfluidization to produce CNF, followed by hydrolysis with oxalic acid. The yield was higher for Method 1.

Morphological analysis of the nanofibrillated quila cellulose showed a fine, homogeneous, uniform network structure. The AFM images of the nanocrystalline celluloses showed small differences for Method 1 and Method 2. These nanocrystals had widths between 10 and 20 nm. FTIR analysis indicated that the microfluidization and acid hydrolysis processes did not affect the molecular form of the nanostructures. X-ray diffraction showed crystallinity values higher than 80%.

Our results indicate the potential of quila to open up new opportunities as a lignocellulosic species for promoting sustainable, environmentally friendly products.

ACKNOWLEDGEMENTS. This study was supported by the Wood Engineering Department of Universidad del Bío-Bío (Chile) and the Biomaterials and Nanotechnology Centre from the same university. We are grateful to the support of members of the Bioproducts and Advanced Materials Nucleus of Catholic University of Temuco (Chile) and our special thanks goes to the Biobased Colloids and Materials, BiCMat research group led by Dr. Orlando Rojas, in University of Aalto, Finland.

REFERENCES

Abraham, E., Deepa, B., Pothan, L.A., Jacob, M., Thomas, S., Cvelbar, U. & Anandjiwala, R. 2011. Extraction of nanocellulose fibrils from lignocellulosic fibres: A novel approach. *Carbohydrate Polymers* **86**, 1468–1475. doi: 10.1016/j.carbpol.2011.06.034

Banga, H., Singh, V.K. & Choudhary, S.K. 2015. Fabrication and Study of Mechanical Properties of Bamboo Fibre Reinforced Bio-Composites. *Innovative Systems Design and Engineering* **6**(1), ISSN 2222-2871.

Beltramino, F. 2016. *Enzymatic-assisted preparation of nanocrystalline cellulose from non-wood fibers*. Pages 4–1 to 4–7. PhD Tesis. Programa de Doctorat d'Enginyeria Tèxtil i Paperera. Universidad Politécnica de Catalunya – España. (in Spanish).

Bolio-López, G.I., Valadez-González, A., Veleva, L. y Andreeva, A. 2011. Cellulose whiskers from agroindustrial residues of banana: obtaining and characterization. *Revista Mexicana de Ingeniería Química* **10**(2), 291–299. ISSN 1665-2738 (in Spanish).

Brinchi, L., Cotana, F., Fortunati, E. & Kenny, J.M. 2013. Production of nanocrystalline cellulose from lignocellulosic biomass: technology and applications. *Carbohydrate Polymers* 2013 Apr 15, **94**(1), 154–169. doi: 10.1016/j.carbpol.2013.01.033

Campos Roasio, J., Peñaloza, R., Kahler, C., Poblete, H. & Cabrera, J. 2003. Bamboo in Chile. Book published by the Technological Research Corporation of Chile, FONDEF Project D98I1002, pp. 41–51. Santiago, Chile (in Spanish).

Canilha, L, Chandel, A.K., Milessi, T.S., Antunes, F.A., Freitas, W.L., Felipe, M.G. & Silva, S.S. 2012. Bioconversion of sugarcane biomass into ethanol: an overview about composition, pretreatment methods, detoxification of hydrolysates, enzymatic saccharification, and ethanol fermentation. *Journal of Biomedicine and Biotechnology* Volume **2012**, Article ID 989572. doi: 10.1155/2012/989572

Chattopadhyay, S.K., Khandal, R.K., Uppaluri, R. & Ghoshal, A.K. 2011. Bamboo fiber reinforced polypropylene composites and their mechanical, thermal, and morphological properties. *Journal of Applied Polymer Science* **119**, 1619–1626. doi:10.1002/app.32826

Chen, W.S., Yu, H.P., Liu, Y.X., Hai, Y.F., Zhang, M.X. & Chen, P. 2011. Isolation and characterization of cellulose nanofibers from four plant cellulose fibers using a chemical-ultrasonic process. *Cellulose* **18**, 433–442. doi: /10.1007/s10570-011-9497-z

Ciolacu, D., Ciolacu, F. & Popa, V.I. (2011. “Amorphous cellulose – structure and characterization”. *Cellulose Chemistry and Technology* **45**(1–2), 13–21.

(CONAF) National Forestry Corporation. 2012. Manual with Measures for the Prevention of Forest Fires (*Technical Report*), Ministry of Agriculture, Santiago, Chile (in Spanish).

Espitia, H.M. 2010. *Isolation of cellulose nanofibers from agro-industrial residues of sugar cane and sugarcane, with potential application in thermoplastic polymer reinforcement* Master's thesis. Universidad Nacional de Colombia, Facultad de Ciencias, Escuela de Química, Sede Medellín – Colombia. https://repositorio.unal.edu.co/handle/unal/69993 (in Spanish).

Fatah, I.Y., Khalil, H.P.., Hossain, M.S., Aziz, A.A., Davoudpour, Y. & Dungani, R. 2014. Exploration of a chemo-mechanical technique for the isolation of nanofibrillated cellulosic fiber from oil palm empty fruit bunch as a reinforcing agent in composites materials. *Polymers* **6**, 2611–2624. doi: 10.3390/polym6102611

Ferraz, P.F.P., Mendes, R.F., Ferraz, G.A.S., Rossi, G., Conti, L. & Barbari, M. 2020. Chemical analyses of lignocellulosic materials residue for cement panels reinforcement. *Agronomy Research* **18**(S1), 815–822. doi: 10.15159/AR.20.155

Fortunati, E., Puglia, D., Monti, M., Peponi, L., Santulli, C., Kenny, J.M. & Torre, L. 2013. Extraction of cellulose nanocrystals from Phormium tenax fibres. *Journal of Polymers and the Environment* **21**, 319–328. doi: 10.1007/s10924-012-0543-1

González, Y., Meza, J., González, O. & Córdova, J. 2013. Synthesis and biodegradation of polyhydroxyalkanoates: plastics of microbial origin. *Revista Internacional de Contaminación Ambiental* **29(**1), 77–115. ISSN 0188-4999 (in Spanish).

Habibi, Y., Lucia, L.A. & Rojas, O.J. 2010. Cellulose Nanocrystals: Chemistry, Self-Assembly, and Applications. *Chemical Reviews* **110**, 3479–3500, 3479. doi: 10.1021/cr900339w

Hideno, A., Abe, K. & Yano, H. 2014. Preparation using pectinase and characterization of nanofibers from orange peel waste in juice factories. *Journal of Food Science* **79**, 1218–1224. doi: 10.1111/1750-3841.12471

Hong, B., Chen, F. & Xue, G. 2013. Preparation and characterization of cellulose nanocrystals from bamboo pulp. *Cellulose Chemistry and Technology* **50**(2), 225–231.

Junka, K, Guo, J, Filpponen, I, Laine, J. & Rojas, O.J. 2014. Modification of cellulose nanifibrils with luminescent carbon dots. *Biomacromolecules* **15**(3), 876–881. doi: 10.1021/bm4017176

Katz, S., Beatson, R.P. & Scallan, A.M. 1984. The determination of strong and weak acidic groups in sulfite pulps. *Svensk Papperstindning* **6**, R48–R53.

Khawas, P. & Deka, S.C. 2016. Isolation and characterization of cellulose nanofibers from culinary banana peel using high-intensity ultrasonication combined with chemical treatment. *Carbohydrate Polymers* **137**, 608–616. doi: 10.1016/j.carbpol.2015.11.020

Kumar, P., Barrett, D.M., Delwiche, M.J. & Stroeve, P. 2009. Methods for Pretreatment of Lignocellulosic Biomass for Efficient Hydrolysis and Biofuel Production. *Industrial & Engineering Chemistry Research* **48**(8), 3713–3729. doi: 10.1021/ie801542g

Li, J., Wang, Y. & Wei, X. 2014. Homogeneous isolation of nanocelluloses by controlling the shearing force and pressure in microenvironment. *Carbohydrate Polymers* Volume **113**, 26 November 2014, pp. 388–393. doi.org/10.1016/j.carbpol.2014.06.085

Li, W., Zhang, Y.C., Li, J.H., Zhou, Y.J., Li, R.S. & Zhou, W. 2015. Characterization of cellulose from banana pseudo-stem by heterogeneous liquefaction. *Carbohydrate Polymers* **132**, 513–519. doi: 10.1016/j.carbpol.2015.06.066

Lin, R., Li, A., Zheng, T., Lu, L. & Cao, Y. 2015. Hydrophobic and flexible cellulose aerogel as an efficient, green and reusable oil sorbent. *RSC Advances* **5**, 82027–82033. doi:10.1039/C5RA15194E

Lu, Q., Cai, Z., Lin, F., Tang, L., Wang, S. & Huang B. 2016. Extraction of Cellulose Nanocrystals with a High Yield of 88% by Simultaneous Mechanochemical Activation and Phosphotungstic Acid Hydrolysis. *ACS Sustainable Chemistry & Engineering* **4** (4), 2165–2172. doi: 10.1021/acssuschemeng.5b01620

Marchessault, R., Morehead, F. & Koch, M.J. 1961. Some hydrodynamic properties of neutral suspensions of cellulose crystallites as related to size and shape. *Journal of Colloid Science* **16**(4), 327–344.

Meile, K., Zhurinsh, A., Briede, L. & Viksna, A. 2018. Investigation of the sugar content in wood hydrolysates with iodometric titration and UPLC-ELSD. *Agronomy Research* **16**(1), 167–175. doi: 10.15159/AR.17.076

Oliveira, P.E., Cunha, A., Reyes, G., Gacitúa, W. & Petit-Breuilh, X. 2016. *Chusquea quila*, a natural resource from Chile: its chemical, physical, and nanomechanical properties. *BioResources* **11**(4), 10057–10069. doi: 10.15376/biores.11.4.10057-10069

Oliveira, P.E., Cunha, A., Pesenti H., Gacitúa, W. & Petit-Breuilh, X. 2018. Exploring an oxidative bleaching treatment for Chilean bamboo: a source of cellulose for biofuel generation and the nanotech industry. *European Journal of Wood and Wood Products* **76**, 1009–1019. doi: 10.1007/s00107-017-1237-0

Pinto, E. & Barrientos, J. 1993. *Flowering Quila (XI Region) /Florecimiento de la Quila (XI Región)*. Technical Report, Corporación Nacional Forestal, Ministerio de Agricultura, Santiago, Chile (in Spanish).

Qinghua, X., Yang, G., Menghua, Q., Kaili, W., Yingjuan, F. & Jian, Z. 2013. Nanocrystalline cellulose from aspen kraft pulp and its application in deinked pulp. *International Journal of Biological Macromolecules* **60**, pp. 241–247. doi: 10.1016/j.ijbiomac.2013.05.038

Rambabu, R., Panthapulakkal, S., Sainb, M. & Dalai, A.K. 2016. Production of nanocellulose fibers from pinecone biomass: Evaluation and optimization of chemical and mechanical treatment conditionson mechanical properties of nanocellulose films. *Industrial Crops and Products* **83**, 746–754. doi: 10.1016/j.indcrop.2015.11.083

Razalli, R.L., Abdi, M.M., Tahir, P.M., Moradbak, A., Sulaiman, Y. & Heng, L.Y. 2017. Polyaniline-modified nanocellulose prepared from Semantan bamboo by chemical polymerization: preparation and characterization. *RSC Advances* **7**(41), 25191–25198.

Salajková, M., Berglund, L.A. & Zhou, Q. 2016. Hydrophobic cellulose nanocrystals modified with quaternary ammonium salts. *Journal of Materials Chemistry* **22**, 19798–19805. doi: 10.1039/C2JM34355J

Schlegel, F. 1993. The problem of flowering. Informe Técnico (*Technical Report*); Revista Chile Forestal **206**, 35–37 (in Spanish).

Segal, L., Creely, J., Martin, Jr.A. & Conrad, C. 1959. An Empirical Method for Estimating the Degree of Crystallinity of Native Cellulose Using the X-Ray Diffractometer. *Textile Research Journal* **29**(10), 786–794. doi: 10.1177/004051755902901003

Safwa, S., Mokhtar, M.N., Naim, M.N., Baharuddin, A.S., Salleh, M.A.M. & Sulaiman, A. 2015. Study on the Preparation of Cellulose Nanofibre (CNF) from Kenaf Bast Fibre for Enzyme Immobilization Application. *Sains Malaysiana* **44**(11), 1541–1550. ISSN 0126-6039

Tang, J., Sisler, J., Grishkewich, N. & Chiu Tam, K. 2017. Functionalization of cellulose nanocrystals for advanced applications. *Journal of Colloid and Interface Science* Volume **494**, 15 May 2017, pp. 397–409. doi: 10.1016/j.jcis.2017.01.077

Theivasanthi, T., Anne Christma, F.L., Toyin, A.J., Gopinath C.B. & Ravichandran, R. 2018. Synthesis and characterization of cotton fiber-based nanocellulose. *International Journal of Biological Macromolecules* **109**, 832–836. doi: 10.1016/j.ijbiomac.2017.11.054

Vanhatalo, K.M. & Dahl, O.P. 2014. Effect of mild acid hydrolysis parameters on properties of microcrystalline cellulose. *BioResources* **9**(3), 4729–4740.

Wang, D. & Shen, S.-J. 1987. *Bamboos of China*. Hardcover, August 1, Timber Press, pp 19–21.
Wang, H.Y., Li, D.G., Yano, H. & Abe, K. 2014. Preparation of tough cellulose II nanofibers with high thermal stability from wood. *Cellulose* **21**, 1505–1515. doi: 10.1007/s10570-014-0222-6
Wang, L., Han, G. & Zhang, Y. 2007. Comparative study of composition, structure and properties of Apocynum venetum fibers under different pretreatments. *Carbohydrate Polymers* **69**(2), 391–397.
Wei, L., Luo, S., McDonald, A. G., Agarwal, U.P., Hirth, K.C., Matuana, L.M., Sabo, R.C. & Stark, N.M. 2017. "Preparation and Characterization of the Nanocomposites from Chemically Modified Nanocellulose and Poly (lactic acid)". *Journal of Renewable Materials* **5**(5), 410–422, 2017.
Zhao, H., Kwak, J.H., Zhang, Z.C., Brown, H.M., Arey, B.W. & Holladay, J.E. 2007. Studying cellulose fiber structure by SEM, XRD, NMR and acid hydrolysis. *Carbohydrate Polymers* **68**, 235–241.
Zimmermann, M., Patt, R. & Kordsachia, O. 1992. ASAM pulping of Douglas-fir followed by a chlorine-free bleaching sequence. *TAPPI J* **74**(11), 129–134.

Agronomy Research **18**(4), 2535–2549, 2020
https://doi.org/10.15159/AR.20.204

Environmental sustainability fruit quality and production in mycorrhizal tomato plants without P fertilizing

G. Palumbo[1], S. Carfagna[2], V. Stoleru[3], V. Torino[1], P.M. Romano[4], F. Letizia[1] and C. Di Martino[1,*]

[1]University of Molise, Department of Agriculture, Environmental and Food, Via F. De Sanctis 1, IT86100 Campobasso, Italy
[2]University of Napoli, Department of Biology, Via Foria 223, IT80137 Napoli, Italy
[3]Ion Ionescu de la Brad, University of Agricultural, UASMV, Iasi, M. Sadoveanu 3, RO700490, Romania
[4]Institute of Agricultural Technical Higher Education 'S. Pardo', IT86035 Larino, CB, Italy
[*]Correspondence: lello.dimartino@unimol.it

Abstract. The influence of root colonization by arbuscular mycorrhizal (AM) fungus *Funelliformis mosseae*, on fruit quality, production and environmental sustainability were evaluated in field-tomato plants grown exposed to P-limited soil 5 µg g^{-1} soil (basal-soil) with nitrate fertilization (50 µg g^{-1} soil), after greenhouse germination and fungus colonization. After 60 days sowing (DAS), when the percentage of mycorrhizal root length (% RLC) raised at about 50%, the plants were transplanted in open field.
During the experiment, the mycorrhization has affected a lot of physiological aspects like vegetative and reproductive growth, improving them and ended the fruiting with a major fruit production that was 50% higher than not mycorrhizal (NM) plants. The ripening process of the fruits was also followed by testing sugars content and ß-Amylase activity in fruits of NM and mycorrhizal (M) plants fruits. At 140 DAS, in the harvesting fruits stage, fruits of M plants showed significantly higher mineral nutrient sugars and organic nitrogen compounds as amino acids and protein, compared to fruits from NM plants. In particular, GLU-GLN-ASP and ASN raised about 35% more than fruits from NM plants, improving nutritional aspect and flavor of the product. THR-ILEU-LEU-VAL and LYS, essential amino acids in man nutrition, increased around 25% more than fruits from NM plants, too. In this contest, lycopene, total carotenoids, ascorbic acid and glutathione (GS) and reduced form (GSH) were also tested in ripe fruits. The overall results suggest that tomato roots colonization by mycorrhizal fungus *Funelliformis mosseae* affects host plant nutritional status, modifying reproductive behavior, fruits production and nutritional quality.

Key words: *Funelliformis mosseae,* mineral nutrients*,* amino acids, mycorrhizal plants, *Solanum lycopersicum.*

INTRODUCTION

The tomato *(Solanum lycopersicum* Mill.) fruit is one of the most popular, as well as one of the most important food, of the Mediterranean gastronomic culture based primarily on quality and nutritional power. Over 40 million metric tons of tomatoes are produced each year on a world basis. The tomato is also popular because it grows well practically everywhere, as well as in the home garden and it preserves the nutritional quality in many dishes both raw and cooked. For its important role in the food market, tomato it was chosen as the ideal specimen for this investigation. The lack of typical flavor in supermarket tomatoes is a frequent complaint from consumers. Flavor is a composite of taste and odor (aroma), a relation exists between the kind of taste that a substance has and its chemical constitution as organic acids, inorganic salts, sugars, amino acids, long chain organic substances etc. Fruit aroma generally comes out by various volatile substances such as esters, aldehydes, ketones, and alcohols, which exist in small quantity in the fruit (El Hadi et al., 2013). The quality of a food product is also defined by its nutritional composition and active substances content, which are not less important than the organoleptic properties. In this contest the mineral and sugars concentration the amino acids pattern, the antioxidant concentration, as lycopene, GDH, carotenoids, vitamin C, citric acid etc., are good indicators of quality and value of the product. Fruit quality and productivity are the result of the environmental conditions and soil fertility (Brunetto et al., 2015). Nowadays, in particular in the Mediterranean area, land for agriculture, are a precious commodity in constant diminution. Therefore, it is essential that these areas can continue to be sustainably cultivated and that the fertility of their land remains intact. It is well knowing that tomato plants growth and reproduction they are greatly affected by phosphorus deficiencies, a condition of many agricultural lands (López-Bucio et al., 2002; Güsewell, 2004). Under these conditions, the colonization of plant roots by symbiotic fungi is highly advantageous (Cavagnaro et al., 2005). AMF are obligate biotrophs, which can form mutualistic symbioses with the roots of around 80% of plant species (Giovannetti, 1980) growing in nursery or field. It is well known that AMF symbiosis can increase plant growth and nutrient uptake, improving yield and fruit quality. The hyphae of AMF penetrate roots and grow extensively between and within living cortical cells, forming a very large and dynamic interface between symbionts (Farahani et al., 2008). The extraradical mycelia, instead, disperse outside the roots to have access to a greater quantity of water and soil minerals for the host plants. the colonization of the fungus and its influence on plant growth are strongly influenced by the mineral component in the soil (Grant et al., 2005). It is well known that the phosphorous soil content affects mycorrhizal development (Jeffries et al., 2003). In *Lotus japonicus* and *Medicago truncultata* selective P carriers, indispensable for phosphate transport through the plant cell arbuscular membrane, are also needed for mycorrhiza development (Harrison et al., 2002; Javot et al., 2007). The widest development of mycorrhizal colonization occurs when soil P concentration is suboptimal for plant growth, but it is often greatly reduced when soil P is largely available (Balaz & Vosatka, 1997), maximizing the use of inorganic fertilizer and the environmental sustainability between plant and soil. The purpose of this investigation was to establish the influence of mycorrhizal colonization on tomato fruit quality and productivity in P-limited soil. In particular, the roots mycorrhizal index and the fruit concentrations of mineral nutrients, total sugars, protein, free amino acids, lycopene, ascorbic acid and glutathione in oxidized were evaluated and reduced form.

MATERIAL AND METHODS

Experimental design

The tomato seeds (*Solanum lycopersicum* L. Desf cv Quorum F1) were separated in two groups: one group (M) was inoculated with spores of the mycorrhizal fungus *Funelliformis mosseae,* (Gerd. and Trappe) while the other one (NM) was not inoculated and used as control. Dry spores of *F. mosseae*, were kindly provided by the 'MS Biotech Spa', (Larino, Campobasso-Italy) in special packs of 100 g on inert powder support. The distribution of the spores in plastic pots (1.2 L) with soil mixture filled with 800 g DW (dry weight) of sterilized (120 °C for 30 min) medium-textured soil [clay : peat : sand 40 : 40 : 20 (v/v/v)] and the germination of the seeds took place in the climatic chamber as best reported by Di Martino et al. (2019).

After 60 days sowing (DAS) May (2016), when the percentage of mycorrhizal root length (% RLC) raised about at 50%, the plants have been transplanted in open field (locality Montefalcone (BN) Italy, elevation 700 m. A low P content soil (5-µg g^{-1}soil) received 90 kg ht (KNO_3) but no P fertilization. To promote the plant engraftment and to compensate the water losses by evaporation, 0.5 liters of water were administered every two days near the plants for the first six days long. Subsequently and until to the end of the experiment (140 DAS), the irrigations were carried out twice a day (at the - 7 a.m. and at the - 7 p.m. for 20 min) - with clear water by drip irrigation. The extension of radical mycorrhization, expressed in percentage of mycorrhizal root length (% RLC), were determined starting from the 28 DAS (the beginning of development and vegetative growth), until to 60 DAS in environmental chamber and successively in open field, until when the harvesting stage correspond in the present experiment at 140 DAS.

To ensure measurement homogeneity, a random number of generator was used to select five plants in each single particle (NM and M plants) (Stefan et al., 2013).

Samplings, plant growth and mycorrhizal colonization analyses

The experimental design envisaged samplings from 21 DAS which is the beginning of development and vegetative growth, to 140 DAS, (harvesting stage, in the ours experiment), at increasing time intervals of two to four weeks. At each sampling, 3 NM and 3 M plants were randomly selected. The three plants were collected and used to be analyzed: the roots were washed with deionized water, dried through paper towels and promptly used for mycorrhizal colonization analysis. At the last sampling (140 DAS), part of the sampled roots were grounded in liquid N_2 to fine powder and stored at -40 °C to be used for elemental analyses. The mycorrhizal colonization was determined as reported by Di Martino et al. (2019).

Free amino acid and protein analyses in fruits

Sixty fruits as sample (collected on five plant selected by random number generator) at 140 DAS (fruits harvesting stage) from M and NM plants, were washed, cut into pieces and seeds discarded. Fruits pieces were then homogenated by minipimer for 5 minutes in ice bath. The homogenized samples were held at -20 °C until analysis.

Drying of 10 g of homogenate in a flow of nitrogen in falkon tubes was solubilized according to Amalraj et al. (2010) with a solubilization buffer consisting of 7 M urea, 2 M thiourea, 2% CHAPS, 50 mM Tris- HCl, pH 8 and left at room temperature for

30 min. Tubes were centrifuged at 14,000 g for 10 min and the supernatant collected and used to determine protein and primary amino acids concentration.

The protein were determined by the Lowry method, using BSA as a standard and expressed in mg g^{-1} FW (Lowry et al., 1951).

The free amino acids in the fruits were determined as reported by Di Martino et al. (2003 and 2006).

Total sugars assay

Refractometric methods was used to obtain only the total amount of sugar 20 g of homogenate (see above) were centrifuged at 15,000 g for 15 min. The total sugars content of supernatants were assayed using a refractometer HI96801 Hanna Instruments.

ß-Amylase activity in fruits

For the enzyme activity raiting, five fruits for sample (collected by random on five different plants (one for plant) from M and NM plants, of the three stages of fruits development were washed, cut into pieces and seeds discarded. Fruits pieces were then crushed into mortars by liquid nitrogen and mixed at a 1:1 (w/v) with an extraction medium as proposed by Di Martino et al. (2019) with some modifications. The extraction buffer contained 50 mM Tris HCl pH 7.5, 15% of glycerol (v/v), 0.25% Triton X-100 (w/v) and 20 mM Na_2SO_3, 1 mM EDTA, 1 mM EGTA, 1 mM DTT, 1 mM phenylmethylsulphonylfluoride, (PMSF). 4% PVP-40 (Sigma Aldrich USA) The homogenate was filtered through four layers of muslin and centrifuged at 15,000 g at 4 °C for 15 min. The protein content of supernatants was determined using the Lowry method (Lowry et al., 1951), before the enzyme activity tests. The protocol Betamyl-3 (Magazine Wicklow, Ireland) was used for the determination of beta amylase activity according to the company instructions. The produced p-nitrophenol was assessed photometrically at 400 nm in a Jasko V-570 spectrophotometer.

Determination of mineral elements concentration in fruits and soil

5 g of NM and M fruits homogenated (see above) were oven dried for a week at 60 °C and ground to powder with a mortar and pestle; 0.1 g of each sample were then transferred into 25 mL beakers. Mineral elements were extracted by digestion of dried homogenate. The mineral elements content in the fruits as well as in the soil were determined as reported by Di Martino et al. (2019).

Lycopene and total carotenoids determination in fruits

About 400 g of fruits homogenate for each samples were lyophilized by vacuum freeze drying for 48 h. Lyophilized samples were used to carotenoids extraction according to the method reported by (Pintea et al., 2003 and Panfili et al., 2004).

Ascorbic Acid determination in fruits

1 g of fruits lyophilized sample (see above) was extracted with 3 mL of 5% *meta*-phosphoric acid. The homogenate was centrifuged at 10,000 g for 10 min at 4 °C and the supernatant was collected for the analysis of AA total by HPLC reverse phase in according to the method reported by Szalai et al. (2014).

Glutathione determination in fruits

Reduced (GSH), oxidized (GSSG) and total glutathione (GSH+GSSG) were determined according to Bashir et al. (2013). Five fruits for sample (collected on five plants (one for plant) selected by random number generator) from M and NM plants, were washed, cut into pieces and seeds discarded. Fruits pieces were then crushed into mortars by liquid nitrogen and to the powdered 5 mL of of 5% sulfosalicylic acid. The homogenates were centrifuged at 15,000 rpm for 15 min at 4 °C. n. For GSH determination, aliquots of supernatant (100–200 µL), were added to the reaction buffer (50 mM Na-phosphate pH 7.00, 0.3 mM EDTA and 0.005% 5,5-Dithiolbis 2-nitrobenzoic acid) in a final volume of 1,150 mL. The mix of reaction was read at 412 nm after 5 min. To the same, were added: 0.02% NADPH and glutathione reductase; 0.001 enzyme unit in a final volume of 1,200 mL. The reaction was run for 30 min at 25 °C. The samples were again read at 412 nm to determine the total glutathione. The values of glutathione concentration were determined against GSH standard curve (10–180 nmol). The used extinction molar coefficient was calculating to be 0.017 cm^{-1} $nmol^{-1}$. The amounts of GSH and GSSG were converted and expressed in µg g^{-1}fw.

RESULTS AND DISCUSSION

Free amino acids and protein concentration in fruits

The influence of mycorrhizal fungus on fruits pathways has been highlighted also by the increase of amino acids and protein abundance compared to the fruits control, although the changes of amino acid pattern in the fruits is also strongly influenced both by the stage of ripeness (Savioli et al., 2012) and the metabolic state of the leaf as source site of metabolite intermediates and precursor molecules for the fruits. In M red fruits at the ripeness, glutamate, glutamine, aspartate and asparagine, represent about 80% of total free protein amino acids in tomato fruits with increase of 20% of total protein on NM red fruits (Fig. 1). In particular glutamine, glutamate, aspartate and asparagine, raised the 35%, 35%, 38% and 40% respectively most of NM fruits. Moreover, a significant increase of alanine 27%, glycine 36% and cysteine 38%, has been registered on the NM fruits with enhancement of 20% total amino acids. Fundamental amino acids as threonine, isoleucine, leucine, valine and lysine also increased in the M fruits, with enhancement of 25% over NM fruits. An interesting note is that among amino acids increased, in the first group cited; glutamate and aspartate impart organoleptic characteristics to the fruits, (Birch, 1987; Cagan, 1987, Bellisle, 1991 and Chaudhari et al., 2000) improving the quality and nutritional, characteristics including the metabolic support for the human gluconeogenesis (Brosnan, 2003) whereas in the second group, glycine and cysteine, as response to oxidative stress represents essential substrates to glutathione pathway (Walquíria et al., 2017).

A glucogenic amino acid is an amino acid that can be converted into glucose through gluconeogenesis The production of glucose from glucogenic amino acids involves these amino acids being converted to alpha keto acids and then to glucose (Nelson & Cox, 2004).

As just said, the fruits amino acids pattern can improve both nutritional than organoleptic property. Studies of organoleptic characteristics of pure amino acids show that various amino acids can be described as being sweet, sour, salty or bitter. Solms (1969) and Stapleton et al. (1999) reported that L-glutamic acid and L- aspartic acid have a unique taste-potentiating characteristics and the participation of amino acids to aroma of foods often surmount the taste properties of the pure products.

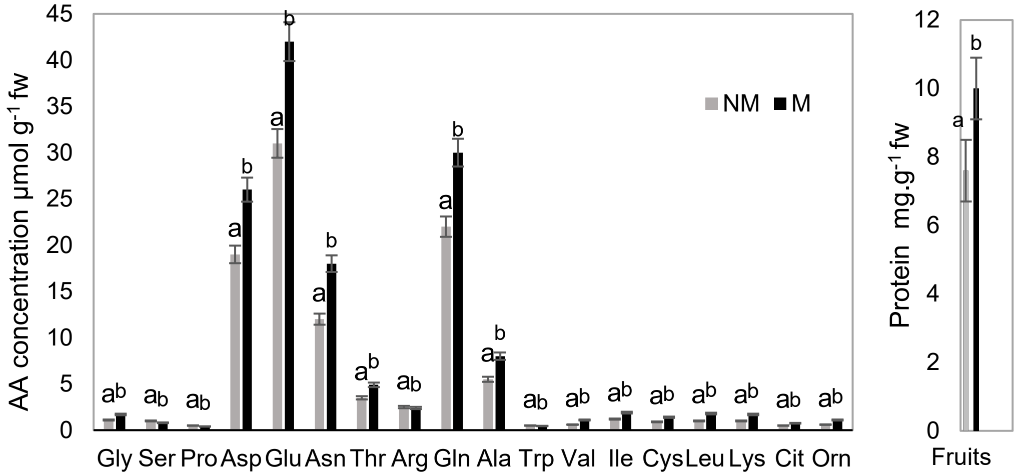

Figure 1. Average of amino acid and protein concentrations in the fruits of NM (grey bars) and M (black bars) tomato plants at 140 DAS. The values are means ± SD of 5 replicates. Bars indicate the standard deviation from five replicates. For every amino acid, values marked by common letters (a, a) are not statistically different, values marked by different letters (a, b) are statistically differen at $P \leq 0.05$ according to Tukey's test.

Sugars total and ß-Amylase activity in tomato fruits

Because the total soluble levels, are an important marker of fruits quality, their fluctuation were detected during the ripening of M and NM tomato fruits in three steps of ripening: Green fruit (G), Breaker (Br) and Red Ripe (RR). The total sugar determined in all fruits examined showed an linear increase during the whole fruits ripening phase reaching 65 and 80% more than the initial stage of maturation for NM and M fruits respectively (Fig. 2, a). Moreover, at RR stage total sugars in M fruits were 30% more than NM fruits. Since the content of total sugars in the fruits during the ripening process is the result of starch hydrolysis and ß-Amylase is the key enzyme that initiates starch degradation in most plant tissues, the ß-Amylase activity was also determined in the three stages of maturation (Fig. 2, b). ß-Amylase activity in all tomato fruits examined showed a maximum of activity at Br stage followed by a decline at the RR stage. Unlike the control, the fruits of M plants showed a significant amylase activity, already from the first stages of ripening of the fruits, indicating an advance on the ripening process with respect NM fruits. Moreover the ß-Amylase level in the fruits control were higher in all stage examined compared to the control.

More specifically they raised the 140; 30; and 50% more then NM fruits in G; Br and RR stage respectively.

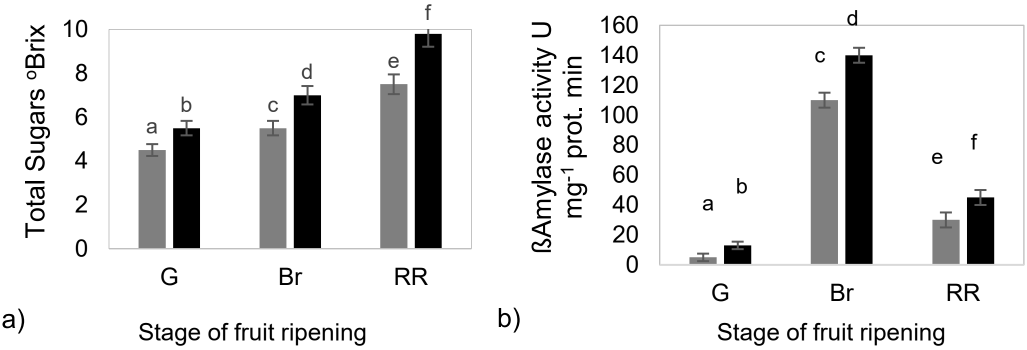

Figure 2. Total sugars content and ß-Amylase activity in NM (grey bars) and M (blak bars) tomato fruits during three stages of ripening process G (green fruits) Br (Breaker stage) RR (Red Ripening stage). Specific activities were expressed in U^{TM} $min^{-1}mg^{-1}$ protein. The values are means ± SD of 5 biological replicates. Values marked by common letters are not statistically different at $P \leq 0.05$ according to Tukey's test.s

Mineral elements concentration in soil and in fruits

Macro (P, K, Ca) and microelements (Fe, Zn, Mn) concentration, in soil and fruits, respectively of M and NM plants were determined at 140 DAS (fruits harvesting stage) and shown in Table 1, at the step when root colonization was at the highest extent (Table 2).

Table 1. Fruits macro (P, K, Ca) and microelement (Fe, Zn, Mn) concentrations in soil and in not mycorrhizal (NM) and mycorrhizal (M) tomato plants at 140 DAS. The values are means ± SD of 4 replicates. Values marked by common letters are not statistically different at $P \leq 0.05$ according to Tukey's test performed between NM and M plants for the same treatment

SOIL	N: (NO_3 50 µg g^{-1}soil) + (NH_4 5 µg g^{-1}soil)					
µg g^{-1}soil	[P]	[K]	[Ca]	[Fe]	[Zn]	[Mn]
Complete elements	240 ± 18	2,600 ± 330	2,200 ± 160	900 ± 80	70 ± 8	600 ± 55
Bioavailable elements	4 ± 0.5	70 ± 8	27 ± 4	12 ± 1	4 ± 0.5	8 ± 1
FRUITS µg g^{-1}dw	[P]	[K]	[Ca]	[Fe]	[Zn]	[Mn]
NM	1,500 ± 250b	2,600 ± 250a	1,500 ± 150b	40 ± 5b	18 ± 2b	17 ± 2b
M	2,200 ± 300a	2,800 ± 250a	2,000 ± 200a	70 ± 5a	30 ± 3a	25 ± 3a

Table 1 shows that macronutrient and micronutrients concentration in tomato fruits was higher in M compared with NM plants in which no significant fungal colonization was found. In particular, for macronutrients, P and Ca, and micronutrients Fe and Zn, there were significant variations between M and NM plants (about 45% and 70% increase respectively). Conversely, there were not significant difference between M and NM plants in about K fruits concentration. In particular the absolute concentration in mycorrhizal tomato fruits for P, Ca, Fe and Zn, 2,200, 2,000, 70 and 30 µg g^{-1}dw fruits respectively compared with soil content 5, 25, 15 and 5 μg g^{-1}soil are in according to the vision that mycorrhizal roots, by means the fungal hyphae, can more widely explore the rhizosphere and catch mineral nutrient, also through an higher nutrient uptake capacity and accumulation in the plant tissues with respect to the not mycorrhizal ones. Because nutrient concentrations in the fruits generally followed the same trend as those in the plant, an enhanced uptake of mineral nutrients from soil, may correspond to an enhancement of mineral concentration in the fruits.

Table 2. Mycorrhization index (% RLC). Mycorrhization Index (% RLC) at increasing time intervals of two to four weeks of M and NM plants during growth in P-limited soil (5 μg g^{-1}soil) The values are means ± SD of 4 replicates. For every (% RLC), values marked by different letters (a, b) are statistically different at $P \leq 0.05$ according to Tukey's test

DAS	21	35	56	84	112	140
NM (%RLC)	3 ± 1a	6 ± 2a	7 ± 2a	6 ± 2a	7 ± 2a	5 ± 1a
M (%RLC)	12 ± 3b	35 ± 5b	50 ± 5b	52 ± 6b	55 ± 5b	58 ± 6b

In fact, in the fruits the macronutrients as well micronutrients concentrations were higher in M compared with NM plants, in particular, P, Ca, for macronutrients, Fe, and Zn for micronutrients that improve the nutritional quality of the fruits. Calcium and phosphate supplements in aliment diet, support proper cellular signaling, proper nerve conduction (Sundelacruz et al., 2019) and a decreased risk of same decreases. Iron, instead present, in red cells is essential for carrying oxygen from the lungs to the body's tissues and in mitochondria in electron, transfer reaction of respiratory chain, zinc is needful for insulin and thyroid function (Baltaci et al., 2019) and collaborates to protect the body from free radicals.

Carotenoids and antioxidants fruits concentrations

For their antioxidant propriety, an increase of lycopene and carotene, in M fruits improve the fruits quality as well as the external appearance providing greater appreciation of the product, in fact, though glutathione as well ascorbic acid (vitamin C) exercising an important influence as an antioxidant and defendes the plant during oxidative damage by scavenging free radicals and ROS (Schulthesis et al., 2002; Elwan & El-Hamahmy, 2009), to a lesser extend, also carotenoid have ROS scavenging activity and the most potent antioxidant among carotenes is lycopene, which imparts also red color to the tomato fruit.

The data in Table 3 shows the Lycopene, total carotenoids, Glutathione and vitamin C concentrations of M fruits compared with NM fruits.

Table 3. Antioxidant substance concentrations in NM and M tomato fruits. Carotenoids, ascorbate and glutation concentration in tomato fruits collected at 140 DAS. The values are means ± SD of 6 replicates. Values marked by common letters are not statistically different at $P \leq 0.05$ according to Tukey's test performed between NM and M plants for the same treatment

Red Fruits	Lycopene μg g^{-1}FW	Tot. Carotenoids μg g^{-1}FW	Ascorbate μg g^{-1}FW	GSH μg g^{-1}FW	GS μg g^{-1}FW
NM	50 ± 7b	65 ± 7b	170 ± 15a	50 ± 6a	20 ± 3a
M	70 ± 8a	90 ± 9a	190 ± 18a	55 ± 7a	22 ± 3a

In M fruits, the lycopene concentration in harvesting stage was 45% higher than NM fruits supported the importance and the function that mycorrhizal fungi have particularly to potentiate the nutritional and nutraceutical quality of tomato fruits through changing of plant secondary metabolism that led to amplify levels of lycopene in fruits obtained from mycorrhizal plants (Giovannetti et al., 2012). In the same tendencies, the value of total carotenoids in the fruits was increased by 40% with the treatment of mycorrhizal fungus over the control (Salem M. Al-Amri, 2013). On the contrary, the same table shows that there were no significant variation in ascorbic acid and glutathione concentration between M and NM plants. The indication that antioxidant compounds as ascorbic acid and glutathione, can maintain in tomato fruits of M and NM an relatively low level, can suggest an low oxidative damage to the biomolecules present in plant systems involved and that mycorrhizal symbiosis in this context does not influence the antioxidant metabolic pathways. In the other hands, an enhancement of their metabolic precursor in treated plant fruit as: cysteine, glycine and glutamate, can prepare the cell to earlier GSH synthesis by stress input (Liu et al., 2018).

Fruiting, fruits ripening and production

M tomato plants also showed an earlier fruiting and fruits production increase. The mean of fruiting date (defined as the date at which 50% of the plants had produced their first fruits) was substantially anticipated in the mycorrhizal condition and occurred at 98 DAS, while the NM plants reached fructification about one week later (Fig. 3). Also the differences in fruits ripening date between NM and M plants, showed the same shift of fruiting date. Indeed, the time needed to reach the red stages was 7 days shorter for the M plants (126 DAS on 133 DAS) compared to NM plants.

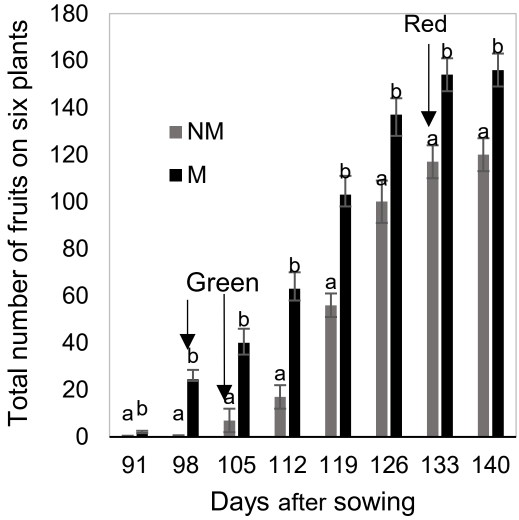

Figure 3. Fruiting evolution, detected as average of the total number fruits present on five plants every week during the reproductive phase in NM (grey bars) and M plants (black bars). The arrows indicate the beginning of fruiting and fruits ripening. The values are means ± SD of 3 replicates. Values marked by common letters are not statistically different at $P \leq 0.05$ according to Tukey's test performed between NM and M plants for the same treatment.

The mycorrhization of *Funelliformis mosseae* increased significantly also the average of fruits number, and fruits weight of mycorrhizal tomato plants compared with control plants: about 155 and 120 fruits, respectively were harvested at 140 DAS as a total amount from five plants and averaged in three replicate (Table 4).

The average of the amount fruits weight harvested from five M plants as above mentioned also increased on the control: 1,700 g and 1,080 g respectively. This led to an increased fruits productivity of the M plants of about 50% on control.

Furthermore, evident differences also were observed for the average of individual fruit weight (of the five plants) 11 and 9 g for M and NM plants respectively in the harvesting stage (140 DAS). (Table 4). Our findings confirm those of other studies as the results of Copetta et al. (2011) who decleared that root mycorrhization induced an increase in growth and number of fruits of a different tomato variety.

Table 4. Fruits production. Average of the total number and total weight fruits harvested from five plants at 140 DAS. The values are means ± SD of 3 replicates. Values marked by common letters are not statistically different at $P \leq 0.05$ according to Tukey's test

Numerical average of fruits collected from five plants	NM	M
Numerical average of total fruits from five plants	120 ± 6b	155 ± 8a
Numerical average of total fruits weight from five plants	1,080 ± 70b	1,700 ±110a
Numerical average weight of one fruit (g) of a100 examined	8 ± 0.6b	11 ± 0.7a

At large extend the ontogenetic cycle of the plant was also favorably affected by mycorrhization. The control plants showed a progressive loss of vigor and half of them died approximately five months after transplanting, whereas the mycorrhizal plants continued to produce fruits for at least five more months (data not shown).

The tomato plants favoured mycorrhiza symbiosis with *Funelliformis mosseae* in soils with phosphorous content 5 μg g^{-1}soil (Table 2), in agreement with the findings that mycorrhizal development is affected by plant nutritional status (Baum et al., 2002; Treseder et al., 2004). The mycorrhizal index (% RLC) reaching 50% at 56 DAS.

The mycorrhization of *Funelliformis mosseae* greatly affected the growth parameters and flowering (data not shown). But in mycorrhizal plants, these alteration of the morphometry also influenced the reproductive growth.

In fact, the mycorrhizal plants being more developed reached the reproductive phase early. Hildebrandt et al. (2002) reported that a treatment of *Glomus intraradices* accelerates the change from vegetative to reproductive phase. the reason could be attributed to the improvement of the nutritional status that positively influences the transition of vegetative meristem to reproductive meristem in tomato, (GU et al., 2010) have identified a group of microRNAs in tomato leaves, which is exclusively induced by AM symbiosis.

The mycorrhizal plants showed a significant advance of flowering, of about ten days on not treated plants, which ended also an early fruiting.

The most interesting evidence obtained in this study was that the mycorrhizal plants, have shown significant increases in the flowering (data not shown) followed significant increases in the tomato fruits number with about 40% more of fruits production compared with no treated plants (Table 4).

The earlier and more pronounced fruiting phase in M plants might result from enhanced capture of mineral nutrients from soil, chiefly immobile ions like P, Ca and Zn, and improved nutrient translocation system that may correspond to an enhancement in yield and mineral concentration in the fruits.

Utkhede (2006) indicated also that M tomato plants produced significantly higher fruits number and weight fruits production compared to the NM plants.

The influence of mycorrhizal fungus on fruits pathways was also evidenced as increase of sugars and amino acids abundance compared to the fruits control, in particular the total soluble solid was detected in three steps during the fruits ripening showing an increase from initial phase (G) to maturity (RR) of 50 and 70% for NM and M fruits respectively.

This trend proceeded with a parallel increase of ß-Amylase activity which hydrolyses starch, increases sugar metabolic levels.

In particular, in NM fruits the substantial lower activity of the enzyme at G stages suggests that ß-Amylase probably detain a more significant function in starch degradation during the late stages, of fruits development. In M fruits instead, significant ß-Amylase activity was already evidenced in early stages of ripening fruits increasing the sugar content already from the first stages of maturation. Moreover, in M fruits ß-Amylase maintaining higher activity levels than NM fruits in all three stages of ripening fruits detected confirming a close relationship between ß-Amylase activity and sugar content in the fruits.

A greater boost to the maturation process in the M fruits can arise from the positive role of ABA in triggering ethylene biosynthesis and ripening of tomato fruits Zhang et al., 2009), furthermore the arbuscular-mycorrhizal (AM) fungus Glomus sp. produces ABA, and ABA concentration in the xylem sap is higher in mycorrhizal than non-mycorrhizal plants (Esch, 1994). In the other hands exogenous ABA accelerates fruits ripening, and fluridone or NDGA treatmentdelayed fruits ripening by inhibition of ABA (Esch, 1994). A greater resource of sugars in M fruits forms adequate carbon skeletons for synthesize a large fraction of primary and essential amino acids, in particular at 140 DAS before the harvesting, giving organoleptic characteristics and nutritional power to the product as well described above, glutamine, glutamate, aspartate and asparagine, raised the 35%, 35%, 38% and 40% respectively most of the control. A significant increase of alanine 27%, glycine 36% and cysteine 38%, was registered, with enhancement of 20% total amino acids. Essential amino acids as threonine, isoleucine, leucine, valine and lysine also increased in the fruits from M plants, with enhancement of 25% over control. An interesting note is that among amino acids increased, in the first group cited; glutamate and aspartate, as well as being indispensable substrates for uman gluconeogenesis, impart organoleptic characteristics to the fruits, improving the quality, whereas in the second group, glycine and cysteine, as response to oxidative stress represents essential substrates to glutathione pathway.

As just said, the fruits amino acids pattern, can improve both nutritional than organoleptic property. Studies of organoleptic characteristics of pure amino acids show that various amino acids can be described as being sweet, sour, salty or bitter. Solms (1969); Stapletonet et al., 1999; Kurihara et al., 2015) reported that L-glutamic acid and L- Aspartic acid have a unique taste-potentiating property and the contribution of amino acids to flavour of foods often exceed the taste properties of the pure compounds. The quality of a fruit is important crossroad between nutritional properties flavor and organoleptic characteristics that are often associated to the color and good appearance of the fruit.

In this contest, lycopene and carotene symbolize the principal carotenoids in tomato fruits that impart color, giving an initial perception of quality. In fact, those important nutrients as also used as a color ingredient in many food formulations, and their increase in M fruits of 45% and 40% of lycopene and carotene makes the fruits more palatable.

For their antioxidant propriety, an increase of lycopene and carotene, in M fruits improve the fruits quality as well as the external appearance providing greater appreciation of the product. Inversely, there was not found difference in ascorbate and glutathione concentration between NM and M plants. For their significant antioxidant characteristic those findings, indicating a low oxidative damage to the biomolecules present in the fruits. In the other hands, an enhancement of their metabolic precursor in treated plant fruit as: cysteine, glycine and glutamate, can prepare the cell to earlier GSH synthesis.

Among the various effects caused, the mycorrhizal fungi could also interact with the training effects of the plant system on quality and productivity. In fact, the mycorrhizal plants had higher fruits yield per plant, moreover the red stages started 7 days earlier and fresh weight was 50% higher than that of the control. The enhancement in fruits yield per plant due to mycorrhizal inoculation might be attributed to enhanced photosynthesis associated with increased P uptake in plants (Dietz & Foier, 1986; Thuynsma et al., 2016), and hence high amounts of assimilates were likely produced to support both symbiosis and fruits development. The acceleration in the velocity of fruits development is possibly achieved because of the compatibility between *Funelliformis. mosseae* and the local ecotype of *Solanum lycopersicum* L that grew in the its natural ecosystem. These results show the importance of achieving a better association between a determined AMF strain and the ecotype of tomato, in order to improve and optimize the production process (Castillo et al., 2009).

CONCLUSIONS

1. Mycorrhizal colonization in tomato plants has been highly extended in our experimental conditions.
2. The fruits nutrients concentrations of M plants were significantly higher than those of NM ones, and it supported also the view that mycorrhiza actively modulate nutrient uptake limiting their interferences and optimizing the growth had better than the plant own roots. Fungal hyphae behave like a very efficient rootstock in the given experimental conditions.
3. The mycorrhization of *Funelliformis mosseae* greatly affected fruits productivity and quality of tomato plants, grown in open field under P limiting conditions by increasing the sugars content and nitrogen metabolism in plants, as well as enhances fruits carotenoid and lycopene concentrations. The increase of mineral nutrients, protein and free amino acid concentrations among which, glutamate, aspartate as well as threonine, isoleucine, leucine, valine and lysine, essential amino acids in man nutrition, suggested that the M fruits tissues had a higher nutritional value and taste property than the NM ones.

These results indicate that the use of AM inoculum of *Funelliformis mosseae* in P-limited soil can improve fruits production and quality, of tomato plants affecting biochemical composition and relative proportion of various mineral nutrients.

ACKNOWLEDGEMENTS. Financial support was provided by University of Molise while the firm 'MS Biotech Spa', Larino, Italy, kindly supplied the fungal spores.

REFERENCES

Amalraj, R.S., Selvaraj, N., Veluswamy, G.K., Ramanujan, R.P., Muthurajan, R., Palaniyandi, M., Agrawal, G.K., Rakwal, R. & Viswanathan, R. 2010. Sugarcane proteomics: establishment of a protein extraction method for 2-DE in stalk tissues and initiation of sugarcane proteome reference map. *Electrophoresis* **31**, 1959–1974.

Balaz, M. & Vosatka, M. 1997. Vescicular - arbuscular mycorrhiza of *Calamagrostisvillosa* supplied with organic and inorganic phosphorus. *Biol. Plantarum* **39**, 281–288.

Baltaci, A.K., Mogulkoc, R & Baltaci, S.B. 2019. Review: The role of zinc in the endocrine system. *Pak. J. Pharm. Sci.* **32**, 231–239.

Bashir, H., Ahmad, J., Bagheri, R. & Nauman, M. 2013. Limited sulphur resource forces *Arabidopsis thaliana* to shift towards non-sulfur tolerance under cadmium stress. *Environ Exp Bot.* **94**, 19–32.

Baum, C., Weih, M., Verwijst, T. & Makeschin, F. 2002. The effects of nitrogen fertilization and soil properties on mycorrhizal formation of *Salix viminalis*. *Forest Ecology and Management* **160**, 35–43.

Bellisle, F., Monneuse, M.O., Chabert, M., Larue-Achagiotis, C., Lanteaume, M.R. & Louis-Sylvestre, J. 1991. Monosodium glutamate as a palatability enhancer in the European diet. *Physiol. Behav*. **49**, 869–873.

Birch, G. 1987. *Structure, chirality, and solution properties of glutamates in relation to taste*. In: "Umami: Basic Taste" Ed. Kawamura, Y. and Kare, M.R. Marcell Dekker, Inc., New York, pp. 173–184.

Brosnan, J.T. 2003 Interorgan Amino Acid Transport and its Regulation. 2nd Amino Acid Workshop American Society for Nutritional Sciences. (A)

Brunetto, G., Wellington, G., De Melo, B., Toselli, M., Quartieri, M., Tagliavini, M. 2015. The Role of Mineral Nutrition on Yields and Fruit Quality in Grapevine, Pear snd Apple. *Rev. Bras. Frutic., Jaboticabal* **37**(4), 1089–1104.

Chaudhari, N., Landin, A.M. & Roper, S.D. 2000. A novel metabotropic glutamate receptor is a taste receptor for monosodium glutamate. *Nature Neurosci* **3**, 113–119.

Cagan, R. H. 1987. Allosteric regulation of glutamate taste receptor function. In "Umami: A Basic Taste" Ed. *Kawamura, Y. and Kare, M.R. Marcel Dekker*. New York, pp. 155–17.

Castillo, C., Sotomayor, L., Ortiz, C., Leonelli, G., Borie, F. & Rubio, R. 2009. Effect of arbuscular mycorrhizal fungi on an ecological crop of chili peppers (*Capsicum annuum* L.). *Chilean Journal of Agricultural Research* **69**, 79–87.

Cavagnaro, T. R., Smith, F.A., Smith, S. & Jakobsen, I. 2005. Functional diversity in arbuscular mycorrhizas, exploitation of soil patches with different phosphate enrichment differs among fungal species. *Plant Cell Environ*. **28**, 642–650.

Copetta, A., Bardi, L., Bertolone, E. & Berta, G. 2011. Fruit production and quality of tomato plants (Solanum lycopersicum L.) are affected by green compost and arbuscular mycorrhizal fungi. *Plant Biosystems.* **145**, 106–115.

Di Martino, C., Fioretto, A., Palmieri, D., Torino, V. & Palumbo, G. 2019. Influence of Tomato Plant Mycorrhization on Nitrogen Metabolism, Growth and Fructification on P-Limited Soil. *Journal of Plant Growth Regulation.* 1–13. doi:10.1007/s00344-019-09923-y

Di Martino, C., Pizzuto, R., Pallotta, M.L., De Santis, A. & Passarella, S. 2006. Mitochondrial transport in proline catabolism in plants: the existence of two separate translocators in mitochondria isolated from durum wheat seedlings. *Planta* **223**,1123–1133.

Di Martino, C., Delfine, S., Pizzuto, R., Loreto, F. & Fuggi, A. 2003. Free amino acids and glycine betaine in leaf osmoregulation of spinach responding to increasing salt stress. *New Phytologist* **158**, 455–463.

Dietz, K.J. & Foyer, C. 1986. The relationship between phosphate and photosynthesis in leaves - Reversibility of the effects of phosphate deficiency on photosynthesis. *Planta.* **167**, 376–381.

Elwan, M.W.M. & El-Hamahmy, M.A.M. 2009. Improved productivity and quality associated with salicylic acid application in greenhouse pepper. *Scientia Hort.* **122**, 521–526.

Esch, H., Hundeshagen, B., Schneider-Poetsch, H.J. & Bothe, H. 1994. Demonstration of abscisic acid in spores and hyphae of the arbuscular-mycorrhizal fungus Glomus and in the N2-fixing cyanobacterium Anabaena variabilis. *Plant Science* **99**, 9–16. doi: 10.1016/0168-9452(94)90115-5

Farahani, A., Lebaschi, H., Hussein, M., Hussein, S.A., Reza, V.A. & Jahanfar, D. 2008. Effects of arbuscular mycorrhizal fungi, different levels of phosphorus and drought stress on water use efficiency, relative water content and praline accumulation rate of Coriander (*Coriandrumsativum* L.). *Journal of Medicinal. Plants Research* **2**, 125–131.

Giovannetti, M. & Mosse, B. 1980. An evaluation of techniques for measuring vesicular arbuscular mycorrhizal infection in roots. *New Phytologist*. **84**, 489–500.

Giovannetti, M., Avio, L., Barale, R., Ceccarelli, N., Cristofani, R., Iezzi, A., Mignolli, F., Picciarelli, P., Pinto, B., Reali, D., Sbrana, C. & Scarpato, R. 2012. Nutraceutical value and safety of tomato fruits produced by mycorrhizal plants. *British Journal of Nutrition* **107**, 242–251.

Grant, C., Bittman, S., Montreal, M., Plenchette, C. & Morel, C. 2005. Soil and fertilizer phosphorus: Effects on plant P supply and mycorrhizal development. *Can J of Plant Sci.* **85**, 15–21.

Gu, M., Xu, K., Chen, A., Zhu, Y., Tang, G. & Xu, G. 2010. Expression analysis suggests potential roles of microRNAs for phosphate and arbuscular mycorrhizal signalling in Solanum lycopersicum. *Physiologica Plantarum* **138**, 226–237.

Güsewell, S. 2004. N:P ratios in terrestrial plants: variation and functional significance. *Tansleyreview New Phytologist* 1**64**, 243–266.

Harrison, M.J., Dewbre, G.R. & Liu, J.A. 2002. Phosphate Transporter from *Medicagotruncatula* Involved in the Acquisition of Phosphate Released by Arbuscular Mycorrhizal Fungi. *The Plant Cell.* **14**, 2413–2429.

Hildebrandt, U., Katharina, J. & Bothe, H. 2002. Towards Growth of Arbuscular Mycorrhizal Fungi Independent of a Plant Host. *Applied and Environmental Microbiology* **68**, 1919–1924.

Javot, H., Pecontroletsa, R.V., Terzaghi, N., Cook, D.R. & Harrison, M.J.A. 2007. Medicagotruncatula phosphate transporter indispensable for the arbuscular mycorrhizal symbiosis. *PNAS* **104**, 1720–1725.

Jeffries, P., Gianninazzi, S., Perotto, S., Turnau, K. & Barea, J.M. 2003. The contribution of arbuscolar mycorrhizal fungi in sustainable maintenance of plant health and soil fertility. *Biol. Fert. Soils.* **37**, 1–16.

Kurihara, K. 2015. Umami the Fifth Basic Taste: History of Studies on Receptor Mechanisms and Role as a Food Flavor. *Biomed Research International*. Volume 2015, Article ID 189402, 1-10. doi: 10.1155/2015/189402

Liu, J., Wang, J., Lee, S. & Wen, R. 2018. Copper-caused oxidative stress triggers the activation of antioxidant enzymes via ZmMPK3 in maize leaves. PLoS ONE, **13**, 1–12. e0203612. https:// doi.org/10.1371

López-Bucio, J., Hernández-Abreu, E., Sánchez-Calderón, L., Nieto-Jacobo, M.F., Simpson, J. & Herrera-Estrella, L. 2002. Phosphate Availability Alters Architecture and Causes Changes in Hormone Sensitivity in the Arabidopsis Root System. *Plant Physiol.* **129**, 244–256.

Lowry, O.H., Rosebrough, N.J., Farr, A.L. & Randall, R.J. 1951. Protein measurement with the Folin phenol reagent. *J Biol Chem*. **193**, 265–275.

Nelson, D.L. & Cox, M.C. 2004. Lehninger, principles of biochemistry 4th edition pp. 723–729.

Panfili, G., Fratianni, A. & Irano, M. 2004. Improved normal-phase high-performance liquid chromatography procedure for the determination of carotenoids in cereals. *J. Agric. Food Ch.* **52**, 6373–7.

Pintea, A., Bele, C., Andrei, S. & Socaciu, C. 2003. HPLC analysis of carotenoids in four varieties of *Calendula officinalisL.* Flowers. *Acta Biologica Szegediensis* **47**, 37–40.
Salem, M. Al-Amri. 2013. Improved growth, productivity and quality of tomato (Solanum lycopersicum L.) plants through application of shikimic acid. *Saudi Journal of Biological Sciences* **20**(4), 339–345.
Savioli, A., Zouari, I., Chalot, M. & Bonfante, P. 2012. The arbuscular mycorrhizal status has an impact on the transcriptome profile and amino acid composition of tomato fruit. *BMC Plant Biol.* **27**, 12–44.
Schultheiss, H., Dechert, C., Kogel, K.H. & Hückelhoven, R. 2002. A small GTP-binding host protein is required for entry of powdery mildew fungus into epidermal cells of barley. *Plant Physiology* **128**, 1447–1454.
Solms, J. 1969. The taste of amino acids, peptides and proteins. *J. Agr. food chem.* **17**, 686–688.
Stapleton, J.R., Roper, S.D & Delay, E.R. 1999. The taste of monosodium glutamate (MSG), L-aspartic acid, and N-methyl-D-aspartate (NMDA) in rats: Are NMDA receptors involved in MSG taste? *Chemical Senses* **24**(4), 449–457.
Stefan, M., Munteanu, N., Stoleru, V., Mihasan, M. & Hritcu, L. 2013. Seed inoculation with plant growth promoting rhizobacteria enhances photosynthesis and yield of runner bean (*Phaseolus coccineus* L.). *Scientia Horticulturae* **151**, 22–29.
Sundelacruz, S., Thurber Moody, A., Levin, M. & Kaplan, D.L. 2019. Membrane Potential Depolarization Alters Calcium Flux and Phosphate Signaling During Osteogenic Differentiation of Human Mesenchymal Stem Cells. *Bioelectricity* **1**,(1). https://doi.org/10.1089/bioe.2018.0005
Szalai, G., Janda, T. & Pál, M. 2014. Routine sample preparation and HPLC analysis for ascorbic acid (vitamin C) determination in wheat plants and Arabidopsis leaf tissues. *Acta Biologica Hungarica* **65**, 205–217.
Thuynsma, R., Kleinert, A., Kossmann, J., Valentine, A. & Hills, P.N. 2016. The effects of limiting phosphate on photosynthesis and growth of Lotus japonicas. *South African Journal of Botany* **104**, 244–248.
Treseder, K.K. 2004. A meta-analysis of Mycorrhizal responses to nitrogen, phosphorus, and atmospheric CO2 in field studies. *New Phytologist* **164**, 347–355.
Utkhede, R. 2006. Increased growth and yield of hydroponically grown greenhouse tomato plants inoculated with arbuscular mycorrhizal fungi *Fusarium oxysporum*f. sp. *Radices-lycopersici*. *Bio Contr.* **51**, 393–400.
Walquíria, F.T., Evandro, B.F., Luís, H.S., Renan, C.U., Klaus, R. & Durval, D. Neto. 2017. Foliar and Seed Application of Amino Acids Affects the Antioxidant Metabolism of the Soybean Crop. *Plant Sci.* doi: 10.3389/fpls.2017.00327
Zhang, M., Yuan, B. & Leng, P. 2009. The role of ABA in triggering ethylene biosynthesis and ripening of tomato fruit. *Journal of Experimental Botany* **60**, 1579–1588. doi:10.1093/jxb/erp026

Agronomy Research **18**(4), 2550–2558, 2020
https://doi.org/10.15159/AR.20.182

Mycobiota of the rhizosphere of raspberry plants (*Rubus idaeus* L.) under the influence of varieties and new fertilizers in conditions of organic production

A. Parfeniuk[1], V. Mineralova[1,*], I. Beznosko[1], A. Lishchuk[1], V. Borodai[2] and V. Krut[3]

[1]Institute of Agroecology and Nature Management of NAAS of Ukraine, Metrologichna, 12, UA03143 Kyiv, Ukraine
[2]The National University of Life and Environmental Sciences of Ukraine, Heroiv Oborony, 15, UA03041 Kyiv, Ukraine
[3]Institute of Microbiology and Virology named after D.K. Zabolotnyi of NAAS of Ukraine, Academician Zabolotny, 154, UA03143 Kyiv, Ukraine
[*]Correspondence: valentinamk@ukr.net

Abstract. The results of studies of influence of raspberry plant varieties and new organic fertilizers on the abundance and species composition of the micromycetes in rhizospheric soil in conditions of organic production are presented. The mycobiota of Joan J and Himbo-Top raspberry varieties during plant ontogeny was analyzed and the species composition of phytopathogenic micromycetes, which are presented in the rhizospheric plant soil, was defined. It was revealed that the following fungi species prevail in the population: *Botrytis cinerea,* Pers*, Aspergillus niger*, V. Tiegh, *Alternaria alternata*, (Fr.) Keissl*, Fusarium sp*. These fungi are producers of mycotoxins that can cause dangerous diseases in animals and humans. There is a stabilizing selection of microorganisms in the phase of separation of buds in inflorescences in the mycobiota of the rhizosphere of plants of raspberry varieties under the influence of the organic fertilizer VITERI with the addition of Basil essential oil.

Key words: raspberry plant, rhizospheric soil, organic fertilizers, essential oils, micromycetes, the abundance, phytopathogens, organic production.

INTRODUCTION

A significant place in the assortment of berry products belongs to raspberries (*Rubus idaeus* L.), whose medicinal and nutritional properties are widely known (Wang & Lin, 2000; Sekizura et al., 2014). In Ukraine, plants of this culture are affected by a large number of diseases. Among them, root and grey mold rots deserve the special attention (Paulus, 1990; Markov, 2017). The causative agents of these diseases reduce the nutritional and marketable quality of berries. In addition, they are able to produce toxins that belong to the biological contamination of biocenoses (Parfeniuk, 2011; Malinovskaia et al., 2017; Dyakov & Levitin, 2018). The cultivation of berry crops, including the everbearing raspberries, while using organic technologies on industrial plantations, provides for the implementation of a set of interrelated agricultural measures. Among them, the fertilizer system and the introduction of sustainable varieties deserve the special attention (Kowalenko, 2006; Buskienė & Uselis, 2008; Emelyanova et al., 2015; Archer et al., 2016; Borodai et al., 2016; Khalil & Jamel, 2017; Sheng et al., 2019; Wendel et al., 2020). Serbian scientists Stojanov et al. (2019) found the positive effect of the organic fertilizer 'Excell Orga' (Angibaud Derome & Spécialités, France) on the growth of raspberry shoots, the productivity and quality of berries, the content of sugars, phenols and flavonoids, antioxidant abilities. New plant protection products, that have been elaborated on the basis of coniferous tree bark, showed good results (Jankevica et al., 2018). The sesame, cinnamon and neem (*Azadirachta indica A.Juss*.) oils are actively used in the practice of plant protection against powdery mildew of raspberries, spotting (*Septoria rubi*) in organic production (Archer et al., 2016). Thymol, Linalool, Limonene, Eugenol, Carvacrol are used for a long period of time - commercial preparations based on vegetable essential oils, which are used as biopesticides. They include basil oil (Archer et al., 2016). The efficiency and selective effect of essential oils of wild weed have been established: *Chenopodiastrum* murale*, Sisymbrium irio, Falcaria vulgaris, Anagallis arvensis, Crepis aspera, Sonchus oleraceus, Notobasis syriaca* against phytopathogens *Alternaria solani, Helminthosporium sativum, Rhizoctonia solani* (Durán-Lara et al., 2020). Organic-mineral fertilizer HELPROST (BTU-Center, Ukraine) has been developed in Ukraine to stimulate the growth of berries, including raspberry plants. However, there is no information about the effect of essential oils and organic fertilizers on the pathogenic mycobiota of the plant rhizosphere at different phases of the everbearing raspberry`s growth. But it is the pathogenic mycobiota that significantly reduces the quality and biological safety of raspberry products. The main indicator of the efficiency of growing raspberries is the amount of harvest, which is due to mineral organic fertilizer. With the exception of this component, the yield will decrease sharply, which is not interesting for production. Therefore, the goal of our research was to increase the biosafety of raspberry agrocenosis by reducing the number of phytopathogenic micromycetes by creating new fertilizers with the addition of essential oils and improving the quality of the crop, which will be obtained with existing technologies.

MATERIALS AND METHODS

On field research was conducted in 2017–2019 on the site of Friendsberry Ltd., located in Myronivskyi district of Kyiv region and characterized by moderate soil and climatic conditions. The microbiological, phytopathological and mycological methods were followed as mentioned in the previous studies (Dudka et al., 1982; Zvyagintsev, 1991; Parfeniuk et al., 2014).

The investigated preparations are among those recommended by Organic Standard Ltd (Ukraine) for use in organic farming. The macro- (NPK) and trace elements are main active substance of the complex organic-mineral fertilizer Viteri 8-4-5 (Zolotov, Ukraine) in an available form for plant. The additional foliar treatment with VITERI fertilizer (1% aqueous solution) and essential oils of Basil and Fennel (0.1% aqueous solution) was carried out to determine the effect of organic fertilizers on the mycobiota of the rhizospheric soil in raspberry agrocenosis during its ontogeny, using known technology (Polianchikov & Kapitanskaia, 2017). Essential oils for scientific research were produced by Arora Aromatics Pvt. Ltd (India) using original technology. The experiment included the following variants:

1. Control 1 - cultivars of raspberries that were grown in organic production by the adopted technology.
2. Control 2 - VITERY - widely known complex organo-mineral fertilizer Viteri 8-4-5 (Ukraine). The main active ingredient of which is macro- (NPK) and microelements in a form that is accessible to the plant. N.P.K fertilizer 8-4-5. The nitrogen contained in this complex organic fertilizer is in both nitrate form, which is immediately available to the plant, and in ammonium form, which is absorbed gradually and has a prolonged effect. Also, due to the ammonium form of nitrogen, VITERI 8-4-5 significantly improves the absorption of phosphorus, which promotes enhanced root growth and increases the drought resistance of the plant.
3. Composition of VITERY organic fertilizer with Basil essential oil.
4. Composition of VITERY organic fertilizer with Fennel essential oil.

Essential oils were not used separately from fertilizers because cultivars of cultivated raspberries are usually grown on complex fertilizers. If the fertilizer not added, the yield will drop sharply and its quality will suffer. This will damage the production even if the essential oil has a positive effect. It should be noted that the number of bushes in each variant averaged 35 pcs.

Studies were conducted in the following phases of raspberry development:

- Phase of growth inflorescence
- Phase of separation of buds in inflorescences of plants
- Phase of intensive fruiting.

The number of micromycetes in the rhizospheric soil of the everbearing raspberry varieties Joan J (British breeding) and Himbo-Top® (Swiss breeding) was determined in different phases of ontogeny due to the influence of the organic fertilizer VITERI and its compositions with essential oils based on commonly known methodology (Zvyagintsev, 1991; Parfeniuk et al., 2014). The number of colonies in Petri dishes was counted using an automatic counter SCAN4000 (Interscience, France). The Czapek Dox Agar was used. One-way analysis of variance (ANOVA) was used to compare the impact of all of the different treatments (Tukey's test for $p < 0.01$ and $p < 0.05$). The experimental results were processed using the STATISTICA 8.0 software package.

RESULTS AND DISCUSSION

It is known that abundance of micromycetes in the raspberry plant rhizosphere, under the influence of abiotic and anthropogenic factors, can significantly change (Kudeyarova, 1999; Nannipieri, 2003; Gadzalo, 2015). Therefore, the number of micromycetes in the rhizospheric soil depending on the raspberry variety and ontogeny phase of the plants was determined (Zvyagintsev, 1991; Parfeniuk et al., 2014).

According to the results, the number of colony-forming units in the rhizospheric soil of Joan J plants before treatment with preparations, in the phase of growth inflorescence, was at the level of control and was in averaged 1,012 thousand CFU g^{-1} of soil regardless of the variant (Fig. 1).

In the phase of separation of buds in inflorescences, the number of CFU in the control variant sharply increased and reached 2,23 thousand CFU g^{-1} of soil. In the same period of plant growth, the number of CFUs in the studied treatments significantly exceeded the control and ranged from 3,03 thousand to 3,84 thousand CFU g^{-1} of soil (Fig. 1).s

It should be noted that the highest number of CFUs was observed in variants, where foliar treatment with VITERI fertilizer was applied with the addition of Fennel essential oil, which indicates about stimulatory activity of this combination in relation to the mycobiota in the rhizosphere of raspberry plants. The highest inhibitory properties in relation to the mycobiota of the rhizosphere of the plants of the variety raspberry Joan J characterized by foliar treatment with VITERI fertilizer in the phase of separation of buds in inflorescences.

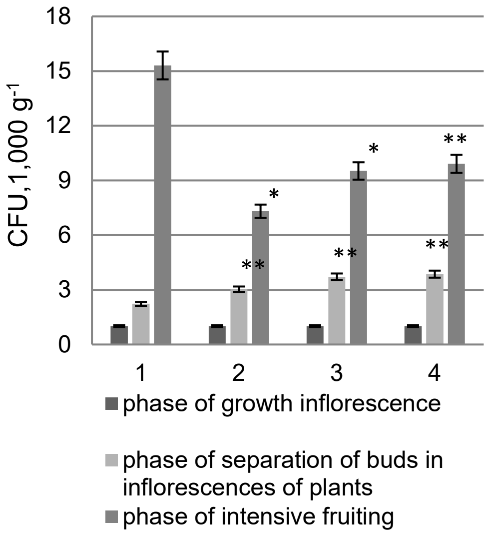

Figure 1. Influence of organic fertilizer VITERI and its compositions with essential oils on the number of micromycetes of rhizospheric soil of Joan J raspberry plants in different phases of ontogeny (1-control, 2-foliar treatment with VITERI fertilizer, 3-foliar treatment with VITERI fertilizer + essential Basil oil, 4-foliar treatment with VITERI fertilizer + essential Fennel oil).

Note: significance of differences compared to the control was a ssessed by one-way ANOVA; * – signific ant differences at $p < 0.05$, ** – significant differences at $p < 0.01$ (Tukey's test).

The highest density of mycobiota in the rhizosphere of plants was observed in the phase of intensive fruiting of raspberries (Fig. 1). During this period, the number of CFUs amounted to 15,3 thousand CFU g^{-1} of soil in the control variant. According to the data, presented in the figure, the greatest inhibition of mycobiota in this period occurred in variants 2 (foliar treatment with VITERI fertilizer) and 3 (foliar treatment with VITERI fertilizer+Basil essential oil), where the number of CFU g^{-1} of soil was in average on 8 and 6 thousand respectively lower than the control.

According to the results of the studies, presented in Fig. 2, it was found that in the rhizosphere of the raspberry plants Himbo -Top, before the tillage, in the budding phase, the number of CFUs was at the level of control and was in averaged 0,787 thousand g^{-1} of soil, which is significantly lower in compared to Joan J (Fig. 1) in the same period of time. But in the phase of separation of buds from inflorescences in control, the number of CFUs sharply increased and had averaged 5,7 thousand CFU g^{-1} of soil. In the variants 2 (foliar treatment with VITERI fertilizer) and 3 (foliar treatment with VITERI fertilizer+Basil essential oil) in the specified period their number was respectively higher on 2 and 1 thousand CFU g^{-1} of soil respectively than at the control. At the same time, in variant 4 (foliar treatment with VITERI fertilizer+Fennel essential oil) in the rhizosphere of Himbo-Top raspberry plants the number of CFUs was significantly lower compared to control and variants 2 and 3.

The results of the research show, that essential oils and their compositions with organic fertilizer VITERI can both suppress and stimulate the formation of mycobiota density in the rhizosphere of raspberry plants (Figs 1, 2).

The given results indicate a significant difference between the influence of different essential oils and their compositions with organic fertilizer VITERI on the density of micromycetes in the mycobiota of the rhizosphere soil of plants of different raspberry varieties. According to the results (Figs 1, 2), a statistically significant difference is particularly evident between control and foliar treatment via essential oils and their compositions with organic fertilizer VITERI in the phase of intensive fruiting. Therefore, the treatment plays a major role in fungal culturable communities.

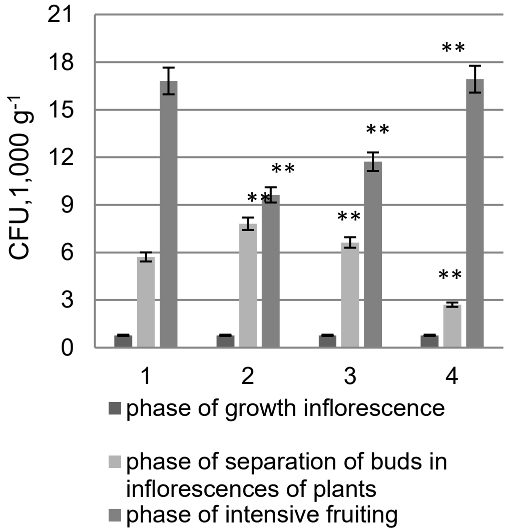

Figure 2. Influence of organic fertilizer VITERI and its compositions with essential oils on the number of micromycetes of rhizospheric soil of Himbo-Top raspberry plants in different phases of ontogeny (1-control, 2-foliar treatment with VITERI fertilizer, 3-foliar treatment with VITERI fertilizer+essential Basil oil, 4-foliar treatment with VITERI fertilizer+essential Fennel oil).

Note: significance of differences compared to the control was a ssessed by one-way ANOVA; * – signific ant differences at $p < 0.05$, ** – significant differences at $p < 0.01$ (Tukey's test).

This process depends on both the variety and the phase of ontogeny of plants. After all, while the number of CFU g^{-1} of soil in the rhizosphere of the Joan J plant varied from 7,3 thousand to 9,9 thousand CFU g^{-1} of soil, depending on the variant and phase of plant development, their number in the rhizosphere of the plant variety Himbo-Top was significantly higher and ranged from 9,6 thousand to 16,9 thousand CFU g^{-1} of soil. It indicates a significant differentiation of raspberry plant varieties according to the mechanisms of synecological relations in the plant-nourishment - microorganism - environment triangle (Figs 1, 2).

The species composition of phytopathogenic micromycetes presented in the rhizospheric soil of the studied varieties was established. The overwhelming majority of pathogens that affected the raspberry plants belonged to known producers of mycotoxins, among which special attention deserves: *Botrytis cinerea, Aspergillus niger, Fusarium grameniarum*, which are producers of mycotoxins (Table 1). These toxins can cause dangerous diseases for humans and animals (Levitin, 2009).

According to the data presented in the Table 2, the phytopathogenic mycobiota in the rhizospheric soil of the raspberry cultivar of the Joan J raspberry plant was represented by following fungi: *Alternaria alternata, Fusarium grameniarum, Aspergillus niger*. The abundance of these micromycetes was in averaged 19% regardless of the variant. Among them, *Aspergillus niger* was the dominant species.

Table 1. Species composition of phytopathogenic micromycetes of mycobiota of raspberry plants of the Joan J and Himbo-Top varieties

Disease	Pathogen	Mycotoxins
Septoriosis	*Septoria rubi*	Only properties
Grey rot	*Botrytis cinerea*	Botrydial
Black mold	*Aspergillus niger*	Aflatoxin
Cladosporiosis	*Cladosporium herbarum*	Only properties
Alternariosis	*Alternaria alternata*	Tentotoxin

Table 2. Spectrum of phytopathogenic micromycetes of the raspberry plants` rhizosphere soil of the Joan J variety

Variants	The proportion of phytopathogenic micromycetes in the mycobiota of the rhizosphere, %		
	phase of growth inflorescence	phase of separation of buds in inflorescences	phase of intensive fruiting
Control	*Alternaria alternata (3)* *Fusarium grameniarum (4)* *Aspergillus niger (12)*	*Botrytis cinerea (14)* *Alternaria alternata (20)* *Fusarium grameniarum (12)*	---
VITERI fertilizer	*Alternaria alternata (3)* *Fusarium grameniarum (4)* *Aspergillus niger (12)*	*Botrytis cinerea (10)* *Alternaria alternata (4)* *Fusarium grameniarum (6)* *Aspergillus niger (60)*	*Aspergillus niger (10)*
VITERI fertilizer + essential Basil oil	*Alternaria alternata (3)* *Fusarium grameniarum (4)* *Aspergillus niger (12)*	*Botrytis cinerea (16)* *Alternaria alternata (12)* *Fusarium grameniarum (14)*	*Fusarium* grameniarum *(10)*
VITERI fertilizer + essential Fennel oil	*Alternaria alternata (3)* *Fusarium grameniarum (4)* *Aspergillus niger (12)*	*Botrytis cinerea (6)* *Alternaria alternata (8)* *Fusarium grameniarum (4)* *Aspergillus niger (48)*	*Fusarium grameniarum (4)* *Aspergillus niger (10)*

Saprotrophic micromycetes were dominating, which include *Penicillium herquei, Penicillium terrestre and Trichoderma viride.* The obtained results give reason to consider that populations of phytopathogenic micromycetes in the rhizosphere soil of plants of these varieties are under conditions of rigid anthropogenic pressure, which in the future may lead to activation of homeostatic processes (Table 2, 3). That is confirmed by the data obtained during the study of mycobiota in the rhizosphere of the Joan J raspberry plants in the budding phase of inflorescences. During this period, the population of phytopathogenic micromycetes ranged from 42 to 80%. While in the mycobiota of the rhizospheric soil of raspberry plants in the control variant, the proportion of phytopathogenic micromycetes was 42% that indicate about stabilizing selection in the population, in the variant with organic fertilizer VITERI it reached 80% that indicate about rigid directed selection of phytopathogenic micromycetes. Foliar treatment of VITERI fertilizer with the addition of Fennel essential oil the number of CFUs of phytopathogenic micromycetes was significantly lower compared to VITERI organic fertilizer and had averaged 66% (Table 2). At the same time, foliar treatment with organic fertilizer VITERI with the addition of essential oil of Basil inhibited the development of phytopathogenic micromycetes in the rhizosphere of plants of the studied variety. The most environmentally safe combination was VITERI+Basil essential oil. In this embodiment, the number of phytopathogenic micromycetes in the rhizospheric mycobiota was 42%, which is close to the stabilizing selection in the mycobiota of the rhizosphere of Joan J raspberry plants.

It should be noted that in the phase of intensive fruiting of raspberry plants in the control variant of the mycobiota of the rhizospheric soil was represented only by saprophytic fungi. The number of phytopathogenic micromycetes on the Joan J variety during this period significantly decreased compared to the phase of separation of buds in the inflorescences and reached an average of 10% in the VITERI variant and 14% in the VITERI variant with the addition of Fennel essential oil (Table 2).

In the mycobiota of the rhizosphere of plants of the Himbo-Top variety of raspberries, the phytopathogenic mycobiota, as in the rhizosphere of the Joan J plants, was represented by following fungi: *Alternaria alternata, Fusarium grameniarum, Aspergillus niger.* But the abundance of these micromycetes was slightly lower, in averaging 14% regardless of the variant (Table 3). Among them, as well as the cultivar of the Joan J variety, the species *Aspergillus niger* dominated. The saprophytic part of the mycobiota was represented by following fungi: *Penicillium herquei, Penicillium terrestre, Trichoderma viride*, whose density reached an average of 86%.

In the rhizosphere of Himbo-Top raspberry plants, a significant increase in phytopathogenic micromycetes was observed, both in the control variant and under the influence of foliar treatment with VITERI organic fertilizer compared to the Joan J variety (Table 3).

Table 3. Spectrum of phytopathogenic micromycetes of the raspberry plants` rhizosphere soil of the Himbo-Top variety

Variants	The proportion of phytopathogenic micromycetes in the mycobiota of the rhizosphere, %		
	phase of growth inflorescence	phase of separation of buds in inflorescences	phase of intensive fruiting
Control	*Alternaria alternata (2)* *Fusarium grameniarum(2)* *Aspergillus niger (10)*	*Botrytis cinerea (10)* *Alternaria alternata (6)* *Fusarium grameniarum (4)* *Aspergillus niger (40)*	---
VITERI fertilizer	*Alternaria alternata (2)* *Fusarium grameniarum(2)* *Aspergillus niger (10)*	*Botrytis cinerea (10)* *Alternaria alternata (4)* *Fusarium grameniarum (6)* *Aspergillus niger (60)*	*Alternaria alternata (20)* *Aspergillus niger (30)*
VITERI fertilizer + essential Basil oil	*Alternaria alternata (2)* *Fusarium grameniarum (2)* *Aspergillus niger (10)*	*Botrytis cinerea (9)* *Alternaria alternata (6)* *Fusarium grameniarum (5)* *Aspergillus niger (35)*	*Botrytis cinerea (10)* *Alternaria alternata (10)*
VITERI fertilizer + essential Fennel oil	*Alternaria alternata (2)* *Fusarium grameniarum (2)* *Aspergillus niger (10)*	*Botrytis cinerea (14)* *Alternaria alternate (10)* *Fusarium grameniarum (4)* *Aspergillus niger (4)*	*Alternaria alternata (10)*

Their number in the variants indicated varied in average from 36 to 80% respectively. In VITERI+Basil essential oil, equilibrium between saprotrophs and phytopathogens was observed, and in VITERI+Fennel essential oil, the number of saprotrophs was almost three times larger than the number of phytopathogenic micromycetes. The results of the studies show that in the phase of separation of buds in inflorescences by foliar treatment with organic fertilizer VITERI with the addition of Basil essential oil in the rhizosphere of plants of both investigated raspberries there is a stabilizing selection in the mycobiota of the rhizosphere.

It should be noted that in the phase of intensive fruiting, almost 80% of the mycobiota of the raspberry plant rhizosphere of the studied varieties were saprotrophic fungi of the genus *Penicillium (Penicillium terrestre, Penicillium breviocompactum and Penicillium ciplicissimum) and Trichoderma viride*. The significant inhibition of phytopathogenic mycobiota in the plant rhizosphere in all variants of the Himbo-Top variety was observed during this period. The control variant was dominated by saprotrophs. At the same time, the number of phytopathogenic micromycetes averaged 50% for the foliar VITERI treatment, while the essential compositions of Basil and Fennel were significantly reduced (up to 20% and 10%, respectively).

CONCLUSIONS

Essential oils and their compositions with organic fertilizer VITERI significantly affect the abundance and biodiversity of micromycetes in the rhizosphere soil of raspberry plants. Foliar treatment with fungal micromycetes in the mycobiota of the rhizosphere of plants of the studied raspberry cultivars is observed during foliar treatment with VITERI organic fertilizer with the addition of Basil essential oil in the phase of bud separation in inflorescences. The number of phytopathogenic micromycetes in the rhizosphere mycobiota of the Joan Jay variety was 42%, and in the mycobiota of the rhizosphere of raspberry plants of the Himbo-Top variety -55%. This indicates the high prospects of this composition for stabilizing the agrocenosis of raspberries and improving the quality and biosafety of growing crops in organic production.

REFERENCES

Archer, L., Carroll, J., Heidenreich, C. & Pritts, M., eds. 2016. Production and IPM Guide for Organic Raspberries and Blackberries. *New York State Integrated Pest Management Program.* Ithaca, N.Y. 59–62.

Buskienė, L. & Uselis, N. 2008. The influence of nitrogen and potassium fertilizers on the growth and yield of raspberries cv. 'Polana'. *Agronomy Research* **6**(1), 27–35.

Borodai, V., Kobrynets, I., Kliachenko, O., Lihanov, A. & Subin, O. 2016. Agroecological aspects of the use of biological products in cultivation *Fragaria vesca* L. *Nauk.visnyk NULES of Ukraine* **234**, 100–108 (in Ukrainian).

Dudka, I., Vasser, S. & Jellanskaja, I. 1982. *Methods of experimental mycology.* In: Bilaj, V. (Ed.). Naukova dumka, Kiev, 548 pp. (in Russian).

Durán-Lara, E., Valderrama, A. & Adolfo, M. 2020. Natural Organic Compounds for Application in Organic Farming. *Agriculture.* 10. 41. 10.3390/agriculture10020041

Dyakov, Yu. & Levitin, M. 2018. *Phitopathogenic fungi infestations*. URSS, Moscow, 260 pp. (in Russian).

Emelyanova, O., Krivorot, A. & Shidlovskiy, A. 2015. The economic efficiency of cultivating raspberry remontant plant when using complex water-soluble fertilizers. *Fruit growing in Belarus: traditions and modernity: international materials scientific conf. dedicated to the 90th Anniversary of the formation of the Institute of Fruit Growing RUE*. Samohvalovichi, pp. 352–356 (in Russian).

Gadzalo, Ya. 2015. *Agrobiology of plant rhizosphere*. In: Gadzalo, Ya. (Ed.), Patika, N. & Zarizhnyak, A., Agrarna nauka, Kiev, 386 pp. (in Russian).

Jankevica, L., Polis, O., Korica, A., Samsone, I., Laugale, V. & Daugavietis, M. 2018. Environmental risk assessment studies on new plant protection products, which have been elaborated from coniferous tree bark. *Agronomy Research* **16**(5), 2056–2067. https://doi.org/10.15159/AR.18.189

Khalil, N. & Jamel, R. 2017. Effect of chemical, organic and bio fertilization on growth and yield of strawberry plant. *Internat. Journal of Advances in Chemical Eng. & Biological Sciences* **4**(1). http://doi.org/10.15242/IJACEBS.ER0117012

Kowalenko, C. 2006. The effect of nitrogen and boron fertilizer applications on Willamette red raspberry growth, and on applied and other nutrients in the plant and soil over two growing seasons. *Canadian Journal of Plant Science* **86**, 213–225. 10.4141/P04-036

Kudeyarova, E. 1999. *Diversity of microbial communities under different anthropogenic loads.* In: Kudeyarova, E.I. (Ed.). Vishaya shkola, Kishineu, 273 pp. (in Russian).

Levitin, M. 2009. Phytopathogenic fungi and human well-being. [Electronic source] – URL: *http://mycol-algol.ru/event_00001/Levitin_event00001.pdf* (in Russian).

Malinovskaia, I. 2017. Influence of organic and mineral fertilizer on the number and physiological and biochemical activity of microorganisms of gray forest soil. *Problemi ekologichnoi biotehnologii* **2**. [Electronic source]. http://ecobio.nau.edu.ua/index.php/ecobiotech/article/view/12194/16294 (in Ukranian).

Markov, I. 2017. *Phytopathology*. In: Markov I.L. (Ed.). Lira-K, Kiev, 480 pp. (in Ukranian).

Nannipieri, P. 2003. Microbial diversity and soil functions. In: Nannipieri, P. (Ed.), Ascher, J. & Ceccherini, M.T. *European Journal of Soil Science* **54**, 655–670.

Parfeniuk, A. 2011. Formation of fungal phytopathogenic background with winter wheat varieties. *Visnyk Lvivskogo Universitetu* **57**, 170–175 (in Ukranian).

Parfeniuk, A., Sterlikova, O., Blaginina, A., Gorgan, T., Beznosko, I., Sahanovskaia, V., Kovtun, V. & Tischenko, G. 2014. *Ecological evaluation of wheat varieties by influence on the formation of populations of phytopathogenic fungi*. Kiev, 39 pp. (in Ukranian).

Polianchikov, S. & Kapitanskaia, O. 2017. Foliar treatment: opportunities and mistakes. In: Polianchikov S. (Ed.). *Agroindustriya* **9**, 32–36 (in Ukranian).

Paulus, O. 1990. Fungal diseases of strawberry. *HortScience* **25**(8), 885–888.

Sekizura, M., Vey Tsi, T., Aomori, T., Okada, Y., Nakamura, K., Apaki, T., Horiuchi, R., Ohti, S., Nakamura, T. & Yamamoto, K. 2014. Effect of a Dietary Supplement Containing Raspberry Ketone on Cytochrome P450 3A Activity. *Pharmaceutica Analytica Acta. Pub Med Journals.* https://doi.org/05. 10.4172/2153-2435.1000302

Sheng, L., Shen, X., Benedict, C., Su, Y., Tsai, H-C., Schacht, E., Kruger, C.E., Drennan, M. & Zhu, M-J. 2019. Microbial Safety of Dairy Manure Fertilizer Application in Raspberry Production. *Front. Microbiol*. **10**, 2276. doi: 10.3389/fmicb.2019.02276

Stojanov, D., Milošević, T., Mašković, P., Milošević, N., Glišić, I. & Paunović, G. 2019. Influence of organic, organo-mineral and mineral fertilisers on cane traits, productivity and berry quality of red raspberry (*Rubus idaeus* L.), *Scientia Horticulturae* **252**, 370–378. https://doi.org/10.1016/j.scienta.2019.04.009

Zvyagintsev, D.G. 1991. *Methods of soil microbiology and biochemistry*. In: Zvyagintsev D.G. (Ed.). MSU, Moskva, 304 pp. (in Russian).

Wang, S. & Lin, H-S. 2000. Antioxidant Activity in Fruits and Leaves of Blackberry, Raspberry and Strawberry Varies with Cultivar and Developmental Stage. *Journal of Agriculture Food Chemistry* **48**(2), 140–146.

Wendel, R., Luciana, P. & Pauletti, R. 2020. Raspberry production with different NPK dosages in South Brazil. *Scientia Horticulturae* **261**. https://doi.org/10.1016/j.scienta.2019.108984

Agronomy Research **18**(4), 2559–2567, 2020
https://doi.org/10.15159/AR.20.205

Experience and prospects for application of by-products of processing of fruits in the production of animal feed

I.A. Plotnikov[1,2,*], M.M. Mukhamedyanov[1], I.A. Domsky[1], O.Yu. Bespyatykh[3] and N.A. Makarova[4]

[1]Russian Research Institute of Game Management and Fur Farming, 79 Preobrazhenskaya street, RU610000 Kirov, Russia
[2]Vyatka State Agricultural Academy, 133 October Avenue, RU610017 Kirov, Russia
[3]Vyatka State University, 12 Orlovskaya street, RU610002 Kirov, Russia
[4]Kirov State Medical University, 112 Karl Marx street, RU610998 Kirov, Russia
[*]Correspondence: bio.vniioz@mail.ru

Abstract. The purpose of the research was to study the feasibility of using by-products of the industrial processing of fruits for the production of full-feed mixed fodders with the possibility of using these mixed feeds as the only feed in the diets of herbivorous fur animals (nutria, brown muskrat, steppe marmot). Studies of chemical composition and nutrition have shown that non-traditional ingredients can be included in the composition of feed. At their expense, you can save up to 30% of leguminous feed, 9% - cake, 1% - meat and bone meal. This allowed us to reduce the cost of the studied batches of feed by 18–21%. Experiments have shown the effectiveness of using such feed in the diets of herbivorous fur-bearing animals. The inclusion of compound feed in the diet allowed to increase the number of commercial offspring per female muskrat by 0.8 heads, compared to the control group. The safety of young animals until the moment of depositing puppies from their mothers was approximately equal in both groups. Young muskrats of the experimental groups had 5.5–6.8% higher values of average daily increments, compared to control analogues. A similar pattern is established in male nutria. Marmots of the experimental group from the very beginning of the experiment were outnumbered by control animals. In July, these differences reached statistically significant values: 4,085 ± 71 g vs. 3,736 ± 73 g ($p < 0.01$). Thus, the marmots of the experimental group recovered faster after winter hibernation.

Key words: compound feed, meal, herbivorous fur-bearing animals, diet.

INTRODUCTION

Fruit processing products are widely used in the food industry. They enrich the human diet with the necessary biologically active and nutritious substances. Rowanberry powder as an unconventional ingredient with high nutritional and biological value was used in the development of gluten-free bread (Dubrovskaya et al., 2017). As supplement to wheat flour, powders of blueberries, rowanberries, pine nuts, sea buckthorn are used (Nilova & Malyutenkova, 2018; Nilova et al., 2019).

By-products of fruit processing are also used in animal feeding. In each region, there are non-traditional sources of feed rich with protein, amino acids, vitamins, inorganic substances, as well as biologically active elements. Using them allows to expand the range of feeds, contributes to increasing the productivity of animals (Mukhamedyanov et al., 2009).

Unclaimed by-products of plant raw materials processing in enterprises for the production of beverages, medicines, and for fruits canning can be promising ingredients for the production of compound feed. Preliminary calculations show that Russia has a sufficient amount of such ingredients to ensure the feeding of all herbivorous fur animals being breed in the country.

It is advisable to use ingredients from by-products of fruit processing that have nutritional value and useful properties in the production of complete feed: black chokeberry [*Aronia melanocarpa* (Michx.) Elliott] (Kokotkiewicz et al., 2010), common apricot [*Prunus armeniaca* L.] (Hayta & Alpaslan, 2011), black currant [*Ribes nigrum* L.] (Djordjević et al., 2013), sea buckthorn [*Elaeagnus rhamnoides* (L.) A. Nelson] (Skalski et al., 2019), cinnamon rose [*Rosa majalis* Herrm.] (Koropachinskiy & Vstovskaya, 2002), rowan [*Sorbus aucuparia* L.] (Klavins et al., 2016), Chinese magnolia vine [*Schisandra chinensis* (Turcz.) Baill.] (Panossian & Wikman, 2008), spiny eleuterococus [*Eleutherococcus senticosus* (Rupr. & Maxim.) Maxim.] (Arouca & Grassi-Kassisse, 2013) and others in the form of meal and flour obtained in the production of various beverages and oils. Biologically active elements that are present in by-products of fruit processing have a positive effect on the functioning of the body's systems and organs, on the productivity of animals (Prikryl et al., 2016; Toporova et al., 2018; Ferraz et al., 2019; Filatov et al., 2019).

The purpose of the research was to study the feasibility of using by-products of the industrial processing of fruits for the production of full-feed mixed fodders with the possibility of using these mixed feeds as the only feed in the diets of herbivorous fur animals.

MATERIALS AND METHODS

The study of compound feeds in experiments with farm animals by the method of Balakirev & Yudin (1994) was carried out at the Russian Research Institute of n.a. Prof. B.M. Zhitkov (VNIIOZ) and animal farm 'Vyatka' (Kirov region, Russia). The study followed the principles of international and Russian declarations and regulations on humane treatment of animals. The subjects of the study were nutria (*Myocastor coypus* Molina, 1782) (Fig. 1) and brown muskrat (*Ondatra zibethicus* Linnaeus, 1776) (Fig. 2) and steppe marmot (*Marmota bobak* Müller, 1776) (Fig. 3).

Figure 1. The nutria (*Myocastor coypus* Molina, 1782) (photo M. Mukhamedyanov).

For inclusion in the diet of experimental fur-bearing animals, batches of compound feeds were prepared with the inclusion of various non-traditional ingredients. Specialists of VNIIOZ and the State Center of Agrochemical Service ‘Kirovsky’ studied the chemical composition and nutritional value of mixed feeds.

Figure 2. The brown muskrat (*Ondatra zibethicus* Linnaeus, 1776) (photo A. Matskova).

Figure 3. The steppe marmot (*Marmota bobak* Müller, 1776) (photo M.V. Plugina).

In all samples the following was determined: initial and hygroscopic moisture. The Kjeldahl titrimetric method for nitrogen determination and the calculation method for crude protein were used (GOST 13496.4-93, 2011). The mass fraction of crude fat was determined by fat-free residue in a Soxhlet apparatus (GOST 13496.15-2016, 2016). The method for crude fiber determination according to Genneberg and Shtoman was used (GOST 31675-2012, 2014). Phosphorus was determined photometrically (GOST 26657-97, 1999). Sulfur was determined by ashing with a mixture of nitric and perchloric acids and then by the turbidimetric method.Calcium, copper, iron, magnesium, manganese, potassium, sodium, zinc were determined by atomic absorption spectrometry (GOST 32343-2013 (ISO 6869: 2000), 2014) on the Spectr 5-3 spectrophotometer. Carotene was determined photometrically (GOST 13496.17-95, 2011). Sample studies were repeated 2–3 times, depending on method requirements.

The compound feed of the control batch included: 76% of wheat and barley grains, 11% of pea grains, 9% of sunflower seed cake, 1.4% of feed limestone (chalk), 1% of vitamin and mineral additives in the form of a premix for rabbits and 1% of meat and bone meal, 0.6% of sodium chloride salt. The dry matter content in this feed was at the level of 86%, the moisture content was 14% respectively.

Instead of part of wheat grain, barley, peas, sunflower seed cake and meat and bone meal, oilseed residues from sea buckthorn pomace (*Elaeagnus rhamnoides* (L.) A. Nelson), cinnamon rose (*Rosa majalis* Herrm.) and flour from pomace of rowan (*Sorbus aucuparia* L.), black chokeberry (*Aronia melanocarpa* (Michx.) Elliott), kernels of common apricot (*Prunus armeniaca* L.), roots of spiny eleuterococus (*Eleutherococcus senticosus* (Rupr. & Maxim.) Maxim.) were included in the experimental batches of compound feed. The quantitative content of ingredients in experimental batches of compound feed is presented in Table 1.

All compound feeds were produced in granular form. The diameter of the granules was 5 mm. Bunker feeders were used for feeding muskrats and marmots, and floor feeders were used for nutria. The animals were kept in cages with a range of metal mesh and a wooden house.

The first experiment was carried out on female muskrats 2 groups were formed (control and experimental), 24 heads in each group. Females were selected into groups on the basis of analogs, taking age (11 months) and body weight (mass) into account. The sisters were evenly divided into groups. The experiment was continued on the young animals obtained from the females after being deposited from their mothers. Out of 120 young animals, 2 groups of 30 females and 30 males in each were formed, taking age, weight and origin into account. The muskrats were kept in cages of 2 heads. The experimental group received compound feed No. 1. The duration of the experiment was 9 months.

The second experiment was carried out on young male nutria. 2 groups of males from among brothers of littermates were formed, 23 heads each, aged 109–112 days and weighing 1,514–1,518 g. The experimental group received compound feed No. 2. The duration of the experiment was 5 months.

The third experiment was carried out on young nutria from the age of 1 month. Females and males were kept separately. With the onset of physiological maturity, 2 groups of stocks were formed, 4 males and 18 females in each group. Experienced animals received compound feed No. 3. The duration of the experiment with the preparatory period was 9.5 months.

The third experiment was carried out on young nutria from the age of 1 month. Females and males were kept separately. With the onset of physiological maturity, 2 groups of stocks were formed, 4 males and 18 females in each group. Experienced animals received compound feed No. 3. The duration of the experiment with the preparatory period was 9.5 months.

The fourth experiment was carried out on 60 marmots at the age of 13 months. 2 groups of 15 females and 15 males in each were formed with equal live weight. The animals were kept in cages in pairs. Experienced animals received compound feed No. 3. The duration of the experiment was 6 months.

The digital materials of the experiments were processed by the method of variation statistics on an IBM personal computer using a package of statistical programs for processing the results of biological research taking into account the Student's criterion (Biostatistica, Excel). The arithmetic mean was calculated, the representativeness error M ± m. The result was considered reliable (statistically significant) at $p \leq 0.05$.

RESULTS AND DISCUSSION

By-products are obtained from fruits of plants that grow in the Volga-Vyatka region of the Russian Federation in the process of industrial processing. In the future meal and flour are produced from their marc. Chemical analysis shows that the content of pectin substances in the marc of Prunus Aronia reaches 1.7%, and organic acids up to 3.2%. The dry matter of Aronia Prunus contains: 11–13% protein with a total amount of amino acids of at least 9.5%, about 6% fat, up to 30% fiber, 7–8% sugars. The content of macronutrients is equal to: 0.65% calcium, 0.32% phosphorus (with an optimal ratio of these elements 2:1), 0.5% potassium and 0.2% magnesium. 9 mg of carotene is contained per kg, trace elements content, mg per kg: iron 228, manganese 86, zinc 41, copper 25.

The dry matter of processed rowan contains: 10% protein, 8% fat, 20% fiber, 14% sugar. Contained in 1 kg: 3.5 g of calcium, 2.5 g of phosphorus, 8 g of potassium, 1.3 g of magnesium, 0.3 g of sulfur, 71 mg of manganese, 296 mg of iron, 26 mg of zinc and 9 mg of copper. In the dry matter of black currant marc there is 12% protein, 18% fat, 23% fiber, 12% sugar. Contained in 1 kg: 5.4 g of calcium, 3.1 g of phosphorus, 5 g of potassium, 1.1 g of magnesium, 0.3 g of sulfur, 23 mg of manganese, 158 mg of iron, 18 mg of zinc and 14 mg of copper.

Apricot kernel flour contains up to 22% sugar, 3% organic acids, 1.5% pectin substances, and up to 25% oil. The dry substance of apricot flour contains: 42% protein, 22% fat, 6.5% fiber, 16% sugar. 1 kg of this flour contains: 3.7 g of calcium, 6.9 g of phosphorus, 1.3 g of potassium, 0.1 g of sodium, 0.3 g of magnesium, 0.2 g of sulfur, 58 mg of iron, 15.5 mg of manganese, 1.5 mg of copper and 2 mg of carotene. Sea buckthorn meal in terms of dry matter contained: 26% protein, 6% fat, 22% fiber and 7% sugar. The mineral content in 1 kg is: 2.5 g of calcium, 3.9 g of phosphorus, 7.3 g of potassium, 1.5 g of magnesium and sulfur, 107 mg of iron, 43 mg of zinc, 4 mg of copper and 2 mg of manganese. The obtained data indicate the possibility of widespread use of by-products of fruits in the composition of compound feeds instead of a certain proportion of legumes, cake, meal and animal feed additives (Plotnikov, 2012; Mukhamedyanov & Plotnikov, 2017).

The composition of experimental batches of feed is shown in the table (Table 1). In 100 g of compound feeds, the content of 1.1–1.3 MJ was determined based on energy nutrition. In the experimental batches of compound feed, in contrast to the composition of the control batch, less than 30% leguminous fodder, 9% - sunflower cake, 1% - meat and bone meal were contained. Due to the inclusion of the studied ingredients in compound feed and a decrease in the content of expensive grains of wheat, barley, peas, as well as the complete exclusion of sunflower seeds cake and meat and bone meal, the total cost of pilot batches of compound feed decreased by 18–21%.

The possibility of using experimental batches of feed was tested in the process of scientific and economic research. The research was performed on domesticated fur animals that are bred in animal farms. In the diet of muskrats and nutria, the studied compound feed was the only food. In the diet of steppe marmots, it was an additional ingredient. Palatability of the combined feed in the control and experimental groups amounted to 97–98%.

Testing in the production conditions of batch No. 1 was carried out in the first study. As a result, it was found that the inclusion of compound feed in the diet allowed to increase the number of commercial offspring per female muskrat by 0.8 heads, compared to the control group. Females who did not receive the studied compound feed gave only 5.4 heads of their offspring. The safety of young animals until the moment of depositing puppies from their mothers was approximately equal in both groups.

The separated young muskrat stock raised on compound feed from batch No. 1 reached body weight by seven months of age: males - 776 ± 14 g, females - 771 ± 17 g, against litter mates raised on compound feed from the control batch: males - 735 ± 12 g, females-722 ± 17 g. The difference in the groups of males and females is statistically significant ($p < 0.05$). Average daily gains of the experimental young stock was more than 5.5–6.8 percent, as compared to the control counterparts.

Table 1. Number of ingredients and chemical composition of experimental batches of feed

Indicators for the composition of ingredients and chemicals	Control	Number of ingredients and composition of experimental granulated feed		
		Batch No. 1	Batch No. 2	Batch No. 3
The composition includes the following ingredients, %:				
grain of wheat and barley	76	50	57	47
pea grain	11	5	-	10
sunflower cake	9	-	-	-
Meal obtained from marc, %:				
sea buckthorns	-	30	21	24
rosehip	-	5	3	-
Flour obtained from marc, %:	-			
rowan	-	-	-	8
black chokeberry	-	-	6	-
apricot kernels	-	-	11	9
Eleutherococcus roots	-	8	-	-
Meat and bone meal	1	-	-	-
Feed limestone (chalk), %	1.4	1.5	1.5	1.5
Sodium chloride salt, %	0.6	0.3	0.5	0.5
Premix for rabbits	1	-	-	-
Chemical composition of produced feed:				
Dry matter content in the feed, %	86	86	84	86
Content in dry matter, %:				
protein	17.6	17.7	17.9	19.1
fat	8.0	6.8	7.9	7.5
fibre	6.8	8.5	8.8	7.6
Macronutrient content in the feed, %:				
calcium	0.78	0.70	0.80	0.60
phosphorus	0.45	0.50	0.49	0.50
magnesium	0.26	0.16	0.18	0.17
potassium	0.69	0.71	0.69	0.77
sodium	0.49	0.40	0.41	0.46
sulfur	0.28	0.10	0.20	0.19
Content of microelements in feed, mg kg^{-1}:				
iron	744	273	396	649
zinc	104	41	49	33
copper	24	17	15	16
manganese	78	32	82	51
Content of carotene in feed, mg kg^{-1}:	14	10	14	16

The second experiment was performed on young males of in-cage nutria. For the experiment two groups of male litter mates were formed: 23 heads at the age of 109–112 days and a body weight of 1,514–1,518 g The experimental group of males was fed with compound feed from batch No. 2. The control group received compound feed of the above composition. For five months of experience, males in the experimental group had a higher average daily gain in body weight. In particular, the value of this indicator in the experimental group was 18.4 ± 0.94 g, and in the control group - 17.9 ± 0.91 g. As a result of the control slaughter, the optimal yield of hot carcass of males was established. A higher value of the output of the hot carcass was recorded in males of the experimental group. It was 48.3%, and in the control group it was 0.4% lower. The average size of the skins that were obtained from males of different groups was equal. It was 2,117 cm^2.

In the third scientific and economic experiment, male and female litter mates received compound feed from experimental batch No. 3 for eight months. To study the reproduction indicators, groups of nutria young stock were formed. The control group included 4 males and 17 females, the experimental group - 4 males and 18 females. In groups animals of the control group were fed with ordinary compound feed, and the experimental group received compound feed from batch No. 3. After 45 days of feeding, in groups 28% of pregnant females were in the control group, and 32% in the experimental group.

To conduct scientific and economic experiments on steppe marmots feeding, two groups of one-year-old young animals of 30 heads were formed. The initial average mass of animals is equal in different groups. The number of females and males in each group was equal. A mixed-sex pair of marmots was kept in an individual cage. Each cage had a house. The experiment was carried out from May to September. After September, marmots prepare for winter hibernation and stop eating food. The compound feed from batch No. 3 was included in the diet of steppe marmots of the experimental group in the amount of 76% of the total nutritional value of the diet. The rest 24% was accounted for by the green mass of grasses. The control group with the same ratio of feed received conventional compound feed. On average, each marmot received 180 g of compound feed and 500 g of green grass mass. The actual consumption of granulated compound feed established by measurements was 98%, and the green grass mass - 70%.

Marmots of the experimental group from the very beginning of the experiment were outnumbered by control animals. In July, these differences reached statistically significant values. Experimental animals weighed 4,085 ± 71 g, and control animals - 3,736 ± 73 g ($p < 0.01$). In September, experimental animals also exceeded control animals by weight, but the difference is not reliable. The average daily gain for the period of weight gain in groups was 16.6 and 16.5 g. As a result, we conclude that marmots of the experimental group who received compound feed prepared according to the recipe No. 3 during the experiment recovered faster after winter hibernation, grew faster and gained the largest live weight. In preparation for hibernation, they were the first to reduce their live body weight, compared to control marmots.

CONCLUSIONS

The results obtained in experiments indicate that the diets of herbivory fur animals can include feed from meal and flour, which are obtained from by-products of industrial processing of fruits (sea buckthorn, cinnamon rose, rowan, black chokeberry, kernels of common apricot, roots of spiny eleuterococus). Due to the introduction of unconventioal ingredients in the composition of compound feeds, up to 30% of leguminous feed was saved, 9% - cake, 1% - meat and bone meal. This allowed to reduce the cost of the studied batches of feed by 18–21%.

The inclusion of new ingredients in compound feed gave a positive effect when growing herbivorous fur animals in cage conditions: nutria, muskrats and marmots. The number of commercial offspring per female of muskrat increased by 0.8 heads, compared with the control group. The set apart young muskrat grown on the experimental compound feed reached body weight by the age of seven months: males -

776 ± 14 g, females - 771 ± 17 g, versus littermates raised on compound feed from the control batch: males - 735 ± 12 g, females - 722 ± 17 g ($p < 0.05$). The average daily gain of the experimental young stock was 5.5–6.8% higher than that of the control counterparts. Male nutria in the experimental group had an average daily gain of 18.4 ± 0.94 g, and in the control group - 17.9 ± 0.91 g. With the content of nutria in the stocks by the 45th day pregnancy was established in 32% of females receiving the experimental feed, and in control - 28%. The marmots of the experimental group weighed 4,085 ± 71 g during the period of maximum weight gain at the age of 16 months, and the control ones weighed 3,736 ± 73 g ($p < 0.01$). All this testifies to the efficiency of using meal and flour from by - products of fruit processing in compound feed for herbivorous fur animals.

REFERENCES

Arouca, A. & Grassi-Kassisse, D.M. 2013. Eleutherococcus senticosus: Studies and effects. *Health* **5**(9), 1509–1515. doi: 10.4236/health.2013.59205

Balakirev, N.A. & Yudin, V.K. 1994. *Methodological guidelines for conducting scientific and economic experiments on feeding fur-bearing animals*. Moscow, NIIPZK, 31 pp. (in Russian).

Djordjević, B., Šavikin, K., Zdunić, G., Janković, T., Vulić, T., Pljevljakušić, D. & Oparnica, C. 2013. Biochemical properties of the fresh and frozen black currants and juices. *J. Med. Food*. Jan, **16**(1) 73–81. doi: 10.1089/jmf.2011.0256

Dubrovskaya, N., Savkina, O., Kuznetsova, L. & Parakhina, O. 2017. Development of gluten-free bread with unconventional raw ingredients of high nutritional value and antimicrobial activity. *Agronomy Research* **15**(S2), 1276–1286.

Ferraz, P.F.P., Ferraz, G.A.S., Schiass,I, L, Nogueira, V.H.B., Barbari, M. & Damasceno, F.A. 2019. Spatial variability of litter temperature, relative air humidity and skin temperature of chicks in a commercial broiler house. *Agronomy Research* **17**(2), 408–417. doi.:10.15159/AR.19.112

Filatov, A., Shemuranova, N., Konopeltsev, I., Plemyashov, K., Anipchenko, P. & Stekolnikov, A. 2019. The role of triterpene acids in boar reproduction. *Theriogenolgy* **137**, 134.

GOST 13496.15-2016. 2016. Forage, compound feed, compound feed raw materials. Methods for mass fraction of crude fat determination. City of Moscow: Standartinform, 9 pp. (in Russia).

GOST 13496.17-95. 2011. Feed. Methods for carotene determination. City of Moscow: Standartinform, 5 pp. (in Russia).

GOST 13496.4-93. 2011. Forage, compound feed, compound feed raw materials. Methods for nitrogen and crude protein content determination. City of Moscow: Standartinform, 15 pp. (in Russia).

GOST 26657-97. 1999. Forage, compound feed, compound feed raw materials. Methods for phosphorus content determination. City of Moscow, 10 pp. (in Russia).

GOST 31675-2012. 2014. Feed. Methods for crude fiber content determination using intermediate filtration. City ofMoscow: Standartinform, 9 pp. (in Russia).

GOST 32343-2013 (ISO 6869: 2000). 2014. Forage, compound feed. Determination of calcium, copper, iron, magnesium, manganese, potassium, sodium and zinc content by atomic absorption spectrometry. City of Moscow: Standartinform, 14 pp. (in Russia).

Hayta, M. & Alpaslan, M. 2011. Apricot Kernel Flour and Its Use in Maintaining Health. *Flour and Breads and their Fortification in Health and Disease Prevention.* Academic Press. 213–221. doi.org/10.1016/B978-0-12-380886-8.10020-0

Klavins, L., Kviesis, J., Steinberga, I., Klavina, L. & Klavins, M. 2016. Gas chromatography–mass spectrometry study of lipids in northern berries. *Agronomy Research* **14**(S2), 1328–1346.

Kokotkiewicz, A., Jaremicz, Z. & Luczkiewicz, M. 2010. Aronia plants: a review of traditional use, biological activities, and perspectives for modern medicine. *J. Med. Food.* Apr. **13**(2), 255–269. doi: 10.1089/jmf.2009.0062

Koropachinskiy, I.Yu. & Vstovskaya, T.N. 2002. *Woody plants of the Asian part of Russia.* Novosibirsk: Publishing House of SB RAS, Branch "Geo", pp. 359–360 (in Russian).

Mukhamedyanov, M.M. & Plotnikov, I.A. 2017. Prospects for industrial technology of breeding of muskrat. *Russian Agricultural Sciences* **43**(5), 427–429. doi: 10.3103/S1068367417050111

Mukhamedyanov, M.M., Plotnikov, I.A. & Solomina, E.S. 2009. Mixed feed from unconventional ingredients for herbivorous furbearers. *Russian Agricultural Sciences* **35**(5), 343–345. doi: 10.3103/S1068367409050164

Nilova, L. & Malyutenkova, S. 2018. The possibility of using powdered sea-buckthorn in the development of bakery products with antioxidant properties. *Agronomy Research* **16**(S2), 1444–1456. doi.org/10.15159/AR.18.055

Nilova, L., Malyutenkova, S. & Kruchina-Bogdanov, I. 2019. The impact of plant powders on acrylamide content in bakery products. *Agronomy Research* **17**(S2), 1401–1413. doi.org/10.15159/AR.19.076

Panossian, A. & Wikman, G. 2008. Pharmacology of *Schisandra chinensis* Bail.: An overview of Russian researchand uses in medicine. *Journal of Ethnopharmacology* **118**, 183–212.

Plotnikov, I.A. 2012. Cage housed marmot's diseases. *Proceedings of the Xth International Scientific Congress in Fur Animal Production*. 21–24 August 2012, Copenhagen, Denmark. *Scientifur* **36**(3/4), 177–179. doi: 10.3920/978-90-8686-760-8_25

Prikryl, M., Vaculik, P., Chladek, L., Libich, L. & Smetanova, P. 2016. The human factor's impact on the process of milking. *Agronomy Research* **14**(5), 1659–1670.

Skalski, B., Kontek, B., Lis, B, Olas, B, Grabarczyk, L, Stochmal, A & Żuchowski, J. 2019. Biological properties of *Elaeagnus rhamnoides* (L.) A. Nelson twig and leaf extracts. *BMC Complement Altern Med* **19**, 148. doi.org/10.1186/s12906-019-2564-y

Toporova, L.V., Bouazid, A.A. & Toporova, I.V. 2018. Energy protein complex from non-standard fruit of fruit trees instead of corn in the rations of broiler chickens. *Feeding of farm animals and feed production* **7**, 33–39 (in Russian).

Agronomy Research **18**(4), 2568–2580, 2020
https://doi.org/10.15159/AR.20.189

Effect of partial substitution of bulk urea by nanoparticle urea fertilizer on productivity and nutritive value of teosinte varieties

H.S.A. Salama[1,*] and H.H. Badry[2]

[1]Crop Science Department, Faculty of Agriculture, Alexandria University, Aflaton street, El-Shatby, EG21545 Alexandria, Egypt
[2]Soil and Water Science Department, Faculty of Agriculture, Alexandria University, Aflaton street, El-Shatby, EG21545 Alexandria, Egypt
[*]Correspondence: heba.salama@alexu.edu.eg

Abstract. The integration of nanoparticle urea (NPU) in the fertilization scheme of forage crops with high nutrients' requirements, like teosinte (*Zea mexicana* L.), would help avoiding the environmental implications associated with the application of high rates of conventional bulk urea (BU), while not depriving the plant from its benefits. The effects of fertilization treatments composed of different percentages of NPU and/or BU, on yield, agronomic characteristics and quality attributes of three cuts of two teosinte local varieties were investigated in a split-split plot design during summers of 2018 and 2019. In general, the application of 50% NPU + 50% BU was similar to 100% BU in the production of highest amount of fresh yield, with the highest values for plant height and stem diameter, in addition to appreciable nutritive value, in terms of high crude protein (66.10 g kg^{-1}) and non-fiber carbohydrates (NFC), and low acid-detergent fiber (284.09 g kg^{-1}) and crude fat (36.97 g kg^{-1}) contents. While the 1st cut was characterized by the highest plant height (58.74 cm in average), stem diameter (7.64 mm in average) and leaf area (130.07 m^2 in average), the 3rd cut produced the highest amount of fresh yield (39.68 t ha^{-1} in average). Variations in quality measures among the three cuts were almost non-significant. Variations in yield and quality were detected between the two tested local varieties. In conclusion, the combined application of 50% NPU with 50% BU is recommended for the production of fodder teosinte in similar environments.

Key words: forage yield, forage quality, nanoparticle urea, nitrogen fertilizers, *Zea mexicana* L.

INTRODCUTION

Fertilization is a basic cultural practice in the farming systems worldwide, upon which the productivity of the different crop species is greatly dependent. Globally, the application of mineral fertilizers is a key management strategy that plays a significant role in enhancing crop productivity and, thus, maintaining sufficient food and feed supplies (Chaudhary et al., 2017).

Nitrogen (N) is the first and most important nutrient required for crop growth and development. As a constituent of chlorophyll, it greatly supports the photosynthesis process (Rathnayaka et al., 2018). In addition, N contributes for biosynthesis of many growth-promoting enzymes and proteins and, thus, plays a crucial role in regulating plant growth especially during the vegetative phase (Iqbal, 2019). Nonetheless, N is a precursor for several chemical compounds that protect the plant against diseases and parasites (Hoffland et al., 2000). Among the different commercial forms of mineral N fertilizers, urea [$CO(NH_2)_2$] is the most widely used, mainly due to its high N content (46% N), in addition to its compatibility with other nutrients (Elemike et al., 2019). However, around 75% of urea applied to the soil is lost (Chhowalla, 2017; Khalifa & Hasaneen, 2018). N fertilizer loss primarily occurs through nitrate leaching, that contaminates ground water leading to eutrophication, and volatilization that increases greenhouse gasses (i.e., nitrous oxides), contributing to the global warming. Nonetheless, the nitrogenous fertilizers' use efficiency in the modern farming systems is reported to be only 45–50% (Iqbal et al., 2019). The high N loss coupled with its low use efficiency forced the farmers to increase the amounts of applied N fertilizers in order to achieve better crop production (Rathnayaka et al., 2018), which resulted in rising the costs of the farming practice, meanwhile, increasing the consequent environmental implications (Chhowalla, 2017; Marchiol, 2019). Therefore, there is a pressing need to improve the N availability for plants, while reducing its harmful effects to the environment.

In this regard, the utilization of nanoparticle fertilizers, especially nanoparticle urea (NPU) was proposed by several researchers (e.g., Chhowalla, 2017; Kottegoda et al., 2017; Rathnayaka et al., 2018) to avoid the problems associated with the application of bulk urea, while not depriving the plant from its benefits. The main drive behind the low N use efficiency of the bulk chemical fertilizers is the lack of synchronization between nutrient release from the fertilizer and its demand by the plant (Marchiol, 2019). As the nanostructured fertilizers are advantaged by the controlled release of nutrients, this will allow for the effective duration of nutrient supply to the plant which would secure optimum fulfillment to its nutrients' needs (Liu & Lal, 2015) without any adverse environmental impacts (Kopittke et al., 2019). When used as foliar application, nanofertilizers have the ability to enter through the porous cell wall of plant cells due to their minute particle size (< 50 nm) allowing for high absorption compared to conventional fertilizers (Benzon et al., 2015). It is evident that applying nanoparticle N fertilizers in conjunction with reduced dosses of conventional N fertilizers can boost the productivity of several cereal crops, e.g., rice, maize and barley (Benzon et al., 2015; Gomaa et al., 2017; Iqbal, 2019). However, their potential with green forage crops is not yet exploited.

Since the area devoted to summer forage crops in Egypt is limited, due to the prioritization of other economic crops like rice, maize and cotton, there is a need to expand the production of high-yielding, high-quality fresh forage crops (Rady, 2018). Teosinte (*Zea mexicana* L.) was believed to be the ancestor of modern maize (*Zea mays* L.) that was indigenous to Mexico and Central America (Gaudin et al., 2011). As a multi-cut forage crop, teosinte is advantaged over other prominent summer forage grasses, like fodder maize, by its special ability to tolerate high temperatures and adverse environmental conditions, and yield high amounts of fresh fodder under stressed conditions (Devkota et al., 2017). In addition, it is suitable for fresh feeding, hay, and silage production (Mohan et al., 2017). However, for improved growth and high fodder productivity, teosinte is known with its high nutrient requirements, especially nitrogen (Kumar et al., 2016), which would entail the unfavorable consequences usually accompanying the application of high doses of conventional N fertilizers. It was therefore, worthwhile to investigate the effect of the integration of nanoparticle urea fertilizer in the fertilization scheme of teosinte, on its fodder productivity and quality. The current study was, thus, designed to evaluate the forage yield and some agronomic characteristics, in addition to the nutritive value of three cuts of two fodder teosinte varieties subject to varying applications of bulk and nanoparticle urea.

MATERIALS AND METHODS

Location

Field trials were conducted during two successive summer seasons (2018 and 2019) at Abis experimental farm, Faculty of Agriculture, Alexandria University, Alexandria, Egypt. Soil of the experimental farm is sandy loam in texture, with 1.80% organic matter, and 100, 30, and 389 ppm available nitrogen, phosphorous and potassium, respectively. The experimental location is arid with hot and dry Mediterranean summer seasons. Precipitation in the summer is zero, and average atmospheric temperature during the two successive seasons are presented in Table 1.

Table 1. Average monthly temperature during summer 2018 and 2019

Month	Average temperature (°C)	
	Summer 2018	Summer 2019
May	24.44	23.24
June	26.11	26.54
July	27.78	28.06
August	28.33	28.06
September	27.78	26.56

Design and treatments

A split-split plot experimental design with three field replications was adopted to investigate the variations in yield, dry matter content, some agronomic characteristics and forage quality parameters among three cuts (sub plots) of two teosinte (*Zea mexicana*) varieties; variety 1 and 2 (sub-sub plots), as affected by five bulk urea (BU) and/or nanoparticle urea (NPU) fertilizer treatments (main plots). The investigated fertilizer treatments were; 100% BU (F1), 75% BU + 25% NPU (F2), 50% BU + 50% NPU (F3), 25% BU + 75% NPU (F4), and 100% NPU (F5). The bulk urea (BU) under investigation was obtained from Abu Qir Fertilizers Company, Alexandria, Egypt, and contained 46% N by weight. Rates of the BU were calculated based on the recommended N fertilization for teosinte in the region, amounting to 280 kg N ha^{-1}.

The NPU was prepared by milling BU over two sieves of 2 mm and 51 µm diameter. Samples with particle size < 51 µm were grinded using Planetary Mono Mill as described by Elkhatib et al. (2015), to a particle size < 30 nm. Scanning electron microscope equipped with energy dispersive spectroscopy (SEM-EDS) (JSM-IT200 Series, JEOL, Japan) was used to determine the particle size of the NPU (Fig. 1). The NPU with diameter < 30 nm was suspended in de-ionized water to prepare a stock solution of 500 mg L^{-1}, which was dispersed by ultrasonic vibration (130 W, 20 kHz) for 25 minutes to avoid nanoparticles aggregation. Four concentrations of NPU, i.e, 200, 150, 100, and 50 mg L^{-1}, representing the 100, 75, 50, and 25% NPU treatment, respectively, were freshly prepared directly before application. To prevent NPU sedimentation, suspensions were continuously mixed using a magnetic stirrer.

Fertilizer treatments were split into three equal doses, applied two weeks after sowing, and two weeks after each of the first and second cuts. At the time of fertilizer treatment application, BU was applied as top dressing, while NPU suspension was applied as foliar spray. The tested varieties were assigned to the sub-sub-plots and sown with the recommended seeding rate, amounting to 48 kg seeds ha^{-1}.

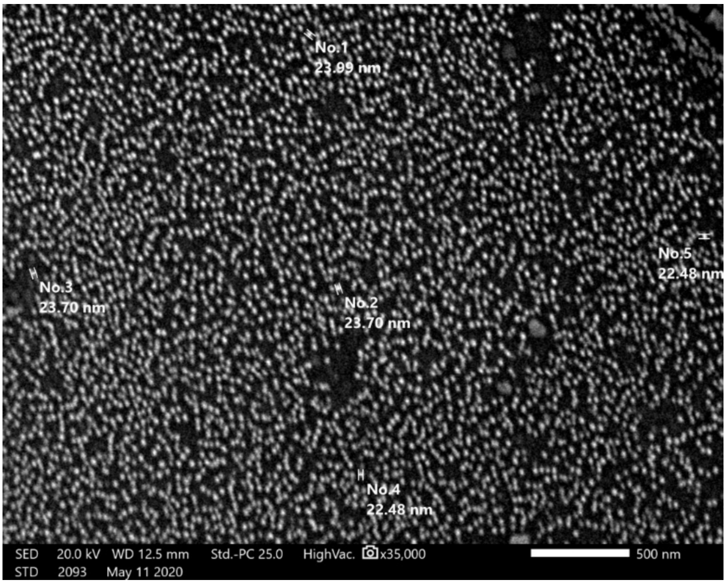

Figure 1. Scanning electron microscopy (SEM) image for nano particle urea (NPU).

Agronomy

Previous crop to teosinte cultivation in both experimental seasons, was wheat drilled on flat plots. After wheat harvesting, soil was plowed using a chisel plow in two perpendicular directions (20–25 cm depth), followed by land levelling, and ridging. Each experimental plot contained 4 ridges, 3 m long and 60 cm apart resulting in a total plot area of 7.2 m^2. A border of four ridges (7.2 m^2) was left between each two successive main plots to separate the fertilizer treatments. Sowing was done on 1^{st} and 10^{th} of May during 2018, and 2019, respectively. Seeds were drilled on the upper third part on one side of the ridge. Phosphorous fertilizer in the form of calcium monophosphate (15.5% P_2O_5) and potassium fertilizer as potassium sulphate (48% K_2O) were applied once before sowing with the recommended rates of 200 and 100 kg ha^{-1}, respectively. Flood irrigation was scheduled on weekly interval and hand weeding was practiced when necessary. At 45 days after sowing (DAS), first cut was taken, then 35 days interval was left before the second and third cuts.

Studied parameters

At each cut, plots were manually harvested using a garden sickle, leaving 5–7 cm above ground level to allow for regrowth. Total fresh yield per plot per cut was weighed on the field. Plant height (cm), stem diameter (mm), and leaf area per plant (cm^2) were calculated as an average of 5 randomly taken plants from the two ridges in the middle of each plot. A representative sub-sample per plot of approximately 750 g fresh matter was dried at 60 °C for 72 h until constant weight was reached to determine the dry matter (DM) content. The dried sub-samples were milled to a 1 mm particle size for forage quality evaluation. Nitrogen content (N) was determined using Kjeldahl procedure

(AOAC, 2012), then crude protein (CP) was calculated as N multiplied by 6.25. Neutral detergent fiber (NDF) and acid detergent fiber (ADF), representing the two prominent dietary fiber fractions, were sequentially analyzed using the semiautomatic ANKOM220 Fiber Analyzer (ANKOM Technology, Macedon, NY, USA) after Van Soest et al. (1991). Both fiber fractions were analyzed without heat stable amylase and expressed including residual ash content. Crude ash (CA) determination was done by incineration of Sub-samples in muffle oven at 550 °C for 3 h (AOAC, 2012). Soxhlet procedure was adopted to determine the crude fat (CF) content of the dried sub samples (AOAC, 2012). Finally, content of non-fiber carbohydrates (g kg^{-1}) was calculated using the following formula:

$$NFC = 1{,}000 - (CP + CF + NDF + CA) \quad (1)$$

Statistics

Analysis of variance for the variations among cuts (C), fertilizer treatments (F), and varieties (V) was done using SAS 9.4 program (SAS Institute, Inc., 2012) - PROC MIXED. Studied factors and their interactions were statistically analyzed using the following model, with only replicates considered random:

$$\begin{gathered} Pijkl = \mu + Ri + Fj + eij + Ck + eijk + Vl + Cj \times Fk + Cj \times Vl \\ + Fk \times Vl + Cj \times Fk \times Vl + eijkl \end{gathered} \quad (2)$$

where μ is the overall mean, R_i is the replicate effect (i = 1,2,3), F_j is the fertilizer treatment effect (j = 1,2,3,4,5), e_{ij} is the experimental error 'a', C_k is the cut effect (k = 1,2,3), e_{ijk} is the experimental error 'b', V_l is the variety effect (l = 1,2), and e_{ijkl} is the experimental error 'c'.

Data of fresh yield, dry matter content and agronomic characteristics will be presented and discussed separately for the two experimental seasons, upon the heterogeneity of variance's error (Hartley, 1950), while data of forage quality parameters will be presented in a combined analysis over the two experimental seasons, upon homogeneity of the variance's error. Least significant difference (L.S.D.) procedure - at 0.05 probability level - was used for means' comparisons.

RESULTS

For all studied parameters, main effects will be presented and discussed only if interaction involving them is not significant.

Yield, dry matter and agronomic characteristics

Analysis of variance revealed that the fresh yield, DM content and agronomic parameters were significantly variable among the tested cuts for both 2018 and 2019 ($p < 0.01$). In addition, fertilizer treatments significantly ($p < 0.01$) affected all parameters except stem diameter, while fresh yield during 2018 and 2019, and agronomic parameters only during 2018 were significantly variable ($p < 0.01$) among the tested varieties. As for the significant interactions, during both seasons, fresh yield was significantly affected by the cut × fertilizer treatment interaction ($p < 0.01$), and agronomic parameters were significantly affected by the fertilizer treatment × variety interaction ($p < 0.01$). Meanwhile, the three-way interaction was declared non-significant for yield, DM and agronomic characteristics ($p > 0.05$).

Highest significant fresh yield was achieved for cut 3, amounting to 39.23 and 40.12 t ha^{-1}, for 2018 and 2019, respectively (Table 2). On the other hand, cut 1 was characterized with the lowest significant amount of fresh yield, 7.07 and 10.95 t ha^{-1}, for the two respective seasons. Applying 100% BU fertilizer resulted in the production of the highest significant fresh yield, which gradually decreased with the decrease in the percentage of BU and increase in the percentage of NPU. Variety 1 was superior to variety 2 concerning the amount of fresh yield, with 27.97 and 31.85 t ha^{-1}, during 2018 and 2019, respectively. Variations in DM content were non-significant among the three cuts and two tested varieties in 2018 and 2019 (Table 2). However, opposite to the fresh yield, the DM content was inversely proportional to the percentage of mineral N fertilizer. Lowest significant DM content was reported for 100% BU fertilizer application, and amounted to 146.05 and 150.23 g kg^{-1} for 2018 and 2019, respectively. On the other hand, the highest significant DM content was reported for the application of 100% NPU fertilizer which was non-significantly different from 75% NPU + 25% BU, and 50% NPU + 50% BU. Fresh yield was significantly affected by the cut × fertilizer treatment interaction during the two growing seasons (Table 3). For all studied fertilizer treatments, cut 1 was inferior to the cuts 2 and 3 concerning the amount of fresh yield production. The application of 100% BU fertilizer produced the highest significant amount of fresh yield for the three cuts. Similarly, partial substitution of BU with NPU fertilizer; i.e. 75% BU + 25% NPU, and 50% BU + 50% NPU, produced as high fresh yield amounts as the application of 100% BU.

Table 2. Means of fresh yield (t ha^{-1}) and dry matter content (g kg^{-1}) as affected by the fertilizer treatment, cut, and variety for the two growing seasons

	Fresh yield		DM	
	Summer 2018	Summer 2019	Summer 2018	Summer 2019
Cut				
C1	7.07^{c*}	10.95^{c}	158.33^{a}	160.52^{a}
C2	31.13^{b}	35.84^{b}	147.83^{a}	145.85^{a}
C3	39.23^{a}	40.12^{a}	161.76^{a}	158.95^{a}
Fertilizer				
F1	34.79^{a}	35.62^{a}	146.05^{b}	150.23^{b}
F2	29.69^{b}	31.48^{b}	153.98^{ab}	150.85^{b}
F3	28.87^{b}	29.74^{bc}	155.79^{ab}	152.69^{ab}
F4	22.04^{c}	27.86^{c}	159.21^{ab}	155.23^{ab}
F5	13.64^{d}	20.15^{d}	164.85^{a}	165.50^{a}
Variety				
V1	27.97^{a}	31.85^{a}	153.82^{a}	152.52^{a}
V2	23.65^{b}	26.09^{b}	158.13^{a}	157.68^{a}

* Means followed by different small letter(s) within the same column, are significantly different according to the L.S.D. test at 0.05 level of probability.

Table 3. Means of fresh yield (t ha^{-1}) as affected by the fertilizer treatment × cut interaction for the two growing seasons

Fertilizer	Summer 2018			Summer 2019		
treatment	Cut 1	Cut 2	Cut 3	Cut 1	Cut 2	Cut 3
F1	10.78^{bA*}	44.94^{aA}	48.66^{aA}	15.85^{bA}	48.95^{aA}	49.68^{aA}
F2	8.54^{bA}	36.88^{aA}	43.64^{aAB}	10.45^{bA}	40.47^{aA}	45.36^{aAB}
F3	8.23^{bA}	36.07^{aA}	42.32^{aAB}	12.85^{bA}	41.62^{aA}	44.95^{aAB}
F4	4.17^{cB}	23.37^{bB}	38.58^{aB}	6.95^{bB}	30.62^{aB}	37.12^{aB}
F5	3.61^{bB}	14.39^{aB}	22.92^{aC}	5.26^{bB}	20.15^{aB}	25.62^{aC}

* Means followed by different small letter(s) within the same fertilizer treatment, and different capital letter(s) within the same cut, for each growing season, are significantly different according to the L.S.D. test at 0.05 level of probability.

Means of the studied agronomic parameters among the three cuts are presented in Table 4. Cut 1 was characterized by the highest significant plant height, stem diameter, and leaf area, amounting to 56.80 m, 7.01 mm, and 129.69 m^2, for 2018, and 60.67 m, 8.26 mm, and 130.45 m^2, for 2019, respectively. Values of the three parameters significantly decreased with advanced cuts, reaching the lowest values for the cut 3.

Table 4. Means of agronomic parameters as affected by the cut for the two growing seasons

Agronomic parameter	Summer 2018			Summer 2019		
	Cut 1	Cut 2	Cut 3	Cut 1	Cut 2	Cut 3
Plant height (cm)	56.80^{a*}	51.68^{b}	42.43^{c}	60.67^{a}	54.30^{b}	48.22^{c}
Stem Diameter (mm)	7.01^{a}	5.50^{b}	4.46^{c}	8.26^{a}	5.92^{b}	4.56^{c}
Leaf area (cm^2)	129.69^{a}	110.76^{b}	94.54^{c}	130.45^{a}	115.85^{b}	101.42^{c}

* Means followed by different small letter(s) within the same row, for each growing season are significantly different according to the L.S.D. test at 0.05 level of probability.

Table 5. Means of agronomic parameters as affected by the fertilizer treatment × variety interaction for the two growing seasons

Agronomic Parameter	Season	Variety	Fertilizer Treatment				
			F1	F2	F3	F4	F5
Plant height (cm)	Summer 2018	V 1	57.71^{aA*}	56.41^{abA}	55.54^{abA}	52.96^{abA}	48.26^{bA}
		V 2	52.47^{aA}	42.46^{bB}	44.03^{abB}	49.84^{abA}	43.33^{bA}
	Summer 2019	V 1	58.26^{aA}	56.10^{aA}	57.01^{aA}	50.31^{abA}	45.67^{bA}
		V 2	55.36^{aA}	45.36^{bB}	50.03^{abA}	47.82^{abA}	40.39^{bA}
Stem diameter (mm)	Summer 2018	V 1	5.29^{bA}	6.85^{aA}	6.35^{abB}	6.20^{abA}	6.37^{abA}
		V 2	5.47^{aA}	5.20^{aB}	4.88^{aB}	4.67^{aB}	5.31^{aA}
	Summer 2019	V 1	6.36^{aA}	6.72^{aA}	7.20^{aA}	6.37^{aA}	7.01^{aA}
		V 2	5.37^{aA}	5.92^{aA}	5.02^{aB}	4.79^{aB}	4.99^{aB}
Leaf area (cm^2)	Summer 2018	V 1	134.22^{aA}	95.67^{bB}	92.68^{bB}	83.62^{bA}	86.97^{bA}
		V 2	149.74^{aA}	142.33^{aA}	143.41^{aA}	99.38^{bA}	88.60^{bA}
	Summer 2019	V 1	146.23^{aA}	100.30^{bB}	101.29^{bB}	99.33^{bA}	95.96^{bA}
		V 2	149.36^{aA}	140.20^{aA}	145.44^{aA}	100.09^{bA}	97.36^{bA}

* Means followed by different small letter(s) within the same variety, and different capital letter(s) within the same fertilizer treatment, for each studied parameter and growing season, are significantly different according to the L.S.D. test at 0.05 level of probability.

Moreover, the three agronomic parameters were significantly variable as affected by the fertilizer treatment × variety interaction during both seasons (Table 5). Plant height for the two varieties gradually decreased with decreasing the percentage of BU fertilizer, however, the application of 50% BU + 50% NPU fertilizer gave similar plant heights to 100% BU fertilizer. Only in case of 75% BU + 25% NPU (during both seasons) and 50% BU + 50% NPU (during 2018) was the variety 1 superior to the variety 2 in plant height. Concerning the stem diameter (Table 5), variety 1 produced thinner stems when 100% BU was applied compared to the other fertilizer treatments during 2018. Meanwhile, variations among the five fertilizer treatments were non-significant for variety 2 during 2018 and both varieties during both seasons. During 2018, when mixtures of BU and NPU fertilizers were used, variety 1 produced thicker stems than variety 2. Moreover, during 2018, variety 1 gave thicker stems, with BU: NPU ratios 50:50% and 25:75% and with 100% NPU as well. Leaf area means of both growing seasons, presented in Table 5, showed that for variety 1, application of 100% BU resulted in significantly higher leaf area values than the other fertilizer treatments, while in case of variety 2, application of 100% BU as well as 75:50% and 50:50% BU: NPU ratios, resulted in higher leaf area values than the other fertilizer treatments with increased proportion of NPU. For the two growing seasons, leaf area of both varieties was significantly similar at 100% BU, 100% NPU and 25% BU + 75% NPU, while, at 75% and 50% BU + complementary NPU percentages, variety 2 gave significantly higher leaf area than variety 1.

Forage quality parameters

Combined analysis of variance for the studied forage quality parameters revealed that CP, ADF and CF contents were significantly variable among the tested fertilizer treatments and varieties ($p < 0.01$). In addition, ADF content was also significantly affected by the cut ($p < 0.01$). Moreover, the three-way interaction cut × fertilizer treatment × variety was significant in case of NFC and NDF contents ($p < 0.01$). Average CP and CF contents for the three cuts were 64.74 and 38.06 g kg^{-1}, respectively (Table 6). Cuts 2 and 3 were characterized by increased ADF contents than cut 1. Fertilizer treatments with 100, 75, and 50% BU resulted in significantly higher CP contents. On the contrary, CF content was higher with fertilizer treatments with increased NPU percentage (100 and 75%). Despite the statistical significance, little variations in ADF content were observed among the five tested fertilizer treatments, where the difference between the highest and lowest values was only 1.87%. Observably, variety 2 was characterized by higher CP content, yet lower ADF and CF contents than variety 1.

Table 6. Means of crude protein (CP), acid detergent fiber (ADF) and crude fat (CF) contents (g kg^{-1}) as affected by the fertilizer treatment, cut and variety combined over the two growing seasons

	CP	ADF	CF
Cut			
C1	64.64^{a}*	267.83^{b}	38.31^{a}
C2	66.13^{a}	315.01^{a}	38.27^{a}
C3	63.45^{a}	303.49^{a}	37.61^{a}
Fertilizer			
F1	68.22^{a}	302.78^{a}	30.63^{c}
F2	67.82^{a}	297.34^{a}	34.21^{b}
F3	66.10^{a}	284.09^{b}	36.97^{b}
F4	60.74^{b}	295.82^{ab}	42.83^{a}
F5	60.86^{b}	297.19^{a}	45.69^{a}
Variety			
V1	62.99^{b}	299.90^{a}	40.09^{a}
V2	66.50^{a}	290.99^{b}	36.04^{b}

* Means followed by different small letter(s) within the same column, are significantly different according to the L.S.D. test at 0.05 level of probability.

With reference to the significant three-way interaction in case of NFC and NDF, Table 7 shows that, generally, variety 2 was characterized with significantly higher NFC, yet lower NDF contents than variety 1 across all cuts and fertilizer treatments. Application of 50% BU + 50% NPU fertilizer, was a common treatment among all tested cuts, that gave significantly high NFC values. Same fertilizer treatment gave low NDF values for cuts 1 and two, while for cut 3, it resulted in high NDF content. The different direction of variation as well as the variable magnitude were probably the main reasons behind the significant three-way interaction.

Table 7. Means of non-fiber carbohydrates (NFC) and neutral detergent fiber (NDF) contents (g kg^{-1}) as affected by the fertilizer treatment × cut × variety interaction combined over the two growing seasons

NFC						
Fertilizer	Cut 1		Cut 2		Cut 3	
treatment	Variety 1	Variety 2	Variety 1	Variety 2	Variety 1	Variety 2
F1	236.53	309.88	207.54	225.35	263.12	307.04
F2	311.68	350.66	221.41	232.55	270.15	299.54
F3	314.85	340.93	233.77	252.92	255.92	296.24
F4	294.49	313.19	247.62	275.39	261.71	276.89
F5	296.82	318.86	247.36	272.63	245.26	280.01
L.S.D.$_{0.05}$	12.58					
NDF						
Fertilizer	Cut 1		Cut 2		Cut 3	
treatment	Variety 1	Variety 2	Variety 1	Variety 2	Variety 1	Variety 2
F1	655.64	578.78	684.43	662.36	631.63	584.64
F2	578.82	533.34	661.10	647.25	621.59	588.36
F3	568.62	548.26	657.39	653.84	630.13	596.30
F4	596.38	578.33	633.05	610.71	622.90	607.67
F5	587.10	567.69	634.40	613.87	634.69	605.49
L.S.D.$_{0.05}$	15.75					

DISCUSSION

Nutrient management is among the most important agronomic practices that needs to be accurately adjusted in order to achieve optimum productivity with satisfactory nutritional value from fodder teosinte (Mohan et al., 2017). The success of using nano fertilizers is highly dependent on the crop species (Elemike et al., 2019). In addition, texture of the experimental soil plays an important role in determining the effectiveness of the nano fertilizer application. As explained by Chhowalla (2017), the examination of nano fertilizer application is recommended in the sandy loam soils, like the experimental location of the current study, where the slow release nature of the NPU becomes an advantage due to the poor native fertilizer retention of the soil. As suggested by Kopittke et al. (2019), including the bulk-sized form (BU) with the nano-sized form (NPU) of the nitrogenous fertilizer under investigation, in the current study, provided a reliable control measure and allowed for a valid interpretation of the results.

The highest significant fresh yield, plant height and leaf area in the current study were observed for the 100% BU treatment. The linear positive effect of nitrogen on crop yield and agronomic characteristics has been previously reported by several researchers (e.g., Bahmaniar & Sooaee Mashaee, 2010; Pannacci & Partolini, 2018; Adamovics et al., 2019), which was attributed to extensive increase in cell growth rate with higher N rates, which resulted in taller plants (Rathnayaka et al., 2018) and higher herbage yield. Observably the application of 50% BU with 50% NPU produced as high fresh yield and tall plants as 100% BU. Similar observations were reported by Liu & Lal (2014), Benzon et al. (2015), and Al-Juthery et al. (2018) for rice, soybean, and wheat respectively, where researchers documented an increase in yield and plant height for mixtures of nano and conventional fertilizers. They attributed this to the improved ability of nano fertilizers to provide the essential nutrients, in addition to enhancing the transportation and absorption of the available nutrients, resulting in better crop growth. An attempt was made by Benzon et al. (2015) to clarify the promoted crop growth and development, noted by the high fresh yield and agronomic characteristics resulting from the combined treatment of nanoparticle and conventional fertilizers. They attributed this to the 'sink strength', known as the ability of a sink to utilize photosynthates towards its own benefit based on its size and activity. As described by Taiz & Zaiger (2006), sink size is known as the total biomass of sink tissue, while sink activity is the uptake rate of photosynthates per unit biomass of sink tissue. As previously mentioned, the ability of nanoparticle fertilizer to enhance the transportation and absorption of nutrients, will be positively reflected on these processes, resulting in better crop growth.

The effect of NPU application, in the current study, was more pronounced in case of dry matter accumulation of the tested varieties, where the DM content significantly increased with increasing the percentage of NPU in the applied fertilizer treatment. Similar results were reported by Rathnayaka et al. (2018) and Manikandan & Subramanian (2016) for rice and maize crops, respectively. This might be partially attributed to the increase in chlorophyll production and rate of photosynthesis accompanying the application of NPU, which allows for better translocation of assimilates and photosynthates to different plant parts resulting in higher DM accumulation (Singh et al., 2017)

In line with the current results, Payghan (2016) reported an increase in the nutritive value of fodder millet, in terms of more CP and less NDF and ADF contents with the combined application of nanoparticle and chemical fertilizers. On the other hand, CF content of the herbage followed an opposite trend in response to the fertilizer treatments, with treatments with increased BU percentage significantly decreasing CF content. This could be attributed to the increase in CP content with increasing N fertilization, which led to decreasing the other chemical components, including CF. A similar negative association between CP and CF contents was reported by Nawar et al. (2020) for sunflower and soybean.

The integration of NPU with BU in the fertilization management of teosinte, allowed to reduce the amount of urea required to reach the optimum productivity and quality from the crop. Similar findings were reported by researchers at the Sri Lankan Institute of Nanotechnology for rice crop (Kottegoda et al., 2017). In agreement with the current results, the researchers stated that rice productivity was significantly enhanced when 50% less conventional urea fertilizer was used in presence of nanoparticle fertilizer application. Nonetheless, it was clear from the current results that complete reliance on NPU would not support the production of teosinte, and that best results on forage yield and quality were achieved with the combined application of BU and NPU. Similar findings were reported by Payghan (2016) for fodder millet.

In comparison to other summer forage relatives, like maize, teosinte is known for its high genetic diversity (Niazi et al., 2015), which partially explains the variations in yield, agronomic characteristics and quality between the two tested varieties. The high yielding variety 1 was characterized by the tallest stems. The positive correlation between high fresh yield and plant height was confirmed for other forage grasses like fodder pearl millet (Habiba et al., 2018) and oat (Amanullah et al., 2004). In an opposite trend to the fresh yield production, variety 2 was characterized by higher nutritive value, in terms of high CP, CP, NFC, yet lower NDF, ADF and CF, thus, might be more recommended for feeding purposes.

Teosinte is characterized by its slow initial growth (Radwan et al., 2000), which might explain the very low amount of fresh yield achieved in the current study on the 1st cut, taken at 45 DAS compared to the 2nd and 3rd cuts. The fresh yield amounts reported by Tarrad et al. (2010) for several teosinte varieties on the 2nd and 3rd cuts, were similar to the current results, while they reported much higher fresh yield on the 1st cut. In their study, the 1st cut was taken at 64 DAS; thus, the plants were allowed to stay longer in the soil and had a better chance to build up a vigorous vegetative growth resulting in a higher amount of fresh yield. Estimation of the yield on dry matter basis is useful for a meaningful comparison among cuts and varieties especially for feeding purposes (Frandsen, 1986). Based on the reported highly significant positive correlation between fresh and dry yields of forage grasses (Knight et al., 1996), the non-significant variations among the three cuts in DM content, suggests that the variations in dry yield will follow the same trend of the fresh yield, with the 1st cut being inferior to the 2nd and 3rd cuts. In partial agreement with the current study, Tarrad et al. (2010) observed that the leaf area of teosinte varieties was the lowest on the 3rd cut, where also the shortest stems were produced. However, same researchers reported the highest leaf area and tallest plants on the 2nd cut, while the current results showed that these were characteristics of the 1st cut.

CONCLUSION

Based on the current results, the integration of nanoparticle urea in the fertilization scheme of fodder teosinte allowed for 50% reduction in the applied conventional urea fertilizer, without sacrificing the yield and quality of the produced forage. The combined application of 50% NPU with 50% BU, resulted in the production of high yield with satisfactory nutritive value, in terms of high crude protein (CP) and non-fiber carbohydrates (NFC), and low fiber and crude fat contents, similar to the addition of 100% BU. This practice was, however, less expensive and safer for the environment. While the 1st cut was characterized by the highest plant height, stem diameter and leaf area, the 3rd cut produced the highest amount of fresh yield. Variations in quality measures among the three cuts were almost non-significant. Variations in yield and quality were detected between the two tested local varieties. In conclusion, the combined application of 50% NPU with 50% BU is recommended for the production of fodder teosinte in similar environments.

REFERENCES

Adamovics, A., Platace, R., Ivanovs, S. & Gulbe, I. 2019. The efficiency of nitrogen fertilizer on the dry matter yield of tall fescue and festulolium grown as feedstock for combustion. *Agronomy Research* **17**(6), 2146–2157. https://doi.org/10.15159/ar.19.204

Al-Juthery, H.W., Habeeb, K.H., Altaee, F.J.K., AL-Taey, D.K. & Al-Tawaha, A.R.M. 2018. Effect of foliar application of different sources of nano-fertilizers on growth and yield of wheat. *Bioscience Research* **15**(4), 3976–3985.

Amanullah, P.S., Zada, K. & Perveen, S. 2004. Growth characters and productivity of oat varieties at Peshawar. *Sarhad Journal of Agriculture* **20**, 5–10.

AOAC. 2012. *International Official Methods of Analysis* (19th Ed.) Association of Official Analytical Chemists. Gaithersburg, MD, USA.

Bahmaniar, M.A. & Sooaee-Mashaee, S. 2010. Influence of Nitrogen and Potassium Top Dressing on Yield and Yield Components as Well as Well as Their Accumulation in Rice *Oryza sativa*. *African Journal of Biology* **9**, 2648–2653.

Benzon, H.R.L., Rubenecia, M.R.U., Ultra, Jr.V.U. & Lee, S.C. 2015. Nano-fertilizer affects the growth, development, and chemical properties of rice. *International Journal of Agronomy and Agricultural Research* **7**(1), 105–117.

Chaudhary, S., Dheri, G.S. & Brar, B.S. 2017. Long-term effects of NPK fertilizers and organic manures on carbon stabilization and management index under rice-wheat cropping system. *Soil and Tillage Research* **166**, 59–66.

Chhowalla, M. 2017. Slow release nanofertilizers for bumper crops. *ASC Central Science* **3**, 156–157.

Devkota, N.R., Ghimire, R.P., Adhikari, D.P., Upreti, C.R., Poudel, L.N. & Joshi, N.P. 2017. Fodder productivity of teosinte (*Euchlaena mexicana* Schrad) at different sowing dates in Western mid-hills of Nepal. *Journal of Agriculture and Forestry University* **1**, 129.

Elkhatib, E.A., Mahdy, A.M. & Salama, K.A. 2015. Green synthesis of water treatment residual nanoparticles using precision milling. *Environmental Chemistry Letters* **13**, 333–339.

Elemike, E.E., Uzoh, I.M., Onwudiwe, D.C. & Babalola, O.O. 2019. The role of nanotechnology in the fortification of plant nutrients and improvement of crop production. *Applied Sciences* **9**(3), 499.

Frandsen, K.J. 1986. Variability and inheritance of digestibility in perennial ryegrass (Lolium perenne), meadow fescue (Festuca pratensis), and cocksfoot (Dactylis glomerata): II. F1 and F2 progeny. *Acta Agriculturae Scandinavica* **36**(3), 241–263.

Gaudin, A., McClymont, S.A. & Raizada, M.N. 2011. The nitrogen adaptation strategy of the wild teosinte ancestor of modern maize, *Zea mays* subsp. parviglumis. *Crop science* **51**(6), 2780–2795.

Gomaa, M.A., Radwan, F.I., Kandil, E.E. & Al-Challabi, D.H.H. 2017. Comparison of some New Maize Hybrids Response to Mineral Fertilization and some Nanofertilizers. *Alexandria Science Exchange Journal* **38**(3), 506–514.

Habiba, H.E., Salama, H.S.A, & Bondok, A.T. 2018. Effect of the Integrated Use of Mineral-and Bio-Fertilizers on Yield and Some Agronomic Characteristics of Fodder Pearl Millet (*Pennisetum Glaucum* L.). *Alexandria Science Exchange Journal* **39**, 282–295.

Hartley, H.O. 1950. The maximum F-ratio as a short-cut test for heterogeneity of variance. *Biometrika* **37**, 308–312.

Hoffland, E., Dicke, M., van Tintelen, W., Dijkman, H. & van Beusichem, M.L. 2000. Nitrogen availability and defense of tomato against two-spotted spider mite. *Journal of Chemical Ecology* **26**, 2697–2711.

Iqbal, M.A. 2019. Nano-Fertilizers for Sustainable Crop Production under Changing Climate: A Global Perspective. *In Sustainable Crop Production*. IntechOpen. doi: 10.5772/intechopen.89089

Khalifa, N.S. & Hasaneen, M.N. 2018. The effect of chitosan–PMAA–NPK nanofertilizer on Pisum sativum plants. 3 *Biotech* **8**(4), 193.

Knight, A.C., Price, J.S. & Gale, G.E. 1996. Mechanical removal of surface moisture from grass. *Grass and Forage Science* **51**, 412–417.

Kopittke, P.M., Lombi, E., Wang, P., Schjoerring, J.K. & Husted, S. 2019. Nanomaterials as fertilizers for improving plant mineral nutrition and environmental outcomes. Environmental Science: *Nano* **6**(12), 3513–3524.

Kottegoda, N., Sandaruwan, C., Priyadarshana, G., Siriwardhana, A., Rathnayake, U.A., Berugoda Arachchige, D.M., Kumarasinghe, A.R., Dahanayake, D., Karunaratne, V. & Amaratunga, G.A. 2017. Urea-hydroxyapatite nanohybrids for slow release of nitrogen. *ACS nano* **11**(2), 1214–1221.

Kumar, B., Dhaliwal, S.S., Singh, S.T., Lamba, J.S. & Ram, H. 2016. Herbage production, nutritional composition and quality of teosinte under Fe fertilization. *International Journal of Agriculture and Biology* **18**(2).

Liu, R. & Lal, R. 2015. Potentials of engineered nanoparticles as fertilisers for increasing agronomic productions. *Science of the Total Environment* **514**, 131–9.

Manikandan, A. & Subramanian, K.S. 2016. Evaluation of zeolite-based nitrogen nano-fertilizers on maize growth, yield and quality on inceptisols and alfisols. *International Journal of Plant and Soil Science* **9**(4), 1–9.

Marchiol, L. 2019 Nanofertilisers. An outlook of crop nutrition in the fourth agricultural revolution. *Italian Journal of Agronomy* **14**(3), 183–190.

Mohan, S., Dar, E.A. & Singh, M. 2017. Fodder quality of teosinte fodder as influenced by nitrogen, phosphorus and zinc application. *International Journal of Pure and Applied Bioscience* **5**, 596–604.

Nawar, A.I., Salama H.S.A. & Khalil H. E. 2020 Additive intercropping of sunflower and soybean to improve yield and land use efficiency: Effect of thinning interval and nitrogen fertilization. *Chilean Journal of Agricultural Research* **80**(2), 142–152

Niazi I.A.K., Rauf S., da Silva J.A.T. & Munir H. 2015. Comparison of teosinte (*Zea mexicana* L.) and inter-subspecific hybrids (*Zea mays* L.× *Zea mexicana*) for high forage yield under two sowing regimes. *Crop and Pasture Science* **66**(1), 49–61.

Pannacci, E. & Bartolini, S. 2018. Effect of nitrogen fertilization on sorghum for biomass production. *Agronomy Research* **16**(5), 2146–2155.

Payghan, H. 2016. Effects of organic, chemical and nano-biological fertilizers on quantitative and qualitative characteristics of millet *(Panicum miliaceum)* varieties. Master's thesis, University of Zabol. http://eprints.uoz.ac.ir/id/eprint/1626

Radwan, M.S., Taha, R.S., Rammah, A.M. & Ibrahim, H.L. 2000. A study of variation and combining ability among exotic and local teosinte accessions. *Egyptian Journal of Plant Breeding* **4**, 189–200.

Rady, H.Y. 2018. Genotypic and Environmental Interaction Effects on Forage Yield and its Related Traits of some Summer Forage Crops. *Journal of Plant Production* **9**(10), 815–820.

Rathnayaka, R.M.N.N., Iqbal, Y.B. & Rifnas L.M. 2018. Influence of Urea and Nano-Nitrogen Fertilizers on the Growth and Yield of Rice (Oryza sativa L.) Cultivar 'Bg 250'. *International Journal of Research Publications* **5**(2), 1–7.

Singh, M.D., Gautam, C., Patidar, O.P., Meena, H.M., Prakasha, G. & Vishwajith. 2017. Nano-Fertilizers is a new way to increase nutrients use efficiency in crop production. *International Journal of Agriculture Sciences* **9**(7), 3831–3833.

Statistical Analysis System. 2012. SAS PC Windows Version 9.4 SAS Institute Inc. Cary, NC, USA.

Taiz, L. & Zeiger, E. 2006. Plant Physiology. 4th Edition. Sinauer Associates, Inc. Sunderland, Massachusetts, USA.

Tarrad, M.M., Rizk, R., Aly, R. & Zayed, E. 2010. Evaluation of some teosinte genotypes under Egyptian conditions. *Egyptian Journal of Agricultural Research* **88**, 265–281.

Van Soest, P.V., Robertson, J.B. & Lewis, B.A. 1991. Methods for dietary fiber, neutral detergent fiber, and nonstarch polysaccharides in relation to animal nutrition. *Journal of Dairy Science* **74**(10), 3583–3597.

Agronomy Research **18**(4), 2581–2591, 2020
https://doi.org/10.15159/AR.20.196

Changes in soil properties and possibilities of reducing environmental risks due to the application of biological activators in conditions of very heavy soils

P. Šařec[1,*], O. Látal[2], P. Novák[3], J. Holátko[4], V. Novák[1], T. Dokulilová[4,5] and M. Brtnický[4,5]

[1]Czech University of Life Sciences Prague, Faculty of Engineering, Department of Machinery Utilization, Kamýcká 129, CZ165 000 Praha 6 – Suchdol, Czech Republic
[2]Agrovýzkum Rapotín Ltd., Rapotín, Výzkumníků 267, CZ788 13 Vikýřovice, Czech Republic
[3]Czech University of Life Sciences Prague, Faculty of Engineering, Department of Agricultural Machines, Kamýcká 129, CZ165 000 Praha 6 – Suchdol, Czech Republic
[4]Mendel University in Brno, Faculty of Forestry and Wood Technology, Department of Geology and Pedology, Zemědělská 1, CZ61 300 Brno, Czech Republic
[5]Mendel University in Brno, Faculty of AgriSciences, Department of Agrochemistry, Soil Science, Microbiology and Plant Nutrition, Zemědělská 1, CZ61 300 Brno, Czech Republic
[*]Correspondence: psarec@tf.czu.cz

Abstract. This study aims at verifying the effect of farmyard manure (FYM) and of selected activators (Z'fix and NeoSol) on changes of soil properties. Their application should lead to improvement of soil physical properties and of organic matter fixation, to reduction of environmental risks, e.g. of tillage energy requirements. Experimental variants (0.7 ha each) were as follows: I (FYM with Z'fix); II (FYM with Z'fix + NeoSol); III (FYM); IV (Control NPK only). FYM was applied at rates: 50 t ha^{-1} (2014); 30 t ha^{-1} (2016). Additional NPK fertilizer (I–IV) was applied according to annual crop nutrient normative. The agent Z'fix was used as an activator of FYM biological transformation (5.5 kg t^{-1}). The agent NeoSol was used as soil activator (200 kg ha^{-1}; annually). In order to verify the effect, cone index, bulk density, tillage implement draft and chemical soil components (Humus, C/N ration and N_{tot}) were measured annually. Compared to the control, the application of FYM combined with the mentioned agents (I–III) increased N_{tot} more than two times. Moreover, it decreased (I–III) bulk density by 8.7%. Tillage implement draft decreased by 3% after the application of FYM with Z'fix (I, II). The study confirmed that FYM application combined with utilization of activators positively influenced soil fertility and helped to reduce environmental risks.

Key words: cone index, implement draft, bulk density, nitrogen, humus, C/N ratio, farmyard manure.

INTRODUCTION

The requirements posed on agricultural production have been raising fast recently. Moreover, these demands are likely to continue rising even faster in the future. The pressure intensifies mostly due to decreasing area of the arable land, the climate change, reduction of livestock farming, changes in crop rotation. For example in the Czech Republic, cattle production has diminished to less than a half of the volume existing 30 years ago (Sálusová, 2018). One of the consequences, even boosted by the intensification of agriculture, is the shortage of valuable soil organic matter (SOM) that contributes to a declining soil production ability on the European scale (Stolte et al., 2016). According to Gardi et al. (2013), this trend leads to a decline of the soil fertility and farmland diversity, as well as to other degradation problems. Walsh & McDonnell (2012) claim that SOM is linked not only to the fertility, but also to other properties, e.g. soil structure. SOM is likewise regarded as inherently reducing soil compaction (Chakraborty & Mistri, 2017). It is a major issue not just in Europe, where around 33 million hectares are reported to be threatened by this phenomenon (Alaoui & Diserens, 2018). Alakukku (1996) claims that the compaction adversely affects hydraulic soil properties, porosity, stability and other soil characteristics. According to Stolte et al. (2016), the compaction significantly affects root growth of plants, because it adversely affects the soil settings important for movement of gas and water. The situation thus often results in reduced crop yields. Amplified soil cone index and bulk density can be detected as a result of harmful soil compaction. Therefore, they are frequently used options of soil compaction measurement (Odey, 2018).

Any organic matters supplied to a degraded soil generally help to rectify its physical attributes (Are et al., 2017). The share of SOM is obviously advanced by applying compost or manure (Panagos et al., 2015). Manure application thus helps to amend the chemical, biological and physical soil characteristics (Ludwig et al., 2007). Liang et al. (2013), McLaughlin et al. (2002) and Peltre et al. (2015) conveyed that manure treatment substantially diminished draft of soil tillage implements. Prolonged application and higher rates produced advanced reduction. It is important in terms of economy and operation, since according to Larson & Clyma (1995), soil tillage operations account for a considerable share of the energy spent in crop production.

In order to rectify soil properties, so-called activators could be applied into any organic material, e.g. deep litter bedding of cattle housing, or straightway to soil. For the present, their effect have been studied only partially. Latest findings nevertheless imply that conditions for cultivating plants may be improved through their use (Borowiak et al., 2016). On one hand, it conveys economic advantages such as a decrease of tillage implement draft resulting in lower fuel consumption (Šařec & Žemličková, 2016). On the other, it may help agriculture to become more sustainable (Šařec & Novák, 2017). On the other hand, repeated application of an activator directly to soil and continuing conventional tillage did not generate any enhancement in terms of physical properties of soil, e.g. water content in soil, soil compaction, density, porosity (Podhrázská et al., 2012). In general, the mentioned works suggest the activators to be verified in different conditions.

This study is focused on assessing the effect of activators and farmyard manure (FYM) on selected soil physical and chemical properties at a five-year field trial.

MATERIALS AND METHODS

During 2014–2018, a field experiment was accomplished at a site near Městec Králové in the Central Bohemia at the altitude 265 m above sea level. The subject of interest was the topsoil (0–0.3 m) from soil type Gleyic Phaeozem. The experimental plot entailed very heavy soil texture. Therefore, the field was hard to till. At the depth from 0 to 0.3 m, the content of clay particles of the size under 0.01 mm accounted for 62% of weight. Particular soil characteristics at the start of the field trial are presented in Table 1.

Table 1. Particular chemical and physical characteristics of soil in the trial field in 2014

	Soil depth (m)	
	0.00–0.30	0.30–0.60
Clay (< 0.002 mm) (%)	48	60
Silt (0.002–0.05 mm) (%)	32	39
Very fine sand (0.05–0.10 mm) (%)	2	1
Fine sand (0.10–0.25 mm) (%)	18	0
Soil texture (USDA)	clay	clay
Humus content (%)	3.89	1.44
Bulk density (g cm^{-3})	1.46	1.48
Total porosity (%)	46.15	43.99
Volumetric moisture (%)	35.65	40.20
CEC - cation exchange capacity (mmol kg^{-1})	278	272
pH (H_2O)	7.50	7.82
pH (KCl)	7.18	7.21

The experimantal plot had a rectangular shape, was about 150 meters wide, and was positioned to avoid headland and to be homogenous. The rectangle was divided lengthwise each 45 meters to form four 0.7 ha variants varying in fertilizer and activator application. The spatial distribution had to be kept basic due to an operational character of the trial. NPK 15-15-15 (Lovofert, Czech Rep.) and cattle manure were the fertilizers applied. NeoSol (PRP Technologies, France) and Z'fix (PRP Technologies, France) were the activators applied. NeoSol was used at the time of stubble cultivation as the activator of biological transformation of soil organic matter. NeoSol composes of a matrix of magnesium and calcium carbonates, and of mineral elements. Z'fix was put at a recommended weekly dose directly into bedding of cattle deep litter housing as the activator of biological transformation of manure. Z'fix is formed by a granular mixture of carbonates and mineral salts. Both these activators are assumed to enhance environment for the transformation of organic matter. They cannot be classified as fertilizers due to their low share of active substances. Different treatments of individual variants and the crops grown are shown in Table 2. Apart from these treatments, all the other operations carried out and material applied did not differ among the variants. Reduced soil tillage technology was employed consisting firstly from shallow disk harrowing and subsequent deeper soil loosening to the depth of at least 20 cm using a tine cultivator.

Table 2. Application rates of individual variants of field trial and crop rotation in the trial field

Variant	Fertilization	Application rates for production year and crop (t ha^{-1})			
		2014/15 silage maize	2015/16 spring barley	2016/17 winter wheat	2017/18 silage maize
I	FYM[A] with Z'fix	50	0	30	0
II	FYM with Z'fix + NeoSol[B]	50 + 0.2	0 + 0.2	30 + 0.2	0 + 0.15
III	FYM	50	0	30	0
IV	Control - NPK only	according to crop demand and local practice			

[A]Farmyard manure of cattle origin; [B]Modified activator NeoSOL has been used with a changed dosage from the year 2017 onwards (formerly PRP SOL).

In order to assess soil physical properties, cone index and bulk density were measured in spring, while tillage draft was measured after harvest each year. Apart from the tillage draft, there were ten repetitions performed annually for each of the variants and variables. The tillage draft measurement was of continuous nature resulting in thousands of records. Only data from starting and final year were evaluated in this article. In order to measure cone index, the PEN 70 penetrometer constructed at the CULS Prague was used. Penetrometer was designed to meet the ASABE standards, i.e. with a tip cone angle of 30°, and tip area of 100 mm^2. Kopecky cylinders (volume of 100 cm^3) were employed in order to acquire undisturbed soil samples and subsequently soil bulk density. The sampling depth reached 0.05 to 0.10 m. The volumetric moisture was attained using Theta Probe (Delta-T Devices Ltd, UK). The draft of chosen farm cultivation machinery was evaluated using drawbar dynamometer with strain gauges S-38 /200 kN/ (LUKAS, the Czech Republic). The measurement was performed after harvest and prior to the first soil tillage operation, i.e. disk harrowing, each year. The drawbar dynamometer was positioned between two tractors. The sample rate of data acquisition system NI CompactRIO (National Instruments Corporation, USA) was set at 0.1 s. Within each variant, multiple machinery passes were performed. The measurements were carried out with the tillage implement either working or towed only. This enabled to discern among the implement draft, rolling resistance, and surface incline influence. The working speed was maintained constant. Acquired data were processed using Trimble Business Center (Trimble, USA), MS Excel (Microsoft Corp., USA) and Statistica (Statsoft Inc., USA).

Soil samples for chemical analysis were taken at two depths (0–0.15 m and 0.15–0.30 m) at the beginning and at the end of the vegetation period, but only the topsoil was assessed in the paper. Soil auger was used to take four summary samples composed of eight partial samples from each variant. The summary samples were dried, cleared of plant and animal residues, sieved and homogenized. The final sample (1 kg) was obtained from the summary samples by quartering.

RESULTS AND DISCUSSION

The paper is focused mainly on comparing starting conditions, i.e. the year 2014, with the resulting conditions after the five trial years, i.e. the year 2018. Fig. 1 display precipitation and monthly average temperatures of the year 2018 compared to the year 2014. In 2018, the weather was both remarkably warm and arid over the entire vegetative period. The preceding years 2016 and 2017 were also warm and short of precipitations.

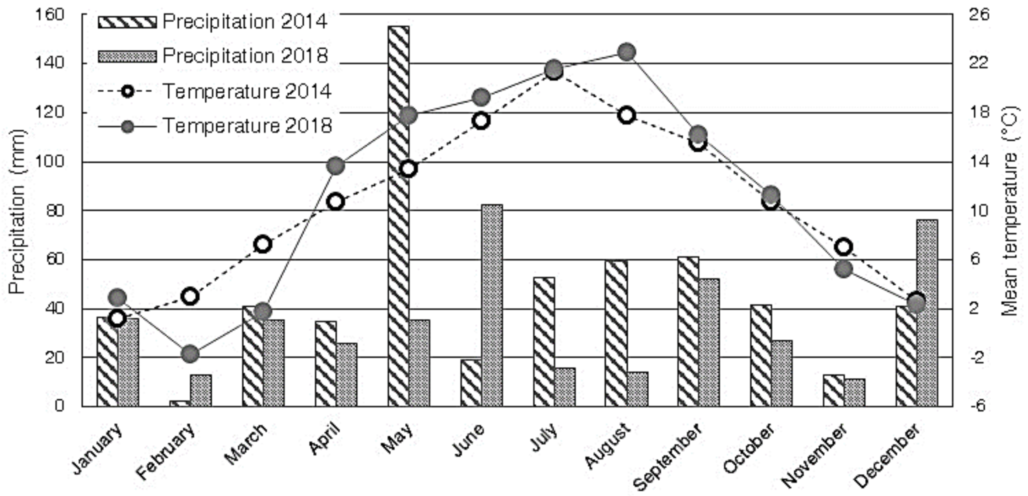

Figure 1. Graph of monthly precipitation and mean temperatures at the experimental site in the years 2014 and 2018.

Table 3. The averages of soil physical properties, and of draft of tillage implements for 2014 and 2018 regardless of trial variants

		2014	2018	Index	*p*
Soil physical properties in spring:					
Vol. moisture at 0.00–0.05 m (%)		17.305[a]	15.570[b]	0.90	0.02992
Bulk density at 0.05–0.10 m (g cm^{-3})		1.384[a]	1.235[b]	0.89	0.00104
Cone index (MPa)	at 0.04 m	0.608[a]	0.540[a]	0.89	0.45405
	0.08 m	0.875[a]	1.333[b]	1.52	0.00025
	0.12 m	1.067[a]	1.450[b]	1.36	0.01236
	0.16 m	1.200[a]	1.746[b]	1.46	0.00487
	0.20 m	1.675[a]	2.087[a]	1.25	0.05361
	0.24 m	2.158[a]	2.568[a]	1.19	0.11921
	0.28 m	2.517[a]	3.061[b]	1.22	0.00524
	0.32 m	2.783[a]	3.422[b]	1.23	0.00103
Draft measurement after harvest:					
Tractor		JD 9570 RT	JD 9570 RT		
Engine power (HP)		570	570		
Implement		tine cultivator	tine cultivator		
Implement type		Köckerling Vario 480	Köckerling Vario 480		
Working width (m)		3	3		
Working depth (m)		10.358[a]	16.529[b]	1.60	0.00000
Working speed (km $hour^{-1}$)		7.026[a]	11.300[b]	1.61	0.00000
Overall implement draft (N)		74.821[a]	78.492[b]	1.05	0.02157
Unit draft (N m^{-2})		240.775[a]	158.290[b]	0.66	0.00000

Concerning statistical evaluation, *t-test* at the significance level of 0.5 was used.

Elementary physical characteristics of soil are depicted in Table 3. Springtime volumetric soil moisture exhibited a statistically significant difference between the two years. This clearly increased the values of cone index, which was susceptible to soil moisture. Illustrative aggregate values at different depths presented in Table 3 display statistically significant differences except at the depths of 0.20 and 0.24 m. On the other hand, overall soil bulk density across the variants decreased. The difference was also significant. Concerning draft measurement after harvest in autumn, immediate conditions were exceptionally favourable for tillage in 2018. Machinery used was the same in both years, but working depth could have been set by 60% deeper in 2018 and the working speed reached by 61% higher value. The overall implement draft thus attained higher value, but the unit draft allowing for the working width and depth was significantly lower in 2018.

Since the conditions substantially differed over the monitored period, the differences of the parameters relative to the average of the control Variant IV provide more information than their absolute values.

Implement draft was measured in a stubble field after the harvest. Manure and other material was applied afterwards. Draft values were evaluated in comparison to the control Variant IV, as is shown in Fig. 2.

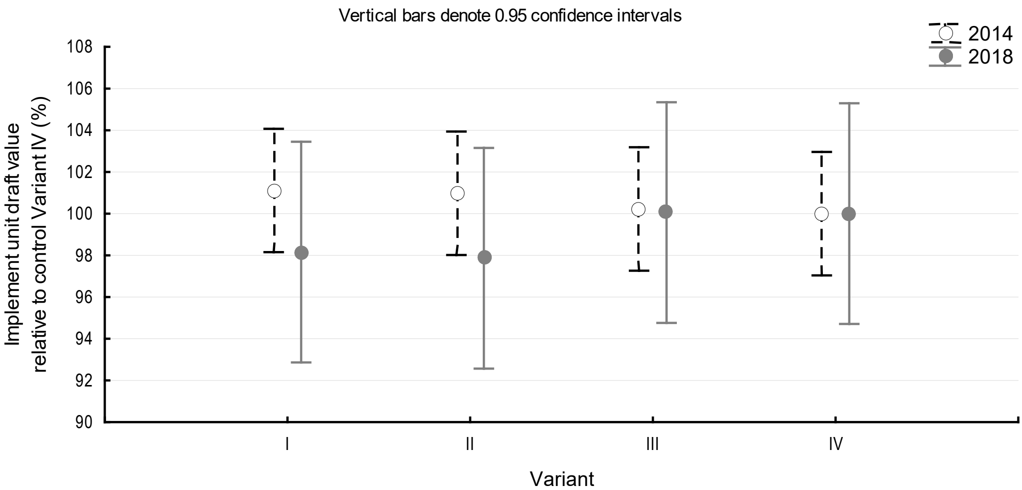

Figure 2. Graph comparing relative differences of implement unit draft values for individual variants in autumn 2014 and 2018 (Variants: I – FYM with Z'fix; II – FYM with Z'fix + NeoSol; III – FYM; IV – Control as 100%).

The *Analysis of Variance* did not confirm any significant differences with respect to the variants, measurement date and the combination of both factors. Generally, average implement draft values decreased relative to the control particularly after the application of FYM with Z'fix (Variants I and II), where the relative decrease attained 3% in average. The findings of Liang et al. (2013), McLaughlin et al. (2002), and Peltre et al. (2015) on draft reduction after manure application are consistent with the trial results, where it was intensified by the influence of activators.

Fig. 3 shows bulk density values related to the average value of respective control Variant IV. As the above mentioned Table 3 already suggested, they differed significantly according to the measurement date. However according to the *Analysis of Variance*, bulk density values did not differ significantly with regard to the variant, nor with regard to its combination with the measurement date. Nevertheless, there is a visible relative bulk density decrease particularly after the application of FYM (Variant III) by 13.4% and after the application of FYM with Z'fix combined with the application of NeoSol (Variant II) by 8.8%. The application of FYM treated with Z'fix (Variant I) presented the lowest decrease. The production of manure using Z'fix requires fewer straw. The manure is consequently more decomposed and thicker. The results are in accordance, though not statistically verified, with Schjønning et al. (1994), who claimed that prolonged time without any fertiliser treatment caused increased soil bulk density and soil strength than manure or inorganic fertilizer treatments, and Jehan et al. (2020), who reported soil bulk density and soil strength having decreased with increase in level of dairy manure. Also Bogunovic et al. (2020) observed a decrease in bulk density after FYM application. On the other hand, Chen et al. (2020) detected no such changes.

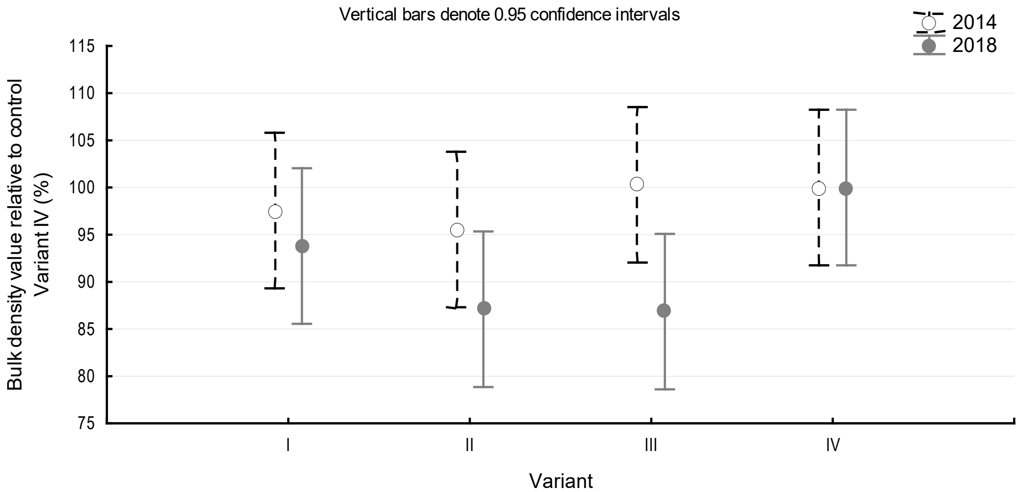

Figure 3. Graph of relative soil bulk density values from the depth of 0.05 to 0.10 m for individual variants in spring 2014 and 2018 (Variants: I – FYM with Z'fix; II – FYM with Z'fix + NeoSol; III – FYM; IV – Control as 100%).

Since cone index depends intensely on soil moisture, it was measured also in spring, when soil moisture was more probable to be homogenous. Cone index values were yet again compared to the control Variant IV, as is presented in Fig. 4. Though actual values increased from 2014 to 2018 (see Table 3), relative differences compared to Variant IV decreased. The *Analysis of Variance* did not find any significant difference for the combination of all the factors in question, i.e. measurement date, variant and depth, nor for the separate factors except for the measurement date. When considering the combinations of the measurement date with the depth or with the variant, differences were statistically significant.

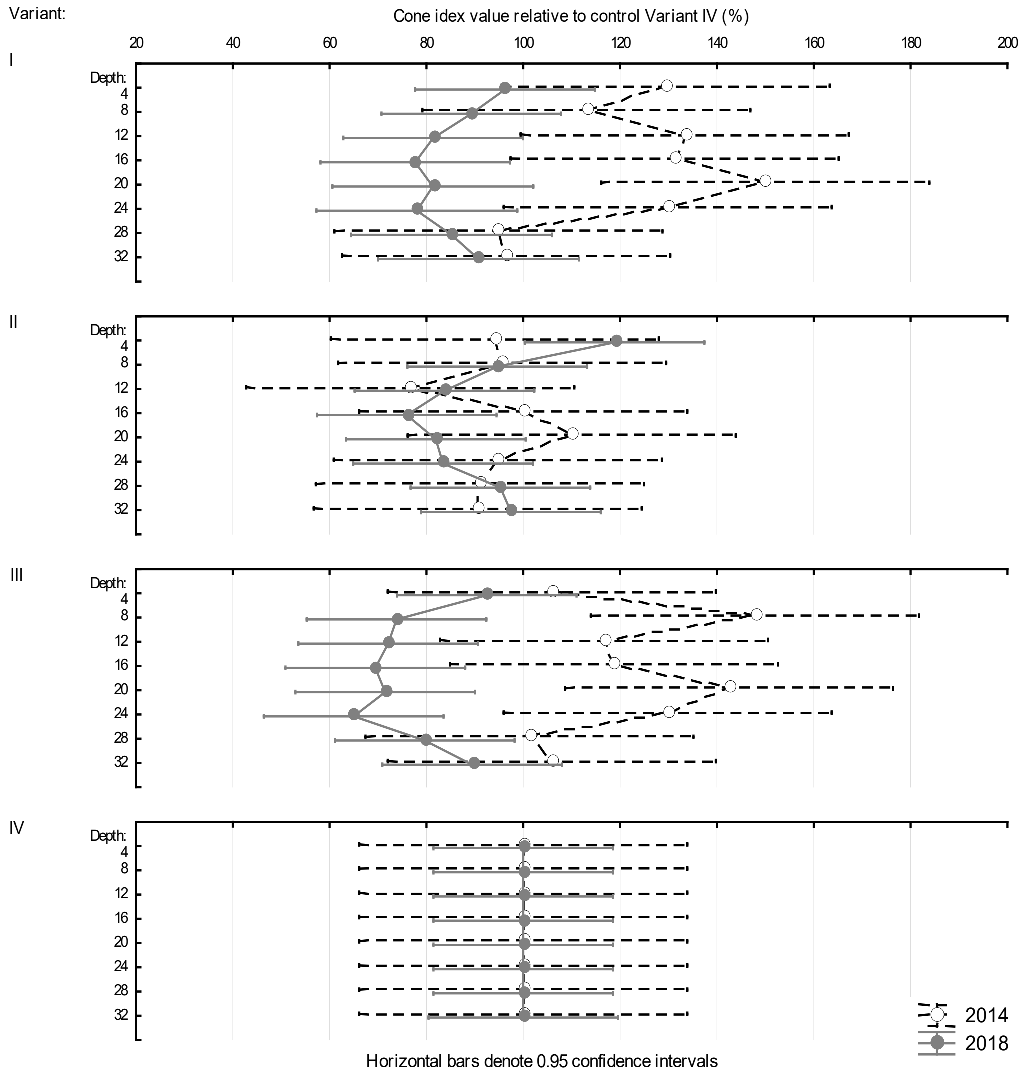

Figure 4. Graph comparing relative differences of cone index values to the depth up to 0.32 m for individual variants in spring 2014 and 2018 (Variants: I – FYM with Z'fix; II – FYM with Z'fix + NeoSol; III – FYM; IV – Control as 100%).

With the *Analysis of Variance* performed separately for each variant using the measurement date and depth as the only factors, the differences were more comprehensible. Within Variant I (FYM with Z'fix) and II (FYM with Z'fix + NeoSol), data formed one homogeneous group. In the case of Variant III (FYM) though, there was a statistically significant difference for the combination of both mentioned factors (*ANOVA*, $n = 160$, $p = 0.04198$) and data formed three homogeneous groups (see Table 4). Compared to the year 2014, the decrease of relative cone index values of the year 2018 for Variant III (FYM) at the depths of 0.08, 0.20 and 0.24 m was statistically significant. This result matches with those of Šařec & Žemličková (2016), Celik et al. (2010) and Luo et al. (2020).

Table 4. Homogenous groups of relative cone index values of Variant III (FYM) according to *Turkey HSD test* (*ANOVA, n* = 160, *P* > 0.05)

Trial date	Depth (cm)	Mean cone index value relative to the control Variant IV (%)	Homogenous groups		
			1	2	3
2018	24	64,9682	****		
2018	16	69,4444	****		
2018	20	71,4859	****	****	
2018	12	72,0930	****	****	
2018	8	73,8255	****	****	
2018	28	79,6460	****	****	
2018	32	89,4479	****	****	****
2018	4	92,4528	****	****	****
2014	28	101,2821	****	****	****
2014	4	105,8824	****	****	****
2014	32	105,8824	****	****	****
2014	12	116,6667	****	****	****
2014	16	118,7500	****	****	****
2014	24	129,8246		****	****
2014	20	142,5000			****
2014	8	147,8261			****

Table 5 presents the results of soil chemical analysis. It is apparent that pH changed particularly when the activators, i.e. Z'fix and NeoSol, were used. The pH reaction could be assessed as neutral to alkaline. The content of total nitrogen increased mainly after FYM with Z'fix application (Variants I and II). C/N ration can be evaluated as high to good and decreasing again particularly after FYM with Z'fix application. Humus content can be rated as good to high one. The FYM combination with the soil activator NeoSol had a beneficial effect on its creation. When considering the humus type, the increased humic over fulvic acids ratios of the Variants I to III can be regarded as beneficial.

Table 5. Results of chemical analysis of soil samples for individual variants in 2014 and 2018 (Variants: I – FYM with Z'fix; II – FYM with Z'fix + NeoSol; III – FYM; IV – Control)

Variant	Year	pH (KCl)	N_{tot} (%)	C/N ratio	Humus (%)	HA/FA ratio[A]
I	2014	6.98	0.3	9.45	4.84	1
I	2018	7.44	0.62	4.43	4.76	1.08
I	*Index*	*1.066*	*2.067*	*0.469*	*0.983*	*1.080*
II	2014	7.07	0.27	10.56	5.01	0.99
II	2018	7.48	0.67	4.57	5.23	1.02
II	*Index*	*1.058*	*2.481*	*0.433*	*1.044*	*1.030*
III	2014	7.1	0.32	9.07	4.94	1.01
III	2018	7.44	0.54	4.92	4.55	1.08
III	*Index*	*1.048*	*1.688*	*0.542*	*0.921*	*1.069*
IV	2014	7.17	0.32	8.66	4.76	1.02
IV	2018	7.01	0.4	6.6	4.55	0.98
IV	*Index*	*0.978*	*1.250*	*0.762*	*0.956*	*0.961*

[A]Humic to Fulvic acids ratio.

The activators of organic matter and their outcomes relate to the topics that are not thoroughly studied. Since the type of organic fertilizers used is altering, i.e. more compost and waste from biogas plants instead of manure and slurry, the increased significance of such activators of organic matter can be anticipated

CONCLUSIONS

The research aimed at the influence of organic fertilizers and activators on particular soil physical and chemical properties was carried out. Generally, the farmyard manure (FYM) and the activators showed positive effect, although not always statistically significant. Significant proved the differences in cone index values compared to the control when applying untreated FYM, where there was a reduction at the depths of 0.08, 0.20 and 0.24 m. After the application of FYM treated with Z'fix, unit implement draft decreased by 3% compared to the control variant. This difference was not confirmed statistically though, and neither were the following ones mentioned. Nonetheless given the average tractive efficiency of around 50% and the fuel requirements of tillage at the level of 20 L ha^{-1}, the 3% reduction in draft would represent 0.3 L ha^{-1} of fuel savings. This application of FYM treated with Z'fix also most of all increased the total nitrogen content. On the other hand, bulk density was mostly reduced by applying untreated FYM. The activators of organic matter should examined further on and at more locations in order to verify the results.

ACKNOWLEDGEMENTS. This study was supported by Research Project of the Technology Agency of the Czech Republic No. TH02030169, and by the Faculty of Engineering, Czech University of Life Sciences Prague under internal grant IGA 2019: 31180/1312/3104.

REFERENCES

Alakukku, L. 1996. Persistence of soil compaction due to high axle load traffic. I. Short-term effects on the properties of clay and organic soils. *Soil and Tillage Research* **37**, 211–222.

Alaoui, A. & Diserens, E. 2018. Mapping soil compaction – A review. *Current Opinion in Environmental Science & Health* **5**, 60–66.

Are, K.S., Adelana, A.O, Fademi, I.O. & Aina, A.O. 2017. Improving physical properties of degraded soil: Potential of poultry manure and biochar. *Agriculture and Natural Resources* **51**, 454–462.

Bogunovic, I., Pereira, P., Galic, M., Bilandzija, D. & Kisic, I. 2020. Tillage system and farmyard manure impact on soil physical properties, CO2 emissions, and crop yield in an organic farm located in a Mediterranean environment (Croatia). *Environmental Earth Sciences* **79**(70), 1–11.

Borowiak, K., Niewiadomska, A., Sulewska, H., Szymanska, G., Gluchowska, K. & Wolna-Maruwka, A. 2016. Effect of PRP SOL and PRP EBV nutrition on yield, photosynthesis activity and soil microbial activity of three cereal species. *Fresenius Environmental Bulletin* **25**, 2026–2035.

Celik, I., Gunal, H., Budak, M. & Akpinar, C. 2010. Effects of long-term organic and mineral fertilizers on bulk density and penetration resistance in semi-arid Mediterranean soil conditions. *Geoderma* **160**, 236–263.

Chakraborty, K. & Mistri, B. 2017. Estimation of soil compaction from bulk density and its effect on crop production. *Indian Journal of Spatial Science* **8**, 101–107.

Chen, S., Zhang, X., Shao, L., Sun, H., Niu, J. & Liu, X. 2020. Effects of straw and manure management on soil and crop performance in North China Plain. *Catena* **187**, 1–11.

Gardi, C., Jeffery, S. & Saltelli, A. 2013. An estimate of potential threats levels to soilbiodiversity in EU. *Global Change Biology* **19**, 1538–1548.

Jehan, S., Iqbal, M., Zahir, Z.A. & Farooq, M 2020. Role of dairy manure in improving wheat yield under deficit irrigation. *Pak. J. Bot.* **52**, 639–644.

Larson, D.L. & Clyma, H.E. 1995. Electro-osmosis effectiveness in reducing tillage draft force and energy forces. *Transactions of ASAE* **38**, 1281–1288.

Liang, A., McLaughlin, N.B., Ma, B.L., Gregorich, E.G., Morrison, M.J., Burtt, S.D., Patterson, B.S. & Evenson, L.I. 2013. Changes in mouldboard plough draught and tractor fuel consumption on continuous corn after 18 years of organic and inorganic N amendments. *Energy* **52**, 89–95.

Ludwig, B., Schulz, E., Rethemeyer, J., Merbach, I. & Flessa, H. 2007. Predictive modelling of C dynamics in the long-term fertilization experiment at Bad Lauchstadt with the Rothamsted Carbon Model. *European Journal of Soil Science* **58**, 1155–1163.

Luo, J., Lin, Z.L., Li, S.Y., Que, Y.X., Zhang, C.F., Yang, Z.Q., Yao, K.C., Feng, J.F., Chen, J.F. & Zhang, H. 2020. Effects of different soil improvement measures on soil physicochemical properties and microbial community structures in mechanically compacted acidified sugarcane field. *Acta Agronomica Sinica(China)* **46**, 596–613.

McLaughlin, N.B., Gregorich, E.G., Dwyer, L.M. & Ma, B.L. 2002. Effect of organic and inorganic soil nitrogen amendments on mouldboard plow draft. *Soil & tillage research* **64**, 211–219.

Odey, S.O. 2018. Overview of engineering problems of soil compaction and their effects on growth and yields of crops. *European Journal of Advances in Enineering and Technology* **5**, 701–709.

Panagos, P., Borelli, P., Meusburger, K., Alewell, C., Lugato, E. & Montanarella, L. 2015. Estimating the soil erosion cover-management factor at the European scale. *Land Use Policy* **48**, 38–50.

Peltre, C., Nyord, T., Bruun, S., Jensen, L.S. & Magid, J. 2015. Repeated soil application of organic waste amendments reduces draught force and fuel consumption for soil tillage. *Agriculture, Ecosystems and Environment* **211**, 94–101.

Podhrázská, J., Konečná, J., Kameníčková, I. & Dumbrovský, M. 2012. Survey of the impact of PRP SOL subsidiary substance on the hydrophysical properties of soil at cultivation of sugar beet. *Listy cukrovarnické a řepařské* **128**, 128–133.

Sálusová, D. 2018. *Czech agriculture from the viewpoint of statistics.* Prague: Czech Statictical Office. 85 pp. (in Czech).

Šařec, P. & Novák, P. 2017. Influence of manure and activators of organic matter biological transformation on selected soil physical properties of Modal Luvisol. *Agronomy Research* **15**, 565–575.

Šařec, P. & Žemličková, N. 2016. Soil physical characteristics and soil-tillage implement draft assessment for different variants of soil amendments. *Agronomy Research* **14**, 948–958.

Schjønning, P., Christensen, B.T. & Carstensen, B. 1994. Physical and chemical-properties of a sandy loam receiving animal manure, mineral fertilizer or No fertilizer for 90 years. *European Journal of Soil Science* **45**, 257–268.

Stolte, J., Tesfai, M., Øygarden, L., Kværnø, S., Keizer, J., Verheijen, F., Panagos, P., Ballabio, C. & Hessel, R. 2016. *JRC Scientific and Technical Reports - Soil Threats in Europe.* Luxembourg: JRC Science Hub. 206 pp.

Walsh, E. & McDonnell, K.P. 2012. The influence of added organic matter on soil physical, chemical, and biological properties: a small-scale and short-time experiment using straw. *Archives of Agronomy and Soil Science* **58**, 201–205.

Agronomy Research **18**(4), 2592–2601, 2020
https://doi.org/10.15159/AR.20.169

Comparing RGB - based vegetation indices from UAV imageries to estimate hops canopy area

K. Starý[1,*], Z. Jelínek[1], J. Kumhálová[1], J. Chyba[2] and K. Balážová[2]

[1]Czech University of Life Sciences Prague, Faculty of Engineering, Department of Machinery Utilization, Kamýcká 129, CZ165 00 Prague, Czech Republic
[2]Czech University of Life Sciences, Faculty of Engineering, Department of Agricultural Machines, Kamýcká 129, CZ165 00 Prague, Czech Republic
[*]Correspondence: staryk@tf.czu.cz

Abstract. Remote estimation of hops plants in hop gardens is imperative in field of precision agriculture, because of precise imaging of hop garden structure. Monitoring of hop plant volume and area can help to predict the condition and yield of hops. In this study, two unmanned aerial vehicles (UAV) - eBee X senseFly UAV equipped with Red Green Blue (RGB) S.O.D.A. camera and Vertical Take-Off Landing (VTOL) UAV FireFly6 Pro by BirdsEyeView Aerobotics equipped with MicaSense RedEdge MX camera were used to acquire images of hop garden at phenology stage maturity of cones (24 th July) before harvest. Seven commonly used RGB vegetation indices (VI) were derived from these RGB and multispectral (MS) images after photogrammetric pre-processing and orthophoto mosaic extraction using Pix4Dmapper software. Vegetation Indices as the Green Percentage Index (G%), Excess of Green Index (ExGreen), Green Leaf Index (GLI), Visible Atmospherically Resistant Index (VARI), Red Green Blue Vegetation Index (RGBVI), Normalised Green Red Difference Index (NGRDI) and Triangular Greenness Index (TGI) were derived from both data sets. Binary model from each of VI was derived and threshold value for green vegetation was set. The results showed significant differences in hop plant area based on the specifications of cameras, especially wavelengths centres, and design and flight parameters of both UAV types. The comparison of various indices showed, that ExG and TGI indices has the highest congruity of estimated vegetation indices in hop garden canopy area for both used cameras. Further processing by Fuzzy Overlay tool proved high accuracy in green canopy area estimation for ExG and TGI vegetation indices.

Key words: unmanned aerial vehicles, hop garden, vegetation indices, canopy area.

INTRODUCTION

Hops with its growing area belongs to the marginal crops; on the other hand, its cultivation is very effective. In addition, hops have an important position in the world brewing industry, especially the Czech one. For this reason, Czech hops is an important export article (Rybáček, 1991).

The crop growth monitoring is one of the most important tasks in agronomy. The results could help to analyse the crop growth process and the growth conditions (Yang et al., 2015). Remote sensing has become a very popular technique in crop information acquiring due to its ability to collect images in various spectra. There are three commonly used remote sensing methods: satellite, ground based and aerial (e.g. UAV = unmanned aerial vehicles). Satellite methods can help to estimate the crop yield, chlorophyll and nitrogen content (Vincini et al., 2016), leaf area index (Xie et al., 2018), etc., but it is limited to its spatial resolution (Kumhálová et al., 2014). The ground-based platform enables to collect data with high accuracy, but it is limited to high workload, which can require long time of measurement (Kumhálová & Matějková, 2017). The fast development in UAV industry and its ability to hold various cameras and sensors have increased the utilization of UAV in field data collecting (Wan et al., 2018). The UAVs are able to hold various cameras and collect accurate data with strong correlation to the ground based collected data (Santos et al., 2020). The camera-based observation is also important for the determination of canopy area, plant volume and the yield of hops. Regardless of the subject of the analysis, the most important aspect is how to identify the green object. There are more options to identify greenness in a crop image. The usual method to identify the greenness is to use the spectral indices (Guijarro et al., 2011). There are many indices used in the agriculture, most of them have been developed for specific purposes. A quick glance at the results usually shows regions with low and high index values. The output of the index is assigned to a colour from a colour scale and generate a false colour image of the monitored area (McKinnon & Hoff, 2017).

Lussem et al. (2018) conducted a research, where they compared results from different spectral indices based on RGB camera (Sony Alpha 6000) imagery with Yara N-Sensor for dry matter yield prediction in the grassland. They selected for their study such spectral indices as Visible Atmospherically Resistant Index (VARI), Normalised Green Red Difference Index (NGRDI) and Normalised Difference Vegetation Index (NDVI). The results showed a good correlation e.g. the value of determination for NGRDI was obtained 0.62 and for VARI 0.63. Other relevant indices were SR (Simple Ratio Index) (0.63) and NDVI (0.65). The NDVI index is most used index worldwide since its introduction in 1974 (Rouse et al., 1974), therefore, there are many researches based on this index, just like another study comparing UAVs RGB based vegetation indices (VARI & TGI) with NDVI (McKinnon & Hoff, 2017). In general, VARI index is mostly dependent on leaf-area while Triangular Greenness Index (TGI) is mostly dependent on chlorophyll and nitrogen. For this reason, these indices may represent some aspects of the NDVI index; on the other hand, the researchers mentioned almost the same count of failures as successes for VARI & TGI indices in comparison to the NDVI index. The processing of the data for vegetation indices calculation has the limits in the threshold selection for detecting the green object and bare soil. These problems help to eliminate the Otsu´s method, which is based on automatic threshold selection for picture segmentation. The result of this procedure is binary image, which can improve the final results derived from vegetation indices (Otsu, 1979). Pádua et al. (2018) used this method for binary image extraction in vineyards.

However, the use of remote sensing is very challenging in hop gardens or vineyards due to the row structure and plant canopies. Within the vineyard plot or hop garden is bare soil or vegetation cover, which may results in presence of inappropriate information such as: inter-row vegetation cover, shadows produced by the plants etc.; when considering the whole hop garden or vineyard. Rybáček (1991) stated that according to historical documents the Czech hop-growing terminology could be sometimes similar to that used in wine-making. Nevertheless, there are many differences in comparison with vineyard. It is the challenge to use similar methods to vineyard-monitoring for deriving green vegetation of hop gardens and calculate its canopy area. Rybáček (1991) described in his study reproduction (propagation) coefficient of the stand (KRP) which depends on the amount of above-ground biomass and the ration of cones to this biomass. This calculation can be good indicator of hops yield. Spectral indices can serve as simply way how to calculate above-ground biomass. The vegetation indices are usually computed over the entire remote-sensed area. In this case, the unrelated information is present and the separation of sensed plants and inappropriate information is required. Pádua et al. (2018) conduct research on this theme, using UAS (Unmanned Aerial System) equipped by RGB camera with resolution of 12 MPx. There were compared thirteen vegetation indices (VI) and computed crop surface model to estimate which index is the best for vineyard vegetation detection. The best vegetation indices were then: ExG, GBVI, RGBVI, GLI & G%.

The main objective of this study is to calculate RGB indices over the selected hop garden and to find out which index is the best for canopy area calculation with regard to the specific structure of hop garden.

MATERIALS AND METHODS

Study area

The study area is an 5.5 ha experimental field located near to Stekník village (N 50°19'28.692"N, E 13°37'22.738"), in the Czech Republic. The hop garden comprised 3 hop varieties - Agnus (1.5 ha), Premiant (2.4 ha) and Sládek (1.6 ha) (see Fig. 1). The conventional hop garden technology with irrigation was used for crop cultivation. The mission was arranged in 24 June 2019 when the hop plants are fully growen with cones developing, and plant hight of 7 m (see Fig. 2).

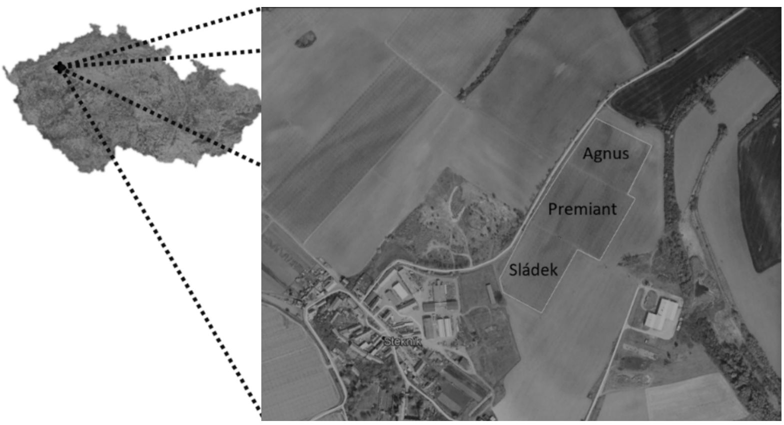

Figure 1. Location of experimental hop garden divided to three parts according to hop variety.

UAV equipment and flight configuration

Aerial survey were conducted using eBee X and FireFly6 Pro (FF6P) drones. The eBee is the fixed-wing drone (senseFly SA, Cheseaux-Lausanne, Switzerland), equipped with a built-in RTK-PPK functionality, and S.O.D.A. camera (Sensor Optimised for Drone Applications; senseFly SA, Cheseaux-Lausanne, Switzerland) with 20 Mpx RGB sensor and 28 mm focal lens. The FF6P is fixed-wing UAV (BirdsEyeView Aerobotics), equipped with multispectral MicaSense RedEdge-MX camera (MicaSense, Inc. Seattle,

Figure 2. Current status of Premiant hop variety in 24 July 2019.

WA, USA) containing five spectral bands and 1.2 Mpx per EO (Earth Observation) band sensor resolution. Spectral properties of cameras used in this study is given in Table 1.

Table 1. Spectral properties of cameras used in this study

Band (nm center)	S.O.D.A. eBee X	MicaSense Red Edge-MX FF6P
BLUE	450 nm (center, 100 nm bandwitdth)	475 nm (center, 20 nm bandwitdth)
RED	520 nm (center, 250 nm bandwitdth)	560 nm (center, 20 nm bandwitdth)
GREEN	660 nm(center, 130 nm bandwitdth)	668 nm (center, 10 nm bandwitdth)
RED EDGE	-	717 nm (center, 10 nm bandwitdth)
NEAR-IR	-	840 nm (center, 40 nm bandwitdth)

This study flight took place in 24 June 2019 between 11:30 a.m. and 1:00 p.m CET for both UAV technology. The eBee X flight was performed at 119 m above take-off height, with speed 15 m s^{-1} in average, and with resulting 2.77 cm spatial resolution of images. The images overlap was 80% longitudinal and 65% lateral. SW eMotion by SenseFly (see https://www.sensefly.com/software/emotion/) was used for setting the flight mission parameters. The FF6P flight was performed at 90 m above take-off height, with speed 16 m s^{-1} in average, and with resulting 7.43 cm spatial resolution of images. The images overlap was 80% longitudinal and 65% lateral.

UAV images processing

Acquired data were processed using Pix4Dmapper (Pix4D SA, Cheseaux - Lausanne, Switzerland), where image calibration, point cloud densification and orthophotomosaics (in WGS 84 UTM Zone 33 coordinate system) were calculated from each of datasets. Orthophotomosaics were then processed in ENVI, ArcGIS SW (ESRI, Redlands, CA, USA) and QGIS SW (Free Software Foundation, Inc., Boston, MA, USA). Selected RGB indices (see Table 2) were calculated for each of varieties and data sets. Green Percentage Index (G%), Excess of Green Index (ExGreen), Green Leaf Index (GLI), Visible Atmospherically Resistant Index (VARI), Red Green Blue Vegetation Index (RGBVI), Normalised Green Red Difference Index (NGRDI) and Triangular Greenness Index (TGI) were chosen to estimate the area of hop plants.

Table 2. RGB vegetation indices used in this study for UAV systems comparison

RGB Spectral Index	Algorithm	References
Green Percentage Index	$G\% = \frac{G}{R + G + B}$	(Richardson et al., 2007)
Excess Green	$ExG = 2 \times g - r - b$	(Woebbecke et al., 1995)
Excess Green- Excess Red	$ExG - ExR$	(Meyer & Neto, 2008)
Green Leaf Index	$GLI = \frac{(G - R) + (G - B)}{2G + R + B}$	(Gobron et al., 2000; Hunt et al., 2013)
Red Green Blue Vegetation Index	$RGBVI = \frac{G2 - (B \times R)}{G2 + (B \times R)}$	(Bendig et al., 2015)
Visible Atmospherically Resistant Index	$VARI = \frac{G - R}{G + R - B}$	(Gitelson et al., 2002)
Normalised Green Red Difference Index	$NGRDI = \frac{G - R}{G + R}$	(Falkowski et al., 2005; Gitelson et al., 2002; Kawashima & Nakatani 1998; Tucker, 1979)
Triangular Greenness Index	$TGI = G - 0.39 \times R - 0.61 \times B$	(Hunt et al., 2013)

Where g = G/(R+G+B); b = B/(R+G+B); *r* = R/(R+G+B); and green (G), red (R) and blue (B) are the reflectance values of each band.

Binary models (0;1) were then derived from resulting indices with the help of threshold based on Otsu´s method (Otsu, 1979). This nonparametric and unsupervised method is based on automatic threshold selection for picture segmentation. In our study the value 0 equals to bare soil and value 1 represent vegetation. Resulted binary rasters were then converted to vector model (polygon shapefiles) for calculating area possibilities for each of varieties and UAV data sets. Excess Green (ExG) and TGI index were used for next image analysis because these indices showed the most accuracy estimation of vegetation cover in hop garden area in comparison with RGB orthophotomosaics. Using Map algebra tool in ArcGIS SW the ExG and TGI indices for each data sets (eBee and FF6P) were deducted from each other with the aim to find out the accuracy of vegetation area calculation. The tool Fuzzy Overlay (Spatial Analyst tool - Overlay; ArcGIS SW) were then used for two model deriving ExG and TGI, which combines the raster of both binary model based on selected index (Fuzzy Overlay of ExG from eBee and ExG from FF6P; and Fuzzy Overlay TGI from eBee and TGI from FF6P). Fuzzy Overlay tool allows the analysis of the possibility of a phenomenon belonging to multiple sets in a multicriteria overlay analysis. Fuzzy Overlay not only determines what sets the phenomenon is possibly a member of, but also analyses the relationships between memberships among multiple sets. The Fuzzy 'Or' Overlay type, which was set for our purposes, will return the maximum value of the sets the cell location belongs to. This technique is useful when you want to identify the highest membership values for any of the input criteria (ArcGIS 10.4, ESRI, 2019). These resulting models derived on the base of Fuzzy Overlay algorithm were compared with each other to determine the accuracy of these models.

RESULTS AND DISCUSSION

Table 3 shows leaf area for each hop variety. The leaf area is derived from both UAV systems: eBee X and FF6P. The results show differences between both sensing which could be caused for various reasons. The eBee X had higher spatial resolution than FF6P and with the Otsu´s binary model for automatic threshold detection the differences between both sensing occurred. The differences between the sensing vary for each indices differently. Similar studies realized in vineyards proved, that UAVs with various cameras spatial resolution could provide accurate data. To provide accurate data, the sensor-related radiometric and spectral calibration are important (Brook et al., 2020). As was confirmed by Pádua et al. (2018) higher accuracy or the least difference is between the ExG and NDVI indices. The ExG as well as TGI indices were used for further processing and in the Table 3 the values are highlighted. The TGI (McKinnon & Hoff, 2017) and ExG indices are mostly dependant on the chlorophyll and nitrogen content, this mean that these indices should be very similar, but even there are differences. These differences are characterized by higher values of TGI index in all variants. These differences, between these two indices, could have occurred due to colour shade change by shadows of the hop canopy, which occurs at any circumstances, due to the technology of hop growing in hop gardens. Another possibility of these differences could be the different colour of leaves (mostly yellow) in the lower layer of hop canopy which is mainly dependant on the hop growth stage and its variety. As proved in the study of Fuentes-Peailillo et al. (2018) the TGI index has best results in canopy cover determination also by different sparse crops in comparison with NDVI. On the other hand the results show that the accuracy of the canopy cover determination depends on the spatial resolution of image. Hunt et al. (2013) proved that the utilization of TGI index has best results in later phenology stages, when it is only affected by leaf chlorophyll content, therefore TGI is the best to detect crop nitrogen requirements. In our study this statement was confirmed, when ExG and TGI were used for further analysis.

Table 3. Leaf area (m^2) derived from eBee X and FF6P UAV systems for individual hop varieties

Index/ Variety	eBee X			FF6P		
	Agnus	Premiant	Sládek	Agnus	Premiant	Sládek
ExGExr	3,374.8	5,223.5	7,711.3	8,227.2	13,478.5	12,081.2
ExG	**5,251.6**	**8,802.0**	**8,089.2**	**3,702.6**	**4,851.4**	**6,117.6**
GLI	709.6	1231.8	478.9	10,579.7	17,166.9	13,947.1
GPI	-	-	-	7,769.1	13,036.3	11,999.7
NGRDI	1,919.2	1,886.7	438.5	8,130.0	13,333.7	11,992.2
RGBVI	-	-	-	9,166.5	15,351.4	13,172.2
TGI	**5,520.0**	**9,240.4**	**8,260.4**	**4,452.3**	**6,278.1**	**6,998.8**
VARI	1,959.3	1,920.3	464.6	8,279.1	13,490.1	12,050.3

The comparison of ExG and TGI from eBee X and FF6P in Table 4 shows, that the green vegetation was mostly identified in both layers. The majority of the vegetation was identified by both UAVs, but the eBee has more unique identification of green vegetation than it is in FF6P layer. This is caused by the difference of both cameras their different spectral properties and by various spatial resolution too. Additional small differences should be caused by the different length and/or position of the shadows of hop canopy caused by impossibility to fly over monitored area at the same time with both UAVs due to law restriction and safety of persons and property.

Table 4. Changes of area of hop garden (m^2) derived from models eBee and FF6P UAVs systems deducted from each other for individual hop varieties. The value 0 = no changes; -1 = green vegetation' was only 'FF6P' layer, 1 = green vegetation' was only in 'eBee' layer

Index/ Variety	Changes	Agnus	Premiant	Sládek
ExGeBee-	-1	283.9	466.0	196.7
ExG FF6P	0	12,792.3	19,835.6	14,122.6
	1	17,77.9	4,355.8	2,040.2
TGIeBee-	-1	381.9	799.8	499.8
TGI FF6P	0	13,065.5	19,328.9	14,184.8
	1	1,406.7	3,706.9	1,674.9

From the previous results (Table 3 & 4) is obvious that it is possible to use standard RGB cameras with high resolution to estimate these indices and leaf area at least in hop gardens and probably in vineyards. This agrees with Lussem et al. (2018) who confirmed the usage of RGB camera in grasslands, but in this case were used different indices namely NGRDI and SR. Pádua et al. (2018) found out similar results with RGB camera utilization. They stated that low-cost RGB camera proved to have enough accuracy for vineyard monitoring. Barbosa et al. (2019) concluded in their study that all of the evaluated vegetation indices, derived for grass monitoring, were affected by lighting condition of the scanned location. We solved similar problems with hop crops.

Thanks to the spatial analyst tool Fuzzy Overlay, the leaf area is presented in Table 5. The leaf area is derived from the multicriterial overlay analysis. This tool utilizes layers ExG from eBee X and FF6P and area from TGI from eBee X and FF6P for the leaf area determination with the highest possible accuracy.

Table 5. Leaf area (m^2) calculated for ExG and TGI model with the help of Fuzzy Overlay tool (combination of layers ExG eBee and ExG FF6P; TGI eBee and TGI FF6P)

Index/Variety	Agnus	Premiant	Sládek
FuzzyExG	5,575.7	10,119.9	8,820.2
FuzzyTGI	5,953.6	13,681.8	7608.7

For selected hops varieties there are also presented comparisons of Fuzzy models. In the Table 6 the changes of hop garden area for models FuzzyExG and FuzzyTGI are presented. The table proves that both models are very accurate, because the differences between the layers are less than 4% in comparison with the common (both layers) area. These changes are also shown in Fig. 3. This figure demonstrate the differences between ExG and TGI fuzzy

Table 6. Changes of area of hop garden (m^2) derived from Fuzzy models (FuzzExG minus FuzzyTGI) for selected hop varieties. The value 0 = no changes; -1 = 'green vegetation' was only TGI layer, 1 = 'green vegetation' was only in ExG layer

Index/ Variety	Changes	Agnus	Premiant	Sládek
FuzzyExG-	-1	385.3	781.6	424.2
TGI	0	14,160.1	22,863.6	15,968.3
	1	93.9	150.8	33.3

models. Differences can be caused by the actual status of individual plants. The results of individual flights can be affected by movement of main stem (bine) and its lateral branches (shoots) which are wrapped around wires. The stem reaches a height of 7 m (upper limit of construction) and grows at an angle, which can caused different lighting condition inside of the hop garden (shadows) (Rybáček, 1991). Other reasons may be different flight altitudes and other camera and drone specifications. However Caruso et al. (2017) in their study reported that the RGB consumer camera mounted on UAV can be sufficient tool for canopy modelling.

The results of Fuzzy Overlay are with agreement with Baidya et al. (2014). They concluded that fuzzy overlay analysis is computationally more expensive but it gives more accurate and consistent results.

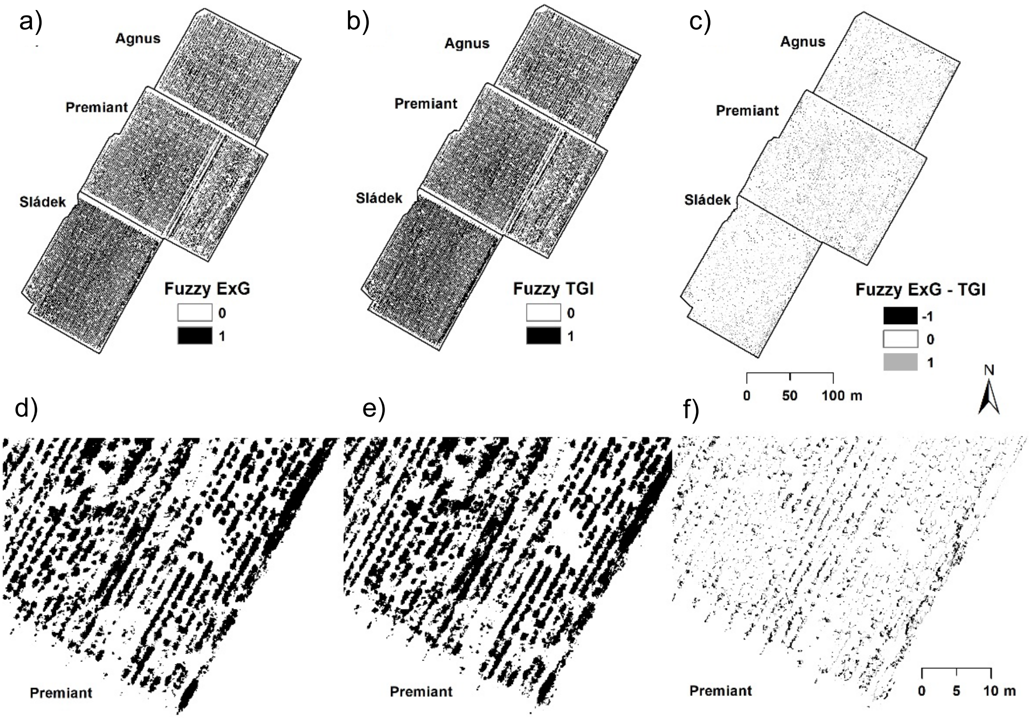

Figure 3. Fuzzy models ExG (a) and TGI (b) and changes of area of hop garden (m^2) derived from Fuzzy models (FuzzExG minus FuzzyTGI) (c) for selected hop varieties. Premiant hop variety Fuzzy models and its changes are shown in detail below - Fuzzy ExG detail (d), Fuzzy TGI detail (e), and changes (Fuzzy ExG - TGI) detail (f).

CONCLUSIONS

The results showed that vegetation indices could be used for the hop plants area monitoring. Hop belongs to the least researched crops, because hop monitoring has its specifics, which must be taken into account.

The comparison of various indices showed, that ExG and TGI indices has the highest congruity of estimated vegetation indices in hop garden area for both used cameras (S.O.D.A. and MicaSense). On the other hand, indices such as: ExGExr, GLI, GPI, NGRDI, RGBVI and VARI did not show significant accordance.

Further processing by Fuzzy Overlay tool proved high accuracy in leaf area estimation for ExG and TGI vegetation indices. Both of these indices had very similar results in crop area detection, because the calculated mutual deviation in detection of hop garden area is smaller than 4%.

Also was confirmed that for the estimation of crop area is possible to use RGB camera and it is not necessary to use more expensive multispectral cameras.

ACKNOWLEDGEMENTS. This study was supported by Czech University of Life Sciences Prague, when conducted under grant IGA no. 2020:31160/1312/3110. Authors would like to thank the Hop Research Institute Co., Ltd. in Žatec and Postoloprty Laboratory Co., Ltd for their time, providing the access to the hop garden and support during this research.

REFERENCES

Baidya, P., Chutia, D., Sudhakar, S., Goswami, Ch., Goswami, J., Saikhom, V., Singh, P.S. & Sarma, K.K. 2014. Effectiveness of Fuzzy Overlay Function for Multi-Criteria Spatial Modeling—A Case Study on Preparation of Land Resources Map for Mawsynram Block of East Khasi Hills District of Meghalaya, India. *Journal of Geographic Information System* **06**, 605–612.

Barbosa, B.D.S., Ferraz, G.A.S., Goncalves, L.M., Marin, D.B., Macield, D.T., Ferraz, P.F.P. & Rossi, G. 2019. RGB vegetation indices applied to grass monitoring: a qualitative analysis. *Agronomy Research* **17**(2), 349–357. https://doi.org/10.15159/AR.19.119

Bendig, J., Kang, Y., Aasen, H., Bolten, A., Bennertz, S., Broscheit, J., Gnyp, M. L. & Bareth, G. 2015. Combining UAV-Based Plant Height from Crop Surface Models, Visible, and near Infrared Vegetation Indices for Biomass Monitoring in Barley. *International Journal of Applied Earth Observation and Geoinformation* **39**, 79–87.

Brook, A., De Micco, V., Battipaglia, G., Erbaggio, A., Ludeno, G., Catapano, I. & Bonfante, A. 2020. A smart multiple spatial and temporal resolution system to support precision agriculture from satellite images: Proof of concept on Aglianico vineyard. *Remote Sensing of Environment* **240**,111679.

Caruso, G., Tozzini, L., Rallo, G., Primicerio, J., Moriondo, M., Palai, G. & Gucci, R. 2017. Estimating biophysical and geometrical parameters of grapevine canopies ("Sangiovese") by an unmanned aerial vehicle (UAV) and VIS-NIR cameras. *Vitis* **56**, 63–70.

Falkowski, M.J., Gessler, P.E., Morgan, P., Hudak, A.T. & Smith, A.M.S. 2005. Characterizing and Mapping Forest Fire Fuels Using ASTER Imagery and Gradient Modeling. *Forest Ecology and Management* **217**, 129–146.

Fuentes-Peailillo, F., Ortega-Farias, S., Rivera, M., Bardeen, M. & Moreno, M. 2018. Comparison of vegetation indices acquired from RGB and Multispectral sensors placed on UAV. *2018 IEEE International Conference on Automation/XXIII Congress of the Chilean Association of Automatic Control (ICA-ACCA)* (1–6). IEEE.

Gitelson, A.A., Kaufman, Y.J., Stark, R. & Rundquist, D. 2002. Novel Algorithms for Remote Estimation of Vegetation Fraction. *Remote Sensing of the Environment* **80**, 76–87.

Gobron, N., Pinty, B., Verstraete, M.M. & Widlowski, J.L. 2000. Advanced Vegetation Indices Optimized for up-Coming Sensors: Design, Performance, and Applications. *IEEE Transactions on Geoscience and Remote Sensing* **38**(6), 2489–2505.

Guijarro, M., Pajares, G., Riomoros, I. & Herrera, P. 2011. Automatic segmentation of relevant textures in agricultural images. *Computers and Electronics in Agriculture* **75**(1), 75–83.

Hunt, E.R., Doraiswamy, P.C., McMurtrey, J.E., Daughtry, C.S.T., Perry, E.M. & Akhmedov, B. 2013. A Visible Band Index for Remote Sensing Leaf Chlorophyll Content at the Canopy Scale. *International Journal of Applied Earth Observation and Geoinformation* **21**, 103–112.

Kawashima, S. & Nakatani, M. 1998. An Algorithm for Estimating Chlorophyll Content in Leave Using a Video Camera. *Annals of Botany* **81**(1), 49–54.

Kumhálová, J. & Matějková, Š. 2017. Yield variability prediction by remote sensing sensors with different spatial resolution. *International Agrophysics* **31**, 195–202.

Kumhálová, J., Zemek, F., Novák, P., Brovkina, O. & Mayerová, M. 2014. Use of Landsat images for yield evaluation within a small plot. *Plant Soil Environment* **11**, 501–506.

Lussem, U., Bolten, A., Gnyp, M.L., Jasper, J. & Bareth, G. 2018. Evaluation of RGB-Based Vegetation Indices From UAV Imagery To Estimate Forage Yield In Grassland. In: *ISPRS TC III Mid-term Symposium "Developments, Technologies and Applications in Remote Sensing*", Volume **XLII**-3, 2018, 7–10 May, Beijing, China, pp. 1215–1219.

Mayer, G.E. & Neto, J.C. 2008. Verification of color vegetation indices for automated crop imaging applications. *Computers and electronics in agriculture* **63**, 282–293.

McKinnon, T. & Hoff, P. 2017. *Comparing RGB-Based Vegetation Indices With NDVI For Drone Based Agricultural Sensing*. AgribotixLLC AGBX021-17, pp. 1–8.

Otsu, N. 1979. A Threshold Selection Method from Gray-Level Histograms. *IEEE Transactions on Systems, Man, and Cybernetics* **9**(1), 62–66.

Pádua, L., Marques, P., Hruška, J., Adão, T., Bessa, J., Sousa, A., Peres, E., Morais, R. & Sousa, J. 2018. Vineyard properties extraction combining UAS-based RGB imagery with elevation data. *International Journal of Remote Sensing* **39**(15–16), 5377–5401.

Richardson, A.D., Jenkins, J.P., Braswell, B.H., Hollinger, D.Y., Ollinger, S.V. & Smith, M.-L. 2007. Use of Digital Webcam Images to Track Spring Green-Up in a Deciduous Broadleaf Forest. *Oecologia* **152**(2), 323–334.

Rouse, J.W., Haas, R.H., Schell, J.A. & Deering, D.W. 1974. Monitoring vegetation systems in the Great Plains with ERTS. In: Freden, S.C., Mercanti, E.P., Becker, M. (Eds.), *Third Earth Resources Technology Satellite-1 Symposium*, Vol. **1**: Technical Presentations, NASA SP-351. National Aeronautics and Space Administration, Washington, DC, pp. 309–317.

Rybáček, V. 1991. *Hop Production*. Elsevier Science Publisher, 286 pp.

Santos, L., Ferraz, G., Diotto, A., Barbosa, B., Maciel, D., Andrade, M. & Rossi, G. 2020. Coffee crop coefficient prediction as a function of biophysical variables identified from RGB UAS images. *Agronomy Research* **18**(S2), 1463–1471. https://doi.org/10.15159/AR.20.100

Tucker, C.J. 1979. Red and Photographic Infrared Linear Combinations for Monitoring Vegetation. *Remote Sensing of Environment* **8**(2), 127–150.

Vincini, M., Calegari, F. & Casa, R. 2016. Sensitivity of leaf chlorophyll empirical estimators obtained at Sentinel-2 spectral resolution for different canopy structures. *Precision Agriculture* **17**, 313–331.

Wan, L., Li, Y., Cen, H., Zhu, J., Yin, W., Wu, W., Zhu, H., Sun, d., Zhou, W. & He, Y. 2018. Combining UAV-Based Vegetation Indices and Image Classification to Estimate Flower Number in Oilseed Rape. *Remote Sensing* **10**(1484), 18.

Woebbecke, D.M., Meyer, G.E., Vonbargen, K. & Mortensen, D.A. 1995. Color indexes for weed identification under various soil, residue, and lighting conditions. *Trans. ASAE* **38**, 259–269.

Xie, Q., Dash, J., Peng, D., Qin, Q., Mortimer, H., Case, R., Pignatti, S., Laneve, G., Pascucci, S., Dong, Y. & Ye, H. 2018. Vegetation indices combining the Red and Red-Edge spectral information for leaf area index retrieval. *IEEE Journal of Selected Topics in Applied Earth Observations and Remote Sensing* **11**(5), 1482–1493.

Yang, W., Wang, S., Zhao, X., Zhang, J. & Feng, J. 2015. Greenness identification based on HSV decision tree. *Information Processing in Agriculture* **2**(3–4), 149–160.

Agronomy Research **18**(4), 2602–2612, 2020
https://doi.org/10.15159/AR.20.215

Evaluation of various legume species and varieties grown in Latvia as a raw material of plant-based protein products

V. Sterna[1,*], S. Zute[1], I. Jansone[1], E. Ence[2] and E. Strausa[2]

[1]Department of Plant breeding and Agroecology, Institute of Agricultural Resources and Economics 'Dižzemes', Dižstende, LV-3258 Talsi district, Latvia
[2]Riga Technical University, Faculty of Engineering Economics and Management, 6 Kalnciema street, LV-1048 Riga, Latvia
[*]Correspondence: vita.sterna@arei.lv

Abstract. Nutrition value of legumes has been traditionally attributed to its high protein content. Protein content of legumes is variable dependent on different species and varieties, and highly affected by environmental factors. Usually protein quality is characterized by its owns amino acid profile in nutritional point of view. Therefore, the present study was conducted to determine the protein contents and amino acid profiles of pea (*Pisum sativum* L), faba beans (*Vicia faba* L) and soya (*Glycine max* L) grown in Latvia and evaluate their potential for food production. Overall results of a five-year analysis (2013–2017) showed that the protein content of peas, faba beans and soybean ranged from 20.0 to 26.1%, 26.6 to 30.5% and 35.9 to 40.9%, respectively. The corresponding values of total crude fat ranged from 0.8 to 1.2%, 0.7–1.3% and 16.6 to 19.3%, respectively. Results of study showed that the protein content of peas, faba beans and soybean was not differed by growing system ($p < 0.05$). The percentage of essential amino acids for pea, faba bean and soya were 34 to 38%, 57 to 59% and 62 to 64% respectively. The composition of pea flakes was preserved protein content of raw material. The pea flakes has high content of lysine of 10.1 g kg^{-1}, phenylalanine+thyrosine of 11.6 g kg^{-1} and the sum of essential amino acids of 66.4 g kg^{-1}. In nutritional point of view, pea flakes could be product with high-quality protein composition.

Key words: protein contents, protein quality, legume seeds.

INTRODUCTION

Legumes are considered the second most important food source after cereals, nutritionally valuable, and providing proteins with essential amino acids, complex carbohydrates, dietary fibre, unsaturated fats, vitamins and essential minerals for human diet (Rebello et al., 2014; Maphosa & Jideani, 2017). Legumes have higher protein content of 20–45% than that of most plant foods, twice the protein content of cereals. Peas and beans are on the lower side of the range with 17–30% proteins while lupins and soybeans are on the higher side with 38–45% protein (Mlynekova et al., 2014; Rebello et al., 2014; Strauta, 2017). Broad variation was stated between locations and traits for genotypes of pulses (Hawhorne, 2006; Kronberga et al., 2016). Pulses become more and more popular due to nutritional value as protein source for food and feed and due to its agricultural service crop properties (Hawhorne, 2006; Lepse et al., 2016; Kirse, 2017).

Furthermore, legumes are gluten free, making them suitable for consumption by celiac disease patients and could be a base for the development of many functional foods to promote human health (Maphosa & Jideani, 2017).

Following global trends in plant-based protein in the diet, there is a growing demand for legume products worldwide[1]. The global legumes market was valued at 44.9 billion USA dollars in 2017 and is expected to reach 75.8 billion USA dollars by 2025, growing at a Compound annual growth rate of 6.77% from 2017 to 2025[2]. The trend is related to the rapid increase in the number of supporters of green and sustainable lifestyle, as well as the actualization of environmental problems through the use of meat products in the diet. More than 40 million tons of crop proteins are imported annually in European Union (EU), representing 80% of EU's crop protein consumption (Petrusán et al., 2016). Mainly, soybeans and corn are imported, while local products such as peas and faba beans are common agricultural commodities in Europe. Partly using EU policy instruments, Germany, France (in cooperation with an Interbranch Organisation), and Poland have set up national plans to support the cultivation of protein crops. Denmark, Austria, and the Netherlands have introduced initiatives to promote plant proteins (Global legumes market 2019–2023, 2019). Vegetal proteins, gluten-free, high-protein content and high-value protein are the key determinants of the value-added products of the future.

Faba beans contain numerous anti-nutritional factors, such as phytic acid, tannins and protease inhibitors, reducing the digestibility of seeds or leading to some pathological conditions (Multari et al., 2015). Raw soybean contains anti-nutrients, including phytic acid (from phytates), which binds and prevents mineral absorption, especially zinc, calcium, and magnesium in the digestive tract (Humer et al., 2015). The preparation method was a key factor governing pulse final nutritional composition, depending on pulse species. Canning led to a greater decrease in proteins, total dietary fibers, magnesium or phytate contents compared to household cooking (Margier et al., 2018).

Extrusion is one of the methods of processing that may affect the nature of grain or seed components, its physical, chemical and nutritional properties (Diaz et al., 2006). It had been found to have minor effect on protein and fat content of peas, faba beans and soya (Strauta, 2017; Kudlinskiene, 2020). The extrusion has a positive effect on nutritional characteristics, because it induces important modifications on starch and proteins, enhancing their digestibility, and reduces the content of trypsin inhibitors, lectins, phytic acid, and tannins, typically present in legumes (Kudlinskiene et al., 2020; Pasqualone et al., 2020). At the same time, the extrusion technology in the food industry provides legumes with a mild taste, as well as faster and more convenient processing in the preparation of a meal. European manufacturers are choosing extrusion processing of legumes for food production, that way offers new food applications for legumes, which have not previously shown great economic importance, such as faba bean or peas (Pasqualone et al., 2020). For instance, a Latvian manufacturer produced extruded pea using local raw material - variety 'Bruno' and looking for new possibilities to offer the consumer a wider range of products with a high-quality protein composition.

[1] https://www.researchandmarkets.com/reports/4749653/global-legumes-market-2019-2023
[2] https://www.hexaresearch.com/research-report/legumes-market

Despite many studies on legume varieties, their productivity and cultivation technologies there are few studies on the latest locally adapted varieties and the amino acid composition of legumes, their suitability for food production.

This study was conducted to collect a five-year analysis of crude protein, crude fat and amino acid compositions of different varieties of pea, faba beans and soya grown in Latvia, and to assest their potentially for food production.

MATERIALS AND METHODS

Materials

The research was conducted at Institute of Agricultural Resources and Economics. The material consisted of three varieties of peas (*Pisum sativum* L), namely 'Selga', 'Almara', 'Lāsma', twelve varieties of faba beans (*Vicia faba* L), namely 'Lielplatone', 'Granit', 'Fuego', 'Jogeva', 'Olga', 'Bobas', 'Laura', 'Isabella', 'Julia', 'Alexia', Boxer', 'Vertigo' and three varieties of soya(*Glycine max* L), namely 'Laulema', 'Annushka', 'Lajma' grown in conventional (C) and organic (O) fields at the Stende Research Centre (lat. 57.1412° N, long. 22.5367° E) from 2013 to 2017. Each field experiment was carried out using a block design with four replicates, plot size was 10 m^{-2}. Legumes grown in an organic farming system have not received additional fertilizer, but in conventional system was provided with additional 0–30 kg N, 50–60 kg P_2O_5 and 75–80 kg K_20 and a conventional pesticide programme applied.

Chemical analyses

After harvesting seeds were dried till 14% moisture, cleaned and sorted using round mesh sieve 50 mm. Mean samples from all (4) replications (0.5 kg) were taken for laboratory testing. Test weight, protein, fat and amino acids composition were determined.

Protein content was determined by the Kjeldahl method, and conversion factor 6.25 was used to convert total nitrogen to crude protein by a standart official method of analysis of LVS EN ISO 20483:2014. *Fat* was extracted with petroleum ether (boiling range of 40–60 °C) by the Soxhlet extraction method and determined gravimetrically by a standart official method of analysis of ISO 6492:1998. The content of *starch* was determined by a standart official method of analysis of LVS EN ISO 10520:2001.

Amino acids. Dried, defatted samples were treated with constant boiling 6N hydrochloric acid in the oven at around 110 °C for 23 h using the Waters AccQ Tag chemistry package. Hydrolyzate was diluted with 0.1% formic acid. Amino acids were detected using reversed-phase HPLC/MS (Waters Alliance 2695, Waters 3100, column XTerra MS C18 5 μm, 1×100 mm). Mobile phase (90% acetonitrile: 10% deionized water) 0.5 mL min^{-1}, column temperature at 40 °C was used. The identity and quantitative analysis of the amino acids (AA) were assessed by comparison with the retention times and peak areas of the standard amino acid mixture.

Free amino acids of extruded pea flakes were determined using GH FID method with Phenomenex Protein Hydroxylate Kit in laboratory BIOR. The sum of essential amino acids (EAA) was calculated as

$$\sum EAA = His + Tyr + Tre + Val + Met + Iso + Leu + Phe + Lys$$

Extrusion of products

The extrusion of pea was conducted in the factory of MILZU! Ltd., and extrusion process was performed using a double-screw extruder. Temperatures for extrusion process were set 78/83/98 °C, screw speed 800 rpm^{-1}. Obtained extrudats were cooked at 130 °C for 10 minutes in conventional oven to receive soft and crispy product. In the final stage of production, the extruded peas were ground to obtain pea flakes.

Data analysis.

SPSS statistical software version 20 was used for data analysis. The following analysis were carried out: Normal distribution (Kolmogorov-Smirnov), homogeneity of variance (Levene's test) and t-test to determine the differences between the means of growing system. The differences were considered statistically significant when $p < 0.05$.

RESULTS AND DISCUSSION

The results of analyzed protein, fat and amino acids of peas, faba beans and soya, grown in Latvia are summarized in Table 1.

Table 1. Mean values of phytochemical content for three legumes over two different growing systems

Species	Growing system	Protein	Fat	Total AA	EAA	EAA/AA
		Mean ± SD (%)		Mean ± SD (g kg^{-1})		(%)
Pea *Pisum sativum* L	C	25.3 ± 2.0^{a}	1.0 ± 0.2	214.8 ± 26.2	79.6 ± 10.2^{d}	34–37
	O	21.9 ± 2.2^{a}	1.1 ± 0.2	204.1 ± 13.2	77.2 ± 5.3^{d}	35–38
Faba beans *Vicia faba* L	C	28.8 ± 3.5^{b}	0.9 ± 0.3	255.6 ± 16.3	91.6 ± 5.1^{e}	57–59
	O	30.4 ± 1.1^{b}	0.9 ± 0.3	255.1 ± 17.9	93.1 ± 5.1^{e}	58–59
Soya *Glycine max* L	C	38.1 ± 1.9^{c}	19.3 ± 0.7	310 ± 11.3	119.7 ± 4.4^{f}	62–63
	O	39.6 ± 1.2^{c}	18.6 ± 0.7	318 ± 9.7	122.8 ± 4.2^{f}	62–64

Different letters indicate significant differences between treatment means.

Results of Table 1 showed that the protein content of peas grown in conventional system was 25.3 ± 2.0% and it was higher than in organic system 21.9 ± 2.2% but diference is not significant ($p > 0.05$). Results of study showed that average protein content of tested varieties are similar with protein content of grey pea 26.9 ± 2.0% (Strauta et al., 2016). The average amount of essential amino acids of peas grown in conventional system was 79.6 ± 10.2 g kg^{-1} it was higher than in organic system and varied more widely over the years and varieties. The results of this study are in line with other, where the protein content of peas and beans reported 17–30% (Mlynekova et al., 2014), in dry pea grains varied between 18.8% and 33.5% depending by variety (Kronberga et al., 2016).

The protein content of faba beans determined higher than protein content of peas, it varied from 26.6% to 31.5% with mean values 28.8 ± 3.5% in samples of conventional fields and 30.4 ± 1.1% in samples of organic fields, it was not affected by growing system ($p > 0.05$). Average of total amino acids content of faba beans determined in conventional system of our study was 255.6 ± 16.3 g kg^{-1}, it was higher than reported in other studies - 232.3 g kg^{-1} (Kudlinskiene et al., 2020). The percentage of essential amino acids in total amino acids for faba bean determined 57–59%, it was higher than for peas and higher as reported for faba bean in other studies - 34–41% (Toews & Wang, 2013) or 31.8–37.7% (Alghamdi, 2009).

The protein content of soybeans determined in this study varied from 35.9% to 40.9% and fat content varied from 16.6% to 19.3%. Results of Table 1 showed that the protein content of soya beans grown in conventional system was 38.1 ± 1.9% and in organic system 39.6 ± 1.2% but diference is not significant ($p > 0.05$). Degola et al. (2019) reported that the protein content in soya bean samples determined from 32.7% to 40.7% and fat content from 18.4% to 21.4% and significantly differed ($p < 0.05$) among growing places in Latvia. The percentage of essential amino acids in total amino acids for soya bean samples was determined from 59% to 62%. The results of this study, when compared protein, fat and percentage of amino acids with values of soya beans mentioned in USDA (2018) database (36.49%, 19.94% and 63.7% respectively) shows that composition of soya grown in Latvia is equivalent in terms of protein and fat content. Grieshop & Fahey (2001) reported that soybeans from China had greather crude protein concentration (42.14%) than those from Brazil (40.86%). Environmental conditions under which soybean are grown have a great impact on chemical composition - diferences in crude protein, amino acid and lipid contents of soybeans were detected both within and among countries (Grieshop & Fahey, 2001).

Protein content of legumes is variable dependent on different species and highly affected by environmental factors. Therefore was compared protein content of species in different years, the results was showed in Table 2.

Table 2. Mean protein content for three legumes for five harvest years

Species	Protein content, mean ± SD %					Average
	2013	2014	2015	2016	2017	
Pea *Pisum sativum* L	22.8 ± 1.9	26.1 ± 2.1	24.5 ± 2.1	26.0 ± 2.0	24.5 ± 2.1	24.37 ± 2.2
Faba beans *Vicia faba* L	26.8 ± 2.1	30.1 ± 2.5	29.6 ± 1.2	24.7 ± 2.1	26.4 ± 2.1	28.0 ± 1.5
Soya *Glycine max* L	*	39.59 ± 2.5	38.1 ± 2.5	*	*	38.8 ± 2.7

*No data.

The results of this study, summarized in Table 2, showed that protein content of legumes was affected by year, the diference for pea and soya beans was significant ($p < 0.05$). Average protein content of twelve varieties of faba beans was not differed significantly, because reaction of each variety on environmental factors was genetically affected due to different ripening times. Differences in protein content of legumes by year can be explained by different amounts of precipitation and air temperature from year to year. Average daily air temperature and cumulative solar radiation during seed filling are especially important for soy ripening. Carrera et al. (2011) also concluded that the environment was the most important source of variation for all traits of soya beans, followed by the genotype x environment interaction.

To characterize potential of varieties grown in same climatic conditions the protein content of different varieties of legumes grown in Latvia was reflected in Fig. 1.

The results of protein summarized in Fig. 1 are in line with other scientific investigations where mentioned that peas and beans are on the lower side of the range with 17–20% proteins while soybeans are on the higher range with 38–45% protein (Maphosa & Jideani, 2017) with the remark that protein content of evaluated varieties was higher than 20%. The results of this five-year study showed that the highest protein content determined in samples of pea variety 'Almara' 26.3 ± 2.2%, but lowest protein content in variety 'Selga'. Most bean varieties evaluated in this study demonstrated average protein content 25–26%. Varieties of faba beans with highest potential to form protein in seeds were 'Jogeva' with average protein content 29.9 ± 2.5%, 'Lielplatone' - 28.0 ± 2.7% and 'Julia' - 27.1 ± 2.6%.

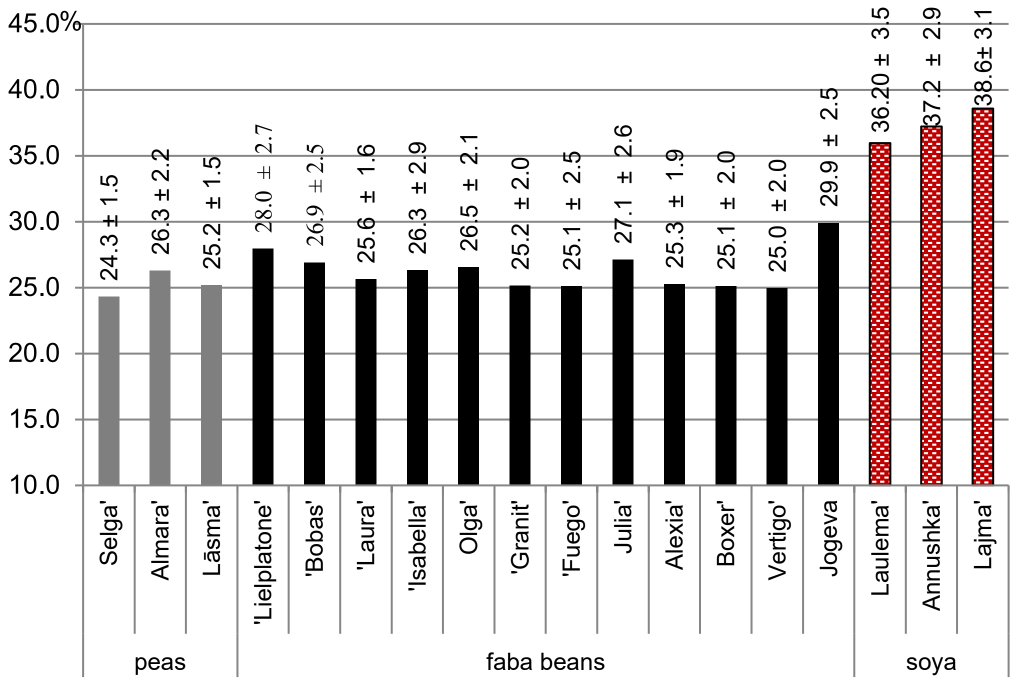

Figure 1. Comparison of protein content of pea, faba beans and soya varieties grown in Stende.

The protein content in samples of soya variety 'Lajma' - 38.6% determined higher than in samples of variety 'Laulema' - 36.2% ($p < 0.05$).

Protein content is not the main indicator of nutrition value of food, more important is composition of amino acids. The analyzed levels of essential amino acids were not always directly related to the protein concentrations of the samples (Goldflus, 2006). Comparison of essential amino acids of pea, beans and soya by years 2014 and 2015 is shown in Fig. 2.

The results of this study showed that content of all amino acids determined higher in the year 2014, especially different were content of Val, Ile, Leu, Phe an Lys in pea and faba bean samples and content of Met, Phe, His and Lys in soya samples. The predominant essential amino acids were leucine, lysine, phenylalanine and valine in all investigated legumes. The results of this study confirms that pulses are low in the essential sulphur containing amino acids - methionine and cysteine (Maphosa & Jideani, 2017; Margier et al., 2018). Fig. 2 shows that content of methionine in peas and faba beans was determined from 3.3 g kg^{-1} to 3.6 g kg^{-1} and the content of methione in soya beans varied from 7.8 g kg^{-1} to 8.2 g kg^{-1}.

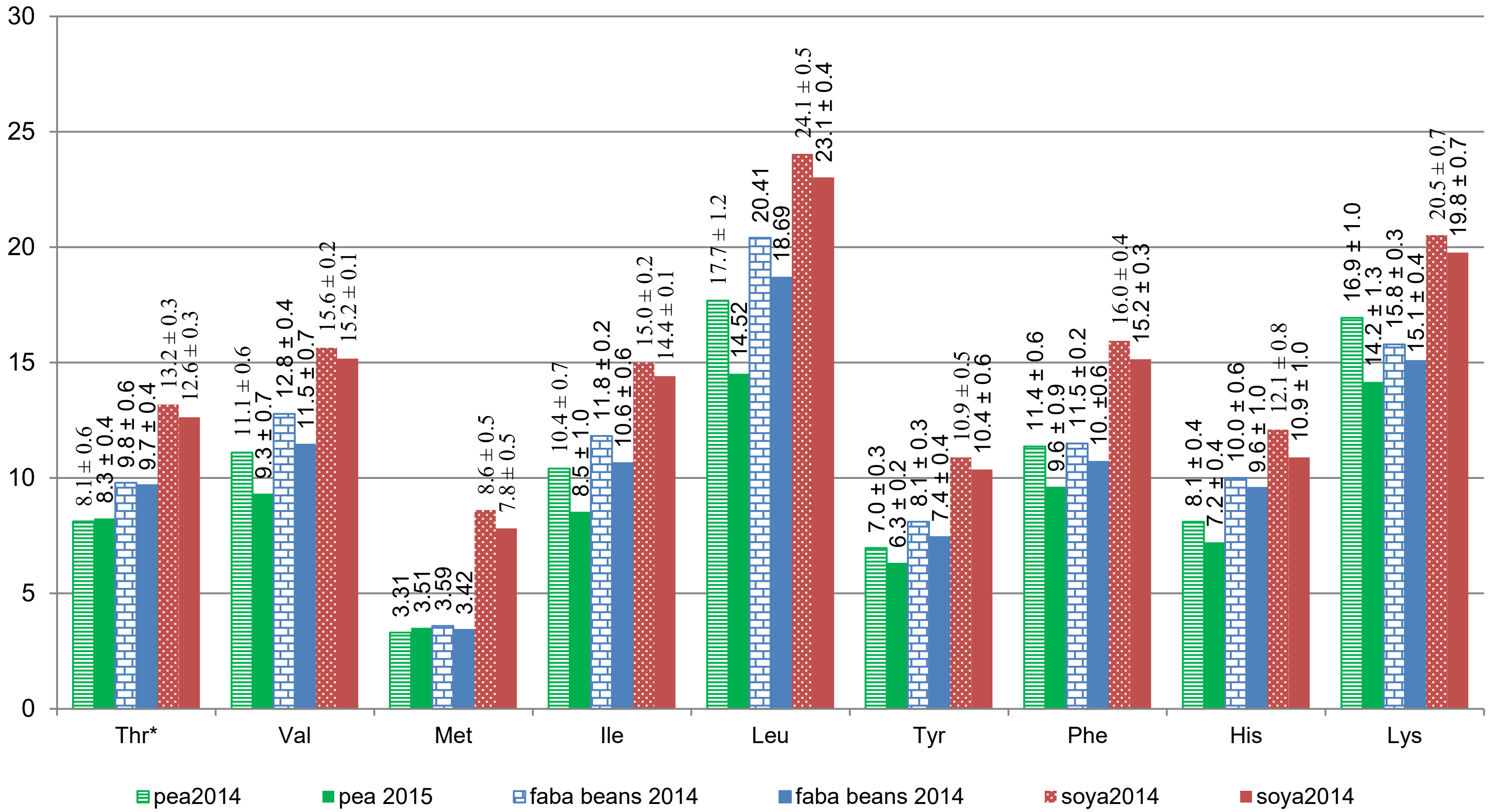

Figure 2. Comparison of essential amino acids content of pea, faba beans and soya in 2014 and 2015 years, g kg^{-1}.

The results of this study showed that content of all amino acids determined higher in The results of this study are in line with other, where evaluated amino acid composition of field beans and mentioned that content of methionine was 0.22 ± 0.01 g 100 g^{-1} content of lysine 1.65 ± 0.01 g 100 g^{-1} or content of leucine was 2.03 ± 0.01 g 100 g^{-1} (Strauta, 2017). Diaz et al. (2006) reported that, content of leucine, lysine, phenylalanine and valine in pea seeds was 14.1 g kg^{-1}; 13.0 g kg^{-1}; 9.5 g kg^{-1} and 9.1 g kg^{-1} respectively while coresponding values of amino acids in faba beans was higher - 18.8 g kg^{-1}; 15.9 g kg^{-1}; 10.9 g kg^{-1} and 12.2 g kg^{-1} respectively.

The content of methionine, phenylalanine and lysine determined in soya samples are significantly higher than content of these amino acids in pea or faba beans samples. The results of this study showed that content of methionine in soya beans was determined from 7.8 g kg^{-1} to 8.2 g kg^{-1}, phenylalanine from 15.2 g kg^{-1} to 15.9 g kg^{-1} and lysine 19.8 g kg^{-1} to 20.5 g kg^{-1}. Diaz et al. (2006) reported that the content of methionine, phenylalanine and lysine in soya meal was 6.5 g kg^{-1}, 23.5 g kg^{-1} and 28.4 g kg^{-1} respectively.

Several factors contribute to limited use of legumes - low yields, poor seed availability, anti-nutrients, their association with bloating and flatulence and their hard-to-cook feature. The development of new legume products could lead to a higher demand of legumes and to increase the production of these legumes by local farmers.

High-temperature short-time extrusion technology (HTST) has become popular in preparing breakfast cereals or snacks of starchy base products like pea and beans.). The plant protein trend has promped innovation in meat substitutes and more than two-thirds of all products included legume ingredients such as adzuki and black beans, chikpeas and lentils with products containin between 9% and 65% legume ingredients (Curtain & Grafenauer, 2019).

Extruded pea flakes for plant-based products manufacturing was prepared. The composition of untreated pea and extruded pea flakes are showed in Table 3.

Table 3. Composition and nutrition value of extruded pea flakes

Nutrients	Untreated	Extruded	Difference*
Protein, %	17.8	17.1 ± 0.2	NS
Fat, %	1.39	1.50 ± 0.1	NS
Starch, %	67.3	67.2 ± 1.5	NS
Dietary fibre, %	8.4	8.0 ± 0.5	NS

*NS – insignificant ($p > 0.05$).

The results of untreated pea and extruded pea flakes summarized in Table 3 are in line with other scientific investigations made on the extrusion of the faba beans and peas - protein and starch are not lost in the extrusion process. In the other studies about extrusion of legumes mentioned that, the protein content of untreated grey pea flour - 26.1 g 100 g^{-1} and extruded pea - 26.9 g 100 g^{-1} was not differed significantly (Strauta, 2017), but in the faba bean samples protein content decreased from 32.5 ± 0.7 g 100 g^{-1} before extrusion to 31.5 ± 0.5 g 100 g^{-1}after extrusion (Strauta & Muizniece-Brasava, 2016) or increased from 232.2 ± 2.0 g kg^{-1} before extrusion to 272.0 ± 3.1 g kg^{-1} after extrusion (Kudlinskiene et al., 2020), but differences were evaluated as insignificant.

World Health Organization recommended daily protein intake is 45 g for an average 60 kg healthy adult female, and 56 g for an average 75 kg male (WHO, 2007). The results of study showed that with 100 g of extruded pea flakes is possible provide about 1/3 of daily protein need. Vegetarians and vegans may need to eat 10–20% more protein than recommended in order to compensate for the lower digestibility of plant-based protein (Petrusan, 2016).

The nutritional value of proteins may differ substantially depending on their amino acid composition and digestibility. Comparison of essential amino acids profile of the extruded pea flakes with recommendations of World Health Organization reflected in Fig. 3.

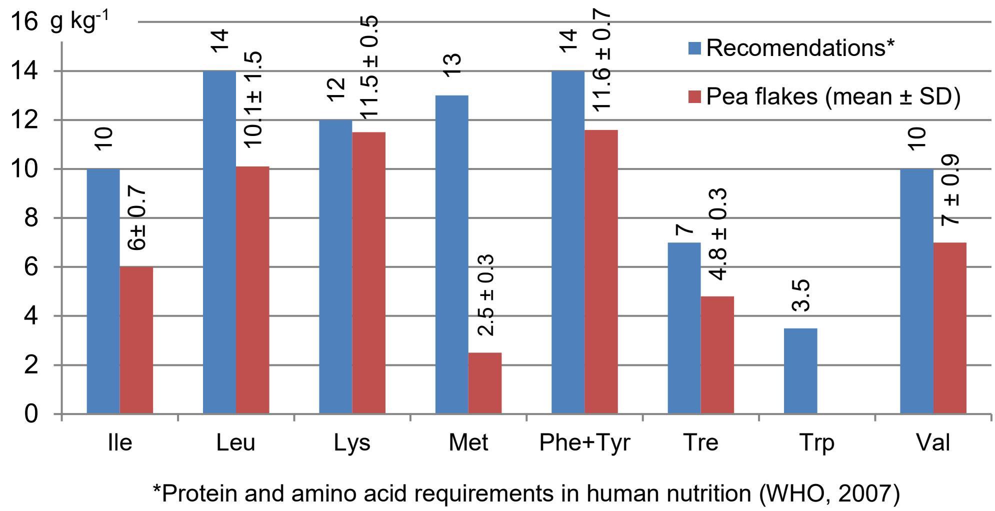

Figure 3. Composition of essential amino acids of extruded pea flakes.

The composition of essential amino acids of extruded pea flakes (Fig. 3.) showed high content of lysine - 11.5 ± 0.5 g kg^{-1}, leucine 10.1 ± 1.5 g kg^{-1} and phenylalanine 6.8 ± 1.0 g kg^{-1} its are close to recommended amount. The results of this study confirms that like other legumes pea flakes are low in the essential sulphur containing amino acid methionine. The content of methionine determined in pea flakes was 2.5 ± 0.3 g kg^{-1}. The composition of amino acids, including content of predominant amino acids lysine, leucine and also methionine of this study were in line with results for extruded grey pea reported by Strauta (2017) - 1.75 ± 0.01 g 100 g^{-1}, 1.76 ± 0.01 g 100 g^{-1} and 0.22 ± 0.01 g 100 g^{-1} respectively. Kudlinskiene et al. (2020) reported no changes in the profile of amino acids of the extruded faba beans, except for the amounts of lysine and histidine. The content of lysine decreased from 16.1 g kg^{-1} in raw material to 15.1 g kg^{-1} in the extruded faba beans, content of histidine decreased from 12.3 g kg^{-1} to 9.8 g kg^{-1} respectively (Kudlinskiene et al., 2020).

When evaluating the extruded product from the point of view of a meat substitute, must be said that protein content (17.1%) of pea flakes was lower, but the sum of essential amio acids (58.2 g kg^{-1}) and contents of lysine (11.5 ± 0.5 g kg^{-1}), leucine (10.1 ± 1.5 g kg^{-1}) or methionine (2.5 ± 0.3) were higher than in the game meat, where corresponding values were - 22.21–23.59%; 27.1–45.7 g kg^{-1}; 5.0–9.5 g kg^{-1}; 5.4–9.0 g kg^{-1}; 1.6–2.5 g kg^{-1} respectively (Strazdina et al., 2011). This comparison is only an insight that encouridges more analysis of the use of peas as a meat substitute.

Since cereals are high in sulfurcontaining amino acids and low in lysine (high in legumes) (Maphosa & Jideani, 2017) for nutritional balance, legumes and cereals are to be consumed in the ratio 35:65, because complemented each other in terms of protein.

CONCLUSIONS

The pea, faba beans and soya grown in Latvia as a raw material for food production has average protein content of five years 24.37 ± 2.2%, 28.0 ± 1.5% and 38.8 ± 2.7% respectively. No difference of protein content of legumes was observed between organic and conventional growing systems.

The percentage of essential amino acids in total amino acids for pea, faba bean and soya determined 34–38%, 57–59% and 62–64% respectively. The soya seeds grown in Latvia are suitable for high quality food production, in addition, procesors are provided with GMO free raw material. Average protein content of soya grown in Stende was 38.1 ± 2.7%, average content of essential amino acids - 122.8 ± 4.2 g kg^{-1}.

The results of extruded pea flakes confirms that protein and starch are not lost in the extrusion process, the protein content of pea flakes was 17.1 ± 0.2%. The composition of essential amino acids of extruded pea flakes showed high content of lysine - 11.5 ± 0.5 g kg^{-1}, leucine 10.1 ± 1.5 g kg^{-1} and phenylalanine 6.8 ± 1.0 g kg^{-1} its are close to recommended amount. There is possibility to produce extruded products using legumes as a raw material of local origin which could be used for high-value plant-based gluten-free protein products production.

ACKNOWLEDGEMENTS. Latvia Ministry of Agriculture is kindly acknowledged to support the study (2013–2018). Data regarding extruded peas conducted by the Milzu! Ltd. with the support from the European Regional Development Fund within the framework of the project 'Latvian Food Industry Competence Centre' in accordance with the contract No. 1.2.1.1/18/A/002 between the Latvian food competence centre Ltd. and the Central Finance and Contracting Agency, concluded on 8th of May, 2019.

REFERENCES

Alghamdi, S.S. 2009. Chemical Composition of Faba Bean (Vicia faba L.) Genotypes under Various Water Regimes. *Pakistan Journal of Nutrition* **8**(4), 477–482.

Carrera, C.S., Reynoso, C.M., Funes, G.J., Martínez, M.J., Dardanelli, J. & Resnik, S.L. 2011. Amino acid composition of soybean seeds as affected by climatic variables *Pesquisa. Agropecuaria Brasileira* **46**(12), 1579–1587.

Curtain, F. & Grafenauer S. 2019. Plant-Based meat substitutes in the flexitarian age: an audit of products on supermarket shelves. *Nutrients* **11**(11), 2603.

Degola, L., Sterna, V., Jansons, I. & Zute, S. 2019. The nutrition value of soybeans grown in Latvia for pig feeding. *Agronomy Research* **17**(5), 1874–1880.

Diaz, D., Morlacchini, M., Masoero, F., Moschini, M., Fusconi, G. & Piva, G. 2006. Pea seeds (*Pisum sativum*), faba beans (*Vicia faba* var.minor) and lupin seeds (*lupines albus* var.multitalia) as protein sources in broiler diets: effect of extrusion on growth performance. *Italian Journal of Animal Science* **5**, 45–53.

Global legumes market 2019–2023, 2019. Acessed 30.04.2020.
https://www.researchandmarkets.com/reports/4749653/global-legumes-market-2019-2023

Goldflus, F.I., Ceccantini, M.I.I. & Santos, W.I.I. 2006. Amino acid content of soybean samples collected in different Brazilian states - harvest 2003/2004. *Brazilian Journal of Poultry Science* **8**(2). Acessed 28.01.2019. http://dx.doi.org/10.1590/S1516-635X2006000200006

Grieshop, C.M. & Fahey, G.C. 2001. Comparison of quality characteristic of soybeans from Brazil, China, and the United States. *Journal of Agricultural and Food Chemistry* **49**(5), 2669–2673.

Hawhorne, W. 2006. Pulses nutritional value and their role in the feed industry. Published by *Pulse Australia* Pty Ltd, pp. 22.

Humer, E, Schwarz, C. & Schedle, K. 2015. Phytate in pig and poultry nutrition. *Animal Physiology Animal Nutrition* **99**(4), 605–625.

Kirse, A. 2017. *Effect of advanced processing methods on the quality of pulse spreads during shelf-life.* PhD Thesis, Latvia University of life Sciences and Technologies, 110.

Kronberga, A., Olle, M., Pereira, M.G., Kokare, A., Konošonoka, I. & Lepse, L. 2016. Evaluation of pea genetic resources for food and feed //*Second International Legume Society Conference*. Legumes for a sustainable World, Troia. Portugal, October 11–14 2016, 95.

Kudlinskienė, I., Gružauskas, R., Daukšienė, A., Dovidaitienė, G., Želvytė, R., Monkevičienė, I., Šližius, E., Urbšienė, D., Racevičiūtė-Stupelienė, A., Ots, M., Kass, M., Žilinskas, H. & Stankevičius, R. 2020. Effect of extrusion on the chemical composition of the faba beans and its influence on Lactation performance of dairy cows. *Zemdirbyste-Agriculture* **107**(1), 87–94.

Lepse, L., Kronberga, A., Olle, M., Kokare, A., KonošonokaI, I., Pereira, M.G. & Bebeli, P. 2016. Evaluation of faba beans genetic resources for food and feed //*Second International Legume Society Conference*. Legumes for a sustainable World, Troia, Portugal, October 11–14, 2016, 93.

Maphosa, Y. & Jideani, V. 2017. The role of legumes in human nutrition In Functional food - improve health though adequate food (Hueda ed), pp. 103–121.

Margier, M., Georgé, S., Hafnaoui, N., Remond, D., Nowicki, M., Du Chaffaut, L., Amiot, M.J. & Reboul, E. 2018. Nutritional composition and bioactive content of legumes: Characterization of pulses frequently consumed in France and effect of the cooking method. *Nutrients* **10**(11), 1668 https://dx.doi.org/10.3390%2Fnu10111668

Multari, S., Stewart, D. & Russell, W.R. 2015. Potential of fava bean as future protein supply to partially replace meat intake in the human diet. *Food Science and Food safety* **14**(5), 511–522. doi: 10.1111/1541-4337.12146

Petrusán, J.I., Rawel, H. & Huschek, G. 2016. Protein–rich vegetal sources and trends in human nutrition: A review. *Current Topics Peptide & Protein Research* **17**, 1–19.

Pasqualone, A., Costantini, M., Coldea, T.E., Summo, C. 2020. Use of legumes in Extrusion: A Review. *Foods* **9**(7), 958 https://www.mdpi.com/2304-8158/9/7/958

Rebello, C.J., Greenway, F.L. & Finley, J.W. 2014. A review of the nutritional value of legumes and their effects on obesity and its related co-morbidities. *Obesity Reviews* **15**(5), 392–407.

Strauta, L. & Muizniece-Brasava, S. 2016. The characteristic of extruded faba beans (*Vicia faba* L.). *Rural Sustainability Research* **36**(331), 42–48.

Strauta, L., Muizniece-Brasava, S. & Gedrovica, I. 2016. Physical and chemical properties of extruded pea product. *Agronomy Research* **14**(S2), 1467–1474.

Strauta, L. 2017. *The use of legumes in the production of extruded food porducts.* PhD Thesis, Latvia University of life Sciences and Technologies, 146 pp.

Strazdina, V., Jemeljanovs, A., Sterna, V. & Vjazevica V. 2011. Evaluation of protein composition of game meat in Latvian farms and wildlife. *Agronomy Research* **9**(Special issue II) 469–472.

Toews, R. & Wang, N. 2013. Physicochemical and functional properties of protein concentrate from pulses. *Food Research International* **52**, 445–451.

USDA 2018. United States Department of Agriculture Food Composition Databases https://www.nal.usda.gov/fnic/databases. Acessed 30.04.2020.

WHO/FAO/UNU, 2007. Protein and amino acid requirements in human nutrition, Report of a Joint WHO/FAO/UNU Expert Consultation, *World Health Organization Technical Report Series* **935**, Geneva.

Agronomy Research **18**(4), 2613–2626, 2020
https://doi.org/10.15159/AR.20.181

Agroecological substantiation of *Medicago sativa* cultivation technology

N. Telekalo* and M. Melnyk

Vinnytsia National Agrarian University, Faculty of Agronomy and Forestry, Soniachna street 3, UA21008 Vinnytsia, Ukraine
*Correspondence: nataliiatelekalo@gmail.com

Abstract. *Medicago sativa* is one of the most productive legumes, which provides high protein production. Application of the biostimulant and microfertilizers is quite relevant and effective. Theoretically substantiates and presents ways to solve the scientific problem of formation of *Medicago sativa* productivity and the impact on them of seed treatment and foliar nutrition, taking into account the conditions of the Forest-Steppe right bankof Ukraine. The research was conducted in the research field of Vinnytsia National Agrarian University in the village of Agronomichne, Vinnytsia district during 2016–2018. Sinyukha variety was sown (2010). There has been established that the use of pre-sowing treatment of seeds and crops of *Medicago sativa* with biostimulant and microfertilizer improves the conditions of growth and development of the crop and increases individual productivity. On the researches it is established that fodder productivity of *Medicago sativa* sowing is provided by application of biostimulators of growth and microfertilizers on crops, genetic potential the culture realized as much as possible on the 2nd year of cultivation. The effect of growth stimulants on *Medicago sativa* productivity was defined and the optimal combination of macro- and microelements in modern complex fertilizers was determined, which contributes to the maximum possible yield of *Medicago sativa* green mass. New technological regulations for the use of bioorganic preparations and components in the technological scheme of *Medicago sativa* cultivation have been developed. It was found that on average for three years of vegetation of *Medicago sativa* sown on gray forest soils in the Forest-Steppe Right Bank, the highest yield of seeds and green mass provides the option of treatment with biostimulator Saprogum® and microfertilizer Wuxal®. Creating optimal conditions for mineral nutrition for *Medicago sativa* plants through the use of bacterial fertilizers and foliar nutrition contributed not only to the formation of high grain yields, but also significantly improved biochemical parameters and, consequently, increased crude protein content in grain, which is important for solving the problem of vegetable protein and balancing the diets of farm animals. The research results are aimed at solving current problems of technological renewal and development of agro-industrial complex on the basis of development of bioorganic models of varietal technology of *Medicago sativa* cultivation with orientation at the level of adequate arable productivity and climate fertility.

Key words: *Medicago sativa*, technology, cultivation, yield, seed quality.

INTRODUCTION

Medicago sativa is one of the most productive and valuable forage crops that are able to help in most regions to address the problem of eliminating plant protein in the diet of animals. An advantage of the use of leguminous perennial dicotyledon plants is their environmental, which is determined by the nitrogen-fixing ability and the enrichment of soil organic matter formed from the root and stem residues (Antoniou Chrystalla et al., 2020; Cen Huifang et al., 2020; Martinez-Hidalgo Pilar et al., 2020; Rezaeian Mohammad et al., 2020). After *Medicago sativa* in the second year of growing in the soil layer 0–20 cm, the number of water-resistant structural units was 41.5%, while in areas where dicotyledon plants were not grown - only 29.8% (Lemus Ramirez et al., 2020; Tucak Marijana et al., 2020). Leguminous perennial dicotyledon plants provide environmentally friendly production, and the agrophytocenoses created by them become an important component of agro-landscapes that provide environmental cleanliness, support human health and safety (Li Danqi et al., 2020; Seddighfar Masoud et al., 2020).

Despite the convincing forage value of *Medicago sativa*, its cultivation in the Forest-Steppe zone of Ukraine is limited. The main reasons for this are the decline of animal husbandry and the transition to monotonous forage, the acidification of soils on which *Medicago sativa* significantly reduces its productivity, forage value of the crop and the duration of economic use. The significant reasons for decrease in the sowing area of *Medicago sativa* include extreme weather conditions, lack of seed sources (El-Zaidy Mohamed et al., 2020; Liu Xiuming et al., 2020; Zhao Yaodong et al., 2020).

Given the current realities, when the emphasis is on reducing the cost of growing crops, micro- and nanotechnology, the use of growth regulators and microfertilizers, the urgent task of plant growing should be to improve cultivation technology *Medicago sativa* on green mass and seeds at the expense of these factors (Hadidi Milad et al., 2020; Li Haiyun et al., 2020). An important element of modern resource-saving technologies for growing crops is the use of new types of fertilizers and biological products - plant growth regulators, liquid complex fertilizers and bacterial enhancersthe efficiency of the use of mineral fertilizers, improving plant nutrition and yield (Cao S. et al., 2020; Wang Jing et al., 2020).The use of these fertilizers and preparations can significantly reduce the volume of application of traditional mineral fertilizers, which significantly reduces the loss of plant nutrients and makes it impossible to pollute the environment (Jiang Peng et al., 2019; Liatukiene Aurelija et al., 2020; Wassie Misganaw et al., 2020).

In the research papers, there is enough information about the complex researches studied the mechanism of the physiological action of growth regulators, both during the treatment of seeds and for foliar nutrition. Plant growth regulators affect growth processes, cause changes in the assimilation apparatus, photosynthesis and carbohydrate metabolism, which improves crop yields (El Husseini, 2019; Xu Hongyu et al., 2020a; Xu Hongyu et al., 2020b). The growing needs of modern agricultural production determine the need to find new ways and methods to improve the crop and its quality (Palamarchuk et al., 2018; Palamarchuk & Telekalo, 2018; Mazur et al., 2018; Mazur et al., 2019; Benabderrahim Mohamed Ali et al., 2020; Sezmis Gurkan & Gursoy Esra, 2020; Yesilayer Nihat et al., 2020). Plant growth regulators are an important component of modern plant growing technologies. Interest in this group of compounds is due to a wide range of their effect on plants, the opportunity is directed to regulate the individual stages of growth and development to mobilize the potential of the plant organism, and accordingly - to enhance yields and quality of agricultural products (Garriga et al., 2020; Min Xueyang et al., 2020). In addition to being used purely, growth regulators can also be used in combination with micro- and macro-elements in foliar nutrition, which is especially important in the critical phases of plant development. Therefore, foliar nutrition during this period has a significant effect, plant viability increases during storage after harvesting, creates better conditions for fertilization and seed formation (Hou Lifeng et al., 2020). However, all of these drugs have been researched mainly in field crops, and for *Medicago sativa*, such researches are practically absent. This requires a detailed study of the application of such environmental measures to improve the productivity of this leguminous perennial plant (Chen Tao et al., 2020; Mbarki Sonia et al., 2020).

The purpose of paper is to research into the efficiency of introduction of biological elements of technology of growing *Medicago sativa*, which involves the use of growth biostimulant and microfertilizer to increase seed productivity and vegetative mass, improve quality of sowing indicators of seeds and chemical composition of green fodder.

MATERIALS AND METHODS

Field experiments were conducted at the experimental field of Vinnytsia National Agrarian University in the village of Ahronomichne Vinnytsia region during 2016–2018. Soils are grey mid-loamy forest. The humus content in the arable layer is 1.85%. The reaction of the soil solution of acidic is pH 5.4. Hydrolytic acidity ranges from 3.5–3.8 mg-eq 100 g^{-1} soil, absorption capacity - 30.7–32.5 mg-eq 100 g^{-1} soil. These soils contain 3.4–5.4 mg 100 g^{-1} of soil available to nitrogen plants, 10–12 mg 100 g^{-1} of mobile phosphorus and 12–14 mg 100 g^{-1} of potassium exchange. Low humus content and the use of organic and mineral colloids from the arable layer do not contribute to the formation of an agronomically valuable structure on these soils.

The investigations were focused on the growth, development and formation of seed yield and green mass and forage productivity of *Medicago sativa* of the Sinyukha variety with the use of new growth biostimulants - Saprogum® and microfertilizers - Wuxal®. The treatment of seeds of *Medicago sativa* growth biostimulant Saprogum® was carried out at a dose of 7 mL L^{-1} of water. The cultivation of *Medicago sativa* Saprogum® growth biostimulant was carried out at a rate of 2.1 L ha^{-1} at a water flow of 300 L ha^{-1}. On the day of sowing, *Medicago sativa* seeds were treated growth biostimulants Saprogum® using PKC-20 Super. Foliar nutrition of *Medicago sativa* microfertilizer Wuxal® was performed at a rate of 3 L ha^{-1}. For control, an option is adopted without biostimulant treatment and without foliar nutrition the microfertilizer.

The acreage of the plot is 30 m², the accounting area - 25 m². Replication in the experiments was 4 times. The sites were located by the method of randomized blocks. Accounting for seed productivity of *Medicago sativa* plants was carried out following with the Methodology of examination of plant varieties. The accounting of the harvest of green mass was carried out by the method of continuous mowing of the grass with the accounting area and weighing. Laboratory germination of seeds of *Medicago sativa* was determined in four repetitions of 100 seeds in Petri dishes on filter paper at a germination temperature of 20 °C. The germination energy of seeds of *Medicago sativa* was determined on the third day of laying the seeds for germination.

Germination of *Medicago sativa* seeds in the laboratory began on the 2nd day after laying for germination and ended on the 7th day. The highest germination energy on the 3rd day after laying the seeds for germination was observed in *Medicago sativa* sowing - 65%. The weight of thousands of seeds was determined by weighing in four repetitions. Determination of biochemical indicators of quality of green fodder was carried out based on the standard methodology of general zootechnical analysis of forages in the certified laboratory of the Institute of feed and agriculture of Podillya NAAS. The solids content was determined by thermostatic-weight method, total nitrogen and crude protein content by Kiel'dalia method, crude fat by Rushkovs'kyi method by the amount of fat-free residue, crude fiber content was determined by Henneberg and Shtoman in the CINAO modification, crude ash - dry ash content, non-nitrogenous extractives (NEC) content - by calculation. Statistical analysis of the experimental data was carried out using the computer program STATICA - 6. Validity of the difference of the experimental data regarding the control was determined using Student's t-criterion.

Saprogum® is a humic preparation made by dispersing the deposits of freshwater lakes (sapropel). Highly humus liquid biostimulator, the main active ingredient of which is physiologically active salts of humic acids, which are easily and quickly absorbed by plants and, as a result, stimulate their growth and development and improve product quality. Agrochemical characteristics of the humic biostimulant Saprogum® are given in Table 1.

Table 1. Agrochemical composition of the biostimulant Saprogum® (on dry matter)

Acidity (pH)	10.0
Total nitrogen,%	1.3
Total phosphorus,%	0.6
Total potassium,%	11.7
Total humic acid carbon,%	10.0
Total humic acid,%	2.0
Copper, mg L^{-1}	6.2
Manganese, mg L^{-1}	100.0
Zinc, mg L^{-1}	2.4

The main active substance of the preparation is physiologically active salts of humic acids. The humic acids of sapropels are in the readily available form (60–80%). Biochemical fractions of sapropels are restored, and therefore have a more effective stimulating effect on plant photosynthesis. Associations of molecules have the smallest size and small molecular weight, which contributes to their active and unobstructed penetration into the roots and leaflets of plants, as a result, stimulate their growth and development and improve product quality.

The preparation is used as a working solution, which is prepared by diluting the initial concentrate with water to obtain the desired concentration of humic acid salts and neutral pH of the solution. Nutrition is carried out in the morning, evening or on cloudy days to prevent burns and intense evaporation of the solution from the leaf surface.

Wuxal® is a complex fertilizer used for foliar fertilization, which provides additional nutrition for all crops to prevent or control the basic nutrients, as well as deficiency of boron and zinc, to support plant growth processes under physiological stress. Wuxal® is great for use on many crops in the early stages of development, when the young root system is not yet able to fully provide the plant with full nutrition, optimizing nutrition, Wuxal® also provides growth, development of plants and their resistance to diseases (Table 2).

Table 2. Agrochemical composition of the microfertilizer Wuxal®

Composition, g L^{-1}	N	P_2O_5	K_2O	SO_3	B	Cu	Fe	Mn	Co	Zn	Mo
Wuxal®	160	160	120	14.0	10	0.21	0.44	0.37	0.008	10	0.028

Benefits of the preparation are excellent buffering properties - at a concentration of 0.2% (200 mL per 100 L of working solution) neutralizes the pH to a neutral level (pH about 7). Compatible with most pesticides and optimizes their action. It provides excellent coverage, adhesion and penetration into the plant. The preparation has well-balanced composition of macronutrients for crops. Suitable for all crops in all climatic zones with high demand for B and Zn. Over-chelating reduces the hardness of water to prepare the working solution.

RESULTS AND DISCUSSION

Productivity of *Medicago sativa* sowing provides the use of growth stimulants and microfertilizers on crops, the genetic potential of the culture is maximally realized in the 2nd year of cultivation, with a long general growing season of 4 years. On average, in the second, fourth year of vegetation, the weight of seeds from one plant of *Medicago sativa*, without treatment with plant growth biostimulant and microfertilizers, was 0.89 g (Table 3).

Table 3. Individual seed productivity of plants of *Medicago sativa* and seed yield depending on the treatment with biostimulant and microfertilizers (average for 2–4 years of vegetation)

Seed treatment	Duration and combination of growth biostimulant and microfertilizer application	Weight of seeds from 1 plant, g	Seed yield, t ha^{-1}
Without treatment seed	Without biostimulant and microfertilizer treatment	0.89 ± 0.02	0.41 ± 0.01
Seed treatment with growth biostimulant Saprogum® (background)	Background + Saprogum® sowing in branching phase	0.93 ± 0.01	0.43 ± 0.02
	Background + Saprogum® sowing in budding phase	0.96 ± 0.02	0.44 ± 0.01
	Background + Saprogum® sowing in branching and budding phase	0.97 ± 0.03	0.44 ± 0.02
	Background + foliar nutrition of Wuxal® sowing in budding phase	0.96 ± 0.02	0.44 ± 0.01
	Background + sowing treatment with growth biostimulant Saprogum® in the branching and budding phase + foliar nutrition in the budding phase with microfertilizer Wuxal®	1.00 ± 0.03	0.46 ± 0.02

$LSD_{0.5}$: A-0.010; B-0.010; AB-0.020.
2016 $LSD_{0.5}$ t ha^{-1}: A-0.010; B-0.010; AB-0.10. 2017 $LSD_{0.5}$ t ha^{-1}: A-0.008; B-0.009; AB-0.16.
2018 $LSD_{0.5}$ t ha^{-1}: A-0.012; B-0.011; AB-0.24.

Note: A – Seed treatment; B – Duration and combination of growth biostimulant and microfertilizer application.

On the variant of sowing treatment with the growth biostimulant Saprogum® in the branching phase, the weight of seeds from one plant was 4.3% higher than on the control and was 0.93 g. When using the growth biostimulant Saprogum® in the budding phase, the yield of seeds from one plant was 0.96 g, which is 7.2% more than in the variant without sowing treatment with growth biostimulant. A similar mass of seeds from one plant was obtained on the variant of sowing by microfertilizer Wuxal® in the budding phase.

Sowing treatment with the growth biostimulant Saprogum® in the branching and budding phase resulted in 0.97 g of seeds being obtained from one plant, which is 8.2% more than the variant without sowing. The highest yield of seeds from one plant was recorded on the variant of sowing treatment with the growth biostimulant Saprogum® in the branching and budding phase by the use of fertilizing the sowing in the budding phase with Wuxal® microfertilizer - 1.0 g, which is 11.0% more than in the variant without sowing treatment with biostimulant and microfertilizers, which is significant at the 5% level of significance. The use of Saprogum® gives a significant increase in seed yield by the value of the average deviation ($LSD_{0.5}$ factor A = 0.010 t ha^{-1}). The application of Wuxal® is significant at the 5% level of significance ($LSD_{0.5}$ factor B = 0.010 t ha^{-1}). Monitoring the productivity of seeds of *Medicago sativa*, depending on the sowing treatment with growth biostimulants and microfertilizers showed that 0.41 t ha^{-1} of seed was harvested without treatment. Sowing treatment with the Saprogum® growth biostimulant during the branching phase led to a seed yield increase of 0.02 t ha^{-1} and a yield of 0.43 t ha^{-1}. Saprogum® in the branching phase, budding phase, dual application of the growth biostimulant in the branching and budding phase, and when treating microfertilizer sowing Wuxal® provided in the budding phaseyield increase by 0.03 t ha^{-1} to 0.44 t ha^{-1}.

The highest seed yield was ensured by the Saprogum® growth stimulation variant in the branching and budding phase by the use of fertilizing the sowing in the Wuxal® microfertilizer budding phase - 0.46 t ha^{-1}, which is 0.05 t ha^{-1} more than without the application growth biostimulants and microfertilizers.The treatment of sowing of *Medicago sativa* with growth biostimulants and microfertilizers has helped to improve the sowing qualities of seeds, including the mass of thousands of seeds, laboratory seed germination and germination energy.

Sowing treatment with the growth biostimulant Saprogum® in the branching phase led to an increase in the mass of thousands of seeds of *Medicago sativa*, by comparison, by 0.02 g to 1.82 g. Saprogum® sowing in the budding phase contributes to the increase in the mass of thousands of seeds by 0.03 g, double sowing in the branching and budding phase - by 0.04 g the use of microfertilizer Wuxal® in the budding phase helped to increase the mass of thousands of seeds of *Medicago sativa* by 0.03 g, which was equivalent to sowing the Saprogum® growth biostimulants in the budding phase. The highest mass of thousands of seeds is provided by the sowing treatment of the Saprogum® growth biostimulant in the branching and budding phas, and the budding phase - by Wuxal® microfertilizer - 1.85 g, which is 0.05 g more than the variant without sowing treatment, which is significant at the 5% level of significance The application of Saprogum® gives a significant increase in the mass of 1,000 seeds by the value of the average deviation ($LSD_{0.5}$ factor A = 0.015 t ha^{-1}). The application of Wuxal® is significant at the 5% significance level ($LSD_{0.5}$ factor B = 0.009 t ha^{-1}) (Table 4).

Table 4. Sowing qualities of seeds of *Medicago sativa* depending on the treatment with biostimulants and microfertilizers (average for 2–4 years of vegetation)

Seed treatment	Duration and combination of growth biostimulant and microfertilizer application	Weight of 1,000 seeds, g	Laboratory germination of seeds, %	Seed germination energy, %
Without treatment seed	Without biostimulant and microfertilizer treatment	1.80	83	56
Seed treatment with growth biostimulant Saprogum® (background)	Background + Saprogum® sowing in branching phase	1.82	86	58
	Background + Saprogum® sowing in budding phase	1.83	86	59
	Background + Saprogum® sowing in branching and budding phase	1.84	87	62
	Background + foliar nutrition of Wuxal® sowing in budding phase	1.83	86	60
	Background + sowing treatment with growth biostimulant Saprogum® in the branching and budding phase + foliar nutrition in the budding phase with microfertilizer Wuxal®	1.85	89	64

$LSD_{0.5}$: A-0.015; B-0.009; AB-0.015. 2016 $LSD_{0.5}$ g: A-0.011; B-0.009; AB-0.04.
2017 $LSD_{0.5}$ g: A-0.007; B-0.009; AB-0.01. 2018 $LSD_{0.5}$ g: A-0.017; B-0.013; AB-0.03.

Note: A – Seed treatment; B – Duration and combination of growth biostimulant and microfertilizer application.

The magnitude of laboratory germination of seeds of *Medicago sativa* with the introduction of a growth biostimulant Saprogum® and microfertilizers Wuxal® increased by 3–6% and amounted to 86–89%. The lowest increase in laboratory germination of seeds compared to the control was found in the variant of sowing cultivation with biostimulant Saprogum® in the branching phase, and the highest in the treatment of sowing with growth biostimulant Saprogum® in the branching phase and budding by the use of fertilizing the sowing phase of microfertilizer budding Wuxal®.

Foliar feeding of sowing of *Medicago sativa* microfertilizer Wuxal® helped to obtain laboratory germination of seeds similar to the sowing treatment with the growth biostimulant Saprogum® separately in the branching or budding phase.

The germination energy of seeds of *Medicago sativa* increased by 2–8%.The smallest increase in the germination energy of seeds of *Medicago sativa* was observed with the introduction of the plant growth biostimulant Saprogum® in the branching phase, and the highest in the variant of sowing cultivation with the Saprogum® growth factor in the branching phase and budding by the use of fertilization of the sowing in the budding phase with Wuxal® microfertilizer, where the seed germination energy was 64%.

In the year of non-cover sowing of *Medicago sativa* on the variant without introduction of growth biostimulant and microfertilizers the yield of green mass was 32.9 t ha^{-1}. Saprogum® growth biostimulant treatment in the branching phase contributed to a 12.9% increase in the green yield of *Medicago sativa* to 37.8 t ha^{-1}. Saprogum® growth budding in the budding phase contributes 12.7% to a green mass yield of up to 37.7 t ha^{-1}, which is 0.1 t ha^{-1} less than when using the Saprogum® growth branch in the branching phase. Double introduction of the growth biostimulant Saprogum® in the branching and budding phase causes the yield of green mass to increase by 13.1% - up to 37.9 t ha^{-1}, which is 0.1 t ha^{-1} and 0.2 t ha^{-1} more, respectively, than at a single introduction to these phases.

Foliar feeding of microfertilizer sowing Wuxal® in the phase of budding of *Medicago sativa* helps to increase the yield of green mass by 13.1% - to the level of 37.6 t ha^{-1}, which is 0.1 t ha^{-1} less than when introduced into the budding phase of the biostimulant growth of Saprogum®. The highest yield of green mass in the first year of vegetation is provided by the sowing treatment of the Saprogum® growth biostimulant in the branching and budding phase by the use of the fertilization in the sowing phase in the Wuxal® microfertilizer budding phase - 38.2 t ha^{-1}, which is 13.9% more than onversion without biostimulant and microfertilizer treatment, 0.6 t ha^{-1} more than when processing microfertilizer sowing Wuxal® in budding phase, 0.5 t ha^{-1} more than in processing with growth biostimulant Saprogum® in budding phase, 0.4 t ha^{-1} - than attreatment with the same preparation in the branching phase and by 0.3 t ha^{-1} more than in the double treatment of sowing with the growth biostimulant Saprogum® in the branching and budding phase (Table 5).

Table 5. The yield of green mass of alfalfa sowing *Medicago sativa* depending on the treatment with biostimulant and microfertilizers (1–4th year of vegetation), t ha^{-1}

Seed treatment	Duration and combination of growth biostimulant and microfertilizer application	1-st year	2-nd year	3-d year	4-th year	Average for all years
Without treatment seed	Without biostimulant and microfertilizer treatment	32.9 ± 0.3	42.7 ± 0.3	35.7 ± 0.1	25.4 ± 0.2	34.2 ± 0.1
Seed treatment with growth biostimulant Saprogum® (background)	Background + Saprogum® sowing in branching phase	37.8 ± 0.2	49.0 ± 0.1	42.5 ± 0.2	30.8 ± 0.2	40.0 ± 0.2
	Background + Saprogum® sowing in budding phase	37.7 ± 0.4	48.7 ± 0.2	42.4 ± 0.3	30.6 ± 0.1	39.8 ± 0.3
	Background + Saprogum® sowing in branching and budding phase	37.9 ± 0.3	50.0 ± 0.3	42.7 ± 0.3	31.1 ± 0.3	40.4 ± 0.3
	Background + foliar nutrition of Wuxal® sowing in budding phase	37.6 ± 0.2	48.9 ± 0.3	42.6 ± 0.2	30.7 ± 0.3	40.0 ± 0.2
	Background + sowing treatment with growth biostimulant Saprogum® in the branching and budding phase + foliar nutrition in the budding phase with microfertilizer Wuxal®	38.2 ± 0.3	50.8 ± 0.2	43.0 ± 0.2	32.0 ± 0.2	41.0 ± 0.3

$LSD_{0.5}$: A-0.09; B-0.09; AB-0.025. 2016 $LSD_{0.5}$ t/ha^{-1}: A-0.010; B-0.010; AB-0.06.
2017 $LSD_{0.5}$ t/ha^{-1}: A-0.008; B-0.015; AB-0.16. 2018 $LSD_{0.5}$ t/ha^{-1}: A-0.019; B-0.016; AB-0.23

Note: A – Seed treatment; B – Duration and combination of growth biostimulant and microfertilizer application.

In the second year of the growing season, the highest yield of green mass was also provided by the option of sowing treatment with the Saprogum® growth biostimulant in the branching and budding phase by the use of fertilizing the sowing in the budding phase by Wuxal® microfertilizer - 50.8 t ha^{-1}, which is 16.0% more than in the version without the introduction of preparations. Saprogum® cultivation treatment with branching and budding promoted green mass yields of 0.8 t ha^{-1} less than the best option and 14.6% more than the control.

Introduction of the Saprogum® growth biostimulant in the branching phase of *Medicago sativa* yields a green mass yield of 1.8 t ha^{-1} less than with the complex application of the Saprogum® and microfertilizer Wuxal® and 12.9% more than in control.

Foliar planting by microfertilizer Wuxal® in the budding phase provides a 12.7% increase in the green yield of *Medicago sativa* than in the control. Saprogum® growth stimulation treatment in the budding phase contributes to a 12.3% increase in green mass yield compared to control.

In the third year of the growing season, the yield of green mass of *Medicago sativa* decreasesits highest value was observed for sowing treatments with a growth stimulant Saprogum® in the branching and budding phase by the use of fertilizing the sowing phase in the Wuxal® microfertilizer budding phase - 43.0 t ha^{-1}, which is 17.0% more than the control. Saprogum® growth and sapling treatment in the branching and budding phase provides a yield of 0.3 t ha^{-1} less green yield, but 16.4% higher than the control. Processing of sowing by microfertilizer Wuxal® in the budding phase, the growth biostimulant Saprogum® in the branching and budding phase allows to obtain the yield of green mass by 16.2; 16.0 and 15.8% more than controls.

In the fourth year of vegetation, the yield of green mass of *Medicago sativa* with the use of growth biostimulant and microfertilizer was 30.6–32.0 t ha^{-1}, which is 17.0–20.6% higher than on the control. The highest yield of green mass was provided by the variant of sowing cultivation of Saprogum® in the branching and budding phase by the use of fertilizing of the sowing in the budding phase by Wuxal® microfertilizer, and the smallest - processing of sapling by the Saprogum® growth biostimulantthe budding phase.

For an average of four years of vegetation of *Medicago sativa*, the highest yield of green mass provides a variant of sowing with a stimulant of growth of Saprogum® in the branching and budding phase by the use of fertilizing of the sowing in the budding phase Wuxal® microfertilizer - 41.0 t ha^{-1}, which is 16.6% more than on the control. The application of Saprogum® gives a significant increase in the yield of green mass by the value of the average deviation ($LSD_{0.5}$ factor A = 0.09 t ha^{-1}). The application of Wuxal® is significant at the 5% level of significance ($LSD_{0.5}$ factor B = 0.09 t ha^{-1}). The green mass yield of 40.4 t ha^{-1} provided the Saprogum® growth stimulant in the branching and budding phases, which is 0.6 t ha^{-1} less than the best case and 15.3% more than the control. 40.0 t ha^{-1} of green mass yields were provided by Saprogum® growth stimulation options for branching and microfertilizer Wuxal® for budding, which is 14.5% more than the control. The smallest increase in the yield of green mass of *Medicago sativa* provides the introduction of a growth stimulant Saprogum® in the budding phase - 14.1% more than in the version without the use of preparations.

The yield of green mass of *Medicago sativa* of Sinyukha variety is closely correlated with plant density ($r = 0.985$), as well as with height ($r = 0.950$), which is significantly at the 1% level of significance. The dependences we found, presented in the form of regression equations, indicated a significant influence of weather conditions on the yield of green mass of the Sinyukha variety (Table 6).

Table 6. Regression dependence of *Medicago sativa* green mass yield between height, plant density and weather conditions (2–4th year of vegetation)

	Regression equation	R_{MH}	R^2	F	F_T
Yield of green mass (Y), t ha^{-1}	$У = 0.1289X_1 + 17.097$	0.986	0.985	232.35	6.70*
	$У = 0.7679X_2 + 21.258$	0.973	0.950	116.47	
	$У = -6.956 - 0.001X_3 + 0.0094X_4$	0.978	0.956	141.52	

Note: Y – Sinyukha; X_1 – plant density, units m^{-2}; X_2 – plant height, cm; X_3 – the amount of precipitation, mm; X_4 – the sum of active temperatures, °C; Rmn – the coefficient of multiple correlation; R^2 – the coefficient of determination; F is Fisher's criterion; F_t – tabular value of Fisher's criterion; * – reliably at 1% significance level.

The productivity of *Medicago sativa* agrophytocenoses on seeds depends on many factors, but the main one is the presence of productive moisture in the soil during the growing season and providing plants with rainfall in critical periods.

The expected results of research are aimed at increasing the level of realization of fodder varietal potential of perennial grasses, namely *Medicago sativa* sowing, increasing the profitability of its production in combination with environmental and social effects. The dry matter content of the green mass of *Medicago sativa* in the non-medicated version was 19.2%. The introduction of a growth biostimulant Saprogum® and microfertilizers Wuxal ® caused a decrease in the dry matter content by 0.4–1.0%. The smallest decrease in the dry matter content of the green mass of *Medicago sativa* was found on the variant of sowing treatment with the growth biostimulant Saprogum® in the branching phase. The greatest reduction of the dry matter content was found on the variant of sowing treatment with the growth biostimulant Saprogum® in the branching and budding phase by the use of fertilizing the sowing in the budding phase with microfertilizer Wuxal®. Reducing the dry matter content of the green mass of *Medicago sativa* by the introduction of a growth biostimulant and microfertilizer caused by the accumulation of moisture in the vegetative mass, similar to the effect of organic and mineral fertilizers on the accumulation of dry substances (Table 7).

Protein content in the completely dry matter of *Medicago sativa* for the application of preparations was 23.4–24.0%. Protein is a major nutrient in feed, so the higher its content, the greater the value of green mass. The highest protein content was observed in the completely dry matter of *Medicago sativa* from the variant of sowing treatment with the growth biostimulant Saprogum® in the branching and budding phase by the use of fertilizing the sowing in the budding phase of microfertilizer 1.2% more than the control 0.2% less protein content was observed in the Saprogum® stimulant treatment in the branching and budding phase. By 0.3% less - on the variant of foliar fertilization of sowing by microfertilizer Wuxal ® in the budding phase, by 0.4% less - on the variant of sowing treatment with the growth biostimulant Saprogum® in the budding phase and by 0.6% less - on the variant of Saprogum® sowing branching phase.

Table 7. Chemical composition of the green mass of *Medicago sativa* depending on the treatment with stimulants and microfertilizers (average for all years of vegetation), %

Seed treatment	Duration and combination of growth biostimulant and microfertilizer application Without biostimulant and microfertilizer treatment	Dry matter	chemical composition on absolutely dry matter				
			protein	fat	cellulose	ash	NES
Without treatment seed	Background + Saprogum® sowing in branching phase	19.2	22.8	2.2	28.5	9.4	37.1
Seed treatment with growth biostimulant Saprogum® (background)	Background + Saprogum® sowing in budding phase	18.8	23.4	2.2	27.9	9.3	37.2
	Background + Saprogum® sowing in branching and budding phase	18.6	23.6	2.3	28.2	9.4	36.5
	Background + foliar nutrition of Wuxal® sowing in budding phase	18.3	23.8	2.2	28.0	9.5	36.5
	Background + sowing treatment with growth biostimulant Saprogum® in the branching and budding phase + foliar nutrition in the budding phase with microfertilizer Wuxal®	18.6	23.7	2.1	28.0	9.3	36.9
	Duration and combination of growth biostimulant and microfertilizer application	18.2	24.0	2.2	27.8	9.4	36.6
$LSD_{0.05}$		0.52	0.06	0.08	0.08	0.07	0.25

Note: A – Seed treatment; B – Duration and combination of growth biostimulant and microfertilizer application.

The fat content of the completely dry matter of *Medicago sativa* did not depend on the sowing treatment with a stimulant and microfertilizer and was in all variants, including controls, 2.1–2.3 %, which was within the margin of error of the experiment. The fiber content of the variant cultivation of *Medicago sativa* without the introduction of growth biostimulant and microfertilizer was 28.5%. Sowing with preparations reduced the fiber content in the absolutely dry matter by 0.3–0.7%. The lowest fiber content was detected on the Saprogum® growth stimulant in the branching and budding phase by the use of the sowing in the Wuxal® microfertilizer budding phase, and 27.8% and the highest on the Saprogum® sowing variant the budding phase is 28.2%.

The ash content did not depend on the cultivation of crops by growth biostimulants and microfertilizers and amounted to 9.3–9.5%. The content of nitrogen–free extractive substances (NES) in the absolutely dry matter of *Medicago sativa* was 36.5–37.2%. The lowest NES content was detected in the feed of *Medicago sativa* from the cultivation variant of the Saprogum® growth biostimulant in the budding phase, as well as its dual use in the branching and budding phase, and the highest in the variant of Saprogum® sowing in the branching phase.

CONCLUSIONS

The highest yield of seeds from one *Medicago sativa* plant was recorded on the variant of sowing treatment with the growth biostimulant Saprogum® in the branching and budding phase by the use of fertilizing the sowing in the budding phase with Wuxal® microfertilizer - 1.0 g, which is 11.0% more than without biostimulant Saprogum® and Wuxal® foliar nutrition.The highest seed yield of *Medicago sativa* also provided the variant of sowing treatment with the Saprogum® growth biostimulant in the branching and budding phase by the use of the fertilization of the sowing in the budding phase with microfertilizer Wuxal® - 0.46 t ha^{-1}.

The highest mass of thousands of seeds is provided by the sowing treatment of the Saprogum® growth biostimulant during the branching and budding phase by the use of fertilization of the sowing phase by the budding Wuxal® microfertilizer - 1.85 g. For an average of four years of vegetation of *Medicago sativa*, the highest yield of green mass provides a variant of sowing with a biostimulant of growth of Saprogum® in the branching and budding phase by the use of feeding of the sowing in the budding phase Wuxal® microfertilizer - 41.0 t ha^{-1}, which is 16.6% more than on the control than on the control without biostimulant Saprogum® treatment and without foliar nutrition the Wuxal® microfertilizer. The highest protein content was observed in the completely dry matter of *Medicago sativa* from the variant of sowing treatment with the growth biostimulant Saprogum® in the branching and budding phase by the use of fertilizing the sowing in the budding phase of microfertilizer Wuxal® 1.2% more than the control.

REFERENCES

Antoniou Chrystalla, Xenofontos Rafaella & Chatzimichail Giannis, Christou Anastasis, Kashfi Khosrow & Fotopoulos Vasileios. 2020. Exploring the Potential of Nitric Oxide and Hydrogen Sulfide (NOSH)-Releasing Synthetic Compounds as Novel Priming Agents against Drought Stress in *Medicago sativa* Plants. *Biomolecules* **10**(1), 120.

Benabderrahim Mohamed Ali, Guiza Marwa & Haddad Mansour. 2020. Genetic diversity of salt tolerance in tetraploid alfalfa (*Medicago sativa L.*). *Acta physiologiae plantarum* **42**(1), 5.

Cao, S., Liang, Q.W. & Nzabanita, C. 2019. Paraphoma root rot of alfalfa (Medicago sativa) in Inner Mongolia, China. *Plant pathology* **69**(2), 231–239.

Cen Huifang, Wang Tingting, Liu Huayue, Tian Danyang & Zhang Yunwei. 2020. Melatonin Application Improves Salt Tolerance of Alfalfa (*Medicago sativa L.*) by Enhancing Antioxidant Capacity. *Plants-basel* **9**(2), 220.

Chen, T., Wang Bo & Power Robert C. 2020. The first archaeobotanical evidence of *Medicago sativa L.* in China: hay fodder for livestock. *Archaeological and anthropological sciences* **12**, 1. doi: 10.1007/s12520-019-00957-7

El Husseini, M.M.M. 2019. Management of the Egyptian alfalfa weevil, *Hypera brunneipennis* (Boheman) (Coleoptera: Curculionidae), in the alfalfa, *Medicago sativa L.,* using the entomopathogenic fungus, *Beauveria bassiana* (Balsamo) Vuillemin. *Egyptian journal of biological pest control* **29**(1), 82.

El-Zaidy Mohamed, Almusalim Abdulrahman & Alsahli Abdulaziz. 2020. Effects of ozone on cell organelles of alfalfa (*Medicago sativa L.*) Seedlings. *Saudi journal of biological sciences* **27**(1), 60–66.

Garriga, M., Ovalle, C. & Espinoza, S. 2020. Use of Vis-NIR reflectance data and regression models to estimate physiological and productivity traits in lucerne (*Medicago sativa*). *Crop & pasture science* **71**(1), 90–100.

Hadidi Milad, Ibarz Albert & Pagan Jordi. 2020. Optimisation and kinetic study of the ultrasonic-assisted extraction of total saponins from alfalfa (*Medicago sativa*) and its bioaccessibility using the response surface methodology. *Food chemistry* **309**, 125786.

Hou Lifeng, Yu Jie & Zhao Lili. (2020). Dark Septate Endophytes Improve the Growth and the Tolerance of *Medicago sativa* and Ammopiptanthus mongolicus Under Cadmium Stress. *Frontiers in microbiology* **10**, 3061.

Jiang, Peng, Shao Jonathan & Nemchinov, Lev G. 2019. Identification of emerging viral genomes in transcriptomic datasets of alfalfa (*Medicago sativa L.*). *Virology journal* **16**(1), 153.

Lemus Ramirez Vicente, Guevara Escobar Aurelio & Garcia Rodriguez Juan Antonio. 2020. Milk production in dairy cows grazing alfalfa (*Medicago sativa*) in the central Mexican highlands. *Revista mexicana de ciencias pecuarias,* **11**(1), 1–18.

Li Danqi, Liu Da & Lv Mengchao. 2020. Isolation of triterpenoid saponins from *Medicago sativa L.* with neuroprotective activities. *Bioorganic & medicinal chemistry letters* **30**(4), 126956.

Li Haiyun, Qiu Yizhi, Yao Tuo, Ma Yachun, Zhang Huirong & Yang Xiaolei. 2020. Effects of PGPR microbial inoculants on the growth and soil properties of *Avena sativa*, *Medicago sativa*, and *Cucumis sativus* seedlings. *Soil & tillage research* **199**, 104577.

Liatukiene Aurelija, Skuodiene Regina & Tomchuk Donata. 2020. Evaluation of agro-biological traits of *Medicago sativa* and M. varia in a Cambisol and Retisol. *Zemdirbyste-agriculture,* **107**(1), 41–48.

Liu Xiuming, Ahmad Naveed & Zhang Jiwei. 2020. Codon-optimized recombinant expression assay for a monomeric 17kda basic fibroblast growth factor (bfgf) in transgenic alfalfa (*Medicago sativa L.):* blueprints towards human therapeutic proteins. *Journal of Botany* **52**(2), 501–507.

Martinez-Hidalgo Pilar, David Flores-Felix Jose & Velazquez Encarna. 2020. High taxonomic diversity of Micromonospora strains isolated from *Medicago sativa* nodules in Western Spain and Australia. *Systematic and applied microbiology* **43**(1), 126043.

Mazur, V.A., Didur, I.M., Pantsyreva, H.V. & Telekalo, N.V. 2018. Energy-economic efficiency of growth of grain-crop cultures in conditions of Right-Bank Forest-Steppe of Ukraine. *Ukrainian Journal of Ecology* **8**(4), 26–33.

Mazur, V.A., Pantsyreva, H.V., Mazur, K.V. & Didur, I.M. 2019. Influence of the assimilation apparatus and productivity of white lupine plants. *Agronomy Research* **17**(1), 206–219.

Mbarki Sonia, Skalicky Milan & Talbi Ons. 2020. Performance of *Medicago sativa* Grown in Clay Soil Favored by Compost or Farmyard Manure to Mitigate Salt Stress. *Agronomy-basel* **10**(1), 94.

Min Xueyang, Jin Xiaoyu & Zhang Zhengshe. 2020. Genome-Wide Identification of NAC Transcription Factor Family and Functional Analysis of the Abiotic Stress-Responsive Genes in *Medicago sativa* L. *Journal of plant growth regulation* **39**, 324–337.

Palamarchuk, V. & Telekalo, N. 2018. The effect of seed size and seeding depth on the components of maize yield structure. *Bulgarian Journal of Agricultural Science* **24**(5), 785–792.

Palamarchuk, V., Honcharuk, I., Honcharuk, T. & Telekalo, N. 2018. Effect of the elements of corn cultivation technology on bioethanol production under conditions of the right-bank forest-steppe of Ukraine. *Ukrainian Journal of Ecology* **8**(3), 47–53.

Rezaeian Mohammad, Moghadam Mahmoud Tohidi & Kiaei Mohammad Mehdi. 2020. The effect of heavy metals on the nutritional value of Alfalfa: comparison of nutrients and heavy metals of Alfalfa (Medicago sativa) in industrial and non-industrial areas. *Toxicological research* **36**(2), 183–193.

Seddighfar Masoud, Mirghazanfari Sayid Mahdi & Dadpay Masoumeh. 2020. Analgesic and anti-inflammatory properties of hydroalcoholic extracts of Malva sylvestris, Carum carvi or Medicago sativa, and their combination in a rat model. *Journal of integrative medicine–jim* **18**(2), 181–188.
Sezmis Gurkan & Gursoy Esra. 2020. Determination of relative feed value, net energy lactation and metabolic energy contents of alfalfa (*Medicago sativa L.*). *Fresenius environmental bulletin* **29**(3), pp.1637–1642.
Tucak Marijana, Cupic Tihomir & Horvat Daniela. 2020. Variation of Phytoestrogen Content and Major Agronomic Traits in Alfalfa (*Medicago sativa L.*) Populations. *Agronomy-basel,* **10**(1), 87. https://doi.org/10.3390/agronomy10010087
Wang Jing, Xu Xing & Ma Dongmei. 2020. Establishment of an efficient alfalfa regeneration system via organogenesis and the co-expression of Arabidopsis SOS genes improves salt tolerance in transgenic alfalfa (*Medicago sativa L.*). *Canadian journal of plant science* **100**(1), 136–139.
Wassie Misganaw, Zhang Weihong & Zhang Qiang (2020). Exogenous salicylic acid ameliorates heat stress-induced damages and improves growth and photosynthetic efficiency in alfalfa (*Medicago sativa L.*). *Ecotoxicology and environmental safety* **191**, 110206.
Xu, Hongyu, L, Zhenyi & Tong Zongyong. 2020a. Metabolomic analyses reveal substances that contribute to the increased freezing tolerance of alfalfa (*Medicago sativa L.*) after continuous water deficit. *Bmc plant biology* **20**(1), 15.
Xu, Hongyu, Tong Zongyong & He, Feng. 2020b. Response of Alfalfa (*Medicago sativa L.*) to Abrupt Chilling as Reflected by Changes in Freezing Tolerance and Soluble Sugars. *Agronomy-basel* **10**(2), 255.
Yesilayer Nihat, Mutlu Gamze & Yildirim Arda. 2020. Effect of nettle (Urtica spp.), marigold (Tagetes erecta), alfalfa (*Medicago sativa*) extracts and synthetic xanthophyll (zeaxanthin) carotenoid supplementations into diets on skin pigmentation and growth parameters of electric yellow cichlid (Labidochromis caeruleus). *Aquaculture* **520**, 734964.
Zhao Yaodong, Ma Wenjing & Wei Xiaohong. 2020. Identification of Exogenous Nitric Oxide-Responsive miRNAs from Alfalfa (*Medicago sativa L.*) under Drought Stress by High-Throughput Sequencing. *Genes* **11**(1), 30.

Agronomy Research **18**(4), 2627–2638, 2020
https://doi.org/10.15159/AR.20.214

Ecological plasticity of buckwheat varieties (*Fagopyrum esculentum Moench.*) of different geographical origin according to productivity

O.V. Tryhub[1], A.V. Bahan[2], S.M. Shakaliy[3,*], Yu.M. Barat[2] and S.O. Yurchenko[2]

[1]Ustymivska Experimental Station of Plant Production of Plant Production Institute nd.a. V.Ya. Yuryev of National Academy of Agrarian Sciences of Ukraine, Ustymivka village, Hlobynskyi district, UA36003 Poltava region, Ukraine
[2]Poltava State Agrarian Academy, Faculty of Agro-Technology and Ecology, Department of Selection, Seed Science and Genetics, 1/3, Skovorody str., UA36003 Poltava, Ukraine
[3]Poltava State Agrarian Academy, Faculty of Agro-Technology and Ecology, Department of Plant Production, 1/3, Skovorody str., UA36003 Poltava, Ukraine
[*]Correspondence: shakaliysveta@gmail.com

Abstract. To determine the ecological plasticity of crop varieties, there are a number of methods that are based on the analysis of the variability of the trait by contrasting years under the conditions. The stability and plasticity of the studied traits of varieties are due to the ability of genetic mechanisms of plants to minimize the consequences of the negative impact of the environment, that is, to resist them. The researches on establishing regularities of manifestation of plasticity, stability and homeostaticity of buckwheat varieties of different ecological and geographical origin were carried out in the conditions of the central part of Ukraine during the period of 2016–2018. The low adaptability of modern buckwheat varieties is a determining factor for low production yields of potentially high-yielding varieties in the sharply contrasting (climatic factors) cultivation conditions. The level of yield (as a complex characteristic) and its main component, the individual productivity of the plant have been determined as the differentiative indicators of modern varieties and new promising breeding material consisting of 35 samples from 5 countries of the world. The analysis of research data has identified a group of varieties (SYN 3/02, Sofiia, Selianochka, Slobozhanka, Yelena, Roksolana, Populiatsiia 7/07, P-330, P-455, P-620, Ametist, Feniks, Ilishevskaia, Batyr and Arno), which have a value as a highly adaptable varietal material for the cultivation conditions and have an increased selective value according to abiotic adaptability indicators and can be used to create a more adaptable material as a potentially more productive as well as more plastic and stable resource for selection.

Key words: buckwheat, yield, plasticity, homeostaticity, stability, breeding value.

INTRODUCTION

Buckwheat is one of the most valuable crops, its importance for humans has recently been substantially redefined, and the areas of application have been greatly expanded (Chrungoo et al., 2016). A number of characteristics affect the value of buckwheat. Grain and plant of this crop contain a complex of compounds that have significant antioxidant properties, essential amino acids and a large vitamin complex (Skrabanja et al., 2004; Harifullina et al., 2010; Jacquemart et al., 2012). Non-waste production and various directions of processed products usage: for nutrition, feed production, pharmacy, as one of the best predecessors in crop rotation, as a fuel with a high heat transfer coefficient, etc are very important for buckwheat products producers (Li et al., 2001; Holasova et al., 2002; Alekseeva et al., 2005). Recently, the environmental aspect of buckwheat production has become very important. High sensitivity of buckwheat plants to most herbicides, even in the residual doses, prompts producers to refuse from toxic chemicals. Their application in buckwheat rotation has been significantly reduced too (Luzhinskaya, 2017; Modern technology, 2018).

The level of world buckwheat production has huge fluctuations over the years, which is associated with the climatic factors and policies of the certain states, macroeconomic and the strategic factors of world buckwheat producers (Kreft, 2001; Zeller, 2001). The final consumers of buckwheat products requires that the producers create products in quantities that can satisfy constant demand and ensure high quality of products (Kalinova et al., 2002; Zhygunov et al., 2016). In turn, in order to obtain certain quantities of buckwheat products of necessary quality, producers want varieties possesing a set of indicators and properties. They are the following: the ability of maximum adaptability to the cultivation conditions, adaptive characteristics, in particular drought resistance and heat resistance, resistance to lodging and simultaneousness of ripening as the factors of variety technological effectiveness (Alekseeva et al., 2005). Scientists from different countries have created varieties capable to satisfy a certain range of requirements, but the issue of abiotic adaptability still remains unsolved (Cawoy, 2006; Fesenko, 2006). A level of yields is an unstable indicator, and plasticity of varieties is low. The constant search for most suitable for practical use varieties is the solution to this problem (Tryhub, 2002; E et al., 2017; Marenych et al., 2019; Muhamedyarova et al., 2020). Such material is the collection ranges, which number more than five thousand samples of different ecological and geographical origin in the whole world (Rufa, 2004; Zhou, 2018). Ukraine has a collection of buckwheat, which consists of varieties and forms of folk selection, breeding varieties, linear material, mutant forms, etc., with a total quantity of more than 2.5 thousand samples originating from more than 30 countries of the world (Tryhub et al., 2018).

Comprehensive assessment of the wide genetic diversity of varieties of different ecological and geographical origin, different types of plants (by ploidy and type of growth) in contrasting environmental conditions allowed to identify genotypes with high levels of adaptive potential.

Factors of ecological plasticity, homeostaticity and stability of varieties are determining indicators of adaptive potential.

The aim of the research was to study the levels of ecological plasticity, homeostaticity and stability of new varieties and possibility to identify these indicators in order to select new varieties (Burdenyuk-Tarasevych et al., 2012).

MATERIALS AND METHODS

The research tasks are the following: to determine the level of productivity and plant individual productivity in varietal material of different ecological and geographical origin; to apply a complex of mathematical and statistical analyzes in order to identify the level of plasticity, homeostaticity and stability of varietal material; to determine the best varieties according to the studied characteristics and recommend them to be used in production and selection studies as a highly adaptive source material.

Thirty-five breeding varieties originating from Ukraine, the Republic of Belarus, the Russian Federation, China and Canada were used for the research. They included the material widely used in production and promising breeding numbers. The researches were carried out at Ustymivska experimental station of plant production in the conditions of the central part of Ukraine (climate is moderate continental with elevated temperatures and unevenly distributed precipitation during the spring-summer period) during 2016–2018. The material was sown by a selection seeder with a row spacing of 45 cm, the seeding rate of 1.8 mln grains per 1 ha, with an area of 15 m^2 in three repetition in the optimal terms - the first decade of May. The mid ripening diploid variety Yelena has been taken as the standard. This variety has increased stability of the yield level and productivity of the plant and high simultaneousness of ripening. In order to obtain a reasonable evaluation of the wide biological diversity of varietal material, diploid and tetraploid varieties of the ordinary and determinate type have been involved in the research. As a differentiating factor for the analysis, the level of grain yield of the experimental samples has been taken, as the resulting indicator of the complex of factors, and its main component is the individual plant productivity in the contrasting environmental conditions. This indicator was determined from a selected sample of 25 plants.

Statistical analysis

The research results have been analyzed in accordance with Eberhart and Rassell methodology (Eberhart & Rassell, 1966), field experiment (with the fundemantals of statistical processing of the research results). Experimental data was also statistically analyzed for the Analysis of variation (ANOVA) and least significant difference (*LSD*) with the determination of the limiting environmental factors X_{opt} and X_{lim}) and the variability level (*R* and *V*), as the characteristics of plasticity, homeostaticity (*Hom*1 and *Hom*2), stability (σ) and breeding value (*Sc*):

$$\text{range of variation } R = X_{opt} - X_{lim}, \text{ (g m}^{-2}\text{)}; \quad (1)$$

$$\text{coefficient of variation } V = \frac{S}{x} \cdot 100, \text{ (\%)}; \quad (2)$$

S – standard deviation; *x* – arithmetic mean.

As characteristics of plasticity homeostatic index:

$$Hom = \frac{x^2}{\sigma}; \quad (3)$$

σ – stability index, which is determined by the level of the linear regression coefficient, index of selection value

$$\text{Breeding value: } S_c = \frac{X \cdot X_{lim}}{X_{opt}}; \quad (4)$$

Hydrothermal coefficient (*HTC*) was calculated by the formula:

$$HTC = \frac{\sum R \cdot 10}{\sum t > 10}; \quad (5)$$

$\sum R$ – amount of precipitation, mm; $\sum t > 10$ – sum of active temperatures (Hangil'din et al., 1981; Iodkovskyy, 1999; Maruhnyak et al., 2010; Man'ko et al., 2012).

RESULTS

The results of studies of the yield level and individual productivity of buckwheat varieties are shown in Table 1. The table describes the average yield and individual productivity of varieties over the research years. It has been determined that the most favorable conditions for buckwheat varieties prevailed in 2016, and the parameters of 2017 and 2018 were more contrasting. Table 2 and 3 describe in each sample the parameters of the limiting factors (X_{opt} and X_{lim}) the level of variability (R) and the coefficient of variation (V, %), and the level of variation (R and V), as the characteristics of plasticity, homeostaticity (Hom_1 *ma* Hom_2), stability (σ) and breeding value (Sc) (Table 1–3).

Table 1. Characteristics of the level of yield and individual productivity of buckwheat [*Fagopyrum esculentum. Moench*] varieties of different ecological and geographical origin in the contrasting environmental conditions

No	The origin of variety		Name	Yield, g m^{-2}				Plant productivity, g			
	country	region		2016	2017	2018	average	2016	2017	2018	average
1	St	Khmelnytskyi	Yelena	283.4	216.8	174.2	224.8	2.5	1.9	1.6	2.0
2	Ukraine	Kyiv	Olha	274.0	200.1	178.1	217.4	2.4	1.8	1.7	2.0
3		Kyiv	Nadiina	232.0	169.3	130.8	177.4	2.1	1.4	1.2	1.6
4		Kyiv	Ruta	195.6	152.7	117.1	155.1	1.7	1.3	0.9	1.3
5		Kyiv	SYN 3/02	322.0	245.0	189.3	252.1	2.4	1.9	1.7	2.0
6		Kyiv	Sofiia	287.0	219.5	176.5	227.7	2.5	1.9	1.5	2.0
7		Sumy	Yaroslavna	288.0	210.2	187.2	228.5	2.7	1.8	1.6	2.1
8		Sumy	Sumchanka	272.0	198.5	177.8	216.1	2.3	1.6	1.4	1.8
9		Sumy	Selianochka	294.4	224.6	201.3	240.1	2.6	2.0	1.8	2.1
10		Sumy	Ruslana	272.6	208.9	177.2	219.6	2.2	1.6	1.4	1.7
11		Sumy	Slobozhanka	276.0	201.4	199.4	225,6	2.3	1.7	1.8	1.9
12		Khmelnytskyi	Podolianka	253.2	184.8	181.5	206.5	2.2	1.6	1.7	1.8
13		Khmelnytskyi	Roksolana	305.0	232.4	208.2	248.5	2.8	2.1	1.8	2.2
14		Khmelnytskyi	Populiatsiia7/07	284.5	217.6	197.9	233.3	2.5	1.9	1,6	2.0
15		Khmelnytskyi	Akademichna	237.0	183.0	131.4	183.8	2.0	1.5	1.0	1.5
16		Poltava	P-330	342.3	250.7	212.4	268.5	3.0	2.2	1.8	2.3
17		Poltava	P-332	271.6	208.2	203.1	227.6	2.2	1.7	1.8	1.9
18		Poltava	P-455	298.0	227.2	207.5	244.2	2.6	2.1	1.8	2.2
19		Poltava	Determinantna 8	257.6	178.8	177.4	204.6	2.1	1.6	1.7	1.8
20		Poltava	P-620	297.6	227.2	203.4	242.7	2.7	2.2	1.8	2.2
21	Belarus	Minsk	Ametist	312.0	237.7	202.8	250.8	2.7	2.1	1.7	2.2
22		Minsk	Lakneia	267.5	195.2	183.3	215.3	2.3	1.8	1.6	1.9
23		Minsk	Feniks	282.0	215.8	162.4	220.1	2.6	1.8	1.3	1.9
24		Minsk	Vlada	264.0	209.7	161.7	211.8	2.1	1.8	1.4	1.8
25		Minsk	Marta	251.7	183.7	173.6	203.0	2.1	1.5	1.6	1.7
26	Russia	Bashkortostan	Ufimskaia	247.0	190.3	170.5	202.6	2.1	1.8	1.6	1.8
27		Bashkortostan	Inzierskaia	196.0	153.0	127.4	158.8	1.7	1.4	1.1	1.4
28		Bashkortostan	Chishminskaia	213.6	155.9	128.8	166.1	1.9	1.3	1.0	1.4
29		Bashkortostan	Ahidel	237.0	173.0	170.4	193.5	2.1	1.5	1.6	1.7
30		Bashkortostan	Ilishevskaia	301.0	229.6	202.1	244.2	2.6	2.1	1.7	2.1
31		Novosybirsk	Natasha	242.6	187.0	147.6	192.4	2.1	1.7	1.3	1.7
32		Tatarstan	Batyr	290.6	211.2	184.6	228.8	2.5	1.8	1.5	2.0
33		Tatarstan	Nikolskaia	221.0	171.6	152.4	181.7	1.9	1.4	1.3	1.5
34	China		BaiChen	214.0	156.2	139.1	169.8	1.9	1.5	1.1	1.5

Table 1 (continued)

35	Canada	Arno	275.6	211.1	197.2	228.0	2.4	1.8	1.6	1.9
Target group										
average			267.4	201.1	175.3	214.6	2.3	1.7	1.5	1.9
min			195.6	152.7	117.1	155.1	1.7	1,3	0.9	1.3
max			342.3	250.7	212.4	268.5	3.0	2.2	1.8	2.3
V			10.3	10.9	12.0	18.3	11,3	11.9	14.3	12.5
R			146.7	98.0	95.3	113.3	1.3	0.9	0.9	1.0
σ			27.5	22.0	21.0	39.2	0.3	0.2	0.2	0.2

Table 2. The expression level of plasticity, stability, homeostaticity and breeding value according to buckwheat varieties yields [*Fagopyrum esculentum. Moench.*]

No	Name	Average, g m^{-2}	Variation level				Homeostaticity		Stability, σ	Breeding value, S_c
			X_{opt} (g m^{-1})	X_{lim} (g m^{-2})	R (X_{opt}-X_{lim}) (g m^{-2})	V, %	Hom_1	Hom_2		
1	Yelena	224.8	283.4	174.2	109.2	21.7	1,036.2	9.5	48.8	138.2
2	Olha	217.4	274.0	178.1	95.9	20.7	1,047.9	10.9	45.1	141.3
3	Nadiina	177.4	232.0	130.8	101.2	22.6	785.8	7.8	40.0	100.0
4	Ruta	155.1	195.6	117.1	78.5	22.3	696.7	8.9	34.5	92.9
5	SYN 3/02	252.1	322.0	189.3	132.7	22.3	1,129.9	8.5	56.2	148.2
6	Sofiia	227.7	287.0	176.5	110.5	21.7	1,049.9	9.5	49.4	140.0
7	Yaroslavna	228.5	288.0	187.2	100.8	20.8	1,100.9	10.9	47.4	148.5
8	Sumchanka	216.1	272.0	177.8	94.2	20.7	1,044.4	11.1	44.7	141.3
9	Selianochka	240.1	294.4	201.3	93.1	20.0	1,199.3	12.9	48.1	164.2
10	Ruslana	219.6	272.6	177.2	95.4	20.9	1,052.9	11.0	45.8	142.7
11	Slobozhanka	225.6	276.0	199.4	76.6	19.5	1,154.6	15.1	44.1	163.0
12	Podolianka	206.5	253.2	181.5	71.7	19.6	1,052.0	14.7	40.5	148.0
13	Roksolana	248.5	305.0	208.2	96.8	20.0	1,240.4	12.8	49.8	169.7
14	Populiatsiia 7/07	233.3	284.5	197.9	86.6	19.8	1,180.2	13.6	46.1	162.3
15	Akademichna	183.8	237.0	131.4	105.6	23.3	789.2	7.5	42.8	101.9
16	P-330	268.5	342.3	212.4	129.9	21.2	1,264.9	9.7	57.0	166.6
17	P-332	227.6	271.6	203.1	68.5	18.6	1,222.7	17.8	42.4	170.2
18	P-455	244.2	298.0	207.5	90.5	19.7	1,238.2	13.7	48.2	170.1
19	Determinantna 8	204.6	257.6	177.4	80.2	20.7	988.2	12.3	42.4	140.9
20	P-620	242.7	297.6	203.4	94.2	20.0	1,211.6	12.9	48.6	165.9
21	Ametist	250.8	312.0	202.8	109.2	20.8	1,205.8	11.0	52.2	163.0
22	Lakneia	215.3	267.5	183.3	84.2	20.2	1,068.4	12.7	43.4	147.6
23	Feniks	220.1	282.0	162.4	119.6	22.7	971.0	8.1	49.9	126.7
24	Vlada	211.8	264.0	161.7	102.3	22.1	959.3	9.4	46.8	129.7
25	Marta	203.0	251.7	173.6	78.1	20.1	1,011.0	12.9	40.8	140.0
26	Ufimskaia	202.6	247.0	170.5	76.5	20.0	1,015.1	13.3	40.4	139.9
27	Inzierskaia	158.8	196.0	127.4	68.6	21.0	755.5	11.0	33.4	103.2
28	Chishminskaia	166.1	213.6	128.8	84.8	21.6	769.6	9.1	35.8	100.2
29	Ahidel	193.5	237.0	170.4	66.6	19.6	987.5	14.8	37.9	139.1
30	Ilishevskaia	244.2	301.0	202.1	98.9	20.3	1,202.7	12.2	49.6	164.0
31	Natasha	192.4	242.6	147.6	95.0	21.9	878.0	9.2	42.2	117.1
32	Batyr	228.8	290.6	184.6	106.0	21.1	1,086.2	10.2	48.2	145.3
33	Nikolskaia	181.7	221.0	152.4	68.6	20.0	906.3	13.2	36.4	125.3
34	BaiChen	169.8	214.0	139.1	74.9	20.8	818.0	10.9	35.2	110.3
35	Arno	228.0	275.6	197.2	78.4	19.3	1,179.4	15.0	44.1	163.1

Table 3. The expression level of plasticity, stability, homeostaticity and breeding value according to individual plant productivity in varietal buckwheat material [*Fagopyrum esculentum Moench.*]

No	Name	Average, g	Variation level				Homeostaticity		Stability, σ	Breeding value, S_c
			X_{opt} (g)	X_{lim} (g)	R (X_{opt}-X_{lim}) (g)	V, %	Hom_1	Hom_2		
1	Yelena	2.0	1.6	2.5	0.9	20.9	9.5	11.0	0.4	1.3
2	Olha	2.0	1.7	2.4	0.7	19.3	10.2	14.9	0.4	1.4
3	Nadiina	1.6	1.2	2.1	0.9	23.4	6.7	7.5	0.4	0.9
4	Ruta	1.3	0.9	1.7	0.8	24.0	5.4	6.8	0.3	0.7
5	SYN 3/02	2.0	1.7	2.4	0.7	19.8	10.1	14.4	0.4	1.4
6	Sofiia	2.0	1.5	2.5	1.0	21.7	9.1	9.5	0.4	1.2
7	Yaroslavna	2.1	1.6	2.7	1.1	22.6	9.1	8.5	0.5	1.2
8	Sumchanka	1.8	1.4	2.3	0.9	22.1	8.0	8.9	0.4	1,1
9	Selianochka	2.1	1.8	2.6	0.8	20.1	10.4	12.3	0.4	1.4
10	Ruslana	1.7	1.4	2.2	0.8	21.0	8.2	10.3	0.4	1.1
11	Slobozhanka	1.9	1.7	2.3	0.6	19.0	10.2	18.0	0.4	1.5
12	Podolianka	1.8	1.6	2.2	0.6	19.1	9.6	15.4	0.4	1.3
13	Roksolana	2.2	1.8	2.8	1.0	20.7	10.8	10.9	0.5	1.4
14	Populiatsiia 7/07	2.0	1.6	2.5	0.9	20.9	9.5	10.9	0.4	1.3
15	Akademichna	1.5	1.0	2.0	1.0	24.5	6.1	6.1	0.4	0.8
16	P-330	2.3	1.8	3.0	1.1	21.2	11.0	9.7	0.5	1.4
17	P-332	1.9	1.7	2.2	0.5	18.7	10.2	20.3	0.4	1.5
18	P-455	2.2	1.8	2.6	0.8	20.3	10.7	13.6	0.4	1.5
19	Determinantna 8	1.8	1.6	2.1	0.5	19.3	9,3	18.5	0.3	1.4
20	P-620	2.2	1.8	2.7	0.9	21.3	10.4	11.2	0.5	1.5
21	Ametist	2.2	1.7	2.7	1.0	21.4	10.1	10.0	0.5	1.4
22	Lacneya	1.9	1.6	2.3	0.7	20.1	9.5	12.9	0.4	1.3
23	Feniks	1.9	1.3	2.6	1.3	24.3	7.8	6.0	0.5	1.0
24	Vlada	1.8	1.4	2.1	0.7	21.5	8.2	11.9	0.4	1.2
25	Marta	1.7	1.5	2.1	0.6	19.3	9.0	15.2	0.3	1.2
26	Ufimskaya	1.8	1.6	2.1	0.5	19.5	9.5	17.3	0.4	1.4
27	Inzerskaya	1.4	1.1	1.7	0.6	21.5	6.5	11.0	0.3	0.9
28	Chishminskaya	1.4	1.0	1.9	0.9	23.4	5.9	6.9	0.3	0.7
29	Agidel’	1.7	1.5	2.1	0.6	19.1	9.0	15.5	0.3	1.2
30	Ilishevskaya	2.1	1.7	2.6	0.9	21.3	10.1	11.0	0.5	1.4
31	Natasha	1.7	1.3	2.1	0.8	22.3	7.6	9.2	0.4	1.0
32	Batyr	2.0	1.5	2.5	1.0	21.8	9.0	8.7	0.4	1.2
33	Nikol’skaya	1.5	1.3	1.9	0.6	20.1	7.7	12.9	0.3	1.1
34	BaiChen	1.5	1.1	1.9	0.8	22.7	6.5	8.6	0.3	0.9
35	Arno	1.9	1.6	2.4	0.8	20.4	9.5	11.9	0.4	1.3

The research of the parameters of plasticity, stability and homeostaticity, as factors determining the level of yield and individual productivity of the plant varieties, was carried out in the contrasting (according to heat and moisture availability) environmental conditions in 2016, 2017 and 2018. It has been defined that the conditions were more extreme in 2017 and 2018, when the level of hydro-thermal coefficient (*HTC*) of the vegetation period ranged from 0.51to 0.68, ‘growth above ground-flowering’ period - 0.37–0.42, ‘flowering- early ripening’ period - 0.56–0.78, ‘early ripening -full ripening’ period - 0.61–0.85 (Table 4). In this case, not only *HTC* level is important, but also the sum of precipitation, and especially the distribution of precipitation by periods.

For example, according to the level of *HTC* during the 'flowering - early ripening' period in 2016, which is generally recognized as optimal, this period is much more arid (0.64) than generally recognized as arid 2017, when the level of *HTC* was 0.78. But such level of *HTC* determined a lower temperature level in 2017 and a slightly higher level of precipitation. Rainfall during the 'flowering - early ripening' period of this year consisted of two heavy rains, with strong winds and had a negative effect on plants.

Table 4. Parameters of weather and climate conditions and level of hydro-climatic coefficient over the research years

Year	Phases of vegetation period											
	'growth above ground-flowering'			'flowering-early ripening'			'early ripening -full ripening'			'growth above ground - full ripening'		
	∑t air	∑ precip	*HTC*	∑t air	∑ precip	*HTC*	∑t air	∑ precip	*HTC*	∑t air	∑ precip	*HTC*
2016	560.6	39.6	0.71	694.4	44.7	0.64	471.6	31.4	0.67	1,726.6	115.7	0.67
2017	531.9	22.5	0.42	621.6	48.5	0.78	432.1	36.6	0.85	1,585.6	107.7	0.68
2018	558.2	20.8	0.37	620.2	34.9	0.56	454.4	27.9	0.61	1,632.8	83.6	0.51

Yields of varieties

The level of research material yields varied in the range of 117.1 to 342.3 g m^{-2} (from 115.1 to 268.5 g m^{-2} according to average data) due to the significant diversity of buckwheat varietal material by ecological and geographical origin and adaptability of certain genotypes to the local environmental conditions.

The most favorable conditions for buckwheat cultivation were in 2016, when the average yield of the target group was 267.4 g m^{-2} with a range of 195.6 to 342.3 g m^{-2}, the least favorable conditions were in 2018, the average yield was 175.3 g m^{-2} with a range of 117.1 to 212.4 g m^{-2}.

According to three-year data, the most yielding varieties were SYN 3/02 (252.1 g m^{-2}), Selianochka (240.1), Roksolana (248.5), Populatsiia 7/07 (233.3), P-330 (268.5), P-455 (244.2), P-620 (242.7), Ametist (250.8), Ilishevskaia (244.2).

Individual productivity of the plant: this indicator, as one of the main components of the characteristics of buckwheat varieties yield, over the years highly repeats tendencies which were established for the previous characteristic. Higher individual productivity was observed in varieties in more favorable weather conditions in 2016 (2.3 g) and a significant decrease was observed in unfavorable 2017 and 2018 (respectively, 1.7 and 1.5 g per plant). For the most part, in the target group, varieties showed_greatest variation in the level of this indicator expression in 2018 (V = 14.3%). The highest average productivity (over 2.0 g $plant^{-1}$) was observed in the samples Yelena, Olha, SYN 3/02, Sofiia, Populatsiia 7/07 and Batyr (2.0 g each), Yaroslavna (2.1 g), P-330 (2.3g), Roksolana, P-455, P-620 and Ametist (2.2 g each).

Plasticity (variability level)

Yield (g m^{-2}): the plasticity level of buckwheat varieties was determined by the level of indicator variation in the contrasting environmental conditions. Hence, the factor of yield change was more important than its physical parameter. The coefficient of variation (V), determined by B.A. Dospekhov's method (1974), was applied in order to get the greater reliability. Varieties Ruta (78.5 g m^{-2}), Slobozhanka (76.6), Podolianka

(71.7), P-332 (68.5), Ufimskaia (76.5), Inzierskaia (68.6), Ahidel (66.6), Nikolskaia (68.6), BaiChen (74.8), Arno (78.4) were the least variable according to the yield level (R).

It has been determined that varieties Slobozhanka (19.5), Podolianka (19.6), Populiatsiia 7/07 (19.8), P-332 (18, 6), P-455 (19.7), Ahidel (19.6), Arno (19.3) had higher plasticity (according to the coefficient of variation) in the contrasting environmental conditions.

Individual plant productivity (g/plant): most varieties had significant fluctuations in the level of indicator expression by years, which is explained by the rather contrasting conditions of the cultivation years.

The highest plasticity (the slightest productivity fluctuation in years with the limiting conditions compared to the optimal ones) was observed in varieties Slobozhanka, Podolianka, P-332, Determinantna 8, Marta, Ufimskaia, Inzerskaya, Ahidel and Nikolskaia. Most of these varieties had a slight level of coefficient variation (*V*) - from 18.7 to 19.5%, with the exception of Inzierskaia (21.5%) and Nikolskaia (20.1%).

Homeostaticity

Yield (g m^{-2}): the indicator determines the genotype response under the variable environmental conditions according to a particular feature. Homeostaticity indicator of the varieties was determined by two methods (Hangil'din et al.,1981; Iodkovskyy, 1999) for more complete description of the material. Most of the research results, regardless of the applyied method, considered varieties Nadiina (Hom_1 - 785.8/Hom_2 - 7.8), Ruta (696.7/8.9), Sofiia (1,049.9/9.5), Yelena (1,036.2/9.5), Academichna (789.2/7.5), Feniks (971.0/8.1), Vlada (959.3/9.4), Chishminskaia (769.6/9.1), Natasha (878.0/9.2), BaiChen (818.0/10.9) to be distinguished by a low rate of response to the changing cultivation conditions.

Some genotypes that had a significant difference in the indicators by the different methods were not taken into account - SYN 3/02 (Hom_1 - 1,129.9/Hom_2 - 8.5), Determinantna 8 (988.2/12.3), Inzierskaia (755.5/11.0), Ahidel (987.5/14.8), Nikolskaia (906.3/13.2).

Individual plant productivity (g/plant): the expression levels of both indicators were quite similar for most varieties. A slight response of the genotype to the environmental factors was observed in the varieties Nadiina (Hom_1 - 6.7/Hom_2 - 7.5), Ruta (5.4/6.8), Sofiia (9.1/9.5), Yaroslavna (9.1/8.5), Sumchanka (8.0/8.9), Ruslana (8.2/10.3), Populiatsiia 7/07 (9.5/10.9), Academichna (6.1/6.1), P-330 (11.0/9.7), Feniks (7.8/6.0), Vlada (8.2/11.9), Inzierskaia (6.5/11.0), Chishminskaya (5.9/6.9), Natasha (7.6/9.2), Batyr (9.0/8.7), BaiChen (6.5/8.6), Arno (9.5)/11.9). Samples Podolianka (9.6/15.4), P-332 (10.2/20.3), Determinantna 8 (9.3/18.5), Lakneia (9.5/12.9), Marta (9.0/15.2), Ufimskaia (9.5/17.3), Ahidel (9.0/15.5), Nikolskaia (7.7/12.9) showed the significant differences in the expression levels of the homeostaticity indicator by the different methods.

Stability

Yield (g m^{-2}): stability of the feature manifestation is a concomitant or additory variety characteristic to plasticity. This indicator describes the organism natural ability to maintain a certain level of expression in the variable environmental conditions, a certain buffer or body strength reserves (Maruhnyak, 2010). According to the obtained data, the varieties SYN 3/02 (56.2), Sofiia (49.4), Selianochka (48.1), Yelena (48.8), Roksolana (49.8), P-330 (57.0), P-455 (48.2), P-620 (48.6), Ametist (52.2), Feniks (49.9), Ilishevskaia (49.6), Batyr (48, 2) produced higher stability over the research years.

Individual plant productivity (g/plant): high level of homogeneity of the target group was observed in terms of the stability of the manifestation level of plant productivity indicator. Only a small number of varieties had an advantage over other samples involved in the research ($\sigma = 0.5$) - Yaroslavna, Roksolana, P-330, P-620, Ametist, Feniks, and Ilishevskaia.

Breeding value

Yield (g m^{-2}): breeding value is an important characteristic of varieties or breeding numbers. It determines the potential material suitability to be involved into breeding process for the creation of new varieties (Klimova, 2013). The distribution of the studied material was carried out according to the breeding value. Varieties - SYN 3/02 (148.2), Selianochka (164.2), Slobozhanka (163.0), Podolianka (148.0), Roksolana (169.7), Populiatsiia 7/07 (162.3), P-330 (166.6), P-332 (170.2), P-455 (170.1), P-620 (165.9), Ametist (163.0), Lakneia (147.6), Ilishevskaia (164.0), Arno (163.1) were included in the group of varieties with the highest level of manifestation.

Individual plant productivity (g $plant^{-1}$): the level of indicator expression in the varieties of the target group ranged from 0.7 to 1.5. The highest indicators were recorded in the varieties Olha, SYN 3/02, Selianochka, Roksolana, P-330, Determinantna 8, Ametist, Ufimskaia, Ilishevskaia (1.4 each), Slobozhanka, P-332, P-455 and P-620 (1.5 each).

DISCUSSION

The scope of research involves the evaluation of the modern varieties both for breeding usage and for use in the production conditions. For this purpose, the integral indicator of plants grain productivity, as the final characteristic of the interaction of the complex of natural biological properties of the organism, and its main component - individual plant productivity was used in the course of the analysis. Taking into account the complexity and interaction of various factors in the formation of the yields, the study of this indicator is only the first step in the evaluation of varietal material suitability for selective introduction and using the level of breeding value as a necessary condition for the initial evaluation of the source material. Recognition of the high breeding value of varieties in terms of yield and individual plant productivity requires a detailed study and description of the biological, morphological and economic characteristics of the samples in the future. For producers, the potential yield in the contrasting environmental conditions is the main indicator of the variety evaluation and its suitability for economic use.

Involvement of representatives of different ecological and geographical groups, various types of ploidy and biology of the plant itself (determinants and indeterminants) into the study allows us to evaluate not only the involved varieties, but also to identify general tendencies and make conclusions about the reasonability of using one or another selection material as the initial varieties and forms. Especially for use in selection, which main tasks are to create new varieties for areas with risky farming (insufficient or unstable moisture availability, uneven distribution of precipitation during the vegetation period, etc.).

Due to the described level of *HTC* during the vegetation period of buckwheat plants, the conditions of the research years made it possible to fully eveluate the yield and productive potential of the varieties and identify varieties, capable of having their high levels in the optimal environmental conditions - Olha, SYN 3/02, Sofiia, Yaroslavna, Selianochka, Slobozhanka, Yelena, Roksolana, Populiatsiia 7/07, P-330, P-455, P-620, Ametist, Feniks, Ilishevskaia, Batyr, Arno. This characteristic is very important for producers and shows the potential opportunities of the realization of yield and productive potential.

It indicates the ability of varieties to produce yields and form plant productivity, subject to the optimal cultivation conditions, that is, to ensure the economic attractiveness of the variety for production.

Another equally important characteristic is the level of variation of the studied parameters, that is, the identification of material with high placticity and stability, as the ability to lower the level of yield and individual productivity to a lesser extent in the extreme limiting environmental conditions (Slobozhanka, Podolianka, P-455) and have an increased expression level of the evaluated characteristics - SYN 3/02, Ruta, Sofiia, Selianochka, Yelena, Roksolana, P-330, P-620, Ametist, Feniks, Ilishevskaia, Batyr, P-332, Ufimskaia, Inzierskaia, Ahidel, Nikolskaia, BaiChen and Arno. Samples, which combine high yield and plant productivity with a high level of plasticity and stability, as a more potentially attractive material for production and selection are of particular value - SYN 3/02, Sofiia, Selianochka, Slobozhanka, Yelena, Roksolana, Populiatsiia 7/07, P-330, P-455, P-620, Ametist, Feniks, Ilishevskaia, Batyr, Arno. An additional characteristic of the resistance or tolerance to the environmental factors is a homeostaticity of the variety, which determines the response rate to such factors.

The research has identified a group of samples that had an increased level of homeostaticity according to variety yield and plant individual productivity - Nadiina, Ruta, Sofiia, Akademichna, Feniks, Vlada, Chishminskaia, Natasha, BaiChen. These varieties are a potential genetic resource for further selection researches.

In the research, the breeding value of the variety material was evaluated according to the yield and individual productivity of the plant, as a characteristic that takes into account the whole range of indicators and descriptions of the plant material and is the final factor for determining the most suitable variety for further breeding use. The group with high level of breeding value includes varieties of different ecological and geographical origin: from Ukraine - SYN 3/02, Selianochka, Slobozhanka, Podolianka, Roksolana, Populiatsiia 7/07, P-330, P-332, P-455, P-620, the Republic of Belarus - Ametist and Lakneia, the Russian Federation - Ilishevskaia, Canada - Arno.

CONCLUSIONS

Comprehensive evaluation of the wide genetic diversity of varieties of different ecological and geographical origin, different types of plants (according to ploidy and type of growth) in the contrasting environmental conditions made it possible to identify genotypes with an increased level of adaptive potential. It has been established that varieties SYN 3/02, Selianochka, Roksolana, Populiatsiia 7/07, P-330, P-455, P-620, Ametist, Ilishevskaia are more attractive for practical use, in observance of the production technology that will significantly eliminate the negative impact of environmental factors and realize the yield and productive potential.

Taking into account the complexity of forming the indicator of yield and significant influence of plant individual productivity on its level, the necessity of applying a number of parameters, in particular, plasticity, homeostaticity and stability for selection practice has been proved. The varieties, which combine a high manifestation level of the studied parameters and can be recommended for further study and use as a valuable starting material, have been identified in the target group - SYN 3/02, Sofiia, Selianochka, Slobozhanka, Yelena, Roksolana, Populiatsiia 7/07, P-330, P-455, P-620, Ametist, Feniks, Ilishevskaia, Batyr, Arno. Most of these varieties have a high breeding value as a result of breeding attractiveness and are recommended for being introduced into the selection practice.

REFERENCES

Alekseeva, E.S., Elahin, I.N., Taranenko, L.K., Bochkareva, L.P., Malina, M.M., Rarok, V.A. & Yacichin, O.L. 2005. *History of culture, botanical and biological features*. *Culture of buckwheat*. V. 1. Drukarnya, P.P., Moschak, M.I., Kamyanec-Podol'skiy, Ukraine, 192 pp.

Burdenyuk-Tarasevych, L., Dubova, O. & Hahula, V. 2012. Evaluation of the adaptive capacity of soft winter wheat varieties in the Forest-steppe conditions of Ukraine. *Selection and seed production* **101**, 3–11.

Cawoy, V., Lutts, S. & Kinet, J.M. 2006. Osmotic stress at seedling stage impairs reproductive development in buckwheat (Fagopyrum esculentum Moench.). *Physiologia plantarum* **128**, 689–700.

Chrungoo, N., Dohtdong, L. & Chettry, U. 2016. Genome Plasticity in Buckwheat. Gene Pool Diversity and Crop Improvement. *Springer International Publishing,* Switzerland, **10**, 227–240.

Eberhart, S.A. & Rassel, W.A. 1966. Stability parametres for comparing varieties. *Crop Sci.* **6**, 36–40.

E, S.Z., Yang, Z.Q., Zeng, X.B., Wang, Y.N., Luo, Z.X., Yuan, J.H., Che, Z.X. & Guo, Y.J. 2017. Effects of Long-Term Fertilization on Nitrogen Fertilizer Use Efficiency in Loessial Soil Region on the Loess Plateau, Northwest China. *Ying Yong Sheng Tai Xue Bao* **28**(1), 151–158. doi: 10.13287/j.1001-9332.201701.011

Fesenko, N.V., Fesenko, N.N., Romanova, O.I., Alekseeva, E.S. & Suvorova, G.N. 2006. *The gene bank and breeding of groat crops. Buckwheat. Theoretical basis of plant breeding* **V**. VIR, St. Peterburg, Russia, 195 pp.

Iodkovskyy, V. 1999. Study of homeostatic varieties of spring wheat. *Selection and seed production* **82**, 48–55.

Jacquemart, A.-L., Cawoy, V., Kinet, J.M., Ledent, J.F. & Quinet, M. 2012. Is buckwheat (*Fagopyrum esculentum Moench*.) Still a Valuable Crop Today? The Europ. *J. Pl. Sc. and Biotechn*. **6**(2), 1–10.

Hangil'din, V. & Litvinenko, N. 1981. Homeostatic and adaptive winter wheat varieties. *Scean-techn. Bull. All-Union Agr. Inst*. **39**, pp. 8–14.

Harifullina, H.H., Herchikov, A.Ya., Shafikov, N.Ya. & Sultanaev, S.H. 2010. The effectiveness of natural buckwheat antioxidants. *Herald of Baskirian Univ*. **5**(2), 291–293.

Holasova, M., Fiedlerova, V., Smcinova, H., Orsak, M., Lachman, J. & Vavreinova, S. 2002. Buckwheat – the source of antioxidant activity in functional foods. *Food research international* **35**, 207–211.

Kalinova, J., Moudry, J. & Curn, V. 2002. Technological quality of common buckwheat (*Fagopyrum esculentum Moench*.). *Roslinna vyroba* **48**, 279–284.

Klimova, O. 2013. Diagnostics for dry resistance of new sugar lines of mays. *Bull. Inst. of Agric. of Steppe zone of NAAS Ukraine* **4**, pp. 64–70.
Kreft, I. 2001. Buckwheat research, past, present and future perspectives – 20 years of internationally coordinated research. *Current advances in buckwheat research proceeding of the 8th International Symposium of Buckwheat*, August 30 – September 2 2001, Chunchon, Republic of Korea, pp. 361–366.
Li, S. & Zhang, Q.H. 2001. Advances in the development of functional foods from buckwheat. *Crit. Rev. Food Sci. Nutr*. **41**, 451–464.
Luzhinskaya, N.A. 2017. Recommendation for growing of buckwheat in 2017. https://mshp.gov.by/information/materials/zem/agriculture/a2a79b4c2e716d60.html
Man'ko, K., Muzafarov, N. & Cehmeystruk, M. 2012. Ecological plasticity of modern varieties of spring barley depending on the background of nutrition. *Selection and seed production* **101**, 264–271.
Marenych, M.M., Hanhur, V.V., Len, O.I., Hangur, Yu.M., Zhornyk, I.I. & Kalinichenko, A.V. 2019. The efficiency of humic growth stimulators in pre-sowing seed treatment and foliar additional fertilizing of sown areas of grain and industrial crops. *Agronomy Research* **17**(1), 194–205. doi.org/10.15159/AR.19.023
Maruhnyak, A., Dac'ko, A. & Maruhnyak, H. 2010. Adaptability and stability of oat varieties in terms of grain quality. *Selection and seed production* **98**, 106–115.
Modern technology for growing buckwheat. 2018. Technology for growing buckwheat.html
Muhamedyarova, L.G., Derkho, M.A., Meshcheriakova, G.V., Gumenyuk, O.A. & Shakirova, S.S. 2020. Influence of bio-humus on soil fertility, productivity and environmental safety of spring wheat grain *Agronomy Research* **18**(2), 483–493, https://doi.org/10.15159/AR.20.152
Rufa, L. 2004. The Development and Utilization of Tartary Buckwheat Resources. Advances in Buckwheat Research. *Proceedings of the 9th International Symposium on Buckwheat, Research Institute of Crop Production*, 18-22 August 2004, Prague 6 – Ruzyně, Czech Republic, pp. 252–258.
Skrabanja, V., Kreft, I., Golob, T., Modic, M., Ikeda, S., Ikeda, K., Kreft, S., Bonafaccia, G., Knapp, M. & Kosmelj, K., 2004. Nutrient content in buckwheat milling fractions. *Cereal Chem*. **81**, 172–176.
Tryhub, O. 2002. *Polymorphism of common buckwheat (Fagopyrum esculentum Moench.) on a level of productivity and adaptability to the conditions of Forest-Steppe of Ukraine*. Candidate of Agricultural Sciences, Institute of Agriculture UAAS, Kyiv, Ukraine, 21 pp.
Tryhub, O., Burdyga, V., Kharchenko, Yu. & Havrylyanchyk, R., 2018. Formation of buckwheat genepool collection in Ukraine and directions of its usage. *Fagopyrum* **35**, 29–35.
Zeller, F. 2001. Buckwheat (Fagopyrum esculentum Moench): utilization, genetics, breeding. *Bodenkultur* **52**, 259–276.
Zhou, M., Tang, Yu, Deng, X., Ruan, Ch., Kreft, I., Tang, Yi. & Wu, Ya., 2018. Overview of Buckwheat Recourses in the World, Buckwheat Germplasm in the World. *Elsevier Ink*., London, UK, pp. 1–9.
Zhygunov, D., Soc, S. & Drozdov, A. 2016. Productivity and quality of buckwheat products. *Grain products and compound feed* **64**, 22–25.

Agronomy Research **18**(4), 2639–2652, 2020
https://doi.org/10.15159/AR.20.233

Case study of non-linear PV inverter devices attached to the LV distribution network

T. Vinnal, H. Puusepp, N. Shabbir, L. Kütt and M. N. Iqbal

Tallinn University of Technology, School of Engineering, Department of Electrical Power Engineering and Mechatronics, Ehitajate tee 5, EE19086 Tallinn, Estonia.
*Correspondence: toomas.vinnal@taltech.ee

Abstract. Every year, more and more solar power plants are connected to the grid, producing electricity in an environmentally sustainable manner. The increasing number of photovoltaic (PV) installations and their integration into the low voltage (LV) distribution network (DN) is having an impact in terms of power quality (PQ). For example, the voltage in the DN can sustain high distortion values. The impact of a PV installation on the LV network is analysed in this research. The field measurements were carried out over a 3-week period at a solar power plant with a total output power of 160 kW in an Estonian rural municipality. The measurement results provide the opportunity to look more closely at the effect of the solar power plant on the supply voltage of the LV DN. Parameters such as voltage variation within a one-minute period, the asymmetry of the voltages and the total harmonic distortion of the voltages are discussed here.

Key words: distribution network, microgeneration, photovoltaic systems, power quality, solar energy, voltage level, voltage quality.

INTRODUCTION

The share of Renewable Energy Resource (RES) in the grid is increasing day by day. It will continue to grow more in the coming decades as most of the countries have plans for generating energy from 100% RES (Tan et al., 2017; Chen & Liu, 2019; Gürtürk, 2019; Hassan et al., 2019). Most of the RES electric producers including the photovoltaic (PV) installation units are directly dependent on environmental or atmospheric conditions (Shabbir et al., 2020) and their energy generation is not smooth rather variable or stochastic in nature (Demolli et al., 2019; Shabbir et al., 2019). Therefore, the usage of RES in such high capacity requires more technical but elaborative solutions. This may cause serious power quality (PQ), reliability and flexibility issues in the grid. For example, the network voltage levels can drop significantly while increased values of harmonic distortions are seen (Ruwaida & Holmberg, 2015). This can be caused by even a single small scale PV producer integrated directly to low voltage (LV) distribution network (DN) power line (Vinnal et al., 2018). Therefore, a large number of similar installations could have a very severe and adverse impact on the grid leading to equipment malfunctioning on the consumer side.

The general operating requirements of an LV distribution network in European DNs are defined within standard EN 50160. As per the standard, the RMS voltage V_n has to remain between ± 10% of the rated voltage during 95% time in a week (Seme et al., 2017). The limits of voltage harmonics tolerable are additionally defined in IEC 61000-2-2 (Meyer & Kilter, 2014). In case these limits are exceeded, the consumer device can sustain damage due to overheating or malfunction. The origins of voltage harmonics in the DN can be traced to current harmonics non-linear devices such as variable speed drives (VFDs), power electronics equipment and an increasing number of solar photovoltaic (PV) and wind RES (Iqbal et al., 2018).

These distortion components are also termed, as harmonic components are usually not significant, compared to the mains frequency voltage component values. Therefore, for the majority of the time, they do not cause equipment loss of function nor failure. Nevertheless, the level of voltage harmonics directly affects the supply voltage quality, capacitors lifetime and power losses in motors and transformers.

The general requirements for connecting a small solar PV to the LV network list frequency and voltage synchronization, and ranges for power factor and voltage unbalance values. The power of a small PV plant is of variable nature, having a diverse effect on these parameters at different times. In extreme cases, the parallel operation of the LV network and PV plant can cause disruptions in the reliable operation of the network. On the other hand, the presence of a PV plant in the distribution can sometimes attribute to the reduction of the harmonics of the phase voltage as compared to the case without having a PV plant. A further drop in total harmonic distortion (THD) values is possible by using switching and semiconductor converters with power factor correction (PFC) (Kopicka et al., 2014).

A high number of papers have been made available on the effects of PQ in the LV distribution network due to the presence of small PV units in the grid. In (Urbanetz et al., 2012) Studied on the effects of the PV generator attached to the LV network found that PV integration in the LV network is beneficial for improving PQ indexes like harmonics and THD. Similarly, the effect of a large PV unit of 1.8 MW connected to the grid is discussed in (Farhoodnea et al., 2012). The presence of such a high power source caused a rise in voltage and flickering and loss in power factor. The harmonic currents and the voltages in LV distribution networks have been elaborated in (Vinnal et al., 2018). A case study on the impact on power quality has been discussed for different PV generators connected to the grid in (Kumary et al., 2014). In (González et al., 2014), PQ parameter measurements at different points in the LV distribution networks showed that the power factor would decrease, voltage and current harmonics remained low but the problems were associated with fluctuations in frequency and increased voltage levels. The problems related to voltage variations and flickering are discussed more in (Pakonen et al., 2016). The evaluation of harmonic distortions associated with PV units is described in (Shi, 2014; Grasso et al., 2018). An integration model of solar PV into the grid has been developed in DigSilent (Jayasekara & Wolfs, 2010), for the analysis of PQ parameters. Studies listed above indicate the significance of PV plants to the PQ indexes and grid operation.

The main focus of this article is to present and analyse selected PQ aspects related to small-scale PV integration in the LV network with particular site case analysis in Estonia. The parameters discussed here are voltage magnitude, fluctuation and harmonics.

The organization of this paper is as follows: section II describes the analysis of PV and LV distribution systems in Estonia along with a description of the measuring site and measurement equipment. The results and discussions are presented in section III. Finally, section IV presents the conclusion and recommendations of this study.

ANALYSIS OF DISTRIBUTION SYSTEM

A. Description of the PV System and LV Network

The measurements were made at a power plant located in Harju County in Estonia. The construction of the power plant began in October 2015 and was completed in one year. An initial payback period of 10 years was estimated for the construction of the plant.

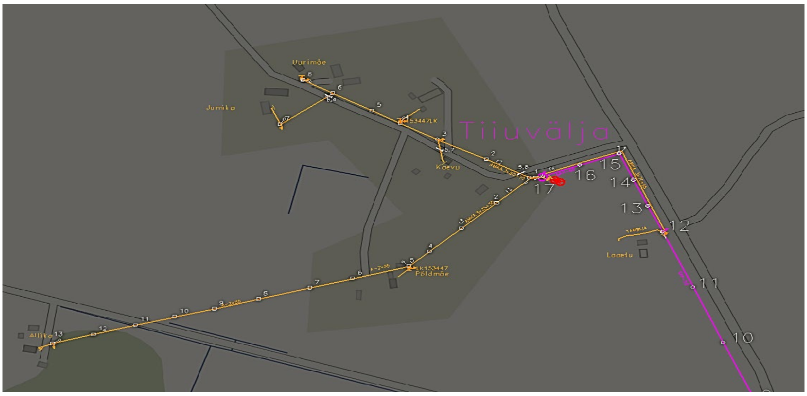

Figure 1. The low-voltage electric network of the considered solar power plant.

This solar power plant is connected to the LV terminals of the 10 / 0.4 kV substation. Fig. 1 shows a map of the low voltage circuit surrounding the substation. The purple colour represents the 10 kV high voltage power line of the substation. The PV panels are shown in Fig. 2 while Fig. 3 shows the transformer along with the LV distribution line.

Figure 2. The PV panels and inverters installation.

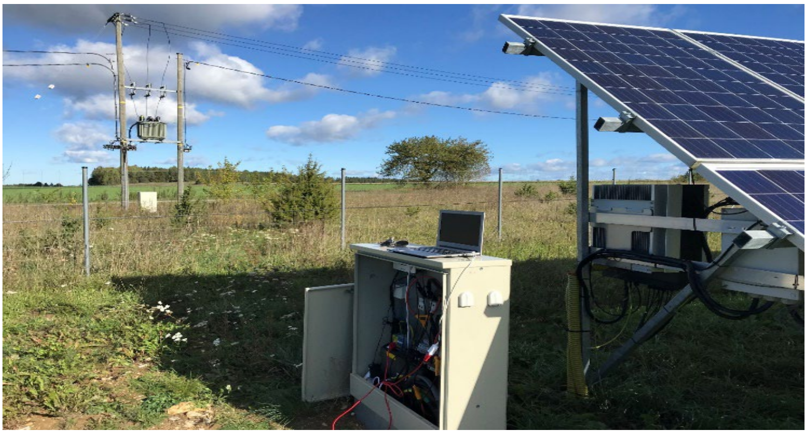

Figure 3. Solar Power Plant point of common coupling (PCC) with a 10 / 0.4 kV substation in the background.

The solar plant includes 668 solar panels with a total output of 177 kW. The total power of the inverters is 160 kVA. There are six inverters - two at 20 kVA and four at 30 kVA.

The entire power plant is divided into six production units by means of six inverters, all of which are concentrated in one main switchboard with circuit breakers. The main switchboard collects all the energy produced and transmits it to a single cable power grid. Separation of inverters into separate production units has created a situation where, for example, if something should happen to one inverter or other devices, 5/6 of the station can continue to run uninterrupted.

B. Instruments and Measurement Procedure

The measurements at the PV station were conducted from September, 2nd until September 25th, 2018 using a three-phase PQ analysed device capable of recording voltage, current, active and reactive power, frequency, voltage asymmetry, as well as the proportion of harmonics of voltage and current up to the 50th harmonic.

Fig. 4 shows the main switchboard and measuring device with four wires for measuring voltage and Rogowski sensors for measuring current. The measurement period for long-term measurements was three weeks and the records over this time at one-minute intervals over the network. The following subchapters present a selection of the data stored by the meter and analysed it.

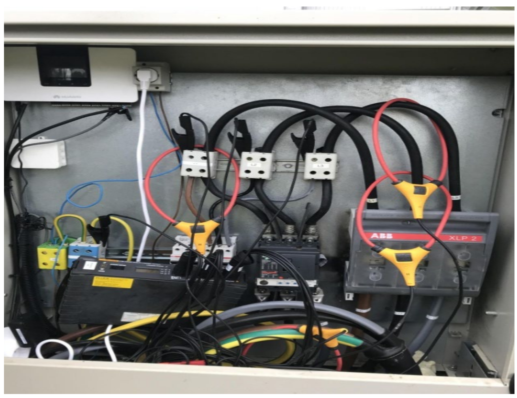

Figure 4. Main switchboard and PQ measurements.

MEASUREMENT RESULTS ANALYSIS

A. Power output ratings

The total power of the inverters of this station is 160 kW and the calculated average power output of the first week was 56.0 kW, in the second week 47.4 kW and in the third week 49.7 kW. Fig. 5 shows the output power of PV panels for the first week. Productivity was steadily high with the weather being rather clear. As only September 15th was low in productivity, the period of measurement can be considered successful.

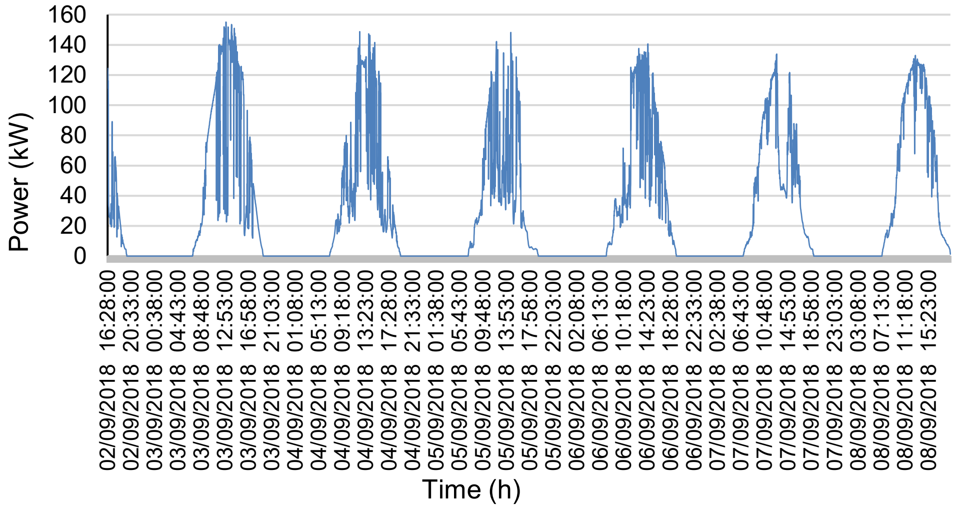

Figure 5. PV plant output power during the first week.

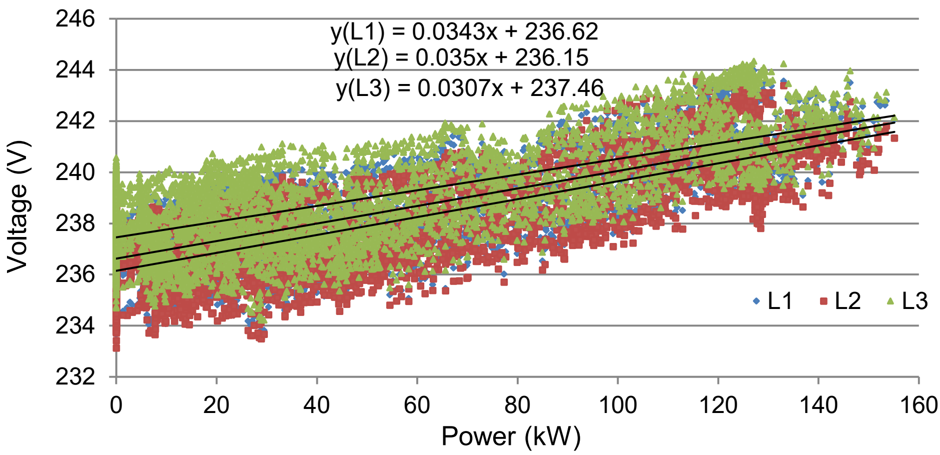

Figure 6. The output voltage of the solar panels, with trend lines corresponding to each of the three LV supply network phases.

Fig. 5 shows that solar power generation is highly cloudiness-dependent and incidental. Fig. 6 shows the weekly voltage dependence of the output voltage. From the graph, it can be seen that as the output of the solar power plant increases, the mains voltage increases. The graphs also present linear trend lines constructed by measuring points, by phase. Trend line equations are written at the legend and their increments over three weeks range from 0.029 P_{out} to 0.039 P_{out}, where P_{out} is the corresponding power output in kW. It can be seen that on average, the voltage rises between 4.6 V and 6.3 V at 160 kW power output.

B. Voltage level and symmetry

The difference between the maximum and minimum voltage values as a function of productivity is shown in Fig. 7. In addition to the average of one minute, the measuring device also recorded the maximum and minimum values of voltages during the same minute. Although the trend lines in the figures are ascending, they are small. Thus, it can be argued that the operation of this solar power plant does not influence the voltage fluctuation for a period of one minute.

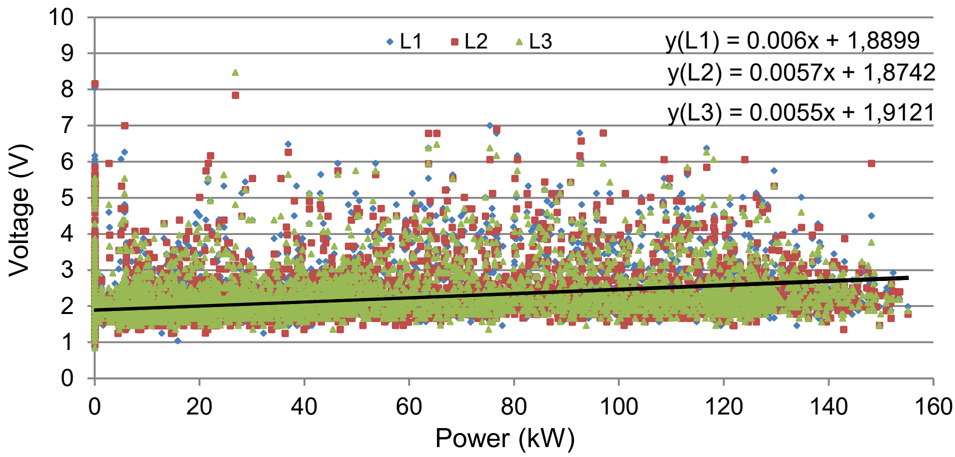

Figure 7. Difference between the minimum and maximum voltages in the LV network.

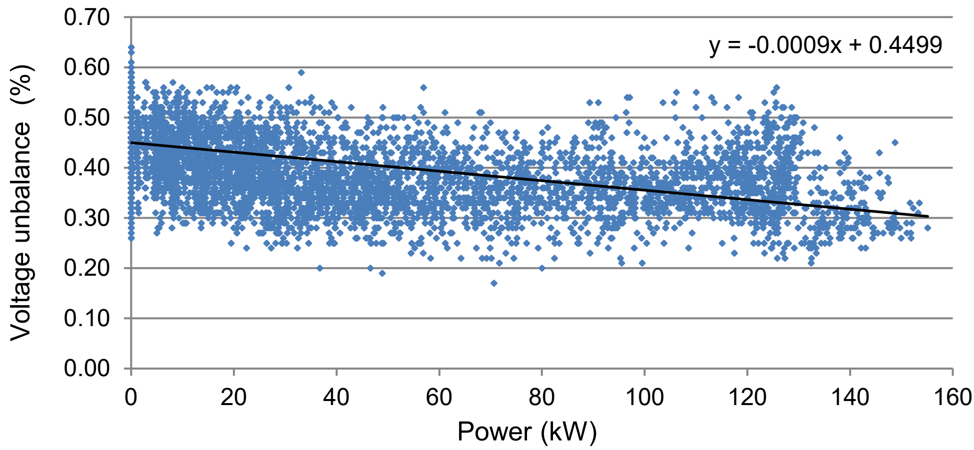

Figure 8. Voltage asymmetry as a function of output power during the first week, also with a trendline describing the relation to PV plant output power.

Fig. 8 shows the dependence of the voltage asymmetry on the output of the solar power plant. It shows visually that the points are horizontal rather than ascending or descending, although the trend line is descending. A decrease in asymmetry with productivity increases can be observed in the arrangement of the measuring points. In the first and third weeks, the average productivity was also higher than in the second week.

C. Voltage distortions

The dependence of the total harmonic distortion on the output power is shown in Fig. 9. The three-week trend line increases are in the range 0.0009 P_{out} to 0.0028 P_{out}, where P_{out} is the corresponding power output in kW. If P_{out} is replaced by the total power of the inverters, the harmonic total distortion of the voltages will increase, on average, between 0.14% and 0.45% at maximum output.

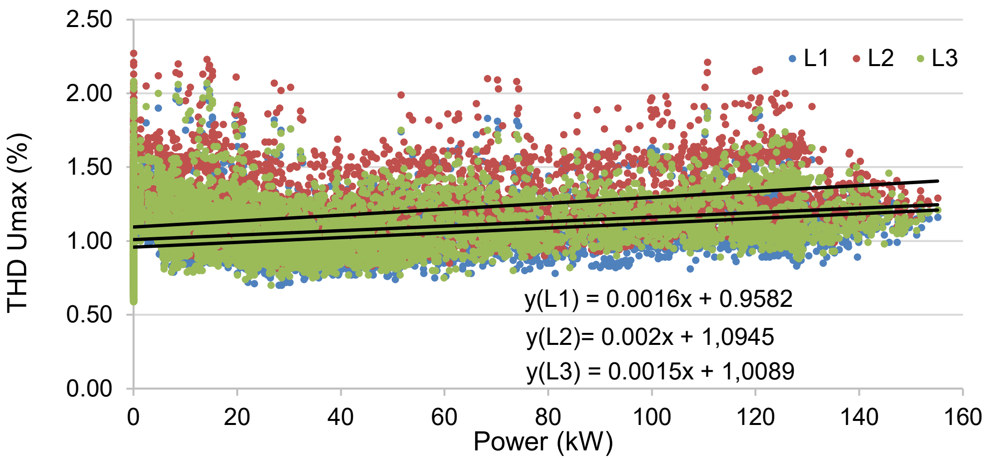

Figure 9. Voltage THD on the output of the solar power plant during the first week, plot based on output power.

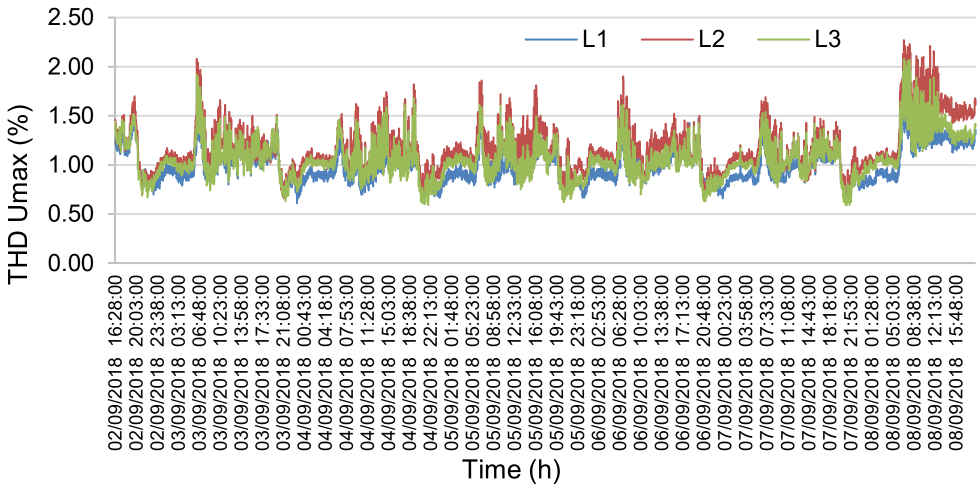

Figure 10. Voltage THD during the first week of measurement, detailed time plot.

Fig. 10 shows the total harmonic distortion of the voltage over three weeks' time. It can be seen from the figure that the level of total harmonic distortion during the night period is much lower than during the daytime. One reason for this may be the operation of the inverters of the solar power plant, but also the fact that consumers in the grid use more devices during the day, which can cause harmonic distortions in the grid.

D. Power output transients

An additional set of measurements were carried out at the PV plant with experimental shutdowns of the power plant. The most effective way to perform the shutdown was to through the use of the main switchboard, which can be seen in Fig. 11. Measurements were made with a PQ analyser unit, which provided recordings with a 1-sec sections of data for every two minutes.

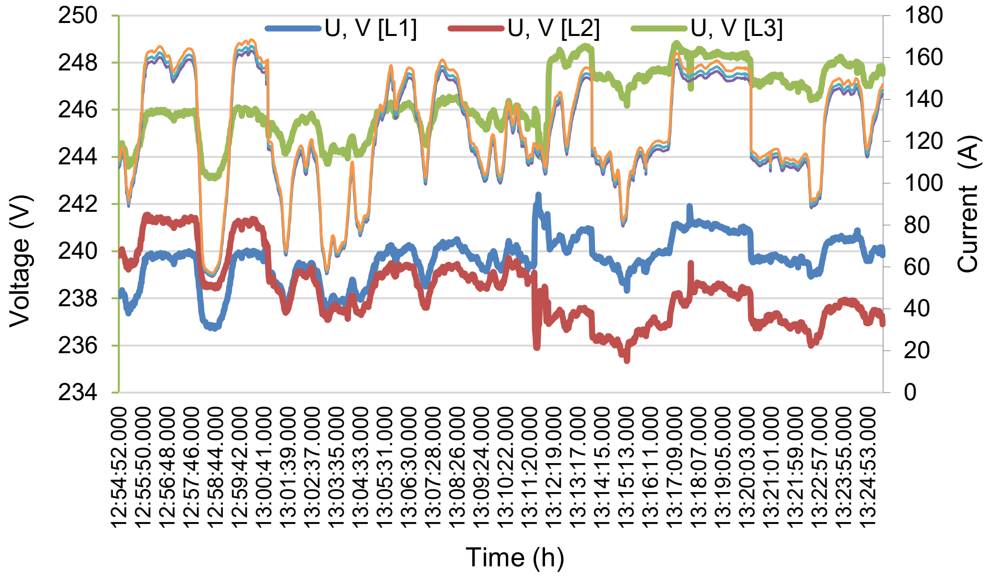

Figure 11. Switching off 2x20 kVA inverters for short periods.

On the main switchboard, two lines from the 20 kVA inverters were connected to one circuit breaker and four lines from the 30 kVA inverter units were connected to the second circuit breaker. Fig. 11 shows the voltage and current measurement data recorded during the shutdown period of the smaller production units. The graph shows that the sharp drop in production also has an immediate effect on the voltage level. As the two smaller inverters together make up only 25% of the total station output rating, it is not possible to clearly distinguish from the graph the moment when the clouds covered the sun for the station.

Fig. 12 shows a section of a period of voltage and current sine waveform. It can be seen in both figures that there is no significant distortion of the sinusoidal current and voltage in the phases. The voltage sine waveform is smoother than the current waveform, but the difference is rather small. The PEN conductor current in Fig. 12 reveals that high-frequency content with a magnitude close to 1 A is present. It can also be seen from

Fig. 12 that the PEN conductor current is in the same phase as the L1 phase current, i.e., when the L1 phase current is at its peak, the PEN conductor current is at its peak value.

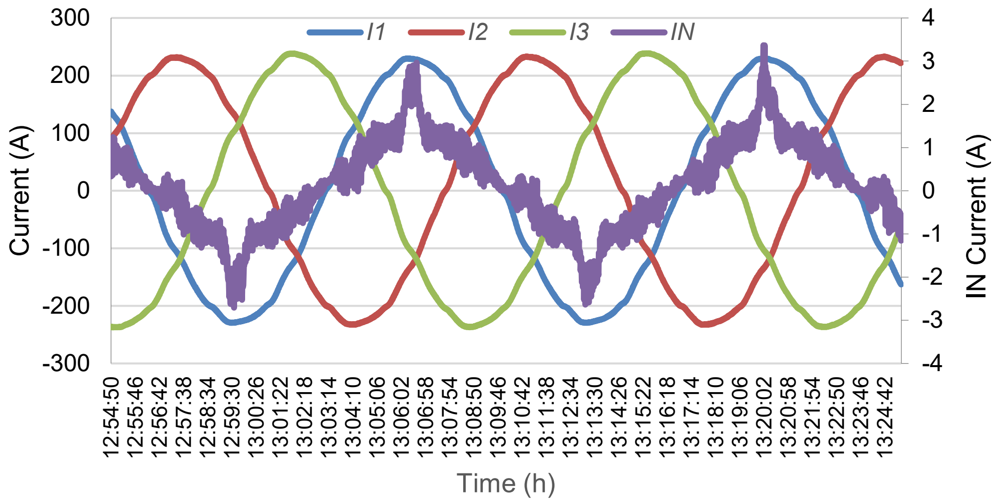

Figure 12. The current shape of three phases and PEN conductor for one period at a high output power.

Fig. 13 presents voltages and currents recorded during the whole station shutdown tests. The first shutdown was at 13:27, the second at 13:33 and the third was at 13:40. From 13:40 to 13:52 the solar power plant was kept isolated from the grid. At the same time, all six inverters were manually switched to idle mode and, at 13:52, the solar power inverters were connected to the mains in idle mode. Starting at 14:08 the inverters began operating in sequence to restore power to the grid.

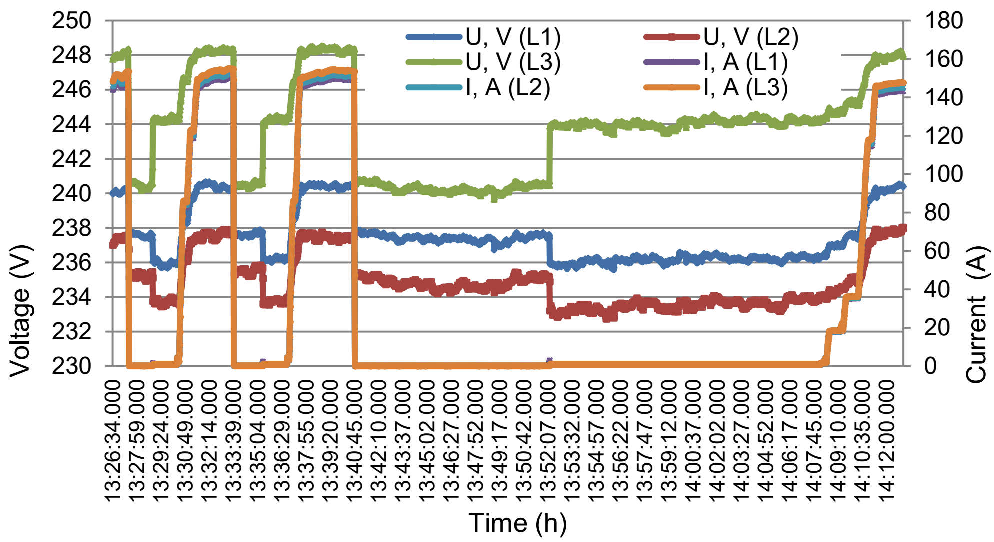

Figure 13. Network voltage and current exiting the station during attempts to disconnect the entire station.

The solar power plant was kept isolated from the grid for a longer period of time and also in idle mode to monitor both modes for extended periods. As a result of these experiments, it became clear that the inverters used in the power plant increase the phase-to-phase voltage difference in the low-voltage grid of the supplying substation. As shown in Fig. 13, when the power plant is switched on the voltages in phases L1 and L2 decrease by about 2 V and in phase L3 increase by about 4 V. As a result, the voltages of the phases L2 and L3 are 10 V instead of the previous 4…6 V.

At 13:28 and 13:35 the graph in Fig 13indicates that after the solar power plant is turned on, the inverters take about 2 minutes to reach full power. While productivity has increased sharply in the first two cases, productivity has increased gradually after being in idle mode. First, the 20 kVA inverters were turned on and then the remaining four 30 kVA inverters.

Fig. 14 shows the total harmonic distortion in the low-voltage grid of the supplying substation recorded during the station shutdown tests. The graph shows that the level of harmonic distortion is lowest when the solar power plant is isolated from the grid. The distortion is then up to 1%. At the time when the solar power plant inverters are turned on in idle mode, the harmonic distortion in the two phases increases by about 0.2%. The figure also shows that as the output of a solar power plant begins to increase, the proportion of total harmonic distortion of the voltage increases to 1.5%.

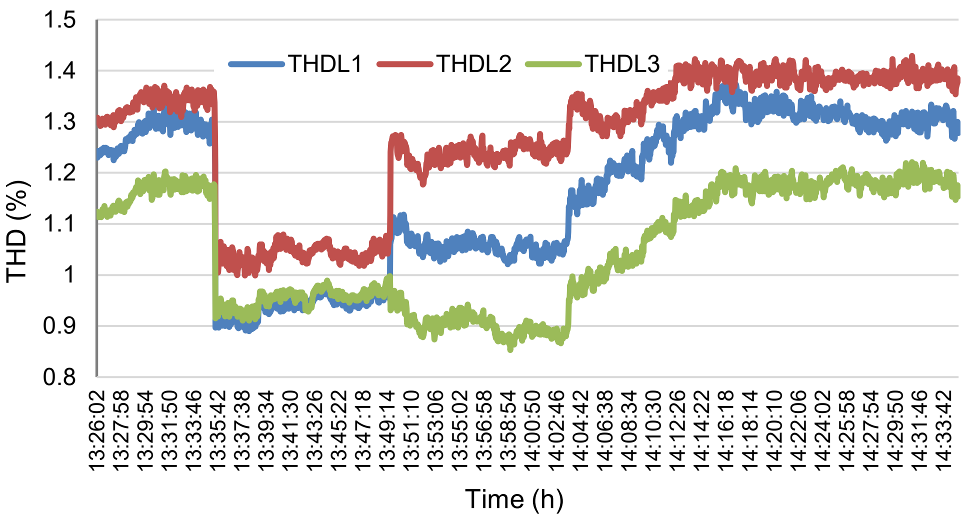

Figure 14. THD of three-phase voltages during disconnection attempts.

Fig. 15 shows the third harmonic level of the low voltage network. Phase L2 levels are approximately 2-fold greater than those of phases L1 and L3. The graph shows that the third harmonic level is independent of the productivity of the solar power plant. The harmonic level rises sharply the moment the inverters are connected to the mains in idle mode and then remains stable between 0.7% and 0.8%. The third harmonic limit stated in the relevant EN 50160 standard is 5%.

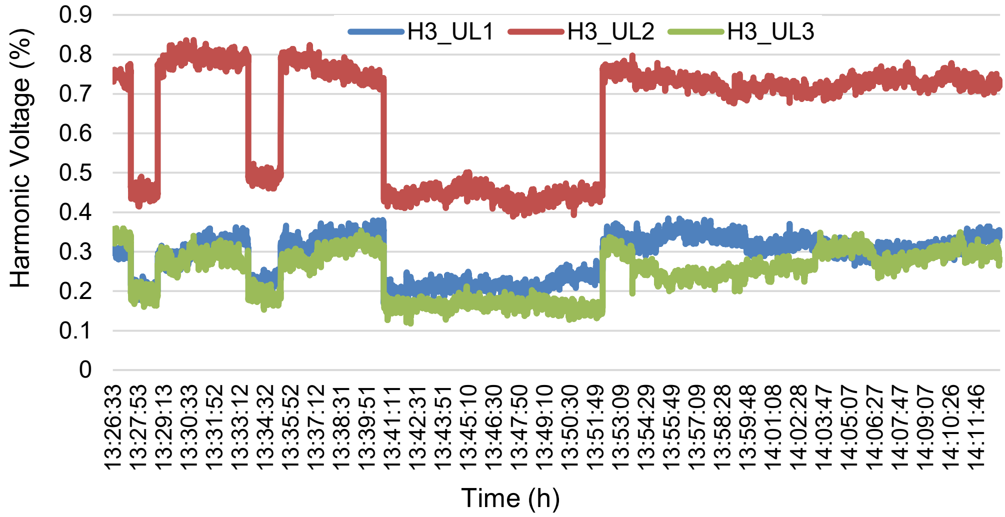

Figure 15. Voltage third harmonic levels during disconnection attempts.

Fig. 16 shows the 11th and 13th voltage harmonic levels of the low voltage network of supplying substation. Unlike the 3rd harmonic, the proportion of these harmonics will not increase until the solar power plant starts supplying electricity to the grid. The 11th harmonic levels are less than 0.9% and the 13th harmonic level below 0.4%. According to the standard EN 50160, the highest levels for the 11th and 13th harmonics are 3.5% and 3.0%, respectively. Similar is valid for the 17th and 19th voltage harmonics trends shown in Fig. 17. These harmonics are up to 0.4%, and the standard EN 50160 allows for 17th harmonics to be 2.0% and 19th harmonics to be 1.5%.

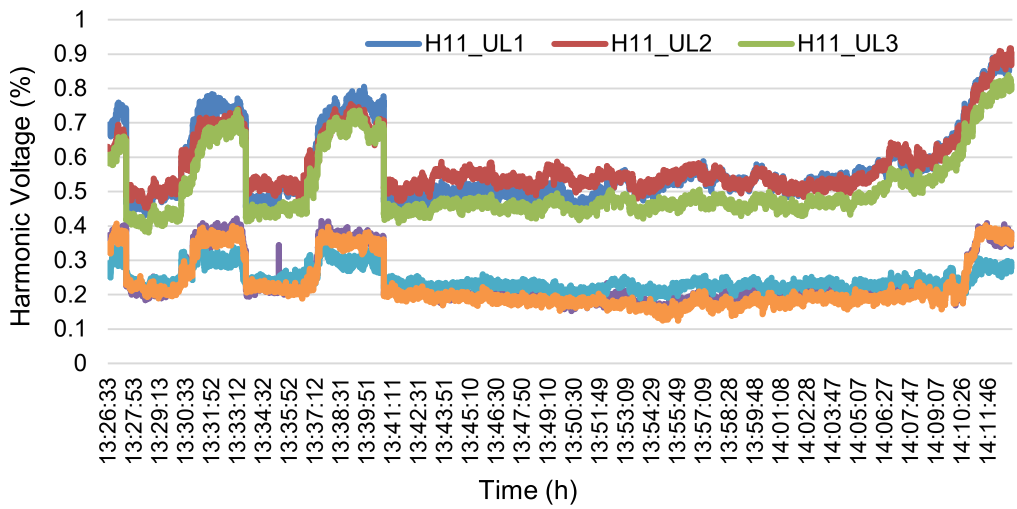

Figure 16. 11th and 13th voltage harmonics levels during disconnection attempts.

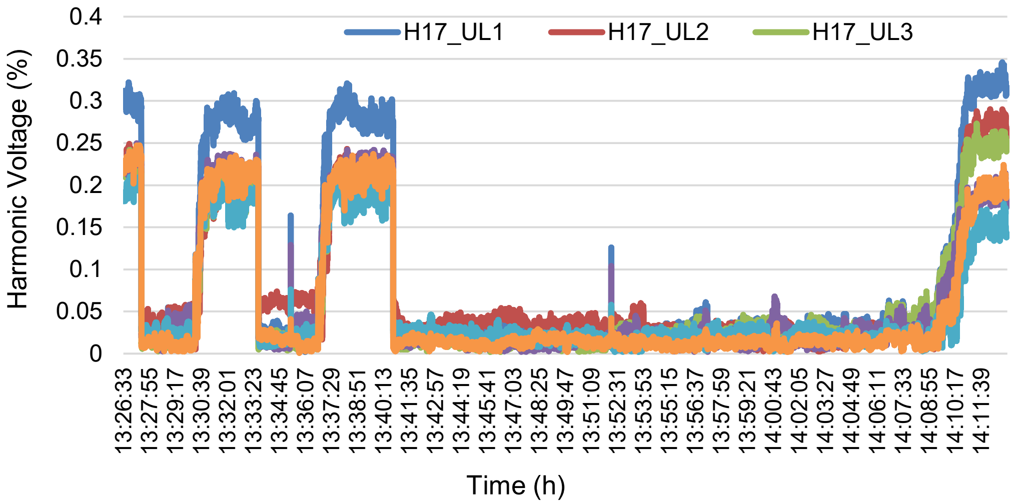

Figure 17. 17^{th} and 19^{th} Voltage harmonics during disconnection attempt.

CONCLUSIONS AND FUTURE WORK

As more and more PV microgeneration systems are installed to the LV grids, power quality issues in the LV networks have to be studied accordingly. While recently the number of studies addressing these problems has increased considerably impact of PV systems upon voltage quality in weak rural LV networks remains unclear.

Results in this paper reflect a 160 kW solar power plant and its impact on the LV network, with the daily average output power for the first week of measurements of is 56 kW, for the second week is 47 kW and for the third week is 50 kW. On average, the phase voltages increased from 236 V to 242 V when the power of the station was close to the maximum. Phase voltages fluctuated between 230 V and 246 V during the three weeks' time. In addition to the voltage increase, as the output power increases the solar power plant has an effect on the rapid change in voltage. The rapid change in power can be caused by clouds.

The measurement records included also the maximum and minimum voltages for one minute. The difference between these values was often up to 8 V over three weeks. Due to the clouds, the output power drop by 130 kW was recorded, resulting in a voltage drop of about 7 V. It is also clear from the figures that at night the mains voltage is more stable than during the day. The standard requires consumers to have a voltage within ± 10% of the rated voltage, or between 207 V and 253 V. As the voltage at the consumer, point depends on the parameters of the lines connecting to the substation, the available data from the substation does not allow an assessment of whether the consumer's supply voltage is above 207 V.

The positive impact of the PV power plant on the low voltage grid is manifested in reducing the voltage asymmetry by increasing the output power. The average reduction in asymmetry at 160 kW output power is from 0.50% to 0.35%, or 0.15%. Voltage asymmetry up to 1% is considered a high-quality indicator, however solar power plant still provides a reduction to it.

The measurements were expected to provide an insight into the effect of solar power inverters on the total harmonic distortion of a voltage. Measurements revealed the smallest voltage total harmonic distortion at the moment when the solar power plant is completely disconnected from the grid. The distortion increased by about 0.2% when the inverters were connected to the grid in idle mode, and when the power was supplied to the grid, the proportion of total harmonic distortion increased further by about 0.3%. This means that due to the solar power plant, the total harmonic distortion in the grid would increase by 0.5%. Since only a few cases had a total harmonic distortion of more than 2% over a 3-week period, these solar power inverters are rather unlikely to cause the permitted values to be exceeded in this particular grid.

The analysis was carried out for both sunny, cloudy and alternating cloudy days. As the measurements were conducted in September, when the intensity of the sun is not at peak, some more measurements in the middle of summer with the highest intensity of the sun and longest daytime are feasible. Measurements should also be carried out on this low-voltage grid in the winter when the solar power plant is in standby rather than in operation for most of the time. These additional measurements would allow a more accurate assessment of the effect of this solar power plant on the low voltage grid.

In addition, tests could be conducted on how a given PV plant will behave when the transformer is shut down. It is also unknown at this time how this solar plant will respond to short circuits in both low voltage and high voltage networks. Attempts to answer these questions would require prior coordination with consumers, as power outages may occur.

ACKNOWLEDGMENTS. This work was supported by the Estonian Research Council grant PSG142.

REFERENCES

Chen, C. & Liu, H. 2019. Medium-term wind power forecasting based on multi-resolution multi-learner ensemble and adaptive model selection. *Energy Conversion and Management* **206** (November 2019), 112492. https://doi.org/10.1016/j.enconman.2020.112492

Demolli, H., Dokuz, A.S., Ecemis, A. & Gokcek, M. 2019. Wind power forecasting based on daily wind speed data using machine learning algorithms. *Energy Conversion and Management* **198**(March), 111823. https://doi.org/10.1016/j.enconman.2019.111823

Farhoodnea, M., Mohamed, A., Shareef, H. & Zayandehroodi, H. 2012. Power quality impact of grid-connected photovoltaic generation system in distribution networks. *SCOReD 2012 - 2012 IEEE Student Conference on Research and Development*, pp. 1–6. https://doi.org/10.1109/SCOReD.2012.6518600

González, P., Romero, E., Miñambres, V.M., Guerrero, M.A. & González, E. 2014. Grid-connected PV plants. Power quality and technical requirements. *9th International: 2014 Electric Power Quality and Supply Reliability Conference, PQ 2014 - Proceedings*, pp. 169–176. https://doi.org/10.1109/PQ.2014.6866804

Grasso, F., Luchetta, A. & Manetti, S. 2018. Measurement of Electric Power Quantities and Efficiency in Nonsinusoidal Conditions.

Gürtürk, M. 2019. Economic feasibility of solar power plants based on PV module with levelized cost analysis. *Energy* **171**, 866–878. https://doi.org/10.1016/j.energy.2019.01.090

Hassan, A., Rehman, A.U., Shabbir, N., Hassan, S.R., Sadiq, M.T. & Arshad, J. 2019. Impact of Inertial Response for the Variable Speed Wind Turbine. *2019 International Conference on Engineering and Emerging Technologies (ICEET)*, pp. 1–6. https://doi.org/10.1109/ceet1.2019.8711826

Iqbal, M.N., Kütt, L. & Shabbir, N. 2018. Modeling of lighting load in residential buildings. *International Journal of Engineering and Advanced Technology* **8**(May), 232–236.

Jayasekara, N. & Wolfs, P. 2010. Analysis of power quality impact of high penetration PV in residential feeders. *AUPEC 2010 - 20th Australasian Universities Power Engineering Conference: "Power Quality for the 21st Century,"* pp. 1–8.

Kopicka, M., Ptacek, M. & Toman, P. 2014. Analysis of the power quality and the impact of photovoltaic power plant operation on low-voltage distribution network. *9th International: 2014 Electric Power Quality and Supply Reliability Conference, PQ 2014 - Proceedings*, pp. 99–102. https://doi.org/10.1109/PQ.2014.6866792

Kumary, S.V.S., Oo, V.A.A.M.T., Shafiullah, G.M. & Stojcevski, A. 2014. Modelling and power quality analysis of a grid-connected solar PV system. *2014 Australasian Universities Power Engineering Conference, AUPEC 2014 - Proceedings*, (October), 1–6. https://doi.org/10.1109/AUPEC.2014.6966605

Meyer, J. & Kilter, J. 2014. Case studies for power quality monitoring in public distribution grids - Some results of working group CIGRE/CIRED C4.112. *9th International: 2014 Electric Power Quality and Supply Reliability Conference, PQ 2014 - Proceedings*, pp. 85–92. https://doi.org/10.1109/PQ.2014.6866790

Pakonen, P., Hilden, A., Suntio, T. & Verho, P. 2016. Grid-connected PV power plant induced power quality problems - Experimental evidence. *2016 18th European Conference on Power Electronics and Applications, EPE 2016 ECCE Europe*, pp. 1–10. https://doi.org/10.1109/EPE.2016.7695656

Ruwaida, Y. & Holmberg, D. 2015. *23 rd International Conference on Electricity Distribution Paper 1017* MAPPING OF HARMONIC LEVELS IN THE LOW-VOLTAGE NETWORK (June), 15–18.

Seme, S., Lukač, N., Štumberger, B. & Hadžiselimović, M. 2017. Power quality experimental analysis of grid-connected photovoltaic systems in urban distribution networks. *Energy* **139**, 1261–1266. https://doi.org/10.1016/j.energy.2017.05.088

Shabbir, N., AhmadiAhangar, R., Kütt, L., Iqbal, M.N. & Rosin, A. 2019. Forecasting Short Term Wind Energy Generation using Machine Learning. *2019 IEEE 60th International Scientific Conference on Power and Electrical Engineering of Riga Technical University (RTUCON)*, pp. 1–4. https://doi.org/10.1109/RTUCON48111.2019.8982365

Shabbir, N., Usman, M., Jawad, M., Zafar, M.H., Iqbal, M.N. & Kütt, L. 2020. Economic analysis and impact on national grid by domestic photovoltaic system installations in Pakistan. *Renewable Energy* **153**, 509–521. https://doi.org/10.1016/j.renene.2020.01.114

Shi, Q. 2014. *Power Quality Impact of Photovoltaic Systems on Residential Distribution Networks*. University of Alberta. https://doi.org/10.1038/132817a0

Tan, K.H., Logenthiran, T. & Woo, W.L. 2017. Forecasting of wind energy generation using Self-Organizing Maps and Extreme Learning Machines. *IEEE Region 10 Annual International Conference, Proceedings/TENCON*, pp. 451–454. https://doi.org/10.1109/TENCON.2016.7848039

Urbanetz, J., Braun, P. & Rüther, R. 2012. Power quality analysis of grid-connected solar photovoltaic generators in Brazil. *Energy Conversion and Management* **64**, 8–14. https://doi.org/10.1016/j.enconman.2012.05.008

Vinnal, T., Jarkovoi, M. & Kutt, L. 2018. Harmonic currents and voltages in lv networks of Estonia : Measurement results, case studies. *2018 IEEE 59th Annual International Scientific Conference on Power and Electrical Engineering of Riga Technical University, RTUCON 2018 - Proceedings*. https://doi.org/10.1109/RTUCON.2018.8659875

Agronomy Research **18**(4), 2653–2664, 2020
https://doi.org/10.15159/AR.20.168

Influence of regional technologies of varying intensity on the bioproductivity of sod-podzolic medium loamy soil in the Central region of the Russian Federation

S.M. Viyugin[1,*], A.V. Kuchumov[2], G.V. Viyugina[3], S.E. Terentyev[4] and I.A. Karamulina[1]

[1]Smolensk State Agricultural Academy, Faculty of Engineering and Technology, Department of Agronomy, Land Management and Ecology, 10/2 B. Sovetskaya Str., RU214000 Smolensk, Russia
[2]Smolensk State Agricultural Academy, Faculty of Economics, Department of Production Management, 10/2 B. Sovetskaya Str., RU214000 Smolensk, Russia
[3]Smolensk State University, Faculty of Natural Geography, Department of Biology and Ornamental Crop Production, 4 Przhevalskogo Str., RU214000 Smolensk, Russia
[4]Smolensk State Agricultural Academy, Faculty of Engineering and Technology, Department of Agricultural Processing Technology, 10/2 B. Sovetskaya Str., RU214000 Smolensk, Russia
[*]Correspondence: vyugin_sm@mail.ru

Abstract. This study is oriented to elucidating the role of the basic elements of regional farming systems in soil-crop complex using agricultural technologies of different levels of cultivation of field crops in the Smolensk Region.
As a result of monitoring carried out in 1991–2008 on a reference site located in the Smolensk Region, negative changes of soil profile were revealed. Degree of soil podzolization increased what contributed to its degradation. All genetic horizons demonstrated deterioration in the basic parameters of soil fertility.
Many years of experience showed a significant influence of the elements of studied technologies on soil acidity parameters, on the level of available phosphorus and exchangeable potassium; the amount of humic compounds was, however, characterized by relative stability.
According to the total grain harvest of winter rye, spring soft wheat and barley, as well as of the green mass of perennial and annual herbs, studied variants were ranged in the following order: intensive, organic, adaptive, and extensive. Organic technology is suitable for getting environmentally friendly products.
Obtained results are recommended to be used in the development of regional technologies of various intensity for the bio-productivity of sod-podzolic medium loamy soil in the Central region of the Russian Federation, as well as in regions with similar soil and climatic conditions. Choice of particular variant is in each case determined by the baseline characteristics of soil, planned level of productivity and harvest quality, availability of material and monetary resources in the economy.

Key words: agrochemical soil parameters, agroecological monitoring, soil bio-productivity, sod-podzolic soil, soil profile, regional technologies, organic technology, crops, six-field field grain and grass crop rotation.

INTRODUCTION

Unstructured intensification of agricultural production leads to an unreasonably high anthropogenic load on agrocoenosis.

As a result, the content of mobile compounds of aluminum, manganese, pesticide residues increases in soil, plants, groundwater and water bodies, aa well as large amount of nitrate nitrogen, and other substances that are toxic to soil and plants and negatively affect crop yields and the quality of crop products (Ladonin et al., 1996; Chernikov et al., 2001; Viyugina & Viyugin, 2003; Stehlík, et al., 2019).

The most important task of the emerging multi-structured agriculture in the Central region of Russia is sustainable increase of agricultural productivity. In the context of heightened environmental and socioeconomic problems, it is necessary to revise the main links of existing farming systems with a view to adapting them to local soil and climatic conditions (Kiryushin, 2011).

The low natural fertility potential of sod and podzolic soils causes the need for intensive development of the agricultural industry with extensive use of chemical and modern treatments of soil (Bahirev, 2016).

However, it is possible to increase the rate of production of high quality agricultural products in the current environment only with the transition to environmentally sound and economically sound systems of fertilizers and pesticides application, providing in addition to high yields extended reproduction of soil fertility and sustainable state of agrocenoses (Kiryushin & Kiryushin, 2015).

In developing regional farming systems, it is necessary to take into account the fact that the interaction between components of agrocenosis should be optimal and not limit potential yields of agricultural crops (Bahirev, 2016; Cherkasov, 2016).

To eliminate negative environmental consequences, with a view to the sustainable development of agricultural production in Russia, a number of scientists have developed scientifically based methodological principles for the design of adaptive landscape farming systems that can improve environmental sustainability of agricultural landscapes, stabilize fertility reproduction and prevent soil degradation, and optimize soil processing system due to its minimization (Kashtanov et al., 1994; Kiryushin, 2011; Viyugin & Viyugina, 2014).

Currently in the Russian Federation, there is official law No. 280-FZ dated August 3, 2018 'On Organic Production and Amendments to Certain Legislative Acts of the Russian Federation' that includes Article 8 'Transition to Organic Agriculture and Organic Production'. The Federal Law on organic agriculture states that the technology of cultivating organic products allows obtaining eco-friendly agricultural products, raw materials and food. In this regard, developing technologies for organic crop cultivation is relevant. Under present-day conditions, organic agricultural production will contribute to solving a large number of problems, since this method provides for an almost complete rejection of mineral fertilizers, pesticides and genetically modified organisms (Akimova & Polushkina, 2015).

The relevance of the long-term experimental studies is that in the modern economic and social situation taking into account environmental contradictions in the Russian Federation, including the Central region of Russia, detailed adaptation of agriculture to multi-level production relations under different soil-climatic conditions is required, when earlier developed methods of farming systems construction do not fully meet the demands of producers.

In this regard, a new methodical approach is relevant in the development and construction of highly effective balanced technologies of crops cultivation in agricultural systems of different intensity determined by different level of material, technical and financial situation of a particular commodity producer in the conditions of the Central region of the Non-Chernozem Zone of the Russian Federation.

The scientific novelty of the multi-year study is that experimental data obtained over 18 years in three rotations of six-field grain and herb crop rotation allowed to study dynamics of the main agrochemical indicators of sod and podzolic soil fertility and productivity of grain and herb crop rotation under the influence of different modifications of regional cultivation technologies of field crops, which are characteristic to farming systems of varying intensity in the conditions of the Central region of the Non - Chernozem Zone of the Russian Federation. The obtained results of the research are recommended to be used in the development of specific regional technologies of crops cultivation on sod-podzolic medium-clay soil in the Central region of the Russian Federation taking into account the initial characteristics of the soil, the planned level of yield and its quality, the availability of material and monetary resources in the economy.

Forecasting optimal land use conditions in agricultural production with the goal of sustainable and cost-effective increase in the fertility of sod-podzolic soils with minimal risks for ecological condition and ecological functions of soils is possible only under the conditions of many years of stationary field experiments laid down in compliance with the basic rules of field experiment methodology (Shatilov, 2001; Shamanaev et al., 2006; Hospodarenko et al., 2018).

OBJECTS AND METHODS

To carry out monitoring studies and the subsequent laying of stationary experiment in 1991, a land plot was selected in the third field of the six-field crop rotation field of Smolensk Agricultural Experimental Agricultural Institute. Results of test sowing and the subsequent accounting of barley crop by working plots showed that the variations in grain yield in repeated plots was insignificant, so this indicates its agrochemical and agrophysical homogeneity.

Before laying a field multifactor experiment for a detailed study of the territorial variability of fertility of sod-podzolic medium loamy soil on July 25, 1991, profile 1 was laid on the reference site. The profile is located at a border check irrigation of the field multifactorial experiment with the extensive variant of agricultural cultivation where no mineral and organic fertilizers or chemical plant protection products against weeds, pests and diseases are provided. In 2008, profile 1a located near profile 1 made in 1991 was laid on the reference site.

Based on the long-term stationary field experience of the Smolensk State Agricultural Academy from 1991 to 2008, agroecological monitoring studies were carried out to study the effect of various modifications of regional technologies for cultivating crops in agricultural systems of varying intensity on the fertility of sod-podzolic soil and the productivity of grain-crop rotation in the conditions of the Central region of the Non-Black Earth Zone of the Russian Federation.

Experimental design included four modifications of regional crop cultivation technologies.

1. Extensive technology - according to experimental scheme, no mineral or organic fertilizers, as well as pesticides were applied. Preparation system included 10–12 cm afterharvesting tillage; 20–22 cm moldboard plowing; early spring harrowing, and 10–12 cm pre-sowing cultivation. Sowing was carried out with a seeding rate established by the number of germinating seeds.

2. Adaptive technology - N55P45K45 kg of AI ha^{-1} were applied in the rotation on average per 1 hectare. Pesticides were added based on average recommended doses. Preparation system included 10–12 cm afterharvesting tillage; 20–22 cm autumn plowing in combination with subsoiling of 32–35 cm; early spring harrowing, and pre-sowing cultivation. Seed was treated with the average dose of fungicide, and weight sowing rate was determined by the number of germinating seeds.

3. Intensive technology - average annual dose of mineral fertilizers was N85P75K75 kg of AI ha^{-1}. Pesticides were added based on maximum recommended doses. Preparation system included 10–12 cm afterharvesting tillage; 35 cm deep nonmoldboard loosening using chisel plow and 10–12 cm disking; early spring harrowing, 10–12 cm complete cultivation, and 8–10 cm pre-sowing cultivation. The seed was treated with the maximum possible dose of fungicide against diseases, and weight sowing rate was determined by the number of germinating seeds.

4. Organic technology - average annual dose of organic fertilizers was 12 t ha^{-1}. Preparation system included 10–12 cm afterharvesting tillage; 20–22 cm autumn plowing; early spring harrowing and 10–12 cm pre-sowing cultivation. According to this technology, heating of seeds with hot air was carried out before sowing. Weight sowing rate was determined by the number of germinating seeds. Agrotechnical methods and biological techniques were used for regulating the phytosanitary state of crops. This technology is designed to produce environmentally friendly products for baby and diet food.

In addition to the methods studied, agrotechnical methods of crop cultivation were common for the Central region of the Non-Chernozem Zone of the Russian Federation, including the Smolensk Region.

In this experiment, varieties cultivated were in the State Register of Breeding Achievements Approved for Use in the Central Region of the Non-Black Earth Zone of the Russian Federation.

In this experiment, nitrophoska, ammonium nitrate, double superphosphate and 60% potassium salt and well-rotted cattle manure were used.

A multifactor field stationary experiment was laid down by split-plot method in 4 repetitions, on sod-medium loamy soil formed on cover loam, with arable horizon thickness of 20–22 cm. Area of an accounting plot was 44 m^2 (5.5×8 m). Soil samples were taken from the arable layer (20–22 cm) at the end of the first, second and third rotation during six-field crop rotation. Samples for analysis were taken from two non-adjacent repetitions from 30 points followed by the formation of a mixed sample for each variant of the experiment. Sample size was determined by E.A. Dmitriev (Dmitriev, 1995; Kiryushin, 2011).

Baseline agrochemical parameters of soil in field experiment were as follows: humus - 1.96%; pH_{ac} - 6.2; Ha - 2.8 cmol kg^{-1} of soil; S - 15 cmol kg^{-1} of soil; mobile phosphorus - 177 mg kg^{-1} of soil, mobile potassium - 220 mg kg^{-1} of soil.

The pattern of crop rotation for this experiment was as follows:

1. Vetch-oatmeal mix for green fodder. 2. Winter rye. 3. Barley with undersowing of clover-timothy mix. 4. Clover-timothy mix of 1 year of use. 5. Clover-timothy mix of 2 years of use. 6. Spring wheat.

The studies were carried out according to the following methods: humus - according to Tyurin in the modification by Central Research Institute of Agrochemical Services [GOST 26113-91]; pH_{KCl} - potentiometrically (GOST 26487-85); mobile phosphorus and potassium - according to Kirsanov [GOST 26207-93]; amount of absorbed bases - according to Kappen-Gilkovits; Kappen hydrolytic acidity in the modification by Central Research Institute of Agrochemical Services (GOST 26212-91). To analyze experimental data, we calculated statistical parameters of samples with quantitative variability of trait and used analysis-of-variance method (Dmitriev, 1995; Dospekhov, 1985; Akimova & Polushkina, 2015).

RESULTS AND DISCUSSION

Before laying a field multifactor experiment, profile 1 was laid for monitoring the patterns of territorial variability of fertility of sod-podzolic medium loamy soil in the reference area.

The following is a description of the morphological features of the genetic horizons of the soil profile 1 started in 1991.

A_p 0–22 is an arable layer, dark gray with a slightly brown hue, loose, penetrated by worms channels and plant roots, there are semi-decomposed parts of root system, lumpy-granular structure is relatively strong, moist, medium loamy with gradual transition to A_1A_2 horizon.

A_1A_2 22–38 is a transitional humus-eluvial, yellow-brown layer, of cloddy-nutty structure, with large number of roots and worm channels, compacted, moist, transition to A_2B horizon is smooth.

A_2B 38–74 is a transitional eluvial-illuvial horizon, yellowish-brown with bright flashes, of weak nutty structure, dense, with rare roots, moist, transition to horizon B is gradual.

B 74–98 is an illuvial horizon, yellow-brown, moist, densified, medium loamy, transition to horizon C is clear.

C 98–155 is a mother rock: clay loam mantle, yellowish-brown, very dense, moist.

Nomenclature of soil according to the 1977 classification is sod-podzolic, slightly podzolized, medium loamy soil on clay loam mantle (Umbric ALBLUVISOKS) (Egorov et al., 1977; Jørgensen, 2014; Naumov, 2016).

In 2008, laying down of the second 1a profile located near profile 1 was carried out. Repeated study of soil profile after 18 years of monitoring studies made it possible to trace changes in the composition and properties of soil at the polygon during many years of stationary field experiment.

Over specified period, the thickness of arable horizon decreased by 2 cm and, accordingly, the thickness of A_1A_2 and A_2B horizons increased what increased the degree of soil podzolization and contributed to its degradation.

The following is a description of the morphological features of genetic horizons in 2008.

A_p 0–20 is an arable horizon, gray with a brown hue, moist, dense, densely penetrated by plant roots and worm channels, of cloddy-lumpy-dusty structure, medium loamy with a gradual transition to A_1A_2 horizon.

A_1A_2 20–40 is a transitional humus-eluvial horizon, pale-whitish in color, of cloddy-nutty structure, with worm channels and roots, compacted, moist, transition to A_2B is gradual.

A_2B 40–76 is a transitional eluvial-illuvial horizon, yellowish-brown with flashes, grayish-whitish powdering of tongued form, of cloddy-nutty structure, dense, moist, root channels are visible, transition to horizon B is gradual.

B 76–96 is an illuvial horizon, yellowish-brown, moist, very dense, medium loamy, transition to the mother rock is clear.

C 96–156 is a mother rock: clay loam mantle, yellowish-brown, very dense, moist.

Nomenclature of soil according to profile No. 1a according to the 1977 classification is sod-podzolic, medium-podzolic, medium loamy soil on clay loam mantle.

A comparative analysis of the dynamics of changes in the agrochemical properties of the genetic horizons of soil profile in 2008 (profile 1a) compared with 1991 (section 1) is shown in Table 1.

Table 1. Agrochemical parameters of the genetic horizons of sod-podzolic medium loamy soil, profile 1a, 2008

Parameters	A_p 0–20 cm		A_1A_2 20–40 cm		A_2B 40–76 cm		B 76–96 cm		C 96–156 cm	
	2008	± to 1991	2008	± to 1991	2008	± to 1991	2008	± to 1991	2008	± to 1991
Humus, %	1.82	-0.20	1.27	0.31	0.50	-0.33	0.27	-0.25	0.21	-
pH_{KCl}	5.57	-0.63	5.37	-0.63	3.39	-0.95	3.18	-1.05	4.13	-0.49
Ha, cmol kg^{-1} of soil	3.04	-0.18	2.52	-0.21	2.95	-0.29	2.62	-0.35	2.95	-0.28
S, cmol kg^{-1} of soil	14.0	-0.8	11.1	-1.0	10.1	-1.2	8.7	-1.4	11.7	-1.1
V, %	82.2	-4.3	81.5	-5.7	77.4	-6.7	76.9	-9.3	79.9	-8.8
P_2O_5 mg kg^{-1}	102	-70	97	-48	84	-36	50	-35	40	-23
K_2O, mg kg^{-1}	90	-30	104	-38	52	-42	41	-34	27	-16

In 2008, humus content in A_p horizon decreased by 9.9%, in A_1A_2 horizon - by 19.6%, in A_2B horizon - by 37.1%, and in horizon B - by 48.1%. Absolute reserves of humus calculated taking into account the thickness of genetic horizons and their density decreased similarly.

Judging by pH_{KCl} value, exchange acidity in A_p horizon increased with the depth along the soil profile by 10.2%, in A_1A_2 horizon - by 8.3%, in A_2B horizon - by 21.9%, and in B horizon - by 24.8%.

In 2008, hydrolytic acidity in horizon A_p increased in comparison with 1991 by 6.2%, in horizon A_1A_2 - by 8.3%, in horizon A_2B - by 9.8%, and in horizon B - by 13.4%. Amount of absorbed bases decreased with the depth of profile from 14.0 to

8.7 cmol kg^{-1} of soil and the degree of soil saturation with bases - from 82.2 to 76.9%.

The content of mobile forms of phosphorus in arable horizon decreased from 172 to 102 mg kg^{-1}, or by 40.7%, in A_1A_2 - by 33.1%, in A_2B - by 30%, in horizon B - by 41.1%. In a similar way, the content of exchange potassium changed along the soil profile.

Summarizing the abovementioned, it should be noted that the deterioration of agrochemical parameters of soil fertility at the monitoring polygon during 18 years of observation is due primarily to the fact that the cultivation of crops was carried out according to extensive technology (variant 1).

The basis of further monitoring studies, from the moment of start in 1991 and up to 2008, was a long-term stationary multi-factorial field experiment of the Smolensk State Agricultural Academy.

Experimental data obtained over 18 years of research in three rotations of a six-field grain-grass crop rotation made it possible to study dynamic changes in basic agrochemical parameters of the fertility of sod-podzolic soil and the productivity of a grain-grass crop rotation under the influence of various modifications of regional cultivation technologies for field crops that are typical for farming systems of varying intensity in the conditions of the Central Region of the Non-Black Earth Zone of the Russian Federation.

Modifications of regional technologies studied in this experiment, with different types and doses of added fertilizers, had an different effect on the soil acidity of arable horizon. Results of these studies in arable horizon are summarized in Table 2. In the variant with extensive technology where no mineral fertilizers are provided, a maximum acidification of a soil solution was specified: for the first rotation by 10.1%, for the second - by 12.4%, and for the third - by 14.2% compared to baseline data.

Table 2. Influence of the modifications of regional technologies on the physicochemical properties of arable horizon of sod-podzolic medium loamy soil

Technologies	Rotation I 1991–1996			Rotation II 1997–2002			Rotation III 2003–2008		
	pH_{KCl}	Cmol kg^{-1} of soil		pH_{KCl}	Cmol kg^{-1} of soil		pH_{KCl}	Cmol kg^{-1} of soil	
		H_a	S		H_a	S		H_a	S
1.	5.57 ± 0.12*	3.0 ± 0.05	14.0 ± 1.1	5.43 ± 0.11	3.2 ± 0.04	13.8 ± 0.9	5.32 ± 0.09	3.4 ± 0.03	13.0 ± 0.8
2.	5.83 ± 0.11	2.7 ± 0.03	15.8 ± 1.3	5.76 ± 0.10	2.5 ± 0.02	16.6 ± 1.4	5.73 ± 0.11	2.3 ± 0.01	17.4 ± 1.4
3.	5.79 ± 0.11	2.4 ± 0.04	17.3 ± 1.5	5.70 ± 0.9	2.2 ± 0.01	18.9 ± 1.6	5.61 ± 0.10	2.0 ± 0.09	20.2 ± 1.8
4.	6.39 ± 0.14	2.2 ± 0.02	19.0 ± 1.7	6.63 ± 0.13	2.0 ± 0.01	24.0 ± 1.9	6.72 ± 0.14	1.8 ± 0.08	26.0 ± 2.1

Note: 1 – extensive; 2 – adaptive; 3 – intensive; 4 – organic; * arithmetic mean error.

Low doses of mineral fertilizers added under crops using adaptive technology contributed to a slight increase in the acidity of soil solution, by crop rotations, respectively: 5.9%, 7.1%, and 7.6%.

Adding increased doses of mineral fertilizers when cultivating crops using intensive technology increased the acidity of soil solution, by crop rotations, respectively: 0.41 units pH_{KCl} (7.1%); 0.50 units pH_{KCl} (8.1%); 0.59 units pH_{KCl} (9.5%). Organic technology including cattle manure as the main fertilizer contributed to a fairly intensive neutralization of soil solution. The value of pH_{KCl} was increased, by crop rotations, respectively: +0.19 units pH_{KCl} (3.1%); +0.43 units pH_{KCl} (6.9%); +0.52 units pH_{KCl} (8.4%).

Hydrolytic acidity of the soil, against an extensive background without fertilizing, increased compared to baseline by 7.1; 14.3 and 21.4% according to crop rotation. When cultivating crops using adaptive technology, parameters of hydrolytic acidity decreased, by crop rotations, by 3.6; 10.7; 17.9%, using intensive technology - by 14.3, 21.4, and 28.6%, respectively.

The most prominent parameters for optimizing soil fertility were noted with using organic technology where the improvement in hydrolytic acidity compared to the extensive technology was, by crop rotations: 21.4, 28.6, and 35.7%.

The data on the influence of different technologies on the amount of absorbed bases are of real interest. Maximum decrease in the amount of absorbed bases compared to the baseline was noted in the arable layer during using extensive technology, respectively, by: 1.0 (3.1%), 1.2 (3.1%), 2.0 (3.1%) cmol kg^{-1} of soil.

Using mineral fertilizers in adaptive technology has led to an increase in the amount of absorbed bases in the arable horizon, by crop rotations, respectively: + 0.8, + 1.6, + 2.4 cmol kg^{-1} of soil. Higher rates of the enrichment of arable horizon with absorbed bases were noted in the variant with intensive technology, by crop rotations, respectively: + 2.3, + 3.9, + 5.2 cmol kg^{-1} of soil.

Regular adding of manure provided by organic technology ensured a substantial increase in the amount of absorbed bases in arable layer, by crop rotations, by: 4.0, + 9.0, + 11.0 cmol kg^{-1} of soil. When adding manure under winter crops, an increase in the amount of absorbed bases in the arable layer was revealed. Therefore, using manure for sod-podzolic soils contributes to the fixation and accumulation of calcium and magnesium in arable layer.

Thus, under the conditions of long-term stationary field experiment, the modifications of regional technology are arranged in the following order according to the degree of influence on the cation exchange properties of soil: extensive, adaptive, intensive, organic. Summarizing the results obtained, it should be noted that soil cultivation with periodic adding of manure and mineral fertilizers in various doses, during three phases of crop rotation, improved the physical and chemical parameters of sod-podzolic soil studied in the course of this experiment.

Dynamic changes in soil humus can demonstrate the effectiveness of technologies used for cultivating crops (Ladonin et al., 1996; Antille et al., 2019).

Table 3 shows the experimental data on the changes in humus content with different modifications of regional technologies during the experiment.

With extensive technology (control variant), there was a sharp decrease in humus in arable layer during the first phase of crop rotation by 0.2%, during the second - by 0.24%, and during the third - by 0.29%. That is, extensive use of soil without adding organic substances and with low yields by crop rotations resulted in intensive degradation of arable horizon.

When adding different doses of mineral fertilizers, there was also a slight decrease in humus content in arable horizon from the baseline (1.96%), by crop rotation with adaptive technology, respectively: by 0.17, 0.13, and 0.07%; with intensive technology - by 0.13, 0.07, and 0.02%. At the same time, adaptive and intensive technologies, during the third rotation as compared with the first one, demonstrated relatively low rates of humus accumulation (0.10 and 0.11%) due to an increase in crop yield and, accordingly, an increase in the number of incoming crop and root residues participating in humification processes.

On an organic background, humus is replenished. During the first rotation the increase in humus content was 0.02%, during the second rotation - 0.11%, and during the third rotation this value was 0.15%.

According to the data in Table 3, during three rotations in the variant with extensive technology where no fertilizers were provided by the experimental scheme, the content of mobile forms of phosphorus decreased: for rotation I - by 7 mg kg^{-1}, for rotation II - by 12 mg kg^{-1}, and for rotation III - by 18 mg kg^{-1}. Adding different doses of mineral fertilizers and manure contributed to a different replenishment of the reserves of mobile phosphorus in arable layer.

Table 3. Influence of the modifications of regional technologies on soil fertility parameters of the arable horizon of sod-podzolic medium loamy soil

Technologies	Rotation I 1991–1996			Rotation II 1997–2002			Rotation III 2003–2008		
	Humus, %	mg kg^{-1} of soil		Humus, %	mg kg^{-1} of soil		Humus, %	mg kg^{-1} of soil	
		P_2O_5	K_2O		P_2O_5	K_2O		P_2O_5	K_2O
1.	1.76 ± 0.02*	170 ± 7.5	207 ± 8.6	1.72 ± 0.03	165 ± 6.6	201 ± 7.8	1.67 ± 0.01	159 ± 5.3	195 ± 8.4
2.	1.79 ± 0.02	187 ± 8.2	239 ± 9.2	1.83 ± 0.05	198 ± 8.9	247 ± 8.2	1.89 ± 0.04	204 ± 8.9	252 ± 8.6
3.	1.83 ± 0.04	205 ± 9.4	257 ± 8.9	1.89 ± 0.05	222 ± 9.7	276 ± 9.2	1.94 ± 0.05	229 ± 7.7	284 ± 9.4
4.	1.98 ± 0.05	181 ± 8.0	229 ± 7.9	2.07 ± 0.08	189 ± 8.3	238 ± 7.9	2.11 ± 0.09	195 ± 8.8	247 ± 8.1

Note: 1 – extensive; 2 – adaptive; 3 – intensive; 4 – organic; * arithmetic mean error.

Obtained experimental data showed that the rate of accumulation of mobile forms of phosphorus was directly dependent on the modification of regional technology.

So, if adaptive technology demonstrated increasing content of mobile phosphorus during first rotation by 10 mg kg^{-1}, during second rotation - by 21 mg kg^{-1} and, finally, during third rotation - by 27 mg kg^{-1}, then with intensive technology the accumulation of mobile phosphorus increased by three rotations, respectively, by 28, 45 and 52 mg kg^{-1}.

When using organic technology, the rate of accumulation of mobile phosphorus by crop rotations was: 4, 12 and 18 mg kg^{-1} of soil.

Data in Table 3 show significantly different at $p < 0.05$ values of mobile potassium content depending on the technology. Extensive technology demonstrated a decrease in mobile potassium of arable layer, by crop rotations, by: 13, 19 and 25 mg ha^{-1}.

Variant with adaptive technology showed an increase in mobile potassium in comparison with the baseline, by crop rotations, by: 19, 27 and 32 mg ha^{-1}.

Maximum content of mobile potassium in arable horizon was noted against the intensive background. The increase in mobile potassium in the first rotation was 37 mg kg^{-1}, in the second rotation - 56 mg kg^{-1}, and in the third rotation - 64 mg kg^{-1}.

Against the organic background, an increase in potassium content was also visible but the intensity of mobile potassium accumulation was much lower in comparison with technologies where adding of mineral fertilizers was provided.

Crop yield formation is determined by the level of agricultural crop cultivation technologies applied.

Crop yield data by rotations are shown in Table 4.

When cultivating crops using extensive technology, crop rotation yields amounted to: rotation I - 12.3; rotation II - 13.1; rotation III - 13.9 thousand of grain units. A certain increase in crop yields by crop rotations with extensive technology was mainly due to the implementation of new varieties, improvement of technological operations and improving the quality of their implementation.

Growth of crop productivity with adaptive technology in comparison with the extensive one, by crop rotations, was: 4.5, 4.6 and 6.1 thousand of grain units with LSD05 equal to 1.1, 1.0 and 1.4 thousand of grain units, respectively.

Table 4. Total crop productivity by crop rotation, tons of grain units

Modifications of regional technologies	Rotation I 1991–1996	Rotation II 1997–2002	Rotation III 2003–2008
Extensive	12.3	13.1	13.9
Adaptive	16.8	17.7	20.0
Intensive	19.2	20.6	22.5
Organic	17.9	19.2	20.2
LSD_{05}	1.1	1.0	1.4

Maximum increase in crop yields was noted for intensive regional technology in comparison with extensive technology, by crop rotations: 6.9, 7.5 and 8.6 thousand of grain units. A similar increase in crop yields was due to improved agrochemical parameters of soil fertility caused by the investment of additional material and financial resources.

Productivity of arable land with using organic technology compared with the extensive one increased by: 5.6, 6.1 and 6.3 thousand of grain units.

The Smolensk Region is well-placed to at least double the output of such products for delivering them for the production of baby food, dietary nutrition for health centers, hospitals, retirement homes, to the industrially developed regions of Russia, as well as to Western countries where producing eco-friendly products is hindered due to industrialization.

CONCLUSION

1. As a result of monitoring conducted on the reference site in 1991–2008, negative changes in soil profile were obvious. The degree of soil podzolization increased what contributed to its degradation. All genetic horizons of the reference site demonstrated the processes of deterioration of the basic parameters of soil fertility.

Deterioration of agrochemical parameters of soil fertility in the reference site during 18 years of observation was due primarily to the fact that the cultivation of crops was carried out according to extensive technology (variant 1).

2. Modifications of regional technologies studied in this experiment have different effect on the dynamic changes in agrochemical parameters of the fertility of arable horizon. Extensive technology led to the acidification of soil solution during the first rotation by 10.1%, during the second - by 12.4%, and during the third - by 14.2%.

Adding mineral fertilizers in different doses that was provided for the cultivation of crops within adaptive and intensive technologies contributed to different increase in the acidity of soil solution by crop rotations. Organic technology with cattle manure as the basic fertilizer contributed to the moderate neutralization of soil solution. $pH_{.KCl}$ increased by crop rotations, respectively, by: 3.1%, 6.9% and 8.4%.

Obtained experimental data revealed that higher rates of accumulation of mobile phosphorus were typical for intensive technology, these values were slightly lower when using adaptive technology.

Organic technology resulted in the following rate of accumulation of mobile phosphorus, by crop rotations: 4, 12 and 18 mg kg^{-1} of soil. Similar dynamics was noted for changes in the content of mobile potassium.

3. Maximum productivity of crops during three rotations of a six-field crop rotation on sod-podzolic medium loamy soil was associated with intensive technology. According to our data, organic technology is recommended for getting environmentally friendly products in the production of baby and diet food.

REFERENCES

Akimova, Y.A. & Polushkina, T.M. 2015. Prospects of the development of organic agriculture in Russia. *Modern problems of science and education*. No. 2 - part 1, pp. 15–18.

Antille, DL, Peets, S., Galambošová, J., Botta, GF, Rataj, V., Macak, M., Tullberg, JN, Chamen, WCT, White, DR, Misiewicz, PA, Hargreaves, PR, Bienvenido, JF & Godwin, RJ 2019. Review: Soil compaction and controlled traffic farming in arable and grass cropping systems. *Agronomy Research* **17**(3), 653–682. https://doi.org/10.15159/AR.19.133

Bahirev, G.I. 2016. *Optimization of arable land as the basis of modern methodology development of ecologically balanced agrolandscapes formation (EBA) of the Federal State Budgetary Scientific Institute - All-Russia Scientific and Research Institute of Arable Farming and Soil Erosion Protection*. Kursk, p. 306.

Cherkasov, G.N. 2016. *Adaptive-landscape systems of agriculture — means of regimes management.* Federal State Budgetary Scientific Institute - All-Russia Scientific and Research Institute of Arable Farming and Soil Erosion Protection., Kursk, p. 306.

Chernikov, V.A., Milashchenko, N.Z. & Sokolov, O.A. 2001. *Environmental safety and sustainable development*. Vol. **3**. Soil resistance to anthropogenic impact. Pushchino: ONTI PNC RAS. 203 pp.

Dmitriev, E.A. 1995. *Mathematical statistics in soil science*. Textbook. Moscow State University Publishing House, Moscow, 320 pp.

Dospekhov, B.A. 1985. *Methods of field experience*. Moscow, Agropromizdat, 416 pp.

Egorov, V.V., Ivanova, E.N. & Fridland, V.M. 1977. *Classification and diagnostics of the soils of USSR*. Moscow, Kolos, 225 pp.

GOST 26212-91 Soils. Determination of hydrolytic acidity by Kappen method modified by CINAO.

GOST 26487-85 Soils. Determination of exchangeable calcium and exchangeable (mobile) magnesium by CINAO methods.

GOST 26213-91 Soils. Methods for determination of organic matter

Hospodarenko, H., Prokopchuk, I., Prokopchuk, S. & Trus, A 2018. Humus content in a podzolized chernozem after a long-term application of fertilizers in a field crop rotation *Agronomy Research* **16**(3), 728–736, https://doi.org/10.15159/AR.18.080

Jørgensen, M.H. 2014. Adaptive tillage systems. *Agronomy Research* **12**(1), 95–100.

Kashtanov, A.N., Lisetskiy, F.N. & Shwebs, G.I. 1994. *Fundamentals of landscape ecological farming.* Moscow, Kolos, 194 pp.

Kiryushin, V.I. 2011a. Theory of adaptive landscape farming and design of agricultural landscapes. Moscow, Kolos, pp. 442–443.

Kiryushin, V.I. & Kiryushin, S.V. 2015. Agrotechnologies. St. Petersburg, *Lan*, pp. 463.

Ladonin, V.F., Viyugin, S.M., Gordeev, Yu.A. 1996. Optimization of using chemicals in biological farming, *Agrochemistry* **2**. 31–37.

Naumov, V.D. 2016. *Geography of soils*. Soils of Russia: textbook, Moscow, Prospect, 340 pp.

Shamanaev, V.A., Viyugin, S.M., Gordeev, A.M., Prudnikov, A.D. & Viyugina, G.V. 2006. *Environmental monitoring*. Smolensk, OOO Smyadyn, 222 pp.

Shatilov, I.S. 2001. Balanced field experiments in agricultural landscape research. Collection of scientific papers. – Oryol, Publishing house OryolSAU, pp. 10–16.

Stehlík, M., Czako, A., Mayerová, M. & Madaras, M. 2019. Influence of organic and inorganic fertilization on soil properties and water infiltration. *Agronomy Research* **17**(4), 1769–1778. https://doi.org/10.15159/AR.19.145

Viyugin, S.M. & Viyugina, G.V. 2014. Influence of agricultural systems of varying intensity on the fertility of sod-podzolic soils: results of monitoring studies at the polygon of Smolensk State Agricultural Academy *// Bulletin of Smolensk State University* No. **1** (25), p. 325–333

Viyugina, G.V. & Viyugin, S.M. 2003. Productivity and stability of agrocoenoses in adaptive agriculture. Smolensk, 107 pp.

Agronomy Research **18**(4), 2665–2676, 2020
https://doi.org/10.15159/AR.20.174

Application of feature selection for predicting leaf chlorophyll content in oats (*Avena sativa* L.) from hyperspectral imagery

W.R. Żelazny[1,2,*]

[1]Crop Research Institute, Division of Crop Management Systems, Drnovská 507/73, CZ161 06 Praha 6 Ruzyně, Czech Republic
[2]Czech University of Life Sciences Prague, Faculty of Engineering, Department of Agricultural Machines, Kamýcká 129, CZ165 00 Praha 6 Suchdol, Czech Republic
[*]Correspondence: wzelazny@vurv.cz

Abstract. Feature selection can improve predictions generated by *partial least squares* models. In the context of hyperspectral imaging, it can also enable the development of affordable devices with specialized applications. The feasibility of feature selection for oat leaf chlorophyll estimation from hyperspectral imagery was assessed using a public domain dataset. A wrapper approach resulted in a simplistic model with poor predictive performance. The number of model inputs decreased from 94 to 3 bands when a filter approach based on the *minimum redundancy, maximum relevance* criterion was attempted. The filtering led to improved prediction quality, with the *root mean square error* decreasing from 0.17 to 0.16 g m^{-2} and R^2 increasing from 0.57 to 0.62. Accurate predictions were obtained especially for low chlorophyll levels. The obtained model estimated leaf chlorophyll concentration from near infra-red reflectance, canopy darkness, and its blueness. The prediction robustness needs to be investigated, which can be done by employing an ensemble methodology and testing the model on a new dataset with improved ground-truth measurements and additional crop species.

Key words: remote sensing, imaging spectroscopy, unmanned aerial vehicles, partial least squares, reproducibility.

INTRODUCTION

The indispensability of chlorophyll for plant photosynthesis (Sims & Gamon, 2002; Main et al., 2011) and its contribution to crop optical properties (Ollinger, 2011) make the estimation of leaf chlorophyll concentration an important remote sensing application. In large-scale assessments, leaf chlorophyll remote sensing is useful for yield prediction (Moharana & Dutta, 2016). At finer spatial scales, it can be used for the delineation of management zones for precision agriculture (Miao et al., 2009). As chlorophyll breaks down under stress, its monitoring provides information about the crop status, and enables a timely intervention to prevent the yield loss (Peñuelas et al., 1995; Sims & Gamon, 2002).

Traditional broad-band optical remote sensing relies on vegetation indexes for assessing crop status (e.g., Basso et al., 2016; Domínguez et al., 2017; Barbosa et al., 2019). Consequently, it is of limited use for estimating the concentrations of individual pigments, such as leaf chlorophyll. Many of these indexes have been adapted for use with hyperspectral imaging products (Miao et al., 2009; Verrelst et al., 2019, often leading to improved results (e.g., Miao et al., 2009). Moharana & Dutta (2016) evaluated ten indexes in terms of rice chlorophyll prediction from proximal spectroradiometric data. Some of the band combinations gave unsatisfactory estimates despite their high performance in other experimental settings, which is a common problem for vegetation indexes. On the other hand, the formulations that excelled during the screening provided realistic maps of rice chlorophyll concentration when applied to EO-1 Hyperion imagery. The limited index transferability across crops can be in part related to differences between plant architectures (Ollinger, 2011). A study involving six crop species evaluated the robustness of relationships between vegetation indexes and leaf chlorophyll with respect to canopy structural parameters. A total of 58 formulations were tested; of this number, only 2 were considered truly robust when applied to both measured and simulated spectra (Zou et al., 2015). Corti et al. (2018) published a meta-analysis intended to identify factors that foster accurate estimation of maize biochemical parameters from optical measurements. Their results suggest that satisfactory predictions can be obtained by avoiding certain families of vegetation indexes-regardless of sensor type, acquisition model, and crop developmental stage. The article indicates that only statistically significant relationships were included in the study, which means that this finding needs to be approached with caution. A recent review by Hatfield et al. (2019) cites additional studies devoted to vegetation indexes suitable for chlorophyll estimation. According to the authors, vegetation indexes should be a first choice in remote sensing applications, as they avoid computational challenges of more sophisticated approaches.

Yet, the main advantage of hyperspectral imagery lies in the possibility of applying 'full-spectrum' methods borrowed from chemometrics and machine learning (Corti et al., 2018; Verrelst et al., 2019). *Partial least squares (PLS) regression* was employed to diagnose chlorophyll levels in winter wheat leaf laboratory samples (Zhang et al., 2012). Scanning of single leaves under controlled illumination allowed the authors to evade the challenges inherent to canopy-level imaging in outdoor conditions, and without doubt contributed to extremely accurate (R statistics up to 0.99) predictions. Unfortunately, unclear study design description undermines the trustworthiness of the findings. Kanning et al. (2018) tested a pushbroom system as a way to overcome some limitations of 2D frame hyperspectral cameras. An experimental winter wheat field was scanned using a UAV, and the measurements subjected to *PLS* modelling. When the model was applied to the pixels of the field orthoimage, the individual nitrogen fertilization treatment levels could be discerned. The estimation quality was sufficient to fit a model for predicting grain yield from the obtained values. Meij et al. (2017) employed *PLS* to predict chlorophyll content in oats from unmanned aerial vehicle (UAV) campaign data. The study also included 25 published vegetation indexes. The *PLS* approach yielded validation predictions inferior to the estimates obtained by using the best of the indexes. Still, according to Verrelst et al. (2019), chemometric methods are in principle more powerful than vegetation indexes for estimating canopy biophysical parameters. The chemometric approach tends, in turn, to be surpassed by machine learning methods, capable of modelling non-linear relationships. A comparison of selected algorithms from both groups demonstrated substantial performance variability within the machine learning family. Robust leaf chlorophyll content predictions for multiple crops were obtained with *kernel ridge* and *Gaussian process regression*. On the other hand, *artificial neural networks*, an approach with a comparable level of sophistication, failed to provide consistently reliable estimates (Caicedo et al., 2014). By applying *support vector machines (SVM)* to maize hyperspectra, Karimi et al. (2008) obtained very good validation estimates for the tasseling stage. The prediction quality was worse, but still satisfactory, for the early growth stage, which the authors attributed to the soil showing through the crop canopy.

Despite its potential, the adoption of imaging spectroscopy remains hindered, in part by the high investment costs involved (Corti et al., 2018). Scene acquisition using a modern 2D camera tends to be slow due to sequential capture of a large number of bands. As a consequence, the speeds of airborne platforms become constrained (Honkavaara et al., 2017) and band registration needs to be performed during the imagery post-processing (Jakob et al., 2017). The voluminous data contained in hyperspectral data cubes require substantial computational capacities and specialized knowledge to process (Yang et al., 2017; Aasen et al., 2018). In the realm of field point spectrometry, similar challenges have been overcome by the development and commercialization of specialized proximity sensors, such as chlorophyll meters (Govender et al., 2009; Miao et al., 2009). These sensors exploit information from limited numbers of pre-selected bands, and have a predictive model embedded in the firmware to perform the computations. A similar route could be taken for imaging spectrometers in order to make the technology more accessible (Govender et al., 2009). One can envision an affordable specialized device capable of capturing narrow-band imagery, as hyperspectral cameras do, comprising bands that were pre-selected to optimize for accurate remote chlorophyll content estimation.

Feature selection methods have proven to be useful for the screening of spectral bands for a variety of applications. In addition to reducing the number of required model inputs, they were shown to improve the prediction accuracy (Ding & Peng, 2005; Mehmood et al., 2012). Fewer computations are required to process data subjected to feature selection, and model interpretation is facilitated (Ding & Peng, 2005). Band pre-selection prior to data acquisition can also address the problem of slow operation of hyperspectral cameras (Yang et al., 2013; Zhang & He, 2013). As demonstrated by the Zhang & He (2013) oilseed rape yield study, substantial reduction of data volume can be attained without impairing model performance. Discarding of 98% of hyperspectral bands had a minimal effect on the quality of nitrogen content prediction in pepper plants, while significantly simplifying the obtained model (Yu et al., 2014). Behmann et al. (2014) proposed an *SVM* model for detecting water stress in barley. The model inputs comprised vegetation indexes, the combinations of which were determined using wrapper feature selection. Increased detection sensitivity was obtained, allowing for earlier drought detection relative to the raw indexes. The aim of the present study is to investigate the effect of two feature selection approaches on the prediction of leaf chlorophyll concentration in oats from hyperspectral imaging data.

MATERIALS AND METHODS

Experimental data

The present study partially replicates and extends the results of Meij et al. (2017), using the same experimental data. Their experiment evaluated the soil-mediated carry-over effects of preceding and cover crops on crop-of-interest status. The data collection took place in summer 2015, which was the second year of the study, and was focused on experimental plots with oats in the grain-filling developmental stage.

The dataset includes narrow-band reflectance spectra of the experimental plots (one averaged spectrum per plot) obtained from UAV imagery. The spectra cover the range of wavelengths from 450 to 915 nm, i.e., between visible blue and near infra-red. The spectral resolution is 5 nm, thus yielding 94 bands. The spectra are accompanied by ground-truth measurements describing the crop's physiological status. They include, among others, SPAD-estimates of leaf chlorophyll concentrations (one averaged estimate per plot), which are the focus of the present study. There are 56 data points in total, labelled as either calibration or validation data in 1:1 proportion. The dataset is in the public domain, and for the purpose of this study, it was downloaded from the Dryad repository (Meij et al., 2018).

Reproduction of the original analysis

In order to obtain a baseline for the assessment of feature selection performance, a reproduction of the Meij et al. (2017) result was prepared. The original study employed vegetation indexes and *PLS* modelling for predicting leaf chlorophyll from the imaging spectra. This paper focuses on the latter approach.

The data partitioning from the original dataset was preserved, and a *PLS regression* model was fitted to the calibration subset. Leaf chlorophyll concentration was modelled as the dependent variable, and the reflectance values for the whole range of the wavelengths as the independent variables. The number of latent variables was tuned using *leave-one-out cross-validation* by calculating the *cross-validation root mean square error (RMSE)* for each value from between 1 and 20. The validation spectra were then fed to the model exhibiting the lowest error, and the generated predictions compared with the SPAD chlorophyll estimates to obtain *validation RMSE, normalized RMSE (NRMSE),* and the R^2 statistics. To reproduce the original validation results, *RMSE* had to be normalized by dividing it by the mean chlorophyll concentration, rather than the standard deviation or range. Likewise, R^2 had to be calculated as the square of the *correlation* coefficient between the predicted and observed values, rather than derived from the sums of squares.

Application of feature selection

Next, the fitting of the *PLS* model to the calibration dataset was repeated, but in addition to the tuning of the latent variable number, feature selection was performed. Two approaches to feature selection were tested: a filter method based on the *minimum redundancy, maximum relevance (MRMR)* criterion, and a forward selection wrapper method.

Under the filtering approach, variables are evaluated independently of model fitting, according to a measure the value of which determines which of them will be discarded (Mehmood et al., 2012). In the *MRMR* method, this measure is the mutual information shared by the candidate feature and the predicted variable, reduced by the average mutual information shared by the candidate feature and the features already accepted for inclusion into the model. The mutual information is a function of the *correlation* coefficient (De Jay et al., 2013).

With wrapping, models are fitted to multiple pre-selected feature subsets, and the fit quality itself serves as the selection performance criterion, making it a computationally more demanding approach (Mehmood et al., 2012). The wrapper forward selection method is analogous to the forward selection in the *stepwise regression:* candidate features are picked one by one from the feature pool, and their influence on the performance of the refitted model is assessed. The variable associated with the highest performance increase is kept in the model, and the process continues iteratively~~,~~ until there is no further improvement.

For each method, the present study aimed to obtain a series of models with the input feature number ranging from 2 to all 94 bands (i.e., no selection). In this way, the influence of feature selection intensity on the prediction quality could be investigated.

Computational reproducibility

The analysis was prepared with reproducibility in mind (Piccolo & Frampton, 2016). It was programmed in the R language (R Core Team, 2019), using the packages pls (Mevik et al., 2019) for model fitting, mRMRe (De Jay et al., 2013) for assessing the *MRMR* criterion, and mlr (Bischl et al., 2016) for model tuning. GNU Make (Stallman et al., 2016) was used as the build tool, and GNU Guix enabled isolation and reproducibility of the software environment for performing the analysis (Courtès & Wurmus, 2015). The computational scripts are available from a Zenodo repository (Żelazny, 2020). On an IA-64 machine~~,~~ the analysis took approximately 100 minutes without parallelization and excluding the time needed to set up the environment. The latter can last hours on the first run, depending on the state of ~~a~~ the Guix store (Courtès & Wurmus, 2015) and availability of pre-compiled package substitutes. It is reduced to minutes on subsequent runs.

RESULTS AND DISCUSSION

Visual data assessment

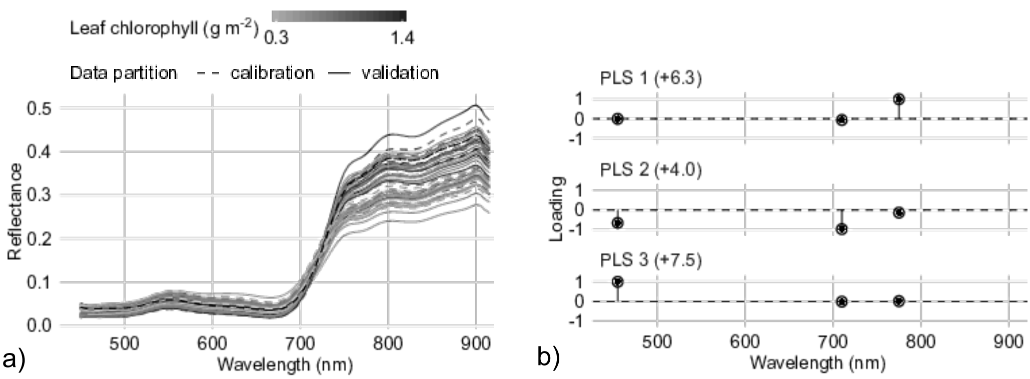

Figure 1. a) Narrow-band spectra of experimental oat plots in the calibration and validation data subsets acquired using an unmanned aerial vehicle. Line hues reflect the differences in SPAD-estimated leaf chlorophyll concentrations. The figure can be rendered in color by running the computational scripts that accompany the article; b) Loadings in the *partial least squares* model for predicting leaf chlorophyll concentrations from the narrow-band spectra. The model is based on three bands obtained from *minimum redundancy, maximum relevance* filtering. Latent variable loadings are given in the parentheses, wavelength loadings are given on the *y* axis.

Fig. 1, a depicts the experimental plot spectra matched to the ground-truth data, analogously to Fig. 4 in Meij et al. (2017). High leaf chlorophyll concentration appears to be associated with increased near infra-red reflectance and a steep red edge–both regions repeatedly considered important for chlorophyll prediction by earlier studies (Govender et al., 2009; Main et al., 2011). On the other hand, contrary to expectation, no apparent red-edge shift can be discerned. The calibration and validation spectra are well mixed in terms of the chlorophyll measurements, as can be expected from the stratified random partitioning, employed by the original study. Regarding the reflectance, the validation subset seems to cover a wider range of values than the calibration subset, but the difference is too small to raise concerns about a mismatch between the partitions.

Reproduction of Meij (Meij et al. (2017)

Despite the variety of existing *PLS* flavours and implementations, the attempt to reproduce the validation results of the Meij et al. (2017) paper turned out to be successful, with only *NRMSE* showing a slight deviation (Table 1, row 'Reproduction'). However, as discussed above, the high number of bands contributing to the model make the 'full-spectrum' approach infeasible for practical application - at least until hyperspectral imagers become affordable (Aasen et al., 2018). In addition, the result of model tuning, which set the number of the latent variables to five, makes an insight into its workings challenging.

Table 1. Tuning parameters and validation statistics of the *partial least squares* models. Each model was calibrated using 28 spectra and validated using another set of 28 spectra

Study	Input bands	Latent variables	*RMSE* (g m^{-2})	*NRMSE* (%)	R^2
Meij et al. (2017)	94	5	0.17	23.82	0.57
Reproduction	94	5	0.17	23.75	0.57
Filter feature selection	19	7	0.21	28.36	0.52
Filter feature selection (truncated)	3	3	0.16	21.84	0.62
Wrapper feature selection	1	1	0.20	28.23	0.43

RMSE = root mean square error, NRMSE = normalized root mean square error.

Feature selection

The *cross-validation* results of models employing filter feature selection exhibit two local error minima (Fig. 2). The absolute minimum corresponds to 19 input bands, a much lower number than for the reference model, but still too high for developing reasonably priced specialized device. What is more, the model shows higher validation error and involves even more latent variables (seven) than the reproduction model (Table 1, 'Filter feature selection').

Conversely, three wavelengths, as in the second minimum, seem a good middle-ground between technical feasibility and expected estimation error. The fact that the number of latent variables in *PLS regression* cannot exceed the number of inputs contributes to the model interpretability. Notable is the improvement of the validation statistics (Table 1, 'Filter feature selection (truncated)'), which corroborates the positive influence of feature selection on prediction accuracy (Mehmood et al., 2012). Although the obtained gains may seem modest, one should consider other advantages offered by feature selection, such as the reduced cost of a specialized imager (Govender et al., 2009), more efficient data acquisition (Yang et al., 2013; Zhang & He, 2013), and smaller volumes of the collected data (Zhang & He, 2013). On a closer examination, the model appears to give accurate predictions for low levels of chlorophyll, but its performance deteriorates above the level of about 0.75 g m^{-2} (Fig. 3). A similar pattern occurred in the Kanning et al. (2018) pushbroom imager study. An attempt to further improve the prediction quality could be made by log-transforming the chlorophyll content values prior to modelling.

Fig. 1, b depicts the band loadings for each latent variable and the latent variable loadings of this model. The chlorophyll content is, thus, predicted as $LCC = 6.3\ PLS_1 + 4.0\ PLS_2 + 7.5\ PLS_3$. The value of the first component $PLS_1 = 0.0\ r_{455} - 0.1\ r_{710} + 1.0\ r_{775}$ corresponds to the near infra-red reflectance, in accordance with the visual assessment, above. The second component $PLS_2 = -0.7\ r_{455} - 1.0\ r_{710} - 0.1\ r_{775}$ includes the bottom part of the red edge and, interestingly, a blue band., it can be interpreted as canopy darkness (low visible albedo), and linked to the absorbance in the photosynthetically-active spectral region. The third component value $PLS_3 = 1.0\ r_{455} + 0.0\ r_{710}\ + 0.0\ r_{775}$ is determined by canopy blueness (blue hue intensity).

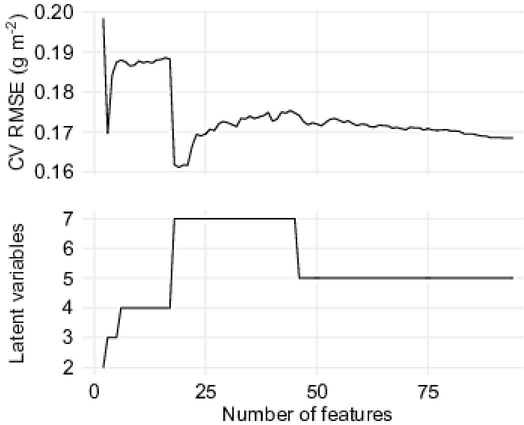

Figure 2. *Cross-validation* prediction performance and tuning results of the oat leaf chlorophyll prediction models according to the number of features selected using the *minimum redundancy*, *maximum relevance* filter. *CV RMSE = cross-validation root mean square error.*

Wavelength combinations similar to the one picked by the filtering algorithm seldom occur in vegetation index formulations. They can be found in the Enhanced Vegetation Index (Gao et al., 2000), the Structure Insensitive Pigment Index (Peñuelas et al., 1995), the Modified Simple Ratio, and the Modified Normalized Difference (mND_{705}) (Sims & Gamon, 2002). No such index was investigated by Meij et al. (2017). In the study by Main et al. (2011), the first three indexes fared poorly when used for predicting chlorophyll content in maize leaves at various developmental stages. The authors attribute this to the weak relationship between the blue spectral region and the leaf chlorophyll concentration.

Regarding mND_{705}, it was among the best-performing indexes in Main et al. (2011), and in Miao et al. (2009) - also a maize study. On the other hand, it occurred to be a poor predictor of chlorophyll content in rice (Moharana & Dutta, 2016). The mND_{705} index formula includes blue reflectance as a way to account for specular reflectance (Sims & Gamon, 2002). The third latent variable of the discussed *PLS* model may play the same role.

Alternatively, it may adjust for Rayleigh scattering. According to Beisl et al. (2008), atmospheric effects occur even in low-altitude airborne remote sensing applications. Although the analysed dataset has been subjected to atmospheric correction, it was based on a single reference panel measurement (Meij et al., 2017). The weakness of this approach is the assumption of constant illumination conditions as individual images are acquired. The blue band information may account for the residual error that still remained after the correction.

The forward selection within the wrapper approach stopped after picking one band (775 nm), thus reducing the *PLS* model to a classical *regression* model with a single independent variable. The selected wavelength lies in the near infra-red spectral region, which agrees with the observation from the visual assessment, above. According to the validation statistics (Table 1 'Wrapper feature selection'), despite its extreme simplicity, the model performs surprisingly well in terms of *RMSE.* However, the low R^2 value puts in question the feasibility of its practical use. Moreover, like the preceding model, it exhibits uneven prediction quality for various levels of chlorophyll (Fig. 3).

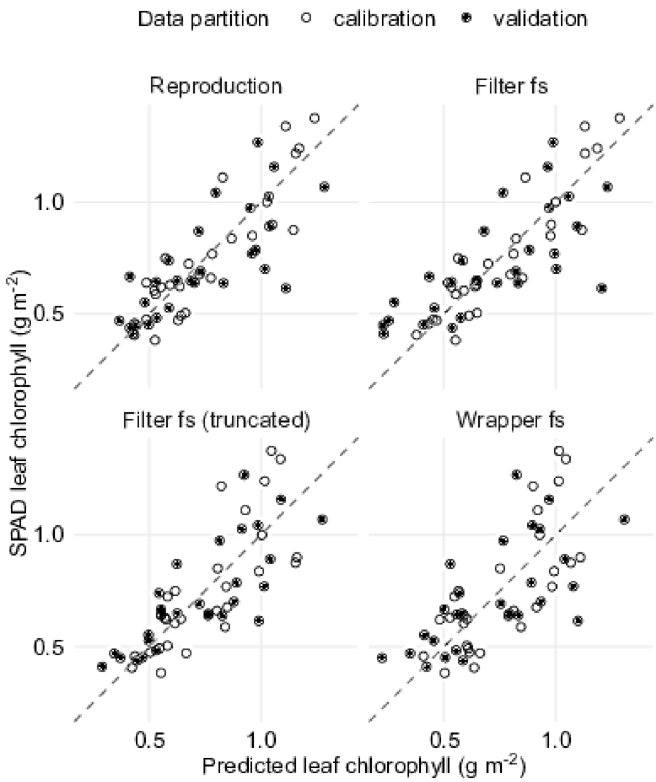

Figure 3. Prediction error patterns of the studied models with respect to the ground-truth data.

In the light of this finding, it can be recommended to avoid wrapper selection for chlorophyll content prediction, especially considering the substantial computational demands of this approach (Ding & Peng, 2005; Mehmood et al., 2012). Conversely, the encouraging results attained with *MRMR* suggest high potential of the filter strategy towards picking highly predictive spectral bands. The *MRMR* criterion seems particularly well-suited to data acquired using optical remote sensing methods. As reflectance measurements exhibit substantial spectral autocorrelation (Karimi et al., 2008; Verrelst et al., 2019), a naive algorithm could pick a set of neighbouring bands, with information content barely exceeding that of a single band. The 'minimum redundancy' aspect of *MRMR* avoids this issue by taking correlations between features into consideration (Ding & Peng, 2005). Still future research might consider examination of feature selection methods from the filter family. The performance of the three classes of methods reviewed by Mehmood et al. (2012): based on loading weights, *regression* coefficients, and variable importance in projection; could be compared, for instance.

Possibilities of assessing and improving study generalizability

The present study illustrates the application of feature selection for obtaining a parsimonious predictive model with high interpretability. Just as omitting model *cross-validation* can lead to over-fitting, a model that performs well on a single validation dataset does not necessarily generalize to new circumstances. This is especially true for unstable models, whose parameters change radically in response to even slight modification of the training data.

In the present study, an improvement of validation statistics was obtained after filtering the spectral bands using the *MRMR* algorithm. As highlighted by De Jay et al. (2013), the algorithm in its original form produces results that are unstable with respect to data modifications. The cited authors proposed an ensemble extension of the filter to stabilize its output.

Ensemble modelling has been shown to improve prediction accuracy, as exemplified by *random forests* (Breiman, 2001), and enable interval estimation, as exemplified by *bootstrap* methods (Wood, 2005). Its obvious application in the discussed study would be to abandon the fixed data partitioning, which was inherited from Meij et al. (2017), in favour of multiple analyses, each based on a different assignment of the data points to the calibration and validation subsets. By the subsequent aggregation of the obtained partial results, the stability of the best performing models could be assessed - not only with respect to the selected wavelengths, but also to their loadings and validation statistics.

Two candidate models fitted to filtered bands were elected by hand for further evaluation based on *CV RMSE* and feature selection intensity as an auxiliary criterion. Repeated data partitioning would result in proliferation of models, making the manual approach unfeasible. Replacing it with an algorithm would necessitate taking both optimization criteria into account, which can be accomplished with aid of *model-based multi-objective optimization* (Horn et al., 2015).

These avenues could not have been taken due to high computational complexity involved, especially if wrapper feature selection were also included. In the future, an adaptation of the analysis for an execution in a high-performance computing environment might be attempted. At that point, an extension of the study to include ensemble modelling would become feasible.

An evident weakness of both the present and the original Meij et al. (2017) study is the fact that the ground-truth data were obtained using a SPAD chlorophyll meter, and thus include spectroscopic estimation errors (Uddling et al., 2007). It is possible that similar errors present in the discussed *PLS* results become masked in the consequence, leading to overoptimistic validation statistics. Therefore, it would be desirable to replicate the study using laboratory analyses for the ground truth, instead.

Spectral responses of leaf pigments differ across plant genotypes. Although the chlorophyll signal is readily discernible in a leaf or canopy spectrum (Ollinger, 2011), the reflectance is modified by additional factors. They include leaf and canopy anatomy and morphology (Asner, 1998; Jacquemoud & Ustin, 2001; Ollinger, 2011) and spectral properties of additional foliar pigments present in the tissues (Jacquemoud & Ustin, 2001; Ollinger, 2011). Research is needed to establish whether feature selection can yield a set of bands that enable calibration of models for chlorophyll content estimation in multiple crops, and how big this set needs to be for the models to be accurate.

CONCLUSIONS

Filtering of bands according to the *minimum redundancy, maximum relevance* criterion can improve the performance of a *partial least squares* model aimed at oat leaf chlorophyll prediction from airborne hyperspectral imagery. Chlorophyll concentration can be estimated from near infra-red reflectance, canopy darkness, and its blueness. The obtained size of the feature space (three bands in the present study) is sufficiently small for the development of affordable single-purpose imagers. Although a wrapper approach based on forward feature selection can yield an even more parsimonious model, the resulting prediction quality is not satisfactory. The robustness of the findings remains to be investigated using an ensemble of dataset partitionings and ground truth obtained from laboratory analyses based on samples collected from multiple crops.

ACKNOWLEDGEMENTS. The work was conducted with ~~the~~ financial support from the Ministry of Agriculture of the Czech Republic, institutional support MZE-RO0418; and from the European Union Erasmus+ Programme. Lammert Kooistra and Jan Clevers read the paper draft and provided valuable remarks. Suggestions from three anonymous reviewers were of immense help to further improve the manuscript.

REFERENCES

Aasen, H., Honkavaara, E., Lucieer, A. & Zarco-Tejada, P. 2018. Quantitative remote sensing at ultra-high resolution with UAV spectroscopy: A review of sensor technology, measurement procedures, and data correction workflows. *Remote Sensing* **10**, 1091.

Asner, G.P. 1998. Biophysical and biochemical sources of variability in canopy reflectance. *Remote Sensing of Environment* **64**, 234–253.

Barbosa, B., Ferraz, G., Gonçalves, L., Marin, D., Maciel, D., Ferraz, P. & Rossi, G. 2019. RGB vegetation indices applied to grass monitoring: A qualitative analysis. *Agronomy Research* **17**, 349–357. https://doi.org/10.15159/AR.19.119

Basso, B., Fiorentino, C., Cammarano, D. & Schulthess, U. 2016. Variable rate nitrogen fertilizer response in wheat using remote sensing. *Precision Agriculture* **17**, 168–182.

Behmann, J., Steinrücken, J. & Plümer, L. 2014. Detection of early plant stress responses in hyperspectral images. *ISPRS Journal of Photogrammetry and Remote Sensing* **93**, 98–111.

Beisl, U., Telaar, J. & Schönermark, M. 2008. Atmospheric correction, reflectance calibration and BRDF correction for ADS40 image data. *The International Archives of the Photogrammetry, Remote Sensing and Spatial Information Sciences* **37**, 7–12.

Bischl, B., Lang, M., Kotthoff, L., Schiffner, J., Richter, J., Studerus, E., Casalicchio, G. & Jones, Z.M. 2016. mlr: Machine learning in R. *Journal of Machine Learning Research* **17**, 1–5.

Breiman, L. 2001. Random forests. *Machine Learning* **45**, 5–32.

Caicedo, J.P.R., Verrelst, J., Muñoz-Marí, J., Moreno, J. & Camps-Valls, G. 2014. Toward a semiautomatic machine learning retrieval of biophysical parameters. *IEEE Journal of Selected Topics in Applied Earth Observations and Remote Sensing* **7**, 1249–1259.

Corti, M., Cavalli, D., Cabassi, G., Gallina, P.M. & Bechini, L. 2018. Does remote and proximal optical sensing successfully estimate maize variables? A review. *European Journal of Agronomy* **99**, 37–50.
Courtès, L. & Wurmus, R. 2015. Reproducible and user-controlled software environments in HPC with Guix. In: *Euro-Par 2015: Parallel Processing Workshops*. Vienna University of Technology, Vienna, pp. 579–591.
De Jay, N., Papillon-Cavanagh, S., Olsen, C., El-Hachem, N., Bontempi, G. & Haibe-Kains, B. 2013. MRMRe: An R package for parallelized mRMR ensemble feature selection. *Bioinformatics* **29**, 2365–2368.
Ding, C. & Peng, H. 2005. Minimum redundancy feature selection from microarray gene expression data. *Journal of Bioinformatics and Computational Biology* **3**, 185–205.
Domínguez, J., Kumhálová, J. & Novák, P. 2017. Assessment of the relationship between spectral indices from satellite remote sensing and winter oilseed rape yield. *Agronomy Research* **15**, 55–68.
Gao, X., Huete, A.R., Ni, W. & Miura, T. 2000. Optical–biophysical relationships of vegetation spectra without background contamination. *Remote Sensing of Environment* **74**, 609–620.
Govender, M., Govender, P.J., Weiersbye, I.M., Witkowski, E.T.F. & Ahmed, F. 2009. Review of commonly used remote sensing and ground-based technologies to measure plant water stress. *Water SA* **35**, 741–752.
Hatfield, J.L., Prueger, J.H., Sauer, T.J., Dold, C., O'Brien, P. & Wacha, K. 2019. Applications of vegetative indices from remote sensing to agriculture: Past and future. *Inventions* **4**, 71.
Honkavaara, E., Rosnell, T., Oliveira, R. & Tommaselli, A. 2017. Band registration of tuneable frame format hyperspectral UAV imagers in complex scenes. *ISPRS Journal of Photogrammetry and Remote Sensing* **134**, 96–109.
Horn, D., Wagner, T., Biermann, D., Weihs, C. & Bischl, B. 2015. Model-based multi-objective optimization: Taxonomy, multi-point proposal, toolbox and benchmark. In: *International Conference on Evolutionary Multi-Criterion Optimization*. Springer, Guimarães, Portugal, pp. 64–78.
Jacquemoud, S. & Ustin, S.L. 2001. Leaf optical properties: A state of the art. In: *8th International Symposium of Physical Measurements & Signatures in Remote Sensing.* CNES, Aussois, pp. 223–332.
Jakob, S., Zimmermann, R. & Gloaguen, R. 2017. The need for accurate geometric and radiometric corrections of drone-borne hyperspectral data for mineral exploration: MEPHySTo – a toolbox for pre-processing drone-borne hyperspectral data. *Remote Sensing* **9**, 88.
Kanning, M., Kühling, I., Trautz, D. & Jarmer, T. 2018. High-resolution UAV-based hyperspectral imagery for LAI and chlorophyll estimations from wheat for yield prediction. *Remote Sensing* **10**, 2000.
Karimi, Y., Prasher, S., Madani, A. & Kim, S. 2008. Application of support vector machine technology for the estimation of crop biophysical parameters using aerial hyperspectral observations. *Canadian Biosystems Engineering* **50**, 13–20.
Main, R., Cho, M.A., Mathieu, R., O'Kennedy, M.M., Ramoelo, A. & Koch, S. 2011. An investigation into robust spectral indices for leaf chlorophyll estimation. *ISPRS Journal of Photogrammetry and Remote Sensing* **66**, 751–761.
Mehmood, T., Liland, K.H., Snipen, L. & Sæbø, S. 2012. A review of variable selection methods in partial least squares regression. *Chemometrics and Intelligent Laboratory Systems* **118**, 62–69.
Meij, B. van der, Kooistra, L., Suomalainen, J., Barel, J.M. & Deyn, G.B.D. 2017. Remote sensing of plant trait responses to field-based plant–soil feedback using UAV-based optical sensors. *Biogeosciences* **14**, 733–749.
Meij, B. van der, Kooistra, L., Suomalainen, J., Barel, J.M. & De Deyn, G.B. 2018. Data from: Remote sensing of plant trait responses to field-based plant–soil feedback using UAV-based optical sensors. doi:10.5061/dryad.75k1d

Mevik, B.-H., Wehrens, R. & Liland, K.H. 2019. *pls: Partial least squares and principal component regression*. https://CRAN.R-project.org/package=pls

Miao, Y., Mulla, D.J., Randall, G.W., Vetsch, J.A. & Vintila, R. 2009. Combining chlorophyll meter readings and high spatial resolution remote sensing images for in-season site-specific nitrogen management of corn. *Precision Agriculture* **10**, 45–62.

Moharana, S. & Dutta, S. 2016. Spatial variability of chlorophyll and nitrogen content of rice from hyperspectral imagery. *ISPRS Journal of Photogrammetry and Remote Sensing* **122**, 17–29.

Ollinger, S.V. 2011. Sources of variability in canopy reflectance and the convergent properties of plants. *New Phytologist* **189**, 375–394.

Peñuelas, J., Baret, F. & Filella, I. 1995. Semi-empirical indices to assess carotenoids/chlorophyll *a* ratio from leaf spectral reflectance. *Photosynthetica* **31**, 221–230.

Piccolo, S.R. & Frampton, M.B. 2016. Tools and techniques for computational reproducibility. *GigaScience* **5**, 30.

R Core Team. 2019. *R: A language and environment for statistical computing*. R Foundation for Statistical Computing, Vienna. https://www.R-project.org/

Sims, D.A. & Gamon, J.A. 2002. Relationships between leaf pigment content and spectral reflectance across a wide range of species, leaf structures and developmental stages. *Remote Sensing of Environment* **81**, 337–354.

Stallman, R.M., McGrath, R. & Smith, P.D. 2016. *GNU Make. A program for directing recompilation*. Free Software Foundation, Boston. 220 pp.

Uddling, J., Gelang-Alfredsson, J., Piikki, K. & Pleijel, H. 2007. Evaluating the relationship between leaf chlorophyll concentration and SPAD-502 chlorophyll meter readings. *Photosynthesis Research* **91**, 37–46.

Verrelst, J., Malenovský, Z., Van der Tol, C., Camps-Valls, G., Gastellu-Etchegorry, J.-P., Lewis, P., North, P. & Moreno, J. 2019. Quantifying vegetation biophysical variables from imaging spectroscopy data: A review on retrieval methods. *Surveys in Geophysics* **40**, 589–629.

Wood, M. 2005. Bootstrapped confidence intervals as an approach to statistical inference. *Organizational Research Methods* **8**, 454–470.

Yang, G., Liu, J., Zhao, C., Li, Z., Huang, Y., Yu, H., Xu, B., Yang, X., Zhu, D., Zhang, X., Zhang, R., Feng, H., Zhao, X., Li, Z., Li, H. & Yang, H. 2017. Unmanned aerial vehicle remote sensing for field-based crop phenotyping: Current status and perspectives. *Frontiers in Plant Science* **8**, 1–26.

Yang, W., Duan, L., Chen, G., Xiong, L. & Liu, Q. 2013. Plant phenomics and high-throughput phenotyping: Accelerating rice functional genomics using multidisciplinary technologies. *Current Opinion in Plant Biology* **16**, 180–187.

Yu, K.-Q., Zhao, Y.-R., Li, X.-L., Shao, Y.-N., Liu, F. & He, Y. 2014. Hyperspectral imaging for mapping of total nitrogen spatial distribution in pepper plant. *PLoS ONE* **9**, e116205.

Zhang, D., Wang, X., Ma, W. & Zhao, C. 2012. Research vertical distribution of chlorophyll content of wheat leaves using imaging hyperspectra. *Intelligent Automation & Soft Computing* **18**, 1111–1120.

Zhang, X. & He, Y. 2013. Rapid estimation of seed yield using hyperspectral images of oilseed rape leaves. *Industrial Crops Products* **42**, 416–420.

Zou, X., Hernández-Clemente, R., Tammeorg, P., Lizarazo Torres, C., Stoddard, F.L., Mäkelä, P., Pellikka, P. & Mõttus, M. 2015. Retrieval of leaf chlorophyll content in field crops using narrow-band indices: Effects of leaf area index and leaf mean tilt angle. *International Journal of Remote Sensing* **36**, 6031–6055.

Żelazny, W.R. 2020. Application of feature selection for predicting leaf chlorophyll content in oats (Avena sativa L.) from hyperspectral imagery (computational scripts). doi:10.5281/zenodo.3573320

Agronomy Research **18**(4), 2677–2686, 2020
https://doi.org/10.15159/AR.20.218

The impact of drainage reclamation on the components of agricultural landscapes of small rivers

V.A. Zubarev[1], Yu.A. Mazhaysky[2] and T.M. Guseva[3,*]

[1]Institute of complex analysis of regional problems of the far Eastern branch of the Russian Academy of Sciences, 4 Sholom Aleichem Str., RU607016 Birobidzhan, Russia
[2]Meshchersky branch of the all-Russian research Institute of hydraulic engineering and land reclamation n. A.N. Kostyakova, 1A Meshcherskaya Str., RU390021 Ryazan, Russia
[3]Ryazan state medical University n. I. P. Pavlova, 22 Lenina str., RU 390000 Ryazan, Russia
[*]Correspondence: guseva.tm@yandex.ru

Abstract. The traditional use of agricultural landscapes of small rivers is agricultural arable land, which requires a number of reclamations and agricultural work. Land drainage has a significant impact on the environment, but these activities were carried out almost without taking into account the requirements of environmental protection. Heavy metals have one of the most significant negative effects on the components of floodplain-channel complexes (floodplain soil, surface water, bottom sediments, macrophytes, hydrobionts). Studies have shown that drainage reclamation leads to a decrease in the content of humus in floodplain soil, collector-drainage runoff, changing the chemical composition of natural water, affects the processes of transit-accumulation of heavy metals from sediments to water. The integrated chemical and ecological assessment of the influence of drainage reclamation on the state of the floodplain soil - water-bottom sediments system showed a critical situation of pollution of agricultural landscapes of water basins with heavy metals. Drainage melioration also negatively affects the state of hydrobionts-aquatic vegetation and fish, heavy metals accumulate in their organisms, which leads to disruption of aquatic flora and fauna life processes.

Key word: agrolandscape of small river, drainage reclamation, collector-drainage water, heavy metals, floodplain soil, surface water, bottom sediments, macrophytes, hydrobionts.

INTRODUCTION

The state of floodplain-channel complexes - agrolandscapes of small rivers located in the Amur river basin in the Far East of Russia is determined by a number of natural factors associated with the instability of the water regime in the monsoon climate, the weak ability of aquatic ecosystems to self-repair, the specific features of the formation of the chemical composition of water within different landscapes, which are influenced by various types of anthropogenesis (Voronov & Makhinov, 2009). The traditional use of agricultural landscapes of small rivers is agricultural arable land, which requires a number of reclamations and agricultural work. Their proper organization is impossible without preliminary research. Land drainage at the initial stage of reclamation construction had a very noticeable impact on the environment, since it was carried out almost without taking into account the requirements of nature conservation. One of the most significant negative effects on the components of the agrolandscapes of small rivers (floodplain soil, surface water, bottom sediments, macrophytes, hydrobionts) is exerted by heavy metals (HM). According to many authors, the group of the most common HM includes iron (Fe), manganese (Mn), copper (Cu), nickel (Ni), zinc (Zn), lead (Pb) and their salts (Nazarov, 2014; Kasiuliene et al., 2016; Dyatel, 2017; Tolkachev et al., 2017; Yashin, 2017; Imeri et al., 2019; Murtic et al., 2019), characterized by long-term storage in water, accumulation in bottom sediments and the aquatic ecosystem as a whole (Israel, 1984; Moore & Ramamurti, 1987; Pais & Jones, 1997; Perevoznikov & Bogdanova, 1999; Kabata-Pendias & Pendias, 2001; Khristoforova, 2007; Tack, 2010; Morais et al., 2012; Chibuike & Obiora, 2014; Lukowski & Wiater, 2016). The danger of HM in the aquatic ecosystem is compounded by the fact that, unlike organic substances, they are not susceptible to decomposition, but are capable of complexation, hydrolysis, and oxidation-reduction processes; they can migrate and accumulate in various components of river ecosystems. Therefore, for an ecological assessment of the agrolandscapes of small rivers under conditions of constant technogenic pressure, along with monitoring the content of HM in ecosystem components, it is necessary to study the features of their accumulation and migration by their components (Dinu, 2010; Mondol et al., 2011, Uddin et al., 2014; Pachura et al., 2016; Fomina et al., 2016; Zubarev & Kogan, 2017; Matveeva et al., 2018). The results of such researches allow us to offer more effective recommendations for the conservation and sustainable use of agrolandscapes of small rivers converted as a result of drainage reclamation.

MATERIALS AND METHODS

The researches were conducted on the territory of the Jewish Autonomous Region, located within the Sredneamurskaya lowland, where, due to the climate, geology, and terrain, in order to create the necessary conditions for agricultural production, large-scale land reclamation was carried out for more than 60 years (Anoshkin & Zubarev, 2018). On the territory of the Jewish Autonomous Region there are 76 drainage and 7 irrigation systems with a total area of 89.1 thousand ha, 36 thousand km of open channels, 2.7 thousand km of closed pottery and polyethylene drainage, 2.4 thousand units of various hydraulic structures were built to remove surface moisture. They are located mainly in the floodplains of small rivers that feed the middle left-bank tributaries of the Amur river and respond most quickly to land reclamation (Fig. 1).

Table 1. Watercourses, in the basins of which drainage reclamation works are carried out, on the territory of the Sredneamurskaya lowland

District	Name of watercourse
Birobidzhanskiy	Uldura, Gryaznushka, Ushumun
Leninskiy	Vertoprashikha, Solonechnaya
Octyabrskiy	Osinovka, Kulemnaya

We identified all watercourses in the basins of which drainage works had been carried out (Table 1). After analyzing the cartographic data, the following watercourses were also selected: the Ushumun river (an analogue of the Uldura river) and the Kulemnaya river (an analogue of the Osinovka river), in the basins of which there was no technogenic influence.

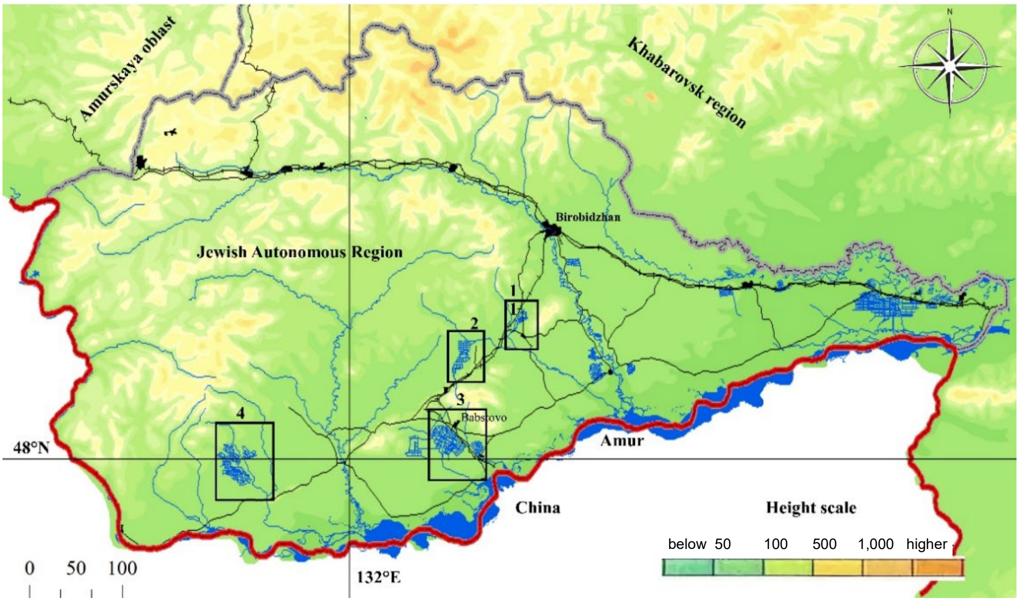

Figure 1. Research areas, southwestern part of the Sredneamurskaya lowland (1–4 - research areas).

These small rivers flow in the southern part of the Jewish Autonomous Region on the territory of the Sredneamurskaya alluvial lowland, they are outside the range of other sources of anthropogenic pollution and are exclusively the receivers of drainage water from drainage reclamation systems. A single method is used to drain floodplains and adjacent territories: land reclamation systems with open trapezoidal collectors and diverting main canals to discharge drainage water into the surface water of selected rivers. The main hydrographic characteristics of the studied small rivers are shown in Table 2.

Table 2. Hydrographic characteristics of small rivers - objects of the research

The name of watercourse	Length, km	Catchment area, km	Width, m	Depth, m
Uldura	15	160	3–5	0.2–0.6
Gryaznushka	32	191	3–5	0.3–0.9
Ushumun	45	260	3–5	1.0–1.5
Vertoprashikha	42	281	3–5	1.0–1.5
Solonechnaya	50	484	3–5	1.0–1.5
Osinovka	50	530	3–5	1.0–1.5
Kulemnaya	40	460	3–5	1.0–1.5

The long-term field researches were carried out to study the impact of drainage reclamation on the components of small river basins. Sampling was carried out at three points: above and below the areas of reclamation activities, as well as directly at the confluence of the drainage channel into the reservoir. Sampling of soil, water, bottom sediments, aquatic vegetation and hydrobionts was carried out in accordance with regulatory documents. 900 samples (350 of water, 225 of soil, 225 of bottom sediments, 50 of aquatic vegetation, and 50 of hydrobionts) were researched.

Sampling of floodplain soil was carried out from the upper horizon. The samples were dried and subjected to grinding, an average sample was formed. The following indicators were determined in each prepared soil sample: humus content by Tyurin I.V., based on the oxidation of soil organic matter by chromic acid to carbonic acid formation, actual acidity - by the potentiometric method, HM gross forms by atomic absorption spectrometry on a 'ThermoElectron SOLAAR 6M' instrument.

When sampling water, a visual inspection of the river state was carried out, the following parameters were determined: water temperature, pH, and oxygen content by the iodometric method. HMs in water were determined by atomic absorption spectrometry on a 'ThermoElectron SOLAAR 6M' instrument. Computer control of the measurement process and information processing was carried out in triplicate with automatic calculation of the confidence interval.

Hydrobionts are a reliable indicators of negative anthropogenic impact, including drainage reclamation, on aquatic ecological systems.For analysis on the content of HM, the highest aquatic plants of the pondweed family - *Potamogeton perfoliatus*, which belong to the group of submerged rooting hydrophytes, were selected and analyzed. To identify the impact of drainage on the aquatic fauna, Lagowski's minnow (*Phoxinus Lagowskii*) was chosen, this species is most often found in small rivers of Sredneamurskaya lowland. Samples of vegetation and fish were dried and subjected to ashing in a muffle furnace. To determine the gross content of HM, all samples were subjected to acid decomposition (HCl) in the 'Mars-6' microwave system. In samples of vegetation and fish, the content of HM was determined by atomic absorption spectrometry on the 'SOLAAR M6' instrument.

All analyzes were performed in triplicate. Statistical processing of the results was carried out using the Microsoft Excel software package.

RESULTS AND DISCUSSION

Drainage reclamation is meant to improve the water regime in waterlogged land and has a significant effect on humus and soil acidity. The researches have shown that the surface fertile horizons of undrained floodplain soil (0–20 cm) contained more humus than reclaimed ones (Table 3). This phenomenon can be explained by the increased aeration of soil under the influence of periodic treatments, leading to an increase in the biological activity of soil and acceleration of the processes of organic matter mineralization, as well as a change from the stagnant water regime to stagnant-flushing one with frequent changes in anaerobic and aerobic conditions.

The researches of soil acidity have shown that in all floodplain soil the pH_{KCl} varies in the upstream in the range of 4.1–4.8, and belongs to the category of 'medium acid' soil. On drainage systems, the pH is classified as 'slightly acidic' - pH - 5.0–6.1 (Table 3). These indicators have a significant impact on transit processes - HM accumulation in soil of agrolandscapes of river basins (Wang et al., 2006).

The research program included the determination of such HMs as iron, manganese, zinc, lead, copper, nickel in the soil of the studied agrolandscapes. Fluctuations in the iron content in the studied soil are very significant. The Fe concentrations in all samples exceed clarke values for soil - 38,000 mg per kg by about 1.5 times. The lowest concentrations of Fe are determined in the floodplains of the Uldura and Gryaznushka rivers, the highest ones - Solnechnaya and Vertoprashikha. When reclaimed within the drained territory, iron concentrations in soil are reduced. In samples that are not subject to the effect of drainage (upstream and downstream), the approximately 80% of total Fe is in the form of ferrous iron and 20% - in ferric iron. When draining by drainage channels, improved aeration conditions are created that contribute to a decrease in humidity and a change in the acidity of floodplain soil towards a weaker acidic pH medium. This led to an increase in ferric iron up to 40%. The increased amount of Fe^{2+} is associated with glue processes, the development of which depends on various factors, which include moisture conditions of the researched area, granulometric composition of soil, chemical and biological processes, as well as the content and forms of organic matter. The Mn content in the researched soil is in the range of 600–700 mg per kg, that is by 1.5 times lower than the average clarke indicator for Russian soil. In floodplain soil not affected by drainage, zinc concentrations were 70–80 mg per kg. In drained floodplain soil, zinc content decreases by 1.5–2 times. The maximum content of gross zinc was observed on the drainage systems of the floodplain soil of the Solonechnaya and Osinovka rivers during the catastrophic flood of 2013. A direct correlation dependence (r = 0.7) between the zinc content and the change in the pH value of the environment for floodplain soil of the Solonechnaya and Osinovka rivers was also established during researches. According to our researches, the concentration of lead in floodplain soil above the drainage area is in the range of 23–25 mg per kg. In soil selected in areas of drainage reclamation, a decrease in lead concentrations in relation to undrained soil. During the flushing type of the water regime (2013–2014), an increase in lead mobility was observed due to the large amount of precipitation. A correlation dependence (r = 0.6) was established between the content of gross forms of lead in the arable horizon and the change in the value of the pH medium, as well as with the amount of precipitation for floodplain soil of the Solonechnaya and Osinovka rivers, which were affected by reclamation. The concentration of gross forms of copper on drainage systems is reduced compared to the background. A correlation dependence (r = 0.7) was established between the content of gross forms of lead, a change in the pH medium, and the volume of precipitation for the floodplain soil of the Solonechnaya and Osinovka rivers, affected by drainage. A fairly uniform distribution of nickel in floodplain soil was noted throughout the researched area, with an average content of 24.3 mg per kg. Long-term drainage and the use of various fertilizers had a weak effect on the content of gross nickel in the soil (Table 4).

Table 3. Average humus content and acidity in floodplain soil of small rivers *

The name of watercourse	Humus, %	pH_{KCl}, un.pH
Floodplain soil - subject to drainage		
Vertoprashikha	5.74 ± 0.3	4.27 ± 0.4
	4.53 ± 0.4	5.13 ± 0.4
Uldura	5.83 ± 0.4	4.42 ± 0.3
	3.70 ± 0.3	5.18 ± 0.5
Gryaznushka	5.68 ± 0.3	4.55 ± 0.3
	3.13 ± 0.2	5.22 ± 0.4
Solonechnaya	5.46 ± 0.4	4.51 ± 0.3
	3.11 ± 0.2	6.21 ± 0.5
Osinovka	5.41 ± 0.3	4.27 ± 0.3
	3.33 ± 0.3	6.02 ± 0.4
Floodplain soil - not affected by drainage		
Kulemnaya	5.47 ± 0.5	4.30 ± 0.3
	5.28 ± 0.4	4.35 ± 0.3
Ushumun	5.64 ± 0.4	4.60 ± 0.4
	5.44 ± 0.4	4.58 ± 0.3

*The note: the numerator is the upper flow, the denominator is the drainage system. For floodplain soil not affected by drainage: the numerator is the upper course, the denominator is the lower course.

Table 4. The average content of gross forms of heavy metals in floodplain soil of small rivers (mg kg^{-1}) *

The name of watercourse	Heavy metals, mg kg^{-1}					
	Fe, 10^3 mg kg^{-1}	Mn, 10^3 mg kg^{-1}	Zn	Pb	Cu	Ni
Floodplain soil - subject to drainage						
Vertoprashikha	51.7 ± 3.0	65.3 ± 3.3	74.3 ± 3.4	25.1 ± 2.0	20.6 ± 2.0	21.6 ± 2.0
	48.9 ± 2.3	55.1 ± 2.8	68.3 ± 3.0	19.2 ± 1.7	19.3 ± 1.7	19.6 ± 1.3
Uldura	47.7 ± 2.6	65.0 ± 3.1	80.1 ± 3.1	24.7 ± 2.2	19.5 ± 2.1	21.6 ± 2.0
	45.0 ± 2.3	57.8 ± 2.0	62.3 ± 3.0	19.9 ± 2.0	17.7 ± 1.6	20.2 ± 1.1
Gryaznushka	47.6 ± 2.5	67.1 ± 3.7	74.0 ± 3.2	24.7 ± 2.9	19.4 ± 1.9	23.1 ± 2.2
	45.0 ± 2.3	53.4 ± 2.9	55.8 ± 2.7	21.6 ± 1.9	17.7 ± 1.7	21.9 ± 1.9
Solonechnaya	53.7 ± 2.6	64.5 ± 3.4	70.8 ± 3.5	24.8 ± 2.1	22.8 ± 2.0	21.0 ± 2.4
	49.1 ± 2.8	46.9 ± 2.3	52.1 ± 2.4	19.1 ± 1.3	17.9 ± 1.8	19.7 ± 1.3
Osinovka	48.0 ± 2.7	65.9 ± 3.1	81.6 ± 3.7	23.9 ± 1.9	19.7 ± 2.5	23.1 ± 2.6
	44.9 ± 2.3	47.1 ± 2.3	51.8 ± 2.7	20.5 ± 1.5	17.4 ± 1.3	21.4 ± 1.7
Floodplain soil - not affected by drainage						
Kulemnaya	48.3 ± 2.4	65.2 ± 3.6	71.1 ± 3.2	23.4 ± 2.1	19.2 ± 1.2	23.1 ± 2.0
	48.3 ± 2.3	64.1 ± 3.3	76.1 ± 2.7	23.4 ± 2.0	19.0 ± 1.8	23.2 ± 2.3
Ushumun	47.0 ± 2.3	62.5 ± 3.4	76.7 ± 3.4	23.4 ± 2.4	19.4 ± 1.7	22.1 ± 2.2
	47.2 ± 2.3	63.3 ± 3.7	77.4 ± 3.5	23.4 ± 2.1	19.9 ± 1.4	23.2 ± 1.8

*The note: the numerator is the upper flow, the denominator is the drainage system. For floodplain soil not affected by drainage: the numerator is the upper course, the denominator is the lower course.

During research, we were studying such important parameters for the migration of heavy metals as temperature, pH, and oxygen content in the water of objects flowing in the territories of drained landscapes (Table 5).

Table 5. Physical and chemical indicators of small rivers in areas of land reclamation *

Indicator	Sampling location		
	Upstream	Drainage channel	Downstream
t, °C	16.1–18.4	20.0–23.1	17.3–21.9
	17.5 ± 1.2	22 ± 1.5	20 ± 1.8
O_2.	8.4–11.8	5.5–8.1	7.6–9.2
mgO_2 dm^{-3}	9.8 ± 1.7	6.7 ± 1.2	8.1 ± 1.4
pH. units	6.1–6.7	7.4–8.5	6.1–8.0
	6.3 ± 0.3	7.8 ± 0.4	6.5 ± 0.3

* The note: in the numerator the minimum and maximum values, in the denominator - the average value of the indicator.

Analysis of the temperature distribution along the longitudinal profile has shown that drainage channels were characterized by higher temperatures of water that can affect the increase in the migratory capacity of HM. The pH value determines the state and mobility of many elements in the aquatic ecosystem, changes the degree of toxicity of pollutants. According to researches the reaction of water changed from slightly acidic to slightly alkaline. In the water of the drainage channel, a decrease in the oxygen content was observed, that led to a change of oxidizing conditions to recovery ones and increased the mobility of HM.

Analysis of the results of the determination of HM in water has shown the following: in surface water taken above the drainage area, the Fe content varies from 1.5 to 2.5 mg dm^{-3}, its amount significantly increases in reclamation channels. The concentration of Fe in the Ushumun and Kulemnaya rivers, not subject to drainage, is almost the same in the upstream and downstream. The high iron content was observed in the water of the drainage channels. According to the results of our researches, the minimum Mn content in the upstream of all watercourses is in the range from 0.1 to 0.6 mg dm^{-3}. The highest concentrations are observed for the water of drainage channels - 1.5–2.5 mg dm^{-3}. In the water of small rivers, above the area of drainage reclamation, low zinc concentrations were revealed, that is explained by its sorption by suspended solids. Under the influence of drainage, there is a change in the pH of water towards a slightly alkaline reaction of the medium, which causes the formation of sparingly soluble zinc hydroxides. In surface water not affected by drainage, the main form of Pb migration is the free form. When the pH of the water changes from 7 to 8, under the influence of drainage reclamation, readily soluble lead hydroxide is formed. The copper content in surface water, above the drainage area, was in the range of 0.0–0.09 mg dm^{-3}. Copper has high complexing ability. In surface water not affected by drainage, the main form of Cu migration is the free form. When the pH of water changes to alkaline values, under the influence of drainage reclamation, the ratio of hydrated forms of copper changes: 30% - Cu^{2+} and 70% - $(Cu\ (OH))^{+}$. In all small rivers, at all sampling points, low nickel concentrations are traced as a result of its sorption, the formation of insoluble compounds, as well as absorption by various organisms. The main form of Ni migration in water is the free form. In areas of drainage reclamation, there is a decrease in lead concentrations at all points relative to the background.

To identify the impact of drainage on hydrobionts, Lagowski's minnow (*Phoxinus Lagowskii*) was chosen, this species is most common in small rivers of the Sredneamurskaya lowland. The results of the researches showed that the accumulation of HM in fish tissues occurs in the downstream of small rivers in the studied area that is associated with the use of land reclamation, accumulation in the soil and further washing out of heavy metals and their compounds contained in fertilizers into rivers. In the gills of Lagowski's minnows, which live in the downstream of the Gryaznushka, Vertoprashikha, and Solonichnaya rivers, iron, manganese, and lead concentrations were found that significantly exceeded the standards for commercial fish. The concentrations of zinc and copper in the gills of minnows from the lower reaches of Gryaznushka, Vertoprashikha and Solonichnaya rivers also exceed the concentrations of these metals in the upstream of the rivers that indicates the accumulation of heavy metals in the lower reaches during land reclamation. Both in the upper and lower reaches of the Ushumun river, the basin of which is the least reclaimed, the concentration of heavy metals (iron, manganese, zinc, copper, lead) in the gills of Lagowski's minnow did not exceed the standard values (Table 6).

The results of the researches showed an intensive accumulation of HM by higher aquatic vegetation (indicator species - *Potamogeton perfoliatus*), selected at different points of small rivers of reclaimed landscapes. According the studied HM, the plants contain Fe to the greatest extent and Ni to the least. According to the content in *Potamogeton perfoliatus*, the elements formed the following decreasing row: Fe > Mn > Pb > Zn > Cu > Ni. The largest accumulations of all HMs in plants were found at the sampling points of the direct inflow of the main canal into the river, this is especially noticeable for the Osinovka and Solonechnaya rivers (Table 7).

Table 6. The concentration of heavy metals in the gills of the Lagowski's minnow (Phoxinus Lagowskii), mg kg^{-1} *

The name of watercourse	Heavy metals Fe	Zn	Mn	Ni	Cu	Pb
Watercourses - subject to drainage						
Gryaznushka	25.0 ± 1.4	7.0 ± 0.9	12.0 ± 1.3	0	0.05 ± 0.002	0
	48.0 ± 2.3	14.5 ± 1.3	24.0 ± 0.9	1.0 ± 0.09	2.5 ± 0.09	2.8 ± 0.08
Vertoprashikha	24.0 ± 1.2	6.7 ± 0.8	11.5 ± 1.1	0	0	0
	45 ± 2.6	10.5 ± 1.1	18.0 ± 1.7	0.3 ± 0.02	1.5 ± 0.07	0.7 ± 0.04
Solonechnaya	21.5 ± 1.3	6.0 ± 0.4	10.3 ± 1.2	0	0	0
	62.4 ± 3.1	28.6 ± 1.7	31.2 ± 2.1	2.3 ± 0.09	4.25 ± 0.2	3.3 ± 0.4
Watercourse - not subject to drainage						
Ushumun	24.0 ± 1.2	6.3 ± 0.4	8.0 ± 1.4	0	0	0
	28.0 ± 1.7	6.5 ± 0.7	10.0 ± 0.9	0	0	0
ПД2К*	30	40	10	20	10	1

*The note: the numerator is the upper course, the denominator is the lower course.
MPC – maximum permissible concentrations of HM for commercial fish (Sanitary rules and regulations 2.3.2.1078-01).

Table 7. The concentration of heavy metals in aquatic plants *Potamogeton perfoliatus*, mg kg^{-1} *

The name of watercourse	Sampling points	Fe· 10^3 mg kg^{-1}	Mn· 10^3 mg kg^{-1}	Zn· 10^3 mg kg^{-1}	Pb mg kg^{-1}	Cu mg kg^{-1}	Ni· 10^{-1} mg kg^{-1}
Watercourses - subject to drainage reclamation							
Solonechnaya	u.c.	7.94 ± 0.6	0.281 ± 0.02	0.117 ± 0.01	3.5 ± 0.2	2.56 ± 0.2	0.3 ± 0.01
	d.c.	17.010 ± 2.6	1.149 ± 0.1	0.624 ± 0.08	11.03 ± 0.6	6.74 ± 0.7	1.6 ± 0.09
	l.c.	10.730 ± 0.1	0.904	0.429 ± 0.02	9.43	3.93 ± 0.4	0.9 ± 0.06
Osinovka	u.c.	7.250 ± 0.6	0.203 ± 0.02	0.178 ± 0.02	2.28 ± 0.2	2.56 ± 0.2	0.3 ± 0.01
	d.c.	18.640 ± 3.4	1.160 ± 0.09	0.663 ± 0.05	10.49 ± 0.7	6.18 ± 0.5	1.4 ± 0.05
	l.c..	16.700 ± 3.0	1.070 ± 0.01	0.351 ± 0.04	8.91 ± 0.6	3.37 ± 0.4	0.8 ± 0.04
Watercourse - not subject to drainage reclamation							
Ushumun	u.c.	5.590 ± 0.4	0.281 ± 0.02	0.117 ± 0.02	3.34 ± 0.4	2.56 ± 0.2	0.3 ± 0.01
	l.c.	5.490 ± 0.4	0.270 ± 0.02	0.186 ± 0.02	3.44 ± 0.1	2.53 ± 0.4	0.3 ± 0.01

*The note: u.c. – upper course; l.c. – lower course; d.c. – drainage channel.

The least impact of drainage is manifested in the downstream of the rivers.

CONCLUSIONS

During drainage reclamation in floodplain soil, conditions are created for improved soil aeration, which leads to a decrease in the humus content and a change in pH from acidic to neutral reaction of the medium. This process contributes to a certain decrease in the concentration of HM in the soil. Conducting drainage reclamation works leads to a decrease in the water quality of all the watercourses considered, as a result of an increase in the concentration of HM in water and bottom sediments. The transformation of landscapes leads to the accumulation of HM in macrophytes and fish, which is potentially dangerous for both the aquatic ecosystem and human health.

REFERENCES

Anoshkin, A.V. & Zubarev, V.A. 2018. Land reclamation and transformation of floodplain-channel complexes at the Sredneamurskaya lowland. *Regional issues* **3–1**, 70–74.

Chibuike, G.U. & Obiora, S.C. 2014. Heavy Metal Polluted Soil: Effect on plants and bioremediation methods. *Appl. Environ. Soil. Sci*. 752708, 12 pp.

Dyatel, A.A. 2017. Ecological and reclamation component of drained lands in the area of impact of the «Khotislavsky» quarry. *Reclamation* **1**(79), 31–38 (in Russian).

Fomina, A.A., Tikhomirova, E.I. & Korableva, A.I. 2016. Analysis of the content of heavy metals in the higher aquatic vegetation of the Volgograd reservoir in the area of the agglomeration of Saratov - Engels. *Bulletin of the Samara Scientific Center of the Russian Academy of Sciences* **2**(3) 822–826. (in Russian).

Dinu, M. 2010. Comparison of Complexing Ability of Fulvic and Humic Acids in the Aquatic Environment with Iron and Zinc Ions. *Water Resources* **37**(1), 65–69.

Israel, Yu.A. 1984. *Ecology and environmental control*. Gidrometeoizdat, Moscow, 560 pp. (in Russian).

Imeri, R., Kullaj, E, Duhani, E. & Millaku, L. 2019. Impact of rootstock on heavy metal bioaccumulation in apple plant grown near an industrial source in Obiliq, Kosovo. *Agronomy Research* **17**(1), 100–110.

Kabata-Pendias, A. & Pendias, H. 2001. *Trace elements in soil and plants (3rd edition*). CRC Press, Boca Raton, 313 pp.

Kasiuliene, A., Paulauskas, V. & Kumpiene, J. 2016. Influence of nitrogen fertilizer on Cd and Zn accumulation in rapeseed (*Brassica napus* L.) biomass. *Agronomy Research* **14**(2), 418–427.

Khristoforova, N.K. 2007. *Fundamentals of Ecology*. Far Eastern University Press, Vladivostok, 454 pp. (in Russian).

Lukowski, A. & Wiater, J. 2016. The content and solubility of lead in arable soil of the Podlasie Province (eastern Poland). *Soil Science Annual* **67**(4), 190–196.

Matveeva, A.Yu., Kutlin, N.G., Kardapoltseva, D.G. & Mullagalieva, A.T. 2018. The effect of anthropogenic stress on the accumulation of heavy metals in the organs and tissues of commercial fish. *Environmental Engineering* **2**, 132–136 (in Russian).

Mondol, M.N., Chamon, A.S., Faiz, B. & Elahi, S.F. 2011. Seasonal Variation of Heavy Metal Concentrations in Water and Plant Samples Around Tejgaon Industrial Area of Bangladesh. *J. Bangladesh Acad. Sci.* **35**(1), 19–41.

Moore, J.V. & Ramamurthy, S. 1987. *Heavy Metals in natural Water: monitoring and evaluation of impact*. Mir, Moscow, 286 pp. (in Russian).

Morais, S., Costa, F.G. & Pereira, M.L. 2012. Heavy metals and human health. In: Oosthuizen J. (ed): Environmental health – emerging issues and practice, pp. 227–246.

Murtic, S., Jurkovic, J., Basic, E. & Hekic, E. 2019. Assessment of wild plants for phytoremediation of heavy metals in soil surrounding the thermal power station. *Agronomy Research* **17**(1), 234–244.

Nazarov, N.N. 2014. Hydrological consequences of drainage reclamation and channel processes. *Geographical Bulletin* **1**(28), 4–10 (in Russian).

Pachura, P., Ociepa-Kubicka, A. & Skowron-Grabowska, B. 2016. Assessment of the availability of heavy metals to plants based on the translocation index and the bioaccumulation factor. *Desalin. Water Treat.* **57**(3), 1469–1477.

Pais, I. & Jones, J.B. 1997. *The Handbook of Trace Elements*. Lucie Press, Boca Raton, 223 pp.

Perevoznikov, M.A. & Bogdanova, E.A.1999. *Heavy metals in freshwater ecosystems*. SRILRF, St. Petersburg, 228 pp. (in Russian).

Tack, F.M.G. 2010. Trace Elements: General Soil Chelistry Principles and Processes. In: Hooda PS (ed): *Trace Elements in Soil*, pp. 9–38.

Tolkachev, G.Yu. 2017. Migration and transformation of forms of heavy metals in the catchment area and in the bottom sediments of the Ivankovo reservoir. *Land reclamation and water management* **6**, 35–40 (in Russian).

Uddin, M.N., Alam, M.S., Mobin, M.N. & Miah, M.A. 2014. An Assessment of the River Water Quality Parameters: A case of Jamuna River. *Journal of Environmental Sciences and Natural Resources* **7**(1), 249–256.

Voronov, B.A. & Makhinov, A.N. 2009. *Current state of water resources in the Far East and their anthropogenic transformation*. The 100th anniversary of the Kamchatka expedition of the Russian Geographical Society of 1908–1910: materials of All-Russian scientific conf. Institute of Volcanology and Seismology, Petropavlovsk-Kamchatsky, Russia, pp. 40–48 (in Russian).

Wang, A.S., Angle, J.S., Chaney, R.L., Delorme, T.A. & Reeves, R.D. 2006. Soil pH effects on uptake of Cd and Zn by Thlaspi caerulescens. *Plant and Soil* **281**(1–2), 325–337.

Yashin, V.M. 2017. The formation of the quality of drainage flow on the Yakhroma floodplain. *Land reclamation and water management* **6**, 21–25 (in Russian).

Zubarev, V.A. & Kogan, R.M. 2017. Ecological Conditions of Watercourses in the Middle Amur Lowland in the Areas of Drainage Reclamation. *Water Resources* **44**(7), 940–951.

INSTRUCTIONS TO AUTHORS

Papers must be in English (British spelling). English will be revised by a proofreader, but authors are strongly urged to have their manuscripts reviewed linguistically prior to submission. Contributions should be sent electronically. Papers are considered by referees before acceptance. The manuscript should follow the instructions below.

Structure: Title, Authors (initials & surname; an asterisk indicates the corresponding author), Authors' affiliation with postal address (each on a separate line) and e-mail of the corresponding author, Abstract (up to 250 words), Key words (not repeating words in the title), Introduction, Materials and methods, Results and discussion, Conclusions, Acknowledgements (optional), References.

Layout, page size and font

- Use preferably the latest version of **Microsoft Word**, doc., docx. format.
- Set page size to **ISO B5 (17.6×25 cm)**, all **margins at 2 cm**. All text, tables, and figures must fit within the text margins.
- Use single line spacing and **justify the text**. Do not use page numbering. Use **indent 0.8 cm** (do not use tab or spaces instead).
- Use font Times New Roman, point size for the title of article **14 (Bold)**, author's names 12, core text 11; Abstract, Key words, Acknowledgements, References, tables, and figure captions 10.
- Use *italics* for Latin biological names, mathematical variables and statistical terms.
- Use single ('…') instead of double quotation marks ("…").

Tables

- All tables must be referred to in the text (Table 1; Tables 1, 3; Tables 2–3).
- Use font Times New Roman, regular, 10 pt. Insert tables by Word's 'Insert' menu.
- Do not use vertical lines as dividers; only horizontal lines (1/2 pt) are allowed. Primary column and row headings should start with an initial capital.

Figures

- All figures must be referred to in the text (Fig. 1; Fig. 1 A; Figs 1, 3; Figs 1–3). Use only black and white or greyscale for figures. Avoid 3D charts, background shading, gridlines and excessive symbols. Use font **Arial, 10 pt** within the figures. Make sure that thickness of the lines is greater than 0.3 pt.
- Do not put caption in the frame of the figure.
- The preferred graphic format is Excel object; for diagrams and charts EPS; for half-tones please use TIFF. MS Office files are also acceptable. Please include these files in your submission.
- Check and double-check spelling in figures and graphs. Proof-readers may not be able to change mistakes in a different program.

References

- **Within the text**

In case of two authors, use '&', if more than two authors, provide first author 'et al.':

Smith & Jones (1996); (Smith & Jones, 1996);

Brown et al. (1997); (Brown et al., 1997)

When referring to more than one publication, arrange them by following keys: 1. year of publication (ascending), 2. alphabetical order for the same year of publication:

(Smith & Jones, 1996; Brown et al., 1997; Adams, 1998; Smith, 1998)

- **For whole books**

Name(s) and initials of the author(s). Year of publication. *Title of the book* (*in italics*). Publisher, place of publication, number of pages.

Shiyatov, S.G. 1986. *Dendrochronology of the upper timberline in the Urals*. Nauka, Moscow, 350 pp. (in Russian).

- **For articles in a journal**

Name(s) and initials of the author(s). Year of publication. Title of the article. *Abbreviated journal title* (*in italic*) volume (in bold), page numbers.

Titles of papers published in languages other than English, should be replaced by an English translation, with an explanatory note at the end, e.g., (in Russian, English abstr.).

Karube, I. & Tamiyra, M.Y. 1987. Biosensors for environmental control. *Pure Appl. Chem.* **59**, 545–554.

Frey, R. 1958. Zur Kenntnis der Diptera brachycera p.p. der Kapverdischen Inseln. *Commentat.Biol.* **18**(4), 1–61.

Danielyan, S.G. & Nabaldiyan, K.M. 1971. The causal agents of meloids in bees. *Veterinariya* **8**, 64–65 (in Russian).

- **For articles in collections:**

Name(s) and initials of the author(s). Year of publication. Title of the article. Name(s) and initials of the editor(s) (preceded by In:) *Title of the collection (in italics)*, publisher, place of publication, page numbers.

Yurtsev, B.A., Tolmachev, A.I. & Rebristaya, O.V. 1978. The floristic delimitation and subdivisions of the Arctic. In: Yurtsev, B. A. (ed.) *The Arctic Floristic Region*. Nauka, Leningrad, pp. 9–104 (in Russian).

- **For conference proceedings:**

Name(s) and initials of the author(s). Year of publication. Name(s) and initials of the editor(s) (preceded by In:) *Proceedings name (in italics)*, publisher, place of publishing, page numbers.

Ritchie, M.E. & Olff, H. 1999. Herbivore diversity and plant dynamics: compensatory and additive effects. In: Olff, H., Brown, V.K. & Drent R.H. (eds) *Herbivores between plants and predators. Proc. Int. Conf. The 38th Symposium of the British Ecological Society*, Blackwell Science, Oxford, UK, pp. 175–204.

Please note

- Use '.' (not ',') for decimal point: 0.6 ± 0.2; Use ',' for thousands – 1,230.4;
- Use '–' (not '-') and without space: pp. 27–36, 1998–2000, 4–6 min, 3–5 kg
- With spaces: 5 h, 5 kg, 5 m, 5 °C, C : D = 0.6 ± 0.2; p < 0.001
- Without space: 55°, 5% (not 55 °, 5 %)
- Use 'kg ha^{-1}' (not 'kg/ha');
- Use degree sign ' ° ' : 5 °C (not 5 ^{O}C).